

**ELG 6369**

**NONLINEAR MICROWAVE DEVICES AND EFFECTS**

**CHAPTER VII**

**MICROWAVE MIXERS**

## A – MIXING PRINCIPLES

### I – Introduction

Mixing is one of the most important functions in telecommunications. Because of cost and signal processing considerations in low frequencies, and for propagation requirements in high frequencies, any transmitter system has to deal with mixing. To mix a signal consists to shift an incident RF signal of frequency  $f_n$  to a signal of frequency  $f_o$  with the help of a local oscillator (LO) or pump of frequency  $f_p$ . Depending on the relative values of input and output frequencies, we can distinguish between up-converter mixers ( $f_o > f_n$ ) and down-converter mixers ( $f_o < f_n$ ).

In the first case, the most used, the output frequency  $f_o$  is called the intermediate frequency (IF); and could be written in the following format

$$f_o = \pm m f_n \pm n f_p \quad m, n = 0, 1, \dots \quad (\text{VII-1})$$

Since the input RF signal is usually small (in terms of magnitude) compared to the LO one, the following notation (derived from Saleh's work) can be used to express the relation between frequencies

$$\omega_n = \omega_o + n\omega_p \quad n = 0, \pm 1, \dots \quad (\text{VII-2})$$

It is important to place the mixing process into a frequency domain perspective. To this end, it is assumed that the angular RF signal had a certain bandwidth, i.e., is centered at  $\omega_{RF}$  with two extra frequency components situated  $\omega_W$  above and below  $\omega_{RF}$  as shown in Figure VII-1.

---

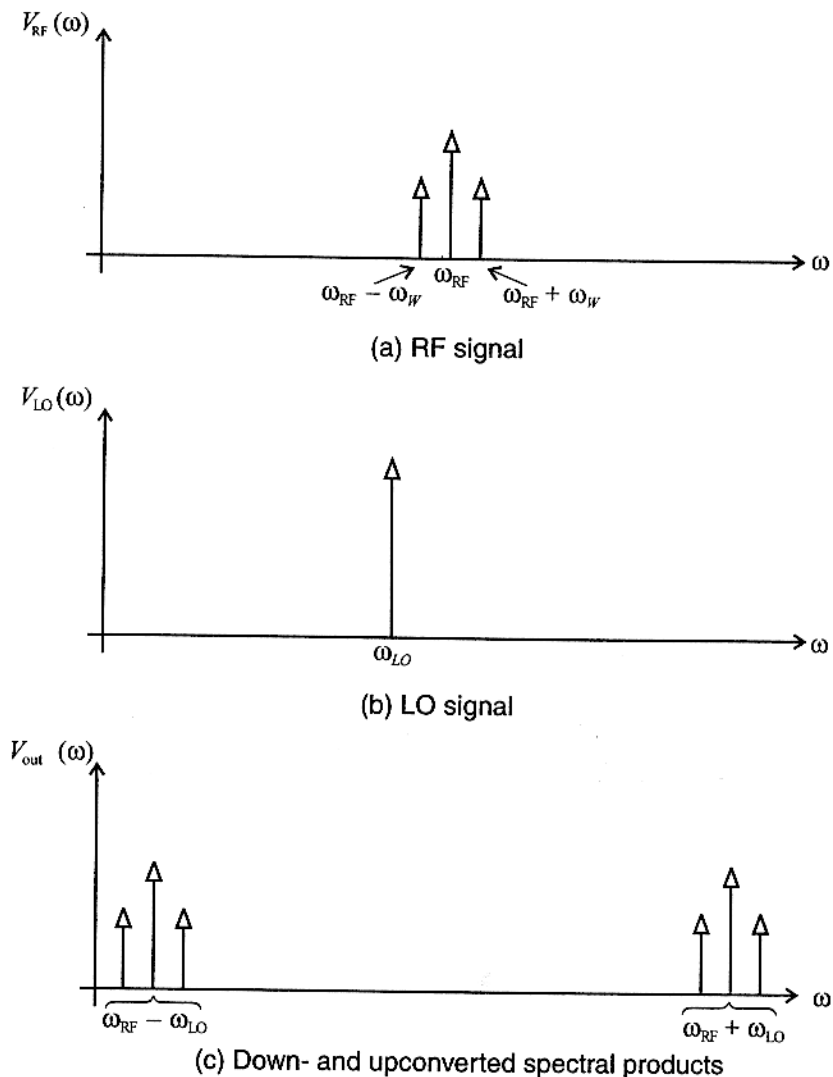


Fig. VII-1. Spectral representation of mixing process.

After performing mixing, the resulting spectrum contains both upconverted and downconverted frequency components. Typically, the upconversion process is associated with the modulation in a transmitter, whereas the downconversion is encountered in a receiver.

---

*The materials you receive for this course are protected by copyright and to be used for this course only. You do not have permission to upload the course materials, including any lecture recordings you may have, to any website. If you require clarification, please consult your professor.*

We have then to specify the kind of mixer in terms of signal, i.e.,

- Lower sideband, or LSB ( $\omega_{RF} - \omega_{LO}$ )
- Upper sideband, or USB ( $\omega_{RF} + \omega_{LO}$ )
- Double sideband, or DSB ( $\omega_{RF} + \omega_{LO}$ ,  $\omega_{RF} - \omega_{LO}$ )

An interrelated issue is the problem of image frequencies mapping into the same downconverted frequency range. To understand this problem, assume an RF signal is downconverted with a given LO frequency. In addition to the desired signal, we have an interferer about IF. In fact, if the desired output frequency is obtained by

$$\omega_{RF} - \omega_{LO} = \omega_{IF} \quad (\text{VII-3})$$

the large LO signal will also generate harmonic; therefore, an image frequency  $\omega_{IM}$  will appear at

$$2 \omega_{LO} - \omega_{RF} = \omega_{LO} + (\omega_{LO} - \omega_{RF}) = \omega_{LO} - \omega_{IF} = \omega_{IM} \quad (\text{VII-4})$$

and combined to the LO signal, will be transformed as

$$\omega_{IM} - \omega_{LO} = \omega_{IF} \quad (\text{VII-5})$$

Since  $\cos(-\omega_{IFT}) = \cos(\omega_{IFT})$ , both frequency spectra are shifted to the same frequency location, as Figure VII-2 illustrates.

To avoid the presence of undesired image signals that can be greater in magnitude than the RF signal, a so-called image filter could be placed before the mixer circuit to suppress this influence,

---

*The materials you receive for this course are protected by copyright and to be used for this course only. You do not have permission to upload the course materials, including any lecture recordings you may have, to any website. If you require clarification, please consult your professor.*

provided sufficient spectral separation is assured. This configuration is known as the image rejection mixer.

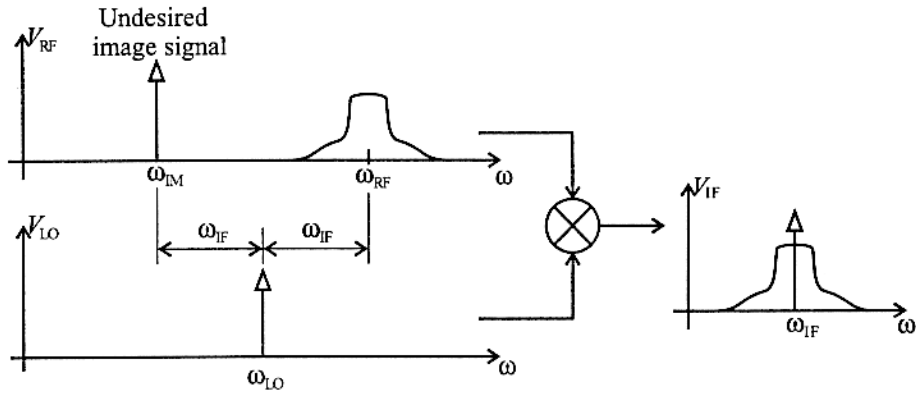


Fig. VII-2. Image frequency.

However, even if the fundamental LO frequency is usually the one used in mixing ( $n = \pm 1$ ), there exist a variety of mixers called "sub-harmonically pumped mixers" which utilize the LO harmonics. They are mainly used in cases where a very high output power combined with a low noise pumping is difficult to achieve (e.g., millimeter band).

## II – Mixer characteristics

### 1. Conversion ratio

The ratio between output and input powers is the mixer conversion ratio. For diode mixers, this ratio is less than unity, and therefore is called conversion loss. While for a transistor mixer, this quantity is noted by the conversion gain since it is usually higher than unity.

### 2. 1 dB compression point

The 1-dB compression point is the input power level for which the conversion ratio varies by 1 dB from its average value. This quantity defines the mixer linearity.

In fact, this parameter is determined when the input/output curve differs from the theoretical linear one by 1 dB. It defines the apparition of intermodulation products, i.e., power transfer from the fundamental output frequency to other output frequencies following equation (VII-2).

### 3. Port isolation

It is essential to isolate the different ports of a mixer, particularly between the large LO signal and the small RF input excitation. In fact, the apparition of a pump power at the input port can significantly reduce the dynamic bandwidth as well as the LO signal itself.

## B- mixer configurations

### I – Diode mixers

In mixing, Schottky diodes are the most widely in centimeter and millimeter ranges. However, Gunn diodes are also used because of their ability to serve both as source (oscillator) and mixing diode. Josephson diodes are also candidates for some special devices. For common use, we can distinguish 4 basic configurations which different characteristics as described in Table VII-1:

- The single ended mixer (one diode).
- The single balanced mixer (two diodes).
- The double balanced mixer (four diodes).

---

*The materials you receive for this course are protected by copyright and to be used for this course only. You do not have permission to upload the course materials, including any lecture recordings you may have, to any website. If you require clarification, please consult your professor.*

Table VII-1. Diode mixer characteristics.

Mixer Type	Characteristics	Typical Applications
Singly balanced, 180-degree ("rat-race") mixer	Approximately 15% RF and LO bandwidth. IF must be less than approximately 15% of the RF/LO frequency. Rejects (2,1) or (1,2) spurious response, but not both. Can be dc biased.	Not a general-purpose circuit. Best used for noncritical applications in integrated components. A poor choice when a broadband IF is needed.
Singly balanced 90-degree mixer, branch-line hybrid	Up to 20% bandwidth. LO- and RF-port bandwidths differ. No inherent IMD/spur rejection. Requires a good, broadband source VSWR over both the RF and LO bands at both ports, or imbalance occurs.	Not a good circuit; used more often than it deserves. Can be used for simple, noncritical applications.
Doubly balanced ring mixer; coupled-line baluns	Multi octave RF and LO bands. Narrowband IF, dc coupled. RF and LO bands can be widely separated.	General-purpose, broadband applications. The star mixer is a better biphasic modulator.
Doubly-balanced ring mixer; "horseshoe" balun	Multi octave RF and LO bands. Broadband IF, dc coupled, which can partially overlap the RF and LO bands. RF and LO bands can be widely separated.	Most common type of general-purpose, commercial mixer. A very compact circuit.
Star mixer with Marchand baluns	Octave RF/LO band. Very broadband, dc-coupled IF but cannot overlap the RF/LO frequency range. RF and LO must cover the same frequency range.	Where the frequency plan allows it, this is a very good choice. High performance, good balance, broad bandwidth are easily achieved. Good biphasic modulator or phase detector.

The materials you receive for this course are protected by copyright and to be used for this course only. You do not have permission to upload the course materials, including any lecture recordings you may have, to any website. If you require clarification, please consult your professor.

## II – Transistor mixers

Although diodes are intensively used in mixing, it is possible to use transistors to design mixers. X- to K-band transistor mixers having 10-15 dB gain are regularly produced, with lower LO power levels than would be required for diode mixers. MESFETs and FET variants (e.g., the high electron mobility transistor, or HEMT) can exhibit conversion gain well into the millimeter-wave region (Table VII-2).

## C – MIXER ANALYSIS

As referred before, since the mixer has two input excitations (RF and LO), such devices have to be analyzed using the large-signal small signal analysis. For analysis clarity, let us use the basic mixing diode, namely the Schottky diode.

### I - Diode mixer analysis

Figure VII-3 shows the block diagram of a diode mixer.

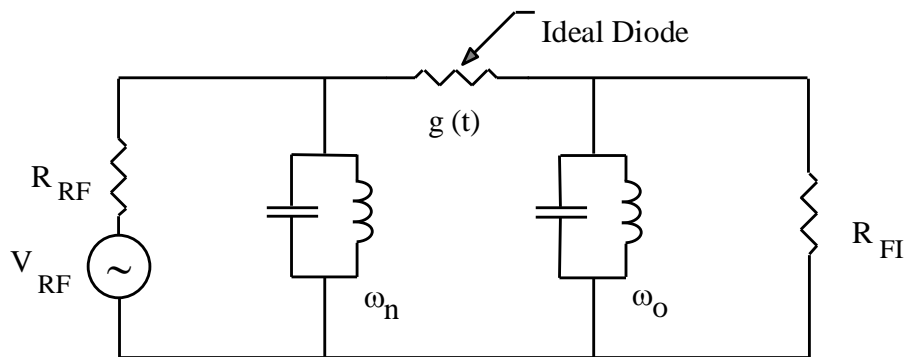


Fig. VII-3. Block diagram of a diode mixer.

*The materials you receive for this course are protected by copyright and to be used for this course only. You do not have permission to upload the course materials, including any lecture recordings you may have, to any website. If you require clarification, please consult your professor.*

Table VII-2. Transistor mixer characteristics.

Mixer Type	Characteristics	Typical Applications
Single-device, single-gate FET mixer	Simple, inexpensive. Provides conversion gain, low noise, low distortion. LO-to-IF isolation may be poor. Best for moderate-bandwidth applications.	Downconverter in receivers. The need for an LO-RF diplexer and IF filters limits applications.
Singe-device, dual-gate FET mixer	Good LO-to-RF isolation without filters. Gain and noise figure are somewhat worse than single-gate mixers; distortion is about the same. Moderate bandwidth.	A nice mixer for low-cost integrated circuits, especially commercial applications.
Singly balanced FET mixer	Essentially the same characteristics as a single-device mixer, but good LO-IF and LO-RF isolation without a diplexer. 3-dB higher LO power, 3-dB better IP. May require baluns.	High-performance IC applications where the number of FETs and the size of the baluns is acceptable. The large number of interconnections makes this a poor choice for hybrid circuits.
Doubly balanced MOSFET mixer	Essentially the same characteristics as a single-device mixer, but has all the benefits of a doubly balanced circuit (see Chapter 3). 6 dB higher LO power, 6 dB better IP. May require baluns.	Essentially the same applications as the singly balanced mixer, but where improved intermodulation rejection justifies the extra complexity and LO power.
Gilbert-cell BJT/HBT mixer	A doubly balanced bipolar mixer. Often works well without baluns. Can be used as a "linear" analog multiplier.	Modulators, signal processing as well as mixing.

The materials you receive for this course are protected by copyright and to be used for this course only. You do not have permission to upload the course materials, including any lecture recordings you may have, to any website. If you require clarification, please consult your professor.

### 1. Large-signal analysis

The purpose for this analysis is to determine the Fourier coefficients of the nonlinear elements  $C_j$  and  $G_j$  of the Schottky diode junction. Thus, the voltage  $V_j(t)$  and the current  $I_j(t)$  of the diode junction can be expressed as

$$V_j(t) = \sum_{k=-\infty}^{\infty} V_{jk} e^{jk\omega_p t} ; \quad I_j(t) = \sum_{k=-\infty}^{\infty} I_{jk} e^{jk\omega_p t} \quad (\text{VII-6})$$

and similarly, the nonlinear element coefficients can be deduced as

$$C_j(t) = \sum_{k=-\infty}^{\infty} C_{jk} e^{jk\omega_p t} ; \quad G_j(t) = \sum_{k=-\infty}^{\infty} G_{jk} e^{jk\omega_p t} \quad (\text{VII-7})$$

### 2. Small-signal analysis

By adding the input small signal to the large pump signal, the diode voltage and current would be equal to

$$V_j(t) = \sum_{k=-N}^N V_{jk} e^{j(\omega_o + k\omega_p)t} \quad (\text{VII-8-a})$$

$$I_j(t) = \sum_{m=-N}^N I_{jm} e^{j(\omega_o + m\omega_p)t} \quad (\text{VII-8-b})$$


---

and therefore, the mixer can be represented by a multifrequency multiport network (Figure VII-4). Based on these relations, the Fourier representation of a resistance  $R_j(t)$  is as follows

$$R_j(t) = \frac{V_j(t)}{I_j(t)} = \sum_{q=-N}^N R_{jq} e^{jq\omega_p t} \quad (\text{VII-9})$$

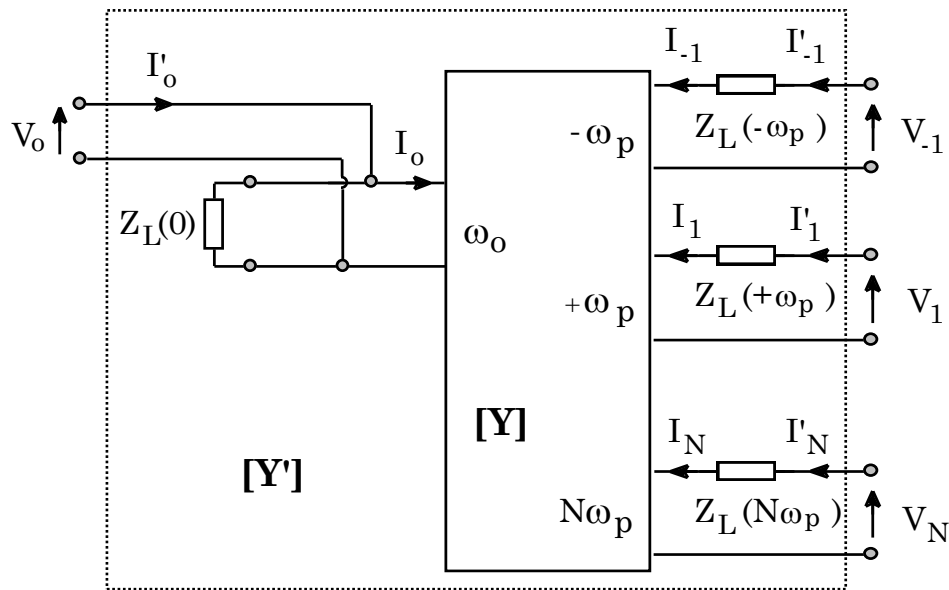


Fig. VII-4. Multifrequency multiport network representation of the diode mixer.

By combining equations (VII-8) and (VII-9), we have

$$\sum_{k=-N}^N V_k e^{j(\omega_o + k\omega_p)t} = \sum_{q=-N}^N \sum_{m=-N}^N R_q I_m e^{j(\omega_o + (q+m)\omega_p)t} \quad (\text{VII-10})$$

Grouping terms of same frequency leads to the following matrix representation

$$\begin{bmatrix} V_{-N} \\ \vdots \\ V_0 \\ \vdots \\ V_N \end{bmatrix} = \begin{bmatrix} R_0 & \cdots & R_{-N} & \cdots & R_{-2N} \\ \vdots & & \vdots & & \vdots \\ R_N & \cdots & R_0 & \cdots & R_{-N} \\ \vdots & & \vdots & & \vdots \\ R_{2N} & \cdots & R_N & \cdots & R_0 \end{bmatrix} \begin{bmatrix} I_{-N} \\ \vdots \\ I_0 \\ \vdots \\ I_N \end{bmatrix} \quad (\text{VII-11})$$

Note that the elements of the matrix include up to  $2N$ th harmonic. Since the time series are purely real, element  $R_j$  should be the complex conjugate of element  $R_{\bar{j}}$ . Therefore, except  $R_0$ , all other elements could be complex. This does not imply that a resistance reacts like a reactance, but we have a phase shift in impedance transfer between frequencies. The final form of the conversion matrix is thus

$$\begin{bmatrix} V_{-N}^* \\ \vdots \\ V_0 \\ \vdots \\ V_N \end{bmatrix} = \begin{bmatrix} R_0 & \cdots & R_{-N} & \cdots & R_{-2N} \\ \vdots & & \vdots & & \vdots \\ R_N & \cdots & R_0 & \cdots & R_{-N} \\ \vdots & & \vdots & & \vdots \\ R_{2N} & \cdots & R_N & \cdots & R_0 \end{bmatrix} \begin{bmatrix} I_{-N}^* \\ \vdots \\ I_0 \\ \vdots \\ I_N \end{bmatrix} \quad (\text{VII-12})$$

Similarly for the conversion matrix of the capacitance

$$I(t) = \frac{dQ(t)}{dt} = C(t) \frac{dV(t)}{dt} + V(t) \frac{dC(t)}{dt}$$

↑↓

$$\sum_{k=-N}^N I_k e^{j(\omega_o + k\omega_p)t} = \sum_{q=-N}^N \sum_{m=-N}^N j(\omega_o + (q+m)\omega_p) V_q C_m e^{j(\omega_o + (q+m)\omega_p)t} \quad (\text{VII-13})$$


---

*The materials you receive for this course are protected by copyright and to be used for this course only. You do not have permission to upload the course materials, including any lecture recordings you may have, to any website. If you require clarification, please consult your professor.*

thus

$$\begin{bmatrix} I_{-N}^* \\ \vdots \\ I_0 \\ \vdots \\ I_N \end{bmatrix} = \begin{bmatrix} \omega_{-N} C_o & \cdots & \omega_{-N} C_{-N} & \cdots & \omega_{-N} C_{-2N} \\ \vdots & & \vdots & & \vdots \\ \omega_o C_N & \cdots & \omega_o C_o & \cdots & \omega_o C_{-N} \\ \vdots & & \vdots & & \vdots \\ \omega_N C_{2N} & \cdots & \omega_N C_N & \cdots & \omega_N C_o \end{bmatrix} \begin{bmatrix} V_{-N}^* \\ \vdots \\ V_0 \\ \vdots \\ V_N \end{bmatrix} \quad (\text{VII-14})$$

or

$$[\mathbf{I}] = [\Omega] [\mathbf{C}] [\mathbf{V}] \quad (\text{VII-15})$$

where  $[\Omega]$  is a diagonal matrix as defined in chapter III. From these results, we can deduce the admittance matrix  $[\mathbf{Y}]$  of a diode, whose elements  $Y_{mn}$  will be equal to

$$Y_{mn} = G_{m-n} + j(\omega_o + m\omega_p) C_{m-n} \quad \omega_m = \omega_o + m \omega_p \quad (\text{VII-16})$$

This admittance matrix is of dimension  $2N \times 2N$  and each  $k^{th}$  line or column refers to the  $k^{th}$  harmonic

$$[\mathbf{Y}] = \begin{array}{c} Line\# \\ \vdots \\ 1 \\ 0 \\ -1 \\ \vdots \\ \dots \end{array} \begin{bmatrix} \vdots & \vdots & \vdots & \vdots & \vdots \\ \cdots & Y_{11} & Y_{10} & Y_{1-1} & \cdots \\ \cdots & Y_{01} & Y_{00} & Y_{0-1} & \cdots \\ \cdots & Y_{-11} & Y_{-10} & Y_{-1-1} & \cdots \\ \vdots & \vdots & \vdots & \vdots & \\ \dots & 1 & 0 & -1 & \cdots \end{bmatrix} \begin{array}{c} Column\# \\ \dots \end{array} \quad (\text{VII-17})$$

Similarly, the overall admittance matrix  $[\mathbf{Y}']$  of the mixer is obtained by including the equivalent impedances  $Z_L(k\omega_p)$  constituted by the impedances  $Z_{RL}(k\omega_p)$  of the linear sub-network and the parasitic elements of the diode (assumed to be linear)

$$[\mathbf{Y}'] = [\mathbf{Y}] + \text{diag} \left\{ \frac{1}{Z_L(k\omega_p)} \right\} \quad (\text{VII-18})$$

From this matrix, it is possible to obtain the mixer parameters. Therefore, for a frequency conversion from a frequency  $\omega_n$  to a frequency  $\omega_m$ , the conversion loss  $L_{mn}$  and the input/output impedances  $Z_{in}$  and  $Z_{out}$  are given by

$$L_{mn} = 4|Y'_{mn}|^2 \operatorname{Re}\{Z_L(m\omega_p)\} \operatorname{Re}\{Z_L(n\omega_p)\} \quad (\text{VII-19})$$

$$Z_{in} = 1/Y_{mm} - Z_L(m\omega_p) \quad (\text{VII-20})$$

$$Z_{out} = 1/Y_{nn} - Z_L(n\omega_p) \quad (\text{VII-21})$$

## II – Transistor mixer analysis

In FET mixers, the two basic configurations are:

- Mixing at the gate based on the nonlinear drain current characteristic near saturation.
- Mixing at the drain based on the nonlinear drain current characteristic near the knee.

### 1. Large-signal analysis

Using a similar procedure as for diodes, the large-signal analysis deals with the determination of the Fourier coefficients of voltage and current quantities both at the gate ( $V_i$  and  $I_i$ ) and drain ( $V_o$  and  $I_o$ )

$$V_i(t) = \sum_{k=-N}^N V_{ik} e^{jk\omega_p t} ; \quad I_i(t) = \sum_{k=-N}^N I_{ik} e^{jk\omega_p t} \quad (\text{VII-22})$$

$$V_o(t) = \sum_{k=-N}^N V_{ok} e^{jk\omega_p t} ; \quad I_o(t) = \sum_{k=-N}^N I_{ok} e^{jk\omega_p t} \quad (\text{VII-23})$$

### 2. Small-signal analysis

As for diodes in small signal analysis, the equivalent circuit of the transistor is a multifrequency multiport network. The difference is the number of ports: { 2(N+1) } instead of { N+1 }. The aim of this part is to determine the conversion matrices of the nonlinear elements.

Let  $[\mathbf{R}_a]$ ,  $[\mathbf{G}_m]$ ,  $[\mathbf{C}_s]$  and  $[\mathbf{C}_d]$  be the conversion matrices of  $R_{ds}$ ,  $G_m$ ,  $C_{gs}$  and  $C_{ds}$  respectively. The mixer admittance transfer matrix  $[\mathbf{Y}]$  is equal to

$$[\mathbf{Y}] = \left[ [\mathbf{Z}_1] + [\mathbf{Z}_c][\mathbf{Z}_6] \right] \left\{ [\mathbf{Z}_A]^{-1} [\mathbf{Z}_B] \right\} + [\mathbf{Z}_c][\mathbf{Z}_5] + [\mathbf{Z}_2]^{-1} \quad (\text{VII-24})$$

with

$$[\mathbf{Z}_A] = [\mathbf{Z}_3][\mathbf{Z}_7]^{-1}[\mathbf{Z}_6] + [\mathbf{Z}_4]$$

$$[\mathbf{Z}_B] = [\mathbf{R}_a] - [\mathbf{Z}_3][\mathbf{Z}_7]^{-1}[\mathbf{Z}_5]$$

$$[\mathbf{Z}_C] = [\mathbf{R}_a][\mathbf{Z}_7]^{-1}$$

$$[\mathbf{Z}_1] = [\mathbf{Z}_{ni}] + [\mathbf{C}_s]^{-1} + j[\Omega]L_s + (R_s + R_i)[\mathfrak{I}]$$

$$[\mathbf{Z}_2] = +j[\Omega]L_s + R_s[\mathfrak{I}]$$

$$[\mathbf{Z}_3] = [\mathbf{C}_d]^{-1} + R_i[\mathfrak{I}] + \{[\mathfrak{I}] + [\mathbf{R}_a][\mathbf{G}_m]\}[\mathbf{C}_s]^{-1} + [\mathbf{R}_a]$$

$$[\mathbf{Z}_4] = R_i[\mathfrak{I}] + \{[\mathfrak{I}] + [\mathbf{R}_a][\mathbf{G}_m]\}[\mathbf{C}_s]^{-1}$$

$$[\mathbf{Z}_5] = [\mathbf{Z}_{no}] + j[\Omega]L_s + [\mathbf{R}_a] + R_s[\mathfrak{I}]$$

$$[\mathbf{Z}_6] = j[\Omega]L_s + R_s[\mathfrak{I}] - [\mathbf{R}_a][\mathbf{G}_m][\mathbf{C}_s]^{-1}$$

$$[\mathbf{Z}_7] = [\mathbf{R}_a] \{ [\mathbf{G}_m][\mathbf{C}_s]^{-1} + [\mathfrak{I}] \}$$

and

$$[\mathbf{Z}_{ni}] = diag \{ Z_{Li}(k\omega_p) \}$$

$$[\mathbf{Z}_{no}] = diag \{ Z_{Lo}(k\omega_p) \}$$

where  $[\mathfrak{I}]$  is the identity matrix. From these relations, one can deduce the conversion gain  $G_{mn}$  of the mixer for a frequency conversion from a frequency  $\omega_n$  to a frequency  $\omega_m$ ,

$$G_{mn} = 4|Y_{mn}|^2 Re \{ Z_{Li}(m\omega_p) \} Re \{ Z_{Lo}(n\omega_p) \} \quad (\text{VII-25})$$

---

*The materials you receive for this course are protected by copyright and to be used for this course only. You do not have permission to upload the course materials, including any lecture recordings you may have, to any website. If you require clarification, please consult your professor.*

The input impedance matrix  $[Z_{in}]$  is thus equal to (with a matched output)

$$[Z_{in}] = [Z_1] + \{[Z_2] + [Z_C][Z_5]\} \{[Z_B]^{-1}[Z_A]\} + [Z_C][Z_6] - [Z_{ni}] \quad (VII-26)$$

The output impedance matrix  $[Z_{out}]$  is similarly equal to (with a matched input)

$$[Z_{out}] = [Z_{out1}] + \{[Z_{out2}][Z_{out3}]^{-1}[Z_{out4}]\} - [Z_{no}] \quad (VII-27)$$

with

$$[Z_{out1}] = [Z_5] + [Z_7][R_a]^{-1}[Z_2]$$

$$[Z_{out2}] = [Z_6] + [Z_7][R_a]^{-1}[Z_1]$$

$$[Z_{out3}] = [Z_4] - [Z_3][R_a]^{-1}[Z_1]$$

$$[Z_{out4}] = [R_d] + [Z_3][R_a]^{-1}[Z_2]$$

## D – APPROXIMATE DESIGN OF SINGLE-GATE FET MIXERS

In diode mixer design, one wishes to minimize conversion loss because low conversion loss guarantees low-noise operation. In FET mixers, high gain is relatively easy to obtain, but other aspects of performance will not be automatically ensured.

Figure VII-5 shows a block diagram of a FET mixer. Because the time-varying transconductance is the primary contributor to mixing, it is important to maximize the range of the

---

*The materials you receive for this course are protected by copyright and to be used for this course only. You do not have permission to upload the course materials, including any lecture recordings you may have, to any website. If you require clarification, please consult your professor.*

FET's transconductance variation and, in particular, the magnitude of the fundamental frequency component of the transconductance.

To maximize the transconductance variation, the FET must be biased close to its turn-on voltage,  $V_t$ , and must remain in its current-saturation region throughout the LO cycle.

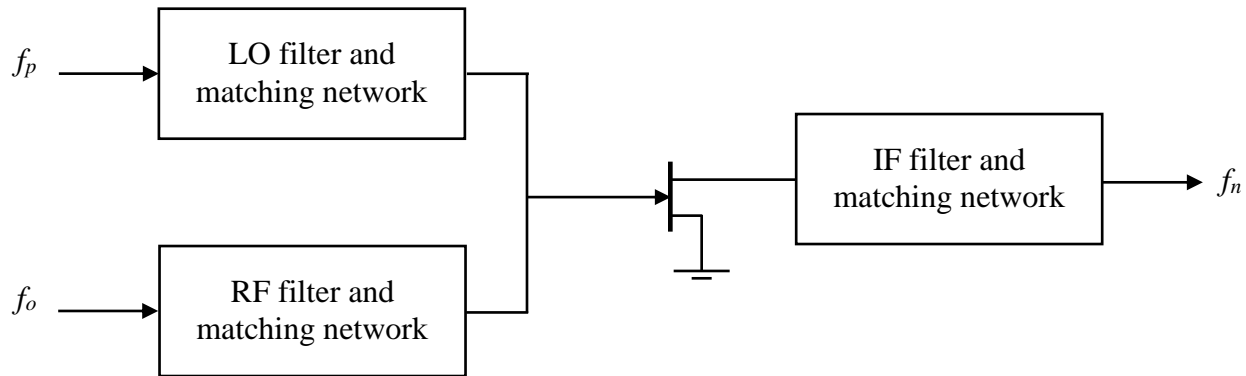


Fig. VII-5. Block diagram of a single-gate FET mixer

Full saturation is achieved by ensuring that the variation of the large-signal drain voltage  $V_d(t)$  under LO pumping is minimal; it is best if it remains constant at its dc value  $V_{dd}$ .

This condition is achieved by short-circuiting the drain at the fundamental LO frequency and all LO harmonics (in fact, short-circuiting the drain will imply a high peak value, which assure a minimal LO voltage across the gate-drain capacitance, so feedback is minimal and the mixer is very stable).

In this case, the drain current has the same half-sinusoidal pulse waveform as the Class-B power amplifier, and the transconductance waveform is similar.

It is therefore best to bias the FET at the same drain voltage it would require if it were used in an amplifier, i.e., near 3V for most small-signal devices. Although the optimum gate bias is usually near  $V_t$ , fine adjustment of the gate voltage must be made empirically as part of the circuit tuning. A usual designed mixer is relatively insensitive to small changes in dc drain voltage.

FET mixers are often conditionally stable, so it is impossible to find source and load impedances that simultaneously match the RF input and IF output ports. Moreover, even when the mixer is unconditionally stable, the output impedance of a mixer having an IF frequency below X-band is very high (over  $1k\Omega$ ), and has only a small reactive component. Since this impedance is much greater than the drain-source resistance of an unpumped FET. Therefore, it is nearly impossible to obtain a conjugate match to such high impedance.

A better choice is to use a resistive load at the IF (selected accordingly to the desired conversion gain). This kind of device is called resistive mixer (Table VII-3). In this case, the mixer's output VSWR will be relatively high. However, theoretical limitations of impedance matching dictate that high output VSWR is unavoidable. Nevertheless, a resistive load, if properly implemented, provides stable operation, flat frequency response, and desired gain.

Table VII-3. Resistive mixer characteristics.

Mixer Type	Characteristics	Typical Applications
Single-device FET resistive mixer	A good circuit for general use. Requires an LO-IF diplexer.	General applications; lack of an IF balun or hybrid makes this mixer somewhat more practical for ICs. Rejects AM LO noise. A nice circuit for RF ICs.
Singly balanced 180-degree mixer	Lower distortion, automatic drain short-circuit for the LO. Requires an IF balun or 180-degree hybrid. Requires filtering to separate the RF and IF.	Especially useful when the IF is low enough to allow a wire-wound transformer for the output balun. In low-frequency mixers using transformers, the IF and RF may overlap.
Doubly balanced ring mixer	Very low distortion but difficult to design optimally at high frequencies because of large layout parasitics. Bandwidth is limited by hybrids.	A very good circuit for general wireless, RF, and lower microwave applications.

---

The materials you receive for this course are protected by copyright and to be used for this course only. You do not have permission to upload the course materials, including any lecture recordings you may have, to any website. If you require clarification, please consult your professor.

## REFERENCES

- [1] S.A. Maas, *Nonlinear microwave circuits*, Norwood MA: Artech House, 1988.
- [2] G.D. Vendelin, A.M. Pavio, U.L. Rohde, *Microwave circuit design using linear and nonlinear techniques*, New York: Wiley & Sons, 1990.
- [3] E.H. Armstrong, "The superheterodyne - its origin, development and some recent improvements," *Proc. IRE*, Vol 12, 540-552, 1924.
- [4] L.C. Peterson, F.B. Llewellyn, "The performance and measurement of mixers in terms of linear-network theory," *Proc. IRE*, Vol 33, 458-476, July 1945.
- [5] H.C. Torrey, C.A. Withmer, *Crystal Rectifiers*, MIT Radiation Lab. Ser., Vol 15, New-York : McGraw-Hill, 1948.
- [6] P.D. Strum, "Some aspects of crystal mixer performance," *Proc. IRE*, Vol 41, 875-889, July 1953.
- [7] E.L. Kollberg, *Microwave and millimeter-wave mixers*, New-York: IEEE Press, 1984.
- [8] S.A. Maas , *Microwave mixers*, Norwood MA: Artech House, 1986.
- [9] A.A.M. Saleh, *Theory of resistive mixers*, Cambridge, MA : M.I.T. Press, 1971.

### **Diode mixers**

- [10] B.J. Clifton, "Schottky-barrier diodes for submillimeter heterodyne detection," *IEEE Trans. Microwave Theory Tech.*, Vol 22, 270-275, Mar. 1974.
  - [11] G.T. Wrixon, "Schottky-diode realization for low-noise mixing at millimeter wavelengths," *IEEE Trans. Microwave Theory Tech.*, Vol 24, 702-706, Nov. 1976.
  - [12] M. McColl, "Conversion loss limitations on Schottky barrier mixers," *IEEE Trans. Microwave Theory Tech.*, Vol 25, N°1, 54-59, Jan. 1977.
  - [13] R.L. Dickman, W.J. Wilson, G.G. Berry, "Super-Schottky mixer performance at 92 GHz," *IEEE Trans. Microwave Theory Tech.*, Vol 29, 788-793, Aug. 1981.
- 

*The materials you receive for this course are protected by copyright and to be used for this course only. You do not have permission to upload the course materials, including any lecture recordings you may have, to any website. If you require clarification, please consult your professor.*

- [14] C. Gupta, J. Del Conte, "Trends in mm-wave mixer designs," *Microwave J.*, Vol 27, 83-92, April 1984.
  - [15] R.J. Mattauch, T.W. Crowe, W.L. Bishop, "Frequency and noise limits of Schottky barrier mixer diodes," *Microwave J.*, Vol 28, 101-116, Mar. 1985.
  - [16] W.L. Bishop, T.W. Crowe, R.J. Mattauch, H. Dossal, "Planar GaAs diodes for THz frequency mixing applications," in *Int. Symp. Space THz Technol.*, Ann Arbor, MI, 1992.
  - [17] M.J. Lazarus, S. Novak, E.D. Bullimore, "New millimeter-wave receivers using self-oscillating Gunn-diode mixers," *Microwave J.*, Vol 13, 43-45, July 1971.
  - [18] F.R. Pantoja, "Homodyne and heterodyne studies of GaAs and InP millimeter-wave Gunn mixers," *IEEE Trans. Microwave Theory Tech.*, Vol 33, 1249-1253, Nov. 1985.
  - [19] G. Vernet, J.C. Henaux, R. Adde, "The Josephson self-oscillator mixer as a submillimeter and far-infrared detector," *IEEE Trans. Microwave Theory Tech.*, Vol 25, 473-479, June 1977.
  - [20] H. How, T.M. Fang, C. Vittoria, A. Widom, "Nonlinear mixer gain calculations for Josephson junctions," *IEEE Trans. Microwave Theory Tech.*, Vol 43, 216-218, Jan. 1995.
  - [21] M. Katoh, Y. Akaiwa, "4-GHz integrated circuit mixer," *IEEE Trans. Microwave Theory Tech.*, Vol 19, N°7, 634-637, July 1971.
  - [22] T. Araki, M. Hirayama, "A 20-GHz integrated balanced mixer," *IEEE Trans. Microwave Theory Tech.*, Vol 19, 638-643, July 1971.
  - [23] G. Begemann, "An X-band balanced fin-line mixer," *IEEE Trans. Microwave Theory Tech.*, Vol 26, 1007-1011, Dec. 1978.
  - [24] H. Ogawa, M. Aikawa, K. Morita, "K-band integrated double balanced mixer," *IEEE Trans. Microwave Theory Tech.*, Vol 28, 180-185, Mar. 1980.
  - [25] W. Hant, "Short millimeter wavelength mixer with low local oscillator power," *IEEE Trans. Microwave Theory Tech.*, Vol 33, 135-142, Feb. 1985.
  - [26] M.T. Faber, J.W. Archer, "Millimeter-wave, shot-noise limited, fixed-tuned mixer," *IEEE Trans. Microwave Theory Tech.*, Vol 33, N°11, 1172-1178, Nov. 1985.
- 

The materials you receive for this course are protected by copyright and to be used for this course only. You do not have permission to upload the course materials, including any lecture recordings you may have, to any website. If you require clarification, please consult your professor.

- [27] M.A. Smith, K.J. Anderson, A.M. Pavio, "Decade band mixer covers 3.5 to 35 GHz," *Microwave J.*, Vol 29, 163-171, Feb. 1986.
  - [28] M.V. Schneider, W.W. Snell, "Harmonically pumped stripline down-converter," *IEEE Trans. Microwave Theory Tech.*, Vol 23, 271-275, Mar. 1975.
  - [29] M. Cohn, J.E. Degenford, B.A. Newman, "Harmonic mixing with an antiparallel diode pair," *IEEE Trans. Microwave Theory Tech.*, Vol 23, 667-673, Aug. 1975.
  - [30] J.D. Büchs, G. Begemann, "Frequency conversion using harmonic mixers with resistive diodes," *IEE J. Microwave Opt. Acoust.*, Vol 2, 71-76, May 1978.
  - [31] R.G. Hicks, P.J. Khan, "Numerical analysis of subharmonic mixers using accurate and approximate models," *IEEE Trans. Microwave Theory Tech.*, Vol 30, 2113-2119, Dec. 1982.
  - [32] W. Yun-Yi, S. Yong-Hui, "A study of W-band subharmonically pumped mixer," *IEEE Trans. Microwave Theory Tech.*, Vol 33, 1340-1345, Dec. 1985.
  - [33] P.H. Siegel, R.J. Dengler, I. Mehdi, J.E. Oswald, W.L. Bishop, T.W. Crowe, R.J. Mattauch, "Measurements on a 215-GHz subharmonically pumped waveguide mixer using planar back-to-back air-bridge Schottky diodes," *IEEE Trans. Microwave Theory Tech.*, Vol 41, 1913-1921, Nov. 1993.
  - [34] S.D. Vogel, "Design and measurements of a novel subharmonically pumped millimeter-wave mixer using two single planar Schottky-barrier diodes," *IEEE Trans. Microwave Theory Tech.*, Vol 44, 825-831, June 1996.
  - [35] E.W. Herold, R.R. Bush, W.R. Ferris, "Conversion loss of diode mixers having image-frequency impedance," *Proc. IRE*, Vol 33, 603-609, Sept. 1945.
  - [36] G.P. Kurpis, J.J. Taub, "Wide-band X-band microstrip image rejection balanced mixer," *IEEE Trans. Microwave Theory Tech.*, Vol 18, 1181-1182, Dec. 1970.
  - [37] L.E. Dickens, D.W. Maki, "An integrated-circuit balanced mixer, image and sum enhanced," *IEEE Trans. Microwave Theory Tech.*, Vol 23, 276-281, Mar. 1975.
  - [38] F. Günes, D.P. Howson, K.J. Glover, "Influence of mixer diode reactances on noise figure and conversion loss," *IEE J. Microwave Opt. Acoust.*, Vol 3, 34-36, Jan. 1979.
- 

*The materials you receive for this course are protected by copyright and to be used for this course only. You do not have permission to upload the course materials, including any lecture recordings you may have, to any website. If you require clarification, please consult your professor.*

- [39] I. Radnovic, B. Jokanovic, "21-24 GHz IRM for link application," *Microwave Engineering Eur.*, Vol 18, 35-40, Feb. 1992.

### ***Transistor mixers***

- [40] J.E. Sitch, P.N. Robson, "The performance of GaAs FET as microwave mixers," *IEEE Proc.*, Vol 61, 399-400, Mar. 1973.
- [41] R.A. Pucel, D. Masse, R. Bera, "Performance of GaAs MESFET mixers at X-band," *IEEE Trans. Microwave Theory Tech.*, Vol 24, 351-360, June 1976.
- [42] O. Kurita, K. Morita, "Microwave MESFET mixers," *IEEE Trans. Microwave Theory Tech.*, Vol 24, 361-366, June 1976.
- [43] P. Harrop, "Gallium arsenide field effect transistor mixers : theory and applications," *Acta Electronica*, Vol 23, N°4, 291-297, 1980.
- [44] M. Sholley, S. Maas, B. Allen, R. Sawires, A. Nichols, J. Abell, "HEMTs mm-wave amplifiers, mixers and oscillators," *Microwave J.*, Vol 28, 121-130, Aug. 1985.
- [45] J.M. Rosário, C.J. Freire, "Design technique for MESFET mixers for maximum conversion gain," *IEEE Trans. Microwave Theory Tech.*, Vol-38, 1972-1979, Dec. 1990.
- [46] T.H. Chen, K.W. Chang, S.B.T. Bui, L.C.T. Liu, G.S. Dow, S. Pak, "Broadband single- and double-balanced resistive HEMT monolithic mixers," *IEEE Trans. Microwave Theory Tech.*, Vol 43, 477-484, Mar. 1995.
- [47] D. Neuf, "Fundamental, harmonic and sampling MESFET mixer circuits," *Microwave J.*, Vol 38, 76-86, Dec. 1995.
- [48] L. Picheta, E.A. Allamando, "Achieve microwave frequency conversion with cold FETs," *Microwaves & RF*, Vol 36, 73-78, Feb. 1997.

---

*The materials you receive for this course are protected by copyright and to be used for this course only. You do not have permission to upload the course materials, including any lecture recordings you may have, to any website. If you require clarification, please consult your professor.*

- [49] S.C. Cripps, O. Nielsen, D. Parker, J.A. Turner, "An experimental evaluation of X-band mixers using dual gate GaAs MESFET's," in Proc. *7th Eur. Microwave Conf.*, 101-104, Copenhagen, 1977.
- [50] C. Tsironis, R. Meierer, R. Stahlmann, "Dual gate MESFET mixers," *IEEE Trans. Microwave Theory Tech.*, Vol 32, 248-255, Mar. 1984.
- [51] T. Sugiura, K. Honjo, T. Tsuji, "12-GHz-band GaAs dual gate MESFET monolithic mixers," *IEEE Trans. Microwave Theory Tech.*, Vol 33, 105-110, Feb. 1985.
- [52] K. Kanazawa, M. Kazumura, S. Nambu, K. Kano, I. Teramoto, "A GaAs double-balanced dual gate FET mixer IC for UHF receiver front-end applications," *IEEE Trans. Microwave Theory Tech.*, Vol 33, 1548-1553, Dec. 1985.
- [53] S.E. Moore, "A dual-gate MESFET mixer using a simplified experimental design approach," *Microwave J.*, Vol 30, 195-199, Nov. 1987.
- [54] O.S.A. Tang, C.S. Aitchison, "A very wide-band microwave MESFET mixer using the distributed mixing principle," *IEEE Trans. Microwave Theory Tech.*, Vol 33, 1470-1478, Dec. 1985.
- [55] S.E. Avery, "Dual mixers," *Microwave J.*, Vol 29, 141-149, Oct. 1986.
- [56] H. Zirath, I. Angelov, N. Rorsman, "A millimeterwave subharmonically pumped mixer based on a heterostructure field effect transistor technology," in *IEEE MTT-S Int. Microwave Symp. Dig.*, Albuquerque, 599-602, 1992.

### **Mixer analysis**

- [57] C.F. Edwards, "Frequency conversion by means a nonlinear admittance," *Bell Sys. Tech. J.*, Vol 35, 1403-1416, Nov. 1956.
  - [58] A.C. Macpherson, "An analysis of the diode mixer consisting of nonlinear capacitance and conductance and ohmic spreading resistance," *IRE Trans. Microwave Theory Tech.*, Vol 5, 43-52, Jan. 1957.
- 

*The materials you receive for this course are protected by copyright and to be used for this course only. You do not have permission to upload the course materials, including any lecture recordings you may have, to any website. If you require clarification, please consult your professor.*

- [59] G.C. Messenger, C.T. McCoy, "Theory and operation of crystal diodes as mixers," *Proc. IRE*, Vol 45, 1269-1283, Sept. 1957.
  - [60] M.R. Barber, "Noise figure and conversion loss of the Schottky barrier mixer diode," *IEEE Trans. Microwave Theory Tech.*, Vol 15, N°11, 629-635, Nov. 1967.
  - [61] J. Lenkowski, "Transients in periodically time-varying circuits," *IEEE Trans. on Circuit Theory*, Vol 14, 426-429, Dec. 1967.
  - [62] D.A. Fleri, L.D. Cohen, "Nonlinear analysis of the Schottky-barrier mixer diode," *IEEE Trans. Microwave Theory Tech.*, Vol 21, N°1, 39-43, Jan. 1973.
  - [63] W.K. Gwarek, *Nonlinear analysis of microwave mixers*, M.S. Thesis, Mass. Inst. Technol., Cambridge, MA, 1974.
  - [64] S. Egami, "Nonlinear, linear analysis and computer aided design of resistive mixers," *IEEE Trans. Microwave Theory Tech.*, Vol 22, 270-275, Mar. 1974.
  - [65] A.R. Kerr, "A technique for determining the local oscillator waveforms in a microwave mixer," *IEEE Trans. Microwave Theory Tech.*, Vol 23, 828-831, Oct. 1975.
  - [66] D.N. Held, A.R. Kerr, "Conversion loss and noise of microwave and millimeter-wave mixers : Part I - Theory ; Part II - Experiment," *IEEE Trans. Microwave Theory Tech.*, Vol 26, 49-61, Feb. 1978.
  - [67] M.E. Hines, "Inherent signal losses in resistive-diode mixers," *IEEE Trans. Microwave Theory Tech.*, Vol 29, 281-292, April 1981.
  - [68] B. Schüppert, "A fast and reliable method for computer analysis of microwave mixers," *IEEE Trans. Microwave Theory Tech.*, Vol 34, 110-119, Jan. 1986.
  - [69] P. Estabrook, B.B. Lusignan, "A mixer computer-aided design tool based in the time domain," in *IEEE Int. Microwave Symp. Dig.*, New-York, 1107-1110, 1988.
  - [70] M.I. Sobhy, F. Bassirat, "Nonlinear modelling and design of microwave mixers," in *IEEE Int. Microwave Symp. Dig.*, New-York, 1111-1114, 1988.
- 

*The materials you receive for this course are protected by copyright and to be used for this course only. You do not have permission to upload the course materials, including any lecture recordings you may have, to any website. If you require clarification, please consult your professor.*

- [71] P.L. Ntake, *A computer-aided design of low-noise parametric down converters and GaAs FET mixers for low-cost satellite microwave receivers*, Ph.D. dissertation, Carleton Univ., Canada, 1977.
  - [72] G.K. Tie, C.S. Aitchison, "Noise figure and associated gain of a microwave MESFET gate mixer," in Proc. *13th Euro. Microwave Conf.*, 579-584, 1983.
  - [73] S.A. Maas, "Theory and analysis of GaAs MESFET mixers," *IEEE Trans. Microwave Theory Tech.*, Vol 32, 1402-1406, Oct. 1984.
  - [74] J. Dreifuss, A. Madjar, A. Bar-Lev, "A novel method for the analysis of microwave two-port active mixers," *IEEE Trans. Microwave Theory Tech.*, Vol 33, 1241-1244, Nov. 1985.
  - [75] W.R. Curtice, "Nonlinear analysis of GaAs MESFET amplifiers, mixers and distributed amplifiers using the harmonic balance technique," *IEEE Trans. Microwave Theory Tech.*, Vol 35, 441-447, April 1987.
  - [76] C. Camacho-Penalosa, C.S. Aitchison, "Analysis and design of MESFET gate mixers," *IEEE Trans. Microwave Theory Tech.*, Vol 35, 643-652, July 1987.
  - [77] M.J. Rosario, J. Costa Freire, "Design technique for MESFET mixers for maximum conversion gain," *IEEE Trans. Microwave Theory Tech.*, Vol 38, 1972-1979, Dec. 1990.
  - [78] F. De Flaviis, T. Rozzi, F. Moglie, A. Sgreccia, A. Panzeri, "Accurate analysis and design of millimeter wave mixers," *IEEE Trans. Microwave Theory Tech.*, Vol 41, 870-873, May 1993.
- 
- [79] M.C.E. Yagoub, H. Baudrand, "Optimum design of nonlinear microwave circuits," *IEEE Trans. Microwave Theory Tech.*, Vol 42, 779-786, 1994.
  - [80] G.L. Matthaei, L. Young, Jones E.M.T., *Microwave filters, impedance matching networks and coupling structures*, London: Artech House, 1980.
  - [81] T.T. Ha, *Solid-state microwave amplifier design*, New-York: Wiley, 1981.
  - [82] K.C. Gupta, R. Garg, R. Chadha, *Computer aided design of microwave circuits*, Dedham MA : Artech House, 1981.

---

*The materials you receive for this course are protected by copyright and to be used for this course only. You do not have permission to upload the course materials, including any lecture recordings you may have, to any website. If you require clarification, please consult your professor.*

- [83] L.D. Abrie, *The design of impedance-matching networks for radio-frequency and microwave amplifiers*, Norwood: Artech House, 1985.
- [84] P.F. Combes, J. Graffeuil, J.F. Sautereau, *Composants, dispositifs et circuits actifs en micro-ondes*, Paris : Dunod Université, 1985.
- [85] L.O., Chua C.A. Desoer, E.S. Kuh, *Linear and nonlinear circuits*, New-York : Mc Graw-Hill, 1987.
- [86] M. Staloff, "Computer-aided design and analysis of microwave transistor amplifiers," *Microwave J.*, Vol 30, 253-268, May 1987.
- [87] S.A. Maas, *C/NL: linear and nonlinear microwave circuit analysis and optimization software*, Butler WI: Artech House, 1990.
- [88] D. Thomas, Jr., G.R. Branner, "Optimization of active microwave frequency multiplier performance utilizing harmonic terminating impedances," in *IEEE Int. Microwave Symp. Dig.*, San-Fransisco, 659-662, 1996.

---

*The materials you receive for this course are protected by copyright and to be used for this course only. You do not have permission to upload the course materials, including any lecture recordings you may have, to any website. If you require clarification, please consult your professor.*

**APPENDIX VII-1**

**MIXER BASICS**

# 50 Years Development of the Microwave Mixer for Heterodyne Reception

Terry H. Oxley, *Life Fellow, IEEE*

*Invited Paper*

**Abstract**—A brief technical historical review of mixer development, in its application as the frequency down-converter for the microwave and millimeter-wave heterodyne receiver, provides the background to discussion of mixer design, technology, and performance characteristics. In general terms, today's mixers designs are based on the 1970s principles, but technology progress in the solid-state frequency-mixing element and associated integrated circuits has been significant, with exploitation of the monolithic potential. Performance advancements have mainly been in the increased frequency capabilities of the planar Schottky barrier diode mixer, broad application of the three terminal devices, and balun implementation.

**Index Terms**—Mixers.

## I. INTRODUCTION

THE terminology “mixer” may be applied to frequency mixing or frequency changing for down-conversion or up-conversion, and refers to a nonlinear element embedded in associated circuitry to provide the appropriate input and output terminals. The most common application is frequency “mixing” applied to heterodyne reception, in which two frequencies beat together in a nonlinear element to produce sum and difference frequencies.

This receiver principle may be traced to the early 1900s for radio reception, but World War II revived interest specifically for military radars at microwave frequencies. The microwave mixer still, today, provides the heart of the heterodyne receiver and is used in all types of microwave systems to meet the needs of both military and civil requirements, e.g., radars of all types, electronic warfare, guided weapons, communication, instrumentation, transportation, radio astronomy, etc. System applications now extend over the frequency range of at least 1–1000 GHz, moving into the terahertz region.

Stimulated by progress in system design techniques demanded by the increasing complexity of military and civil requirements, mixer research and development (R&D) has continued with much technology advancement in the semiconductor device frequency-mixing element and associated circuitry, progressing through the main phases of the traditional

waveguide/coaxial configurations, the hybrid microwave integrated circuit (MIC) and the monolithic microwave integrated circuit (MMIC). The advent of the front-end low-noise amplifier has impacted on the original mixer prime design aim of low noise (high sensitivity) for many applications, introducing the use of more complex mixer designs with dynamic-range upper limit suppression of intermodulation products being an important characteristic.

The paper will present and discuss some generalized advancement in mixers, resulting from the large R&D effort applied to microwave and millimeter-wave receivers over the period from 1950 to 2000, much from personal experience.

## List of Symbols

- Compression point (CP): Upper limit of dynamic range expressed in terms of 1-dB compression in output power as a function of input power. May be expressed as mixer  $L_c$  or  $r.f$  to  $i.f$ . receiver overall gain.
- Double-sideband (DSB): Operation of the receiver when it is receiving usable signals in both the signal and image bands.
- Dynamic range: Power difference between the minimum detectable signal and maximum signal that can be accepted before a specified compression can take place.
- FET: Field-effect transistor.
- $F_i.f$ : Noise figure of the  $i.f$ . amplifier.
- HBT: Heterojunction bipolar transistor.
- HEMT: High electron-mobility transistor.
- $1/f$ : Flicker or low-frequency noise. Noise corner ( $n/c$ ) being defined as the onset of ONF ( $N_r$ ) increase with decrease of  $i.f$ .
- $i.f.$ : Intermediate frequency.
- $I$ : Image frequency, where  $I = l.o. - i.f.$  when signal  $= l.o. + i.f.$
- Image recovery (enhancement): Recovery of image power generated by the mixer with reconversion to  $i.f.$  power leading to enhanced receiver overall noise figure or mixer conversion loss.
- Image rejection (suppression): Suppression of  $r.f.$  input signals at the image frequency.
- Intercept point (IP3): Upper limit of dynamic range, expressed as a measure of the third-order intermodulation products generated by a second input signal arriving at the signal port along with the desired signal.

Manuscript received July 2, 2001.

The author, retired, was with GEC Research Ltd., Marconi Research Center, GT. Baddow, Chelmsford, Essex CM2 8HN, U.K. He is now at Railside, Station Lane, Farnsfield, Newark, Notts. NG22 8LB, U.K. (e-mail: t.oxley@ieee.org).

Publisher Item Identifier S 0018-9480(02)01968-3.

- $Lc/Gc$ : Mixer conversion loss/conversion gain: ratio of available signal power at radio frequency to the available output power at intermediate frequency.
- *l.o.*: Local oscillator.
- MESFET: Metal–semiconductor FET
- MISFET: Metal–insulator–semiconductor FET
- $Nr$ : Noise ratio of the mixer nonlinear element: ratio of available noise power to that of a resistor equivalent to the mixer output resistance, at room temperature. Contributions are thermal, shot and flicker noise.
- $ONF$ : Overall noise figure: sensitivity of a heterodyne receiver expressed as  $ONF = Lc(Fif + Nr - 1)$  assuming local-oscillator noise sidebands are suppressed.
- *r.f.*: Radio frequency.
- Single-sideband (SSB): Operation of the receiver when it is receiving a useful signal in the signal band only.
- $Plo$ : Local-oscillator power.

### *Explanation of Mixer Circuits*

*Single-Ended Mixer (SEM)*: is the most basic and comprises a single-port circuit embedding a single mixing element with both *r.f.* and *l.o.* coupled externally. A merit is simplicity, but has the disadvantages of *r.f.* loss due to external *r.f./l.o.* coupling, and no suppression of *l.o.* noise sidebands or intermodulation products.

*Single-Balanced Mixer (SBM)*: combines two single-ended mixers via a four-port 3-dB coupler (balun), such that the *l.o.* noise sideband products are balanced out. The circuit provides isolation between *r.f.* and *l.o.* ports, suppression of *l.o.* A.M. noise products and even-order modulation products. The coupler (balun) defines many characteristics, particularly *r.f.* bandwidth (may provide 90° or 180° phase difference between output ports, each with particular merits).

*Double Balanced Mixer (DBM)*: comprises four mixing elements connected as a quad, in ring, bridge or star form, and two baluns. Inherent characteristics provide cancellation of *l.o.* A.M. noise, broad bandwidth, high isolation between all ports, suppression of even harmonics of *r.f.* and *l.o.* signals (high rejection of even-mode harmonics and reduction of the total number of possible intermodulation products), high signal handling (thus, high dynamic range), and thus, high dynamic range, low *i.f.* impedance, and finally, the merit of a potential compact structure. Balun designs are of prime importance for accessing the quad terminals, both in design and implementation for performance and achieving the potential compact mixer structure.

*Double–Double Balanced Mixer (DDBM)*: an extension of the DBM that comprises eight mixing elements and separate *r.f.*, *l.o.*, and *i.f.* baluns, providing higher dynamic range and facilitates overlapping *r.f.* and *i.f.* bandwidths.

*Image Rejection Mixer (IRM)*: normally combines two identical mixers (SEM, SBM, or DBM) in a phasing arrangement such that the image is out-phased or rejected, while the desired signals are unaffected. Also, may be achieved by a signal bandpass filter that rejects the image frequency and coupled to absorb image power generated by the mixer.

*Image Recovery (Enhancement) Mixer*: is basically an IRM phasing circuit in which the image power generated in one mixer is converted to *i.f.* by the other mixer and vice versa, for  $Lc$  en-

hancement. Also may be achieved by a signal bandpass filter that reflects the mixer image power in the correct phase. Short-circuit image termination is preferable to open-circuit image termination to minimize and provide acceptable impedance levels. An image recovery circuit inherently provides image rejection, but not vice versa.

*Antiparallel Sub-Harmonic Mixer (SHM)*: is a special case of a harmonic mixer when the *l.o.* is one-half the fundamental frequency with two mixing elements of opposite polarity connected in shunt to produce a full-wave antiparallel arrangement and a symmetrical *I–V* characteristic. Unlike the harmonic mixer, the circuit suppresses the fundamental mixing products between *l.o.* and signal and many higher order mixing products, and will provide down conversion from all sidebands where the sub-multiple is even with suppression of odd-order products, implying the capability of a similar conversion loss to that obtained from a fundamental mixer. *l.o.* A.M. noise sidebands are suppressed.

*Image Rejection Harmonic Mixer (IRHM)*: combines the IRM and SHM and provides suppression of harmonic intermodulation products.

## II. WAVEGUIDE/COAXIAL MIXER

The early traditional mixers of the 1950/1960s era incorporated a resistive element that was mainly based on the 1940/1950s technology; basically consisting of an encapsulated point-contact diode produced by a tungsten whisker wire in pressure contact with a bulk p-type silicon (Si) semiconductor chip (epitaxial Si was introduced during the 1960s by some manufacturers). The structure was essentially a metal–semiconductor device based on the physical mechanism described by the Schottky theory of rectification [1]. The devices were encapsulated in standardized outlines and plug-in mounted in waveguide/coaxial-line single-ended and balanced mixer configurations (coupling provided by magic tee, slot coupler, rat race, etc.). In this period, however, many devices were designed to meet stringent ONF, *r.f.*, and *i.f.* impedance specifications at selected signal frequencies, to meet the requirements of system fixed tuned mixer mounts. Diode encapsulations included the 3-GHz IN21 and 10-GHz IN23 ceramic capsules, the 3- and 10-GHz coaxial type (U.K.), the 16-GHz IN78 and 35-GHz IN53 coaxial types, the 35-GHz integral waveguide (U.K.), and the millimeter-wave sharpless wafer plug-in waveguide (some outlines required opposite polarity types for balanced mixers). Toward the late 1960s, novel miniature reversible capsule outlines [e.g., metal–quartz–metal (MQM)] introduced greater flexibility and broader frequency capability.

### A. Point-Contact Diode Status

Much of the point-contact work after the 1950s concentrated on achieving a production status of the earlier developed types. A greater theoretical understanding and a high degree of fabrication sophistication were achieved during this period, which led to the optimization of the semiconductor material properties with controlled surface treatment, and development of specialized techniques for forming the intimate metal–semiconductor interface of the wire–semiconductor contact. It should be men-

tioned, however, that an ideal forward  $I$ - $V$  characteristic ( $n = 1$ ) was never achieved with this technology and the  $I$ - $V$  ideality factor ( $n$ ) was typically 1.5; reverse voltage breakdown was in the 1–2-V region. The early performance characteristics of about 9.5 dB ONF ( $Fif = 2$  dB, 45 MHz *i.f.*,  $Plo = 1.0$  mW) and 14 dB ONF, at 10 and 35 GHz, respectively ( $Lc$  typically 6.0 dB and diode noise ratio typically 1.6 at 10 GHz), were the subject of steady development progress over the years.  $Plo$  ranged from 0.5 to 2.0 mW, with an input 1-dB CP of about –18 dBm. R&D also focused on millimeter-wave devices, exploring higher electron-mobility semiconductor rectifying junctions, and developing miniature encapsulations. From studies on semiconductor materials, it was found that bulk n-type germanium (Ge) in conjunction with a titanium wire offered potential performance merits (a satisfactory wire metal–gallium arsenide combination was never established), and the late 1950s/1960s saw the development of a range of Ge point-contact mixers [2], [3]. In many cases, Ge retrofits for the Si established types were developed providing 8.5 dB ONF at 10 GHz and 11 dB ONF at 35 GHz ( $Fif = 2$  dB). The miniature reversible capsule types that were later introduced (including advanced metal–semiconductor techniques) achieved 6.5 dB ONF ( $Fif = 2$  dB, 45 MHz *i.f.*) at 10 GHz, 8.5 dB ONF at 35 GHz [2], and about 14 dB  $Lc$  at 140 GHz.

### B. Image Recovery

The potential of image recovery to enhance receiver noise figure was explored with point-contact diodes by SSB techniques, using a high- $Q$  filter located in the signal line. The studies did provide a better understanding of the process, but such circuits were not found to be practical, mainly as the result *r.f.* filter losses, implied narrow-band operation and the nonideal diode  $I$ - $V$  characteristic of the point-contact diode [2]. The mechanism, however, was observed with systems incorporating a high- $Q$  transmit–receive (t.r.) cell (t.r. gas discharge valve) for receiver overload protection and, for some applications, it was practice to adjust the distance between the cell and mixer for optimum overall noise figure.

### C. Tunnel (Backward) Diode

Additional to the metal–semiconductor, considerable research interest was expressed during the 1960s in the backward diode (a modified tunnel diode), for low flicker noise mixer applications (Doppler radars) and low drive mixers using solid state *l.o.*'s. Initially produced as retrofits for many Si point-contact mixers by employing a gallium (p-type dopant) plated gold whisker wire pulse bonded to the n-type Ge chip [4], [5], planar Ge backward diodes were developed in the late 1960s with an aluminum (p-type dopant) evaporated contact; producing a 3- $\mu\text{m}$ -diameter junction with overlay. Their performance characteristics featured a low drive level ( $Plo = 100 \mu\text{W}$ ) with 8 dB ONF ( $Fif = 2$  dB, MHz *i.f.*) at 10 GHz, and a 1/ $f$  noise corner  $\approx 100$  kHz (compared with 1–5-MHz range for point-contact technology). A major disadvantage was a poor upper limit dynamic range.

### D. Early Schottky Barrier Diode

The planar metal–semiconductor mixer diode, commonly known as the Schottky barrier, was introduced during the late 1960s. The process of evaporating the metal contact to produce the small area of the point-contact diode, without the need for the forming procedure, overcame the point-contact limitations on choice of metal and semiconductor material and, in conjunction with advancing semiconductor epitaxial expertise, the technology permitted the use of higher mobility materials e.g., epitaxial n-type Si, epitaxial n-type gallium arsenide (GaAs) in combination with a range of metals, such as gold, titanium, nickel, etc. (Ge was not considered due to the lack of epitaxial techniques); epitaxial techniques introducing the application of lower doped ( $10^{16} \text{ cm}^{-3}$  region) layers than with bulk semiconductors ( $10^{18} \text{ cm}^{-3}$  region). The technology produced improved diode  $I$ - $V$  characteristics compared with point-contact technology for equivalent operating frequency, i.e., higher  $I$ - $V$  reverse voltage breakdown ( $>6$  V) and near ideal forward  $I$ - $V$  characteristics ( $n$  values  $< 1.1$ ), with resulting diode noise ratio of  $\approx 1.05$  (MHz *i.f.* range),  $Plo$  range 1–10 and 2–20 mW for Si and GaAs, respectively, and input 1-dB CP about –5 to 0 dBm. These advances led to greater flexibility in mixer design, allowing a broader operational *l.o.* power range with potential of optimizing impedance levels (beneficial for  $50\text{-}\Omega$  transmission systems) and higher dynamic range. Although essentially a planar device being studied in conjunction with planar transmission lines for MICs, considerable attention was given to the development of retrofit devices for point-contact outlines for application in the pretuned mixer configurations of existing equipments, achieving, e.g., 7-dB ONF ( $Fif = 2$  dB, 45 MHz *i.f.*) at 10 GHz. Although wire-bonded chip techniques were used, a favored approach was use of a semiconductor chip with a matrix of 3–5- $\mu\text{m}$ -diameter junctions that were probed by a pointed wire, generally termed the multidot (honeycomb) technique; the principle is still used today at submillimeter-wave and terahertz frequencies.

### E. Spike Burnout

In the early years of the t.r. radar system, the receiver was protected from overload damage by a t.r. cell and the power leakage was in the form of voltage/time pulse consisting of a nanosecond spike followed by a flat response of the pulselength. The spike width under these conditions was, in general, shorter than the mixer diode thermal constant, and it was the energy within the spike that caused the damage; thus, it was normal practice to specify t.r. cells and mixer diode burnout ratings in terms of spike energy. The mechanism was extremely complex, the effect could be catastrophic, occur with time at an energy level below that which produced catastrophic damage, or be a recoverable temporary deterioration in sensitivity during the transmit pulse. Simulated spike leakage by dc or coaxial line were used for non-*r.f.* diode testing specifications, but unfortunately, a reliable correlation was never established and dynamic tests were considered to be more meaningful. The physical cause of diode burnout was usually accepted to be the result of high temperatures produced at the junction leading to diffusion or melting, thus, with much dependency on junction area and

the choice of metal–semiconductor; in practice, no significant difference was observed between silicon and germanium devices. The point-contact diode presented little maneuverability for high burnout design. The event of the Schottky-barrier diode, however, with its larger contact area for equivalent microwave performance and versatility of a range of contact metals offered great promise, but early experience with t.r. radar systems did not realize the assumed potential, thus triggering further studies. These indicated the influence of barrier metals and semiconductor material and its orientation, and that by selection significant improvements compared with point-contact technology could, in fact, be realized. For example, 10-GHz GaAs Schottky diodes could be designed notwithstanding t.r. cell leakage levels of about 1 erg/spike compared with about 0.2 erg/spike for point-contact technology [6]. Over this period much attention was also given to improving receiver protection by the application of solid-state devices; varactor limiters in conjunction with t.r. cells, p-i-n switches, p-i-n switch/limiter combinations, etc., and considerable improvement was made in reducing/eliminating narrow spike leakage [7]. Also, the advent of the *r.f.* amplifier implied that the low-noise transistor became the criterion for receiver reliability [8]. Later years placed the emphasis on pulse damage with testing procedures exploring burnout effects for continuous, single, and successive microwave pulses for a range of pulse shapes/pulsewidths, etc. [9].

### III. MIC

Production of point contact mixers continued into the late 1970s (possibly the 1980s) to meet requirements of established systems. R&D, however, was phased out during the late 1960s, when advances in planar semiconductor devices complemented by development of planar transmission lines introduced the feasibility of the miniature planar hybrid MIC.

#### A. Diode Technology

The event of MICs stimulated many advances in Si and GaAs Schottky barrier device technology (the higher electron mobility of GaAs being beneficial above about 12 GHz). Early semiconductor epitaxial technology utilized 0.2- $\mu\text{m}$  layers, and this progressed rapidly to thinner layers. The late 1970s saw the introduction of the “Mottky” (Mott) diode for millimeter-wave frequencies (defined as the limiting case of a Schottky diode, such that the depletion layer extends through the epitaxial layer) [1], [10], barrier metals were explored for optimum barrier height depending on application. Early diode chips employed 20- $\mu\text{m}$ -diameter contacts to facilitate wire bonding; later techniques used smaller junctions (3–10  $\mu\text{m}$ ) with 10–20- $\mu\text{m}$  overlays. Much attention, however, during the late 1960s and early 1970s, was given to developing planar Schottky diodes for frequency ranging applications up to about 100 GHz in a form suitable for embedding in planar transmission lines e.g., microstrip, stripline, fin-line, etc., with emphasis placed on providing a pretesting capability structure. Leadless inverted device (LID) ceramic and quartz carriers, beam leaded devices, and flip chip were all explored in preference to application of direct-circuit wire-bonded chips. Additional to optimizing

the rectifying junction, significant development was applied to minimizing the stray capacitance associated with the metal overlay of the dielectric layer linked with contacting the junction. Finger geometries were used for beam lead devices [11], [12], some using glass-bridge techniques for rugged structures, with application into the millimeter-wave frequencies [13]. Mott coplanar structures were designed for flip-chip bonding [14] and, during the 1980s, the planar doped barrier (PDB) diode (a majority carrier rectifying structure where the degree of asymmetry in the *I/V* characteristic may be independently controlled), was offered as an alternative to the Schottky barrier diode for low drive, reduced flicker noise, improved burnout [15], and also with application to the SHM [15], [16].

#### B. Mixer Circuits

The late 1960s saw the studies of mixer circuits using many planar transmission media, e.g., fin-line, microstrip, stripline, image guide, with the development of experimental balanced Schottky barrier diode single-ended and single-balanced MIC mixers (mainly using branch arm, rat race, Lange 3-dB couplers) up to about 12 GHz, demonstrating 6.5 dB ONF ( $F_{if} = 1.5$  dB) at 10 GHz, and application to experimental integrated heterodyne receiver subsystems in the late 1960s. These techniques were extended as early as 1972, to development of millimeter-wave microstrip and fin-line circuit media and mixers; e.g., 30–40-GHz SBMs with ONF about 10 dB ( $F_{if} = 1.5$  dB) and at 90-GHz SEMs with  $L_C < 14$  dB [17], [18].

Also of significance was the exploitation of interest in mixer circuit designs now realizable by planar MIC techniques, such as the DBM, IRM, and SHM, which were not practicable with waveguide/coaxial-line transmission media. A great deal of development attention was given to the DBM in the early 1970s, using discrete Schottky barrier diodes to form the quad or by encapsulated quad structures. The main problem of accessing the diode-quad terminals (at low frequencies by conventional center-tapped toroid transformers), was overcome by transmission-line baluns in three-dimensional structures or broadside coupled lines for the *r.f.* and *l.o.* and fine wire chokes with miniature decoupling capacitors for the *i.f.* [19]. The concept launched much interest in broad-band balun design and configurations to eliminate via-holes and back metallization of structures; new ideas still being introduced in the late 1980s/early 1990s with coplanar waveguide, slot-line baluns applied to DBM and DDBM circuits [20], [21] (the latter demonstrated in monolithic technology also applicable to MIC). The original basis realized many broad-band mixer designs within the *r.f.* region of at least 1–26 GHz and *i.f.* band of at least 10 GHz, many with *r.f.-i.f.* band overlap.

The potential merits of the antiparallel diode SHM (using wire-contacted diodes) were demonstrated for millimeter-wave frequencies in the early 1970s [22], with the principle applied to many following applications where pumping at one-half the signal frequency was an advantage for limited available *Plo*. Also, wide-frequency separation between *r.f.* and *l.o.* implied high isolation between these ports. Later years saw extensive MIC exploitation of the circuit basis at microwaves and millimeter waves with both diode and transistor elements, e.g., in 1991 application of the high electron-mobility transistor

(HEMT) [23]. The characteristics of the PDB diode were attractive for this type of mixer [15], [16].

### C. Image Recovery/Rejection

The MIC topology reopened interest during the 1970s in image-recovery mixers to enhance receiver performance, and using the basis of SSB operation, many R&D studies were carried out to improve the understanding and achieve practical realization [24]–[26]. Circuits combined single-balanced and DBM designs, with the effect of image termination studied in some depth. Quad diode mixers designed for the low-impedance levels associated with image short circuit (in preference to image open circuit predicted theoretically for best  $L_C$ ) became the preferred choice, and many research workers demonstrated better than 1-dB improvement in mixer conversion loss up to about 12 GHz [24]–[26].

The introduction of the low-noise *r.f.* amplifier (LNA), however, offered improved receiver ONF performance compared to the potential of image-recovery mixers and drew attention to the requirement for high-power-level second-stage image (noise) rejection mixers, with many system needs focusing on the upper limits of the mixer dynamic range such as IP3 (together with high isolation between ports and broad *r.f./i.f.* bandwidths). A combination of these characteristics became at least of equal importance to mixer design as high sensitivity, and further work on image recovery was thus phased out, with much development applied to the less complex IRM; specifically the phasing basis for low *i.f.*'s (megahertz region) or broad-band *r.f.* Many diode-based image rejection (some with image enhancement) subsystems units were developed for frequencies up to 40 GHz during the 1970s, using two-diode and quad-diode mixers, typically achieving 6.5 dB ONF ( $F_{if} = 1.5$  dB, MHz *i.f.*) at 10 GHz and 8 dB at 35 GHz, with image rejection about 20 dB. Some followed into production stages. The potential of the IRHM was reported in 1982 [27].

### D. GaAs MESFET Mixers

Extensive studies were carried out during the 1970s on active single- and dual-gate GaAs MESFET mixer designs and, in general, these demonstrated the feasibility of conversion gain (thus reducing ONF dependency on  $F_{if}$ ) [28]; circuit studies included the SBM, DBM, and application to the IRM [29]. HEMT mixers for millimeter-wave frequencies were studied in the 1980s [30]. The broad-band active distributed mixer circuit, based on distributed amplification, was demonstrated in 1984 [31]. In general, although there was significant R&D progress with MESFET mixers showing broad potential application, the medium noise figure coupled with poor  $1/f$  characteristics, tended to limit their application and, in general, they were not accepted as being competitive with the Schottky barrier diode for many hybrid mixer circuits.

## IV. MMIC

The MIC technologies and techniques formed the origin of many complex MIC subsystems developed after the 1970s and were applied to production in the 1980s; application of new developments is still continuing today. Advancements in MMIC

technology, however, during the 1980s, realized its potential for further miniaturization with the prospects of low cost high-volume production.

### A. GaAs

GaAs monolithic mixers were reported in the early 1970s [32], but it was not until the 1980s that the technology was sufficiently advanced to practically compete with the MIC. In the early days, it was common practice for GaAs MMIC circuits to be produced as individual chips, sometimes being individually packaged, but with increasing interest being given to interconnection for multifunction circuits. Diode technology was developed extensively during the 1980s, attention being given to interdigital finger geometry and air-bridge techniques for diode designs, with operation up to about 100 GHz, and many MMIC mixers based on MIC SBM design principles were developed during the 1980s within the *r.f.* range of 1–100 GHz. These presented comparable performance to the MIC; e.g., SBM typically 6.5 dB ONF and 7.5 dB ONF ( $F_{if} = 1.5$  dB, MHz *i.f.*) at 10 and 94 GHz, respectively ( $P_{lo} = 10$  mW).

The prospects of the GaAs MMIC to realize receiver-integrated structures including mixer and amplifiers using the same technology, together with exploiting the rapid advances in LNA transistors, re-encouraged interest in the three-terminal devices as the mixing element, with much emphasis in the 1980s/1990s being applied to passive (resistive) operation, i.e., device operated as a variable resistance element [33], where studies had demonstrated the potential of improved  $1/f$  noise, lower dc power consumption, and better intermodulation products (higher dynamic range) compared with the active device. For example, studies on MESFET-, MISFET-, HEMT-, HBT (GaAs/InP)-based structures, reported IP3 characteristics typically 20 dBm for the SEM [34], [35] and studies of  $1/f$  noise reported noise corners of <10 MHz for MESFET and 10–30 MHz for HEMT millimeter-wave technologies [36]. The Schottky diode formed from the gate-source/drain of transistor structures found interest as the mixing element using MESFET-, HEMT-, HBT-based technologies, to realize monolithic integration compatibility with processing several receiver circuit functions on a single chip [37]–[39]. Generally, it was shown that the MESFET may offer the merits of a low-cost process, HEMT low-noise figure, and HBT low  $1/f$  noise and low drive.

Of particular significance to the progress of MMIC mixers (diode and transistor circuits) for broad-band SBM and DBM applications was the monolithic implementation of the balun, with the design aims of low loss, miniaturization (smallest possible line lengths), wide-band, and compatibility with integration of the whole mixer on a single chip; advancements are still continuing today. Some examples may include: 1) lumped-element (narrow bandwidths) [40]; 2) broad-band Marchand and side-coupled type baluns for octave bandwidths [41]; 3) compact wide-band active *l.o.* port balun with gain [43]; 4) broad-band Marchand with spiral-shaped equal-length coupled lines [42]; and 5) compact planar spiral structures that behave like a bifilar balun [44].

The potential advantages offered by MMIC mixer technology, particularly with three-terminal devices, are now

being exploited across the range of mixer circuits. For example: 1) down-converters that may combine a combination of mixer, *r.f.*, *i.f.*, and *l.o.* amplifier circuit functions [45]; 2) antiparallel diode SHMs [46]; 3) IRMs realized by signal filter for narrow-band *r.f.* or gigahertz *i.f.*'s applications to meet simplicity and low-cost requirements, such as DBS reception [47] and, more recently, HEMT SHM MMIC single-chip 38–38.6-GHz transceivers [48]; 4) IRMs using phasing techniques for broad-band *r.f.* or megahertz *i.f.* applications, in 1986, as a single-chip MMIC 4-GHz down-converter utilizing two Schottky barrier diode DBM's [49] and, more recently, broad-band 24–44-GHz DBM harmonic IRMs [50]; and 5) active HEMT distributed mixers with application to broad-band receivers [51].

### B. Silicon

Discrete Si and GaAs Schottky barrier mixer diodes achieve similar ONF characteristics up to about 12 GHz, with Si providing the lower barrier height (thus, *Plo*) and better  $1/f$  noise (100-kHz noise corner compared with 500-kHz noise corner for GaAs). Si offers useful application into the millimeter-wave frequency region, but due to its higher electron mobility, GaAs provides the higher cutoff frequency and better performance, particularly at frequencies above about 40 GHz, and with the advent of GaAs MMICs it has predominated as the technology basis. The superior  $1/f$  characteristics of Si, however, may offer a better ONF performance for some applications (e.g., FMCW radar) up to approximately 100 GHz.

Due to its potential for low cost, small size, and reproducibility for multicircuit integration there has been a continuing progressive interest in Si to challenge GaAs for monolithic circuits, including application to frequency conversion. Silicon bipolar-based technology active mixers have provided attractive characteristics, e.g., a silicon bipolar MMIC SEM with approximately 15-dB gain at 11 GHz for  $-5$ – $0$ -dBm *Plo*, possible applications up to 20 GHz [52], and a 2-GHz active DBM silicon Gilbert cell (emitter-coupled-transistor pair) with approximately 15-dB *Gc*, SSB ONF 16 dB,  $-18$ -dBm IP3 for 0-dBm *Plo* and possible operation up 6 GHz [53]. Progressive research is continuing into Si- and SiGe-based monolithic integrated millimeter-wave circuits (SIMMWICs), and associated coplanar Schottky diode SBM circuits have been reported exhibiting approximately 8.0-dB *Lc* at 77 GHz [54].

### V. APPLICATION ABOVE 100 GHz

Applications above about 100 GHz, promoted mainly by radio astronomy, but finding exploitation in spectroscopy, satellite remote sensing, etc., is a specialized field, but mixer technology and many design principles are based on the lower frequencies. Cryogenic cooled receivers have a particular attraction for many applications. The mixer can be characterized by conversion loss *Lc*, by noise temperature *Tm*, and *i.f.* amplifier noise temperature *Tif*. Although other mixer elements are available, generally, low-parasitic GaAs Schottky barrier (Mottky) diode single-ended mixers are employed, with quasi-optical diplexing techniques to couple the *l.o.* and signal. Mixer mounts normally utilize waveguide horn-feed forms

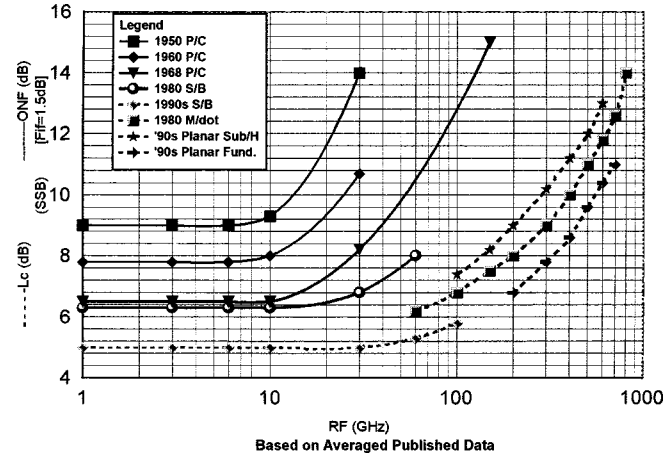


Fig. 1. Conversion loss (*Lc*) and overall noise figure (ONF) as a function of radio frequency (*r.f.*).  
Based on Averaged Published Data

TABLE I  
COMPARISON OF POINT CONTACT AND SCHOTTKY BARRIER DIODE  
1970/1980s CHARACTERISTICS (10 GHz *r.f.*)

I-V "n"	SSB ONF	<i>Lc</i>	<i>Plo</i>	In CP	<i>Nr</i>	$1/f$ n/c
Si P/C	1.5	7.3	5	0.5 to 2	-18	1.25
Ge P/C	1.3	6.5	4.5	0.3 to 1	-20	1.15
Si S/B	1.05	6.3	4.5	1 to 10	-5 to 0	1.05
GaAs S/B	1.05	6.3	4.5	2 to 20	-5 to 0	1.05
	dB	dB	mW	dBm		
	$Fif=1.5dB$					i.f.=45MHz

of construction or may employ open structure (quasi-optical) techniques or printed antenna. The advent of the Schottky barrier diode in the 1960s was fully exploited for radio astronomy using the low parasitic whisker contacted multidot (honeycomb) technology. Typical room-temperature *Lc* values of 6.0 dB in the 100-GHz frequency region for fundamental operation were achieved in the early 1970s with 2–3- $\mu$ m-diameter junctions and 6.5 dB for subharmonic mixing in the 200-GHz region in the late 1970s with 1.5- $\mu$ m-diameter junctions. Since then, steady advancements have been made both in device and receiver submillimeter-wave technologies and techniques. The 1980s saw application up to about 1000 GHz using the same earlier technology basis [55], and the 1990s further improvement in room-temperature conversion loss. Currently, however, developments of high-quality low-parasitic planar air-bridge diodes have promoted the interest in planar technologies beyond 100 GHz [56], [57], and this technology, utilizing MIC-waveguide techniques, is providing a competitive performance to the wire-contacted diode single-ended mixer. Further, application to the SHM is providing an alternative option to fundamental operation for frequencies as high as 640 GHz [58]. Recent work is exploring the potential of the MMIC [59], [60]. Terahertz frequencies, however, generally still employ advanced low-parasitic whisker-contacted techniques (0.25-micrometer-diameter anodes) [61].

TABLE II  
COMPARISON OF IP3 CHARACTERISTICS

Type	Device	r.f.	Lc	SSB NF	Plo	Input IP3	Ref
SEM	Diode	S/ Barrier	10	5.5	5.5	10	5 to 10*
SEM	Passive	GaAs MESFET	10	6.5	6.6	10	21.5*
SEM	Active	GaAs MESFET	10	-6	5	10	16*
SEM	Passive	GaInAs MISFET	10	7	7	20	30
SEM	Passive	S-D PsMESFET	10	6.9		10.5	25.5*
SEM	Passive	PHEMT	60	10		10	[64]
SBM	Passive	PHEMT	60	8.5		10	30
SEM	Passive	InP HEMT	94	10*	10	10	20
SEM	Active	InP HEMT	94	0.8	9	10	8
SBM	Diode	InP HEMT S/diode	94	10	10	10	13
			GHz	dB	dB	dBm	dBm
				*Plo=3.4dBm	Fif = 0dB		*Output

The progress of low-noise HEMT amplifiers exceeding 100 GHz, however, as at lower frequencies, could make mixer noise performance a secondary consideration, with the dynamic-range characteristic becoming of primary concern, implying the desirability for the application of more complex mixer configurations.

## VI. PERFORMANCE DISCUSSION

Comparisons of mixer data can present problems. Mixer sensitivity may be expressed in terms of DSB or SSB noise figure (or noise temperature), with or without *i.f.* amplifier noise contribution, for megahertz or gigahertz range of *i.f.*'s or by conversion loss/gain. Designs may be for broad-band or narrow-band *r.f.* and *i.f.*. Integration may imply probe measurement techniques [62].

Historically, point-contact mixers were specified (by approved standards) in terms of SSB overall noise figure, with suppression of *l.o.* noise sidebands (*l.o.* filter), at a specified *i.f.* amplifier noise figure and frequency, and with reference to the mixer signal terminals. This basis tended to hold into the 1980s, including some early packaged MIC mixers, but largely as the result of multicircuit integration, conversion loss has become common practice to interpret resistive mixer performance (although recognized that it may not reflect possible degrading sensitivity contribution of the device generated noise *Nr*).

Fig. 1 presents a very generalized picture to indicate the overall trend of room-temperature resistive mixer achievable sensitivity performance over the period 1950 to 2000. The 1950s–1980s are depicted by SSB ONF (*Fif* = 1.5 dB), and by *Lc* for the 1990s Schottky barrier diode and frequencies

above 100 GHz, based on available averaged published meaningful data (DSB data corrected by adding 3 dB).

At frequencies below 100 GHz, the ONF improvement for the point-contact diode from the 1950s to approximately 1970 is clearly shown, with the late 1960s provided a very acceptable performance up to at least 40 GHz (1968 data is predominantly Ge). The event of the Schottky barrier diode did not provide a great ONF advantage over the Ge point contact up to about 12 GHz, the benefit being derived from *Plo* flexibility, *Nr* near 1.0, improved upper limit dynamic range, and reduced *1/f* noise (and, of course, planar structure), but became significant at higher frequencies (data includes Si and GaAs, predominantly GaAs above approximately 40 GHz). Approximate calculation of *Lc* for the 1968 point contact and 1980 Schottky barrier data, indicates an *Lc* about 5 dB up to about 12 GHz, comparable with the 1990 Schottky barrier technology. The flattening of conversion loss above about 30 GHz in the 1990s may be attributed to the progress in device technology to minimize planar stray capacitive parasitics, applied to both the MIC and MMIC basis. It should be noted that the data is predominantly for SEM configurations, thus presenting the device sensitivity capability.

Table I provides a broad summary of 1970/1980s point contact (representing the status toward the end of development) and Schottky diode performance characteristics at 10 GHz, indicating the characteristic merits of the Schottky barrier technology.

With consideration of frequencies above 100 GHz, the Fig. 1 1980 data represents the wire-contacted multidot GaAs Schottky (Mottky) diode SEM structures of that period. Recent planar technology is now almost performance competitive with wire-contacted structures up to about 650 GHz, and the 1990s data represents predominately planar technology. Although

TABLE III  
COMPARISON OF Lc/NF AND IP3/CP CHARACTERISTICS

	Type	Device	r.f.	Lc	SSB NF	IF	Plo	In IP3	In CP	Ref
<b>SBM</b>	<b>Passive</b>	<b>FET</b>	<b>2-27</b>	<b>6-15</b>		<b>1G</b>	<b>17</b>	<b>24-37</b>	<b>18.5</b>	[66]
<b>SBM</b>	<b>Active</b>	<b>FET</b>	<b>1.1</b>	<b>-16.7</b>	<b>5.2</b>	<b>130M</b>	<b>0</b>	<b>7.5*</b>		[70]
<b>SBM</b>	<b>Passive</b>	<b>PHEMT</b>	<b>50 to 100</b>	<b>11.6</b>		<b>50M</b>	<b>4</b>		<b>0</b>	[41]
<b>SBM</b>	<b>Passive</b>	<b>PHEMT</b>	<b>77</b>	<b>8.8</b>		<b>50M</b>	<b>4</b>		<b>0</b>	[41]
<b>DBM</b>	<b>Diode</b>	<b>S/B</b>	<b>6 to 18</b>	<b>5 to 8.5</b>		<b>1G</b>	<b>10</b>		<b>6</b>	[20]
<b>DBM</b>	<b>Passive</b>	<b>FET</b>	<b>2 to 8</b>	<b>8 to 9</b>			<b>23</b>	<b>30</b>		[66]
<b>DBM</b>	<b>Passive</b>	<b>FET</b>	<b>4 to 18</b>	<b>8 to 12</b>		<b>1 to 2G</b>	<b>7</b>	<b>&gt;18</b>		[42]
<b>DBM</b>	<b>Diode</b>	<b>FET s/diode</b>	<b>6 to 18</b>	<b>5 to 10</b>			<b>15</b>		<b>&gt;8</b>	[67]
<b>DBM</b>	<b>Diode</b>	<b>PHEMT s/diode</b>	<b>14 to 32</b>	<b>6 to 9</b>	<b>6 to 9</b>	<b>dc-8G</b>	<b>11</b>	<b>18</b>	<b>11</b>	[68]
<b>DDBM</b>	<b>Diode</b>	<b>S/B</b>	<b>1 to 18</b>	<b>8.5</b>		<b>M</b>	<b>20</b>	<b>25</b>		[19]
<b>DDBM</b>	<b>Diode</b>	<b>S/B</b>	<b>6 to 20</b>	<b>7.5</b>		<b>2 to 7G</b>	<b>17</b>	<b>20</b>	<b>8.5</b>	[21]
<b>SHM</b>	<b>Diode</b>	<b>S/B</b>	<b>26 to 36</b>	<b>10 to 12</b>			<b>11</b>	<b>13</b>	<b>2.5</b>	[69]
<b>SHM</b>	<b>Passive</b>	<b>HEMT</b>	<b>10</b>	<b>6.5</b>		<b>0.1 to 2G</b>	<b>12</b>		<b>10</b>	[23]
<b>SHM</b>	<b>Passive</b>	<b>PHEMT</b>	<b>10</b>	<b>8</b>	<b>8.5</b>	<b>1G</b>	<b>16</b>	<b>13</b>	<b>-2</b>	[46]
<b>SHM</b>	<b>Active</b>	<b>PHEMT</b>	<b>10</b>	<b>-5</b>	<b>12</b>	<b>1G</b>	<b>16</b>	<b>10</b>	<b>-2.5</b>	[46]
			GHz	dB	dB	Hz	dBm	dBm	dBm	
					<b>Fif=0dB</b>			<b>* Output</b>		

there is a wide spread in available data, the 1990s data tends to fall into two categories: the fundamental operation SEM and the antiparallel SHM, with the SEM indicating the better performance by a factor of almost 2:1. Although progress is being made with the MMIC, it is not yet competitive with the hybrid planar configurations, e.g., 16.5 dB  $L_c$  at 180 GHz for a subharmonic InP HEMT diode mixer [60].

In general, the three-terminal device mixer has not presented a significant noise-figure performance advantage over the Schottky barrier diode, the passive transistor mixer  $L_c$  performance falls well within the spread of diode mixers for frequencies below 100 GHz. The active device sensitivity can only be expressed meaningfully in terms of ONF, but active gate-fed mixers may require less  $P_{lo}$  and display the better ONF performance. The passive (resistive) transistor characteristics have, however, indicated a particular benefit in terms of dynamic range upper limit defined by IP3, thus, useful application to the high-level second-stage mixer for LNA microwave receivers. There is a widespread in published IP3 data (this may be quoted at output or input) for various three-terminal device technologies and circuit designs, and the potential of the transistor compared with the Schottky barrier diode may best be compared for the SEM. Some published IP3 data based on references in this paper is summarized in Table II, and some example comparisons of  $L_c/NF$  and IP3/CP characteristics are indicated in Table III for a range of mixers.

With reference to Table II, [63] also presents a comparison of spike-doped PsMESFET, ion-implanted MESFET, power PsHEMT, and n-p-n HBT as a ratio measure of two-tone third-order intercept to  $P_{lo}$ , and indicates ratios of 22.0, 13.9, 14.2, and 10.2, respectively, compared with zero for a typical diode; [64] presents IP3 data for 60-GHz resistive pseudomorphic HEMTs (pHEMTs) with reactive feedback between gate and drain, with application to direct conversion receivers (converts r.f. signal direct to baseband); and [38] presents a comparison of resistive, active, and Schottky mixer configurations compatible with InP HEMT technology.

With reference to Table III, [70] combines two dual-gate FET with built-in active baluns for personal-communication-system applications; [67] and [68] utilize transistor Schottky diodes (monolithic processing integration compatibility). Although not included as a Table III characteristic, the SHM provides >55 dB r.f. to l.o. isolation compared with the 15–30-dB range for the other mixers. In general terms, IP3 for the broad-band (e.g., 1–18 -GHz region) DBM falls in the range of 15–30 dBm (10–20 -dBm  $P_{lo}$ ) for a passive transistor quad compared with about 15 dBm (10-dBm  $P_{lo}$ ) for a diode quad, with similar  $L_c$  in the 6.5–9.0-dB range.

Current transistor mixer technologies and techniques embrace many options including circuit and modes of operation, and a detailed performance data analysis is outside the scope of this paper. Unfortunately, generally sensitivity based on  $L_c$

data tends to lack *ONF* qualification, of particular significance for megahertz and below intermediate-frequency applications, where there appears little information on flicker-noise characteristics of the transistor mixer for its various operational modes (referenced reports indicate  $1/f$  noise corners in the 10–30-MHz range for low flicker-noise passive transistors [36], compared with the 100–500-kHz range for 10-GHz Schottky barrier diodes [15]).

## VII. SOME CONCLUSIONS

As the result of extensive R&D investment, mixer technology and techniques have advanced considerably since the traditional mixer of 50 years ago incorporating point-contact technology, particularly through the significant steps of the Schottky barrier diode and transistor, applied to the MIC and MMIC.

Currently, the MMIC performance characteristics compete with those of the MIC and offer the mixer designer the miniaturization and reproducibility advantages of MMIC technology, with the capability to meet a wide range of system needs up to approximately 100 GHz, thus providing a specific choice of mixer circuit and embedded frequency-mixing element depending on application.

Noteworthy mixer technology and performance progress is being made above 100 GHz where sensitivity is still of prime importance, and planar technology is offering almost competitive performance to the wire-contacted multidot structure. Advances, however, of low-noise HEMT amplifiers exceeding 100 GHz, may soon imply the desirability for receiver second-stage high-level mixers.

## REFERENCES

- [1] H. C. Torrey and C. A. Whitmer, *Crystal Rectifiers*. New York: McGraw-Hill, 1948.
- [2] T. Oxley, "Recent advances in germanium microwave mixer diodes," presented at the IERE/IEE Microwave Applicat. Semiconduct. Symp., London, U.K., July 2, 1965, Paper 30.
- [3] G. C. Messenger and C. T. McCoy, "Theory and operation of crystal diodes and mixers," *Proc. IRE*, vol. 45, pp. 1269–1273, Sept. 1957.
- [4] S. T. Eng, "Low-noise properties of microwave backward diodes," *Trans. IRE Microwave Theory Tech.*, vol. MTT-9, pp. 419–425, Sept. 1961.
- [5] T. H. Oxley and F. Hilsden, "The performance of backward diodes as mixers and detectors at microwave frequencies," *J. Inst. Electron. Radio Eng.*, vol. 31, no. 3, pp. 181–191, Mar. 1966.
- [6] G. H. Swallow *et al.*, "Some aspects of high burnout gallium arsenide Schottky diodes," *GEC J. Sci. Technol.*, vol. 40, no. 3, pp. 126–131, 1973.
- [7] C. H. Hamilton, "High power passive semiconductor limiting," in *Proc. Military Microwave Conf.*, vol. 80, 1980, pp. 380–385.
- [8] J. J. Whalen and R. T. Kemerley, "X-band burnout characteristics of GaAs MESFETs," in *IEEE MTT-S Int. Microwave Symp. Dig.*, 1982, pp. 286–288.
- [9] C. M. Glenn and R. V. Garver, "Mixer burnout," *Appl. Microwave*, pp. 118–125, Spring 1990.
- [10] N. J. Keen, "The Mottky diode: A new element for low noise mixers at millimeter wavelengths," in *Proc. Advisory Group Aerosp. Res. Develop. Conf.*, vol. 245, Sept. 1978.
- [11] N. P. Cerniglia *et al.*, "Beam leaded Schottky barrier diodes for low noise integrated circuit mixers," *IEEE Trans. Electron Devices*, vol. ED-15, pp. 674–678, Sept. 1968.
- [12] S. Jamison *et al.*, "Beam-lead Schottky-barrier planar mixer diodes for millimeter wave applications," in *IEEE MTT-S Int. Microwave Symp. Dig.*, 1981, pp. 331–333.
- [13] M. J. Sisson, "The development of millimeter wave mixer diodes," *Radio Electron. Eng.*, vol. 52, pp. 534–542, Nov./Dec. 1987.
- [14] R. K. Surridge *et al.*, "Planar GaAs Mott low noise mm-wave (35 and 85 GHz) mixer diodes," in *11th European Microwave Conf.*, 1981, pp. 871–875.
- [15] M. J. Kearney and I. Dale, "GaAs planar doped barrier diodes for mixer and detector applications," *GEC J. Res.*, vol. 8, no. 1, pp. 1–12, 1990.
- [16] S. Dixon *et al.*, "Subharmonic mixer using planar doped barrier diodes," in *IEEE MTT-S Int. Microwave Symp. Dig.*, 1982, pp. 27–29.
- [17] P. J. Meier, "Two new integrated-circuit media with special advantages at millimeter wavelengths," in *IEEE MTT-S Int. Microwave Symp. Dig.*, May 1972, pp. 221–223.
- [18] T. H. Oxley *et al.*, "Hybrid microwave integrated circuits for millimeter wavelengths," in *IEEE MTT-S Int. Microwave Symp. Dig.*, May 1972, pp. 221–223.
- [19] D. Neuf *et al.*, "Multi-octave double balanced mixer," *Microwave J.*, Jan. 1973.
- [20] D. Cahana, "A new, single plane, double-balanced mixer," *Appl. Microwave*, pp. 78–83, Aug./Sept. 1989.
- [21] J. Eisenberg *et al.*, "Double-double balanced MMIC mixer," *Appl. Microwave*, pp. 101–108, Fall 1991.
- [22] M. V. Schneider and W. W. Snell, "Harmonically pumped stripline down-converter," *IEEE Trans. Microwave Theory Tech.*, vol. MTT-23, pp. 271–275, Mar. 1975.
- [23] H. Zirah, "A subharmonically pumped resistive dual-HEMT-mixer," in *IEEE MTT-S Int. Microwave Symp. Dig.*, 1991, pp. 875–878.
- [24] D. Neuf, "A quiet mixer," *Microwave J.*, pp. 29–32, May 1973.
- [25] B. R. Halford, "An experimental study of image termination methods for low-noise mixers," in *IEEE MTT-S Int. Microwave Symp. Dig.*, 1976, pp. 85–88.
- [26] T. H. Oxley *et al.*, "Phasing type image recovery mixers," in *IEEE MTT-S Int. Microwave Symp. Dig.*, 1980, pp. 270–273.
- [27] D. Weiner *et al.*, "The image rejection harmonic mixer," in *IEEE MTT-S Int. Microwave Symp. Dig.*, 1982, pp. 36–38.
- [28] S. C. Cripps *et al.*, "An experimental evaluation of X-band GaAs FET mixers using single and dual-gate devices," in *IEEE MTT-S Int. Microwave Symp. Dig.*, 1977, pp. 285–287.
- [29] S. C. Cripps *et al.*, "An S-band dual gate MESFET image rejection mixer," in *IEEE MTT-S Int. Microwave Symp. Dig.*, 1978, pp. 300–302.
- [30] S. A. Maas, "Low-noise 45 GHz HEMT mixer," in *15th European Microwave Conf.*, 1985, pp. 607–610.
- [31] O. S. A. Tang and C. S. Aitchison, "A microwave distributed MESFET mixer," in *14th European Microwave Conf.*, 1984, pp. 483–487.
- [32] G. R. Antell, "Monolithic mixers for mm-wavelengths," presented at the European Microwave Conf., Stockholm, Sweden, 1971, Paper C2/3.
- [33] M. Mradmanesh and N. A. Barakat, "State of the art S-band resistive FET mixers," in *IEEE MTT-S Int. Microwave Symp. Dig.*, 1994, pp. 1435–1438.
- [34] S. A. Maas, "A GaAs MESFET mixer with very low intermodulation," *IEEE Trans. Microwave Theory Tech.*, vol. MTT-35, pp. 425–429, Apr. 1987.
- [35] K. W. Chang *et al.*, "Zero bias GaInAs MISFET mixers," in *IEEE MTT-S Int. Microwave Symp. Dig.*, 1989, pp. 1027–1030.
- [36] J. Geddes *et al.*, "A millimeter wave passive FET mixer with low  $1/f$  noise," in *IEEE MTT-S Int. Microwave Symp. Dig.*, 1991, pp. 1045–1047.
- [37] R. Shimon *et al.*, "Low cost coplanar 77 GHz single-balanced mixer using ion-implanted GaAs Schottky diodes," in *IEEE MTT-S Int. Microwave Symp. Dig.*, 1998, pp. 1439–1442.
- [38] R. S. Virk *et al.*, "A comparison of W-band MMIC mixers using InP HEMT technology," in *IEEE MTT-S Int. Microwave Symp. Dig.*, 1997, pp. 1301–1304.
- [39] K. W. Kobayashi *et al.*, "An 18–22 GHz down-converter based on GaAs/AlGaAs HBT-Schottky diode integrated technology," *IEEE Trans. Microwave Guided Wave Lett.*, vol. 7, pp. 106–108, Apr. 1997.
- [40] J. Putnam and R. Puente, "A monolithic image-rejection mixer on GaAs using lumped elements," *Microwave J.*, pp. 107–116, Nov. 1987.
- [41] K. Kamozaki *et al.*, "50–100 GHz octave band MMIC mixers," in *IEEE RFIC Symp. Dig.*, 1997, pp. 95–98.
- [42] M. C. Tsai *et al.*, "A compact wideband balanced mixer," in *IEEE Microwave Millimeter-Wave Monolithic Circuits Symp. Dig.*, 1994, pp. 135–138.
- [43] J. Schellenberg and H. Do-ky, "Low-loss, planar monolithic baluns for K/Ka-band applications," in *IEEE MTT-S Int. Microwave Symp. Dig.*, 1999, pp. 1733–1736.
- [44] M. Shimozawa *et al.*, "A parallel connected Marchand balun spiral shaped equal length coupled lines," in *IEEE MTT-S Int. Microwave Symp. Dig.*, 1999, pp. 1737–1740.

- [45] R. S. Virk *et al.*, "A  $K_u$ -band frequency converter using 0.25 PHEMT technology," in *IEEE MTT-S Int. Microwave Symp. Dig.*, 2000, pp. 639–642.
- [46] M. Ventresca and M. C. Tsai, "An active PsHEMT sub-harmonically pumped mixer," in *IEEE MTT-S Int. Microwave Symp. Dig.*, 1994, pp. 1641–1644.
- [47] T. Sekiguchi *et al.*, "Ultra small sized low noise block downconverter module," in *IEEE MTT-S Int. Microwave Symp. Dig.*, 1992, pp. 447–452.
- [48] Y.-L. Kok *et al.*, "A  $K_a$ -band monolithic single-chip transceiver using sub-harmonic mixer," in *IEEE RFIC Symp. Dig.*, 1998, pp. 235–237.
- [49] T. J. Holden *et al.*, "A monolithic 4 GHz image rejection frequency converter," in *IEEE GaAs Integrated Circuit Symp. Dig.*, pp. 187–191.
- [50] K. Kawakami *et al.*, "A millimeter-wave broadband monolithic even harmonic image rejection mixer," in *IEEE MTT-S Int. Microwave Symp. Dig.*, 1998, pp. 1443–1446.
- [51] R. Heilig *et al.*, "A monolithic integrated MEMT frontend in CPW technology from 10–50 GHz for measurement systems or broadband receivers," in *IEEE MTT-S Int. Microwave Symp. Dig.*, 1995, pp. 211–214.
- [52] I. Kipnis, "Silicon bipolar MMIC for frequency-conversion application up to 20 GHz," in *IEEE MTT-S Int. Microwave Symp. Dig.*, 1987, pp. 855–858.
- [53] J. N. Wholey and I. Kipnis, "Silicon bipolar active mixer," *Appl. Microwave*, pp. 108–117, Spring 1990.
- [54] K. M. Strohm *et al.*, "Monolithic integrated coplanar SIMMWIC 77 GHz mixer," in *26th European Microwave Conf. Dig.*, 1996, pp. 293–296.
- [55] B. J. Clifton, "Receiver technology for the submillimeter-wave region," *Infrared Phys.*, vol. 25, no. 1/2, pp. 267–272, 1985.
- [56] J. L. Hesler *et al.*, "Fixed-tuned submillimeter wavelength waveguide mixers using planar Schottky-barrier diodes," *IEEE Trans. Microwave Theory Tech.*, vol. 45, pp. 653–658, May 1997.
- [57] P. H. Siegel, "A 640 GHz planar-diode fundamental mixer/receiver," in *IEEE MTT-S Int. Microwave Symp. Dig.*, 1998, pp. 407–410.
- [58] I. Mehdi *et al.*, "An all solid-state 640 GHz subharmonic mixer," in *IEEE MTT-S Int. Microwave Symp. Dig.*, 1998, pp. 403–406.
- [59] P. H. Siegel *et al.*, "Design and measurement of a 210 GHz subharmonically pumped GaAs MMIC mixer," in *IEEE MTT-S Int. Microwave Symp. Dig.*, 1992, pp. 603–606.
- [60] Y.-L. Kok *et al.*, "A 180 GHz monolithic sub-harmonic In-P HEMT diode mixer," *IEEE Microwave Guided Wave Lett.*, vol. 9, pp. 1051–1059, Dec. 1999.
- [61] T. W. Crowe *et al.*, "GasAs devices and circuits for terahertz applications," in *IEEE MTT-S Int. Microwave Symp. Dig.*, 1999, pp. 929–932.
- [62] A. Pham *et al.*, "Comparison of air coplanar microprobes for on-wafer measurement at  $W$ -band," in *IEEE MTT-S Int. Microwave Symp. Dig.*, vol. 3, 1997, pp. 1659–1662.
- [63] M. J. Schindler *et al.*, "A comparison of GaAs transistors as passive mode mixers," in *IEEE MTT-S Int. Microwave Symp. Dig.*, 1994, pp. 937–940.
- [64] K. S. Ang *et al.*, "Monolithic resistive mixers for 60 GHz direct conversion receivers," in *IEEE RFIC Symp. Dig.*, 2000, pp. 35–38.
- [65] C.-Y. Chang *et al.*, "A decade bandwidth resistive FET singly balanced MIC mixer," in *IEEE MTT-S Int. Microwave Symp. Dig.*, 1999, pp. 311–314.
- [66] S. Weiner *et al.*, "2 to 8 GHz balanced MESFET mixer with +30 dBm input 3rd order intercept," in *IEEE MTT-S Int. Microwave Symp. Dig.*, 1988, pp. 1097–1100.
- [67] W. R. Brinlee *et al.*, "A novel planar double-balanced 6–18 GHz MMIC mixer," in *IEEE MTT-S Int. Microwave Symp. Dig.*, 1994, pp. 9–11.
- [68] C. J. Trantanella, "Ultra small MMIC mixers for  $K$ - and  $K_a$ -band communications," in *IEEE MTT-S Int. Microwave Symp. Dig.*, 2000, pp. 647–650.
- [69] H. Gu, "A novel uniplanar balanced subharmonic pumped mixer for low-cost broadband millimeter-wave transceiver design," in *IEEE MTT-S Int. Microwave Symp. Dig.*, 2000, pp. 631–634.
- [70] H. Koizumi *et al.*, "A GaAs single balanced mixer MMIC with built-in active balun for personal communications systems," in *IEEE Microwave Millimeter-Wave Monolithic Circuits Symp.*, 1995, pp. 77–80.



**Terry H. Oxley** (M'73–SM'78–F'92–LF'99) CEng, MIEE, was born in St. Leonards-On-Sea, Sussex, U.K., in 1924.

In 1946, he joined the GEC Hirst Research Center (HRC) following wartime service in the Royal Navy. Since 1950, he has been professionally involved in the microwave field of solid-state devices and circuits. In 1970, he became Head of the HRC Microwave Component Department, where he was responsible for microwave and millimeter-wave R&D. In 1980, he joined Marconi Electronic Devices

Ltd., Lincoln, U.K., where he was the Development Manager responsible for microwave and millimeter-wave R&D. In 1985, he joined GEC Research Ltd., based at the Marconi Research Center (MRC), GT. Baddow, Chelmsford, Essex, U.K., as the Microwave Research Coordinator reporting to the Managing Director. In 1988, he retired from GEC Research Ltd., and has continued his microwave engineering involvement as a consultant on an independent basis. He has authored over 100 scientific papers.

Mr. Oxley was the recipient of numerous awards, including Her Majesty's Silver Jubilee Medal (for contribution to advancements in microwave components), the GEC Nelson Gold Medal (for Company technical achievement), the IEEE Microwave Theory and Techniques Society (IEEE MTT-S) Meritorious Service Award, and the IEEE Region 8 Section Volunteer Award.

**Mixers for Wireless Circuits**

**ELEC 483 - Wireless Technology**

**Brian Frank**

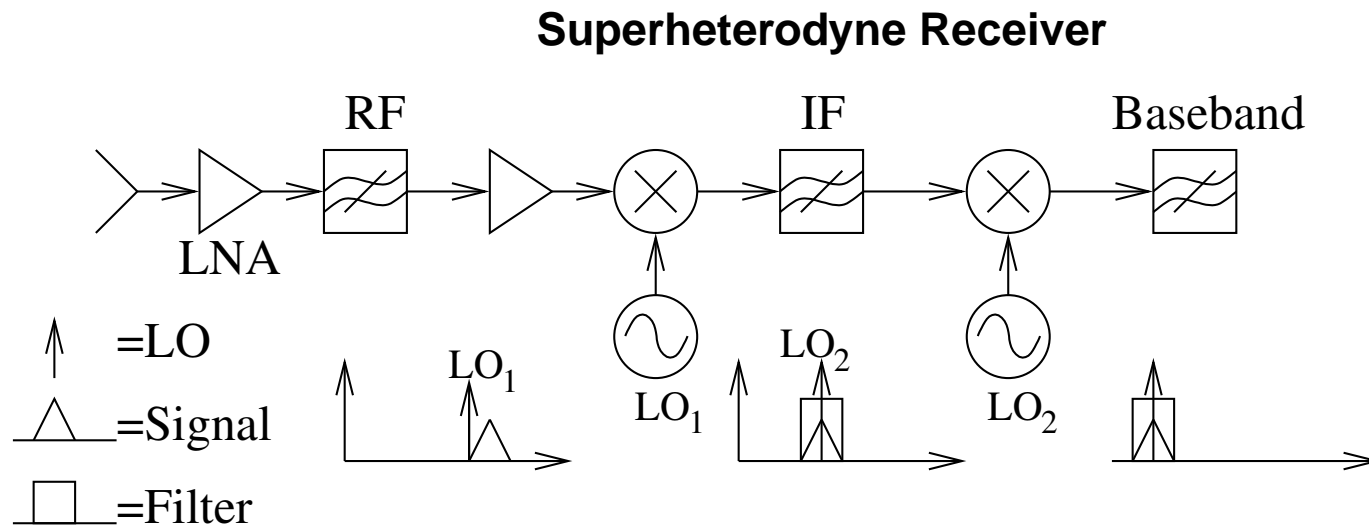
**2003-2004**

### Overview

- What do mixers do?
- How do they work?
- What types are there?
  - Transistor mixers (FET)
  - Diode mixers
  - Balanced/double balanced mixers

### Mixers - Where did they come from?

- First presented by Armstrong as part of superheterodyne receiver (improvement over direct downconvert receiver of the time)
- RF signal converted to intermediate frequency (IF) where fixed frequency filter and narrowband amplifier cleaned up signal
- Solves problem of poor frequency stability of oscillator which plagues direct downconvert systems
- MIT's Radiation Laboratory (vital to WWII radar effort) improved mixer by using diodes
- FET devices made it possible to create mixers with conversion gain, rather than conversion loss (power of IF relative to power of RF)



### What is a mixer?

- Shift the frequency of an input signal to a new frequency using a carrier from a local oscillator (LO)
- From basic trigonometry, multiplying two sinusoidal signals

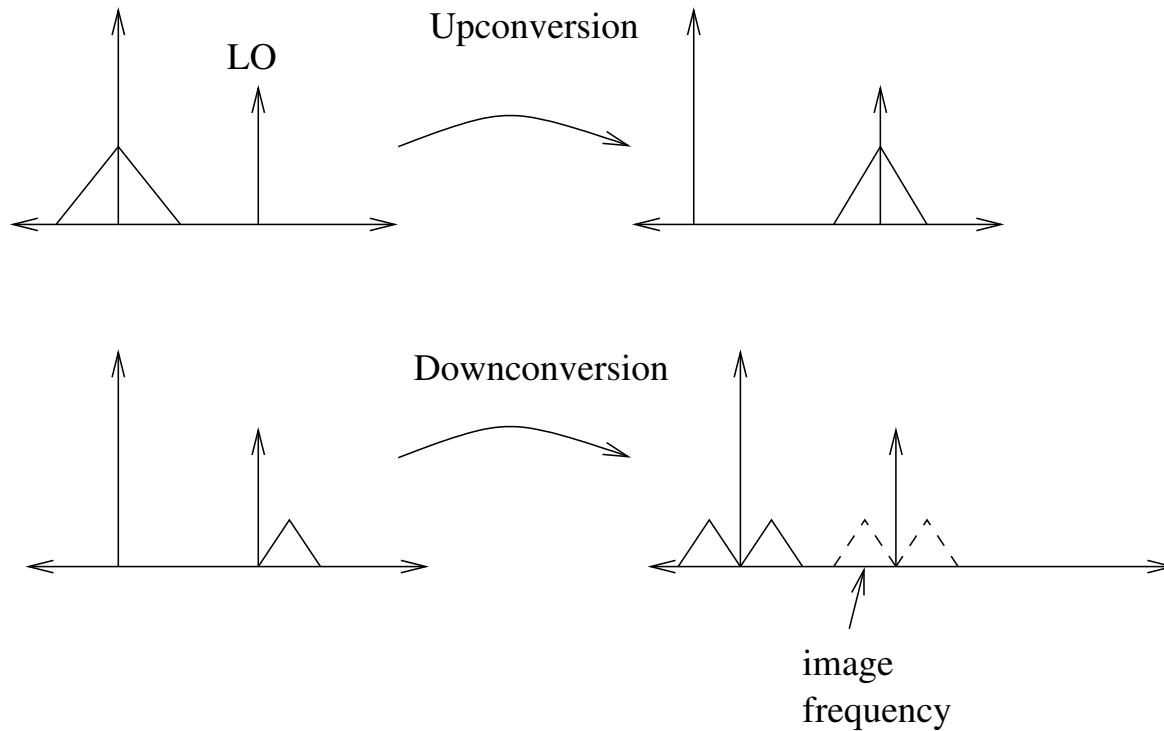
$$\begin{aligned}V_1 &= A_1 \cos \omega_1 t \\V_2 &= A_2 \cos \omega_2 t\end{aligned}\tag{1}$$

results in

$$V_1 V_2 = \frac{1}{2} (\cos(\omega_1 + \omega_2)t + \cos(\omega_1 - \omega_2)t)\tag{2}$$

- We have one signal at a low frequency (difference between two frequencies), and one at a high frequency (sum of two frequencies) each with 1/2 voltage of original

### Mixing



### Conversion gain/loss

- Conversion gain/loss tells us the ratio of the power of the desired output signal (whether at the high or low frequency) to the power of the input signal
- Passive mixers (e.g. diode mixers) have minimum of 6 dB conversion loss (i.e. output signal has half the voltage of the input)
- Active mixers (using transistors) can amplify as they frequency convert, resulting in conversion gain
- Mixer may be either an upconvert (shifts up in frequency) or downconvert mixer (shifts down in frequency)

### How do we implement a mixer?

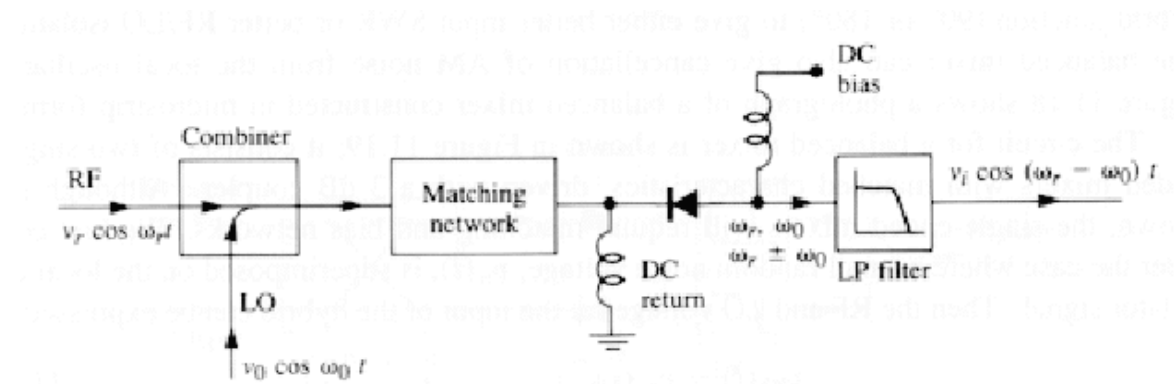
- Use non-linearity of a device
- Requires either diode or transistor
- Use a large signal (LO) to vary impedance (reflection coefficient) of mixing device

### Diode mixers

- Earliest, simplest, and fastest mixers
- Several topologies possible including a single diode mixer, single balanced mixer, double balanced mixer, subharmonic mixer, etc.
- Use Schottky diodes for high frequencies (fastest, lowest conversion loss of passive mixers, largest bandwidth)

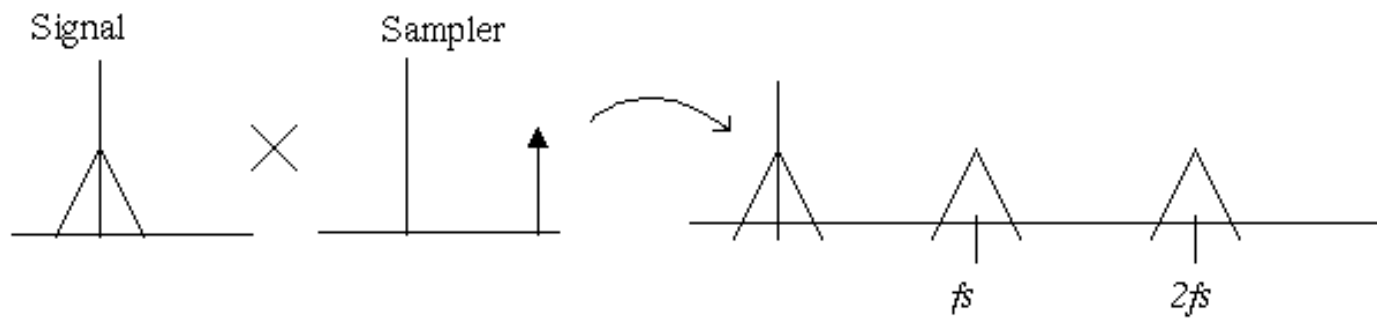
## Single diode mixer

- Simple, low power, fast
- Problem: isolation between signals (filters required)
- Operation: add RF and LO using coupler, feed into diode, use matching networks and filters to isolate signals



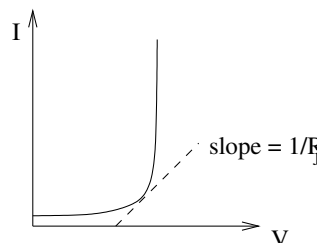
### Diode mixing

- Ideally, want the diode to be lossless switch with a duty cycle of zero
- Want diode to conduct for an infinitesimally small period of time at a frequency corresponding to the LO frequency
- Recall: if we sample a signal at a sampling frequency of  $f_s$  then our output signal in the frequency domain is simply the sampled signal with images repeated every  $f_s$
- If the sampling signal is not a perfect delta function, but is rather itself a square wave with a certain duty cycle, then the signal is multiplied by a time shifted sinc function, rather than a delta function.



### Diode as a switch

- We want the diode to look like  $Z_{in} = \infty$  for half of the cycle, and  $Z_{in} = 0$  for the other half
- In terms of reflection coefficient, we want it to be  $\Gamma = 1$  for half the cycle, and  $\Gamma = -1$  for the other half.
- If we bias a Schottky diode close to threshold voltage, then a large applied LO voltage will cause the diode to swing between being very conducting (low impedance), and off (high impedance)
- Is not truly an open and short circuit, so a matching network is used



### Diode harmonics

- We will get not only our desired output, but also other harmonics
- These harmonics cut out by the stubs and filters:
  - The signal filter is an open circuit at image and frequencies higher than the signal
  - The short-circuited stub shorts even harmonics of the LO
  - The open-circuited stub shorts odd harmonics of the LO
  - The IF filter shorts everything except the IF

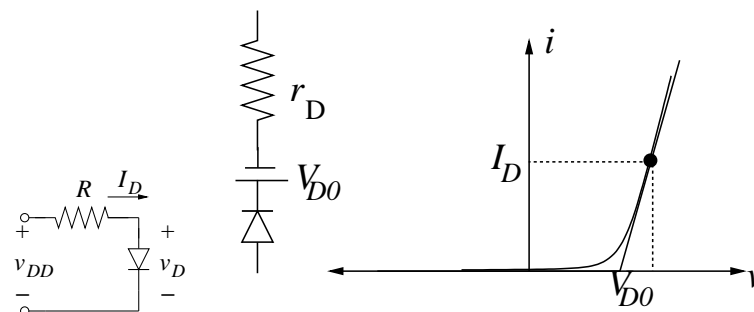
## Diode mixer model

- Assume that we have a diode biased at a certain  $V_D$ , with  $I_D = I_S e^{V_D/nV_T}$
- If we apply a small signal voltage  $v_d(t)$  on top of a large LO signal  $V_D$ , our total diode voltage is  $v_D = V_D + v_d(t)$ , so the diode current is

$$i_D(t) = I_S e^{(V_D+v_d(t))/nV_T} \quad (3)$$

$$= I_S e^{V_D/nV_T} e^{v_d(t)/nV_T} \quad (4)$$

$$= I_D e^{v_d(t)/nV_T} \quad (5)$$



## Diode mixer model (cont'd)

- If  $v_d/nV_T \ll 1$  (which means  $v_d \leq 10 \text{ mV}$ ), then we can expand the exponential into

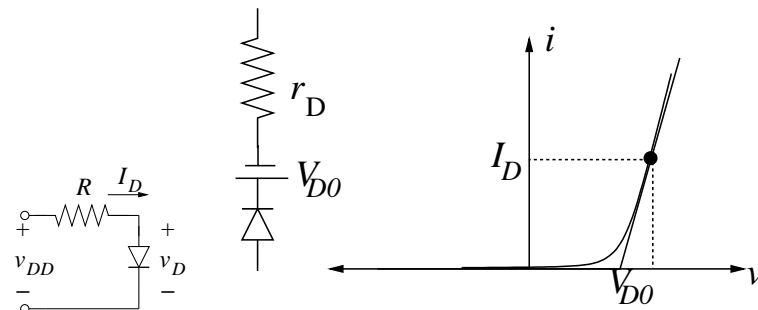
$$i_D(t) \approx I_D \left( 1 + \frac{v_d(t)}{nV_T} \right) \quad (6)$$

$$\approx I_D \frac{I_D}{nV_T} v_d(t) \quad (7)$$

$$\approx I_D + i_d(t) \quad (8)$$

so that we have the total diode current as the sum of the large signal current  $I_D$ , and a small signal diode current  $i_d(t)$

- Notice that  $i_d(t) = v_d(t)g_d$ , where  $g_d = I_D/nV_T = r_d^{-1}$ . Hence we have a small signal current that is the *product* of the small signal RF voltage and the large LO signal  $I_D$



### Diode mixer model (cont'd)

- The output current is the sum of the large LO signal, and a term that is the product of the LO and the small signal -  $v_d g_d = v_d I_D / nV_T$
- Since  $I_D$  is related to the input LO voltage by  $I_D = I_S e^{V_D/nV_T}$ , there will be other harmonics produced as well
- Since a diode can be modeled as a nonlinear device with a particular Taylor series, our discussion about nonlinearities for amplifiers applies here as well (e.g. third order intermodulation products)

### FET Mixers

- Operation similar to diode operation, but more flexibility
- For common source FET with small signal  $v_g$  applied to gate, small signal output at drain is  
$$v_d = v_g g_m R_{out}$$
- Since  $g_m$  can be expressed as

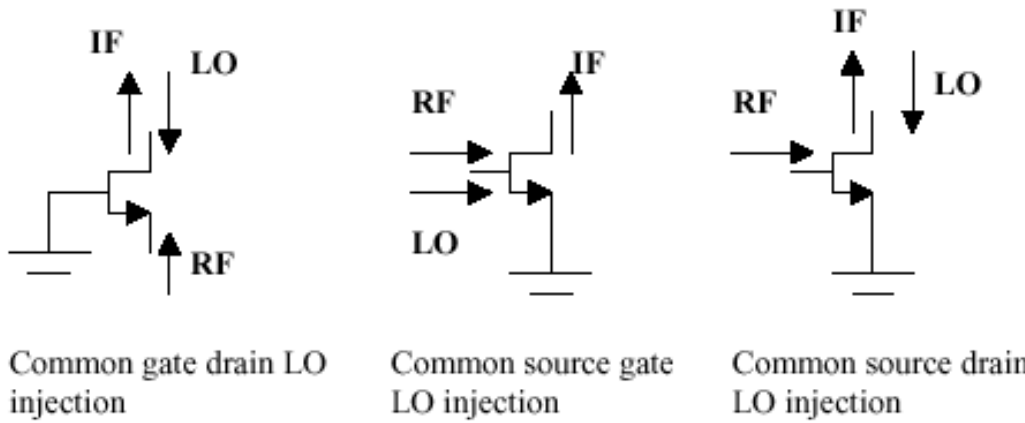
$$\begin{aligned} g_m &= \mu_n C_{ox} W/L (V_{GS} - V_t) \\ &= \sqrt{2\mu_n C_{ox} \frac{W}{L}} \sqrt{I_D} \end{aligned} \tag{9}$$

we see that our output will be composed of the product of the output current  $I_D$  and the small RF signal  $v_g$

- FETs also provide gain, so the output frequency converted signal can be larger than the input signal (due to  $g_m R_{out}$ )
- Bipolar mixers not common (smaller swing, increased noise figure)

### FET Mixer Configurations

- Mixing action may be provided in several ways
  - LO and IF applied both to the gate
  - One applied to the gate and one to the drain
  - One to the drain and one to the source
- As long as appropriate matching networks and filters are applied at the appropriate ports, mixing will occur
- Choice of configuration depends upon the application

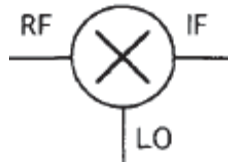


# RF Mixers

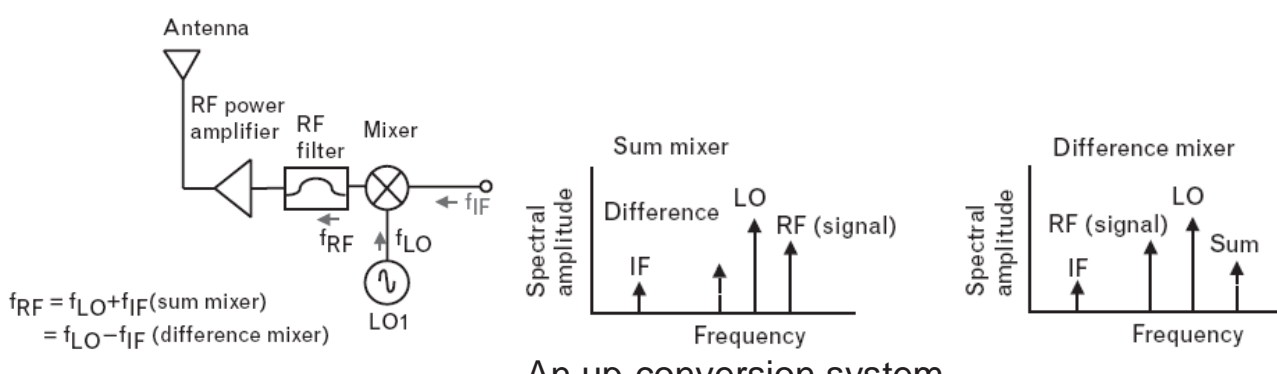
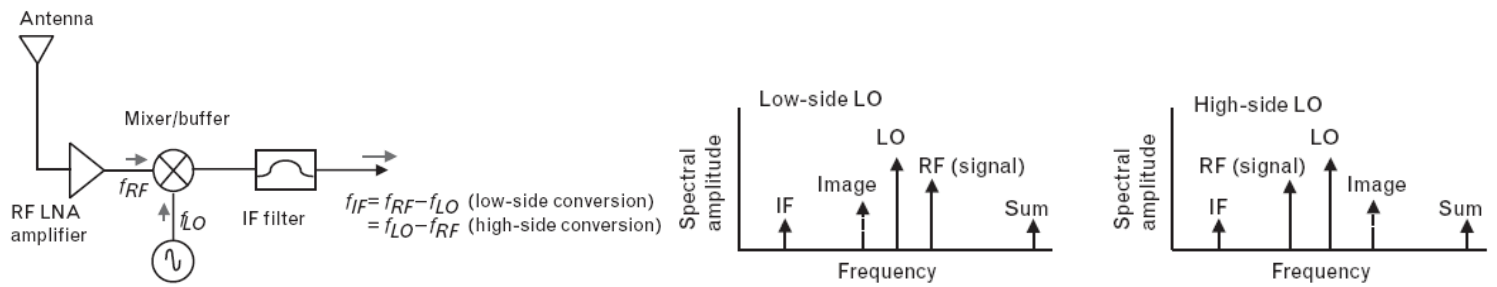
Julian Rosu, YO3DAC / VA3IUL, <http://www.qsl.net/va3iul>

**RF Mixers** are 3-port active or passive devices. They are designed to yield both, a sum and a difference frequency at a single output port when two distinct input frequencies are inserted into the other two ports.

In addition to this, a Mixer can be used as a phase detector or as a demodulator.



The two signals inserted into the two input ports are usually the Local Oscillator signal, and the incoming (for a receiver) or outgoing (for a transmitter) signal. To produce a new frequency (or new frequencies) requires a nonlinear device. In a mixing process if we want to produce an output frequency that is lower than the input signal frequency, then it is called *down-conversion* and if we want to produce an output signal that is at a higher frequency than the input signal, it is referred to as *up-conversion*.



A common misunderstanding about mixers is that a Mixer is only a nonlinear device.

- Actually an RF Mixer is fundamentally a linear device, which is shifting a signal from one frequency to another, keeping (faithfully) the properties of the initial signal (phase and amplitude), and therefore doing a linear operation.

From the moment that we use a nonlinear device to perform the mixing operation, Mixers have relatively high levels of intermodulation distortion, spurious responses, and other undesirable nonlinear phenomena.

- In contrast to frequency multipliers and dividers, which also change signal frequency, Mixers theoretically preserve the amplitude and phase without affecting modulation properties of the signals at its ports.

### **Important Mixer properties are:**

Conversion Gain or Loss, Intercept point, Isolation, Noise Figure, High-order spurious response rejection and Image noise suppression.

**1. Conversion Gain or Loss** of the RF Mixer is dependent by the type of the mixer (active or passive), but is also dependent by the load of the input RF circuit as well the output impedance at the RF port. Also is dependent by the level of the LO.

The typical conversion gain of an active Mixer is approximately +10dB when the conversion loss of a typical diode mixer is approximately -6dB.

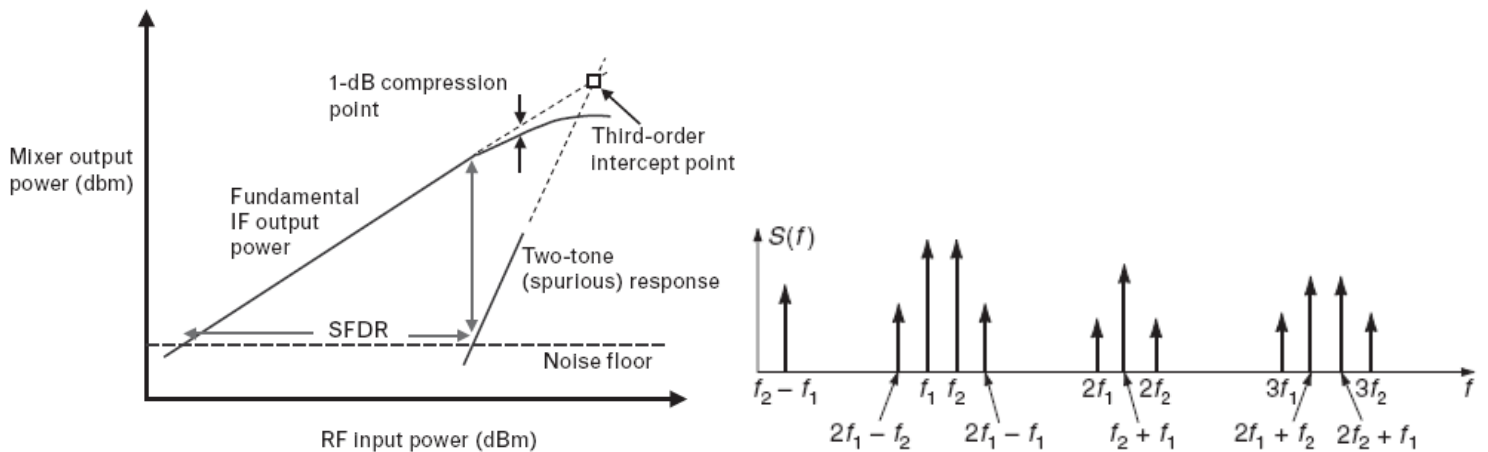
The Conversion Gain or Loss of the RF Mixer measured in dB is given by:

Conversion<sub>[dB]</sub> = Output IF power delivered to the load<sub>[dBm]</sub> – Available RF input signal power<sub>[dBm]</sub>

**2. Input Intercept Point (IIP3)** is the RF input power at which the output power levels of the unwanted intermodulation products and the desired IF output would be equal.

- From an RF System point of view, a Mixer linearity is more critical than Noise Figure.

The Third-Order intercept point (IP3) in a Mixer is defined by the extrapolated intersection of the primary IF response with the two-tone third-order intermodulation IF product that results when two RF signals are applied to the RF port of the Mixer.



**3. Spurious products** in a Mixer are problematic, and Mixer vendors frequently provide tables showing the relative amplitudes of each response under given LO drive conditions.

One way to reduce such products is to short-circuit the higher harmonics of the LO at the intrinsic Mixer terminals to lower the power in such responses.

Reducing the second or third harmonic of the local oscillator reduces its harmonic products by 20 to 25 dB and 10 to 15 dB, respectively.

**4. Isolation** is the amount of local oscillator power that leaks into either the IF or the RF ports. There are multiple types of isolation: LO-to-RF, LO-to-IF and RF-to-IF isolation.

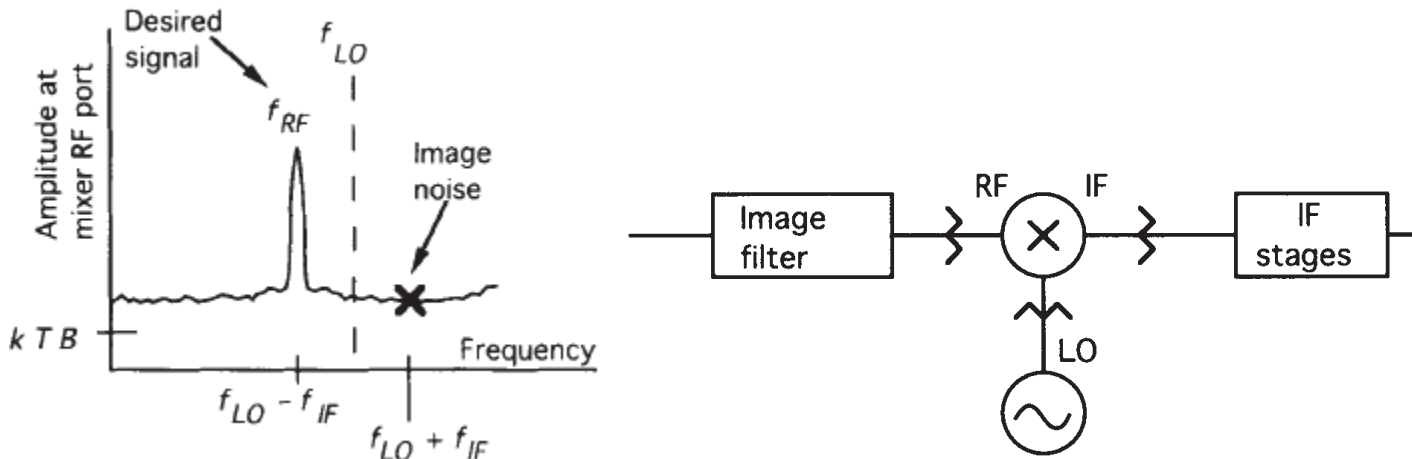
**5. Noise Figure** is a measure of the noise added by the Mixer itself, noise as it gets converted to the IF output.

- For a passive Mixer which has no gain and only loss, the Noise Figure is almost equal with the loss.
- In a mixer noise is replicated and translated by each harmonic of the LO that is referred to as Noise Folding.

In addition to the degradation in system Noise Figure introduced by the conversion loss of the Mixer, noise sources within the Mixer device itself further corrupt the Noise Figure. For example, the effect of  $1/f$  noise in MESFETs can be severe if the IF frequency is below the corner frequency of the flicker noise (normally less than 1 MHz), as this noise will add to the output.

- A Mixer will convert energy in the upper or lower sidebands with equal efficiency. Consequently the noise in the side band with no signal will be added to the IF output, which will increase the Noise Figure at the IF port by 3dB, no matter how good the preceding component noise figure is. An Image Filter at the RF input of the Mixer could suppress this noise.

Also there are some particular Image Reject mixers that suppress the image noise by their topology.



The wideband noise of the Local Oscillator is another parameter that can raise the IF noise level, degrading in this way the overall Noise Figure. So, the wideband noise separated from the LO frequency by  $\pm f_{IF}$  spacing will mix to produce noise at IF frequency.

- Any noise that is near a multiple of the LO frequency can also be mixed down to the IF, just like the noise at the RF. This noise conversion process is related, *but not the same as*, the LO-to-RF isolation.
- Noise at frequencies of  $\pm f_{IF}$  spacing from the LO harmonics also contributes to overall system Noise Figure.
- Wideband LO noise is down-converted to IF with much higher conversion loss than the desired signal and image noise.

- A Band Pass Filter between LO and the Mixer could help reducing the wideband LO noise.
- In case of Mixers, the Noise Figure is defined for both the image and RF responses, and the output noise is generated by the input termination includes only the noise arising from the principal frequency transformation of the system.

When a Single Sideband Noise Figure at the RF input is to be determined, the output noise arising from the input termination, at the image frequency is not included.

Furthermore, it is impossible to measure directly the noise figure thus defined, because noiseless image terminations are difficult to obtain. The use of a filter to eliminate the image response (only to do accurate NF measurement) does not help because it changes the image-frequency embedding impedance, and hence changes the noise temperature. So, an alternate definition of *SSB Noise Figure* has found more common use.

When a noisy LO signal is applied to the Mixer, its noise components at the RF and image frequencies are down converted and appear at the IF port, just as if they had been applied to the RF input. It is important to pick the IF frequency high enough so that noise at the RF and image frequencies are well separated from the LO and can be filtered effectively.

- SSB NF assumes signal input from only one sideband, but noise inputs from both sidebands. Measuring SSB noise figure is relevant for Superheterodyne receiver architectures in which the image frequency is removed by filtering or cancellation.
- DSB NF includes both signal and noise inputs from both sidebands. A DSB NF is easier to measure; wideband excess noise is introduced at both the signal and image frequencies. It will be 3 dB less than the SSB noise figure in most cases.

This is perhaps more relevant for Direct Conversion receivers where the image cannot be filtered out from the signal.

### **Mixers can be divided into several classes:**

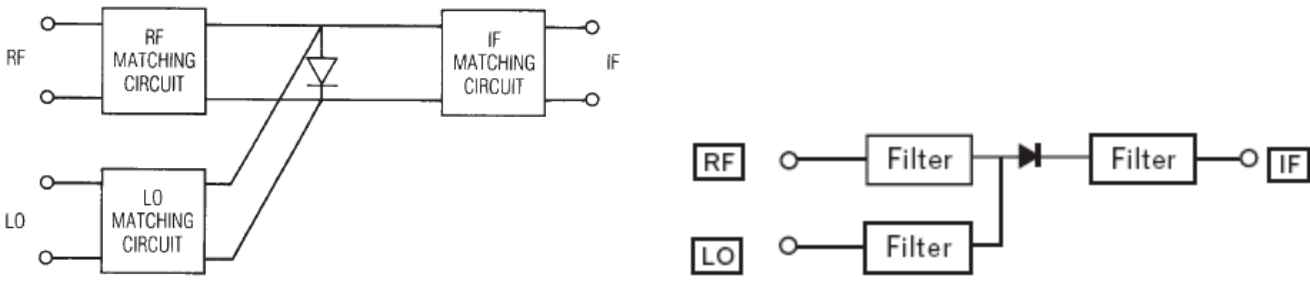
1. Single-device Mixer
2. Single Balanced Mixer
3. Double Balanced Mixer.

1. **Single-device Mixer** which is using one nonlinear component (one diode, or one transistor) has the disadvantage of not attenuating local oscillator AM noise and always requires an injection filter.

Single-device mixers need to follow some general design rules for best performance.

- To get the maximum conversion gain the LO node should be a short circuit at the RF and IF frequencies, while the RF node should be a short circuit at the LO frequency to prevent the LO leakage into the RF port.

Single-device Mixer using one diode is primarily a process of matching the pumped diode to the RF input and IF output, terminating the diode properly at LO harmonics and unwanted mixing frequencies (other than the RF and IF), and isolating the RF, LO, and IF ports. That isolation, and in some cases the termination, can be provided by using filters, a balanced structure, or both. The choice depends on the frequency range and the intended application.



The diode used for mixing can be modeled at the RF frequency as a resistor and capacitor in parallel. The resistor is usually in a range of 50 to 150 ohms and the capacitor between 1 and 1.5 times the junction capacitance. The IF output impedance is usually between 75 ohms and 150 ohms. At low IF frequencies the output impedance is almost pure resistive.

As the LO level increases, both RF and the LO input impedances decrease.

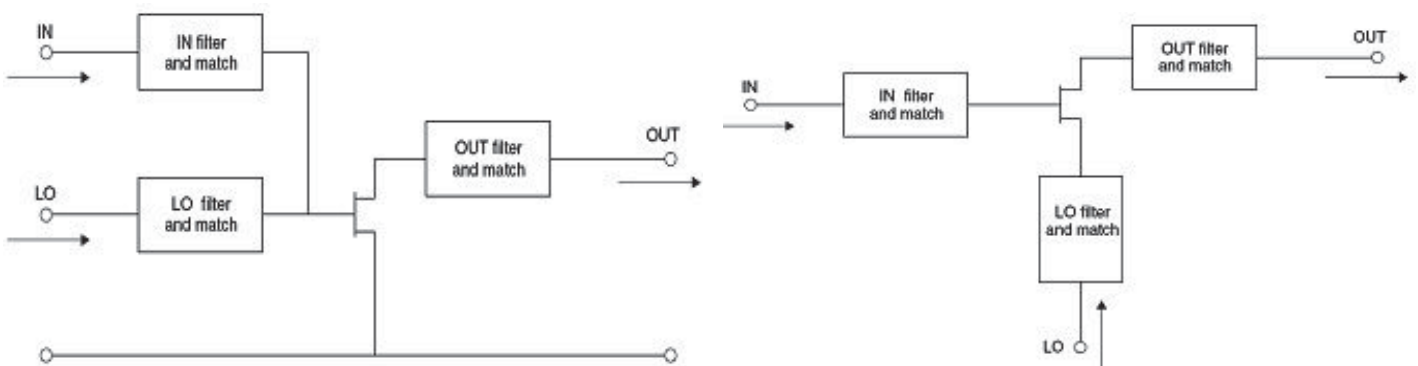
The RF and IF input impedances mentioned above (high or low end on the range) are affected by the IF port termination on unwanted and LO harmonics frequencies. The diode's termination at the image frequency is the most critical of all the terminations at unwanted mixing frequencies.

- Terminating the IF port in a reactance at image frequency can improve the conversion efficiency of the Mixer.

For selecting the mixing diode have to look for the cut-off frequency of the diode, for series resistance  $R_s$  and junction capacitance  $C_j$ . Minimizing both  $R_s$  and  $C_j$  is necessary to achieve low conversion loss and distortion, but they are inverse trade-offs.

- Sometimes it helps to apply a DC bias to a single-diode mixer which can reduce the required LO power and provides a degree of freedom for adjusting the mixer's input and output impedances.

In active Single-device design case (i.e. one-transistor Mixer), to prevent oscillations the IF node should be a short circuit at both LO and RF frequencies, and RF should be low impedance at IF frequency. This also prevent that the noise at the IF frequency is not amplified and added to the output.

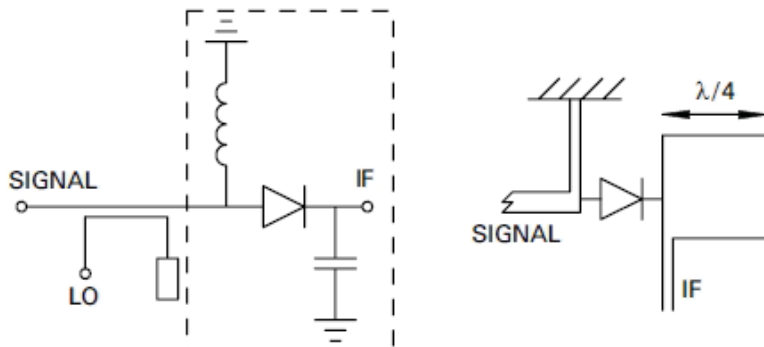


Single-device Mixers using FETs (two approaches for LO input)

The input filters, which are necessary to achieve RF-to-LO isolation and prevent radiation of the LO back through the antenna or other RF input, should attempt to short-circuit all unwanted frequencies (i.e., those other than the RF-and-LO) so there are no interfering voltages appearing at the input.

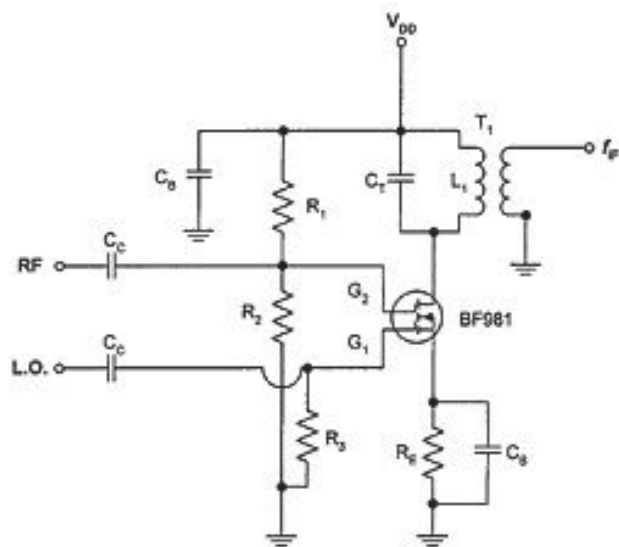
The input should be matched to the RF to maximize conversion gain and noise figure, and if possible, to the LO as well for LO power transfer. The image frequency should be short-circuited (if possible), as well as the IF, so neither noise nor spurious signals are amplified by the device. It is important that the device not behave as an amplifier at the IF, especially if the IF is low where the device gain is high.

- As a general rule in active Mixer design, all undesired frequencies should be short-circuited at both the input and the output to minimize distortion, noise, and for stability.
- The IF port impedance at IF frequency should be relative high for best conversion gain, but in this way decreasing the IM distortion performance.
- The IF port should provide enough rejection of the LO frequency in order to do not overload any further IF amplifiers down the chain.
- FET mixers, especially single-gate FET mixers with LO and RF applied to the gate, have more serious LO-to-RF isolation problem because the LO signal is amplified by the FET.



Single-device Mixers using one Diode

A dual-gate MOSFET will give much improvement for LO-to-RF isolation (approximately 20dB).



Dual-gate MOSFET Mixer

**2. Balanced Mixers** are grossly divided into two classes, called Singly-Balanced Mixers (SBM) and Doubly-Balanced Mixers (DBM).

- **Singly-Balanced mixers** use two devices, and are usually realized as two single-device mixers connected via a 180-degree or 90-degree hybrid.

Double balanced mixers usually consist of four un-tuned devices interconnected by multiple hybrids, transformers or baluns.

The advantages of balanced mixers over single-device mixers are:

- Rejection of spurious responses and intermodulation products.
- Better LO-to-RF, RF-to-IF and LO-to-IF isolation.
- Rejection of AM noise in the LO

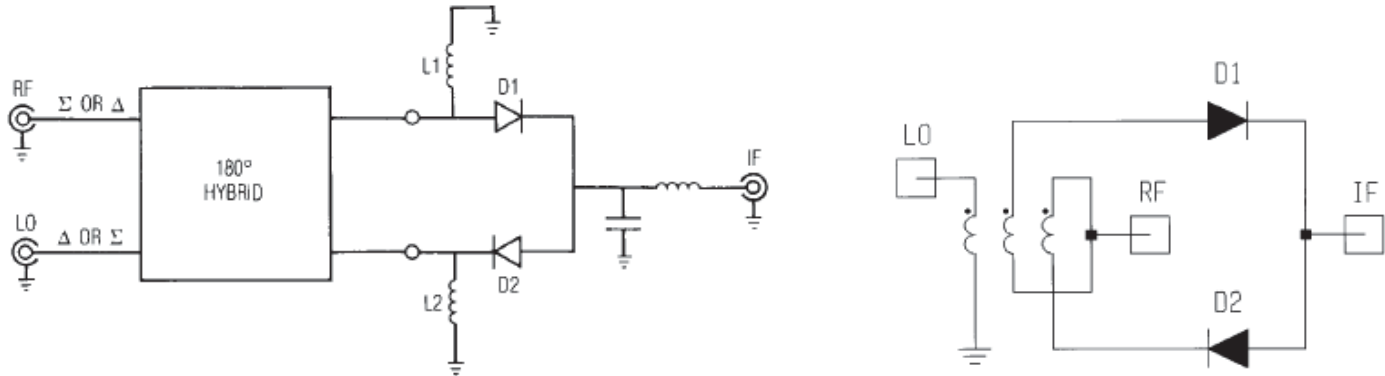
The disadvantage of balanced mixers is their greater LO power requirements.

Balanced mixers often used to separate the RF and LO ports when their frequency overlaps and filtering is impossible. In practice a perfect doubly balanced mixer give 10-30dB isolation without any filtering (depends by frequency and structure)

A Singly-Balanced Mixer consists of two single-diode mixing elements, which may be two diodes or two transistors.

In a singly-balanced diode Mixer it is essential that the DC path through the diodes to be continuous.

If the diodes are open-circuited at DC, the Mixer it will not work. Often, the hybrid provides that path.



In single-balanced using a quadrature hybrid the LO power reflected from the individual mixers does not return to the LO port, but instead exits the RF port; similarly, reflected RF power exits the LO port.

The LO-to-RF and RF-to-LO isolation is therefore equal to the input return loss of the individual mixers at the LO and RF frequencies, respectively; the port isolation of the quadrature hybrid mixer depends primarily on the input VSWRs of the two individual mixers, not on the isolation of the hybrid itself. Isolation of 10dB is typical.

If the RF port termination has a poor VSWR at the LO frequency, the circuit's balance can be upset and the LO pumping of the individual mixers becomes unequal.

The same, a poor LO port termination at the RF frequency can upset RF balance.

The even LO harmonics rejection depends by which port is used for LO input (Sigma or Delta).

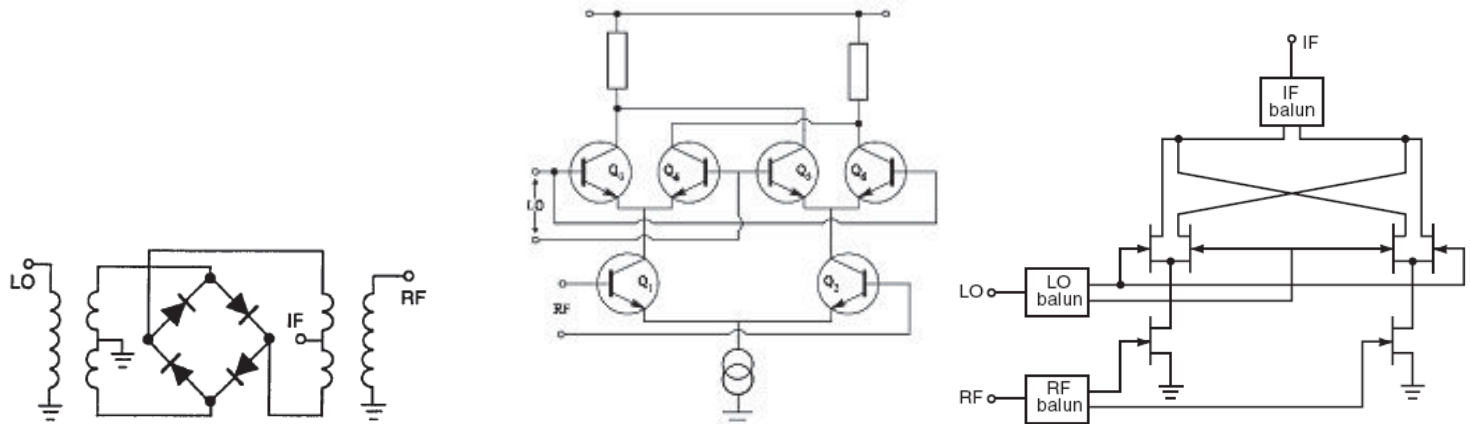
Whatever input is used for LO the mixer reject the even LO harmonics that mix with the even RF harmonics.

- To reduce the overall Noise Figure of the Mixer the two diodes shall be well matched. Diodes can be matched on RF characteristics (conversion loss, IF impedance and VSWR), but are more easily matched on DC parameters (junction capacitance, series resistance and forward voltage) that can be measured readily for all diode outlines, including beam lead types.

- **Doubly-Balanced Mixers** have higher conversion loss (or lower gain) than Singly-balanced Mixers and lower limit in maximum frequency, but has broader bandwidth.

The two most common types of doubly balanced mixers are the Ring Mixer and the Star Mixer.

The Ring Mixer is more suitable for low-frequency applications, in which transformers can be used, but it is also practical at high frequencies.



Double-balanced Mixers (Diodes, BJTs, FETs)

Ring Double-balanced Mixers can be described by treating its nonlinear components (diode or transistors) as switches, which are turned ON and OFF by the LO. This approach assumes that the conductance waveform of the diodes is a square wave, which is approximately true, as long as the LO level is great enough and its frequency is not too high.

- In Double-balanced diode Mixers because of the symmetry, even-order spurious responses are also rejected.
- Because the RF voltage is split between four diodes, the RF power in each diode is one-quarter that of a single-balanced mixer, so the 1-dB compression point and third-order intercept point are almost 6 dB higher.
- However, four times as much LO power is now required to pump the diodes to the same degree.
- The conversion loss is the same, because the RF power is split four ways and the IF power recombined four ways; therefore, the increase in intercept point provides a true increase in dynamic range due to the increase in output compared to a single diode.

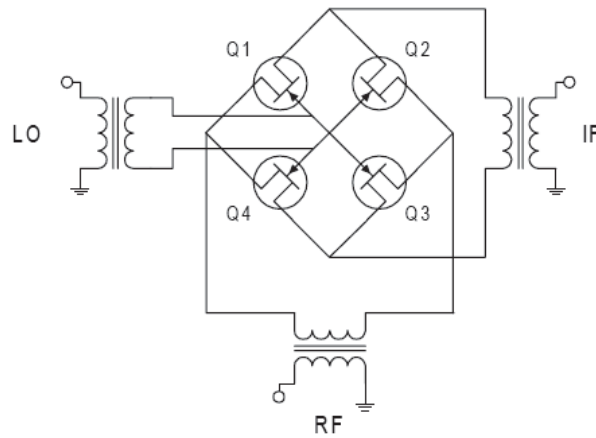
Beyond about +10dBm LO power, the increase in intercept point does not rise as fast as the LO power, because the ON diodes begin to limit the LO voltage across the OFF diodes, which are in parallel. To each diode, the RF current is indistinguishable from the LO current, and the total RF swing is therefore limited in the OFF condition. This can be improved by using two or more diodes in series in place of the single diodes shown.

- Many of the advantages of balanced structures, such as improved isolation, reduced spurious response, and improved intercept point, can be achieved for Active Mixers in the same way as for Diode Mixers.

Symmetric or anti-symmetric pairing of identical basic mixers provides an effective means to attenuate some unwanted frequency components in the spectra of the input and output signals.

The suppression is especially needed for the large local oscillator signal, which could saturate or seriously reduce the performances of an IF amplifier stage, but it is important for components with smaller amplitude also. Intermodulation within external systems of these unwanted components could mix with wanted signal and produce spurious signals that can interfere with other circuits of the system.

- Double-balanced FET Mixers can be designed for both passive and active use.
- Active FET Mixers based on Gilbert-cell architecture with biased semiconductor devices, can work with low LO levels and often provide conversion gain, but with decreased linearity compared to passive mixers.
- Passive FET Mixers, usually based on FET quads, provide good linearity but require high LO levels and exhibit high conversion loss.



The operation of this type of Mixer is similar to that of a conventional diode-based Double-balanced Mixer. The main difference is that the FET Mixer has six terminals, compared to the four terminals of the Double-balanced diode Mixer.

During the positive half-cycle of the LO signal to the FET mixer, two of the FETs are in conduction while the other two are turned off. As a result, the secondary winding of the RF balun is connected to the secondary winding of the IF balun through the FETs that are switched on. During the LO signal's negative half-cycle, the FETs which were on during the positive half-cycle are turned off and vice versa.

This results in a reversal of the polarity of the RF signal reaching the IF balun.

The frequency at which the FETs are turned on and off is determined by the frequency of the LO signal. This is mathematically equivalent to a multiplication of the RF and LO signals, resulting in the generation of sum and difference frequencies at the IF port. Compared to diode mixers, FET mixers have better P1dB compression point performances.

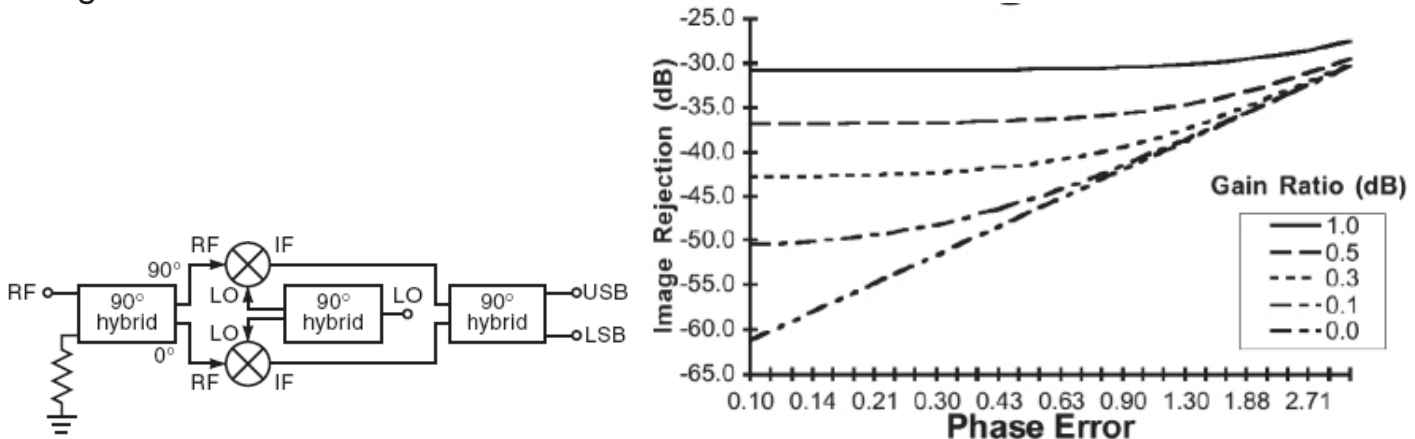
The linearity performance of a FET mixer, as evaluated in terms of the third-order intercept point, is affected by variations in the load impedance. Thus, the most predictable performance occurs with a purely resistance termination as the load. This type of stable termination can be achieved by terminating the mixer with a filter, but the filter appears purely resistive only within its 3-dB passband. As the filter's impedance rises beyond its passband, the mixer's intercept performance degrades.

- In an active FET mixer, the devices are biased for gain, but at the expense of intercept-point performance.
- Passive mixers require higher LO power levels, but provide better third-order-intercept performance.

### Image-Reject Mixers

The Image-rejection Mixer is realized as the interconnection of a pair of balanced Mixers. It is especially useful for applications where the image and RF bands overlap, or the image is too close to the RF to be rejected by a filter.

The LO ports of the balanced mixers are driven in phase, but the signals applied to the RF ports have 90 degrees phase difference. A 90-degrees IF hybrid is used to separate the RF and image bands.



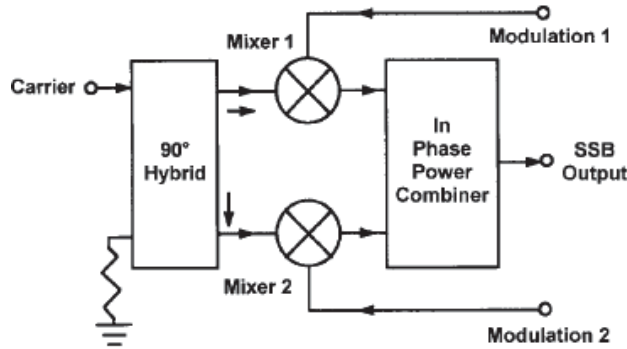
- Image Rejection improves with higher LO.
- Image rejection depends more strongly on phase mismatch.

### Single-Sideband (SSB) or In-Phase/Quadrature (I/Q) Mixers

SSB or I/Q modulators are useful in discriminating and removing the lower sideband (LSB) or upper sideband (USB) generated during frequency conversion, especially when sidebands are very close in frequency and attenuation of one of the sidebands cannot be achieved with filtering.

- With an I/Q modulator, one of the sidebands is attenuated along with its carrier.

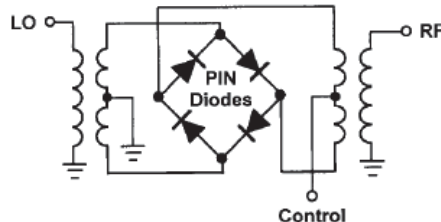
I/Q modulators basically consist of two Double-balanced Mixers. The Mixers are fed at the LO ports by a carrier phase-shifted with 90 degrees (0 degrees to one mixer and 90 degrees to the other mixer). Modulation signals are fed externally in phase quadrature to the two mixers IF ports. The modulated mixers outputs are combined through a two-way in-phase combiner.



The circuit forms a phase cancellation network to one sidebands and a phase addition network to the other sideband. The carrier is also attenuated and is directly dependent on the LO-to-RF isolation of the two mixers.

Phase and amplitude imbalance errors affect the side band suppression.

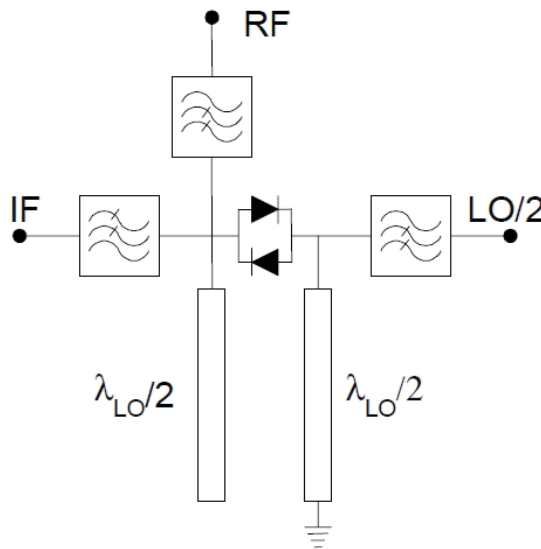
- A diode Double-balanced Mixer can be used as a **DC-controlled attenuator** if PIN diodes are used instead of Shottky devices in its ring.



### Sub-harmonic Mixers

A Sub-harmonic Mixer has an LO input at frequency = LO/n. They are useful at higher frequencies when it can be difficult to produce a suitable LO signal (low phase noise, tuning range and output power all become more difficult to achieve with increasing frequency, whilst cost increases).

- Sub-harmonic mixers use anti-parallel diode pairs.
- These mixers produce most of their power at “odd” products of the input signals.
- Even products are rejected due to the I-V characteristics of the diodes.
- Attenuation of even harmonics is determined by diodes “balance”.
- Diode “match” is critical.



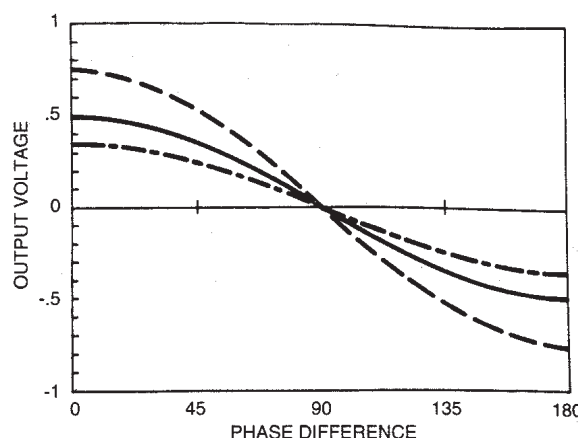
- The short circuit  $\lambda_{LO}/2$  stub at the LO port is a quarter of a wavelength long at the input frequency of LO/2 and so is open circuit. However, at RF frequency this stub is approximately a half wavelength long, so providing a short circuit to the RF signal.
- At the RF input the open circuit  $\lambda_{LO}/2$  stub presents a good open circuit to the RF but is a quarter wavelength long at the frequency LO/2 and so is short circuit.
- The IF is normally far enough away from the RF frequency to allow easy realization of an IF filter presenting an open circuit output to the RF port.

### Mixers as Phase Detectors

In a Double-balanced Mixer the output at the IF port contains the sum and difference of the frequencies of the signals input to the LO and RF ports.

- If the RF and LO signals have identical frequencies, then their difference is zero Hz, or DC, which is the desired output for a phase detector. Their sum, which is twice the input frequency, can be selectively filtered out if it is not already beyond the frequency response of the IF port.

The voltage at the IF port will be DC and will vary as the cosine of the phase difference between the LO and RF signals. Null readings for IF voltage are thus obtained whenever the phase difference between the LO and RF signals is equal to  $n\pi/2$  with  $n = \pm 1, \pm 3, \dots$ , while maximum and minimum readings are obtained for phase difference equal with  $n\pi$  where  $n = 0, \pm 1, \pm 2, \dots$



Practical mixers that are used as phase detectors they often display some characteristics which differ from those of idealized mixers.

The characteristics of most interest are DC offset and/or mixer-induced phase shift of the signals due to circuit imbalance. Parameters that affects these characteristics are: frequency, LO and RF drive levels, load resistance, and temperature.

- The origin of DC offset voltages is a combination of diode imbalance and transformer asymmetry and can come from either or both input signals. In addition to isolation and LO drive level, DC offset is also affected by the load resistance and temperature.
- Even after the effects of DC offset have been minimized, it is still possible that a null reading will be obtained at some relative phase other than PI/2 (90 degrees). This is because the mixer itself may change the relative phase of the two input signals due to the fact that the electrical length from the LO-to-IF port is not identical to that from the RF-to-IF port.
- Frequency affects the DC offset by virtue of its effect upon isolation.
- Higher the isolation between ports, lower the DC offset.
- Also, as conversion loss decreases, maximum output DC voltage increases.

#### References:

1. *RF Circuit Design for Wireless Applications* – U. Rohde, D. Newkirk
2. *Microawave Mixers* - Stephen Maas
3. *Nonlinear Microwave and RF Circuits* - Stephen Maas
4. *RF Design Guide* – P. Vizmuller
5. *RF Circuits Design - Theory and Applications* - Ludwig, Bretschko
6. *Practical Rf Circuit Design for Modern Wireless Systems* – R. Gilmore, L. Besser
7. *RF Circuit Design* - W. Davis, Krishna Agarval
8. *Microwave Journal Magazine* – 1997 - 2007



## Mixers

A Mixer is an analogue device that can multiply two signals together and also provides the difference of the two signals. They are composed of a non-linear device (a diode or a transistor) and passive couplers devices to inject the input mixing signals into the non-linear device that will perform the mixing. Current technology state-of-the-art in mixer realization shows that the bandwidth of mixers are limited by the passive devices and not by the diode or transistors, which have bandwidths exceeding the requirements.

Bandwidth of the mixer will be limited by the bandwidth of the couplers.

The multiplication process begins by inputting two signals:

$$a = A \sin(\omega_1 t + \phi_1) \text{ and signal } b = B \sin(\omega_2 t + \phi_2)$$

The resulting multiplied signal will be:

$$a.b = AB \sin(\omega_1 t + \phi_1) \sin(\omega_2 t + \phi_2)$$

This can be multiplied out thus:

$$\text{Using this trig identity } \dots \sin A \sin B = -\frac{1}{2} [\cos(A + B) - \cos(A - B)]$$

$$\text{Where } A = (\omega_1 t + \phi_1) \text{ and } B = (\omega_2 t + \phi_2)$$

$$= -\frac{AB}{2} [\cos((\omega_1 t + \phi_1) + (\omega_2 t + \phi_2)) - \cos((\omega_1 t + \phi_1) - (\omega_2 t + \phi_2))]$$

$$= -\frac{AB}{2} [\cos((\omega_1 + \omega_2)t + (\phi_1 + \phi_2)) - \cos((\omega_1 - \phi_1)t - (\phi_1 - \phi_2))]$$

Sum frequency  
(removed by filtering)

Difference frequency ie  
I.F

## Mixer Definitions

**(1) Conversion Gain:** This is the ratio (in dB) between the IF signal (usually the difference frequency between the RF and LO signals) and the RF signal.

**(2) Noise Figure:** Noise figure is defined as the ratio of SNR at the IF port to the SNR of the RF port.

**(i) Single sideband (SSB):** This assumes the only noise from the signal  $\omega_1$  and not the image frequency  $\omega_1 - 1$ , this would be the case if a band-pass filter was added in front of the mixer eg.

RF = 1694 MHz, LO = 1557MHz to give an IF of 137MHz.

Also an image IF will add to 137MHz from an RF of 1420MHz ie 1557MHz-1420MHz = 137MHz as shown in

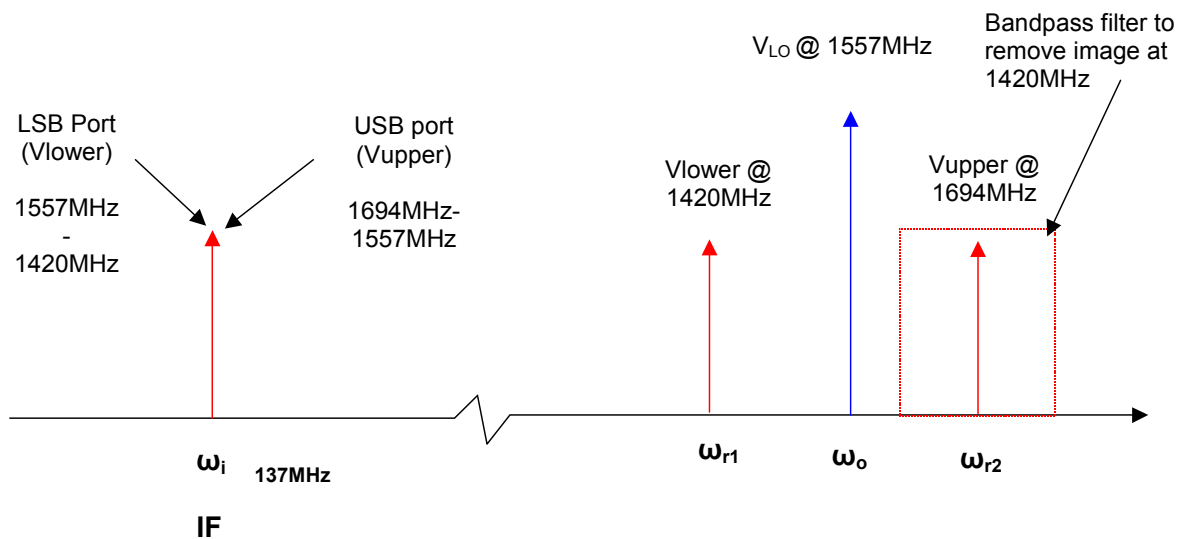
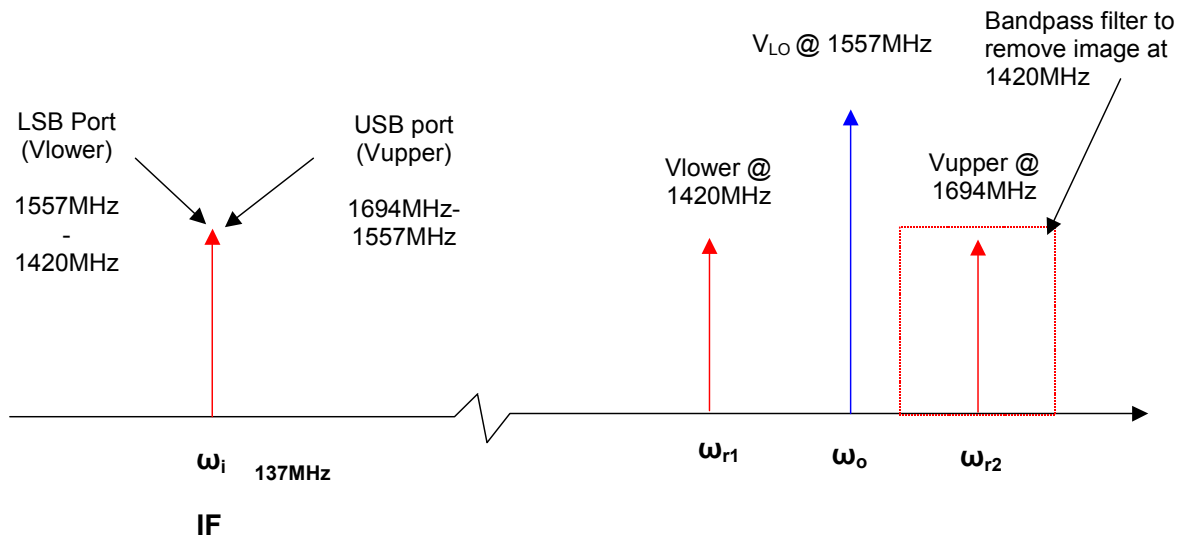


Figure 1.





**Figure 1 Single-sideband conversion of image noise to IF of 137MHz. The image response at 1420MHz will also produce a signal at the IF and (in the absence of a carrier) will down convert noise. This is overcome by adding a band-pass filter at 1694MHz.**

In this situation the addition of a band pass filter at 1694MHz will eliminate the image response.



**(ii) Double sideband (DSB):** In DSB both sidebands are available thus it has twice as much power available at the IF port compared to the SSB signal. As a result, its conversion loss is 3dB less than that of an SSB signal, as shown:

$$P_{(IF)_{DSB}} = 2 P_{(IF)_{SSB}} \text{ and conversion loss is given by}$$

$$(LC)_{DSB} = (LC)_{SSB} - 3(dB) \text{ or in terms of loss ratios } (LC)_{DSB} = \frac{(LC)_{SSB}}{2}$$

### DSB to SSB Noise Figure

$$Fm = 1 + (LC - 1) \frac{T}{T_0} \quad \text{Where } T = \text{temperature of mixer, } T_0 = \text{room temperature (273°K)}$$

$$\text{For DSB, } (LC)_{DSB} = \frac{(LC)_{SSB}}{2} \quad \text{Therefore, } Fm_{(DSB)} = 1 + \left( \frac{(LC)_{SSB}}{2} - 1 \right) \frac{T}{T_0}$$

At room temperature, ie  $T = T_0$

$$Fm_{(DSB)} = \frac{(LC)_{SSB}}{2} \text{ in other words } Fm_{(DSB)} \text{ is half or 3dB less than } Fm_{(SSB)}$$

$$Fm_{(DSB)} = Fm_{(SSB)} - 3(dB)$$

### Isolation

These parameters define how much signal leakage will occur between pairs of ports. ie RF to LO, LO to IF and RF to IF. So if for example RF to IF isolation was specified at 35dB this means that the RF at the IF port will be 35dB lower than the RF applied to RF port.

Most systems will specify some form of spurious specification on the output so RF and LO signals may cause problems leaking through the mixer to the IF port and may require additional filtering at IF to remove.

## Linearity

### (i) 1dB Compression point

Like other non-resistive networks, a mixer is amplitude-nonlinear above a certain input level resulting in a gain compression characteristic as shown in Figure 2.

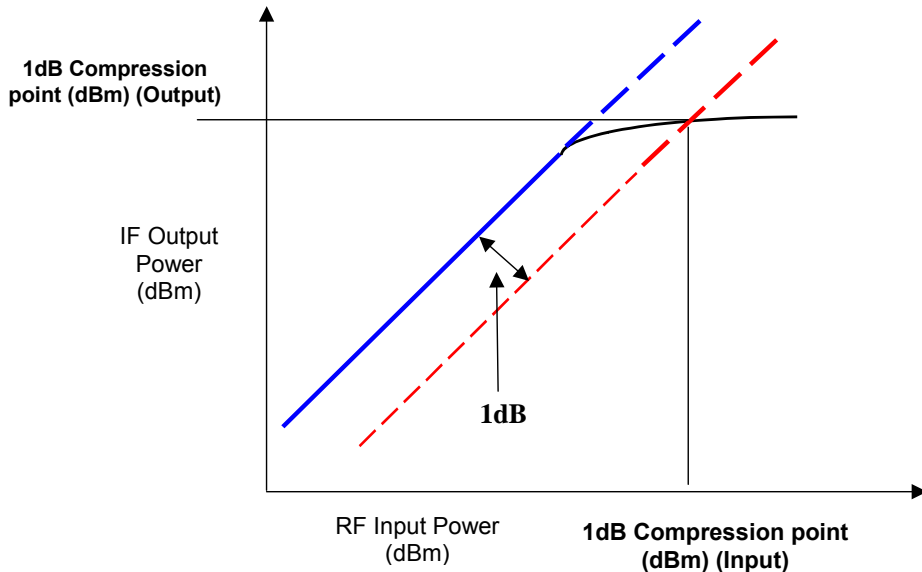


**Figure 2 Typical gain compression characteristic for a non-linear Amplifier/Mixer, showing the measurement of the 1dB compression point.**

Above this point the If fails to track the RF input power level – normally a 1dB rise in RF power will result in a 1dB rise in the IF power level. The 1dB compression point is measured by plotting incident RF power against IF power as shown in the figure above.

Most mixers have the 1dB compression point specified at the input ie the single-tone input signal level at which the output of the mixer has fallen 1dB below the expected output level.

For typical double balanced mixers this figure is ~ 6dB below the LO power level. (So performance can be improved by overdriving the LO port).

The 1dB compression point gives rise to the **dynamic range** of the mixer, which is the difference between the 1dB compression point and the minimum discernable signal (MDS – this is dependant on the noise floor of the device).

### (ii) Intermodulation (IM3) performance

This parameter is the same as specified for amplifiers and measured in a similar way. It is measured by applying two closely spaced input tones at frequencies  $F_1$  and  $F_2$ . Third order products from the mixing of these tones with the LO (at frequency  $F_{LO}$ ) occur at frequencies given by:  $(2F_1 \pm F_2) \pm F_{LO}$  and  $(2F_2 \pm F_1) \pm F_{LO}$ . In the case of the mixer, the third order products of most interest are  $(2F_1 - F_2) - F_{LO}$  and  $(2F_2 - F_1) - F_{LO}$  as they fall in, or close to the IF band.

The IM3 performance is often summarised by giving the 3<sup>rd</sup> Order Intercept point (IM3 Intercept) as shown in the compression characteristic of Figure 3, where the IM3, IM5 plots intersect with the extrapolated gain plot (blue dotted line). As a rule of thumb the IM3 intercept point is approximately 10dB above the 1dB compression point.

This figure of merit gives an indication of the mixer's signal handling capability. In particular it provides an indication of the levels of third order products a mixer is likely to produce under multi-tone excitation.

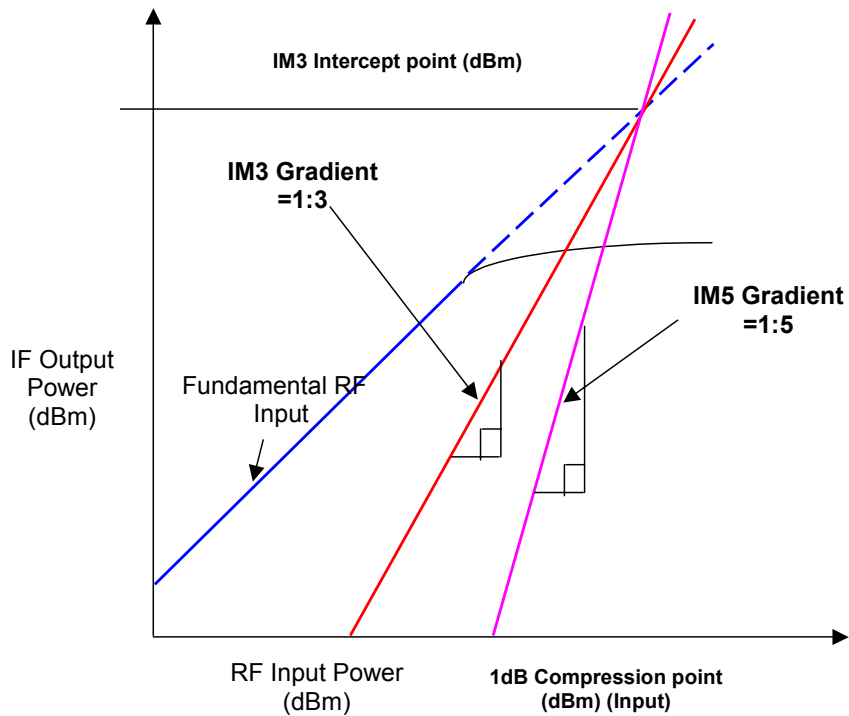


**Figure 3 IM3 gain compression characteristic, as a rule of thumb the IM3 intercept point is approximately 10dB above the 1dB compression point.**

The IM3 and IM5 graphs will intercept the fundamental graph at the intercept point. (Note the IM2 intercept point will be different and usually a lot higher).



Again, for mixers the measurement is referred to the input ( $IP_{3,in}$ ) and is given by:-

$$IP_{n,in} = \frac{IMR}{(n-1)} + \text{Input power(dBm)}$$

Where IMR = Intermodulation ratio (The difference in dB between the desired output and spurious signal) and n = the IM order.

Typically, for double balanced mixers  $IM_{3,in}$  is  $\sim 14$ dB greater than the single tone 1dB compression point and  $\sim 8$ dB greater than the LO power.

### Mixer Types

Mixers can be first divided into active or passive. Passive mixers primarily use Schottky diodes, or are FET resistive mixers, that use the resistive channel of a MESFET to provide low-distortion mixing with the same conversion loss as a diode mixer. Active mixers use FET or bipolar devices.

Although single-device mixers are used occasionally, most practical mixers are balanced, and require baluns or hybrids, that determine the bandwidth and overall performance of the mixer.

Diode mixers have an important advantage over FETs and bipolar devices: a Schottky-barrier diode is inherently a resistive device, and as such has very wide bandwidth. The bandwidths of diode mixers are limited primarily by the bandwidths of the baluns, not the diodes. FETs, in contrast, have a high-Q gate-input impedance, causing difficulties in achieving flat, wide bandwidth.

Diode mixers usually have 5-8 dB conversion loss, while active mixers usually can achieve at least a few dB of gain. Although properly designed active mixers can achieve somewhat lower noise figures than diode mixers, most systems can tolerate a relatively noisy mixer, so the diode mixer's loss and noise are rarely a significant disadvantage. Broadband diode mixers usually do not require more local-oscillator (LO) power than active mixers, but narrowband active mixers may have an LO-power advantage. Finally, balanced active mixers always require an IF hybrid or balun; diode mixers generally do not. When the IF frequency is low, the resulting large size of the IF balun may be troublesome, especially in monolithic circuits. Finally, even balanced active mixers require matching and filtering circuits, while balanced diode mixers largely do not.

Active mixers have a few important advantages over diode mixers besides their superior gain and noise figure. High-quality diodes are often difficult to produce in FET monolithic circuit technologies, so active FET mixers often are easier to integrate. Diodes in such technologies usually consist of a FET gate-to-channel junction, which usually is a very poor diode. Dual-gate FET mixers offer inherent LO-RF isolation, even in single-device circuits, although noise figure and gain usually are slightly worse than in single-gate FET mixers.



### Singly Balanced Diode Mixers:

Advantages:

- Provide either LO or RF Rejection (20-30 dB) at the IF output
- Rejection of certain mixer spurious products depending on the exact configuration
- Suppression of Amplitude Modulated (AM) LO noise

Disadvantages:

- Require a higher LO drive level

### Doubly Balanced Diode Mixers:

Advantages:

- Both LO and RF are balanced, providing both LO and RF Rejection at the IF output
- All ports of the mixer are inherently isolated from each other
- Increased linearity compared to singly balanced
- Improved suppression of spurious products (all even order products of the LO and/or the RF are suppressed)
- Reasonable conversion loss on signal RF (about 7dB)
- Consumes no power except for the losses incurred in conversion
- Broadband in nature and therefore suited to multi-band designs
- High intercept points

Disadvantages:

- Require a higher LO drive level
- Require two baluns
- Relative high noise figure, about the same as the conversion loss
- Ports highly sensitive to reactive terminations.
- High quality, high speed diodes which will take the necessary saturating current and large reverse voltages across the non-conducting diodes are an absolute must where performance counts
- Diodes need to be well "matched"
- The transmission line transformers require great care in design and construction. The actual construction will determine the bandwidth.

### Double Doubly Balanced Diode Mixers:

Advantages:

- Increased linearity

Disadvantages:

- Increased complexity (3 baluns and 8 diodes are required)
- Higher level of LO drive must be provided

Note: for increased linearity an alternative approach is to use a FET resistive mixer. This can yield even higher linearity than the double doubly balanced topology whilst having a simpler circuit configuration.

### Active FET Mixers:

Active FET Mixers are transconductance mixers using the LO signal to vary the transconductance of the transistor.

Advantages:

- Provide conversion gain
- Lower noise figure than passive mixers

### Single gate FET Mixers:

Advantages:

- Low component count.
- Good for X-Band designs

Disadvantage:

- some form of diplexing is required to separate the LO and RF inputs which are incident on the same port.

### Dual gate FET Mixers:

Advantages:

- No LO and RF diplexing is required,
- LO and RF signals are inherently isolated

Disadvantage:

- Shortage of suitable devices at higher frequencies.

### Image Reject Mixers:

Image reject mixers comprise two balanced mixers, of any topology, driven in quadrature by the LO signal as shown in . The RF drive to each mixer is in-phase (split by a in-phase hybrid eg Wilkinson power Divider) and the IF output is combined in quadrature.

Advantages:

- Possible to achieve 20 dB of image frequency rejection

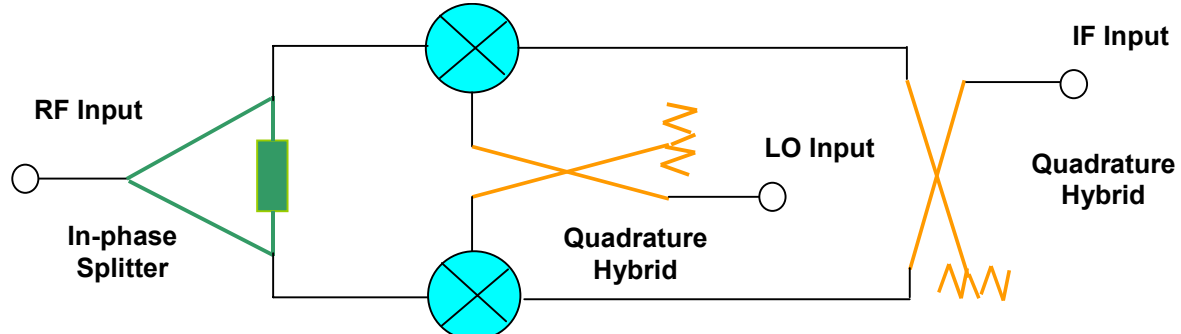


**Figure 4 Schematic diagram of an image reject mixer. Here the mixers are fed with the LO drive in quadrature, and the RF fed in phase (Split using a Wilkinson power splitter for example). The two IF's from the mixers are combined in quadrature.**



The table shown below in Table 1 gives a summary of key features/advantages for each active and passive mixer type.

	LO rejection	RF rejection	Rejection of spurious	Suppression of AM noise	LO power level	Linearity	Conversion loss on signal RF	Broadband	IP point	NF	Complexity	Diplexing	Image freq rejection
Single diode					Low	Poor	Low	✓					
Singly balanced diode	✓*	✓*	certain	✓	high								
Doubly balanced diode	✓	✓	even	✓	High	Better	7dB	✓	High	Rel high	4diode 2balun		
Double doubly balanced diode	✓	✓	even	✓	Very high	Increased					8diode 3balun		
Active FET							Gain			Lower than passive			
Single gate FET											required		
Dual gate FET											Not req.		
Image reject											2 mixers, 3 hybrids		20dB

\* LO or RF rejection to choose

**Table 1 Comparison Table of mixer types and their characteristics**



## Design Seminar



Agilent EEs of  
Customer Education  
and Applications

### Fundamentals of Mixer Design



**Agilent Technologies**  
Innovating the HP Way

#### Abstract

The mixer is used in nearly all RF/Microwave systems for frequency translation. This seminar explains how mixers provide this function and why they often generate so many spurious outputs as well. Issues such as single vs. double balanced, active vs. passive, nonlinear vs. switching mode mixers will be discussed. Mixer performance measures such as image rejection, conversion gain, gain compression, intercept and intermodulation, noise figure, dynamic range, and isolation will be explained.



## About the Author



**Steve Long**

- University of California, Santa Barbara
- Professor, Electrical and Computer Engineering
- Consultant to Industry



Page 2

### BIOGRAPHICAL SKETCH

Stephen Long received his BS degree in Engineering Physics from UC Berkeley and MS and PhD in Electrical Engineering from Cornell University. He has been a professor of electrical and computer engineering at UC Santa Barbara since 1981. The central theme of his current research projects is rather practical: use unconventional digital and analog circuits, high performance devices and fabrication technologies to address significant problems in high speed electronics such as low power IC interconnections, very high speed digital ICs, and microwave analog integrated circuits for RF communications. He teaches classes on communication electronics and high speed digital IC design.

Prior to joining UCSB, from 1974 to 1977 he was a Senior Engineer at Varian Associates, Palo Alto, CA. From 1978 to 1981 he was employed by Rockwell International Science Center, Thousand Oaks, CA as a member of the technical staff.

Dr. Long received the IEEE Microwave Applications Award in 1978 for development of InP millimeter wave devices. In 1988 he was a research visitor at GEC Hirst Research Centre, U.K. In 1994 he was a Fulbright research visitor at the Signal Processing Laboratory, Tampere University of Technology, Finland and a visiting professor at the Electromagnetics Institute, Technical University of Denmark. He is a senior member of the IEEE and a member of the American Scientific Affiliation.



Basic engineering problem:

*Choosing the right mixer for the task...*



Learning Objectives:

- Understand operating principles of the mixer
- What makes a good mixer?
- Choices: Nonlinear/switching mode; single/double balance; active/passive
- Specify performance: Gain, NF,  $P_{1\text{dB}}$ , TOI, SFDR, isolation, image rejection
- Review some mixer design examples

[Always see the NOTES pages for Exercises throughout...](#)



Page 3

There are many different mixer circuit topologies and implementations that are suitable for use in receiver and transmitter systems. How do you select the best one for a particular application? Why does the choice depend on the application and technology available?



## Why study mixers?

- Receivers
  - up or down conversion
  - demodulation of SC SSB or SC DSB
  - input must support large dynamic range
  - AGC
- Transmitters
  - up conversion
  - modulation: amplitude and phase
  - input has optimum signal level for high performance



Page 4

Mixers have a wide variety of applications in communication systems.

The superheterodyne receiver architecture often has several frequency translation stages (IF frequencies) to optimize image rejection, selectivity, and dynamic range. Direct conversion receiver architectures such as used in pagers use mixers at the input to both downconvert and demodulate the digital information. Mixers are thus widely used in the analog/RF front end of receivers. In these applications, often the mixer must be designed to handle a very wide dynamic range of signal powers at the input.

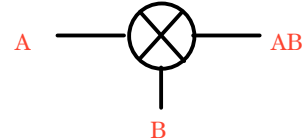
The mixer can be used for demodulation, although the trend is to digitize following a low IF frequency and implement the demodulation function digitally. They can also be used as analog multipliers to provide gain control. In this application, one input is a DC or slowly varying RSSI signal which when multiplied by the RF/IF signal will control the degree of gain or attenuation.

In transmitter applications, the mixer is often used for upconversion or modulation. In this application, the input signal level can be selected to optimize the overall signal-to-noise ratio at the output.



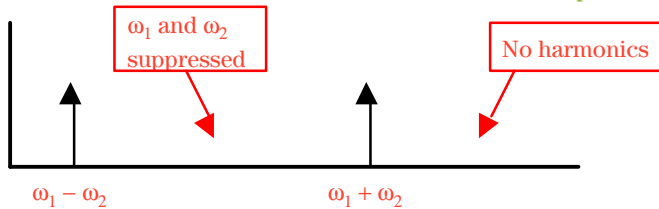
## What is a mixer?

- Frequency translation device
- Ideal mixer:
  - Doesn't "mix"; it multiplies



$$(A \sin \omega_1 t)(B \sin \omega_2 t) = \frac{AB}{2} [\cos(\omega_1 - \omega_2)t - \cos(\omega_1 + \omega_2)t]$$

Downconvert      Upconvert



Page 5

A mixer doesn't really "mix" or sum signals; it multiplies them.

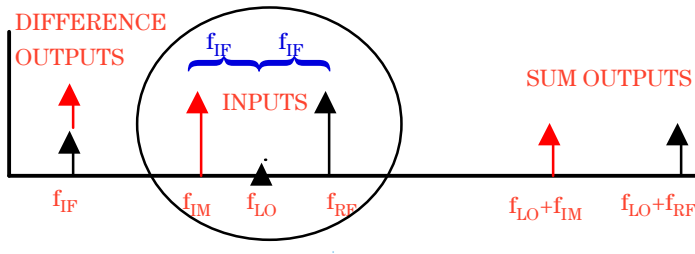
$$(A \sin \omega_1 t)(B \sin \omega_2 t) = \frac{AB}{2} [\cos(\omega_1 - \omega_2)t - \cos(\omega_1 + \omega_2)t]$$

Note that both sum and difference frequencies are obtained by the multiplication of the two input sinusoidal signals. A mixer can be used to either *downconvert* or *upconvert* the RF input signal, A. The designer must provide a way to remove the undesired output, usually by filtering.



## Images

- Two inputs (RF & **Image**) will mix to the same output (IF) frequency.
- The image frequency must be removed by filtering
- $f_{IF}$  and  $f_{LO}$  must be carefully selected
- Image rejection ratio:  $\text{dB}(P_{IF \text{ desired}}/P_{IF \text{ image}})$



 Agilent Technologies

Page 6

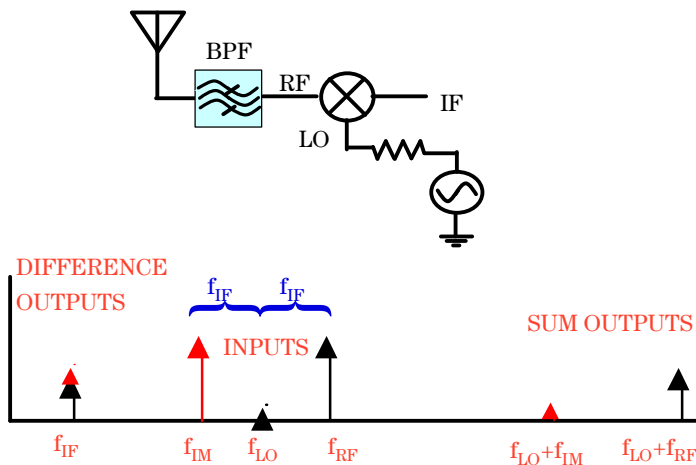
Even in an ideal multiplier, there are two RF input frequencies ( $F_{RF}$  and  $F_{IM}$ ) whose second-order product has the same difference IF frequency.

$$F_{RF} - F_{LO} = F_{LO} - F_{IM} = F_{IF}$$

The two results are equally valid. One is generally referred to as the “*image*” and is undesired. In the example above, the lower input frequency is designated the image.



## Image rejection preselector



Agilent Technologies

Page 7

A *bandpass preselection filter* is often used ahead of the mixer to suppress the image signal. The IF and LO frequencies must be carefully selected to avoid image frequencies that are too close to the desired RF frequency to be effectively filtered.

In a receiver front end, out-of-band inputs at the image frequency could cause interference when mixed to the same IF frequency. Also, the noise present at the image would also be translated to the IF band, degrading signal-to-noise ratio.

Alternatively, an *image-rejection mixer* could be designed which suppresses one of the input sidebands by phase and amplitude cancellation. This approach requires two mixers and some phase-shifting networks.

So far, the spectrum exhibited by the ideal multiplier is free of harmonics and other spurious outputs (*spurs*). The RF and LO inputs do not show up in the output. While accurate analog multiplier circuits can be designed, they do not provide high dynamic range mixers since noise and bandwidth often are sacrificed for accuracy.



## Mixer operating mechanisms

- Nonlinear transfer function
  - use device nonlinearities creatively!
  - useful at mm-wave frequencies
- Switching or sampling
  - a time-varying process
  - preferred; fewer spurs



Page 8

High performance RF mixers use nonlinear characteristics to generate the multiplication. Thus, they also generate lots of undesired output frequencies.

Three techniques have proven to be effective in the implementation of mixers with high dynamic range:

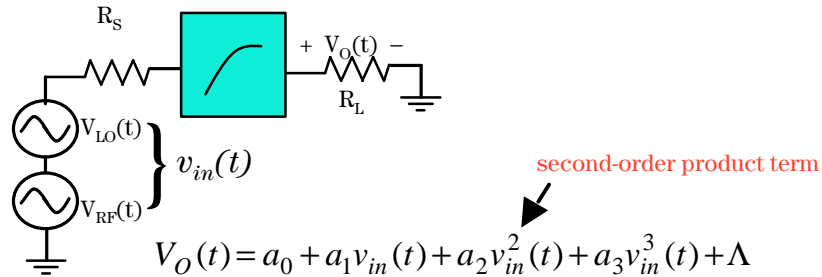
1. Use a device that has a known and controlled nonlinearity.
2. Switch the RF signal path on and off at the LO frequency.
3. Sample the RF signal with a sample-hold function at the LO frequency.

The nonlinear mixer can be applicable at any frequency where the device presents a known nonlinearity. It is the only approach available at the upper mm-wave frequencies. When frequencies are low enough that good switches can be built, the switching mixer mode is preferred because it generates fewer spurs. In some cases, sampling has been substituted for switching.



## Nonlinear mixer operation

Any diode or transistor will exhibit nonlinearity in its transfer characteristic at sufficiently high signal levels.



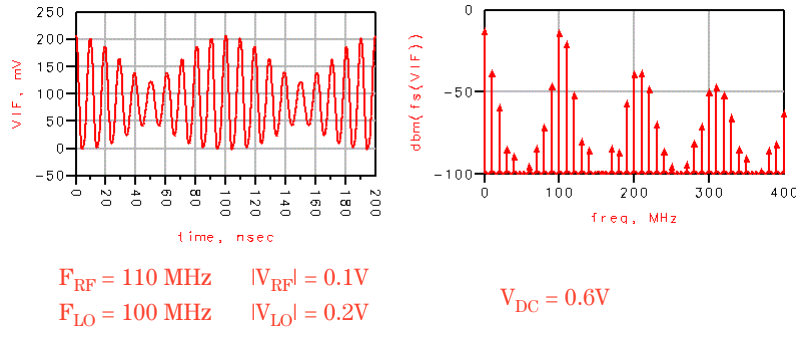
We see that our output may contain a DC term, RF and LO feedthrough, and terms at all harmonics of the RF and LO frequencies. Only the second-order product term produces the desired output.

In addition, when  $v_{RF}$  consists of multiple carriers, the power series also will produce cross-products that make the desired output products dependent on the amplitude of other inputs.

Spurious output signal strengths can be decreased when devices that are primarily square-law, such as FETs with longer gate lengths, are used in place of diodes or bipolar transistors.



## Unbalanced diode mixer output

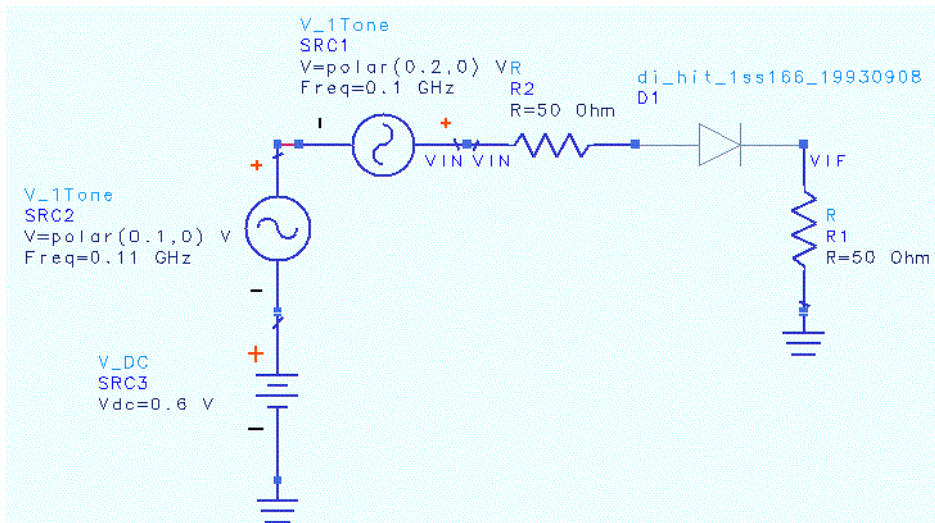


 Agilent Technologies

Page 10

We can see that there are a lot of spurious outputs generated. Ideally, we would like to see outputs only at 10 MHz and 210 MHz. So, we prefer the switching type mixer when the RF and LO frequencies are low enough that we can make decent switches. This takes us up through much of the mm-wave spectrum.

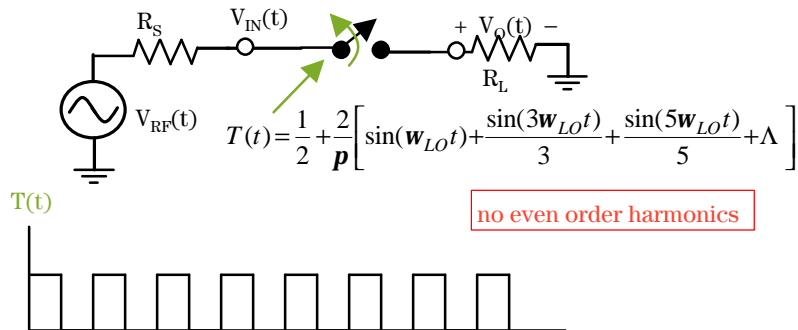
[See ADS example file diode1.dsn]





## Switching or sampling mixers

- Let  $V_{IN}(t) = V_R \cos(\omega_{RF}t)$
- Multiply by the LO switching function  $T(t)$



Agilent Technologies

Page 11

This simple switch is operated by the LO. If the LO is a square wave with 50% duty cycle, it is easily represented by its Fourier Series. The symmetry causes the even-order harmonics to drop out of the LO spectrum. When multiplied by a single frequency cosine at  $\omega_{RF}$  the desired sum and difference outputs will be obtained as shown in the next slide. Note that everything is single-ended; there is no balancing on this design.

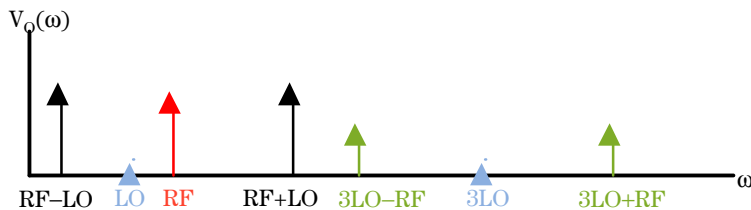
There will be harmonics of the LO present at  $3\omega_{LO}$ ,  $5\omega_{LO}$ , etc. that will also mix to produce outputs called “spurs” (an abbreviation for spurious signals). These harmonics also convert broadband noise that is generated internal to the mixer (or that is allowed into the mixer input in the absence of a preselection filter) into the IF output band.



## Mixer output

$$V_o(t) = \frac{V_R}{2} \cos(\omega_{RF}t) + \frac{2V_R}{P} \left[ \cos(\omega_{RF}t) \sin(\omega_{LO}t) + \underbrace{\cos(\omega_{RF}t) \sin(3\omega_{LO}t)}_{3} + \Lambda \right]$$

RF feedthrough      2nd-order product      4th-order spurs



Page 12

The product of  $V_{RF}(t)T(t)$  produces the desired output frequencies at  $\omega_{RF} - \omega_{LO}$  and  $\omega_{RF} + \omega_{LO}$  from the second order product.

Odd harmonics of the LO frequency are also present since we have a square wave LO switching signal. These produce spurious 4th, 6th, ... order products with outputs at

$$n\omega_{LO} - \omega_{RF} \text{ and } n\omega_{LO} + \omega_{RF} \quad \text{where } n \text{ is odd.}$$

We also get *RF feedthrough* directly to the output.

None of the LO signal should appear in the output if the mixer behaves according to this equation. But, if there is a DC offset on the RF input, there will be a LO frequency component in the output as well. This requirement is not unusual, since many mixer implementations require some bias current which leads to a DC offset on the input.

**EXERCISE 1:** Use the diode in the nonlinear diode mixer simulation as a switch. Put a square wave LO in series with the RF generator and simulate the output spectrum using transient analysis. (solution in ADS file ex1)

[See ADS example files **swmix2.dsn** and **diode1.dsn**]



## Isolation between ports

- The mixer is not perfectly unilateral -  
leakage between:
  - LO to IF
  - LO to RF
  - RF to IF
- Determine the magnitude of these leakage components at the IF and RF ports using harmonic balance.
- Use the mix function to select frequencies.



Page 13

Isolation can be quite important for certain mixer applications. For example, LO to RF leakage can be quite serious in direct conversion receiver architectures because it will remix with the RF and produce a DC offset. Large LO to IF leakage can degrade the performance of a mixer postamp if it is located prior to IF filtering.

**EXERCISE 2:** Modify the data display swmix2.dds to measure the LO to IF,

LO to RF, and RF to IF isolation. Express these isolations as power ratios.

(solution in ADS display file ex2.dds)



## Conversion gain or loss

- Generally expressed as a voltage gain or as a transducer power gain

$$A_V = \frac{V_{IF}}{V_{IN}}$$

$$\text{ConvGain} = \frac{\text{Output power at } F_{IF}}{\text{RF available input power}} = \left( \frac{\frac{v_{IF}^2}{2R_L}}{\frac{v_{RF}^2}{8R_S}} \right)$$



Page 14

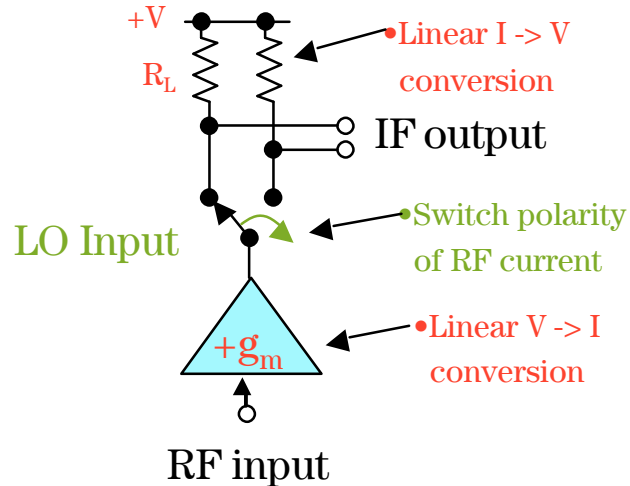
*Conversion gain* is usually defined as the ratio of the IF output power to the available RF source power. So we can be compatible with ADS output format, in these equations, the voltages are peak amplitudes, not RMS. If the source and load impedances are different, the power gain must account for this as shown. Voltage gains are also useful, especially in RFIC implementations of mixers.

*Active or passive implementations* can be used for the mixer. Each has its advantages and disadvantages. The passive implementations using diodes as nonlinear elements or switches or FETs as passive switches always exhibit conversion loss rather than gain. This can impact the overall system noise performance, so if noise is critical, an LNA is usually added before the mixer.

We see that the simple switching mixer has low conversion gain because the voltage gain  $A_V$  is only  $1/\pi$ . Also, the RF feedthrough problem and in most instances, an LO feedthrough problem exist. All of these deficiencies can be improved by the use of balanced topologies which provide some cancellation of RF and LO signals as well as increasing conversion gain.



## Ideal Single-balanced mixer



 Agilent Technologies

Page 15

The RF feedthrough can be eliminated by using a differential IF output and a polarity reversing LO switch.

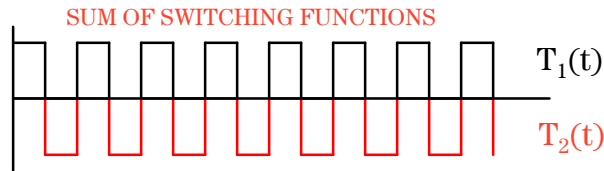
The polarity reversing LO switching function is shown in the next slide.



## LO Switching Function T(t)

$$T_1(t) = \frac{1}{2} + \frac{2}{p} \left[ \sin(\omega_{LO}t) + \frac{1}{3} \sin(3\omega_{LO}t) + \dots \right]$$

$$T_2(t) = -\frac{1}{2} + \frac{2}{p} \left[ \sin(\omega_{LO}t) + \frac{1}{3} \sin(3\omega_{LO}t) + \dots \right]$$



$$T(t) = T_1(t) + T_2(t)$$



Page 16

When added together, the DC terms (1/2 & -1/2) cancel. The DC term was responsible for the RF feedthrough in the unbalanced mixer since the  $\cos(\omega_{RF}t)$  term was multiplied only by  $T_1(t)$ .

$$V_{IF}(t) = AV_R \cos(\omega_{RF}t) \frac{4}{p} \left[ \sin(\omega_{LO}t) + \frac{1}{3} \sin(3\omega_{LO}t) + \frac{1}{5} \sin(5\omega_{LO}t) + \dots \right]$$

Second-order term:

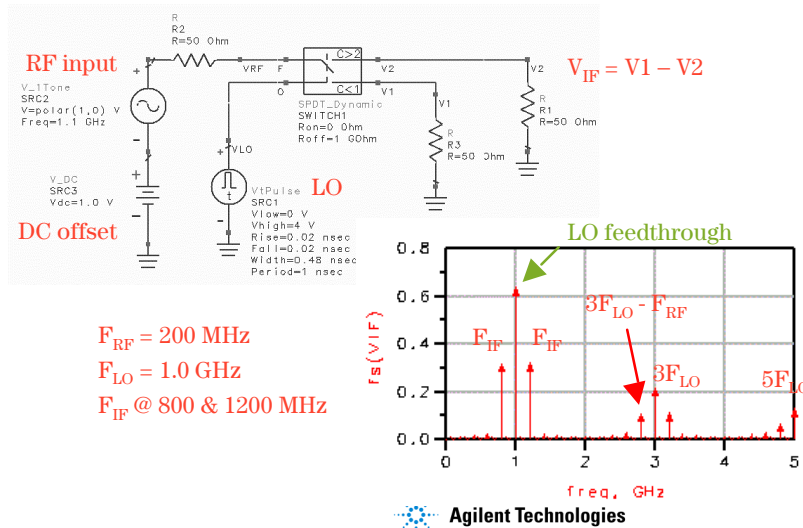
$$\frac{2AV_R}{p} [\sin(\omega_{RF} + \omega_{LO})t - \sin(\omega_{RF} - \omega_{LO})t]$$

Here we see that the ideal conversion gain  $(V_{IF}/V_R)^2 = A^2 (2/\pi)^2$  (if  $A=1$ ) is 6 dB greater than for the unbalanced design.

But, we can still get LO feedthrough if there is a DC current in the signal path. This is often the case since the output of the transconductance amplifier will have a DC current component. This current shows up as a differential output.



## Output spectrum: SB mixer



As you can see, the output spectrum of the single-balanced switching mixer is much less cluttered than the nonlinear mixer spectrum. This was simulated with transient analysis using an ideal switch. The behavioral switch model has an on-threshold of 2V and an off-threshold of 1V. The LO was generated with a 4V pulse function and the duty cycle was set to 50%. The output is taken differentially as  $V_{IF} = V_1 - V_2$ .

Note the strong LO feedthrough component in the output. This is present because of the DC offset on the RF input which produces a differential LO voltage component in the output.

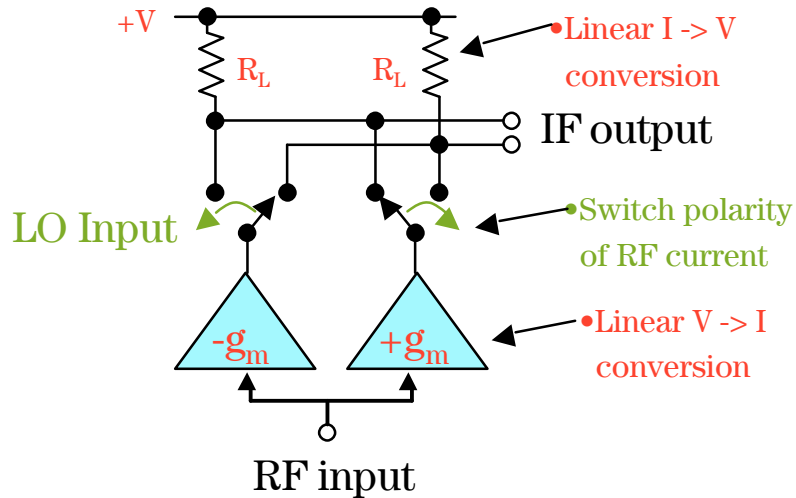
[See ADS example file **swmixer1.dsn**]

**EXERCISE 3:** Set the DC offset voltage to 0 and resimulate. Observe that the LO feedthrough is gone. Compare  $V_1$  and  $V_{IF}$  vs time with and without the DC offset. Use markers to measure the IF output power and calculate the conversion gain. (solution in ADS file ex3)

This LO component is highly undesirable because it could desensitize a mixer postamplifier stage if the amplification occurs before IF filtering. Eliminating the LO component when a DC current is present requires *double-balancing*.



## Ideal Double Balanced Mixer



Agilent Technologies

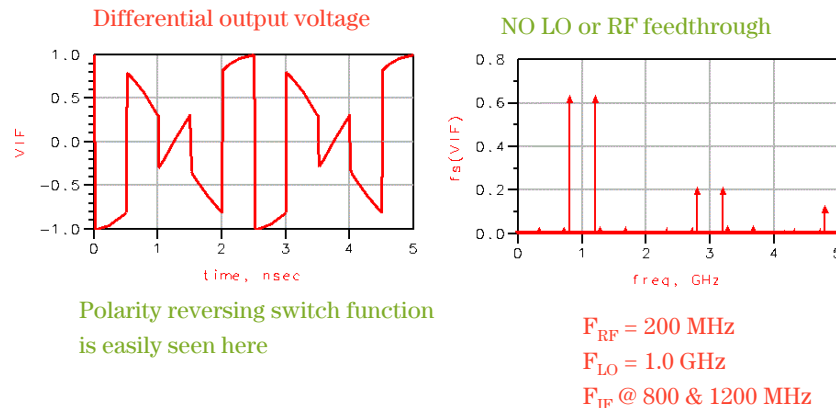
Page 18

An ideal double balanced mixer consists of a switch driven by the local oscillator that reverses the polarity of the RF input at the LO frequency[1] and a differential transconductance amplifier stage. The polarity reversing switch and differential IF cancels any output at the RF input frequency since the DC term cancels as was the case for the single balanced design. The double LO switch cancels out any LO frequency component, even with currents in the RF to IF path, since we are taking the IF output as a differential signal and the LO shows up now as common mode. Therefore, to take full advantage of this design, an IF balun, either active (a differential amplifier) or passive (a transformer or hybrid), is required. The LO is typically suppressed by 50 or 60 dB if the components are well matched and balanced.

To get the highest performance from the mixer we must make the RF to IF path as linear as possible and minimize the switching time of the LO switch. The ideal mixer above would not be troubled by noise (at the low end of the dynamic range) or intermodulation distortion (IMD) at the high end since the transconductors and resistors are linear and the switches are ideal.



## Output Spectrum: DB mixer



Agilent Technologies

Page 19

The differential output voltage and frequency spectrum are simulated using a transient analysis in ADS. The polarity switching action can be clearly seen in the output voltage. There is no LO or RF feedthrough in this ideal DB mixer, even with a DC current in the signal path.

[See ADS example file: **swmixer3.dsn**]

In real mixers, there is always some imbalance. Transistors and baluns are never perfectly matched or balanced. These nonidealities will produce some LO to IF or RF to IF feedthrough (thus, isolation is not perfect). This is usually specified in terms of a power ratio relative to the desired IF output power: dBc

Secondly, the RF to IF path is not perfectly linear. This will lead to intermodulation distortion. Odd-order distortion (typically third and fifth order are most significant) will cause spurs within the IF bandwidth or cross-modulation when strong signals are present. Also, the LO switches are not perfectly linear, especially while in the transition region. This can add more distortion to the IF output and will increase loss due to the resistance of the switches.



## Mixer Performance Specifications

- Image rejection
- Conversion gain: voltage or power
- Port-to-port isolation: dBc
- Large signal performance:
  - gain compression:  $P_{1dB}$
  - intermodulation distortion spec: third-order intercept (TOI)
- Small signal performance: noise figure
- Operating range: Spurious-free dynamic range



Page 20

We have already discussed image rejection, conversion gain and isolation. Other performance specifications relate to the mixer's ability to work with very weak and very strong signals.

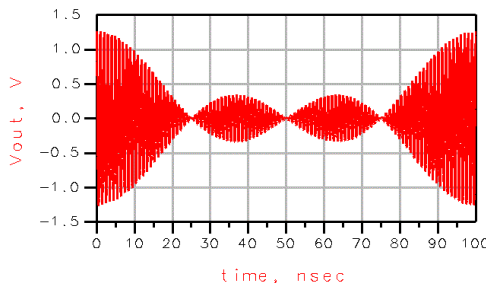
We would like to maximize mixer performance by:

1. maximize linearity in the signal path
2. idealize switching: high slew rates
3. minimize noise contributions



## Large-signal mixer performance

- Signal statistics
  - 4 sources
  - $P_{av\text{s}} = 0 \text{ dBm}$
  - in phase @  $t=0$
- $Df = 10 \text{ MHz}$



- Peak signal voltage, not average power dictates when distortion becomes excessive.



Page 21

In receiver applications, a mixer is often exposed to several signals within its preselected input bandwidth. It is important to understand that it is the peak signal voltage, not average signal power, that dictates when distortion becomes excessive in an amplifier or mixer. In the example above, 4 carriers, each with 0 dBm average power, are applied to the input. Each signal is separated by 10 MHz and all 4 are in phase at  $t = 0$ . As can be seen above, these signals will appear in phase periodically, with 4 times the peak signal voltage of a single carrier. While we are fond of expressing the large-signal performance in terms of an input power in dBm, let's remember that the time domain instantaneous signal peaks are what stress the system. Real signals are likely to be much more complex than this, so the probability of having a large peak like this is less likely in a real application. But, even infrequent overdrive and distortion generation can degrade bit error rates.

[See ADS example file sigs.dsn]



## Gain Compression

- Conversion gain degrades at large input signal levels due to nonlinearity in the signal path.
- Assume a simple nonlinear transfer function:

$$V_{RF}(t) = v_{in} - a_3 v_{in}^3$$

$$V_{RF}(t) = V_R \left( 1 - \underbrace{\frac{3a_3 V_R^2}{4}} \right) \sin(\omega_{RF} t) + \underbrace{\frac{1}{4} a_3 V_R^3}_{\text{Gain compression}} \sin(3\omega_{RF} t)$$

Gain compression      Third-order distortion

- This distortion then gets mixed to the IF frequency



Page 22

*Gain compression* is a useful index of distortion generation. It is specified in terms of an input power level (or peak voltage) at which the small signal conversion gain drops off by 1 dB.

The example above assumes that a simple cubic function represents the nonlinearity of the signal path. When we substitute  $v_{in}(t) = V_R \sin(\omega_{RF} t)$  and use trig identities, we see a term that will produce gain compression:

$$1 - 3a_3 V_R^2/4.$$

If we knew the coefficient  $a_3$ , we could predict the 1 dB compression input voltage. Typically, we obtain this by measurement of gain vs. input voltage. The reduced amplitude output voltage then gets mixed down to the IF frequency.

We also see a cubic term that represents the third-order *harmonic distortion* (HD) that also is caused by the nonlinearity of the signal path. Harmonic distortion is easily removed by filtering; it is the *intermodulation distortion* that results from multiple signals that is more troublesome to deal with.

Note that in this simple example, the fundamental is proportional to  $V_R$  whereas the third-order HD is proportional to  $V_R^3$ . Thus, if  $P_{out}$  vs.  $P_{in}$  were plotted on a dB scale, the HD power will increase at 3 times the rate that the fundamental power increases with input power. This is often referred to as being “well behaved”, although given the choice, we could easily live without this kind of behavior!



## Use Harmonic Balance simulation

**HARMONIC BALANCE**

```

HarmonicBalance
HB1
MaxOrder=8
Freq[1]=LOfreq
Freq[2]=RFfreq
Order[1]=7
Order[2]=3
UseKrylov=yes
SweepVar="P_RF"
Start=-15
Stop=10
Step=1
Other=

```

- Highest order of IM products
- Fundamental Frequencies: put highest power source first
- Number of harmonics of sources [1] & [2]
- Sweep P\_RF in 1 dB steps from -15 dBm
- Can be used to pass variables to data display



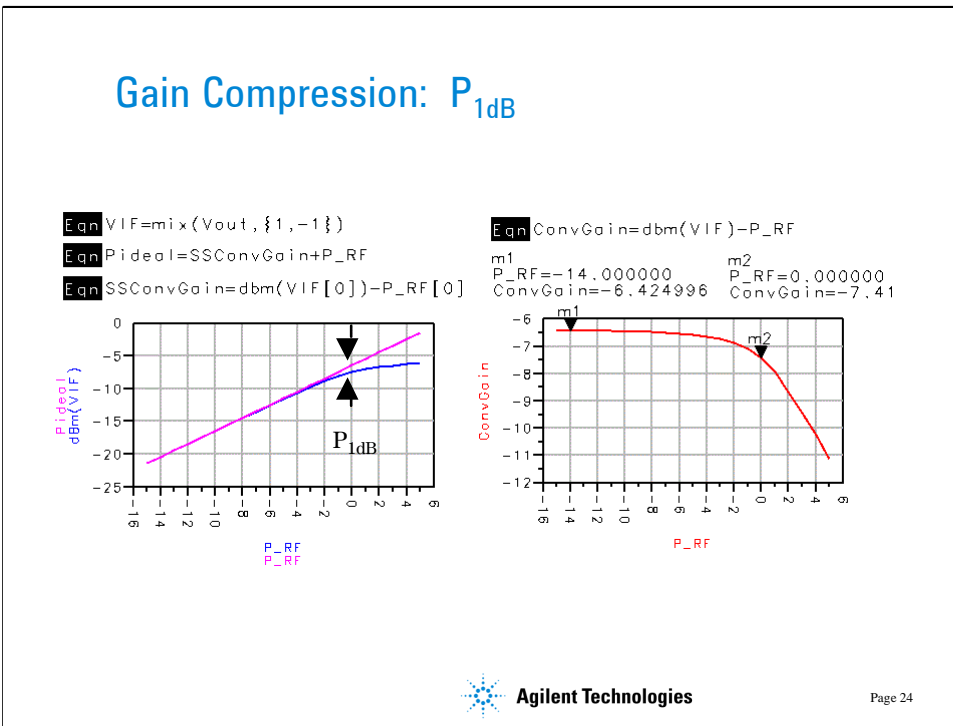
Agilent Technologies

Page 23

Harmonic balance is the method of choice for simulation of mixers. By specifying the number of harmonics to be considered for the LO and RF input frequencies and the maximum order (highest order of sums and differences) to be retained, you get the frequency domain result of the mixer at all relevant frequencies. To get this information using SPICE or other time domain simulators can often require a very long simulation time since at least two complete periods of the lowest frequency component must be generated in order to get accurate FFT results. This becomes a serious problem with two-tone input simulations. Concurrently, the time step must be compatible with the highest frequency component to be considered.

Maximum order corresponds to the highest order mixing product ( $n + m$ ) to be considered ( $nf[1] \pm mf[2]$ ). The simulation will run faster with lower order and fewer harmonics of the sources, but may be less accurate. You should test this by checking if the result changes significantly as you increase order or number of harmonics.

The frequency with the highest power level (the LO) is always the first frequency to be designated in the harmonic balance controller. Other inputs follow sequencing from highest to lowest power.



The RF mixer behavioral model in ADS has been used to illustrate the gain compression phenomenon. The input RF power ( $P_{RF}$ ) was swept from -15 dBm to +5 dBm. On the left, we see the simulated IF output power vs. the ideal output power. Ideal output power is calculated from the small signal conversion gain, simulated at the lowest  $P_{RF}$  input power level,  $P_{RF}[0]$ . Here, the index [0] refers to the first entry in the data set for  $P_{RF}$ , -15 dBm. The  $dBm(VIF[0])$  function is used to convert the corresponding first entry in the IF voltage data set IF to power.

VIF is the output voltage at the IF output frequency and must be selected from many frequencies in the output data set. This frequency is selected by using the *mix* function. In this example, LOfreq = 1 GHz and RFfreq = 0.85 GHz. If we are interested in the downconverted IF frequency, 150 MHz, we can select it from:

$$V_{IF} = \text{mix}(Vout, \{1, -1\}).$$

The indices in the curly brackets are ordered according to the HB fundamental analysis frequencies. Thus,  $\{1, -1\}$  selects LOfreq – RFfreq.

Other equations are added to the display panel which calculate the conversion gain

$$\text{ConvGain} = \text{dBm}(VIF) - P_{RF}.$$

Here we can identify the 1 dB gain compression power to be about 0 dBm.

**[Refer to ADS example RFmixer\_GC]**



## Intermodulation distortion

- IMD consists of the higher order signal products that are generated when two RF signals are present at the mixer input. The IMD will be down and up converted by the LO as will the desired RF signal.
- IMD generation is a good indicator of large signal performance of a mixer.
- Absolute accuracy is highly dependent on the accuracy of the device model, but the relative accuracy is valuable for optimizing the circuit parameters for best IMD performance.



Page 25

The gain compression power characterization provides a good indication of the signal amplitude that the mixer will tolerate before really bad distortion is generated. You should stay well below the  $P_{1dB}$  input level.

Another measure of large-signal capability is the intermodulation distortion. Intermodulation distortion occurs when two or more signals are present at the RF input to the mixer. The LO input is provided as before. These two signals can interact with the nonlinearities in the mixer signal path (RF to IF) to generate unwanted IMD products (distortion) which then get mixed down to IF.



## Intermodulation Distortion

- Let's consider the 3rd order nonlinearity:  $a_3 v_{in}^3$

- two inputs:  $v_{in} = V_1 \sin(w_1 t) + V_2 \sin(w_2 t)$

$$V_{out3} = a_3[V_1^3 \sin^3(\mathbf{w}_1 t) + V_2^3 \sin^3(\mathbf{w}_2 t) + \\ 3V_1^2 V_2 \sin^2(\mathbf{w}_1 t) \sin(\mathbf{w}_2 t) + 3V_1 V_2^2 \sin(\mathbf{w}_1 t) \sin^2(\mathbf{w}_2 t)]$$

## - Agilent Technologies

Page 26

Let's consider again the simple cubic nonlinearity  $a_3 v_{in}^3$ . When two inputs at  $\omega_1$  and  $\omega_2$  are applied simultaneously to the RF input of the mixer, the cubing produces many terms, some at the harmonics and some at the IMD frequency pairs. The trig identities show us the origin of these nonidealities. [4]

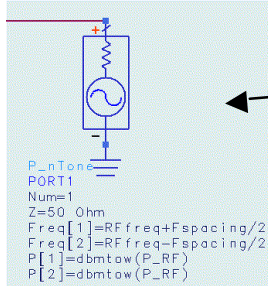
We will be mainly concerned with the third-order IMD. This is especially troublesome since it can occur at frequencies within the IF bandwidth. For example, suppose we have 2 input frequencies at 899.990 and 900.010 MHz. Third order products at  $2f_1 - f_2$  and  $2f_2 - f_1$  will be generated at 899.980 and 900.020 MHz. Once multiplied with the LO frequency, these IMD products may fall within the filter bandwidth of the IF filter and thus cause interference to a desired signal. IMD power, just as HD power, will have a slope of 3 on a dB plot.

In addition, the cross-modulation effect can also be seen. The amplitude of one signal (say  $\omega_1$ ) influences the amplitude of the desired signal at  $\omega_2$  through the coefficient  $3V_1^2V_2a_3/2$ . A slowly varying modulation envelope on  $V_1$  will cause the envelope of the desired signal output at  $\omega_2$  to vary as well since this fundamental term created by the cubic nonlinearity will add to the linear fundamental term. This cross-modulation can have annoying or error generating effects at the IF output.

Other higher odd-order IMD products, such as 5th and 7th, are also of interest, but may be less reliably predicted unless the device model is precise enough to give accurate nonlinearity in the transfer characteristics up to the  $2n-1^{\text{th}}$  order.



## IMD simulation



- Use a two-tone generator at the mixer input.
- The two input frequencies are separated by Fspacing and each have an input power of P\_RF dBm.
- Large MaxOrder and LO Order are needed for accurate HB TOI predictions with highly nonlinear elements
- Oversampling (Param menu) should also be increased cautiously

```

HB1
MaxOrder=10
Freq[1]=LOfreq
Freq[2]=RFfreq+Fspacing/2
Freq[3]=RFfreq-Fspacing/2
Order[1]=11
Order[2]=3
Order[3]=3
Oversample[1]=2
Oversample[2]=2
Oversample[3]=2
UseKrylov=yes

```



Agilent Technologies

Page 27

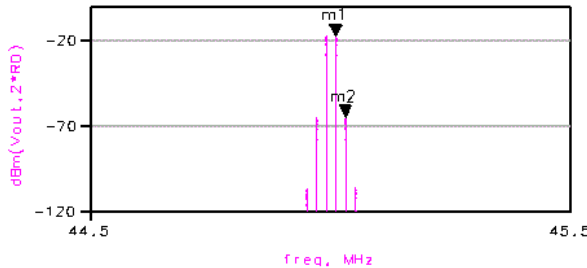
The IMD simulation is performed with a two-tone generator at the RF input. The frequency spacing should be small enough so that both fall within the IF bandwidth. You should keep in mind that both of the generator tones are in phase, therefore the peak voltage will add up periodically to twice the peak of each source independently. Because of this, you will expect to see some reduction in the  $P_{1dB}$  on the order of 6 dB.

Often accurate IMD simulations will require a large *maximum order* and *LO harmonic order* when using harmonic balance. In this case, a larger number of spectral products will be summed to estimate the time domain waveform and therefore provide greater accuracy. This will increase the size of the data file and time required for the simulation. Increase the orders in steps of 2 and watch for changes in the IMD output power. When no further significant change is observed, then the order is large enough. Simulation of very low power levels is subject to convergence errors and numerical noise[6].

Sometimes, increasing the *oversampling ratio* for the FFT calculation (use the *Param* menu of the HB controller panel) can reduce errors. This oversampling controls the number of time points taken when converting back from time to frequency domain in the harmonic balance simulation algorithm. A larger number of time samples increases the accuracy of the transform calculation but increases memory requirements and simulation time. Both order and oversampling should be increased until you are convinced that further increases are not worthwhile.



## IF output spectrum



Third-order intermodulation products at  $2f_1 - f_2 - f_{LO}$  and  $2f_2 - f_1 - f_{LO}$  will be present in the IF output.

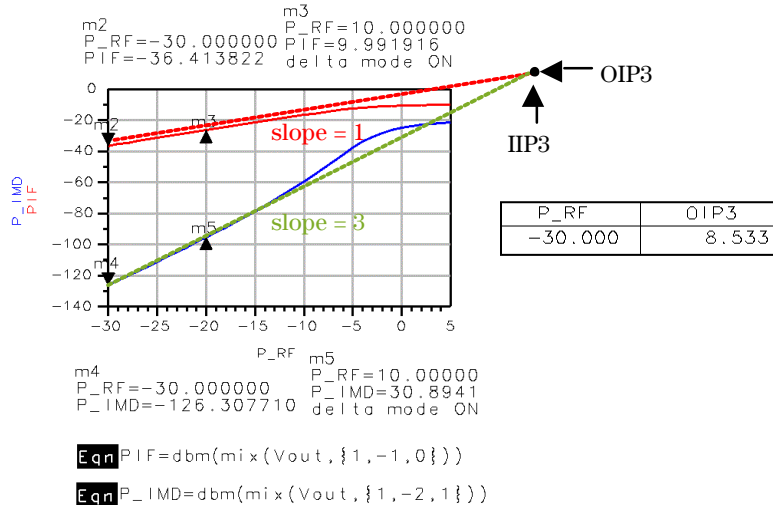


Note that the third-order (m2) and fifth-order products are quite close in frequency to the desired signal (m1). This means that they are often impossible to remove by filtering.

The two IMD sidebands should be approximately of equal power if the simulation is correct. If not, increase the order of the LO in the HB controller and see if this makes the sidebands more symmetric.



## Third-order intercept definition



**Agilent Technologies**

Page 29

A widely-used figure of merit for IMD is the *third-order intercept* (TOI) point. This is a fictitious signal level at which the fundamental and third-order product terms would intersect. In reality, the intercept power is 10 to 15 dBm higher than the  $P_{1\text{dB}}$  gain compression power, so the circuit does not amplify or operate correctly at the IIP3 input level. The higher the TOI, the better the large signal capability of the mixer.

It is common practice to extrapolate or calculate the intercept point from data taken at least 10 dBm below  $P_{1\text{dB}}$ . One should check the slopes to verify that the data obeys the expected slope = 1 or slope = 3 behavior. In this example, we can see that this is true only at lower signal power levels.

$$\text{OIP3} \equiv (\text{PIF} - \text{PIMD})/2 + \text{PIF}.$$

Also, the input and output intercepts are simply related by the gain:

$$\text{OIP3} = \text{IIP3} + \text{conversion gain.}$$

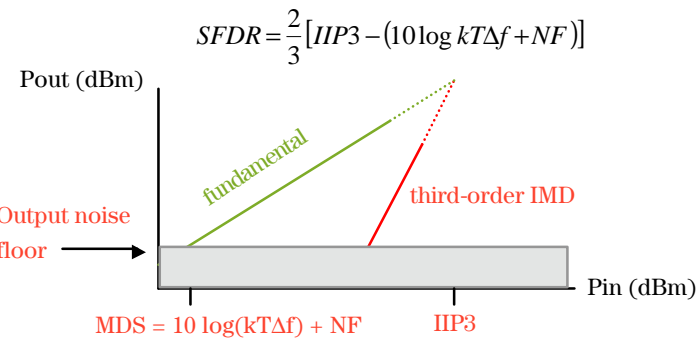
In the data display above, equations are used to select out the IF fundamental tone and the IMD tone, in this case, the lower sideband. The mix function now has 3 indices since there are 3 frequencies present: LO, RF1 and RF2.

[See ADS example file: RFmixer\_TOI]



## Noise figure & SFDR

- We have been concentrating on the large signal limitations of the mixer. Noise determines the other end of the mixer dynamic range.
- Spurious-free dynamic range:  $NF = 10 \log_{10} \left[ \frac{(S/N)_{in}}{(S/N)_{out}} \right]$



 Agilent Technologies

Page 30

*Noise figure* is defined as the ratio between the input and output S/N ratio.

$$NF (\text{dB}) = 10 \log[(S/N)_{in}] / [(S/N)_{out}]$$

Any real mixer or amplifier will degrade S/N because noise is added to the signal. The *minimum detectable signal* (MDS) power is determined by noise and corresponds to a signal whose strength just equals the noise. The thermal noise power in bandwidth  $\Delta f$  is  $10 \log(kT\Delta f)$  where  $k$  is Boltzmann's constant and  $T$  is absolute temperature. Thus,

$$MDS (\text{dBm}) = 10 \log(kT\Delta f) + NF$$

since the system generated noise adds to the thermal noise ambient.

The maximum signal power is limited by distortion, which we describe by IIP3. The *spurious-free dynamic range* (SFDR) is a commonly used figure of merit to describe the dynamic range of an RF system. If the signal power is increased beyond the point where the IMD rises above the noise floor, then the signal-to-distortion ratio dominates and degrades by 3 dB for every 1 dB increase in signal power. If we are concerned with the third-order distortion, the SFDR is calculated from the geometric 2/3 relationship between the input intercept and the IMD.

It is important to note that the SFDR depends directly on the bandwidth  $\Delta f$ . It has no meaning without specifying bandwidth.



## Determining Noise Figure

- Use harmonic balance simulator for mixer NF.
  - takes into account any nonlinearities and harmonics that could mix noise down into the IF band.
  - If  $P_{RF} \ll P_{LO}$ , either a 1-tone generator or a passive termination can be used at the input with equal accuracy.
  - Noise Figure is calculated.
    - Ideal filter (centered on RF) is added in simulation.
    - Noise contributors within mixer are listed by value
    - For passive switching mixers,  $NF @ - ConvGain$



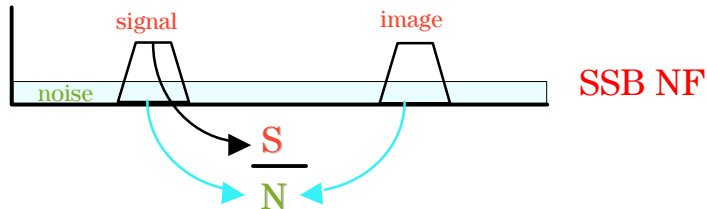
Page 31

The harmonic balance simulator will take into account wideband noise that is generated in the mixer. Some of this noise gets mixed down to the IF frequency from the harmonics of the LO. If the RF signal is of small amplitude, the harmonics that it might generate can be neglected, and either a 1-tone generator or a passive termination can be used. The predictions will be the same. Note that it is essential that the input generator frequency and the HB input analysis frequency be the same.



## SSB or DSB Noise Figure?

- There are two definitions used for noise figure with mixers - often a source of confusion.
- SSB NF assumes signal input from only one sideband, but noise inputs from both sidebands.
- Relevant for heterodyne architectures



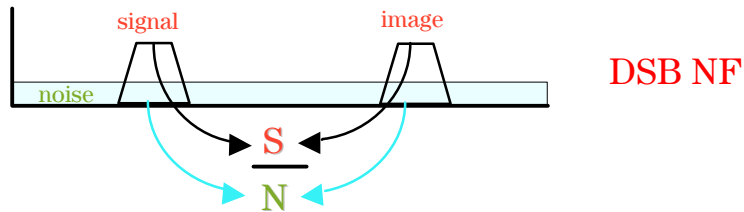
Page 32

Measuring SSB noise figure is relevant for superhet receiver architectures in which the image frequency is removed by filtering or cancellation. Noise figure is generally measured with a wideband noise source that is switched on and off. The NF is then calculated from the “Y factor” [4] and gain does not need to be known. With a SSB measurement, the mixer internal noise shows up at the IF output from both signal and image inputs, but the excess noise is only introduced in the signal frequency band.



## SSB or DSB Noise Figure?

- DSB NF includes both signal and noise inputs from both sidebands. Appropriate for direct conversion architectures.



Page 33

A DSB NF is easier to measure; wideband excess noise is introduced at both the signal and image frequencies. It will be 3 dB less than the SSB noise figure in most cases. This is perhaps more relevant for direct conversion receivers where the image cannot be filtered out from the signal.

Either type of measurement is valid so long as you clearly specify what type of measurement is being made.



## Passive or Active Mixers?

- Passive nonlinear devices or switches
  - conversion loss, not gain
  - high tolerance to IMD
  - external baluns or transformers needed
- Active mixers
  - can provide conversion gain
  - active baluns - better for IC implementation
  - more difficulty in achieving good IMD performance



Page 34

Passive mixers are widely used because of their relative simplicity, wide bandwidth, and good IMD performance. The transformers or baluns generally limit the bandwidth. They must introduce some loss into the signal path, however, which can be of some concern for noise figure. In this case, an LNA can be introduced ahead of the mixer, usually with some degradation in IMD performance.

Active mixers are preferred for RFIC implementation. They can be configured to provide conversion gain, and can use differential amplifiers for active baluns. Because of the need for additional amplifier stages in the RF and IF paths with fully integrated versions, it is often difficult to obtain really high third-order intercepts and 1 dB compression with active mixers.



## Mixer circuit examples

- OK, now let's look at some examples
- 2 mixer circuits will be reviewed:
  - diode DB quad:
    - familiar and widely used
    - wide bandwidth, limited by baluns
  - Low IMD FET mixer:
    - not as well known, but good performance

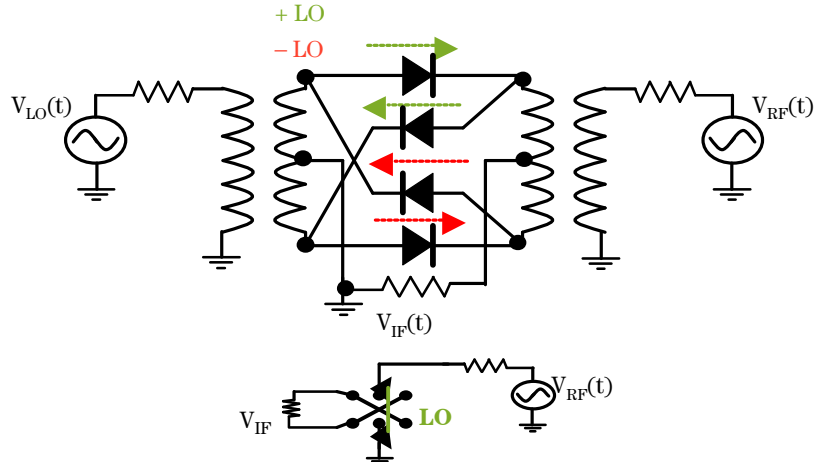


Agilent Technologies

Page 35



## Diode DB quad mixer



 Agilent Technologies

Page 36

The diode double-balanced quad mixer is a very popular design and available in a wide variety of frequency bandwidths and distortion specs. The MiniCircuits™ catalog [7] is full of these. The diodes act as a polarity reversing switch as seen in the bottom of the figure. When the top of the LO transformer is positive, the blue path is conductive and will ground the top of the RF transformer. When the top is negative, the red path is conducting and the RF polarity reverses. Both LO and RF feedthrough are suppressed by the symmetry and balancing provided by the transformers. The LO signal at the RF and IF ports appears to be a virtual ground for either LO polarity.

Since the LO signal must switch the diodes on and off, a large LO power is required, typically 7 dBm when one diode is placed in each leg, 17 dBm with two diodes per path! With this much LO power, even with good isolation, there may still be significant LO in the IF output.

When the diodes are conducting with LO current  $\gg$  RF current, the mixer should behave linearly. At large RF signal powers, the RF voltage modulates the diode conduction, so lots of distortion will result in this situation. The diodes are also sensitive to RF modulation when they are biased close to their threshold current/voltage. For both reasons, we prefer high LO drive with a fast transition (high slew rate - a square wave LO is better than sine wave) between on and off. The IMD performance is very poor with small LO power.



## Design procedure

- Determine correct RF and LO impedances to match through the diode ring to the 50 ohm IF load. Transformer ratios can be swept using HB or XDB.
- Sweep LO power to maximize conversion gain and gain compression
- Or, buy one from MiniCircuits™!



Page 37

The RF and LO impedances at the diode ring theoretically should be determined and matched at all of the relevant harmonics. [8] For most designs, optimizing the transformer ratios with the IF port connected to 50 ohms should be sufficient, since we cannot select impedances at each frequency independently, and this approach would not be possible for a broadband design such as this.

Exercise 4. Modify the gain compression simulation (diodeDBQ\_GC) to evaluate conversion gain and P1dB as a function of LO power. Use the XDB simulator with a parameter sweep. (solution: ADS file diodeDBQ\_ex4)

Exercise 5. Sweep the RF transformer turns ratio to find the best ratio for conversion gain and P1dB. (solution: ADS file diodeDBQ\_GC\_OPT)

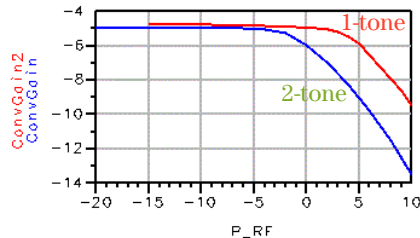


## Diode mixer performance

```

Eqn P_IMD=dbm(mix(Vout,{-1,2,-1}))
Eqn PIF=dbm(mix(Vout,{-1,1,0}))
Eqn ConvGain=PIF-P_RF

```

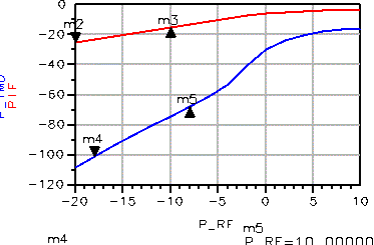


$P_{1dB} = +5 \text{ dBm}$   
 $P_{1dB} = 0 \text{ dBm}$

$P_{RF}$	OIP3
-20.000	16.729
-18.000	16.011
-16.000	15.264
-14.000	15.190
-12.000	14.745
-10.000	14.530

$m^2$   
 $P_{RF}=-20.000000$   
 $PIF=-24.993328$

$m^3$   
 $P_{RF}=10.000000$   
 $PIF=10.003541$   
 delta mode ON



$m^4$   
 $P_{RF}=-18.000000$   
 $P_{IMD}=-101.000153$   
 delta mode ON

$m^5$   
 $P_{RF}=10.000000$   
 $P_{IMD}=33.2558$   
 delta mode ON



Agilent Technologies

Page 38

A harmonic balance simulation can be used to estimate the mixer performance. With the DB diode mixer, the currents in the diodes are half wave, so a high number of LO harmonics and maximum order and some oversampling of the FFT operation are necessary to reproduce this waveform and therefore get reasonable accuracy on the third-order product. Gain compression is not as sensitive to the LO order.

Gain compression behavior depends strongly on the signal statistics as discussed earlier. There is about 5 dBm difference in  $P_{1dB}$  between single and two tone simulations.

We see that the third order IMD predictions are not “well behaved”; the slope is 33.2 dB/decade instead of 30. This puts our TOI calculation in doubt, but it is still useful for design optimizations. We can also see that the OIP3 prediction depends upon the RF input power level.

Noise figure of these passive switched mixers is usually close to

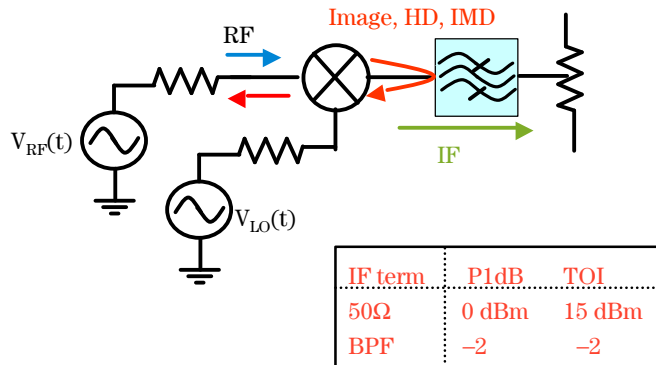
$$NF = -\text{ConvGain}$$

Thus, for a -5 dB Conversion Gain, a noise figure of about 5 dB is expected.

[See ADS example files **diodeDBQ\_TOI** and **diodeDBQ\_GC**]



## Need good match at each port



Page 39

Since these passive diode switch mixers are bilateral, that is, the IF and RF ports can be reversed, the performance of the mixer is very sensitive to the termination impedances at all ports. A wideband resistive termination is needed to absorb not only the desired IF output but also any images, harmonics, and IMD signals. If these signals are reflected back into the mixer, they will remix and show up at the RF port and again at the IF port. The phase shifts associated with the multiple replicas of the same signals can seriously deteriorate the IMD performance of the mixer.

A simulation was carried out using a bandpass filter in the IF port as shown above. The  $P_{1dB}$  was degraded by 2 dB and the third-order IMD power was not well behaved. A calculated TOI showed nearly 17 dB degradation.

Thus, it is important to terminate. Terminations can consist of:

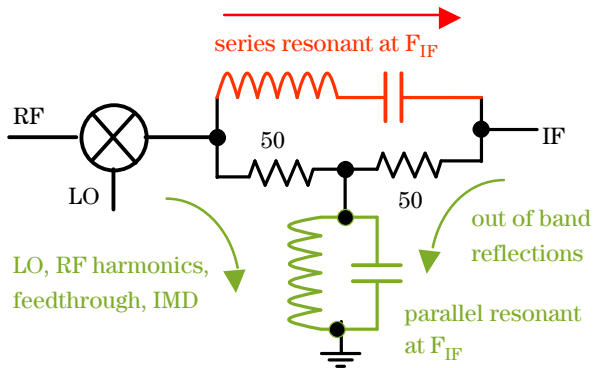
1. Attenuator. Obviously not a good idea if NF is important
2. Wideband amplifier with good S11 or S22 return loss
3. Diplexer. A passive network that separates frequencies but provides  $Z_0$  termination for all components.

[See ADS example file: **diodeDBQ\_TOI\_BPF**]



## Mixer termination methods

- Passive diplexer



Agilent Technologies

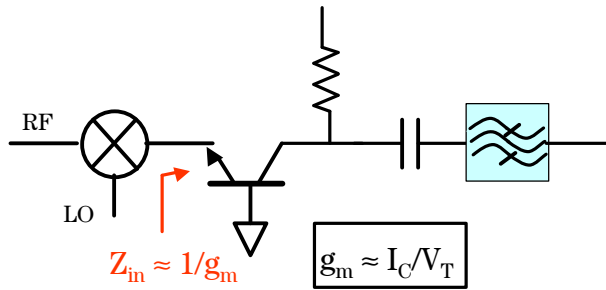
Page 40

This passive diplexer provides a low-loss forward path through the series resonant branch. At  $F_{IF}$ , the parallel resonant branch has a high impedance and does not load the IF. Outside of the IF band (you need to set the Q for the design to control the bandwidths) the series resonant branch presents a high impedance to the signals and the parallel resonant branch a low, but reactive impedance. At these frequencies, above (through C) and below  $F_{IF}$  (through L), the resistors terminate the output. The farther away from  $F_{IF}$  you are, the better the match.



## Mixer termination methods

- Active wideband termination



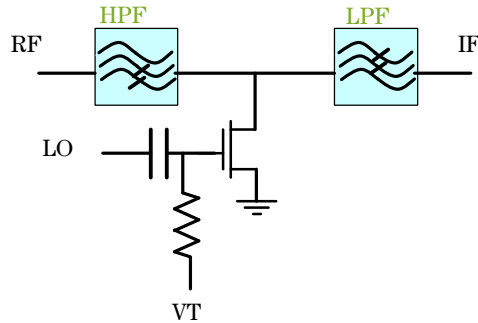
Page 41

This common base stage provides a wideband resistive impedance provided the maximum frequency at the input is well below the  $f_T$  of the transistor. The bias current can be set to provide a 50 ohm input impedance. Alternatively, one can bias the device at higher current levels and add a series resistor at the input. Of course, this degrades noise, but will improve IMD performance. The amplifier must be capable of handling the complete output power spectral density of the mixer without distorting.



## Low IMD FET mixer

- LO modulates channel resistance
- Channel resistance is very linear at small VDS
- LPF and HPF act as diplexer



Page 42

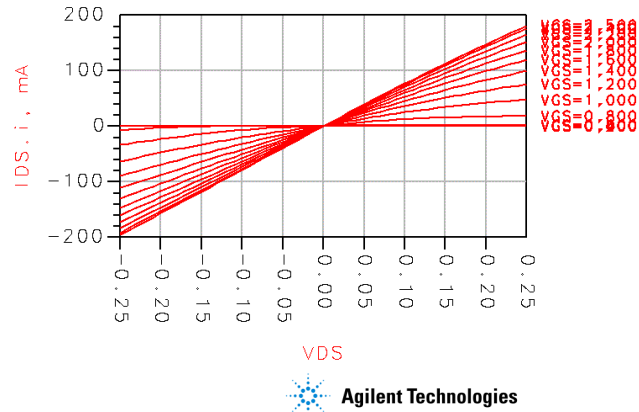
Another popular mixer utilizes only one FET in its simplest form. [10] The LO signal switches the FET on and off. The gate is biased close to threshold. The channel resistance of the FET therefore becomes time dependent and provides a switching mixer behavior. The RF input and IF output are separated by high pass (HPF) and low pass (LPF) filters respectively.

The surprising thing about this design is the high P1dB and TOI that it can deliver. On the down side, one must do some balancing to get rid of significant LO to IF feedthrough.



## ID - VDS of MOSFET

- Highly linear at low VDS
- Device width and LO voltage can be optimized for performance



Agilent Technologies

Page 43

The mixer RF to IF path will be quite linear if the total drain voltage (VDS) remains small. As can be seen from the DC simulation, the MOSFET exhibits quite linear channel resistance up to at least a VDS of + and - 0.25V.

[See ADS example files: **MOSFET\_IVtest**]



## Design process

- Select nominal FET channel width and optimize the source and load impedances for conversion gain
- Design input (HPF) and output (LPF) networks which present these impedances to the FET drain
- Optimize FET width and matching impedances for highest  $P_{1dB}$



Page 44

The design procedure for this mixer requires that the optimum impedances be presented to the RF and IF ports where they join at the drain. These networks can also act as diplexer to some degree, helping to separate RF from the IF output and vice-versa. A 1-port impedance block can be placed in each path and ADS used to optimize the conversion gain. These impedances will provide an initial estimate of the optimum RF and IF impedances.

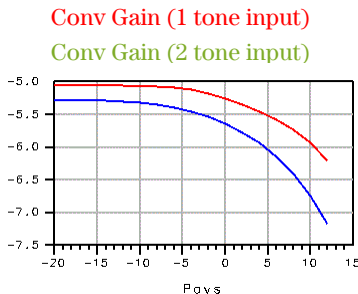
Alternatively, a current probe can be placed in series with the RF and IF paths to the drain. The V/I at each connection can be analyzed at each frequency and optimum impedances inferred.

Next, high-pass and low-pass networks can be designed to present these impedances, at least at the fundamental frequencies. ADS can again be used to optimize the conversion gain. Device width may also be varied to improve  $P_{1dB}$ .

[See ADS design files: **fet1opt1tone** and **fet1optmatch**]

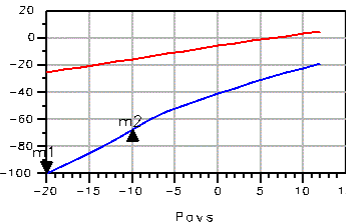


## FET mixer performance



P<sub>1dB</sub> = + 12 dBm  
P<sub>1dB</sub> = + 7 dBm

P <sub>avs</sub>	OIP3
-20.000	11.808
-18.000	11.877
-16.000	11.841
-14.000	11.696
-12.000	11.452



m1  
P<sub>avs</sub>=-20.000000 P<sub>avs</sub>=10.000000  
PIMD=-99.461604 PIMD=32.116890  
delta mode ON  
Eqn PIMD=dbm(mix(Vload, {-1,2,-1}))



Agilent Technologies

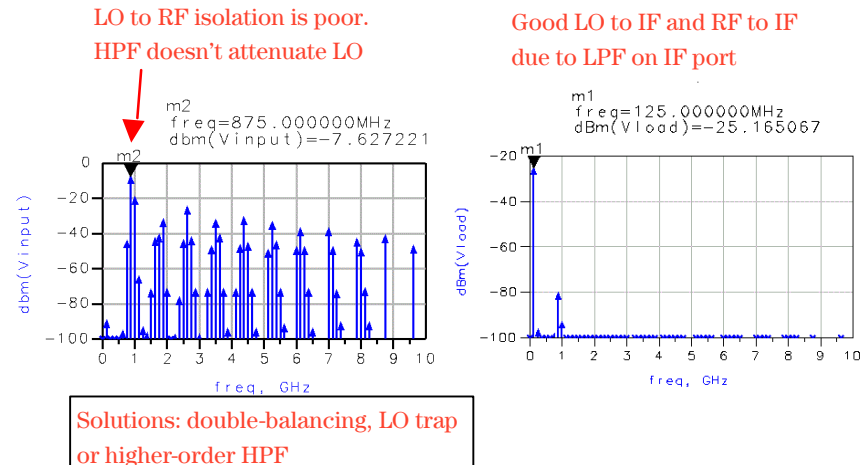
Page 45

The mixer performance was simulated. Surprisingly, we see that the P<sub>1dB</sub> is higher than that simulated for the diode mixer. The OIP3 is also reasonably high.

[See ADS design files fet1\_GC, fet1\_GC2 and fet1\_TOI]



## FET mixer isolation



Agilent Technologies

Page 46

So far, so good. But, now we see the problem with this design. There is a very large LO feedthrough to the IF port due to the large CGD of the MOSFET. You could try to reduce this by designing a better HPF or inserting a resonant LO trap in the output. Probably a better way is to use double-balancing, although this will require 4 FETs and some transformers.

[See ADS design files fet1\_ISO]



## Conclusion

### Learning objectives:

- Understand operating principles of the mixer
- What makes a good mixer?
- Choices: nonlinear/switching mode; single/double balance; active/passive
- Specify performance: Gain, NF,  $P_{1\text{dB}}$ , TOI, SFDR, isolation
- Mixer examples - numerous other possibilities



Agilent Technologies

Page 47



## Exercises

1. Use ADS to evaluate the performance of a single-balanced or double-balanced FET mixer based on the mixer example in this seminar. You will need to add transformers to do this. Evaluate and compare the conversion gain, isolation, P1dB, and TOI with the single FET version.

### Further resources:

- Go through the ADS example files, modify them for your own design work.

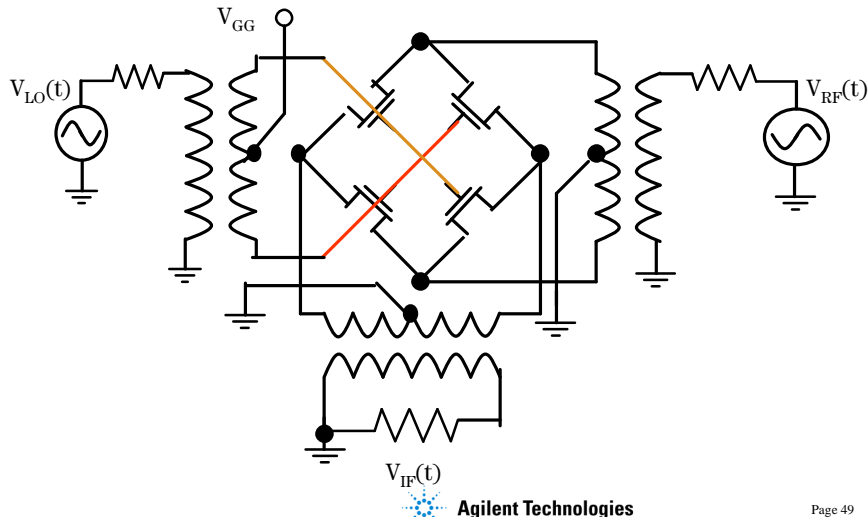


Page 48



## Exercises

2. Refer to the notes page...



 Agilent Technologies

Page 49

The mixer shown above is the FET equivalent of the diode ring mixer. This was first described by Ed Oxner [10] and can provide impressive large signal performance with a sufficiently strong LO voltage. The substrate connection of the MOSFETs can be grounded or connected to a negative supply to reduce the gate capacitances.

Using the MOSFET model from the previous ADS examples, design this mixer and evaluate all of the important mixer performance measures.

[10] Oxner, E. S., "Commutation Mixer Achieves High Dynamic Range," RF Design, pp. 47-53, Feb. 1986.



## References

- [1] Gray, P. R. and Meyer, R. G., *Design of Analog Integrated Circuits*, 3rd Ed., Chap. 10, Wiley, 1993.
- [2] Gilbert, B., "Design Considerations for BJT Active Mixers", Analog Devices, 1995.
- [3] Lee, T. H., *The Design of CMOS Radio-Frequency Integrated Circuits*, Chap. 11, Cambridge U. Press, 1998.
- [4] Hayward, W., *Introduction to Radio Frequency Design*, Chap. 6, American Radio Relay League, 1994.
- [5] Razavi, B., *RF Microelectronics*, Prentice-Hall, 1998.
- [6] Maas, S., "Applying Volterra Series Analysis," *Microwaves and RF*, p. 55-64, May 1999.
- [7] Minicircuits RF/IF Designers Handbook, [www.minicircuits.com](http://www.minicircuits.com)
- [8] Maas, S., "The Diode Ring Mixer", *RF Design*, p. 54-62, Nov. 1993.
- [9] Maas, S., "A GaAs MESFET Mixer with Very Low Intermodulation," *IEEE Trans. on MTT*, MTT-35, pp. 425-429, Apr. 1987.



Page 50

## References

- [1] Gray, P. R. and Meyer, R. G., *Design of Analog Integrated Circuits*, 3rd Ed., Chap. 10, Wiley, 1993.
- [2] Gilbert, B., "Design Considerations for BJT Active Mixers", Analog Devices, 1995.
- [3] Lee, T. H., *The Design of CMOS Radio-Frequency Integrated Circuits*, Chap. 11, Cambridge U. Press, 1998.
- [4] Hayward, W., *Introduction to Radio Frequency Design*, Chap. 6, American Radio Relay League, 1994.
- [5] Razavi, B., *RF Microelectronics*, Prentice-Hall, 1998.
- [6] Maas, S., "Applying Volterra Series Analysis," *Microwaves and RF*, p. 55-64, May 1999.
- [7] Minicircuits RF/IF Designers Handbook, [www.minicircuits.com](http://www.minicircuits.com)
- [8] Maas, S., "The Diode Ring Mixer", *RF Design*, p. 54-62, Nov. 1993.
- [9] Maas, S., "A GaAs MESFET Mixer with Very Low Intermodulation," *IEEE Trans. on MTT*, MTT-35, pp. 425-429, Apr. 1987.



## End of Design Seminar...



Page 51

## **Mixers Examples**

**ELEC 483 - Wireless Technology**

**Brian Frank**

**2003-2004**

### Mixer Topologies

- Topology differences due to use of hybrids/baluns to achieve isolation between three ports and rejection of harmonics
  - Single diode/FET
  - Single balanced diode/FET mixers
  - Double balanced diode/FET mixers
  - Triple balanced diode/FET mixers
- Mixers evaluated by isolation between ports, spurious response rejection, loss

### Spurious response

- All real nonlinear devices will produce additional harmonics due to higher order terms
- General nonlinear device has voltage transfer function given by a Taylor series

$$v_{out} = a_0 + a_1 v_{in} + a_2 v_{in}^2 + a_3 v_{in}^3 + \dots \quad (1)$$

- We usually desire the mixing produced by the  $a_2 v_{in}^2$  term since usually

$$v_{in} = v_{RF} + v_{LO} \quad (2)$$

### Second and third order harmonics

- Second order term gives

$$(v_{LO} + v_{RF})^2 = v_{LO}^2 + v_{RF}v_{LO} + v_{RF}^2 \quad (3)$$

and so  $v_{in}^2$  will give us a  $v_{LO}v_{RF}$  term, but also a second order harmonic at  $2\omega_{RF}$  due to  $v_{RF}^2$  and at  $2\omega_{LO}$  due to  $v_{LO}^2$

- Third order term gives

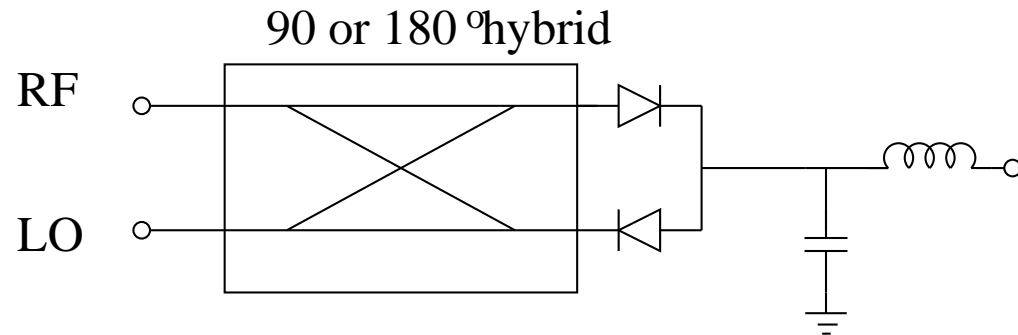
$$(v_{LO} + v_{RF})^3 = v_{LO}^3 + 2v_{RF}^2v_{LO} + 2v_{RF}v_{LO}^2 + v_{RF}^3 \quad (4)$$

which gives us harmonics at  $2\omega_{LO} + \omega_{RF}$  and  $2\omega_{RF} + \omega_{LO}$

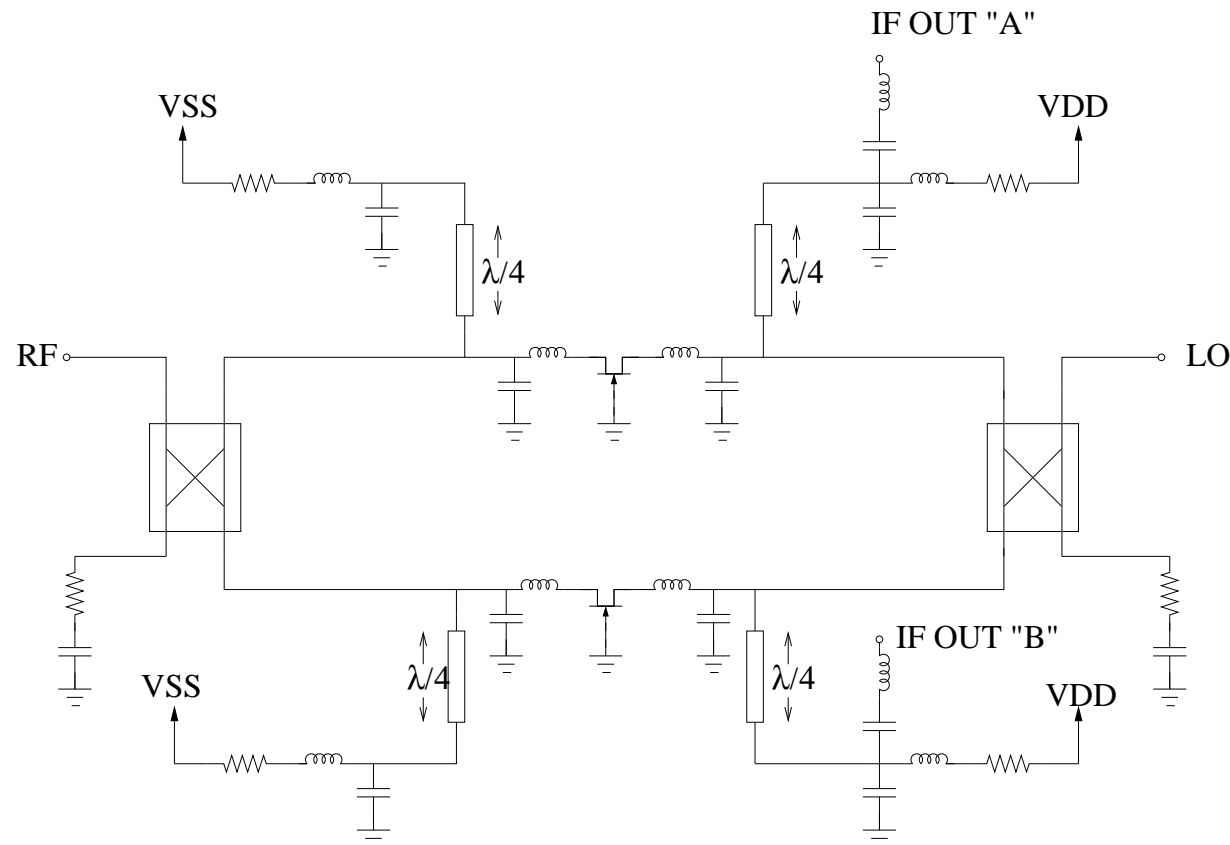
- Similarly, higher order terms will give higher order harmonics  $m\omega_{RF} + n\omega_{LO}$  where  $m, n$  are integers

### Single balanced mixers

- Hybrid or balun used to isolate any two of IF, RF, and LO ports
- Choice of  $90^\circ$  and  $180^\circ$  hybrids
- E.g. single balanced mixer with  $180^\circ$  hybrid rejects  $(m, n) = (2, 2)$  and either  $(2, 1)$  or  $(1, 2)$  depending on whether the LO is injected into the  $\Delta$  port or the  $\Sigma$  port



### Example: Single balanced FET mixer

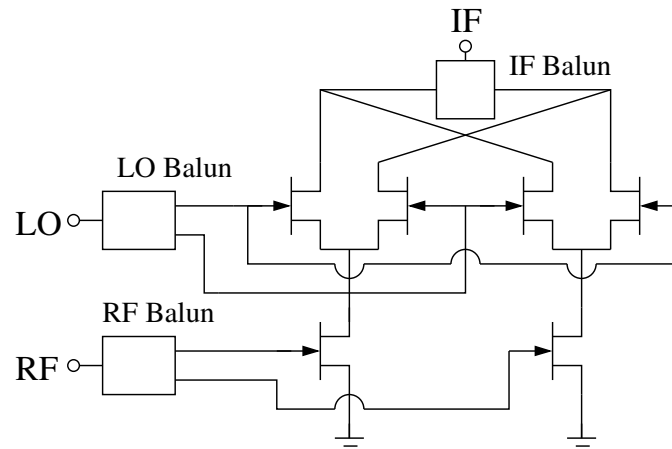


### Double balanced mixers

- IF, RF, and LO ports mutually isolated so IF, RF, and LO bands may overlap
- Double balanced mixers reject all  $(m, n)$  responses where  $m$  or  $n$  or both are even
- More complex

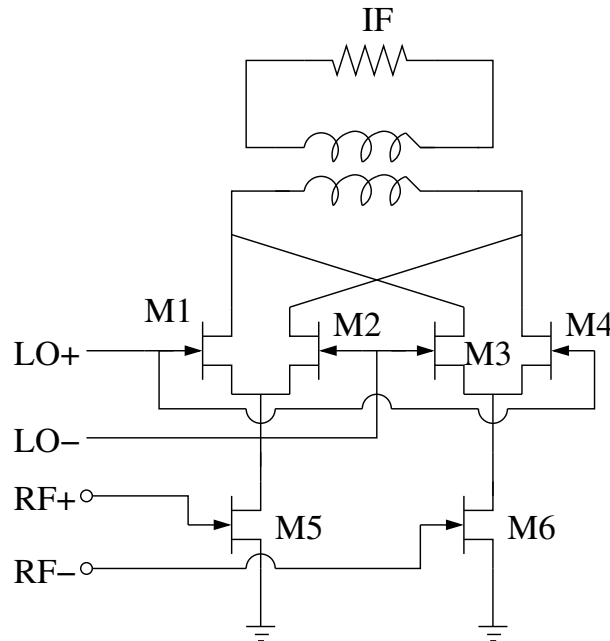
### Double balanced mixer example: Gilbert mixer

- Two single balanced mixers combined
  - Operates as alternating switch - LO alternates which FET is on
  - Lower FET is essentially a common source amplifier for the RF
- Interconnection at output causes drains of FETs to be virtual grounds for LO and RF and even-order spurious responses and *intermodulation products*

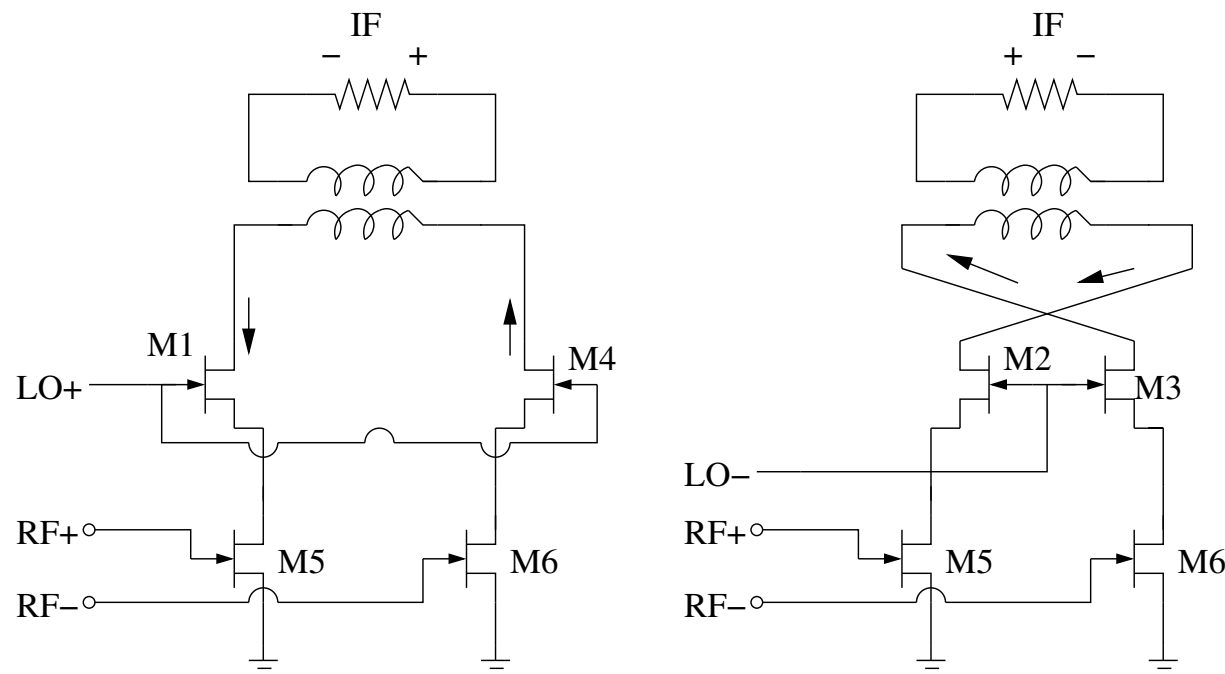


### Gilbert mixer analysis

- The gilbert cell mixer can also be drawn as below
- The large LO signal alternately turns on M1 and M4, then M2 and M3
- The small RF signal sets the direction of small signal current flow



## Gilbert mixer analysis



### Intermodulation and Intercepts

- The nonlinear effects that produce spurious responses also produce *intermodulation* whereby an input of two closely spaced frequencies  $\omega_1$  and  $\omega_2$  will result in an output containing harmonics of these two
- If we return to our Taylor series, we have that

$$v_{out} = a_0 + a_1 v_{in} + a_2 v_{in}^2 + a_3 v_{in}^3 + \dots \quad (5)$$

where  $v_{in} = v_{RF} + v_{LO}$

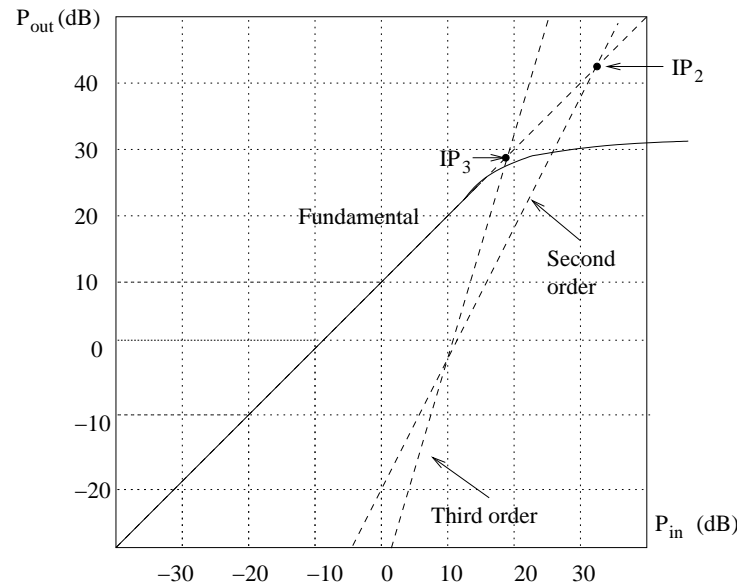
- If  $v_{RF}$  is some combination of two signals at  $\omega_1$  and  $\omega_2$  then:
  - The  $v_{in}^2$  term will result in harmonics at  $2\omega_1$ ,  $2\omega_2$ ,  $\omega_1 - \omega_2$  and  $\omega_1 + \omega_2$  (*second-order harmonics*)
  - $v_{in}^3$  term results in harmonics at  $3\omega_1$ ,  $3\omega_2$ ,  $2\omega_1 + \omega_2$ ,  $2\omega_2 + \omega_1$ , etc. (*third-order harmonics*)
- Need to find good measure of how significant the distortion due to these products are

### Harmonics and output power

- As input power increases, output power will increase (relatively) linearly
- Since the output harmonics go as  $v_{in}^2$ ,  $v_{in}^3$ , etc., increasing the input power will result in a much larger increase in these harmonics than in the fundamental
- Eventually there is more power in the harmonics than in the fundamental
- Can plot these harmonics on a power in vs. power out scale
- This is valid for amplifiers and for mixers (just that for mixers the output power is a different frequency than the input)

### Second and third order intercepts

- Plot of input vs. output power
- Fundamental signal increases with slope of 1
- Second and third order harmonics increase with slope of 2 and 3, respectively





## How to select a mixer

---

Select the proper mixer for your needs. There are hundreds of models available. Under-specify and face marginal performance, over-specify and pay for more than you need. Here's the proper approach.

Mixers are abundant in electronic systems ranging from inexpensive consumer products to sophisticated military hardware. You'll find them in entertainment equipment as well as communications gear, test instruments, radar units and countermeasure systems. Mini-Circuits offers over 400 different off-the-shelf mixer models with thousands of variations available. Different connector configurations, tighter specs, and reliability testing are available on request. Non-optimum mixer selection bears a penalty: under-specify and face marginal performance; over-specify and pay extra for unnecessary performance characteristics.

### Making the right choice

Simply stated, there are three basic steps:

- (1) Deciding on a surface-mount, connector, or plug-in version.
- (2) Selecting the mixer "Level", which is the LO (local oscillator) drive power in dBm required for the application.
- (3) Picking a model that extends over the frequency range involved.

The sequence of these steps follows the manner in which mixer information is accessed when selecting "Frequency Mixers" in the Product Selection menu on the Mini-Circuit website. A general presentation will be given for each of these steps, and then pertinent technical considerations will be discussed in more detail.

At the start it is important to understand your specific needs, so it is strongly recommended that you organize the requirements for your application and put them in writing. Ascertain what frequency ranges (LO, RF, and IF) are involved, and the LO drive you have available. Some applications might specify other factors, such as the acceptable amount of harmonic distortion (caused by mixing of LO and single-tone RF harmonics) and/or two-tone, third-order intermodulation (IM) distortion.

#### I. DETERMINE THE TYPE OF PACKAGE AND CONNECTIONS: SURFACE-MOUNT, PLUG-IN, OR WITH COAXIAL CONNECTORS.

Generally, the user has evaluated the system requirements and will know beforehand whether the mixer is to be mounted on the user's PC board or needs to have coaxial connectors. Mini-Circuits has three types of package available: Users typically install surface-mount components via reflow soldering, and many of such products are aqueous-washable. All plug-in (through-hole) mounting units have at least 4 pins to ensure a mechanically rugged connection to the user's PC board. Some mixers are made with hermetically sealed ceramic diode "quads". Various off-the-shelf mixers are available with BNC or SMA connectors, and specials can be provided with N or TNC connectors. Many connectorized units are available with an optional mounting bracket, as shown on the data sheets. Please describe your connector and bracket requirements when ordering.

## II. DETERMINE THE LO LEVEL REQUIRED.

In applications that specify distortion at a particular value of RF input signal power, such a specification might be the governing factor in determining the choice of mixer level; i.e. Level 7, Level 10, Level 17, etc. As a first-order guide for diode mixers, the LO power should be 10 dB greater than the highest input signal level anticipated. Mini-Circuits High-IP3 mixers utilize field-effect transistors, and among most of those mixers it is sufficient to choose one with LO power 3 dB **less than** the RF power.

In many cases these first-order guidance numbers may be modified. The trade-off is generally between performance and cost. Keep in mind that it is desirable to select the lowest level mixer that will meet the application because it will be more economical to use, and it should result in the least amount of LO leakage within the user's system.

Mini-Circuits offers a wide range of mixers of different levels, from 3 to 27. Referring to Fig. 1, and the discussion on 1 dB compression point on Page 3, select the mixer level for your requirement. For active mixers, which incorporate an amplifier in one of the internal signal paths, as well as for image reject mixers, see the individual data sheets for this information.

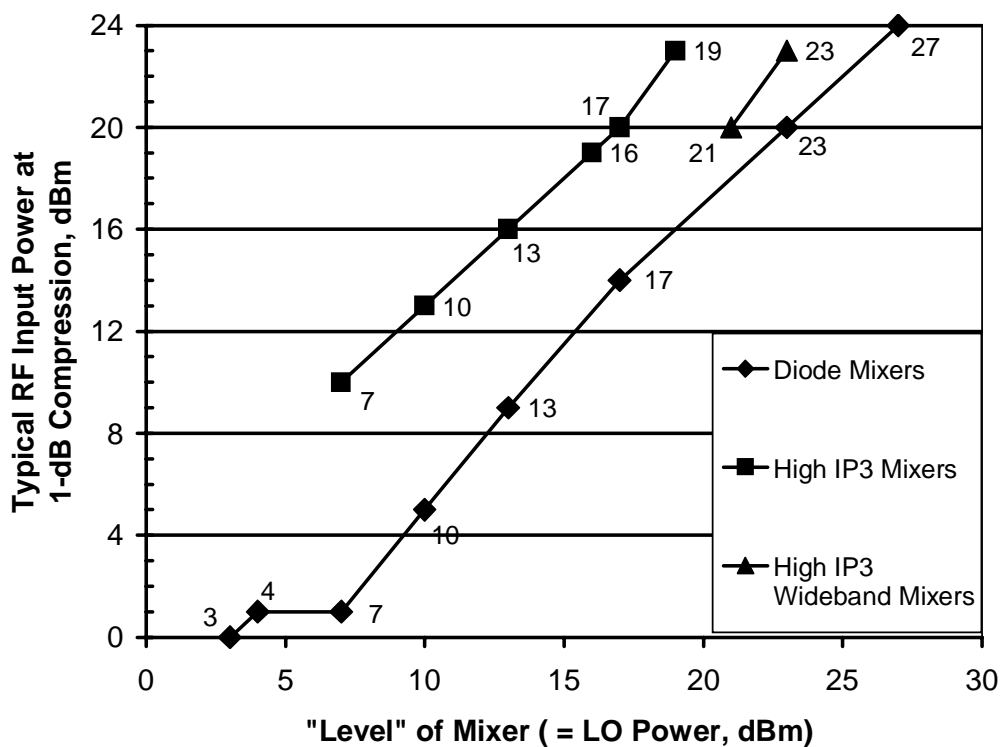


**Figure 1**      Typical RF Input Power at 1-dB Compression of  
Mini-Circuits Mixers Designed for Various LO Levels

### **III. DETERMINE THE FREQUENCY RANGE REQUIRED AND SELECT A MODEL.**

Mini-Circuits offers extremely wideband mixers with a considerable amount of frequency overlap between models. Determine the required frequency range of operation. Then select the mixer whose frequency range specification best "straddles" the range you need. For optimum performance, it is good practice to select a mixer whose midband frequency range (identified by lower-case letter "m" in the specifications) covers the intended operation. Aside from that, all Mini-Circuits mixers perform to specifications with good margin over their entire frequency range. Further, many users operate them outside the specified band with good results, and can still expect to receive high-performing mixers with unit-to-unit repeatability.

#### **1-dB compression point is key to choosing mixer level**

What does the 1dB compression point signify? As RF input level is increased, IF output should follow in a linear manner. Eventually, however, IF output increases at a lower rate until the mixer IF output becomes nearly constant.

The RF input power at which the IF output power deviates from linearity by 1 dB is termed the 1-dB compression point. Fig. 1 on Page 2 displays the RF input level at 1-dB compression for each level of mixers of the different types. The 1-dB compression point is useful in comparing dynamic range, maximum output, and two-tone performance of various mixers. It is a basis on which the user can choose mixer level.

The 1-dB compression point, which is one definition for the high end of a mixer's linear range, is relatively simple to test. It is therefore included on data sheets supplied by Mini-Circuits and by other mixer manufacturers. But, in some applications mixer linearity may be specified otherwise, in accordance with the intended application. For a receiver as an example, two-tone, third-order intermod may be critical. For video applications, percent distortion or intermodulation intercept point may be specified, and in an attenuator measurement system, compression at a given RF input power might be important. A systems engineer needs a convenient means of relating the criterion for a particular application to the published 1-dB compression point. The following linearity criteria will now be discussed in that regard.

1. Maximum RF input power anticipated.
2. Percent distortion.
3. Intermodulation intercept point.
4. Two-tone third-order intermodulation, dBc, at a given RF input in dBm per tone.
5. LO drive power available.
6. No particular spec to meet.

#### **1. MAXIMUM RF INPUT POWER ANTICIPATED.**

If you know this number, simply select the lowest level mixer whose RF input level at 1-dB compression exceeds your requirement for RF input power. For example, if the maximum encountered RF level is +5 dBm, select a Level 13 mixer, rated at +9 dBm typical RF input for 1-dB compression.

## **2. PERCENT DISTORTION.**

The percent distortion is usually specified in terms of voltage. Thus, a 0.1% distortion figure means 0.999 of the desired voltage appears at the mixer output. Next, convert this voltage ratio to a power ratio in dB by squaring and taking ten times the log. The resultant figure is the amount of compression for the specified RF input level. Now this must be extrapolated to 1-dB compression for a corresponding RF input level. As a rule of thumb, extrapolation may be achieved by assuming a linear relationship in dB, between compression and RF input level. Thus, a ten-times increase in compression corresponds to ten-times increase in RF input level.

Let's illustrate with the 0.1 percent distortion example, and say it is specified at -10 dBm RF input. The 0.1 percentage corresponds to a relative 0.999 voltage output; squaring this yields 0.998 power ratio or -0.009 dB. We therefore know that 0.1% distortion at -10 dBm input means the maximum allowable compression is 0.009 dB (stated as a positive number). Extrapolating, using the rule-of-thumb relationship, we state that 0.09 dB compression corresponds to an RF of 0 dBm, and 0.9 dB compression corresponds to a maximum allowable RF input level of 10 dBm. So, which mixer is appropriate? A Level 17 mixer, with +14 dBm RF input level at the 1-dB compression point.

## **3. INTERMODULATION INTERCEPT POINT.**

This is a figure of merit relating to the level of intermodulation products generated by a mixer, amplifier, or other mildly nonlinear device. An intercept point can be defined for a second-order, third-order, fifth-order, or other product. For a diode mixer, as a rule-of-thumb, two-tone third-order intercept point (IP3) is approximately 15 dB above the 1-dB compression point. For a FET mixer, the rule-of-thumb is 10 dB. So, if the intercept point value is given, merely subtract the corresponding number of dB from it and pick a mixer having at least that value of 1-dB compression point.

## **4. TWO-TONE, THIRD-ORDER INTERMODULATION.**

For a mixer, two-tone, third-order intermodulation intercept point (IP3) is usually specified with respect to the RF input. Intermodulation (IM) level on the other hand, is measured at the output, either as power in dBm or as dBc relative to the desired IF signal. To find Input IP3 given the output IM power in dBm, first calculate Output IP3 as:

$$IP3_{OUT} (\text{dBm}) = |IM3_{OUT} (\text{dBm}) - P_{OUT} (\text{dBm})| / 2 + P_{OUT} (\text{dBm}).$$

In this formula  $P_{OUT}$  is the power of the desired IF output signal,  $IM3_{OUT}$  is the power of the third-order intermodulation product in dBm, and  $|IM3_{OUT} - P_{OUT}|$  is the absolute value of the difference in dB between the third-order IM product at the output and the desired IF output.

If output IM is given in dBc, the formula is:

$$IP3_{OUT} (\text{dBm}) = |IM3_{OUT} (\text{dBc})| / 2 + P_{OUT} (\text{dBm}).$$

To convert the Output IP3 obtained from these formulas to Input IP3, add the conversion loss value (a positive number, in dB).

Once the output intercept point is calculated, simply subtract 15 dB or 10 dB (see Paragraph 3 above) to find the 1-dB compression point, and select among mixers having that value of 1-dB compression point or higher.

## **5. LO DRIVE POWER AVAILABLE.**

The LO drive is critical since the function of the LO drive is to switch the mixer diodes fully on and off for lowest distortion. So, for optimum performance, select the mixer level to match the LO drive. Mini-Circuits conveniently identifies its mixer levels by the LO drive requirement; thus a Level 7 mixer refers to a LO drive level of +7 dBm. If there are constraints on the LO power available, select the closest mixer level that is lower than the available LO power. For example, if +12 dBm LO drive is available, select a Level 10 mixer.

## **6. NO PARTICULAR SPEC TO MEET.**

Suppose no linearity spec or criterion is given for your application. Choose a Level 7 mixer. Why? Because it is the most popular and offers the widest choice of models at lowest cost.

## **Frequency range is the final deciding factor**

Once the package style and mixer level have been decided you may find a wide variety of models from which to choose. You may notice models with overlapping frequency ranges. Why? So you can choose the optimum mixer for your requirement.

Frequency specs for RF and LO on most of the mixer data sheets are given in three ranges. The lower frequency range, L, covers the lowest specified frequency to one decade (or in some cases, one octave) higher. The upper frequency range, U, starts one octave below the highest frequency. Mid-range, M, covers the frequency range between L and U. For example, a mixer specified from 0.5 to 500 MHz could offer a low-frequency range of 0.5 to 5 MHz, an upper frequency range of 250 to 500 MHz, and a mid-range of 5 MHz to 250 MHz. Try to select a mixer with the highest low-frequency limit for which the mid-range matches your application. Be sure that the IF frequency range covers your requirements, including whether you need it to go down to DC.

## **What about "Specials"?**

When a particular model has been selected the user must determine if the model will meet the electrical performance criteria the user has generated. All MCL mixers are characterized, and a significant number of performance curves and tabulated data describing the models are given on the data sheets and the "View Data" pages on the website. The performance curves on the data sheets describe typical performance. Sometimes the system designer requires higher isolation, lower conversion loss, temperature tracking of conversion loss, unit to unit tracking of conversion loss, selection of higher order harmonic products, less than 100 microvolts of phase-detector DC offset, larger specified bandwidths, etc. Mini-Circuits offers these special performance criteria and many more. Our high volume production enables us to select units to customer specifications at extremely low cost. Mini-Circuits maintains a highly documented system to handle specialized customer requirements.

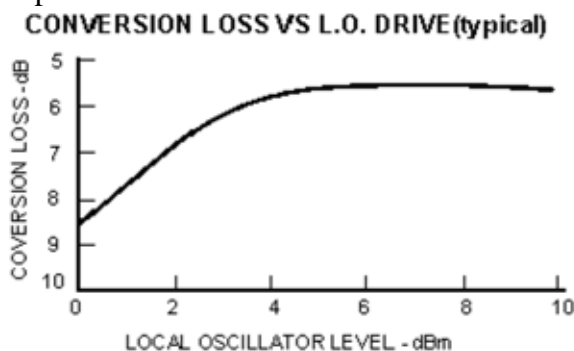
In summary, contact us about "specials" and we'll do our best to satisfy your needs without excessive cost or delivery date extension. Sometimes, "special" means shipping a quantity of mixers within a very short time span; since Mini-Circuits is the largest manufacturer of mixers in the world, you may be pleasantly surprised by the quick response. Try us.

## Practical questions relevant to selecting a mixer

Here are frequently asked questions and their answers.

### ***Q. How critical is LO level in a mixer application?***

**A.** The purpose of the LO signal is to switch the mixer diodes on and off. Mixer manufacturers select fixed LO levels so they can test and specify at each particular level. In practice, however, LO drive can vary with minimal effect on mixer performance. For example, a Mini-Circuits SRA-1 unit is specified at +7 dBm LO level; if the LO drive was only 3 dBm perhaps a 0.5 dB increase in conversion loss might take place. Or, a high-level SRA-1H might experience a 0.3-dB increase in conversion loss if LO level was +14 dBm instead of the specified +17 dBm LO. The curve below illustrates how conversion loss varies with LO power for a Level 7 mixer.



### ***Q. I notice Mini-Circuits offers many series of mixers, such as the ADE, MCA1, SIM, SRA, SYM, TFM, ZX05, etc. including over 450 models. Why so many models?***

**A.** Mixers are used in systems covering communications, weapons, test instruments, radar, data transmission and countless other applications. A mixer manufacturer can opt to produce a dozen models and thus, in a sense, force the design engineer to compromise specific system needs by offering a rather narrow selection. Mini-Circuits approach is to offer a wide variety so the designer can buy just what is needed, and thus neither compromise system performance nor pay for more than is really needed. That's why Mini-Circuits offers more off-the-shelf models than all other manufacturers combined. But that's not enough. As needs change, new models will become available. For example, the recent demand for higher density packaging has been filled by Mini-Circuits surface-mount mixers such as ADE, MCA1, and SIM series, more than doubling packaging density on a PC board. Finally, although we list over 450 off-the-shelf models, we can supply a great number of variations (such as connector configurations, tighter specs, etc.) at our customers' request.

### ***Q. What's the difference between "Level 7", "Level 10", and "Level 27" mixers?***

**A.** The different levels of mixers are determined by the LO drive required for a particular application. Thus, each level of mixer has been optimized for a given LO drive, and will offer low distortion even at the maximum input level specified for the mixer. The higher the level of mixer, the lower the distortion expected. It is obvious that the highest level mixer could satisfy most requirements. However, high LO drive would be necessary and the cost of a level 27 mixer is higher than a lower level mixer. Thus, rather than over-specify, select the level of mixer that will optimize your system.

### ***Q. I don't have enough LO drive even for a level 3 mixer. What can I do?***

**A.** Level 3 mixers, although specified for +3dBm LO, will operate well with LO drive as low as 0 dBm. However, there is some degradation: about 0.5 to 1.5 dB additional conversion loss among

various Level 3 models. Also, the upper frequency limit might be slightly reduced and there may be increase in two-tone, third-order IM.

***Q. I am operating over a wide bandwidth and my LO drive level changes by about 3 dB. How should I take this into account when I select a mixer?***

**A.** The preferred approach would be to determine your lowest LO drive level over the band and then select a mixer for this drive level. Remember that as LO level increases over the nominal (to +10 dBm for a level 7 mixer), conversion loss remains flat and thus optimum performance will be maintained and not degraded.

***Q. From my requirement for intercept point, I have selected a Level 13 mixer. Can I apply a +7dBm LO drive and expect the high performance specified in the data sheets?***

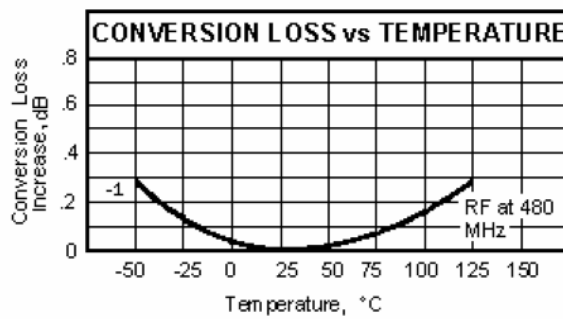
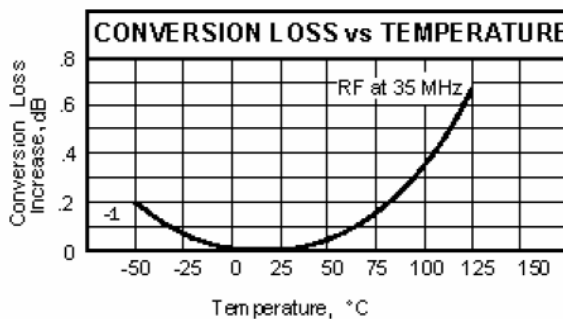
**A.** No. Performance to the specifications take place when the mixer diodes are driven fully "on" by the LO drive. Therefore, when LO drive is insufficient, the diodes operate on a lower-current portion of their I-V characteristic curve. The resulting increase in diode non-linearity increases distortion of the output signal. That is why Mini-Circuits offers so many different mixer levels, so that the user can choose optimally.

***Q. I need a mixer with flat conversion loss over my frequency range spec. How do I go about selecting a model?***

**A.** Conversion loss over the midrange response of a mixer is usually flat. So select a mixer that has a midrange response covering the frequency range you need. Also, the VSWR of the mixer (especially the RF and IF ports) should be checked in order to minimize mismatch errors which could compromise the conversion loss flatness.

***Q. I expect wide temperature extremes for my latest RF design project and mixer conversion loss vs. temperature concerns me. What advice can you offer?***

**A.** For extremely cold environments (down to -55°C), to maintain flat conversion loss, pick a mixer that operates a minimum of two octaves below your lowest frequency of operation. For example, if your application involves operation at 30 MHz, select a mixer that extends to 7.5 MHz or lower. Why? The permeability of the ferrite core in the mixer transformer will drop at reduced temperature, resulting in higher losses or frequency fall-off at the low end of the band. In extremely high-temperature environments, the mixer diodes will be the predominant factor affecting conversion loss. Diode impedance will change and cause mixer mismatch to upset flat conversion loss. So, select a mixer whose upper frequency is an octave higher than that of your application. For example, if you are concerned with high-temperature performance at 500 MHz, select a mixer good up to 1000 MHz (such as the SRA-2CM or TFM-2).



***Q. Do you supply a mixer with a specified maximum VSWR?***

**A.** Generally, a maximum VSWR spec is not given in the mixer data sheets. You can find typical performance data of mixers including VSWR on our website. As a general rule, try to select a mixer whose midrange covers your frequency band of interest. If you need to specify a maximum VSWR requirement, Mini-Circuits can screen and test to meet your needs.

***Q. My application involves maximum RF input signal levels of -20 dBm. I notice the 1- dB compression point specification of many mixers is at +1 dBm and higher. Should this spec be of concern to me?***

**A.** Yes, if two-tone, third-order IM is critical or if receiver response to unwanted signals is important. The 1-dB compression point is related to the intercept point, which is a "figure-of-merit" of the linearity or distortion characteristic of a mixer. It also indicates the susceptibility of the mixer to unwanted signals.

***Q. I need a mixer that nominally operates at + 10 dBm LO drive but requires protection against sudden surges of RF input power as high as 200 mW. What mixer should I select?***

**A.** To avoid damage from a 200 mW input signal, choose a Level 17 mixer. Reason: a Level 17 mixer contains eight diodes, and is rated at 200 mW maximum RF power. But, there is a penalty. For minimum distortion, you'll require +17 dBm LO drive, which may be higher than your original intent. Or, you can operate at a lower LO drive and accept an additional conversion loss of 1.0 to 1.5 dB.

***Q. I have an application requiring an RF frequency response from 100 Hz to 10 MHz. I don't see any mixers specified with an RF this low. What can I do?***

**A.** One of the characteristics of double-balanced mixers (DBM) is that for most models IF response extends down to DC. All ports of the DBM are balanced and isolated from each other. Therefore, if the high-frequency response of the IF port is sufficient to handle the RF signal in your application, simply connect the RF input signal to the IF port and take the IF output from the RF port. Make sure the RF frequency response of the mixer will accommodate the IF frequency requirements, since in this configuration the IF (formerly the RF) does not go down to DC.

Disadvantages? Yes. Generally, the linearity characteristic will not be as good as with the signal connected in the conventional manner. Also, there is a danger that transients at the RF port (previously the IF port) can damage the diodes internal to the mixer.

# Selecting high linearity mixers for wireless base stations

Stephanie Overhoff, Field Applications Engineer  
Maxim Integrated Products, Inc.

*Today's communication systems like wireless base stations make strong demands on receiver sensitivity and large-signal performance. This article focuses on mixers, and describes key mixer performance issues and the basic parameters specified in data sheets. The article explains how to select the best mixer to optimize the receive channel.*

## Introduction

The communication standards for wireless base stations—e.g., GSM, UMTS, and (now) LTE—define minimum specifications for various parameters including receiver sensitivity and performance in the presence of large signals. These key requirements make heavy demands on every functional block of the radio in a wireless base station. In the receive signal path, mixer performance has a major impact on the receiver's sensitivity and large-signal performance. This article describes key mixer performance issues and parameters to help you select the best mixer for your receive channel.

## A wireless base-station receiver

To start, we first analyze the block diagram of a typical receiver used in wireless base stations (**Figure 1**). These receivers are called superheterodyne receivers

because the received signal undergoes two consecutive downconversions to lower frequencies. As shown, the signal is received by the antenna and then filtered by RF filter 1, which is normally used to filter out trash signals. This filter output is then amplified by an LNA (low-noise amplifier), which normally has a very low noise figure.

The amplified signal is again filtered, this time by RF filter 2, which limits the frequency range while filtering out unwanted signals that can limit the mixer's performance. The filtered and band-limited signal is then fed to the first mixer, where it is downconverted to an IF frequency by mixing with an LO's (local oscillator's) signal. Depending on the receiver's architecture, this IF signal can be further downconverted to a second, lower-IF frequency, and then demodulated for processing in the baseband.

We now examine the mixers in this receiver chain. The mixers' parameters should be investigated because they have a major effect on the receiver's sensitivity and large-signal performance.

## Mixer parameters

The noise figure of a mixer describes the degradation in SNR (signal-to-noise ratio) from input to output. That ratio is normally expressed in the logarithmic measure of decibels (dB), as shown in Equation 1:

$$NF = 10 \log \frac{SNR_{RF}}{SNR_{IF}} \quad [dB] \quad (\text{Eq. 1})$$

A second important parameter is the conversion gain (or alternatively, conversion loss). Conversion gain gives an important indication whether the mixer configuration is active or passive. Passive mixers have insertion loss (called conversion loss) because they include no components for amplifying the signal. Active mixers, however, have active components and provide conversion gain.

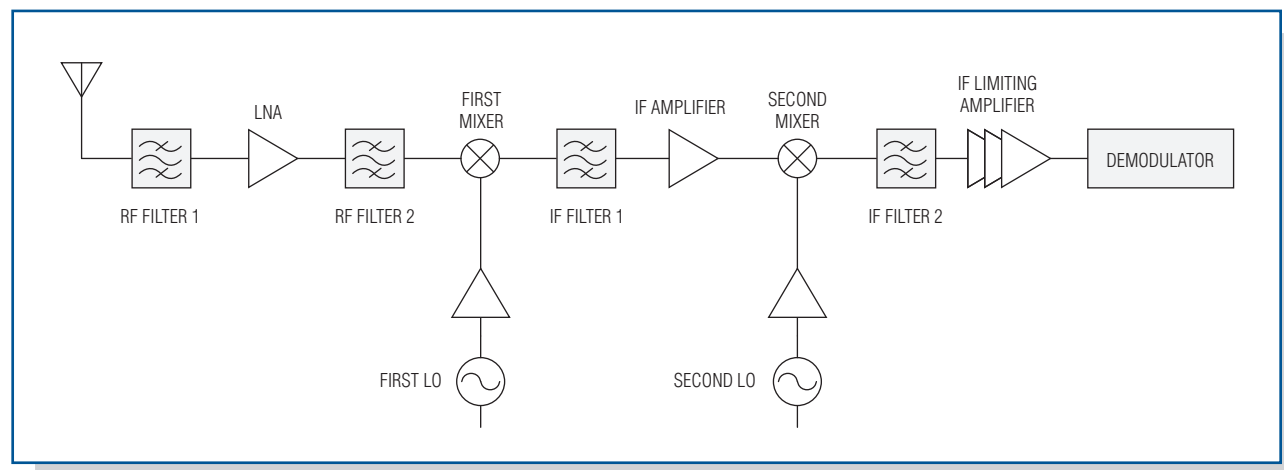


Figure 1. Block diagram of a typical wireless base-station receiver.

An active mixer can be realized in either of two configurations: as an integrated mixer based on a balanced (Gilbert cell) design; or as a passive mixer that is combined with an IF amplifier stage to provide gain instead of loss. Because the integrated mixer has gain, it requires no external IF amplifier stage to make up for insertion loss.

$$\text{Conversion gain / loss} = G = \frac{P_{\text{RF}}}{P_{\text{IF}}} \quad [\text{dB}] \quad (\text{Eq. 2})$$

Conversion gain (or loss) is a logarithmic measure expressed in dB, as seen in Equation 2. It is frequency dependent, and should be specified over the mixer's entire operating frequency range. To ensure optimal receiver performance, the variation of conversion gain/loss over the specified frequency range should be as small as possible.

Because wireless base stations usually operate in a fluctuating temperature environment, the conversion gain/loss should also be specified over the operating temperature range, again with as small a variation as possible. This temperature range is important because under normal conditions a small variation with temperature allows a smaller headroom, which is useful in system planning.

The large-signal behavior of a mixer is described by a mixer parameter called the “1dB compression point,” also called compression point (IP<sub>1dB</sub>), and the second- and third-order intercept points (IP<sub>2</sub> and IP<sub>3</sub>). The IP<sub>1dB</sub> compression point predicts the level of input power at which the mixer gain is reduced by 1dB, with respect to the linear expression in Equation 3:

$$P_{\text{OUT}} = G \times P_{\text{in}} \quad (\text{Eq. 3})$$

A mixer should also be able to convert a weak signal when two large signals of nearly the same frequency are applied to the mixer's input. This behavior is normally described by the third-order intercept point (IP<sub>3</sub>), which together with the noise figure describes the dynamic range of the mixer. A large IP<sub>3</sub> indicates a high-linearity mixer. The mixer's data sheet should also specify intercept points for the mixer's input and output. Using Equation 4, you can calculate the OIP<sub>3</sub> (output intercept point) from the IIP<sub>3</sub> (input intercept point), and vice versa:

$$\text{OIP}_3 = \text{IIP}_3 + G \quad (\text{Eq. 4})$$

Where OIP<sub>3</sub> is the intercept point at the mixer's output, IIP<sub>3</sub> at the input, and G is the conversion loss or gain. The OIP<sub>3</sub> for a passive mixer is, therefore, reduced by the mixer's conversion loss. This insertion loss requires compensation in either the RF or IF gain stages in order to establish the receiver's desired overall noise figure. (The noise figure is an additional parameter that must be accounted for in the receiver design.)

## Passive vs. active mixers

A major advantage of passive mixers is that they can also be used as frequency upconverters. In other words, their input signals can be converted to a higher frequency. An upconverter is normally employed in a transmitter chain, where it converts an IF signal to the final transmit frequency. Because a passive mixer can be used in the transmit chain as well as the receiver chain, you need to order and stock only one component.

A “direct downconversion receiver” directly downconverts input signals to the baseband without requiring an IF signal. For these receivers, the mixer's data sheet should specify another important parameter called port-to-port isolation. This parameter measures the amount of isolation between the LO's signal and the mixer's input signal. If port-to-port isolation is not large enough, the LO can mix with itself, producing a DC offset at the mixer output that degrades the receiver's performance.

Because a mixer converts frequencies, it generates new frequencies called mixer spurs. Spurs should be investigated thoroughly, especially those at (2RF - 2LO), (3RF - 3LO), and higher orders that affect the receiver by coinciding with its IF frequencies. This behavior is usually described in a mixer's data sheet by the 2 x 2 and 3 x 3 parameters.

Besides these various parameters, you must also consider the level of integration. Some applications can benefit by integrating the mixer core with an LO amplifier, baluns, and LO switch.

## A common PCB receiver layout yields design flexibility

Today the development effort can be reduced by using one layout for different frequency ranges. A receiver designed for a 900MHz GSM system can then be used for an 1800MHz GSM system, just by changing a few key components.

A family of pin-compatible mixers is ideally suited for applications in which a common PCB layout accommodates multiple frequency bands for the wireless infrastructure. The ultimate goal is to develop a single layout for a multistandard wireless base station that handles GSM, UMTS, WiMAX™, and LTE.

A passive mixer like the **MAX2029** in the receiver chain, for example, can downconvert the receiver signal, while another identical mixer in the transmitter can upconvert the IF signal to the final transmit frequency. The circuit in **Figure 2** integrates all the external components: LO buffer amplifier, baluns, and LO switch.

Used as a downconverter, the MAX2029 delivers 36.5dBm of IIP<sub>3</sub>, 27dBm of IP<sub>1dB</sub>, 6.5dB of conversion loss, and a

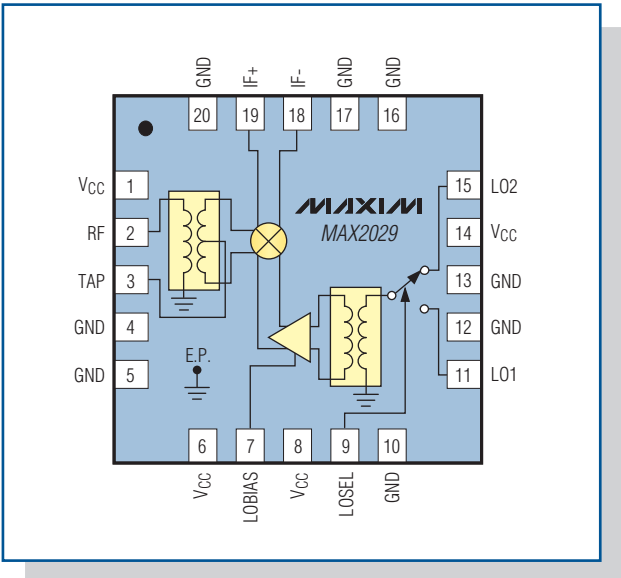


Figure 2. Block diagram of a passive mixer.

6.7dB noise figure. Because the MAX2029's SiGe process technology enables impressive performance, it is well suited for base-station applications in which high linearity and a low noise figure are critical.

The 2RF - 2LO rejection (72dBc with a -10dBm RF input signal) enables simpler and more cost-effective filters by easing the requirements for filtering the close-in harmonics. The MAX2029 expands the frequency range at the lower end from 815MHz to 1000MHz. As one member of a pin-compatible mixer family, which includes the **MAX2039** and **MAX2041**, the MAX2029 allows the creation of a single PCB layout for receivers that handles different frequency ranges and different communication standards.

Active mixers can take the form of either a balanced (Gilbert cell) design, or a passive mixer combined with an IF amplifier stage. The **MAX9986**, for example, represents the second configuration. Its low noise figure allows less RF gain ahead of the mixer stage, which in turn enables better overall linearity for the receiver. Again, as more gain is added in front of the mixer to minimize the cascaded noise figure, the mixer's linearity must be higher to maintain overall receiver linearity.

A similar article appeared in German in *Elektronik Informationen* in July 2008, and in English in *High Frequency Electronics Magazine* in October 2009.

WiMAX is a trademark of the WiMAX Forum.

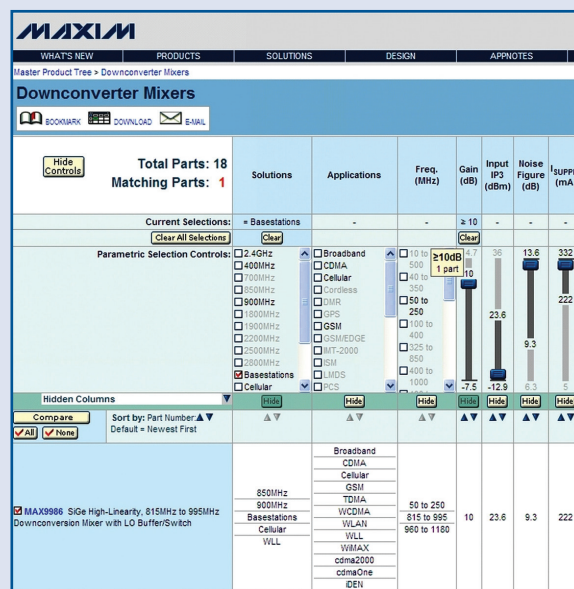
## Choose the right mixer

When searching the Internet for a mixer, the challenge is to sift through all the specifications listed for the various mixers. Then you must make an optimum choice. Fortunately, a web-based parametric search tool will help you do just that. The parametric search enables design engineers to quickly find the right IC for an application. A single page shows all the search criteria for filtering information and all the corresponding parts. Changing any of these criteria updates the parts list immediately. Search features include single-click filtering, sliding filter controls, multilevel sorting, and abundant tool tips. There is no easier way to find the right part for an application.

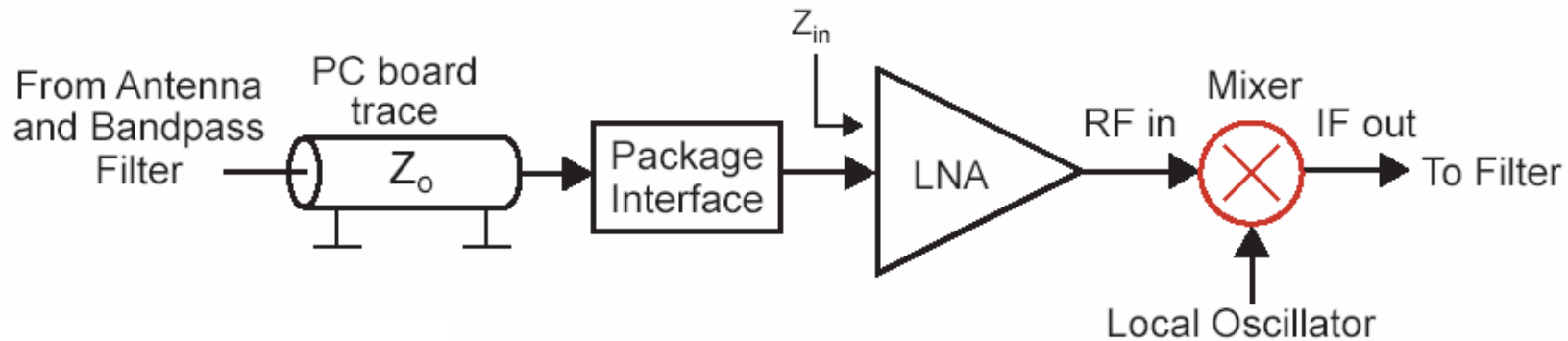
**Figure 3** shows the search results for an active mixer with 10dB gain, designed especially for base stations. The part proposed is a MAX9986. An additional click on that component leads the user directly to the component's QuickView homepage, where the associated data sheet, application notes, and other information can be found.

A parametric search with this web tool from Maxim reveals the number of products that match a specific combination of filter settings—before the user makes the first click. The “smart” search algorithm shows

only valid criteria. The user cannot make selections that eliminate all parts. Built using the latest Web 2.0 technologies, this [parametric search](#) requires no plug-ins on the user's system



# Mixer Design Overview

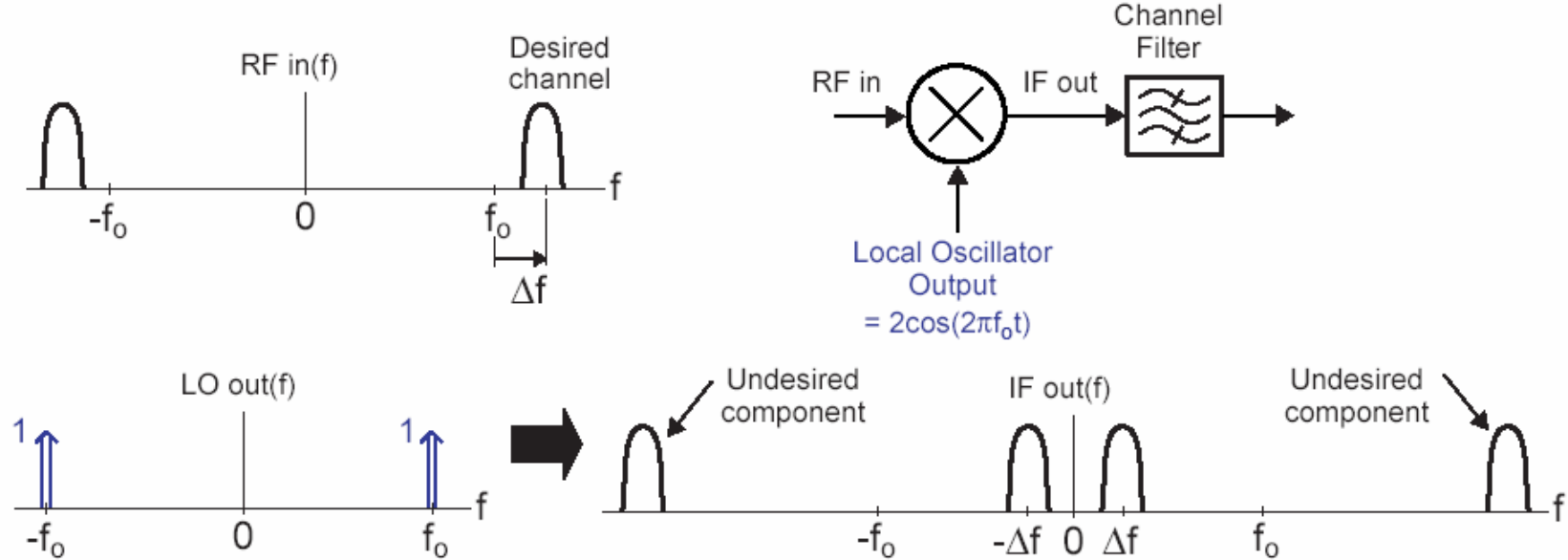


- ❑ Noise Figure – impacts receiver sensitivity
- ❑ Linearity (IIP3) – impacts receiver blocking performance
- ❑ Conversion gain – lowers noise impact of following stages
- ❑ Power match – want maximize voltage gain rather than power match for integrated designs
- ❑ Power – want low power dissipation
- ❑ Isolation – want to minimize interaction between the RF, IF, and LO ports
- ❑ Sensitivity to process/temp variations – need to make it manufacturable in high volume

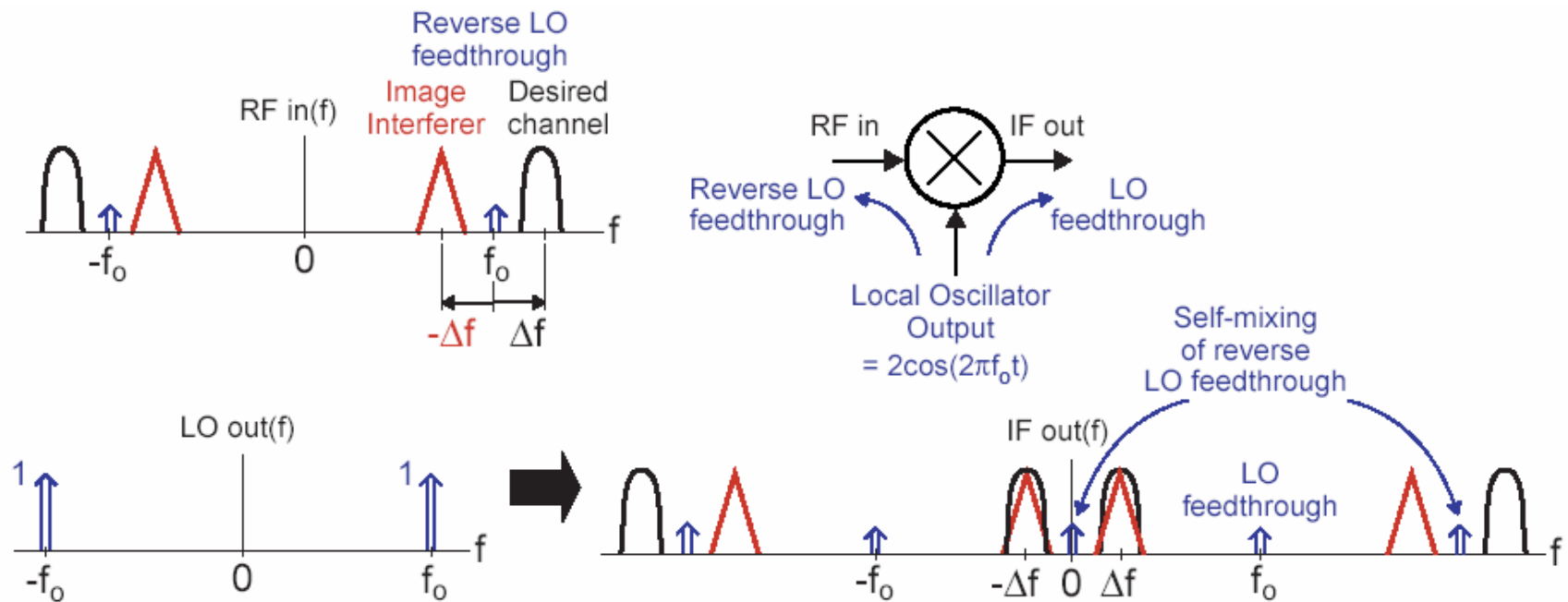
# Types of Mixer

- ❑ Multiplication through device non-linearity
- ❑ Multiplication through switching
  - Active mixers
  - Passive mixers

# Ideal Mixer Behavior

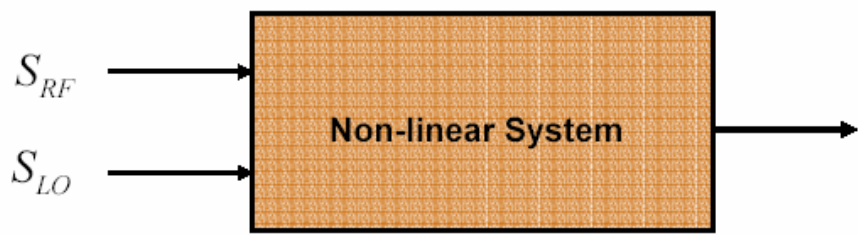


# Non-Ideality in Mixers



- ❑ **Image problem**
- ❑ **LO feedthrough**
- ❑ **Self mixing due to reverse LO feedthrough**

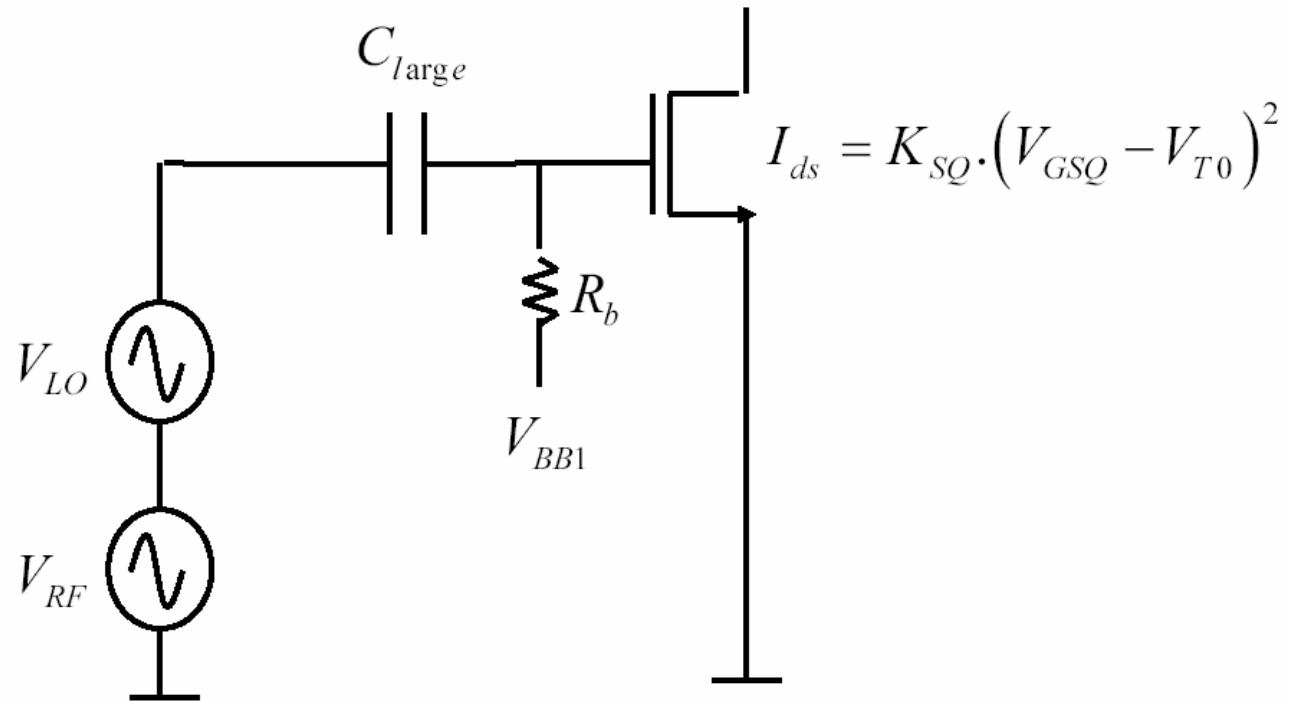
# Mixer Based on Non-Linearity



$$\begin{aligned}S_{MIX} = & a_1 S_{RF} + a_2 S_{RF}^2 + a_3 S_{RF}^3 + \dots \\& + b_1 S_{LO} + b_2 S_{LO}^2 + b_3 S_{LO}^3 + \dots \\& + c_1 S_{RF} S_{LO} + c_2 S_{RF}^2 S_{LO} + c_3 S_{RF} S_{LO}^2 + \dots\end{aligned}$$

- Drain current of an MOSFET exhibits a square dependence on gate overdrive
- Collector current of an BJT exhibits a exponential dependence on base-emitter voltage drive

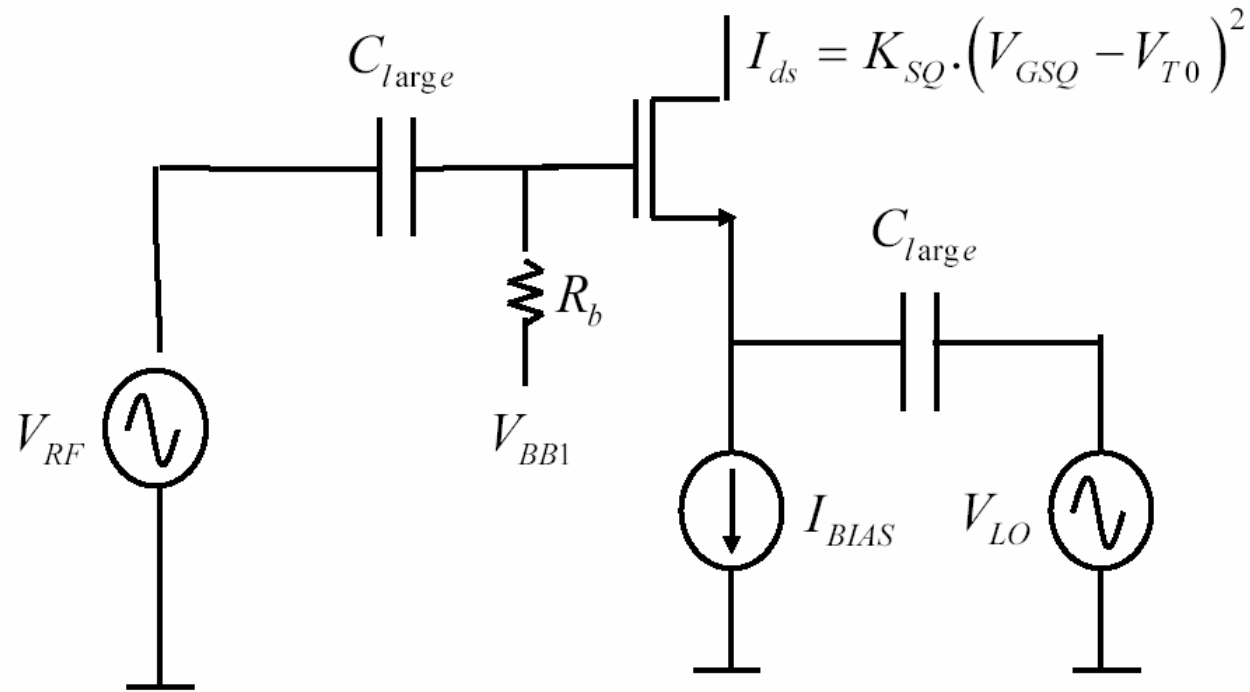
# Single-Device Mixer Using MOSFET (Square-Law Mixer)



$$\begin{aligned} I_{ds} &= K_{SQ} \cdot (V_{bias} + V_{RF} + V_{LO} - V_{T0})^2 \\ &= K_{SQ} \cdot \left\{ (V_{bias} - V_{T0})^2 + (V_{RF} + V_{LO})^2 + 2(V_{bias} - V_{T0})(V_{RF} + V_{LO}) \right\} \end{aligned}$$

$$i_{ds}(\omega_{LO} \pm \omega_{RF}) = K_{SQ} \cdot V_{RF} \cdot V_{LO} \left\{ \boxed{\cos(\omega_{LO} - \omega_{RF})t} + \cos(\omega_{LO} + \omega_{RF})t \right\}$$

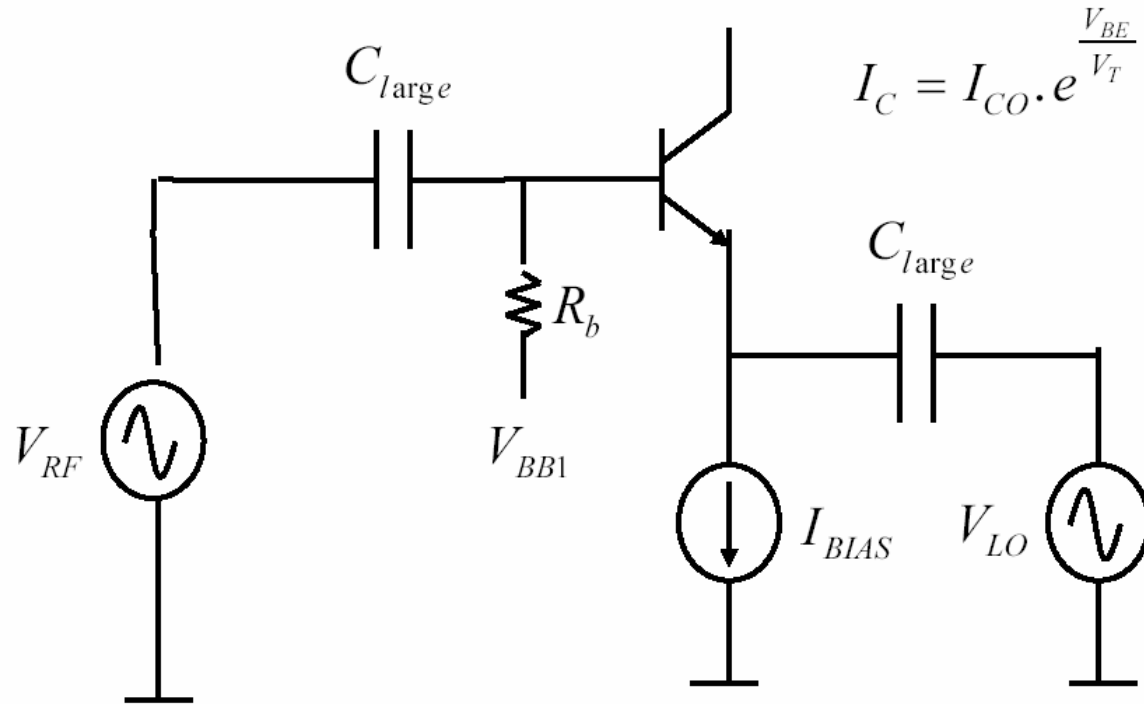
# Practical Configuration for Single-Device Mixer



$$i_{ds}(\omega_{LO} - \omega_{RF}) = K_{SQ} \cdot V_{RF} \cdot V_{LO} \cdot \cos(\omega_{LO} - \omega_{RF})t$$

$$\begin{aligned} \text{Transconductance-conversion-gain} &= G_c = \frac{i_{ds}(\omega_{IF} = \omega_{LO} - \omega_{RF})}{V_{RF}(\omega_{RF})} \\ &= K_{SQ} \cdot V_{LO} = \frac{\mu C_{ox} W}{2L} \cdot V_{LO} \end{aligned}$$

# Single-Device Mixer Using BJT



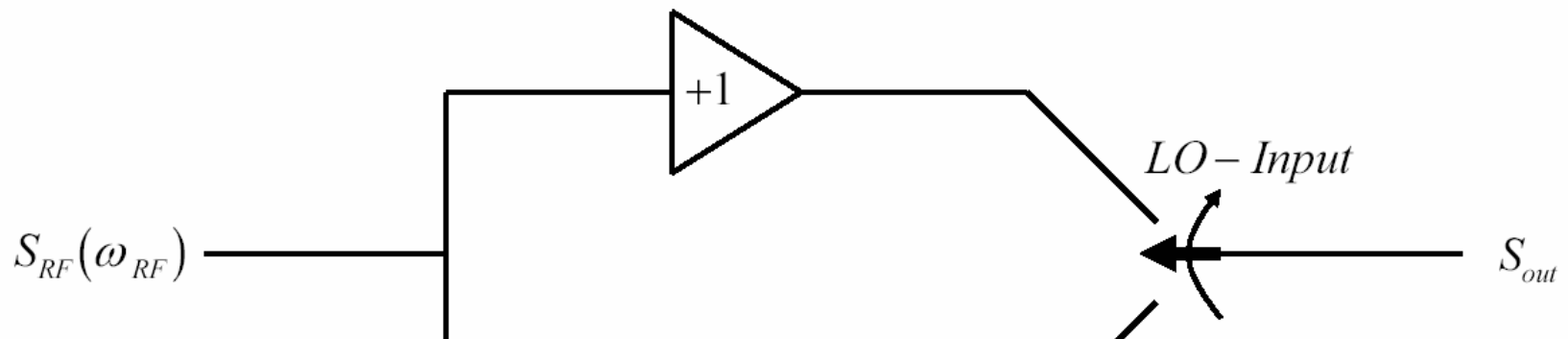
$$I_C = I_{CO} \cdot e^{\frac{V_{RF} - V_{LO}}{V_T}} = I_{CO} \cdot \left\{ 1 + \left( \frac{V_{RF} - V_{LO}}{V_T} \right) + \left( \frac{V_{RF} - V_{LO}}{V_T} \right)^2 + \dots \right\}$$

$$\text{Transconductance-conversion-gain} = G_c = \frac{i_C (\omega_{IF} = \omega_{LO} - \omega_{RF})}{V_{RF}(\omega_{RF})} = \frac{I_{CO}}{V_T^2} \cdot V_{LO}$$

# Design Considerations for Mixer Based on Device Non-Linearity

- ❑ Design simplicity
- ❑ Noise Figure
  - The square law MOSFET mixer can be designed to have very low noise figure
- ❑ Linearity
  - By operating the square law MOSFET mixer in the square law region the linearity of the mixer can be improved considerably
  - BJT mixer is less linear as it produces a host of non-linear components due to the exponential nature of the BJT mixer
- ❑ Power Dissipation
  - Very low power dissipation due to single device operation
- ❑ Power Gain
  - Reasonable power gain can be achieved
- ❑ Isolation
  - Poor isolation from LO to RF port – by far the biggest short coming

# Mixing Through Switching



$$S_{out} = S_{RF} \cdot \cos(\omega_{RF} t) \otimes \{ \dots \text{ (switches)} \dots \}$$

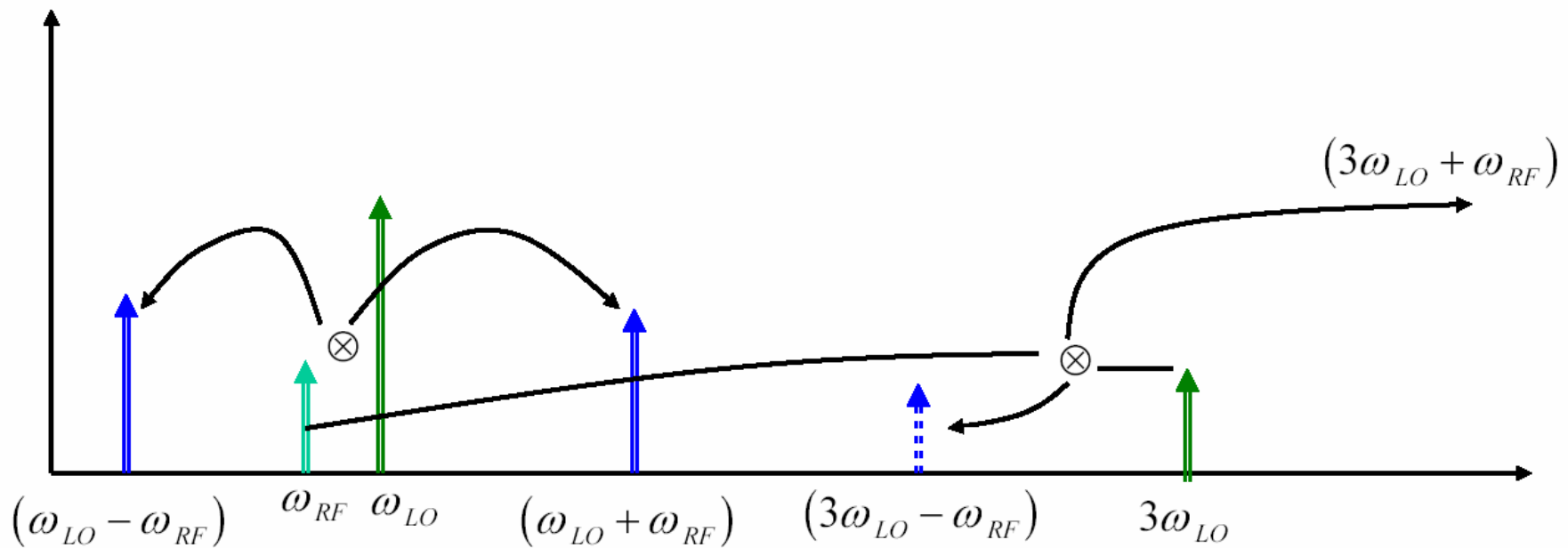
A timing diagram below the equation shows a series of rectangular pulses. The top pulse is labeled '+1' and the bottom pulse is labeled '-1'. These pulses represent the state of the second switch over time.

$$S_{out} = S_{RF} \cdot \cos(\omega_{RF} t) \otimes \left\{ \frac{4}{\pi} \cos(\omega_{LO} t) - \frac{4}{3\pi} \cos(3\omega_{LO} t) + \frac{4}{5\pi} \cos(5\omega_{LO} t) - \dots \right\}$$

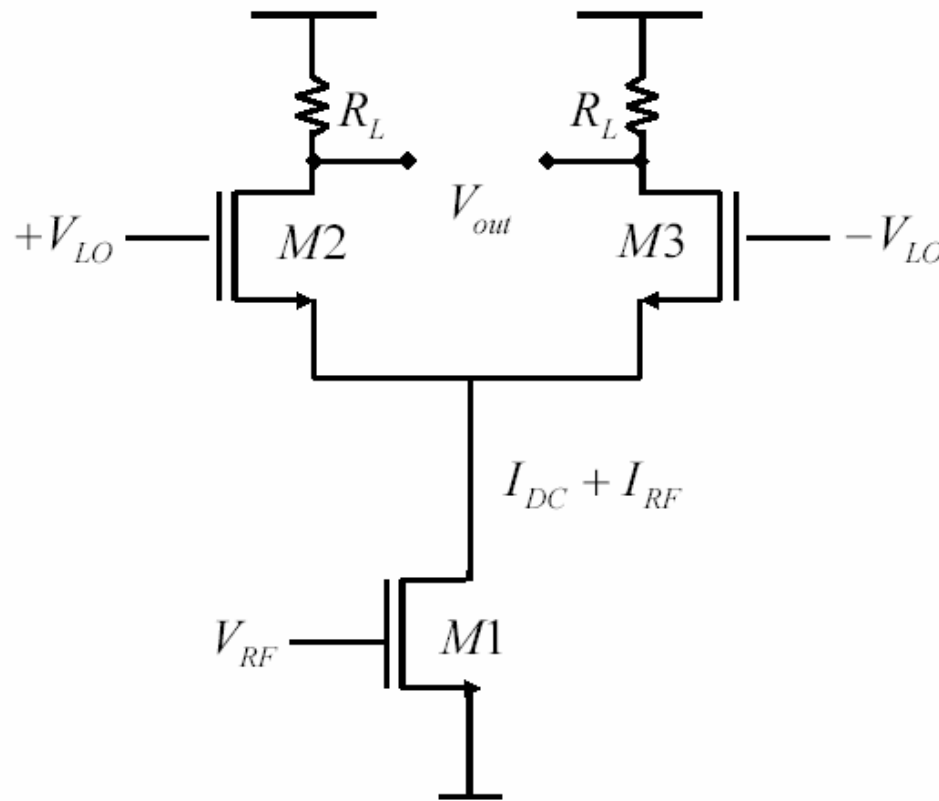
# Spectral Components Due to Mixing

$$S_{out} = S_{RF} \cdot \cos(\omega_{RF}t) \otimes \{ \dots \text{ } \overset{+1}{\underset{-1}{\boxed{\text{ }}}}\text{ } \dots \text{ } \dots \text{ } \dots \text{ } \dots \text{ } \dots \}$$

$$S_{out} = S_{RF} \cdot \cos(\omega_{RF}t) \otimes \left\{ \frac{4}{\pi} \cos(\omega_{LO}t) - \frac{4}{3\pi} \cos(3\omega_{LO}t) + \frac{4}{5\pi} \cos(5\omega_{LO}t) - \dots \right\}$$

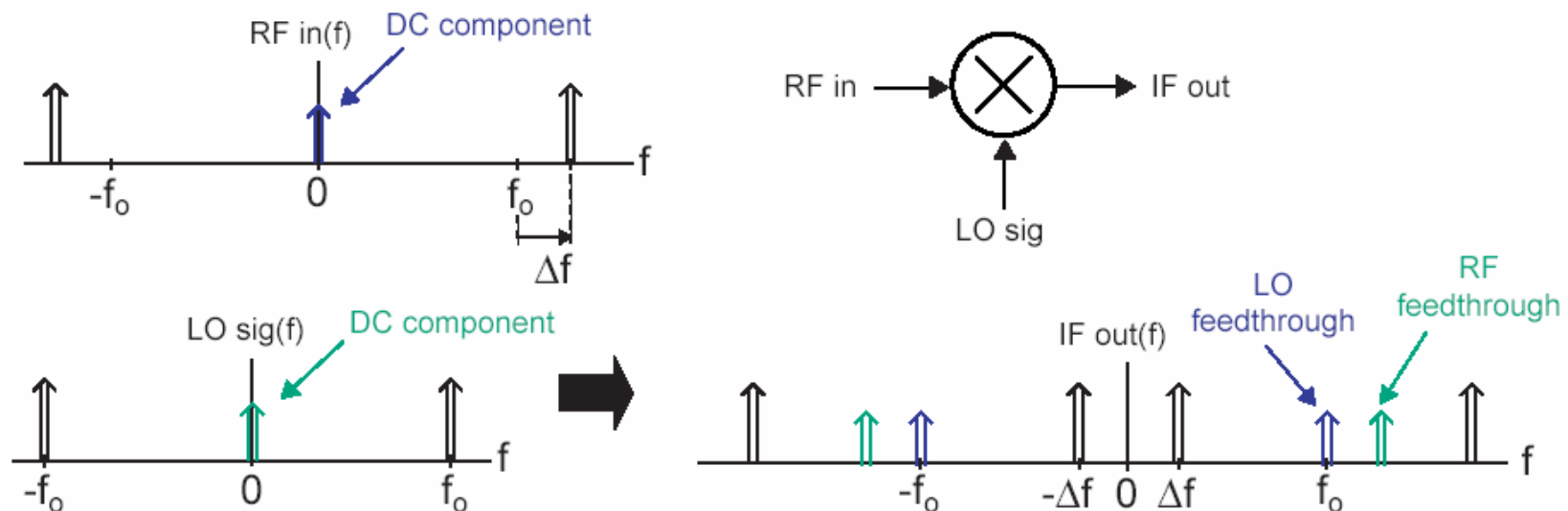


# Simple Switching Mixer (Single-Balanced Mixer)



- M1 acts as a transconductance to convert the RF voltage signal to a current
- M2 and M3 commute the current between the two output branches.

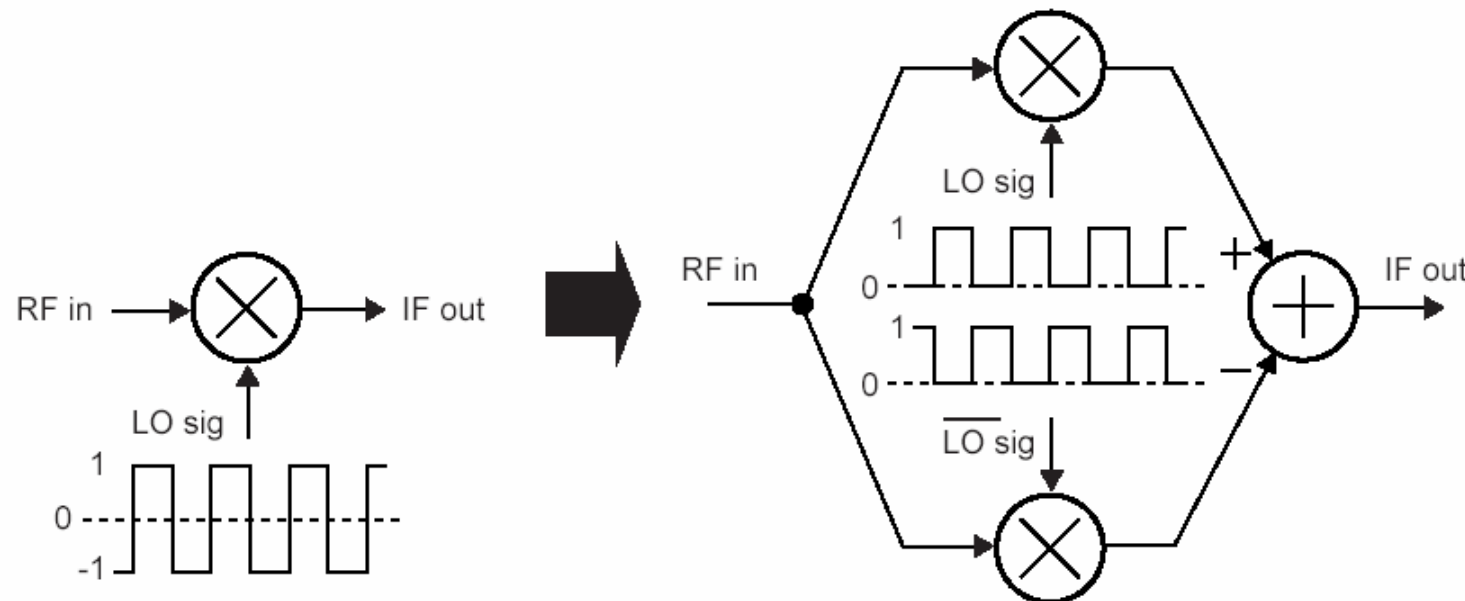
# The Issue of Balance in Mixers



- A balanced signal is defined to have a zero DC component
- Mixers have two signals of concern with respect to this issue – LO and RF signals
  - Unbalanced RF input causes LO feedthrough
  - Unbalanced LO signal causes RF feedthrough
- Issue – transistors require a DC bias

# Achieving Balanced LO Signal with DC Baising

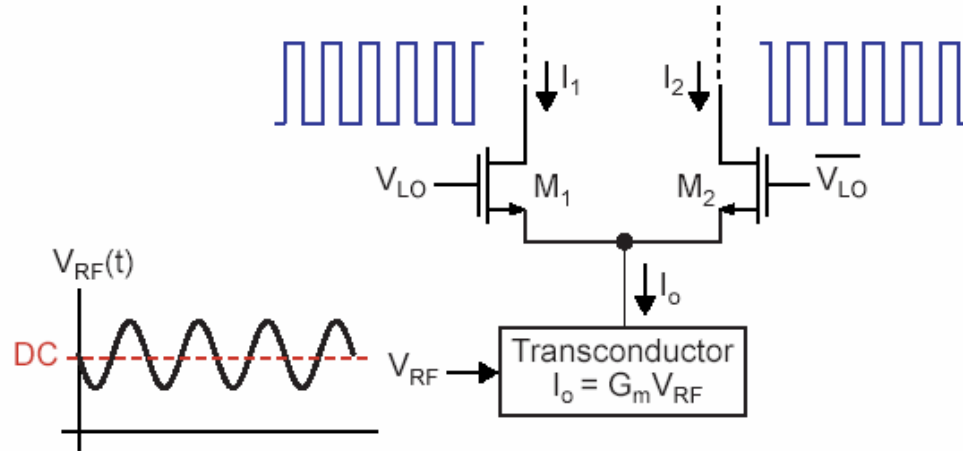
- Combine two mixer paths with LO signal 180 degrees out of phase between the paths



$$RF(t) \cdot [LO(t) - \overline{LO(t)}] = RF(t) \cdot LO(t) - RF(t) \cdot \overline{LO(t)}$$

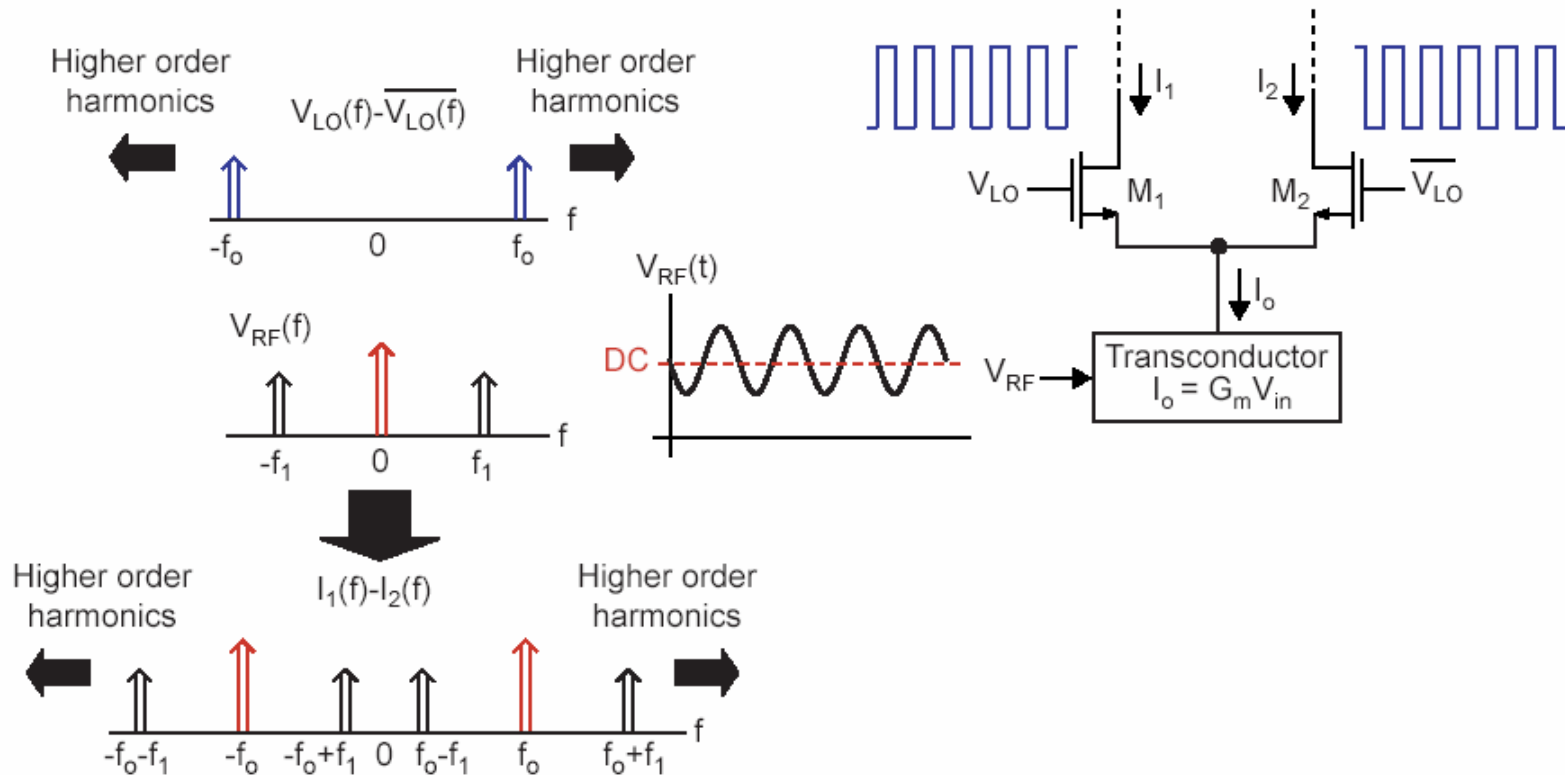
- DC component is cancelled

# Single-Balanced Mixer



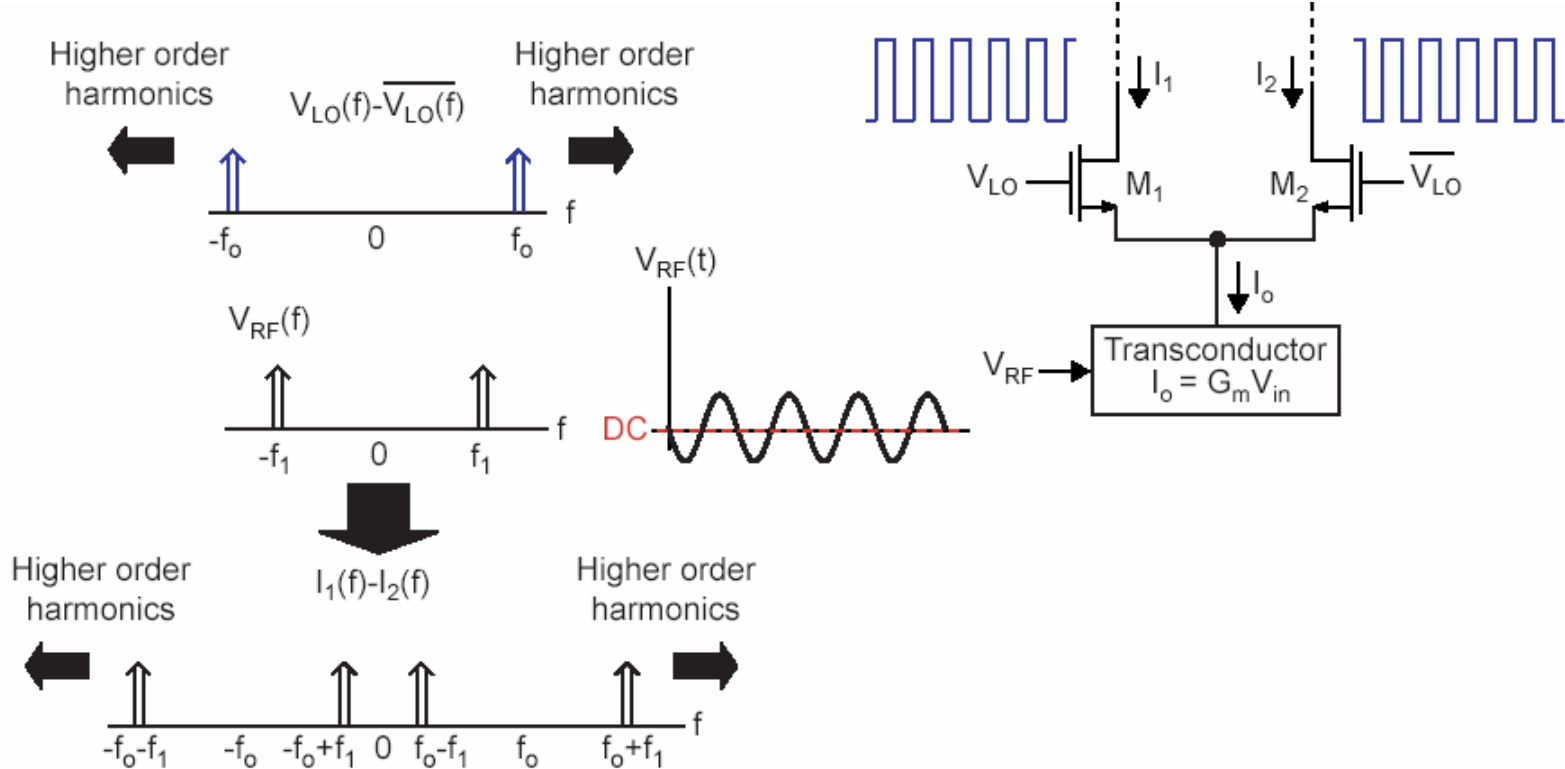
- Works by converting RF input voltage to a current, then switching current between each side of differential pair
- Achieves LO balance using technique on previous slide
  - Subtraction between paths is inherent to differential output
- LO swing should be no larger than needed to fully turn on and off differential pair
  - Square wave is best to minimize noise from  $M_1$  and  $M_2$
- Transconductor designed for high linearity

# LO Feedthrough in Single-Balanced Mixers



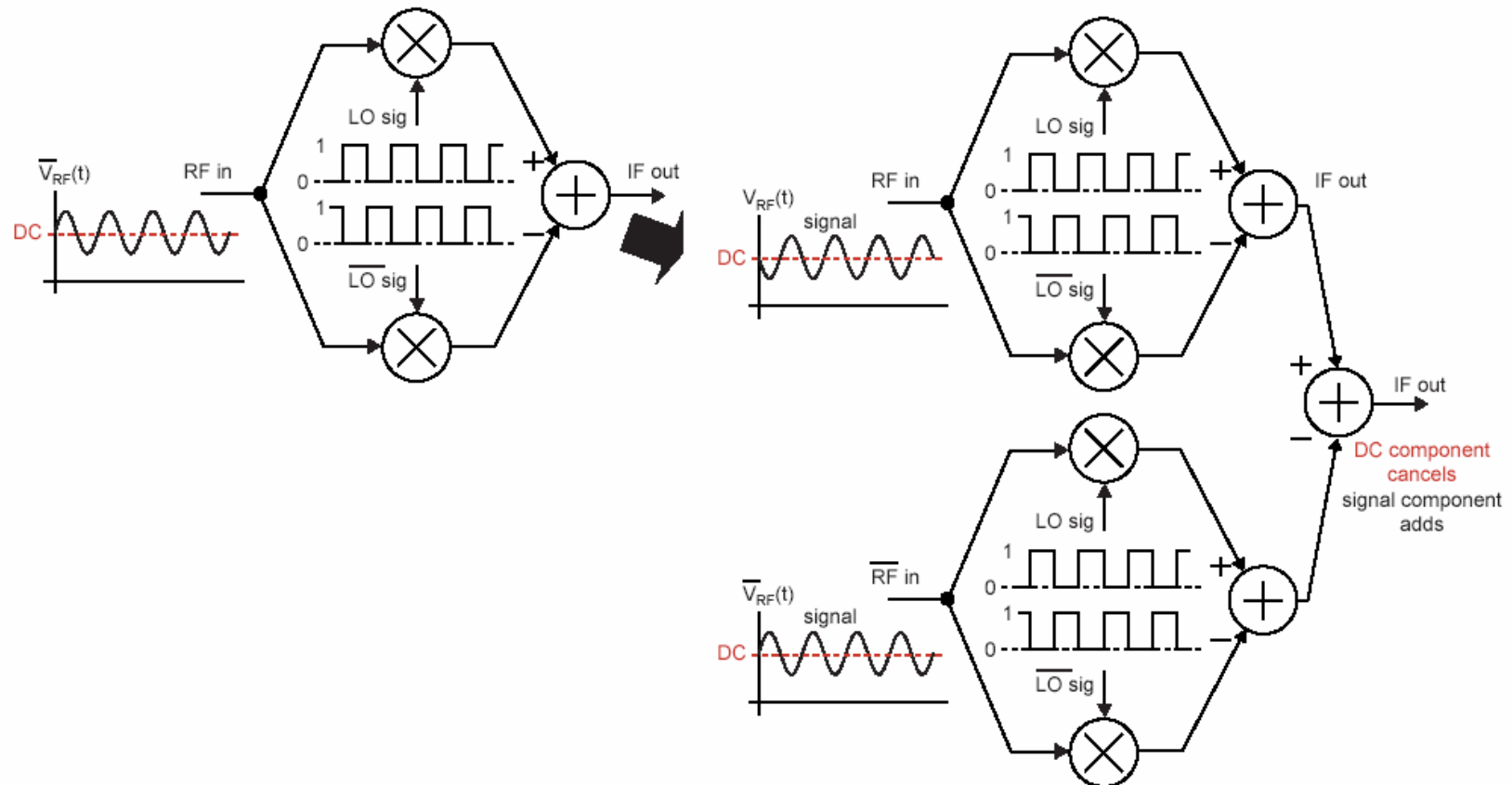
- DC component of RF input causes very large LO feedthrough
  - Can be removed by filtering, but can also be removed by achieving a zero DC value for RF input

# Ideal Double-Balanced Mixer



- DC values of LO and RF signals are zero (balanced)
- LO feedthrough dramatically reduced!
- But, practical transconductor needs bias current

# Achieving Balanced RF Signal with Biasing

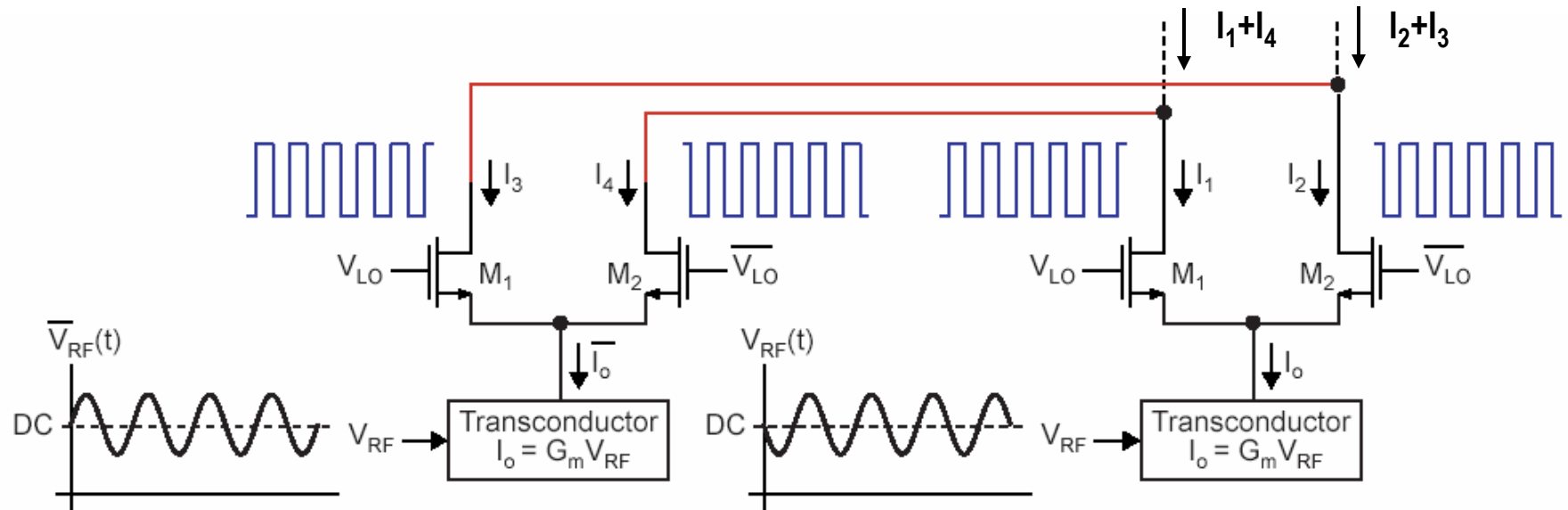


$$[RF(t) - \overline{RF(t)}] \cdot [LO(t) - \overline{LO(t)}]$$

$$\Downarrow RF(t) \cdot [LO(t) - \overline{LO(t)}] = RF(t) \cdot LO(t) - RF(t) \cdot \overline{LO(t)}$$

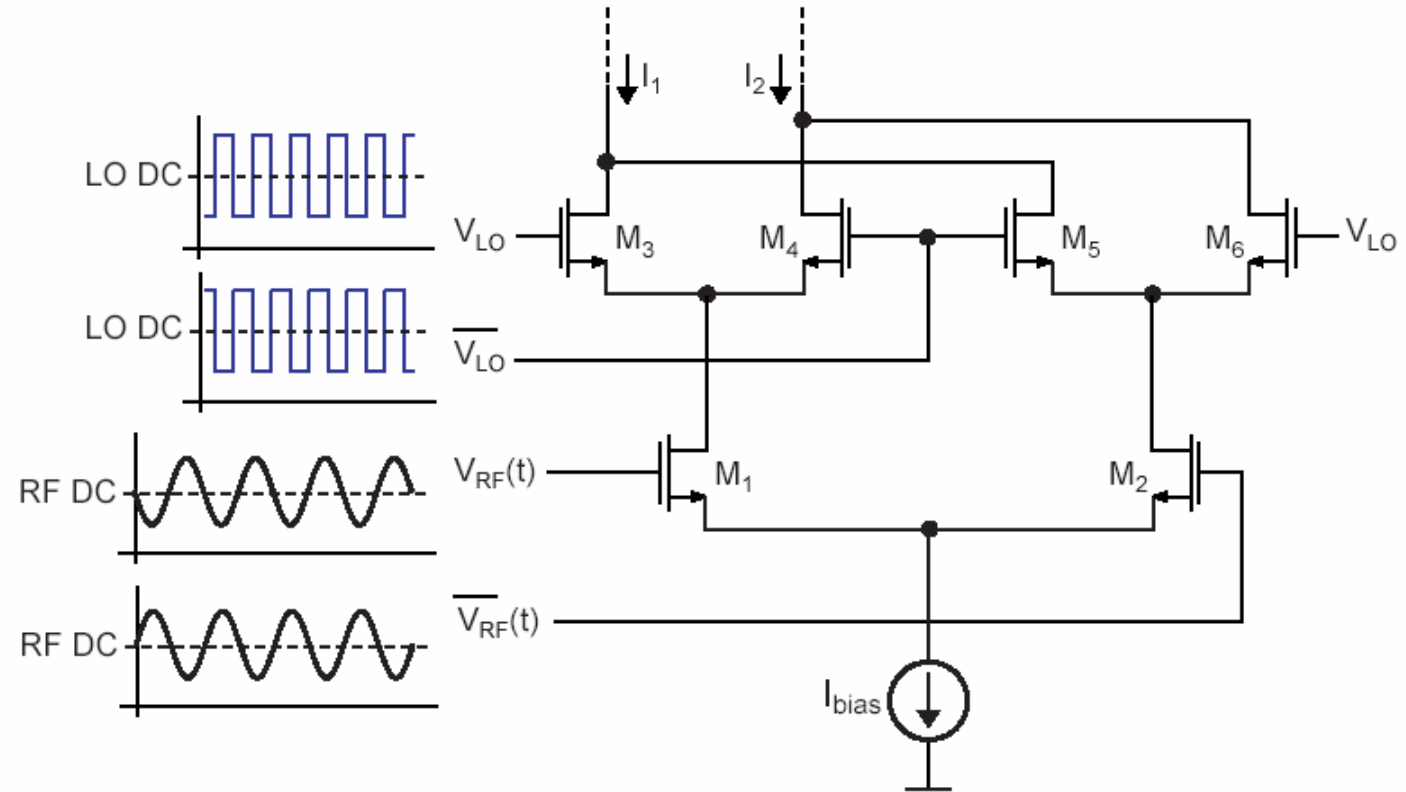
$$\Downarrow \overline{RF(t)} \cdot [LO(t) - \overline{LO(t)}] = \overline{RF(t)} \cdot LO(t) - \overline{RF(t)} \cdot \overline{LO(t)}$$

# Double-Balanced Mixer Implementation



- Applies technique from previous slide
  - Subtraction at the output achieved by cross-coupling the output current of each stage

# Gilbert Cell (Four Quadrant) Mixer

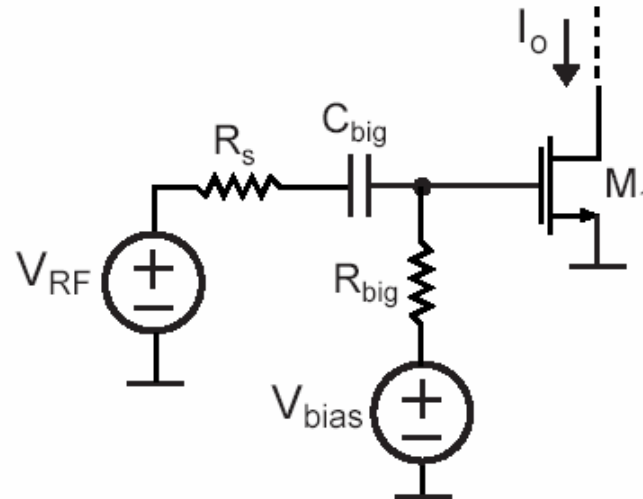


- Use a differential pair to achieve the transconductor implementation
- This is the preferred mixer implementation for most radio systems!

# Mixer Voltage Conversion Gain

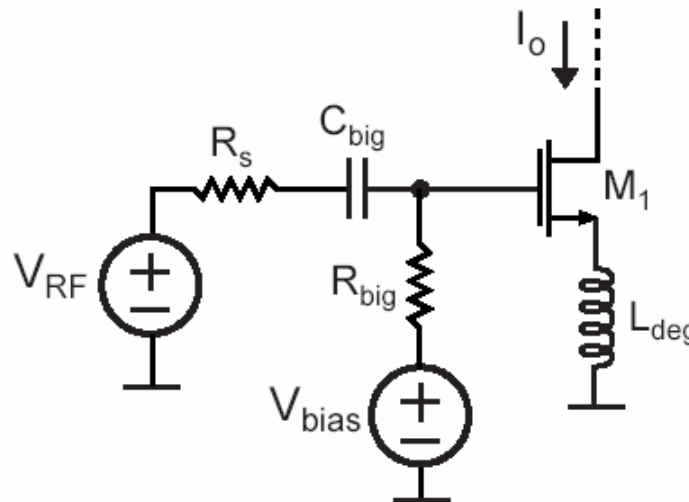
- ❑ Voltage conversion gain of a mixer depends on several factors
  - Input transconductance
  - Multiplication factor
  - Load resistance

# Common-Source Transconductance Stage in Mixer



- Apply RF signal to input of common source amp
  - Transistor assumed to be in saturation
  - Transconductance value is the same as that of the transistor
- High  $V_{bias}$  places device in velocity saturation
  - Allows high linearity to be achieved

# CS Transconductance Stage with Degeneration



- Add degeneration to common source amplifier
  - Inductor better than resistor
    - No DC voltage drop
    - Increased impedance at high frequencies helps filter out undesired high frequency components
  - Don't generally resonate inductor with  $C_{gs}$ 
    - Power match usually not required for IC implementation due to proximity of LNA and mixer

# Transconductor Stage in Mixer

$$g_{m\_Effective} = \frac{1/j?_0 C_{gs}}{Z_{in}|_{?0}} g_m = G_m$$

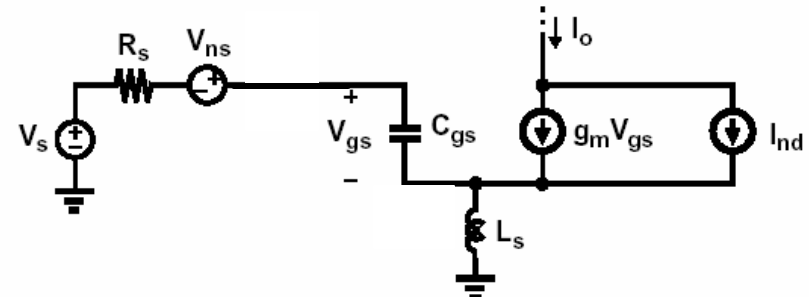
$$= Q_{in} g_m$$

$$= \frac{g_m}{?_0 C_{gs} (R_s + \frac{g_m}{C_{gs}} L_s)}$$

$$= \frac{g_m}{?_0 C_{gs} (R_s + ?_T L_s)}$$

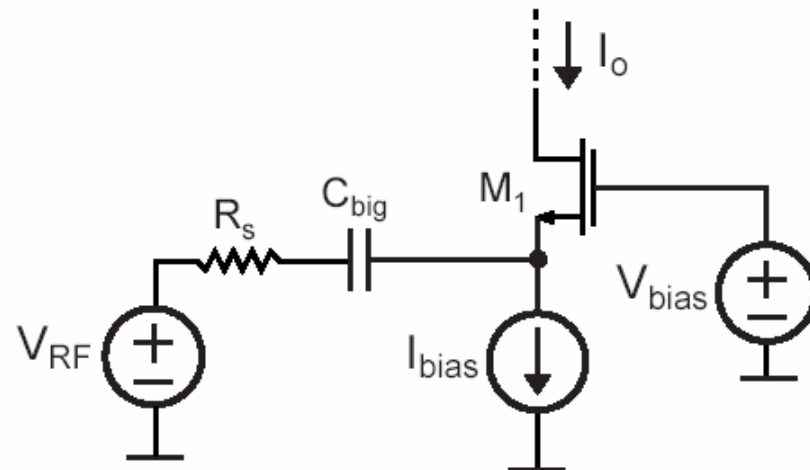
$$\gg \frac{1}{?_0 L_s}$$

For  $?_T L_s \gg R_s$ , highly linearly transconductance, only depends  $L_s$



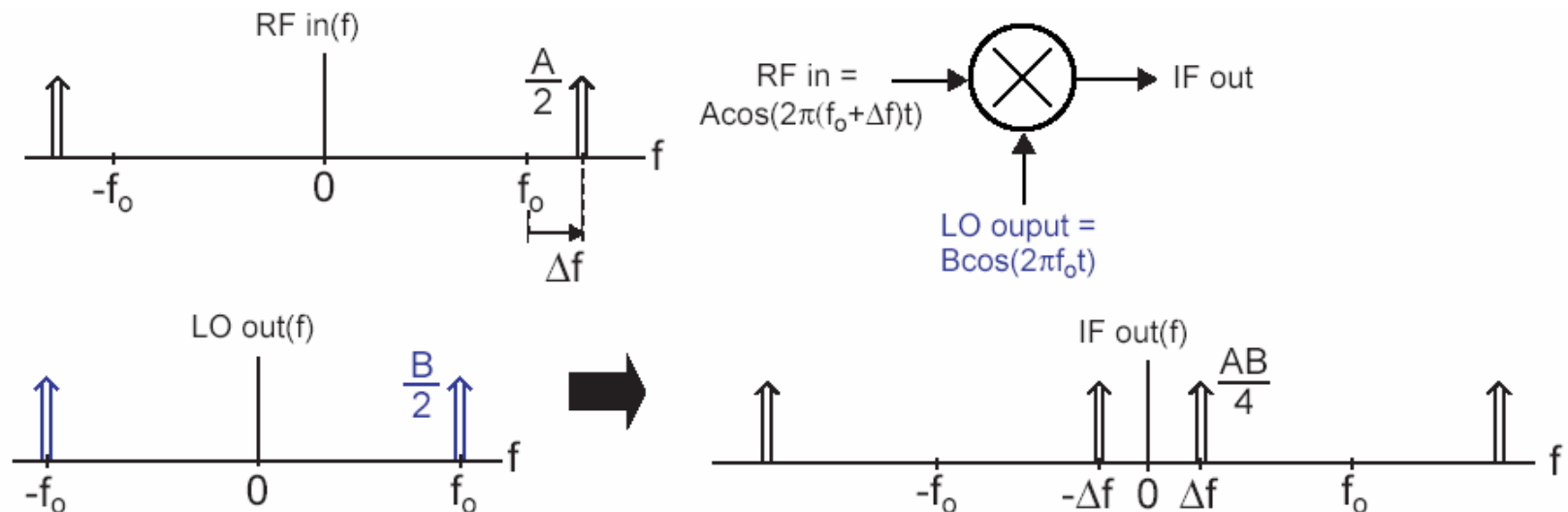
Note that:  $Q_{in} = \frac{I}{?_0 C_{gs} (R_s + \frac{g_m}{C_{gs}} L_s)} = \frac{?_0 L_s}{R_s + \frac{g_m}{C_{gs}} L_s}$

# Common-Gate Transconductance Stage in Mixer



- Apply RF signal to a common gate amplifier
- Transconductance value set by inverse of series combination of  $R_s$  and  $1/g_m$  of transistor
  - Amplifier is effectively degenerated to achieve higher linearity
- $I_{bias}$  can be set for large current density through device to achieve higher linearity (velocity saturation)

# Mixer Multiplication Factor



- **Defined as voltage ratio of desired IF value to RF input**
- **Example: for an ideal mixer with RF input =  $A \sin(2\pi(f_o + \Delta f)t)$  and sine wave LO signal =  $B \cos(2\pi f_o t)$**

$$IF\ out(t) = \frac{AB}{2} \left( \cos(2\pi(\Delta f)t) + \cos(2\pi(2f_o + \Delta f)t) \right)$$
$$\Rightarrow \text{Voltage Conversion Gain} = \frac{AB/2}{A} = \frac{B}{2}$$

# Mixer Voltage Conversion Gain

- If the *sinusoidal LO swing* is sufficiently large to completely switch the current, we can approximate the LO by a square wave
- Consider only the fundamental term in LO

$$\begin{aligned} i_{out} &= i_{RF} \cos(w_{RF} t) \cdot \frac{4}{p} \cos(w_{LO} t) \\ &= \frac{1}{2} \left\{ \frac{4}{p} i_{RF} \cos[(w_{RF} - w_{LO})t] + \frac{4}{p} i_{RF} \cos[(w_{RF} + w_{LO})t] \right\} \end{aligned}$$

- After the low-pass filter,

$$\begin{aligned} i_{out} &= \frac{2}{p} i_{RF} \cos[(w_{RF} - w_{LO})t] \\ &= \frac{2}{p} g_{m\_eff} v_{RF} \cos[(w_{RF} - w_{LO})t] \end{aligned}$$

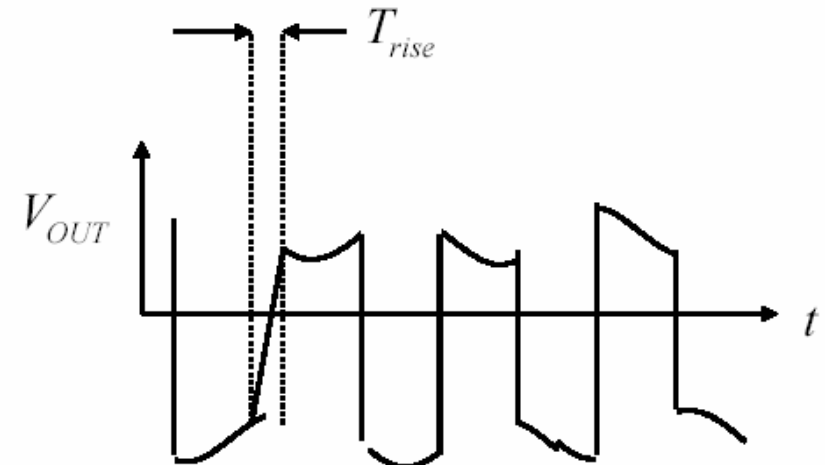
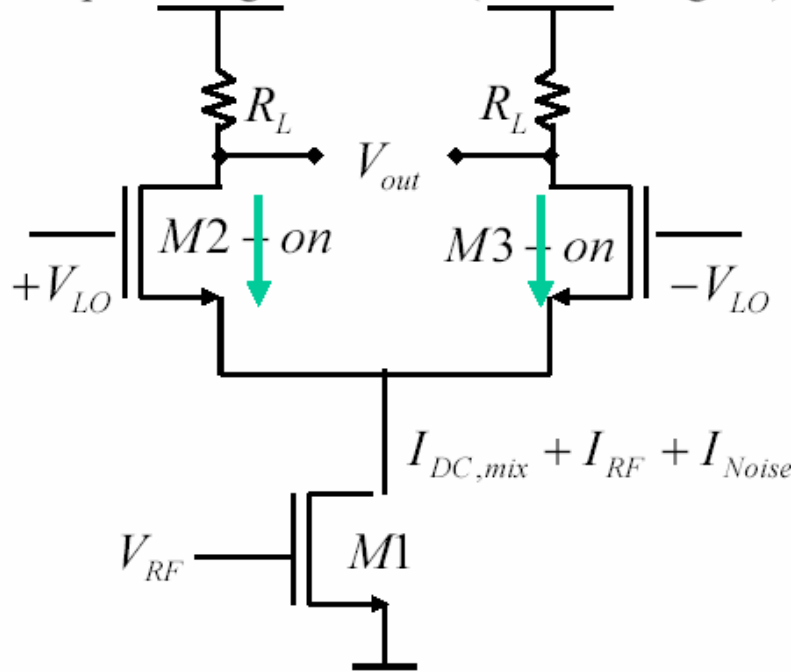
$$P\ Gain = i_{out} R_{out} = \frac{2}{p} g_{m\_eff} R_{out}$$

# Mixer Noise Analysis

- Three contributors to mixer noise
  - Transconductance stage
  - Switching pairs
  - Load resistance

# Design Consideration for Minimizing Mixer NF

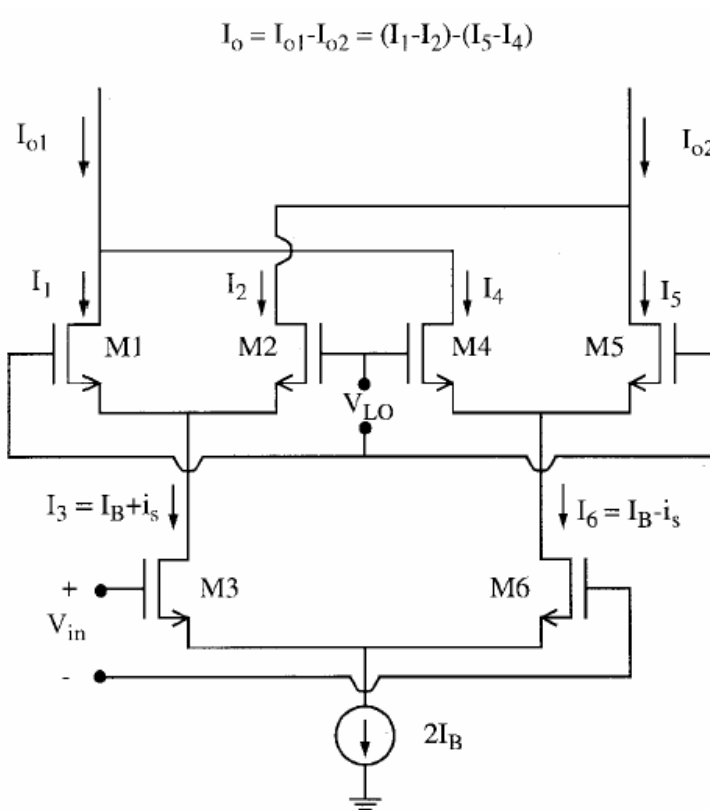
- Optimizing the mixer (for noise figure):



$$g_m \propto \sqrt{W} \dots \text{fixed} - I_{DC}$$
$$\omega_T \propto \frac{1}{\sqrt{W}} \dots \text{fixed} - I_{DC}$$

- Design the transducer for minimum noise figure
- Noise from M2 and M3 can be minimized through fast switching of M2 & M3 by
  - making LO amplitude large to ensure complete ( $> 90\%$ ) current commuting
  - making M2 and M3 as small as possible (i.e. increasing fT of M2 and M3)

# NF Expression for Double-Balanced Mixer [1]



(NF)<sub>SSB</sub>

$$= \frac{\alpha}{c^2} + \frac{2(\gamma_3 + r_{g3}g_{m3})g_{m3}\alpha + 4\gamma_1\bar{G} + 4r_{g1}\bar{G}^2 + \frac{1}{R_L}}{c^2 g_{m3}^2 R_s} \quad (44)$$

where

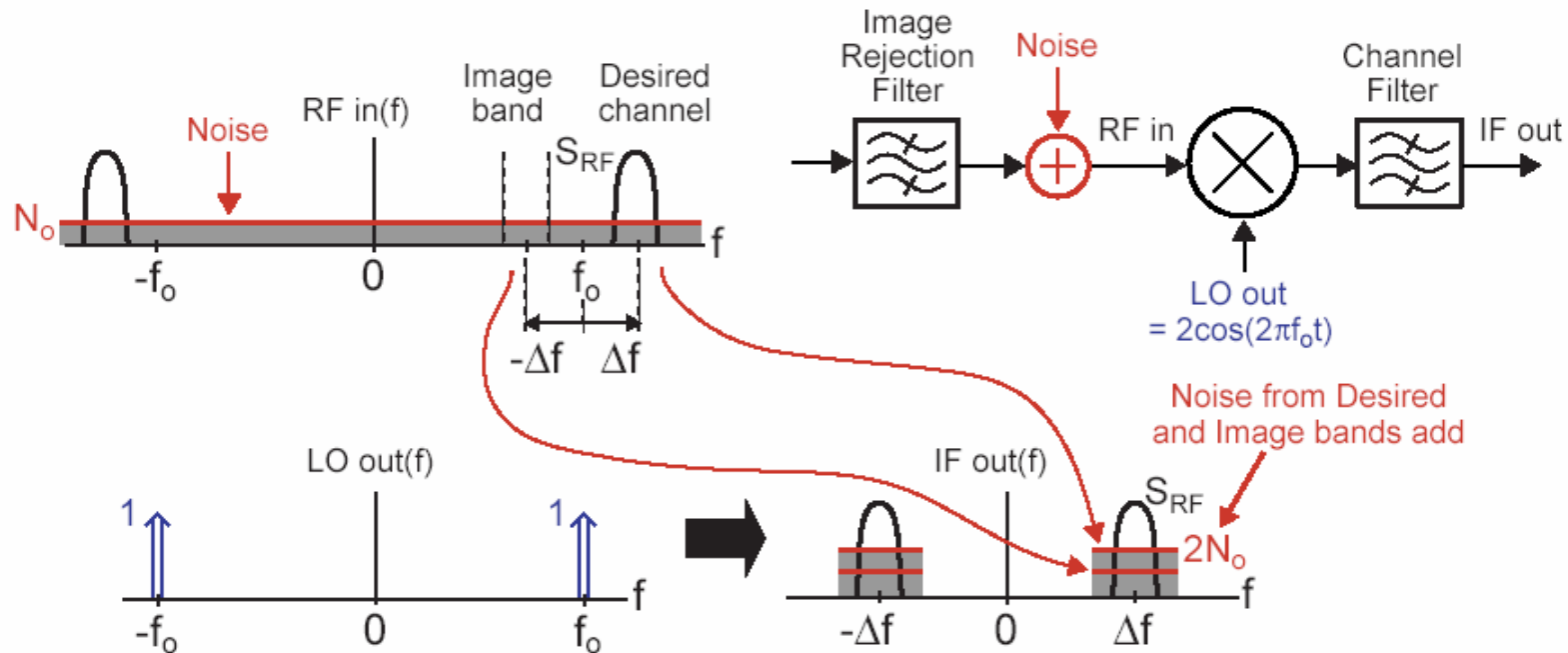
$$c \cong \frac{2}{\pi} \left( \frac{\sin(\pi \Delta f_{LO})}{\pi \Delta f_{LO}} \right) \quad (18)$$

$$\alpha \cong 1 - \frac{4}{3}(\Delta f_{LO}) \quad (25)$$

$$\bar{G} = \frac{1}{\pi V_o} \int_{-V_x}^{V_x} \left( \frac{dI_{o1}}{dV_{LO}} \right) dV_{LO} = \frac{2I_B}{\pi V_o}. \quad (33)$$

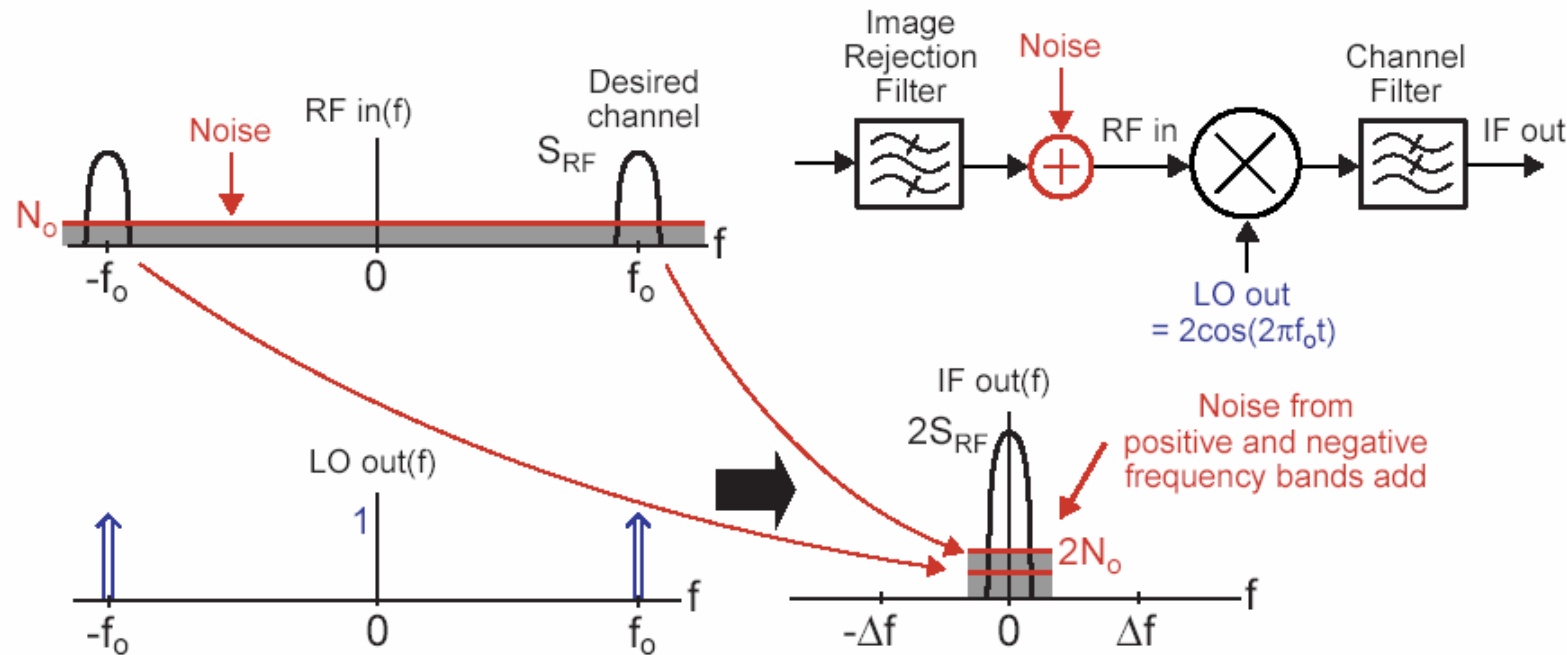
$$\bar{G}^2 \approx 16 \left( \frac{\ln(\sqrt{2} + 1)}{\sqrt{2}} - \frac{1}{3} \right) \cdot \frac{K_1^{1/2} I_B^{3/2}}{\lambda T_{LO}} = 4.64 \cdot \frac{K_1^{1/2} I_B^{3/2}}{\lambda T_{LO}} \quad (40)$$

# Mixer NF for Single-Sideband Systems



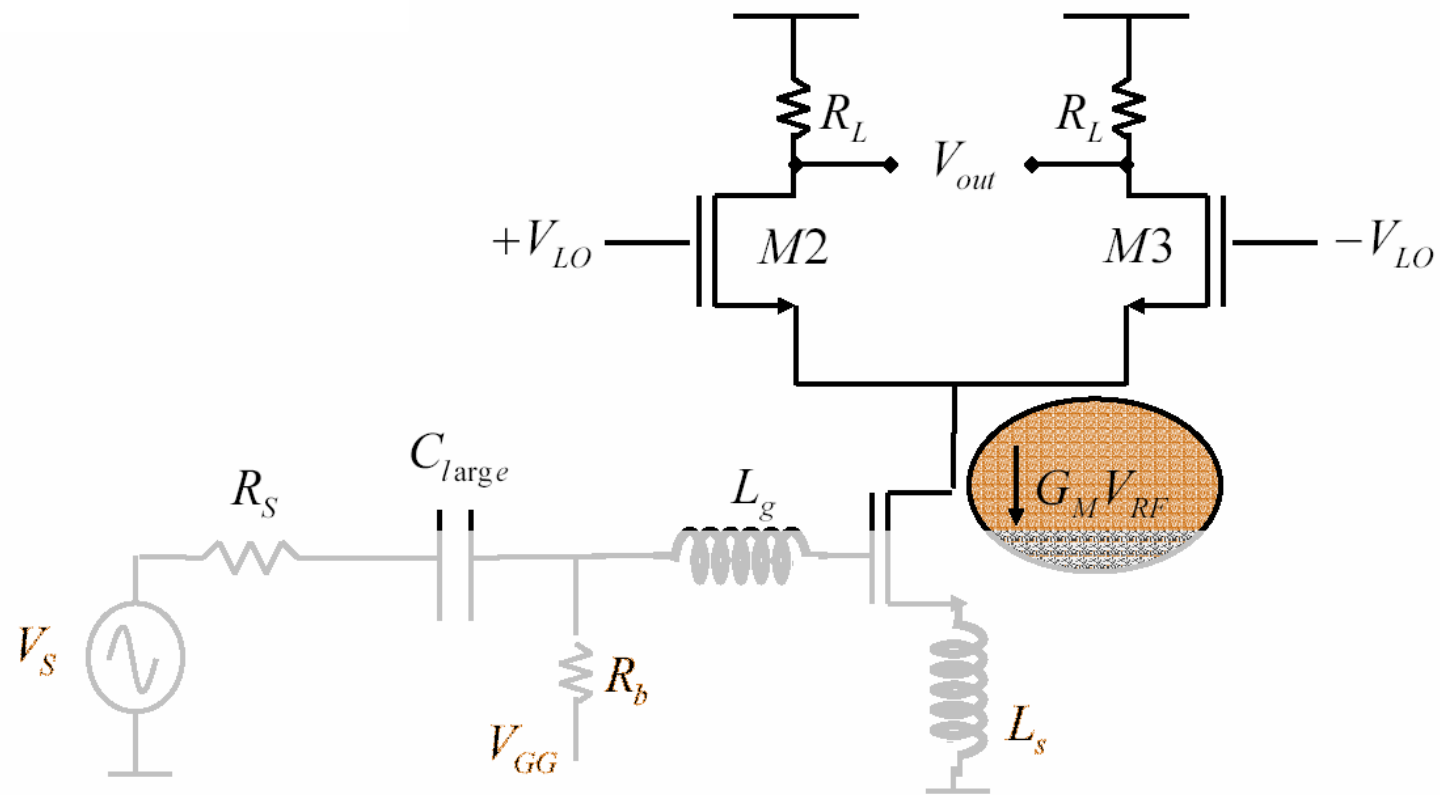
- Issue – broadband noise from mixer or front end filter will be located in both image and desired bands
  - Noise from both image and desired bands will combine in desired channel at IF output
    - Channel filter cannot remove this
  - Mixers are inherently noisy!

# Mixer NF Double Sideband Systems



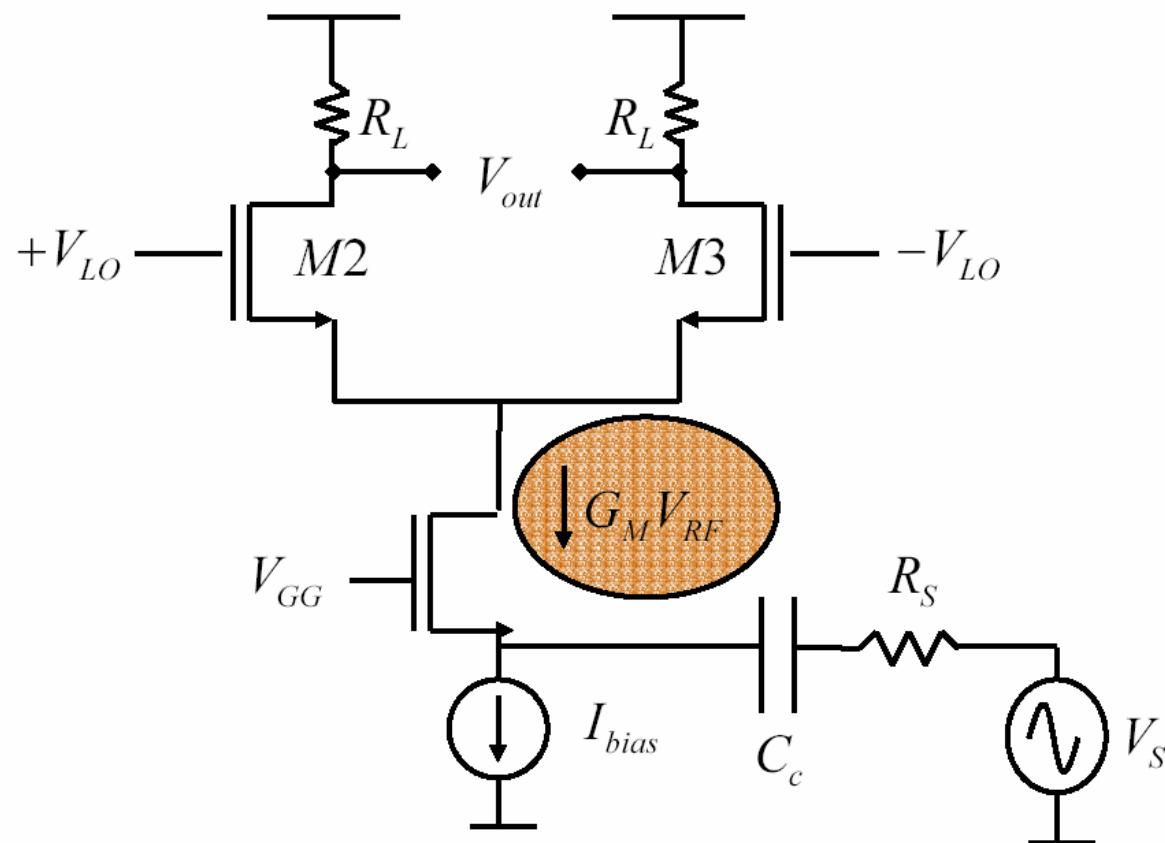
- For zero IF, there is no image band
  - Noise from positive and negative frequencies combine, but the signals do as well
- DSB noise figure is 3 dB lower than SSB noise figure
  - DSB noise figure often quoted since it sounds better
- For either case, Noise Figure computed through simulation

# Design Consideration for Mixer Linearity



- Linearity of the Mixer primarily depends on the linearity of the transducer ( $I_{tail}=G_m \cdot V_{rf}$ ). Inductor  $L_s$  helps improve linearity of the transducer.
- The transducer transistor  $M1$  can be biased in the linear law region to improve the linearity of the Mixer. Unfortunately this results in increasing the noise figure of the mixer (as discussed in LNA design).

# Design Consideration for Mixer Linearity



- Using the common gate or common base stage as the transducer improves the linearity of the mixer. Unfortunately the approach reduces the gain and increases the noise figure of the mixer.

# Measured IIP<sub>3</sub> for a 0.8-mm SB Mixer [2]

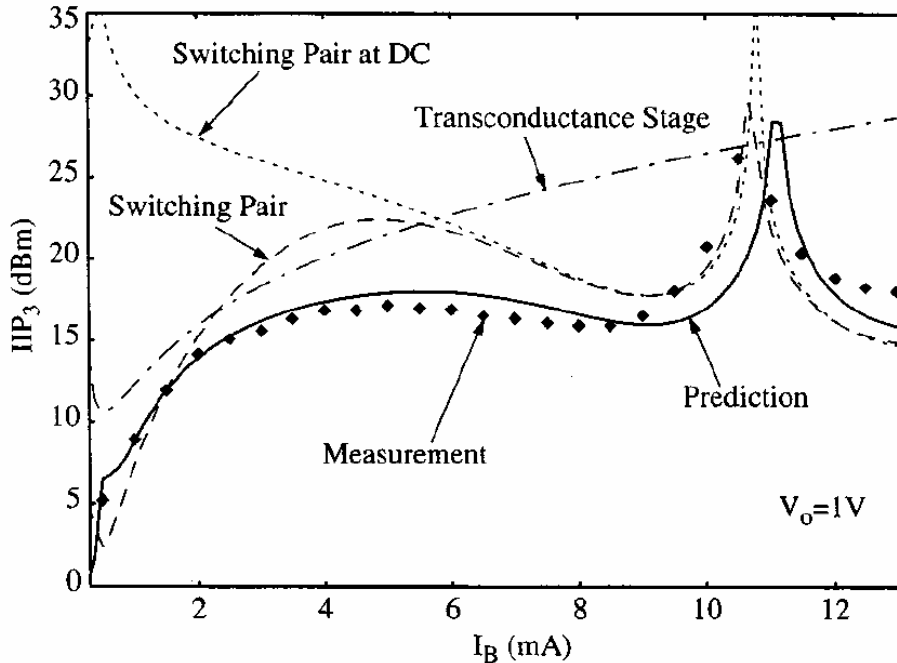


Fig. 20. Intermodulation measurements versus bias current for a fixed LO amplitude  $V_o = 1$  V.

- At high bias current, the switching pair nonlinearity dominates
- At low bias current, the transconductance stage nonlinearity dominates
  - For short channel devices, the transconductance stage nonlinearity dominates
  - IIP<sub>3</sub> is proportional to  $(V_{RF\_DC} - V_{th})$

## Measured IIP3 for a 0.8-mm SB Mixer [2]

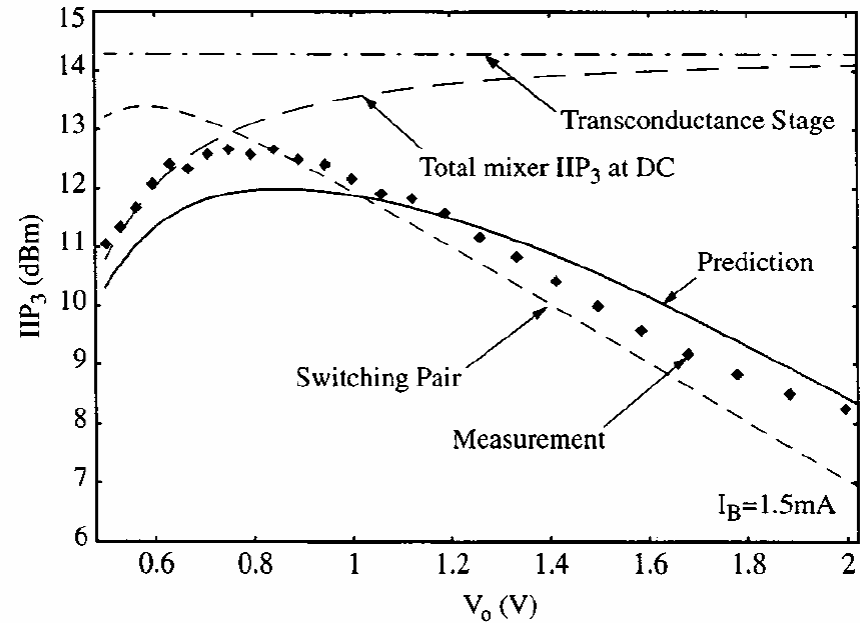
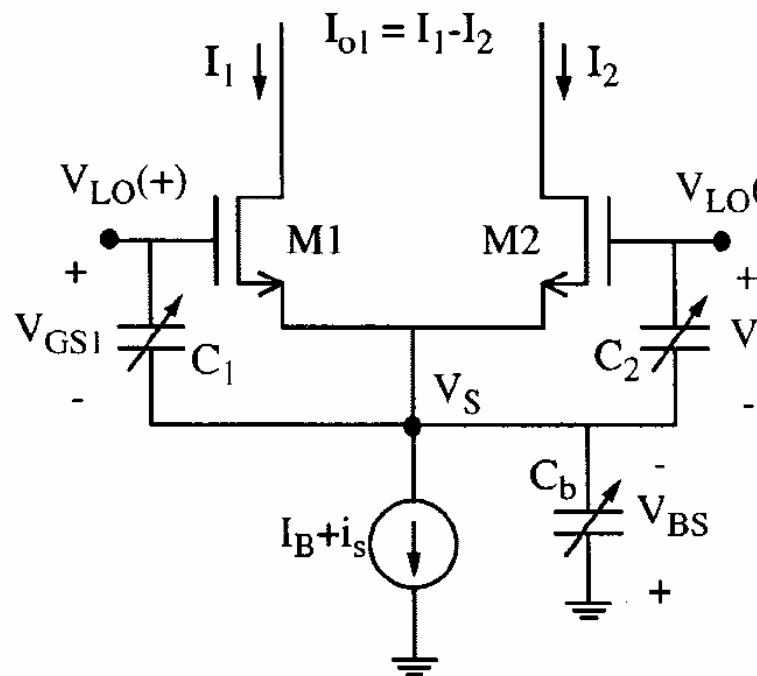
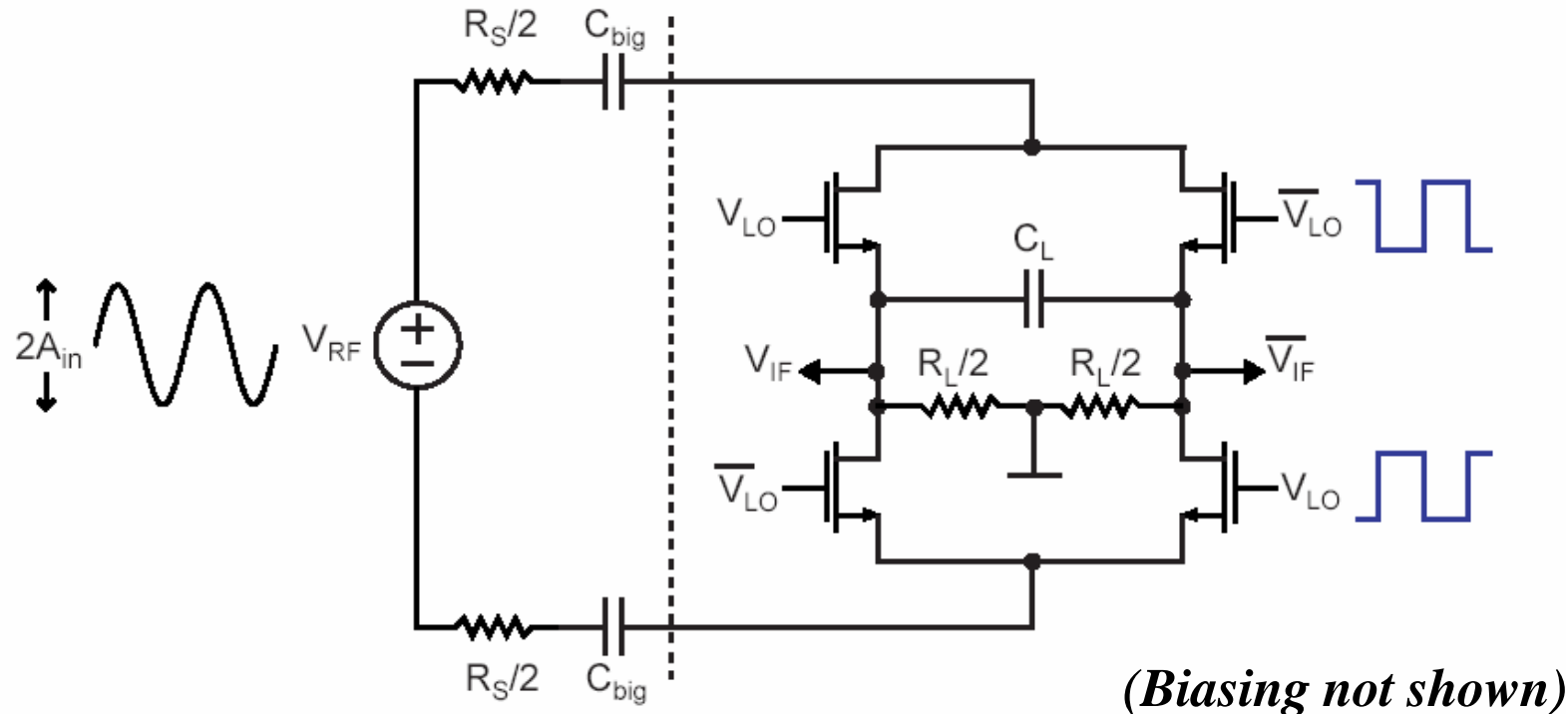


Fig. 21. Intermodulation measurements versus LO amplitude for a fixed bias current  $I_B = 1.5$  mA.

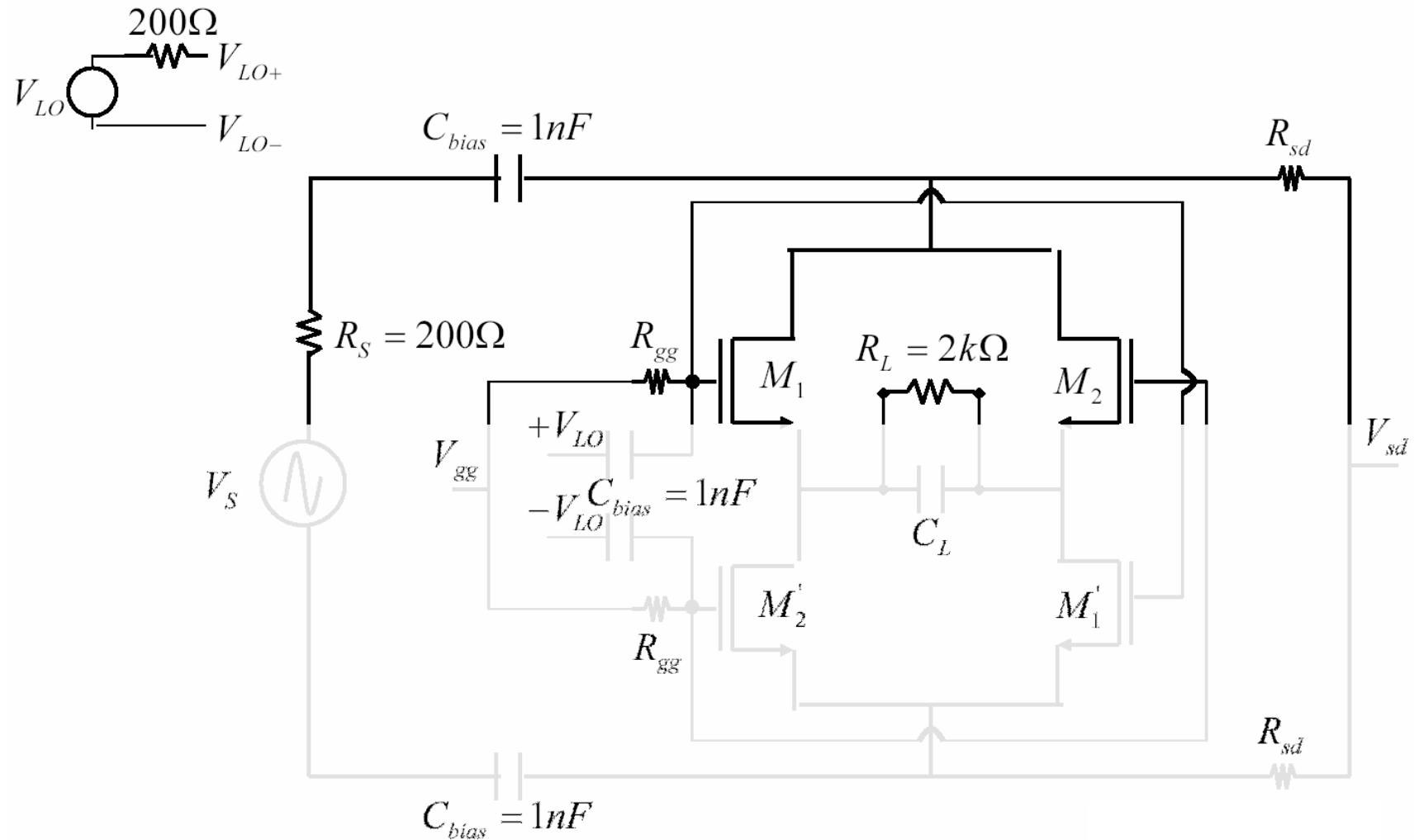
- ❑ At high frequencies, excessively large LO amplitude degrades IIP3 due to parasitic capacitive coupling which is nonlinear
- ❑ For low-voltage design (< 2V), this is usually not a big concern

# Passive Mixers



- ❑ Very high linearity (assuming the current are completely commuted)
  - 20–30 dBm of IIP3 achievable
- ❑ High noise figure (noise due to the the switching devices)
  - 20–30 dB of NF
- ❑ Voltage conversion loss

# Passive Mixers with Biasing Shown



## References

1. M. T. Terrovitis and R. G. Meyer, "Noise in Current-Commuting CMOS Mixers" *IEEE Journal of Solid-State Circuits*, Vol. 34, No. 6, June 1999.
2. M. T. Terrovitis and R. G. Meyer, "Intermodulation Distortion in Current-Commutating CMOS Mixers," *IEEE Journal of Solid-State Circuits*, Vol. 35, No. 10, October 2000.
3. Prof. M. Perrott, MIT  
<http://ocw.mit.edu/OcwWeb/Electrical-Engineering-and-Computer-Science/6-776Spring-2005/CourseHome/index.htm>
4. Prof. L. Larson, UC San Diego  
ECE 265A and 265B lecture notes

**APPENDIX VII-2**

**DIODE MIXERS**



## BALANCED SCHOTTKY DIODE MIXERS

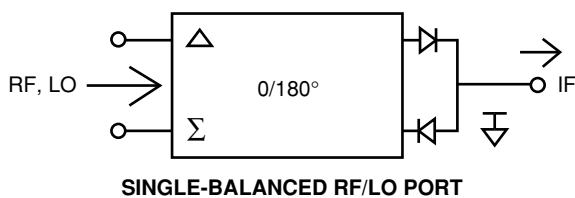
### Questions and Answers about...

#### SINGLE-, DOUBLE- AND TRIPLE-BALANCED SCHOTTKY DIODE MIXERS

##### Q1: What are the differences between single- and double-balanced mixers?

**A1:** Before explaining this difference we should mention that a one-diode or unbalanced mixer is often used in economical receiver front ends, where tunable or fixed bandpass filters can easily separate the LO, RF and IF energy coupled to and from the diode. Early wideband receivers utilized two diodes in a single-balanced mixer circuit with a  $90^\circ$  hybrid to couple RF and LO power to a pair of diodes. This technique allowed overlapping LO and RF bandwidths without filters, but the isolation was dependent on how well the diodes were impedance matched. Broadband  $180^\circ$  hybrid balanced mixers eliminated this problem. The figure below shows the equivalent circuit and the single-tone intermodulation table of the MITEQ Model SBB0618LA1 biasable single-balanced mixer with 0 dBm LO applied to the in-phase port of the  $180^\circ$  hybrid and -10 dBm RF at the delta port. In this mode of operation only the RF energy is balanced or applied out of phase to each diode, with a subsequent reduction or cancellation of even harmonic mixing products (i.e.,  $\text{LO} \pm 2\text{RF}$ ,  $\text{LO} \pm 4\text{RF}$ ).

Alternately, in any single-balanced mixer one could choose to apply the LO to the  $180^\circ$  port and observe suppression of the even harmonic LO products instead ( $2\text{LO} \pm \text{RF}$ ,  $4\text{LO} \pm \text{RF}$  etc.). The circuit and resulting products are shown below:



RF HARMONIC				
	$\Delta = \text{RF } (-10 \text{ dBm})$	$\Sigma = \text{LO } (0 \text{ dBm})$		
3	45	46	41	
2	38	42	41	
1	0	17	15	
	1	2	3	

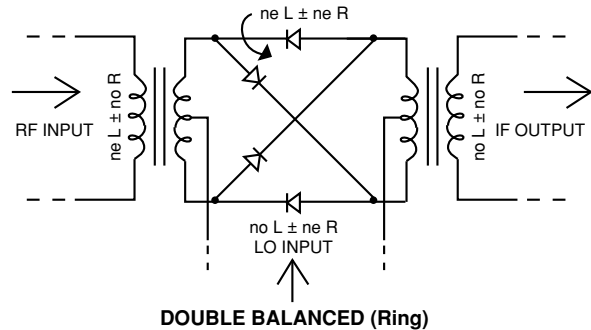
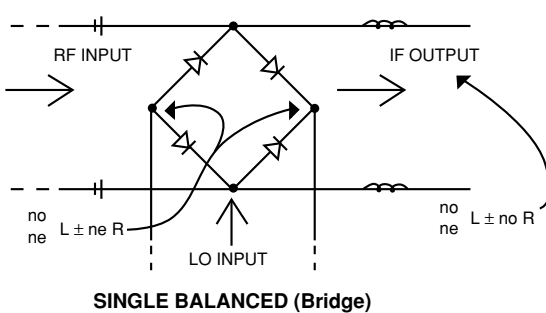
LO HARMONIC

RF HARMONIC				
	$\Delta = \text{LO } (0 \text{ dBm})$	$\Sigma = \text{RF } (-10 \text{ dBm})$		
3	49	53	40	
2	28	44	28	
1	0	30	15	
	1	2	3	

LO HARMONIC

Both single-balanced mixer configurations, however, suppress any RF or noise energy that may be present with the LO (common mode or noise rejection). In addition, single-balanced mixer circuits are particularly easy to bias and monitor the diode currents.

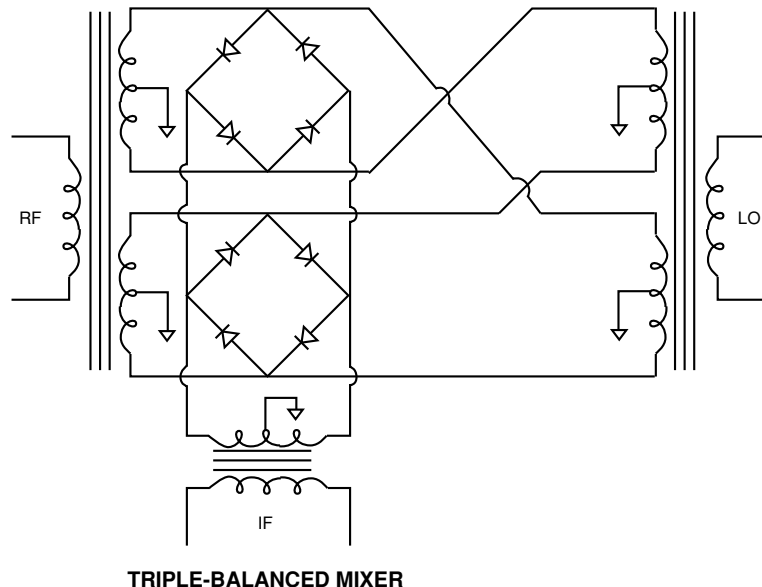
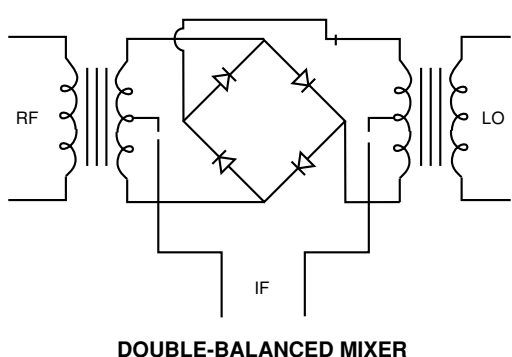
Alternately, one could also make an easily biasable single-balanced mixer with multi octave bandwidth coverage using a diode bridge (shown below). This appears very similar to the ring double-balanced mixer (also shown), but the key difference is that all even order products are canceled in the output of the double-balanced, whereas only even products of the RF are canceled in the single-balanced circuit. The MITEQ Model SBB0218LR5 uses this circuitry for RF coverage from 2 to 18 GHz and 2 to 26 GHz, however the IF output cannot overlap the RF coverage.



The double-balanced mixer circuit provides mutual isolation of LO, RF and IF energy, without filters, because of the combined properties of the ring diode circuit and wideband baluns. This results in suppression of all even-order harmonic mixing products of both the LO and RF (i.e.,  $2LO \pm RF$ ,  $LO \pm 2RF$ ,  $2LO \pm 2RF$ , etc.). The double-balanced mixer, however, requires 3 dB more LO power than the two-diode single-balanced circuit assuming, of course, that the same barrier voltage diode is used in each case.

**Q2: What are the major differences between triple- (or double-double) and double-balanced mixers?**

**A2:** The triple-balanced mixer employs two diode quads (eight junctions in total) fed by two power splitters at the RF and LO microwave baluns. The architecture allows both quads to be coupled together with mutual LO-to-RF isolation. The most significant advantage of this circuit is that the output IF signal is available at two separate balanced and isolated terminals with large bandwidth (typical 0.5 to 10 GHz). The IF signal and return path are isolated from both the RF and LO ports, thus allowing for overlapping frequencies at all three ports. A slight disadvantage of this circuit is that it will not yield a DC IF. In contrast, the standard microwave double-balanced mixer often uses diplexing techniques to separate the IF signal from the LO band. As a result, a microwave double-balanced mixer cannot support widely overlapping RF and IF frequencies while maintaining a DC response at the IF port. The theoretical single-tone spur product port cancellation relations are the same for each mixer circuit, however, in practice the triple-balanced mixer and only certain designs of double-balanced mixers with high port isolation yield the best spur suppression (MITEQ DM Series).



**Q3: For what applications are triple-balanced mixers best suited?**

**A3:** They are especially valuable for translating large bandwidth segments from one frequency range to another with low intermodulation distortion. The high IF-to-LO and IF-to-RF isolation of this class of mixers makes the conversion loss flatness much less dependent on IF frequency mismatches that almost always exist at the RF and LO ports. Recently MITEQ perfected a triple-balanced 4 to 40 GHz RF/LO mixer with a 0.5 to 20 GHz IF (Model TB0440LW1). Many customers are using this mixer with several fixed LOs to downconvert the 26 to 40 GHz portion of the millimeter band into existing receivers in the 0.5 to 18 GHz range. This mixer is also useful for upconverting the 0.5 to 18 GHz band into a fixed Ku-band second converter, thus eliminating the image response without tunable preselectors.



## BALANCED SCHOTTKY DIODE MIXERS (CONT.)

### Q4: For what applications are microwave double-balanced mixers best suited?

**A4:** Double-balanced mixers are most utilized in lower cost applications where there is no requirement for overlapping RF and IF frequencies and moderate LO power is available. In addition, the DC-coupled output of the double-balanced design makes it a prime candidate as a building block for phase detectors, I/Q modulators and demodulators that operate over narrow or extremely wide bandwidths. Lower frequency torroid balun type mixers below 2 GHz often have excellent LO-to-RF balance or isolation (40 to 50 dB) and, therefore, function well as low offset phase demodulators or high carrier rejection I/Q modulators. Conventional microwave double-balanced mixers with tapered line baluns seldom exceed 20 dB LO-to-RF isolation. The MITEQ DM Series of double-balanced mixers uses a unique balun (patent pending) that yields 30 dB minimum LO-to-RF isolation over multi octave bandwidths and 40 dB typical over communication bands (Models DM0208LW2, DM0416LW2). In addition, the 4 to 16 GHz version has a DC to 4 GHz IF range with 30 dB minimum isolation to the RF and LO ports.

### Q5: How much LO power is required for double- and triple-balanced mixers?

**A5:** Nonbiasable double-balanced mixers with so-called "zero bias" silicon Schottky diode quads will operate with +3 to +6 dBm LO power. Schottky diodes made with other junction metals and base semiconductor material, such as gallium arsenide (GaAs), can operate up to +23 dBm of LO power. The required LO power is usually determined by the desired input 1 dB compression point of the mixer and is typically specified at 5 dB above this level. Triple-balanced mixers typically require 3 dB more LO power than single-quad mixers since there are twice as many diode junctions.

### Q6: What is meant by single- and two-tone intermodulation products?

**A6:** Using amplifier terminology, a single-tone input at a frequency ( $f_1$ ) can produce outputs at the harmonic frequencies ( $2f_1, 3f_1, 4f_1 \dots mf_1$ ). Each harmonic has an input-to-output power slope equal to the order of the product (m). For example, if we double the input power (3 dB increase), we expect to see the 2nd harmonic frequency increase in power by 6 dB, the 3rd by 9 dB, etc.

In the case when two nonharmonically related tones are simultaneously fed into an amplifier, the output spectrum becomes more complex. The two tones can mix with each other due to the nonlinear transfer in the amplifier, and produce new additional signals (two-tone intermodulation products) of the order  $m \pm n$ . Certain products are of particular interest because no amount of input filtering can eliminate them, such as the two-tone third order (i.e.,  $2f_1 \pm f_2$  and  $f_1 \pm 2f_2$ ). In this case, we recognize this as third order because  $m + n = 3$ .

The former discussion is applicable to mixers with the additional complexity that the power supply for a mixer is not DC, but a time-varying voltage classified as the LO signal. The LO does not switch the mixer in a sinusoidal fashion, but rather as a square wave and, therefore, an additional set of harmonics are present at the output of the device. Single-tone spurs are not only harmonically related to the frequency of the RF input signal ( $f_{RF}$ ), but are also related to the harmonics of the LO input signal ( $f_{LO}$ ). The output spurious signals are typically classified by their order (i.e.,  $mf_{RF} \times nf_{LO}$ ) and represented in a spur table or  $m \times n$  matrix chart.



## BALANCED SCHOTTKY DIODE MIXERS (CONT.)

The two-tone third-order outputs of a mixer are defined the same way as for an amplifier, but are usually referred to the input. The LO shifts the third-order product into the IF range by the relation:

$$(m_1 f_{RF1}, \pm m_2 f_{RF2}) \pm n \text{ LO}$$

The rules for determining the RF input to IF output power slope of each RF intermodulation product remain the same for all LO harmonics.

### **Q7: What determines the level of undesired single- and multitone intermodulation products in a mixer?**

**A7:** This is a rather complex question that requires knowledge of the mixer circuit used, power ratio between the LO and applied RF, the order of the product, the degree of mixer circuit balance and the terminating impedances at each port, including out-of-band responses.

In general, mixer intermodulation products at multiples of the RF frequency are produced when the RF power level is sufficient to affect the conducting state of the diode or semiconductor used for the mixer switching action. Intermodulation products at multiples or harmonics of the LO frequency are caused by the nonsinusoidal resistance variation of the diodes due to the exponential forward voltage/current characteristic. Typically, RF harmonics can be reduced by increasing the LO power and mixer circuit complexity (i.e., single, double or triple balanced). Basically, when the incoming RF is subdivided between many diodes and the individual output IFs are recombined, each diode will generate disproportionately less intermodulation. However, each time we double the amount of diodes, both the LO power and the RF dependent intercept powers will double (+3 dB).

More recently, MESFETs (metal epitaxial semiconductor field effect transistors) have been utilized for passive mixing by applying the LO signal to the gate source junction and RF/IF to the drain source junction. The principal advantage of these mixers is much lower levels of the single-and two-tone third-order products for a given amount of LO power. For example, a typical Schottky diode mixer has a 3 dB greater input IP<sup>3</sup> power level than the LO power, but the MESFET version is 10 dB higher. The MITEQ Model SBF0812HI3 (8 to 12 GHz) has an input IP<sup>3</sup> level of +33 dBm when using +23 dBm LO.

Intermodulation levels in most mixers are influenced by external and internal terminating impedances at the RF, IF and LO ports. Internally terminated and load insensitive mixers are also available, including a new MITEQ design that redirects reflected IF, RF and sum energy to separate ports (patent pending).

In general, a good practice is to:

1. Use a mixer requiring a high or medium drive level.
2. Use a mixer with the high interport isolation (i.e., good balance).
3. Have broadband resistive terminations at all ports (beyond the desired pass bands). If this is not possible, use a broadband termination at the IF or RF port.
4. Compare each mixer design by measuring data in the system reflection environment actually encountered.



## BALANCED SCHOTTKY DIODE MIXERS (CONT.)

### Q8: What are the differences between the DB and DM Series of double-balanced mixers?

**A8:** The DB Series of mixers utilize the more conventional tapered ground microstrip balun (invented in 1972 at RHG by present MITEQ personnel). This balun is ideally suited for extremely broadband microwave applications (2 to 18 and 1 to 30 GHz), requiring modest LO-to-RF isolation (20 dB typical). The major limitations of this design relate to the high and unsymmetric balun leg impedances, making it difficult to achieve high IF frequency coverage with DC capability.

More recently at MITEQ, we have perfected a new more symmetric balun which yields typical LO-to-RF isolation of 35 dB over 4 to 1 bandwidth ratios. This design is synthesized from double- and triple-tuned microwave filter theory and, therefore, has much higher out-of-band rejection than conventional double-balanced mixers. In addition, the IF capability is greatly extended. For example, the Model DM0520LW1 has an IF coverage of DC to 8 GHz with simultaneous RF and LO coverage of 5 to 20 GHz.

### Q9: What advantage does the new DM and FDM mixer baluns offer for narrow RF bandwidth applications?

**A9:** In general, the new balun design exhibits best performance at band center and, therefore, the narrower band units yield progressively better LO-to-RF isolation (45 dB typical for 10 percent bandwidth units). In addition, the spurious mixing products of these microwave units are similar to that expected from VHS/UHF double-balanced mixers having similar isolation. The 10 percent RF bandwidth units typically have the same RF skirt selectivity as a two-pole filter, thus reducing the system input preselection requirements (see Model FDM0325HA1).

Another advantage of the FDM design is that the LO and IF coverage are relatively broadband and one can choose an IF frequency that causes the RF image response to fall on the skirt of the balun, thus yielding image rejection without the usual more expensive matched mixers and hybrid circuit topology.

Finally, special versions of the FDM design can be optimized for simultaneous image rejection and image recovery in selected communication bands requiring relatively high IF frequencies. The typical conversion loss in this mode is 3.5 dB.

### Q10: What is the principle advantage of even harmonic mixing?

**A10:** Aside from requiring an LO at half the normal frequency, one can achieve ultra-high (-55 to -60 dB) rejection of the LO leakage out the RF port relative to the input power. This means an input isolator can often be eliminated, but more important, for linear upconverter or modulation requirements, the carrier rejection can be maintained at high levels. Some customers employ pairs of I/Q even harmonic up- and downconverter mixers for lower cost data links. The principle disadvantages of the even harmonic mixer are slightly higher (2 dB) conversion loss, more LO power sensitivity and, of course, doubling of the LO phase noise.

## Questions and Answers about...

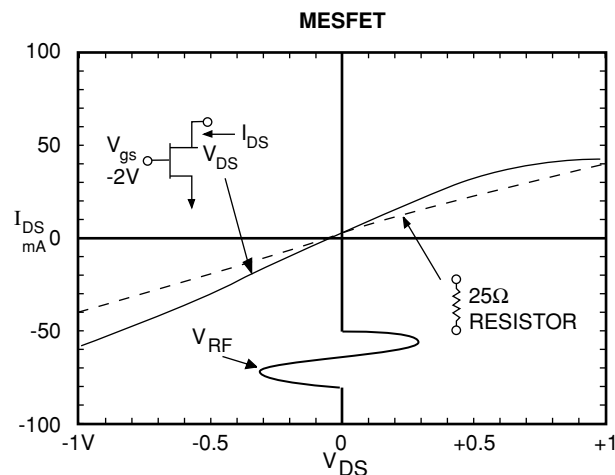
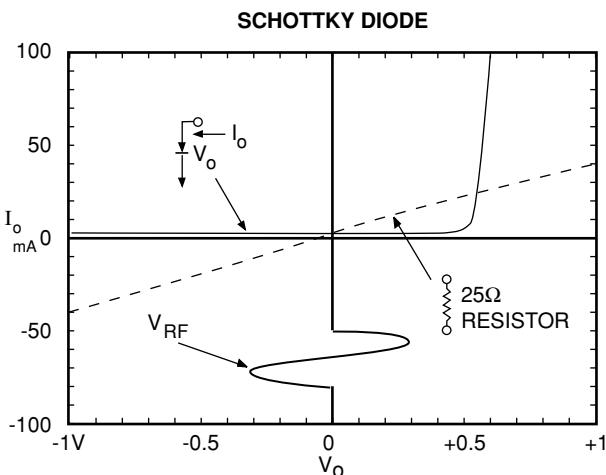
## MESFET MIXERS

**Q1: What does MESFET mean?**

**A1:** Metal Epitaxial Semiconductor Field Effect Transistor (i.e., the gate electrode is a metal to semiconductor junction similar to a Schottky diode).

**Q2: Why use a MESFET for mixing instead of a Schottky diode?**

**A2:** The principal advantage of a FET mixer is a reduction in the third-order distortion, thus yielding improved single-tone (i.e., LO  $\pm$  3RF) and two-tone (2RF, - RF<sub>2</sub> - LO) intermodulation products relative to a Schottky diode mixer that operates at the same LO power. The figure below illustrates the source of mixing distortion (E/I characteristic) of a Schottky diode and a typical MESFET.



The dotted sine wave represents an applied RF signal across each semiconductor junction at the instant that the LO voltage is zero (in the case of the MESFET curve a fixed negative bias on the gate results in the E/I VD curve shown). The most significant difference in the two curves is how they each compare to an ideal fixed 50 ohm resistor, shown by the dotted straight line. The resistor, of course, would yield no distortion in the resulting current sine wave. We notice that the deviation from a straight line for the Schottky diode is considerably greater, thus yielding a poor IP<sub>3</sub> at this bias point. The measured IP<sub>3</sub> of both mixers is the average of the instantaneous IP<sub>3</sub> distortion at each LO operating voltage. The input IP<sub>3</sub> of a MESFET mixer is typically 10 dB or greater than the LO power. A general rule for Schottky diode mixers is 3 dB greater than the LO power (the intercept powers of mixers are usually specified relative to the maximum signal power at the input). The third-order intercept point of amplifiers is, therefore, relative to the output port.

In addition, the linear mixing region of a Schottky diode is approximately 5 dB below the applied LO power since both the RF signal and LO signal exist at the same terminal. However, a FET mixer, configured in the passive mode, has the LO applied to the gate and controls the drain to source channel resistance with low power. RF and IF signals that are present at the drain cannot easily modulate the channel resistance and, therefore, produce an RF 1 dB compression point approximately equal to the LO power. At the lower switching rates (UHF and VHF frequencies) the power difference is more dramatic (e.g., a FET switch controls +25 dBm RF with microwatts of gate power).

Another difference between the MESFET and the Schottky diode is that the latter is a two-terminal device and, therefore, requires filters or multiple diodes and balanced circuits to separate the LO, RF and IF circuits (this is essential when signal LO and RF bandwidth overlap). The MESFET is a three-terminal device and allows decoupling between the LO (gate to source) and RF/IF circuitry (drain to source). Single- and double-balanced FET mixer circuits also exist.

### **Q3: What are the disadvantages of a MESFET mixer relative to the Schottky device?**

**A3:** There are two, cost and LO VSWR, particularly for broad bandwidth applications. At the present time, the fabrication process for making 4 silicon diodes in a quad configuration is considerably less costly than that of 4 GaAs MESFETs, therefore, if the P1 dB or IP<sup>3</sup> requirements are moderate (up to +10 and +20 dBm respectively), a Schottky diode device is adequate. For P1 dB and IP<sup>3</sup> of greater than +17 and +27 dBm, the MESFET cost may be justified in view of the extra cost of an LO amplifier needed for the Schottky device. The Schottky device will typically require LO powers of +24 dBm to achieve IP<sup>3</sup> of +27 dBm, whereas the MESFET mixer requires only +17 dBm LO power.

Another difficulty of designing octave and multi octave bandwidth MESFET mixers is impedance matching the FET gate circuit to a 50 ohm source impedance. Unlike the Schottky mixer, the FET gate circuit is not driven into full conduction during LO operation, but rather swings from pinch-off to zero bias and thus always has a high reflection coefficient. For narrow bandwidth applications, one can impedance match to the low series resistance of the gate and achieve large voltage swings with little LO power (a desirable condition). More recently at MITEQ, we have achieved octave bandwidth operation with 15 dB or more gate return loss by employing balanced circuitry. This technique has been employed to make a series of octave high level (P1 dB = +23 dBm input) MESFET mixers from 6 to 18 GHz that are suitable for a second-stage image rejection mixer following a high-gain low-noise RF preamplifier.

### **Q4: What are the differences between active and passive FET mixing?**

**A4:** Active FET mixers are typically DC biased like an amplifier and employ a dual gate or two series FETs. The LO and RF signals are applied to separate gates and the IF signal (or sum frequency) is coupled from the drain. This circuit yields low IP<sup>3</sup> and moderate gain with high shot noise at low IF frequencies.

Passive FET mixers have conversion loss and noise similar to Schottky diode mixers. The RF signal is applied across the drain source channel of the MESFET without any DC drain voltage. The LO signal is fed to the gate, effectively modulating the channel resistance. This produces a mixing action with the sum and difference appearing across the drain source. External or self gate biasing is used to prevent forward gate conduction from the LO signal, however, since no average current is drawn, the main noise source in this mixing is thermal.



## MESFET MIXERS (CONT.)

### Q5: Are there preferred frequency ranges for MESFET mixers?

**A5:** No, since the advantage of their high IP<sup>3</sup> with moderate LO power has been proven at UHF through millimeter bands.

### Q6: Where should MESFET mixers be used?

**A6:** In any application requiring high dynamic range. For example, in receiver front end downconverters where one or more high level RF signals result in intermodulation distortion spurs (such as in EW, radar or communication front ends). MESFET mixers are also well suited to second-stage mixing following a low-noise, high-gain RF pre-amplifier. In the latter usage a filter or imageless mixer must be used to reject the added noise. A typical communication example is in any wireless cable TV link where up to 60 tones will be frequency multiplexed onto a single carrier. In this case, the Schottky diode mixer is no match for the spur handling capability of the MESFET mixer.

### Q7: What about the relative cost of Schottky diode versus MESFET mixers?

**A7:** Broadband double- and triple- (double-double) balanced Schottky mixers are a mature technology and are available from many suppliers. Therefore, diode mixers are more likely to be the winner in any moderate quantity cost contest where LO power is easily available. In addition, the unbiased Schottky diode does not require a separate DC power supply. However, when the issue is maximum RF power handling with low LO power, the comparison is not always obvious. Particularly, when a separate LO amplifier may be required to supply the extra 6 dB needed to make the Schottky diode mixer perform at the same signal powers as the FET mixer. Typical cost ratios put the MESFET mixer 2 to 4 times higher in unit price to that of the Schottky mixer. This can often compensate the cost of an LO amplifier or the enhancement in overall system performance.

### Q8: Is the MESFET mixer more susceptible to burnout from a high power RF pulse or CW signal when compared to a conventional Schottky ring?

**A8:** Quite the contrary, since the RF is applied across the channel (drain source) of the FET, the FET power dissipation is more like the limits for the DC supply power in a FET amplifier. The CW RF power limit of a typical 10 GHz balanced MESFET mixer is approximately 1 watt (the CW power limit of a typical Schottky ring mixer is about 300 mW). Thus, in some system applications, an RF limiter is not required.

### Q9: What about the noise level of FET versus Schottky diode mixers?

**A9:** When using FETs in the passive mode (no average drain current), the 1/f and thermal noise is very similar to GaAs Schottky diode mixers, i.e., corner frequency (defined as the point where the 1/f noise equals the thermal noise) is about 100 kHz.

### Q10: Are MESFET mixers more temperature sensitive than Schottky diode mixers?

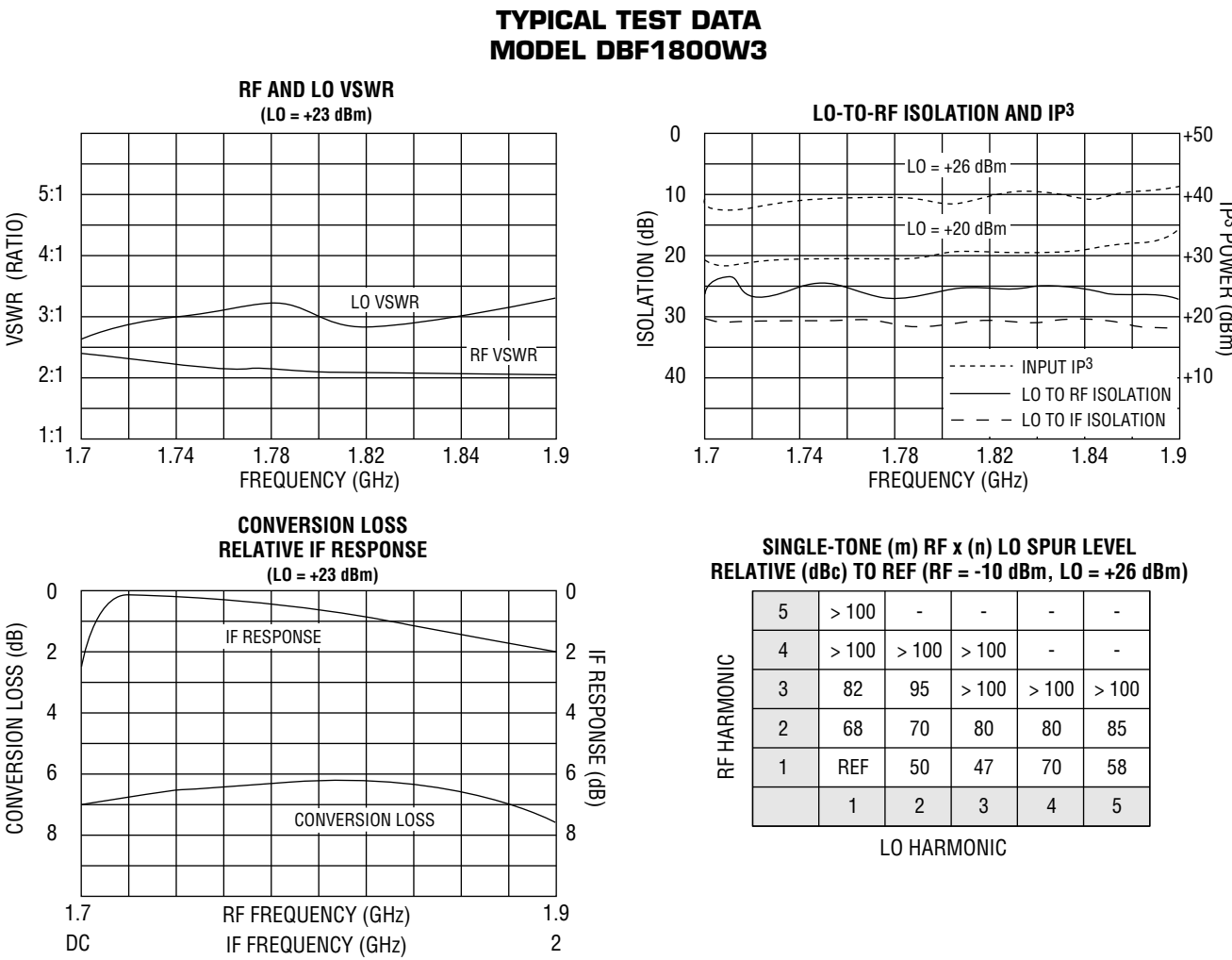
**A10:** No, particularly if one employs zener voltage regulating diodes in the MESFET gate bias circuit. Each type mixer will then commonly have a conversion loss variation of +0.25 dB for a temperature variation of +50°C when using a constant LO power.

**Q11:** Are there passive modes of operation for the MESFET mixer other than LO on gates and RF/IF on the drain source?

**A11:** It is possible to get very low conversion loss (-3 to 0 dB) by applying LO between the drain and source and RF to the gate with IF output at the drain. In this mode of operation, the LO periodically powers the FET into the active amplifier region and one obtains normal amplifier gain less the Fourier LO switching coefficient (approximately -6 dB). The input IP<sub>3</sub>, burnout and noise figure for this mode of operation are all considerably lower than drain source mixing. The lower limit of noise figure for this mode of operation is 3 dB because of the image response.

**Q12:** What are the performance characteristics of a typical MITEQ narrow bandwidth MESFET mixer?

**A12:** The curves below show averaged measured data on four L-band units:



# Schottky Diode-Based Mixers Design and Optimization at Millimetre and Submillimetre-wave Bands

J.V. Siles<sup>1</sup>, J. Grajal<sup>1</sup>, V. Krozer<sup>2</sup>, and B. Leone<sup>3</sup>

<sup>1</sup>Universidad Politécnica de Madrid, Departamento de Señales, Sistemas y Radiocomunicaciones,  
E.T.S.I. Telecomunicación, Ciudad Universitaria S/N, 28040 Madrid, Spain  
Phone: +34 91.336.73.58, E-mail: {jovi,jesus}@gmr.ssr.upm.es

<sup>2</sup>Orsted-DTU Technical University of Denmark, Orsted Plads,  
building 348, DK-2800 Kgs. Lyngby, Denmark

<sup>3</sup>European Space Agency ESA/ESTEC, Keplerlaan, Noordwijk, The Netherlands

**Abstract** — In this paper we present some design and optimization aspects for Schottky-based mixers at the millimetre and submillimetre-wave bands by using an in-house mixer CAD tool. This simulator takes into account both the external circuit and a physical model for the semiconductor device. For mixer analysis, proper time-frequency conversion techniques have been implemented, which combine good accuracy and low computational cost. This CAD tool allows the joint optimization of the Schottky diode and the external circuit. Another important advantage is the possibility to study and optimize the internal structure of the Schottky diode for optimum performance.

## I. INTRODUCTION

The use of Schottky diodes for mixing applications at the millimetre and submillimetre-wave bands has experienced a big progress. In this sense, the development of the fabrication processes, making possible anode areas below  $1 \mu\text{m}^2$ , has led to less restrictive requirements regarding LO power [1].

In order to guarantee good operation conditions, Schottky mixers demand LO powers in the 1 mW range. This is a clear disadvantage with respect to other technologies such as SIS (Semiconductor Insulator Semiconductor) and HEB (Hot Electron Bolometer) mixers. In addition, Schottky mixers have worse noise performance than HEB and SIS. However, the great advantage of Schottky mixers is that they can operate well at room temperature, although optimum performance is achieved when they are cooled.

In this paper we analyse some important Schottky mixers design and optimization aspects through an in-house numerical mixer CAD tool. This tool, which is described in [2] and [3], couples the external circuit simulator with a drift-diffusion physical numerical model of the Schottky diode employing harmonic balance techniques (HB). An in-depth study of multi-tone HB techniques was performed to select the proper one for mixer analysis [3]. An *Almost Periodic Fourier Transform* (APFT) method was finally selected to do the time-frequency conversions in HB. It supports non-commensurable LO and RF frequencies and is suitable for systems with memory that are

not described by algebraic equations (this is the case of the numerical model of the Schottky diode). A description of the implemented APFT is provided in [3].

In comparison with commercial programmes, our CAD tool has the advantage of employing a system with memory instead of memoryless one [4]. This is the case of *Libra* commercial CAD. Furthermore, other CADs are based on approximate approaches, as admittance matrix techniques. In this context, the advantage of our mixer CAD tool is that no assumptions or approximations are made regarding LO and RF powers.

## II. CAPABILITIES OF THE MIXER CAD TOOL

A joint optimization of both the external circuit and the Schottky diode is mandatory to achieve this optimum performance. The use of drift diffusion-based physical model for the Schottky diodes makes possible an in-depth study of the influence of the internal structure of the Schottky diode. Most of the physical effects and limitations (barrier lowering, tunnelling, non-constant recombination velocity, carrier velocity saturation, ...) that occur in the semiconductor device are included in this model. This is essential to achieve the best possible mixer performance. Our mixer CAD tool allows this joint optimization by considering all possible design parameters:

- External circuit
  - LO and RF frequencies
  - LO and RF pump powers
  - Bias voltage
  - Loads at LO, RF, IF and image frequencies
  - Loads at other frequencies
- Schottky diode
  - Layer profile (doping and length)
  - Anode area
  - Physical effects: tunneling, barrier lowering, carrier velocity saturation, ...

The simulator offers the possibility to carry out a great number of mixer analyses: Optimization of the IF impedance, conjugate-matching of LO and RF

impedances, image enhancement, LO power sweep, RF power sweep, anode area sweep, bias voltage sweep, etc. The provided output results are the conversion loss, the rectified current, matched impedances, voltages and currents at each frequency component, internal distribution of carriers in the diode, etc.

### III. MIXER DESIGN AND OPTIMIZATION ASPECTS

In this section, we present the results for room temperature Schottky diode-based mixers at 100 GHz, 400 GHz and 585 GHz. The optimization goal is to achieve minimum conversion losses with the minimum possible LO power because, as it was previously introduced, the available LO power represents the main limitation for the performance of Schottky mixers at these frequency bands.

#### A. DC Bias and LO Power

Figs. 1 and 2 show the joint effect of varying both the DC bias and the LO power in the conversion loss for a 100 GHz mixer and a 400 GHz mixer. In both cases, it can be depicted that the conversion loss decreases rapidly with LO power until a region of constant loss is reached. This is a very interesting aspect of Schottky mixers in the sense that, fixed the RF power, the IF power is constant with the LO power. In addition, when DC bias is applied, the LO power requirements to reach this region of minimum loss are lower. However, if bias is quite high, the conversion loss starts to grow above a certain LO power. This can be noticed in Fig. 1 for a 0.8 V bias voltage. Therefore, there will be a trade-off between bias and LO power.

For the 400 GHz mixer a high doping ( $1 \cdot 10^{18} \text{ cm}^{-3}$ ) has been selected to avoid the carrier velocity saturation effect at high frequencies [5]. LO power requirements for minimum loss are a bit lower in the 400 GHz mixer with respect to the 100 GHz mixer because a lower anode area has been considered.

The IF impedance has been optimized for each bias voltage at a 1.5 mW LO power. However, it is shown in Fig. 3 that the conversion loss at a certain bias voltage does not depend so much on the IF impedance at this frequency of operation. This provides an extra degree of freedom in the sense that, after the manufacturing process, it will be possible to adjust the mixer bias for optimum performance without the need to modify the IF impedance.

#### B. Anode Area and Doping

Analogous to the LO power and the bias voltage, the anode area and the epitaxial layer doping of the Schottky diode must be concurrently optimized.

At low frequencies, the best performance is obtained for low doping levels, as can be appreciated in Fig. 4. In addition, for a  $1 \cdot 10^{17} \text{ cm}^{-3}$  doping, the conversion loss is almost constant with the anode area so it is not necessary a joint optimization of both the area and the doping.

At high frequencies, there are two effects that affect negatively to the performance of the Schottky-based mixers.

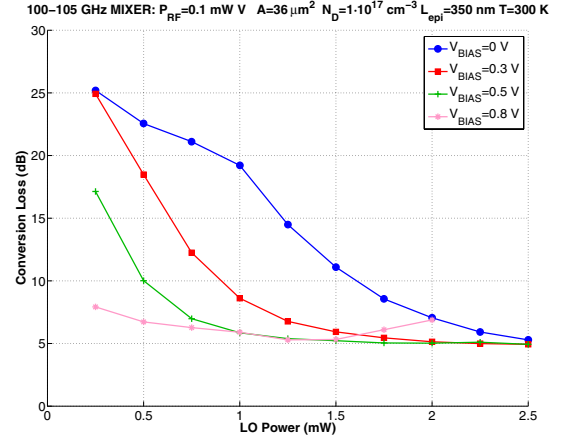


Fig. 1. 100-105 GHz Mixer. Joint influence of DC bias and LO power on conversion loss.

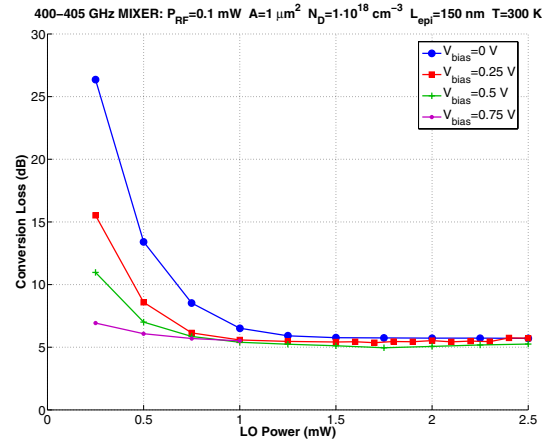


Fig. 2. 400-405 GHz Mixer. Joint influence of DC bias and LO power on conversion loss.

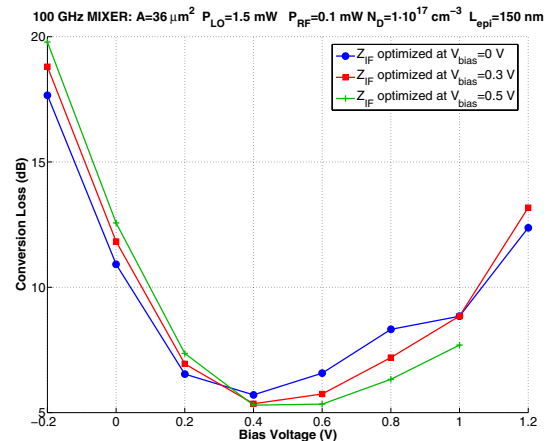


Fig. 3. 100-105 GHz Mixer. Influence of DC bias and IF impedance on conversion loss.

The first one is the shunting effect of the junction capacitance over the junction resistance [6]. This effect is directly proportional to the frequency and to the capacitance. Furthermore, the capacitance is directly proportional to the anode area and to the square root of the epilayer doping. Therefore, for high anode areas, a better performance will be obtained by reducing the doping, as can be seen in Fig. 7. This way, the capacitance is also reduced and the shunting effect is lower. However, the best way to improve performance by reducing the shunting effect at high frequencies is to reduce the area [6].

The second effect is the carrier velocity saturation [5]. Such effect may represent an important issue in Schottky mixers at high frequencies unless a high epitaxial layer doping is selected in the Schottky diode. For anode areas below  $1 \mu\text{m}^2$  the shunting effect is minimized and the more important limitation on the mixer performance is the carrier velocity saturation. Consequently, in this situation lower conversion losses will be achieved for higher dopings (Figs. 7 and 6).

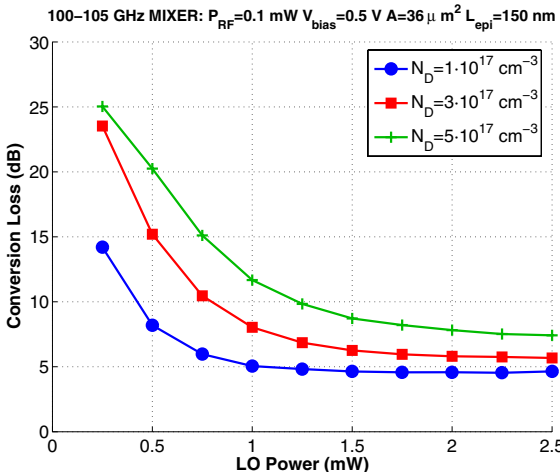


Fig. 4. 100-105 GHz Mixer. Influence of doping on conversion loss.

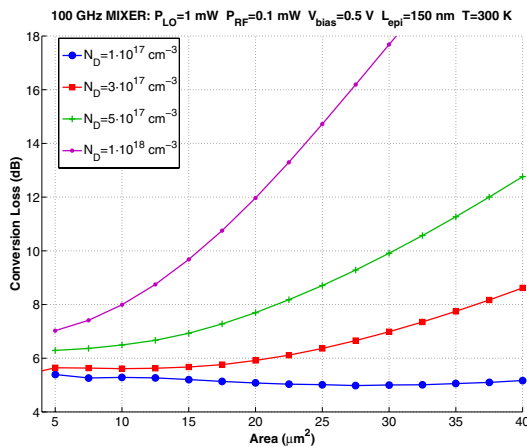


Fig. 5. 100-105 GHz Mixer. Joint influence of anode area and doping on conversion loss.

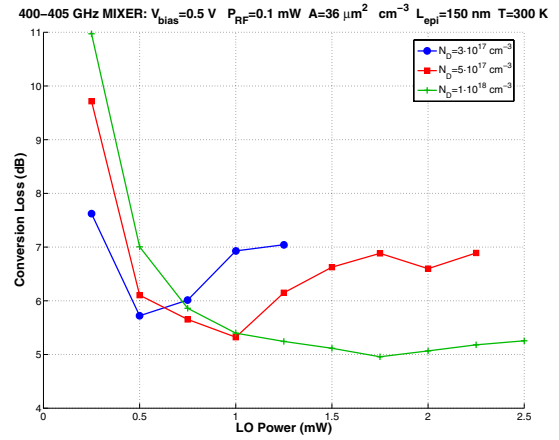


Fig. 6. 400-405 GHz Mixer. Influence of doping on conversion loss.

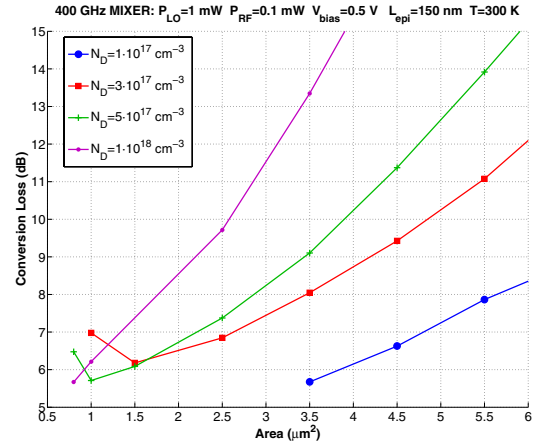


Fig. 7. 400-405 GHz Mixer. Joint influence of anode area and doping on conversion loss.

### C. Image Enhancement

One of the best known methods of reducing the conversion loss of a mixer is to terminate the diode in a reactance at the image frequency ( $f_Y$ ). If this *image enhancement* is performed properly, power that would be otherwise dissipated in the image termination is converted to the intermediate frequency (IF). This results in an improvement in efficiency [1].

Image enhancement is generally achieved by using an image-reject filter. But this filter is extremely difficult to realize due to the high selectivity required because of the fact that, in general, the LO and image frequencies are very close one of each other. Thus, it is complicated to synthesize simultaneously the LO and image frequency impedances and it is common in practice to use the LO impedance value as well for the image frequency. Fig. 8 shows for a 585 GHz mixer that, by selecting the same impedance value for both the LO and the image frequency, no significant additional loss is added with respect to the case:  $Z(f_Y) = 50 \Omega$ . Obviously, there is no image enhancement in any of these cases. However, if  $Z(f_Y) = 0 + j \cdot 300 \Omega$  is selected, there is an improvement of around 1 dB due to the image enhancement. Further studies about this effect on mixers performance can be found in [3].

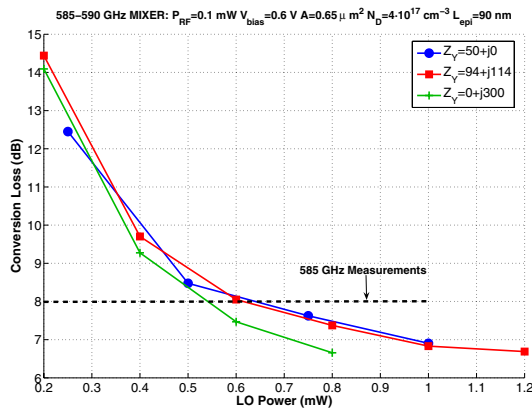


Fig. 8. 585-590 GHz Mixer. Influence of the impedance at the image frequency (Image Enhancement).

#### D. Validation

The objective of this section is simply to prove that simulated results are close to measurements. For this purpose, the 585 GHz mixer above has been analyzed using the circuit characteristics published in [7]. Unfortunately, only the conversion loss ( $\sim 8 \text{ dB}$ ) for a non-specified LO power level within the range 0.2-1 mW is reported in [7].

Impedances at the rest of frequencies have been fixed to  $50 \Omega$ . Results are presented in Fig. 8. It can be noticed that the 8 dB measured conversion loss is achieved for a LO power of around 0.6 mW according to simulations.

A larger amount of data from measurements will be necessary to have a complete validation of the mixer CAD tool. Further efforts are being made in this sense. However, the mixer CAD tool is conceptually equal to a previously reported and validated CAD tool for multiplier analysis so those validation results, which can be found in [8] and [9], can be extended to the mixer case.

#### IV. CONCLUSION

In this paper, we have presented some important design and optimization aspects for Schottky diode-based mixers at millimetre and submillimetre-wave bands.

For this purpose we have employed an in-house numerical mixer CAD tool that is based on a physical drift-diffusion model of the Schottky diode that allows taking into account most of the physical effects and limiting mechanism of Schottky mixers, such as the carrier velocity saturation and the shunting effect of the capacitance at high frequencies.

It has been demonstrated that it is essential a concurrent optimization of the design parameters of both the external circuit (bias, LO power, impedances, etc) and the Schottky diode (anode area, doping, ...). The image enhancement, a well-known method to improve the mixer performance, has been also analysed.

Simulation results corresponding to 100 GHz, 400 GHz and 585 GHz mixers have been presented. The results from the 585 GHz mixer have been compared with measurements with good agreement.

The mixer CAD tool represents a complement to a previous existent simulation tool for the analysis of multiplier circuits. As a result, a complete simulation tool

is available for the design of receivers up to Terahertz frequencies.

#### ACKNOWLEDGEMENT

The authors would like to thank the partial financial support of the European Space Agency to this work, under contract GSTP-3 ref. RIDER1 15293/01/NL/NF.

#### REFERENCES

- [1] S. Maas, *Microwave Mixers (Second edition)*. Artech-House, Inc. Boston-London, 1986.
- [2] J. Grajal, V. Krozer, E. Gonzalez, F. Maldonado, and J. Gimero, "Modelling and design aspects of millimeter-wave and submillimeter-wave Schottky diode varactor frequency multipliers," *IEEE Transactions on microwave theory and techniques*, vol. 48, pp. 910-928, April 2000.
- [3] J. V. Siles, J. Grajal, V. Krozer, and B. Leone, "A CAD tool for the design and optimization of Schottky diode mixers up to Terahertz frequencies," *Proceedings of 16th International Symposium on Space Terahertz Technology, Göteborg, Sweden*, May 2005.
- [4] P. Heron and M. Steer, "Jacobian calculation using the Multidimensional Fast Fourier Transform in the harmonic balance analysis of nonlinear circuits," *IEEE Transactions on Microwave Theory and Techniques*, vol. 38, no. 4, pp. 429-431, 1990.
- [5] E. Kollberg, T. Tolmunen, M. Frerking, and J. East, "Current saturation in submillimeter-wave varactors," *IEEE Transactions on Microwave Theory and Techniques*, vol. 40, pp. 831-838, May 1992.
- [6] T. Crowe, R. Mattauch, H. Roser, W. Bishop, W. Peatman, and X. Liu, "Gaas schottky diodes for thz mixing applications," *Proceedings of the IEEE*, vol. 80, pp. 1827-1841, November 1992.
- [7] K. Hui, J. Hesler, D. Kurtz, W. Bishop, and T. Crowe, "A micro-machined 585 GHz Schottky mixer," *IEEE Microwave and Guided Wave Letters*, vol. 10, pp. 374-376, September 2000.
- [8] J. Grajal, J. V. Siles, V. Krozer, E. Sbarra, and B. Leone, "Analysis and design of schottky diode multiplier chains up to Terahertz frequencies," *In Proc. ESA Microwave Technology Techniques Workshop: Preparing for Future Space Systems*, May 2004.
- [9] J. Grajal, J. V. Siles, V. Krozer, E. Sbarra, and B. Leone, "Performance evaluation of multiplication chains up to THz frequencies," *In Proc. 29th International Conference on Infrared and Millimeter Waves 12th International Conference on Terahertz Electronics*, September 2004.

---

# Low Cost Mixer for the 10.7 to 12.8 GHz Direct Broadcast Satellite Market

## Application Note 1136

---

### Introduction

The wide bandwidth requirement in DBS satellite applications places a big performance demand on the individual components in the low noise block downconverter. This application note describes a low cost, wide bandwidth passive mixer for 10.7 to 12.8 GHz DBS applications with low LO drive requirements. The mixer uses the Hewlett-Packard HSMS-8202 dual mixer diode in the SOT-23 package.

### DBS Frequency Conversion Scheme

Considering the broad RF bandwidth requirements of many of the DBS services such as Astra, the 10.7 to 12.7 GHz RF band must be downconverted to an IF which is generally 950 to approximately 2300 MHz. Attempting to translate the entire 2 GHz of RF bandwidth down to a 1.35 GHz wide IF does have its challenges. Most important besides the bandwidth issue is image rejection and LO radiation back out the antenna port of the LNA. A typical LNB uses two LO frequencies, one at 9.75 GHz and one at 10.6 GHz. With a 9.75 GHz LO, the 10.7 to 12.1 GHz band will be downconverted to 950 to 2350 MHz. With the 10.6 GHz LO,

the 11.7 to 12.8 GHz band down-converts to 1100 to 2200 MHz.

### Mixer Topologies

A very common mixer topology is the 90 degree branch line hybrid as shown in Figure 1.

The hybrid is a 4 port device with the LO and RF being fed into two adjacent ports and the two mixer diodes which are connected in series are connected to the remaining two ports. Each section of the square is 90 degrees in length. The IF is extracted from the junction of the two diodes. Proper filtering of the RF and LO is needed at the IF port. The operation of this mixer is covered in an existing Hewlett-Packard application Note AN-1052 [1]. This mixer provides good input VSWR at the LO and RF ports but has limited bandwidth and port to port isolation.

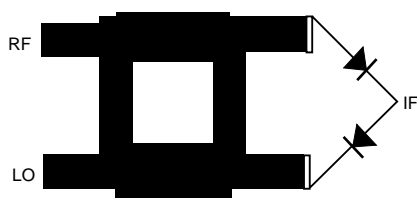
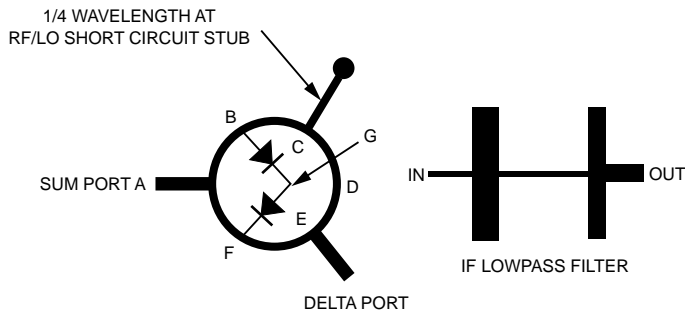


Figure 1. Branch Line Hybrid Mixer

Another mixer configuration is the hybrid ring mixer which is sometimes called a rat race mixer. According to Maas [2], the rat race mixer has a wider bandwidth as compared to other mixer types, making it appropriate for the very wide bandwidth of the typical DBS system. A typical rat race mixer is shown in Figure 2.

The Rat Race Mixer is comprised of six quarterwave length  $70 \Omega$  transmission lines in a circle. Each transmission line is 90 degrees in length for a total perimeter of 540 degrees or 1.5 wavelength.

The operation of the hybrid ring is as follows. A signal incident at port A is divided into two paths. The signals that arrive at ports B and F are both delayed by 90 degrees but arrive in phase and hence the name Sum port. A signal incident at the E port travels around the ring with a 90 degree delay to port F and a 270 degree delay to port B. The signals that arrive at ports B and F are out of phase when fed from port E and hence port E is called the Delta port. Normally the mixer diodes are driven with the LO fed out of phase through the delta port and the RF is fed in-phase at the Sum port.



**Figure 2. Rat Race Mixer**

The rat race mixer also provides port to port isolation. A signal incident at port A will split and the signals that arrive at port E will be out of phase and cancel providing some isolation. In a similar manner a signal incident at port E will divide and arrive again out of phase at port A providing isolation. This isolation could be in the 10 to 30 dB range. Best isolation will occur at the frequency where each segment of the rat race mixer is 90 degrees in length. As the frequency is varied from the nominal design frequency, the isolation and basic mixer performance will get worse.

Having a good handle on the best ports for both the RF and LO, attention must now be turned to the IF port. The IF can actually be extracted from the mixer in several locations. Based on the phasing through the ring, it appears that port C would offer some RF to IF or LO to IF isolation. This may suggest that port C may be a good choice. Some textbooks suggest the use of port D for the IF but based on the phase relationships, it does not appear to be the optimum port. Another option is to pull the IF at the junction of the two mixer diodes at point G. This point is usually RF and LO grounded. If one were to use an open circuited stub at this point to place point G at a low potential at

the RF and LO frequencies, then the IF could still be extracted at this point. The mixer in this application makes use of this method. A four section low pass filter provides an additional 25 to 30 dB attenuation of both the RF and LO frequencies at the IF port.

A quarterwave length (@ RF and LO) short circuited stub placed at port C places the ring coupler at a low impedance at the IF. According to the theory, this stub should improve conversion efficiency but was found to be unnecessary with the design presented in this application note.

## Mixer Design

### Ring Coupler

The first item to design is the ring coupler. As discussed in the previous section, the wide RF bandwidth is downconverted to the IF in two segments. The actual frequency at which the band is split depends on a couple of factors. One is image rejection of available RF filtering and the other is LO to RF port radiation. Image rejection is determined primarily by the bandpass filter at the RF port of the mixer. Radiated LO from the LNA antenna port is influenced by several factors. The first is the reverse gain of the LNA at the LO frequency. The second would be the LO to RF port isolat-

tion of the mixer. The third factor is the rejection of the LO frequency by the RF port filtering. Considering that the lowest RF frequency is 10.7 GHz and one of the suggested LO frequencies is 10.6 GHz, suggests that the RF port filtering will be a challenge. Therefore, it is best to design the mixer for best performance at the 10.6 GHz LO frequency. The ring coupler was designed to be 540 degrees in length at 10.6 GHz. The characteristic impedance of the transmission line is  $70\ \Omega$ .

### Diode Match

For low cost, the Hewlett-Packard HSMS-8202 in a surface mount SOT-23 plastic package containing two matched Schottky diodes was chosen for the application. Although a plastic packaged part has greater parasitic elements than a typical ceramic package, the parasitics can be tuned out.

The  $70\ \Omega$  characteristic impedance of the ring coupler dictates that each port be  $50\ \Omega$  for best performance. Typically the diodes are connected directly to ports B and F with no matching networks. Considering the bandwidth requirement of the mixer, a matching network was designed within the space confines of the ring coupler. The challenge is to match each diode as best as possible from 9.75 GHz (the lowest LO frequency) to 12.8 GHz (the top of the RF band).

The model for each diode in the SOT-23 package is shown in Figure 3.

The equivalent circuit takes into account the nominal +7 dBm LO drive and the package parasitics. Each HSMS-8202 consists of two of these diodes in series with the anode of one diode and the

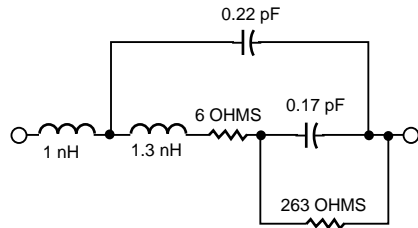


**Figure 3. Diode Equivalent Circuit**

cathode of the second diode connected together and brought out to a third terminal. It is this third terminal that will be used as the IF port. For best mixer performance, the IF port of the diode should be presented with a low impedance at the RF and LO frequencies. This low impedance keeps the RF and LO signals from propagating out the IF port and consequently making conversion loss worse. The low impedance is accomplished by placing an open circuited stub on the printed circuit board at the IF terminal of the diode. A trapezoidal open circuited stub is used in the design and its length and angle were optimized using EESOF Libra.

A small length of transmission line was used to provide a better impedance match to the diodes over the 9.75 to 12.8 GHz frequency range. Its length and width were optimized with EESOF Libra. The HSMS-8202 and its associated matching networks are shown in Figure 4.

With the LO being injected into the Delta port, the phase of the voltages present at the diodes is out of phase but since the diodes are connected to the ring coupler in opposite orientation from each other they can be viewed as being turned on simultaneously. This means that the model for the diode package and the matching network must assume that the diodes are on at the same time and

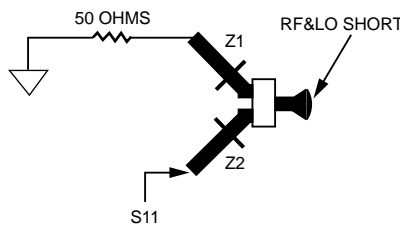


**Figure 4. HSMS-8202 and Matching Networks**

should be modeled as such.

As shown in Figure 4, both diodes share the trapezoidal open circuited stub as a common RF and LO short. Each diode leg must then be matched individually to as near  $50\ \Omega$  as possible. Since both diodes are identical, then it follows that identical matching networks be used.

The circuit shown in Figure 4 was optimized using EESOF Libra. One of the diodes and its corresponding matching structure is terminated in  $50\ \Omega$  with the other leg used by the simulator to determine best match. Both Z1 and Z2, which are identical, and the trapezoidal open circuited stub were optimized for best return loss, S11. The fact that the entire matching networks and diodes must fit within the ring coupler does limit the physical size of the networks. According to EESOF Libra, S11 optimized at approximately 10 dB from 9.75 to 12.8 GHz.

The resultant matching network Z1 and Z2 are series transmission lines of  $0.035"$  width by  $0.200"$  in length. The additional stubs that are placed on Z1 and Z2 were later determined empirically to improve conversion loss. They are  $0.020"$  by  $0.120"$  and placed approximately  $0.140"$  from the ring

coupler. These dimensions are for a dielectric material of  $0.020"$  thickness and a dielectric constant of 2.5. Complete artwork is contained in Figure 10 at the end of this application note.

## Construction

The completed mixer is shown in Figure 5. The Sum port is dc connected to the ring coupler. The Delta port is ac coupled with a  $1\text{ pF}$  chip capacitor at the ring coupler. The small value chip capacitor should help reduce IF leakage out the Delta port when used for LO injection.

A small wire is used to dc couple in the IF low pass filter. In actual systems, the connection from the mixer to the IF is quite often through a feedthrough pin to an adjacent printed circuit board where the IF amplifiers are located. Another option is a zero ohm resistor across the ring coupler.

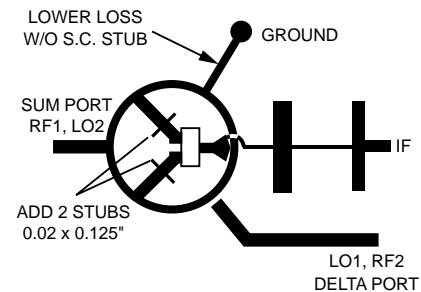


**Figure 5. Ku Band Mixer using HSMS-8202**

## Performance

Conversion loss was initially measured using the Delta port as the LO port. As was later determined, the mixer had slightly less conversion loss at the low end of the frequency range when the Sum port was driven with the LO. The performance of both configurations is shown in Figures 6 and 7.

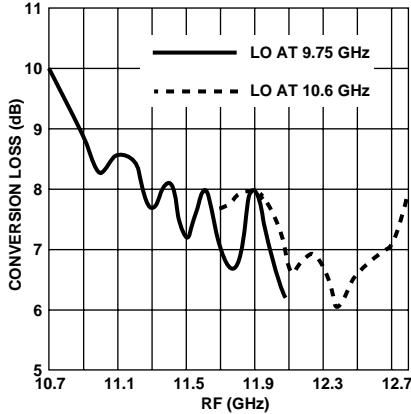


Figure 6. Conversion Loss with +1 dBm LO @ Delta Port

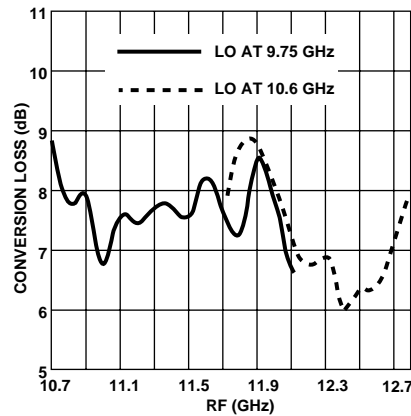


Figure 7. Conversion Loss with +5 dBm LO @ Sum Port

+1 dBm LO was found to produce minimum conversion loss when the Delta port was the LO port. When injecting the LO into the Sum port, it was found that +5 dBm was required to produce minimum conversion loss.

Based on the frequency of minimum conversion loss and the performance at the band edges, it appears that the ring may be centered somewhat high in frequency. Considering that the ring and diode matching networks must cover 9.75 to 12.7 GHz, a nearly 3 GHz of bandwidth, the perfor-

Table 1. LO to RF and LO to IF Isolation

Configuration	LO Frequency (GHz)	LO to RF Isolation (dB)	LO to IF Isolation (dB)
LO in Sum Port @ +5 dBm	9.75	25.4	40.3
	10.6	30.5	37.8
LO in Delta Port @ +1 dBm	9.75	25.8	48.0
	10.6	32.5	46.0

mance can still be considered very good. The improved higher end performance might well offset the usual gain and noise figure rolloff of the LNA.

LO to RF port and LO to IF port isolation was tested for both configurations and the results are shown in Table 1.

Based on the LO to RF isolation data, it appears that the ring coupler was optimized properly for 10.6 GHz rather than 9.75 GHz. Comparing the isolation data and the previous conversion loss data may suggest that the center frequency is even higher than 10.6 GHz. The next iteration should be centered somewhat lower in frequency to improve the low end RF performance.

The LO to IF isolation was measured with a four section low pass filter at the IF port. The low pass filter with its inductive input places a high impedance to the RF and LO at the junction of the mixer diodes and the trapezoidal bypass capacitor. As the data shows, the basic mixer has better LO to IF isolation when the LO is fed into the Delta port.

Conversion loss versus LO power was measured for both mixer schemes. For test purposes, the RF frequency is 12.2 GHz and the LO frequency is 10.6 GHz. The per-

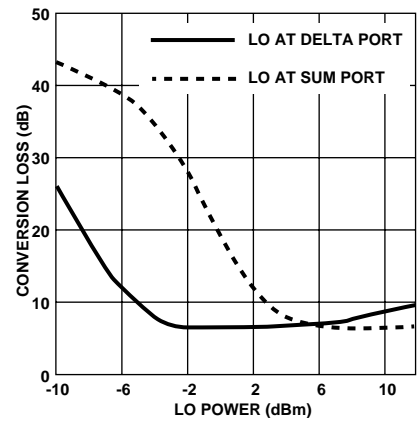


Figure 8. Effect of LO Power on Mixer Performance

formance is shown in Figure 8. Normally, one would not expect as radical a difference in performance between feeding the Sum or the Delta port. Further investigation showed that the Delta port has a very good return loss as compared to the Sum port when used as the LO port. The mixer was originally optimized for best conversion loss when the Delta port was used to feed the LO. The resultant bench tuning optimized the mixer for delta port LO feed with the RF at the Sum port. The Delta port return loss with a 10.6 GHz LO measured 11.5 dB at a +1 dBm LO and 14.7 dB at +5 dBm LO power. The same measurement on the Sum port revealed return losses of only 2 dB or slightly less. Converting the return loss to a resultant mismatch loss suggests at least a 4.2 dB – 0.3 dB = 3.9 dB

potential difference in drive level required. This correlates well with the 4 dB difference observed in LO drive requirements for feeding the Sum versus the Delta port.

### Dual Channel LNB

The mixer may be used as part of a dual channel LNB as shown in Figure 9. A power divider is used to feed the LO to both mixers. Approximately +5 to +6 dBm LO power is required at the input to the power divider. This insures adequate LO drive to each mixer.

The most important parameter of the two channel mixer is the channel to channel isolation. Poor channel to channel isolation results in the appearance of co-channel interference in the received TV signal. The channel to channel isolation is influenced by the LO power divider and its ability to couple energy from one mixer to the other. From the system point of view, the concern is how far down in amplitude will the RF1 signal be when it cross couples from channel 1 over into channel 2 through the LO power divider and shows up as undesired downconverted IF output at the IF2 port.

The RF to LO isolation has been measured at approximately 25 dB. A well designed LO power divider may have only 15 dB of port to port isolation. Therefore, the undesired RF1 signal that is incident on the LO port of the channel 2 mixer is 40 dB below the normal RF1 or RF2 signal level. The question that remains is how well does this undesired RF1 signal (which is now at the same port as the normal LO signal at channel 2 mixer) downconvert to an IF signal at the IF2 port?

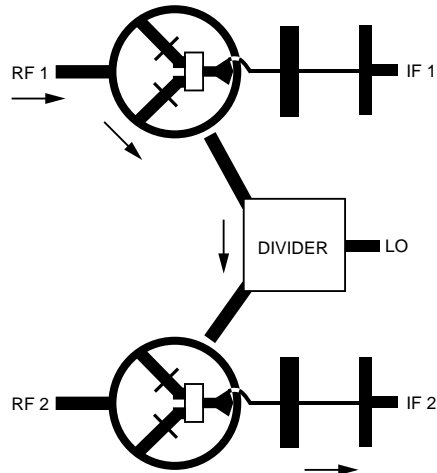


Figure 9. Dual Channel Downconverter

Table 2. Conversion Loss with RF and LO incident on same port

Mixer Configuration	LO Frequency (GHz)	RF Frequency (GHz)	Conversion Loss (dB)
RF and LO @ Delta Port	9.75	10.7	25
	9.75	11.7	27
	10.6	12.0	24
	10.6	12.8	24
RF and LO @ Sum Port	9.75	10.7	23
	9.75	11.7	20.5
	10.6	12.0	23
	10.6	12.8	23

The mixer was tested for this situation by coupling in a -20 dBm RF signal (simulating the interfering signal from the adjacent channel mixer) along with the normal +1 dBm LO into the Delta port of the mixer. Conversion loss was measured. The results are shown in Table 2 for both mixer configurations.

The mixer exhibits from 10 to 15 dB greater conversion loss when the RF and LO are fed into the same port. Slightly greater conversion loss is obtained when the LO is injected into the Delta port.

Therefore, the interfering signal from the adjacent channel will be at a level approximately 50 to 55 dB below the desired signal at the IF output port.

The mixer provides this type of rejection for the same reason that a balanced mixer provides AM LO noise cancellation. Normally the diodes are LO driven from the Delta port which causes the LO voltage to have a 180 degree phase difference at the two diodes. Since the diodes are reversed, the junction conductance waveforms across each diode (generated as a

result of the large-signal termed the LO) are in phase. With the RF fed into the Sum port, the RF voltage is in phase at the diodes. Since the junction conductance waveforms are in phase along with the RF voltage, then the IF voltages must also be in phase. The IF voltages add and produce the desired IF output. If there is AM noise riding on the LO signal or any other small-signal also incident on the LO port, the situation changes. The undesired small-signal, which enters the Delta port, arrives at the diodes out of phase and therefore cancels at the IF port.

## Conclusion

The HSMS-8202 has been shown to produce very good performance in DBS applications when used in a rat race type mixer. The mixer also provides a good solution for dual channel systems.

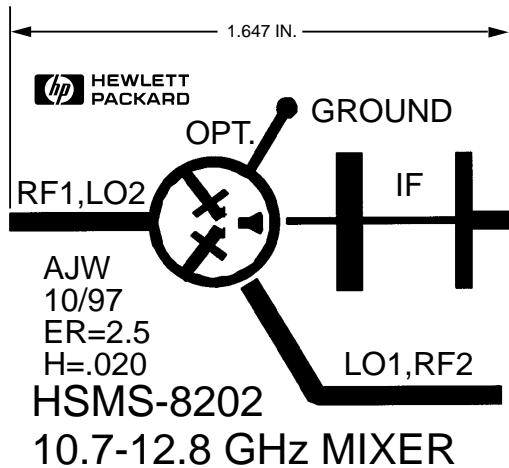


Figure 10. Artwork for DBS Mixer

---

## References

- [1] *A Low Cost, Surface Mount X-Band Mixer*, Hewlett-Packard Application Note 1052, 5091-4934E (7/92)
- [2] *Microwave Mixers*, Stephen A. Maas, Artech House, Inc., © 1986

[www.hp.com/go/rf](http://www.hp.com/go/rf)

For technical assistance or the location of your nearest Hewlett-Packard sales office, distributor or representative call:

**Americas/Canada:** 1-800-235-0312 or  
(408) 654-8675

**Far East/Australasia:** Call your local HP sales office.

**Japan:** (81 3) 3335-8152

**Europe:** Call your local HP sales office.

Data Subject to Change

Copyright © 1998 Hewlett-Packard Co.

Printed in U.S.A. 5966-2488E (7/98)

# Conversion Loss and Noise of Microwave and Millimeter-Wave Mixers: Part 1—Theory

DANIEL N. HELD, MEMBER, IEEE, AND ANTHONY R. KERR, ASSOCIATE MEMBER, IEEE

**Abstract**—An analysis is presented for the conversion loss and noise of microwave and millimeter-wave mixers. The analysis includes the effects of nonlinear capacitance, arbitrary embedding impedances, nonideality of microwave diodes, and shot, thermal, and scattering noise generated in the diode. Correlation of down-converted components of the time-varying shot noise is shown to explain the “anomalous” noise observed in millimeter-wave mixers. Part 1 of the paper presents the theoretical basis for predicting mixer performance, while Part 2 compares theoretical and experimental results for mixers operating at 87 and 115 GHz.

## I. INTRODUCTION

THE BASIC principles of frequency conversion using crystal diodes were first studied in depth by Torrey and Whitmer [1] in 1948. Since then attempts at a more accurate analysis of microwave mixer performance have been limited by the complexity of the nonlinear problem and by a lack of understanding of the noise properties of pumped diodes. Practical developments in the design of mixers and mixer diodes have resulted in a number of commonly used designs whose conversion loss and noise figure are often within a few decibels of the theoretical best values predicted for idealized switching mixers. This paper and its companion paper (Part 2) attempt to close the gap between theory and practice.

Following Torrey and Whitmer's original work, the assumption of a sinusoidal local oscillator (LO) voltage across an exponential resistive diode was often used, with its implicit assumption that the diode was short-circuited at all harmonics of the LO. The effects of the parasitic series resistance and capacitance (assumed constant) of the mixer diode were investigated using approximate methods by Sharpless [2], Messenger and McCoy [3], Mania and Stracca [4], and Kerr [5]; and a new and intuitive approach to mixer analysis was taken by Barber [6], who approximated the diode by a switch whose pulse-duty ratio determined the conversion properties of the mixer. However, all these approaches required simplifying assumptions about the termination of higher order sidebands and ignored the effects of the nonlinear diode capacitance. Agreement between theory and experiment was at best within a few decibels in conversion loss and noise figure.

An important work by Saleh [7] in 1971 studied the effects of local oscillator waveforms and higher order sideband

terminations on resistive mixers, and demonstrated that these characteristics must be considered if an accurate analysis is to be made. The problem of a more exact analysis of a microwave mixer has been tackled recently by Egami [8], who performed a numerical nonlinear analysis for a known diode and embedding impedance, followed by a small-signal conversion loss analysis. Egami assumed a constant junction capacitance and used a harmonic balance technique to solve the nonlinear problem, considering three harmonics of the local oscillator.

In recent years considerable misunderstanding has arisen on the subject of mixer noise. The correlation properties of shot noise in vacuum tube mixers were understood by Strutt [9] in 1946 and since then van der Ziel and Waters [10], [11], Kim [12], and Dragone [13] have further developed this theory. The misunderstanding seems to have arisen with the assumption, by Messenger and McCoy [3], that a mixer and a passive attenuator have similar noise properties and that the temperature of this equivalent attenuator is “the time average of the static noise characteristic” of the diode. This led to a widely held belief that for a Schottky diode mixer, the noise-temperature ratio [3]  $t \approx 1$ , and to the subsequent observation of an “anomalous” component of noise in millimeter-wave mixers [14].

In the present paper the large-signal nonlinear problem and the small-signal linear problem are presented in forms suitable for computer solution. Arbitrary embedding impedances are allowed at the harmonics of the LO and at all the sideband frequencies, and any diode capacitance law can be assumed. The shot-noise theories of Strutt [9], van der Ziel [11], Kim [12], and Dragone [13] are extended to include the effects of arbitrary sideband terminations, as well as thermal (Johnson) noise and scattering noise, resulting in a noise correlation matrix which is compatible with the formulation of the small-signal mixer analysis. The microwave properties of small Schottky-barrier diodes are discussed, and it is shown that skin effect, thermal time constants, and depletion layer fringing effects can all be significant in determining the mixing properties of the diode.

The theory presented in this paper is experimentally verified in a companion paper (Part 2) in which theoretical loss and noise predictions for millimeter-wave mixers are shown to be in good agreement with experiment.

## II. NONLINEAR ANALYSIS

The small-signal loss and noise properties of a mixer are governed by the large-signal current and voltage waveforms

Manuscript received February 18, 1977; revised May 12, 1977.

D. N. Held was with the Department of Electrical Engineering, Columbia University, New York, NY 10027. He is now with the Jet Propulsion Laboratory, California Institute of Technology, Pasadena, CA 91103.

A. R. Kerr is with the NASA Institute for Space Studies, Goddard Space Flight Center, New York, NY 10025.

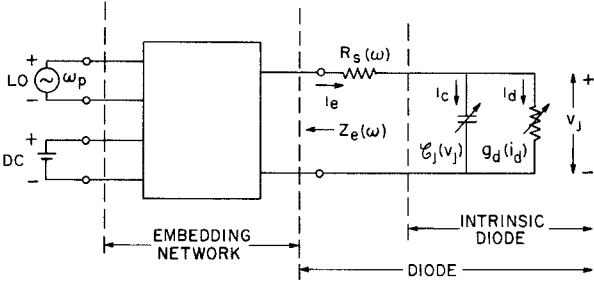


Fig. 1. Equivalent circuit of the mixer. The intrinsic diode  $C_j$  and  $g_d$  is nonlinear and is characterized in the time domain, while the diode series resistance  $R_s$  and the embedding impedance  $Z_e$  are linear and are best represented in the frequency domain.

produced at the diode by the LO. The steady-state large-signal response of the mixer circuit of Fig. 1 can be described in terms of the Fourier coefficients of the voltage and current  $v_j$  and  $i_e$ . Thus

$$v_j(t) = \sum_{k=-\infty}^{\infty} V_k e^{jk\omega_p t}, \quad V_k = V_{-k}^* \quad (1)$$

$$i_e(t) = i_c(t) + i_d(t) = \sum_{k=-\infty}^{\infty} I_{ek} e^{jk\omega_p t}, \quad I_{ek} = I_{e-k}^* \quad (2)$$

where  $\omega_p$  is the LO frequency. Two sets of boundary conditions must be satisfied simultaneously by these quantities. The first, imposed by the diode, is most easily expressed in the time domain, while the second set, imposed by the embedding network, is for our purposes more conveniently considered in the frequency domain. At the diode

$$i_d = i_0 [\exp(\alpha v_j) - 1] \quad (3)$$

and

$$i_c = C_j \frac{dv_j}{dt} \quad (4)$$

where

$$C_j = C_{j0} \left( 1 - \frac{v_j}{\phi} \right)^{-\gamma} \quad (5)$$

and

$$\alpha = q/\eta kT. \quad (6)$$

From (3) the incremental conductance of the diode

$$g_d = \frac{di_d}{dv_j} = \alpha(i_d + i_0) \approx \alpha i_d. \quad (7)$$

The embedding network requires that

$$V_k = -I_{ek}[Z_e(k\omega_p) + R_s(k\omega_p)], \quad k = \pm 2, \pm 3, \dots, \pm \infty \quad (8a)$$

$$V_{\pm 1} = V_p - I_{e\pm 1}[Z_e(\pm\omega_p) + R_s(\pm\omega_p)] \quad (8b)$$

$$V_0 = V_{dc} - I_{e0}[Z_e(0) + R_s(0)] \quad (8c)$$

where  $V_p$  and  $V_{dc}$  are the LO and dc-bias voltages, respectively. The frequency dependence of  $R_s$  is due to skin effect and is discussed in Section V.

Methods for solving the nonlinear mixer problem have been described by several authors [15]–[17]. However, only that of Gwarek [17] appears capable of handling the case in which the diode capacitance is a function of junction voltage and in which a large number (six or seven) of harmonics of the LO are considered. Using an IBM 360/95 computer, we have found that with Gwarek's method convergence is achieved in about two seconds. The degree of convergence of the solution is determined using the convergence parameter described by Kerr [16]. It is assumed that there is one unique steady-state solution; the possibility of multiple solutions, mentioned in [16] is beyond the scope of this work.

Having determined the LO waveforms at the diode, (3)–(7) give  $i_d(t)$ ,  $g_d(t)$ , and  $C_j(t)$ . These may be expressed as Fourier series:

$$i_d(t) = \sum_{k=-\infty}^{\infty} I_k \exp(jk\omega_p t), \quad I_k = I_{-k}^* \quad (9)$$

$$g_d(t) = \sum_{k=-\infty}^{\infty} G_k \exp(jk\omega_p t), \quad G_k = G_{-k}^* \quad (10)$$

and

$$C_j(t) = \sum_{k=-\infty}^{\infty} C_k \exp(jk\omega_p t), \quad C_k = C_{-k}^*. \quad (11)$$

These quantities, together with the embedding impedance  $Z_e(\omega)$ , determine the small-signal properties of the mixer.

### III. SMALL-SIGNAL ANALYSIS

Knowing the Fourier coefficients of the diode capacitance and conductance, it is possible to construct the small-signal conversion matrix for the diode [1], [17]. This matrix interrelates the various sideband frequency components of the small-signal current and voltage  $\delta I_m$  and  $\delta V_m$  shown in Fig. 2. The subscript notation for the sideband quantities follows that of Saleh [7]; subscript  $m$  indicates frequency  $\omega_0 + m\omega_p$ , where  $\omega_p$  and  $\omega_0$  are the LO and intermediate frequencies. Thus  $Z_{em} = Z_e(\omega_m) = Z_e(\omega_0 + m\omega_p)$ . The conversion matrix  $Y$  is a square matrix defined by

$$\delta I = Y \delta V$$

where

$$\delta I = [\dots, \delta I_1, \delta I_0, \delta I_{-1}, \dots]^T$$

and

$$\delta V = [\dots, \delta V_1, \delta V_0, \delta V_{-1}, \dots]^T. \quad (12)$$

For convenience, the row and column numbering of all matrices and vectors in this paper will correspond with the sideband numbering. For example,

$$Y \equiv \begin{array}{ccccc} \text{row \#} & : & \left[ \begin{array}{ccccc} & \vdots & \vdots & \vdots & \vdots \\ 1 & \cdots & Y_{11} & Y_{10} & Y_{1-1} & \cdots \\ 0 & \cdots & Y_{01} & Y_{00} & Y_{0-1} & \cdots \\ -1 & \cdots & Y_{-11} & Y_{-10} & Y_{-1-1} & \cdots \\ \vdots & & \vdots & \vdots & \vdots & \ddots \\ & & & & & \end{array} \right] \\ & & \cdots & 1 & 0 & -1 & \cdots & \text{column \#} \end{array}$$

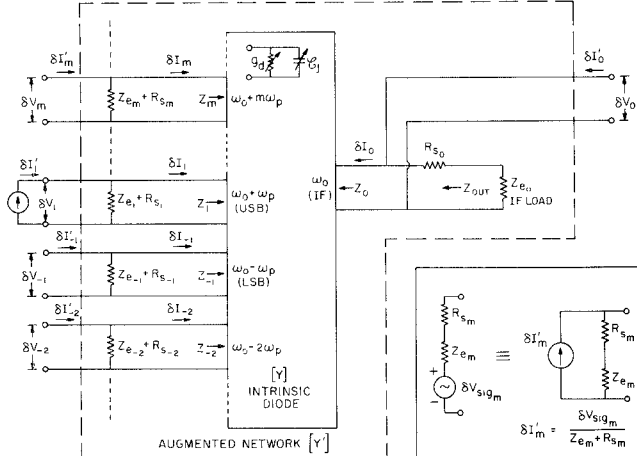


Fig. 2. Small-signal representation of the mixer as a multifrequency linear multiport network. The voltage and current  $\delta V_m$  and  $\delta I_m$  at any port  $m$  are the small-signal components at frequency  $(\omega_0 + m\omega_p)$  appearing at the intrinsic diode; each port represents one sideband frequency. The conversion matrix  $Y$  is the admittance matrix of the intrinsic diode. The augmented network (broken line) includes all the sideband embedding impedances  $Z_{e_m}$  and is characterized by the augmented admittance matrix  $Y'$ . During normal mixer operation the equivalent signal current generator  $\delta I'$  is connected at port 1 of the augmented network, the other ports being open-circuited. In the noise analysis, equivalent noise current sources  $\delta I'_{S_m}$  and  $\delta I'_{T_m}$  are connected to all ports. The inset shows the relation between the signal source  $\delta V_{sig_m}$  at the  $m$ th sideband and its equivalent source  $\delta I'_m$ .

Using this notation the elements of  $Y$  are given by [1], [17]

$$Y_{mn} = G_{m-n} + j(\omega_0 + m\omega_p)C_{m-n} \quad (13)$$

where  $G_k$  and  $C_k$  are the Fourier coefficients of the diode conductance and capacitance as defined in (10) and (11).

It is convenient to form an augmented  $Y$  matrix,  $Y'$ , which is the admittance matrix of the multiport network outlined by the broken line in Fig. 2. This augmented network contains the whole mixer, including all its external terminating impedances  $Z_{e_m}$ , but does not contain signal sources associated with these terminations. Signal sources are replaced by equivalent current sources  $\delta I'_m$  connected across  $(Z_{e_m} + R_{s_m})$  as shown in Fig. 2 (inset). The ports of the augmented network are all normally open-circuited. For the augmented network

$$\delta I' = Y' \delta V \quad (14)$$

where the elements of  $\delta I'$  are defined in Fig. 2, and

$$Y' = Y + \text{diag} \left[ \frac{1}{Z_{e_m} + R_{s_m}} \right]. \quad (15)$$

Inverting (14) gives

$$\delta V = Z \delta I' \quad (16)$$

where

$$Z = (Y')^{-1}. \quad (17)$$

#### A. Mixer Port Impedances

To determine the port impedance  $Z_m$ , defined in Fig. 2, the corresponding embedding impedance  $Z_{e_m}$  is open-circuited,

enabling  $Z_m$  to be measured at port  $m$  of the augmented network. It follows that

$$Z_m = Z'_{mm,\infty} \quad (18)$$

where the subscript  $\infty$  indicates that  $Z'_{mm}$  (the  $mm$ th element of  $Z'$ ) is evaluated with  $Z_{e_m} = \infty$ . In particular the IF output impedance is (see Fig. 2)

$$Z_{\text{out}} = Z_0 + R_{s_0} = Z'_{00,\infty} + R_{s_0}. \quad (18a)$$

For a microwave mixer the embedding impedance at all frequencies other than the IF is defined by the mixer geometry. However, the IF load impedance  $Z_{e_0}$  can usually be adjusted for optimum performance using a matching circuit. Throughout the rest of this paper it will be assumed that the IF port is conjugate-matched,<sup>1</sup> and IF-matched  $Y'$  and  $Z$  matrices will be implied.

#### B. Conversion Loss

The conversion loss of a mixer

$$L = \frac{\text{Power available from source } Z_{e_1}}{\text{Power delivered to load } Z_{e_0}}. \quad (19)$$

For the purposes of analysis  $L$  may be expressed as the product of three separate loss components:

$$L = K_0 L K_1 \quad (20)$$

where

$$\begin{aligned} K_0 &= \frac{\text{Power delivered to } (Z_{e_0} + R_{s_0})}{\text{Power delivered to } Z_{e_0}} \\ &= \frac{\text{Re } [Z_{e_0} + R_{s_0}]}{\text{Re } [Z_{e_0}]} \end{aligned} \quad (21)$$

$$L = \frac{\text{Power available from } (Z_{e_1} + R_{s_1})}{\text{Power delivered to } (Z_{e_0} + R_{s_0})} \quad (22)$$

and

$$\begin{aligned} K_1 &= \frac{\text{Power available from } Z_{e_1}}{\text{Power available from } (Z_{e_1} + R_{s_1})} \\ &= \frac{\text{Re } [Z_{e_1} + R_{s_1}]}{\text{Re } [Z_{e_1}]} \end{aligned} \quad (23)$$

$K_0$  and  $K_1$  account for loss in the series resistance at the IF and signal frequencies, while  $L$  is the conversion loss of the intrinsic mixer with no series resistance. Using (22) and (16),

$$\begin{aligned} L &= \frac{1}{\text{Re } [\delta V_0 \delta I_0^*]} \frac{|\delta I'_1|^2 |Z_{e_1} + R_{s_1}|^2}{4 \text{Re } [Z_{e_1} + R_{s_1}]} \\ &= \frac{1}{4 |Z'_{01}|^2} \frac{|Z_{e_0} + R_{s_0}|^2}{\text{Re } [Z_{e_0} + R_{s_0}]} \frac{|Z_{e_1} + R_{s_1}|^2}{\text{Re } [Z_{e_1} + R_{s_1}]} \end{aligned} \quad (24)$$

From (20), (21), (23), and (24), the conversion loss

$$L = \frac{1}{4 |Z'_{01}|^2} \frac{|Z_{e_0} + R_{s_0}|^2}{\text{Re } [Z_{e_0}]} \frac{|Z_{e_1} + R_{s_1}|^2}{\text{Re } [Z_{e_1}]} \quad (25)$$

<sup>1</sup> Note that although a conjugate-match at the IF port results in maximum power transfer, the signal port should not in general be conjugate-matched for minimum conversion loss [7].

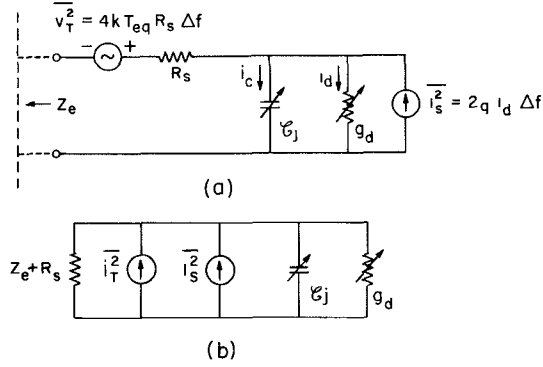


Fig. 3. (a) Noise equivalent circuit of the mixer. (b) The equivalent circuit with the thermal noise source  $\overline{v_T^2}$  transformed to a current source  $\overline{i_T^2}$  given by equation (27). The sideband components of the noise sources  $\overline{i_T^2}$  and  $\overline{i_S^2}$  can then be treated in the same way as the equivalent external small-signal currents  $\delta I'_m$  in Fig. 2.

Equation (25) may be generalized to give the conversion loss from any sideband  $j$  to any other sideband  $i$ .

$$L_{ij} = \frac{1}{4|Z'_{ij}|^2} \frac{|Z_{e_i} + R_{s_i}|^2}{\text{Re}[Z_{e_i}]} \frac{|Z_{e_j} + R_{s_j}|^2}{\text{Re}[Z_{e_j}]} \quad (26)$$

#### IV. MIXER NOISE

The sources of noise in a Schottky diode are 1) thermal noise in the series resistance, 2) shot noise generated by current flow across the barrier, and 3) noise due to phonon scattering and, in gallium arsenide, intervalley scattering [22]. In room-temperature mixers shot and thermal noise predominate, with scattering noise contributing typically only 5–10 percent to the overall mixer noise, as is shown in Part 2 of this paper. We have not attempted an exact analysis of scattering noise but assume that it can be approximated by an increase in the noise temperature of the series resistance.

The equivalent circuit of the diode including noise sources is shown connected to the embedding network in Fig. 3(a). Fig. 3(b) shows the same circuit transformed to a configuration more compatible with the mixer equivalent circuit of Fig. 2; the thermal noise source  $\overline{v_T^2}$  has been replaced by an equivalent current source  $\overline{i_T^2}$ . As seen by the intrinsic diode ( $g_d$  and  $\mathcal{C}_j$ ),

$$\overline{i_T^2} = \frac{4kT_{eq}R_s\Delta f}{|Z_e + R_s|^2} \quad (27a)$$

but, as seen by the IF load impedance  $Z_{eo}$ ,

$$\overline{i_T^2} = \frac{4kT_{eq}R_s\Delta f}{|Z_0|^2} \quad (27b)$$

where  $Z_0$  is the output impedance of the intrinsic diode as defined in Fig. 2. The shot-noise current source

$$\overline{i_S^2} = 2qi_d\Delta f. \quad (28)$$

##### A. Shot Noise

The diode shot noise given by (28) is a function of the instantaneous flow of current  $i_d$  across the barrier, produced

by the LO. Since  $i_d(t)$  is periodic, the shot-noise current can be regarded as a stationary white noise current modulated at the LO frequency  $\omega_p$ . The properties of this modulated shot noise have been studied by Strutt [9], Kim [12], van der Ziel [11], and Dragone [13], and the present analysis is based on their work.

First, we shall consider the *unmodulated* shot-noise current to be composed of pseudosinusoidal currents [18], [19]  $\delta\mathcal{I}_{S_m} \exp[j(\omega_0 + m\omega_p)t + j\phi_m]$  at each of the sideband frequencies  $\omega_m = \omega_0 + m\omega_p$ ,  $m = 0, \pm 1, \dots, \pm \infty$ . All other frequency components of the noise can be disregarded since they cannot contribute to the IF output of the mixer. Next, consider each of the currents  $\delta\mathcal{I}_{S_m}$  to be modulated by the local oscillator ( $\omega_p$ ), generating modulation products at all the frequencies  $\omega_m + n\omega_p$ ,  $n = 0, \pm 1, \pm 2, \dots, \pm \infty$ , which are the sideband frequencies  $\omega_{m+n}$ . The modulation products are present at the terminals of the intrinsic diode and will be converted to the output frequency as described by (16). Clearly their individual outputs will be correlated. The random phase variable  $\phi_m$  is preserved in these output components but is eliminated when we finally consider a finite bandwidth and take the ensemble average of a set of pseudosinusoidal currents in a narrow band about each of the frequencies  $\omega_m$ .

Let  $\delta I'_{S_m}$  denote the complex amplitude of the pseudosinusoidal noise current at sideband frequency  $\omega_m$ .  $\delta I'_{S_m}$  contains components due to the modulation products of all the currents  $\delta\mathcal{I}_S$  and is therefore the shot-noise input current at port  $m$  of the mixer, which corresponds to a signal input current  $\delta I'_m$  in Fig. 2. The vector  $\delta I'_S$  is defined as  $[\dots, \delta I'_{S_0}, \delta I'_{S_1}, \delta I'_{S_{-1}}, \dots]^T$ . Equation (16) now enables the IF output noise voltage due to shot noise to be determined:

$$\delta V_{S_0} = \mathbf{Z}_0 \delta I'_S \quad (29)$$

where  $\mathbf{Z}_0$  is the zeroth row of the square matrix  $\mathbf{Z}$ . Taking the ensemble average<sup>2</sup> of  $|\delta V_{S_0}|^2$  (which corresponds considering a nonzero bandwidth),

$$\langle |\delta V_{S_0}|^2 \rangle = \mathbf{Z}_0 \langle \delta I'_S \delta I'^{\dagger}_S \rangle \mathbf{Z}_0^{\dagger}. \quad (30)$$

The square matrix  $\langle \delta I'_S \delta I'^{\dagger}_S \rangle$  is known as the *correlation matrix* for the mixer, since the  $(m,n)$  element describes the correlation between the components of shot noise at sideband frequencies  $\omega_m$  and  $\omega_n$ . Dragone [13] has evaluated this matrix, obtaining

$$\langle \delta I'_{S_m} \delta I'^{*}_{S_n} \rangle = 2qI_{m-n}\Delta f \quad (31)$$

where  $I_{m-n}$  is one of the Fourier coefficients of the local oscillator current  $i_d(t)$  as defined in (9).

A different approach leading to the same result has been taken by van der Ziel [11] in his analysis of shot noise in mixers. The shot noise, caused by electrons crossing the depletion layer of the diode, is considered as a series of impulsive deviations from the noiseless diode current. The

<sup>2</sup> The symbol  $\langle \dots \rangle$  denotes statistical (or ensemble) average as opposed to time average which is denoted by an overbar. Superscripts  $T$  and  $\dagger$  denote, respectively, the transpose and the complex conjugate transpose of a matrix or vector.

spectrum of each current impulse is flat and the phase is linear with frequency, its slope depending on the time of occurrence of the impulse. The different frequency components  $\omega_m$  are down-converted according to (16) and have phases related to the time of occurrence of the impulse and to the LO phase. Summing the separate effects of all such impulses gives the output voltage due to shot noise, including the effects of correlation between the components. Van der Ziel gives the example of a simple two-port mixer as an illustration of the effect of shot-noise correlation.

### B. Thermal Noise

It was shown above ((27) and Fig. 3) that the thermal noise generated in the series resistance of the diode can be regarded as a noise current source  $i_T^2$  across the terminals of the intrinsic diode.

Since  $R_s$  is assumed to be time-invariant, down-converted thermal noise will have no correlated components; quasinsoidal components  $\delta I'_{T_m}$  at the sideband frequencies  $\omega_m$  give rise to an output voltage (using (16))

$$\delta V_{T_0} = \mathbf{Z}_0 \delta \mathbf{I}_T \quad (32)$$

where  $\delta \mathbf{I}_T = [\dots, \delta I'_{T_1}, \delta I'_{T_0}, \delta I'_{T_{-1}}, \dots]^T$ , and  $\mathbf{Z}_0$  is a row of the matrix  $\mathbf{Z}$ .

Taking the ensemble average of  $|\delta V_{T_0}|^2$  gives

$$\langle \delta V_{T_0}^2 \rangle = \mathbf{Z}_0 \langle \delta \mathbf{I}_T \delta \mathbf{I}_T^\dagger \rangle \mathbf{Z}_0^\dagger. \quad (33)$$

The square matrix  $\langle \delta \mathbf{I}_T \delta \mathbf{I}_T^\dagger \rangle$  is again the correlation matrix (cf. (30)), but since  $\delta I'_{T_m}$  and  $\delta I'_{T_n}$  are uncorrelated for  $m \neq n$ , it is a diagonal matrix with the elements

$$\langle \delta I'_{T_m} \delta I'^*_m \rangle = \frac{4k T_{eq} R_{s_m} \Delta f}{|Z_{e_m} + R_{s_m}|^2}, \quad m \neq 0 \quad (34a)$$

$$= \frac{4k T_{eq} R_{s_0} \Delta f}{|Z_0|^2}, \quad m = 0. \quad (34b)$$

### C. Total Mixer Noise

Combining the shot and thermal noise output voltages given by (30) and (33) gives the total noise output voltage appearing across the series combination of the IF load and the diode series resistance (see Fig. 2):

$$\langle \delta V_{N_0}^2 \rangle = \mathbf{Z}_{01} \{ \langle \delta \mathbf{I}_S \delta \mathbf{I}_S^\dagger \rangle + \langle \delta \mathbf{I}_T \delta \mathbf{I}_T^\dagger \rangle \} \mathbf{Z}_{01}^\dagger \quad (35)$$

where the shot and thermal noise correlation matrices  $\langle \delta \mathbf{I}_S \delta \mathbf{I}_S^\dagger \rangle$  and  $\langle \delta \mathbf{I}_T \delta \mathbf{I}_T^\dagger \rangle$  are given by (31) and (34). It is assumed here that the effects of scattering noise are fairly small and are equivalent to a small increase in the value of the equivalent noise temperature of the diode series resistance  $T_{eq}$  in (27) and (34). The magnitude of this increase can be estimated from the current waveform of the pumped diode and from measurements on the dc biased diode, as described in Part 2 of this paper.

The equivalent input noise temperature  $T_M$  of a two-frequency mixer (no external image termination) may be defined in terms of a noiseless but otherwise identical mixer:  $T_M$  is the temperature to which the source conductance of

the noiseless mixer must be heated in order to deliver to the IF load the same noise power as the noisy mixer delivers when its source conductance is maintained at absolute zero temperature. For a three-frequency mixer (having external terminations at the signal, image, and intermediate frequencies), the single-sideband mixer noise temperature  $T_{M_{SSB}}$  is defined in the same way, but with the stipulation that the image conductance of both the noisy and noiseless mixers be maintained at absolute zero temperature.<sup>3</sup>

The effective mean-square input noise current necessary to produce the noise voltage  $\langle \delta V_{N_0} \rangle$  at the output, is found using (16):

$$\langle \delta I_{N_0}^2 \rangle = \langle \delta V_{N_0}^2 \rangle / |Z'_{01}|^2. \quad (36)$$

This corresponds to input current source  $\delta I'_1$  in Fig. 2 and is associated with the impedance  $(Z_{e_1} + R_{s_1})$ . The corresponding mean-square noise voltage associated with the source impedance  $Z_{e_1}$  is  $\langle \delta I_{N_0}^2 \rangle |Z_{e_1} + R_{s_1}|^2$ . The effective input noise temperature of the mixer  $T_M$  is the temperature to which  $\text{Re}[Z_{e_1}]$  must be heated to generate an equal noise voltage. Hence, using (36),

$$T_M = \frac{\langle \delta V_{N_0}^2 \rangle}{4k\Delta f} \frac{|Z_{e_1} + R_{s_1}|^2}{|Z'_{01}|^2 \text{Re}[Z_{e_1}]} \quad (37)$$

$\langle \delta V_{N_0}^2 \rangle$  is given by (35) in terms of the internal shot and thermal noise sources of the diode and  $Z'_{01}$  is an element of the matrix  $\mathbf{Z}$  defined in (17).

The single sideband noise figure of the mixer is defined as

$$F_{SSB} = 1 + \frac{T_M}{T_0} \quad (38)$$

where  $T_0 = 290$  K by convention.

## V. THE MICROWAVE SCHOTTKY DIODE

The Schottky diode is conventionally represented as shown in Fig. 1. The series resistance is assumed equal to its dc value and independent of frequency, while the capacitance exponent  $\gamma$  (5) is assumed independent of voltage. For a diode of the kind used for microwave and millimeter-wave mixers these assumptions are not generally valid, and it is important to include the departures from ideality in the nonlinear and small-signal analyses if accurate results are to be obtained.

### A. Series Resistance

There are three effects which cause the series resistance  $R_s$  of a diode to differ from the value determined from the dc  $\log I-V$  curve. These are 1) thermal time-constants in the diode, 2) RF skin effect in the diode material, and 3) the voltage dependence of the depletion-layer width.

It has been shown by Decker and Weinreb [20] that the incremental junction resistance of a diode, measured at a

<sup>3</sup> For the three-frequency mixer a double-sideband noise temperature  $T_{M_{DSB}}$  is frequently used. For cases in which the signal and image conversion loss  $L_{01}$  and  $L_{0-1}$  are equal  $T_{M_{DSB}} = \frac{1}{2} T_{M_{SSB}}$ . If  $L_{01} \neq L_{0-1}$ , which is particularly probable when a high IF is used, then  $T_{M_{DSB}} = T_{M_{SSB}} / (1 + L_{01}/L_{0-1})$ .

low frequency (audio or dc), contains a negative component caused by heating of the diode by the test signal. Thus

$$r_{lf} \triangleq \frac{dv_j}{di_d} = \left. \frac{\partial v_j}{\partial i_d} \right|_T + \left. \frac{\partial v_j}{\partial T} \right|_{i_d} \cdot \frac{dT}{di_d} \quad (39)$$

$$= r_{hf} + \left. \frac{\partial v_j}{\partial T} \right|_{i_d} \cdot \frac{dT}{di_d}. \quad (40)$$

The second term on the RHS of (39) is the (negative) component of the low-frequency junction resistance which results from the diode temperature varying in phase with the test signal. At higher frequencies, above about 10 MHz for our 2.5- $\mu\text{m}$  GaAs diodes, thermal time constants in the diode prevent its temperature from varying appreciably and only the term  $r_{hf}$  is measured. It follows that the value of the series resistance  $R_s$  deduced from the dc log  $I-V$  curve is lower than the true constant temperature value which would be observed at microwave frequencies. For our millimeter-wave diodes the error in  $R_s$  is 1–3  $\Omega$  [20], [23].

The RF skin effect contributes an additional resistance  $R_{\text{skin}}$  in series with the diode.  $R_{\text{skin}}$  is proportional to  $\sqrt{f}$  and can be estimated if the diode geometry and resistivity are known [24]. The diode contact wire is also likely to have a significant skin resistance, which should be included in  $R_{\text{skin}}$ . For our 2.5- $\mu\text{m}$  GaAs diodes  $R_{\text{skin}}$  is 2–3  $\Omega$  at 100 GHz.

The width of the depletion layer in a diode depends on the junction voltage and, therefore, the component of series resistance contributed by the undepleted epitaxial material will also be voltage-dependent. In the present paper we have assumed that this voltage dependence has negligible effect on the performance of the mixer.

### B. Junction Capacitance

The simple diode capacitance law, (5), is derived in many texts [21] for planar diodes. If the doping profile at the barrier (or junction) is uniform or linear with distance, the exponent  $\gamma$  has the value  $\frac{1}{2}$  or  $\frac{1}{3}$ , respectively. However, for the very small diameter diodes used at millimeter wavelengths the assumption of a planar device is no longer valid: fringing effects at the edge of the depletion layer are significant and the shape of the depletion layer is voltage-dependent [21]. The simple capacitance law, (5), can still be used provided the exponent  $\gamma$  is allowed to be voltage dependent, i.e.,  $\gamma \rightarrow \gamma(v_j)$ .

## VI. APPLICATION TO PRACTICAL MIXERS

The mixer analysis presented in the preceding sections assumes a knowledge of the diode and embedding impedance at all harmonics of the LO and at all the sideband frequencies  $\omega_0 + k\omega_p$ ,  $k = 0, \pm 1, \pm 2, \dots, \pm \infty$ . In practice the number of frequencies which can be considered is limited by the ability to make meaningful measurements or calculations of the embedding impedance beyond some frequency limit, and by the size of complex matrix which can be inverted by available computers. The computer time required to solve the nonlinear problem increases rapidly with the number of LO harmonics. It is necessary therefore

to work with a finite number  $N$  of LO harmonics and a corresponding number ( $N + 1$ ) of sideband frequencies. The infinite series and matrices of Sections II–IV can then be replaced by finite ones. The electrical implication of such a truncation is that all higher harmonics or sidebands are either open- or short-circuited. In particular, truncation of the  $Y$  matrix in (12) implies that all higher sidebands are short-circuited. This is likely to be a good approximation for millimeter-wave mixers because the mean junction capacitance approaches a short circuit for very high frequencies. A similar situation results from ignoring frequencies above  $N\omega_p$  in the nonlinear analysis. Using Gwarek's method it is tacitly assumed that the junction voltage  $v_j$  has no components above frequency  $N\omega_p$ . Again this should be a good approximation provided  $N$  is high enough.

## VII. CONCLUSION

The nonlinear, small-signal, and noise analysis given in Sections II–V provides the means for accurately determining the performance of microwave and millimeter-wave mixers. In the companion paper, Part 2, the analysis is applied to mixers operating at 87 and 115 GHz. Good agreement with measured results is obtained, and the “anomalous” mixer noise [14] is shown to be primarily shot noise for which the phase relations of down-converted components must be taken into account.

## REFERENCES

- [1] H. C. Torrey and C. A. Whitmer, *Crystal Rectifiers*. (MIT Radiation Lab. Series, vol. 15). New York: McGraw-Hill, 1948.
- [2] W. M. Sharpless, “Wafer-type millimeter-wave rectifiers,” *Bell Syst. Tech. J.*, vol. 35, pp. 1385–1402, Nov. 1956.
- [3] G. C. Messenger and C. T. McCoy, “Theory and operation of crystal diodes as mixers,” *Proc. IRE*, vol. 45, pp. 1269–1283, 1957.
- [4] L. Mania and G. B. Stracca, “Effects of the diode junction capacitance on the conversion loss of microwave mixers,” *IEEE Trans. Communications*, vol. COM-22, pp. 1428–1435, Sept. 1974.
- [5] A. R. Kerr, “Low-noise room-temperature and cryogenic mixers for 80–120 GHz,” *IEEE Trans. Microwave Theory Tech.*, vol. MTT-23, pp. 781–787, Oct. 1975.
- [6] M. R. Barber, “Noise figure and conversion loss of the Schottky barrier mixer diode,” *IEEE Trans. Microwave Theory Tech.*, vol. MTT-15, pp. 629–635, Nov. 1967.
- [7] A. A. M. Saleh, *Theory of Resistive Mixers*. Cambridge, MA: MIT Press, 1971.
- [8] S. Egami, “Nonlinear, linear analysis and computer aided design of resistive mixers,” *IEEE Trans. Microwave Theory Tech.*, vol. MTT-22, pp. 270–275, Mar. 1974.
- [9] M. J. O. Strutt, “Noise figure reduction in mixer stages,” *Proc. IRE*, vol. 34, no. 12, pp. 942–950, Dec. 1946.
- [10] A. van der Ziel and R. L. Waters, “Noise in mixer tubes,” *Proc. IRE*, vol. 46, pp. 1426–1427, 1958.
- [11] A. van der Ziel, *Noise: Sources, Characterization, and Measurement*. Englewood Cliffs, NJ: Prentice-Hall, 1970.
- [12] C. S. Kim, “Tunnel diode converter analysis,” *IRE Trans. Electron Devices*, vol. ED-8, no. 5, pp. 394–405, Sept. 1961.
- [13] C. Dragone, “Analysis of thermal shot noise in pumped resistive diodes,” *Bell Syst. Tech. J.*, vol. 47, pp. 1883–1902, 1968.
- [14] A. R. Kerr, “Anomalous noise in Schottky-diode mixers at millimeter wavelengths,” *IEEE MTT-S Int. Microwave Symp., Digest of Technical Papers*, pp. 318–320, May 1975.
- [15] D. A. Fleri and L. D. Cohen, “Nonlinear analysis of the Schottky-barrier mixer diode,” *IEEE Trans. Microwave Theory Tech.*, vol. MTT-21, pp. 39–43, Jan. 1973.
- [16] A. R. Kerr, “A technique for determining the local oscillator waveforms in a microwave mixer,” *IEEE Trans. Microwave Theory Tech.*,

- vol. MTT-23, pp. 828-831, Oct. 1975.
- [17] W. K. Gwarek, "Nonlinear analysis of microwave mixers," M.S. thesis, MIT, Cambridge, Sept. 1974.
- [18] S. O. Rice, "Mathematical analysis of random noise," *Bell Syst. Tech. J.*, vol. 23, no. 3, pp. 282-332, July 1944.
- [19] V. R. Bennet, *Electrical Noise*. New York: McGraw-Hill, 1960.
- [20] D. R. Decker and S. Weinreb, private communication.
- [21] S. M. Sze, *Physics of Semiconductor Devices*. New York: Wiley, 1969 (see p. 90 *et seq.*).
- [22] W. Baechtold, "Noise behavior of GaAs field-effect transistors with short gates," *IEEE Trans. Electron Devices*, vol. ED-19, pp. 674-680, 1972.
- [23] D. N. Held, "Analysis of room temperature millimeter-wave mixers using GaAs Schottky barrier diodes," Sc.D. dissertation, Department of Electrical Engineering, Columbia University, New York, 1976.
- [24] J. A. Calviello, J. L. Wallace, and P. R. Bie, "High performance GaAs quasi-planar varactors for millimeter waves," *IEEE Trans. Electron Devices*, vol. ED-21, pp. 624-630, Oct. 1974.

# Conversion Loss and Noise of Microwave and Millimeter-Wave Mixers: Part 2—Experiment

DANIEL N. HELD, MEMBER, IEEE, AND ANTHONY R. KERR, ASSOCIATE MEMBER, IEEE

**Abstract**—The theory of noise and conversion loss in millimeter-wave mixers, developed in a companion paper, is applied to an 80-120-GHz mixer. Good agreement is obtained between theoretical and experimental results, and the source of the recently reported "anomalous noise" is explained. Experimental methods are described for measuring the embedding impedance and diode equivalent circuit, needed for the computer analysis.

## I. INTRODUCTION

IN Part 1 of this paper [1] the theory of microwave and millimeter-wave mixers was presented in a form suitable for analysis by digital computer. The present paper gives the results of such an analysis, comparing computed and measured conversion loss, noise, and output impedance for an 80-120-GHz mixer under various operating conditions.

The significance of this work in relation to earlier work is discussed in the introduction to Part 1, the salient points being that this method of analysis gives unprecedented agreement between theory and experiment and that the "anomalous noise" [2] reported in millimeter-wave mixers is entirely accounted for.

The analysis requires a knowledge of the embedding impedance seen by the diode at a finite number of frequencies, and of the equivalent circuit of the diode, including

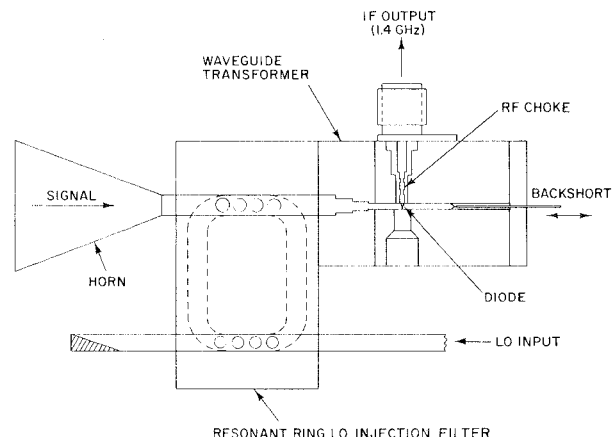


Fig. 1. Cross-section of the 80-120-GHz mixer used in this work.

noise sources. Experimental methods for determining these input quantities are described in Sections II and III. The mixer analysis is described in Section IV and typical sets of theoretical and measured results are shown to be in good agreement. Section V discusses the sources of mixer noise and loss, and small-signal power flow in the mixer.

The mixer used for these experiments is the room-temperature 80-120-GHz mixer described in [3] and is shown here in Fig. 1. It uses a 2.5- $\mu\text{m}$ -diameter GaAs Schottky diode in a quarter-height waveguide mount. The diode was made by Professor R. J. Mattauch at the University of Virginia.

Manuscript received February 18, 1977; revised May 12, 1977.

D. N. Held was with the Department of Electrical Engineering, Columbia University, New York, NY 10027. He is now with the Jet Propulsion Laboratory, California Institute of Technology, Pasadena, CA 91103.

A. R. Kerr is with the NASA Institute for Space Studies, Goddard Space Flight Center, New York, NY 10025.

- vol. MTT-23, pp. 828-831, Oct. 1975.
- [17] W. K. Gwarek, "Nonlinear analysis of microwave mixers," M.S. thesis, MIT, Cambridge, Sept. 1974.
- [18] S. O. Rice, "Mathematical analysis of random noise," *Bell Syst. Tech. J.*, vol. 23, no. 3, pp. 282-332, July 1944.
- [19] V. R. Bennet, *Electrical Noise*. New York: McGraw-Hill, 1960.
- [20] D. R. Decker and S. Weinreb, private communication.
- [21] S. M. Sze, *Physics of Semiconductor Devices*. New York: Wiley, 1969 (see p. 90 *et seq.*).
- [22] W. Baechtold, "Noise behavior of GaAs field-effect transistors with short gates," *IEEE Trans. Electron Devices*, vol. ED-19, pp. 674-680, 1972.
- [23] D. N. Held, "Analysis of room temperature millimeter-wave mixers using GaAs Schottky barrier diodes," Sc.D. dissertation, Department of Electrical Engineering, Columbia University, New York, 1976.
- [24] J. A. Calviello, J. L. Wallace, and P. R. Bie, "High performance GaAs quasi-planar varactors for millimeter waves," *IEEE Trans. Electron Devices*, vol. ED-21, pp. 624-630, Oct. 1974.

# Conversion Loss and Noise of Microwave and Millimeter-Wave Mixers: Part 2—Experiment

DANIEL N. HELD, MEMBER, IEEE, AND ANTHONY R. KERR, ASSOCIATE MEMBER, IEEE

**Abstract**—The theory of noise and conversion loss in millimeter-wave mixers, developed in a companion paper, is applied to an 80-120-GHz mixer. Good agreement is obtained between theoretical and experimental results, and the source of the recently reported "anomalous noise" is explained. Experimental methods are described for measuring the embedding impedance and diode equivalent circuit, needed for the computer analysis.

## I. INTRODUCTION

IN Part 1 of this paper [1] the theory of microwave and millimeter-wave mixers was presented in a form suitable for analysis by digital computer. The present paper gives the results of such an analysis, comparing computed and measured conversion loss, noise, and output impedance for an 80-120-GHz mixer under various operating conditions.

The significance of this work in relation to earlier work is discussed in the introduction to Part 1, the salient points being that this method of analysis gives unprecedented agreement between theory and experiment and that the "anomalous noise" [2] reported in millimeter-wave mixers is entirely accounted for.

The analysis requires a knowledge of the embedding impedance seen by the diode at a finite number of frequencies, and of the equivalent circuit of the diode, including

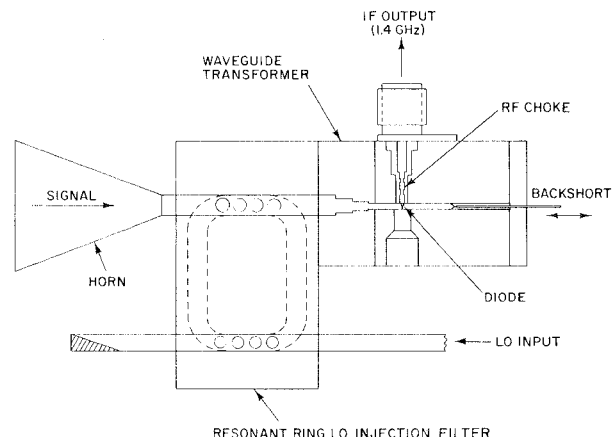


Fig. 1. Cross-section of the 80-120-GHz mixer used in this work.

noise sources. Experimental methods for determining these input quantities are described in Sections II and III. The mixer analysis is described in Section IV and typical sets of theoretical and measured results are shown to be in good agreement. Section V discusses the sources of mixer noise and loss, and small-signal power flow in the mixer.

The mixer used for these experiments is the room-temperature 80-120-GHz mixer described in [3] and is shown here in Fig. 1. It uses a 2.5- $\mu\text{m}$ -diameter GaAs Schottky diode in a quarter-height waveguide mount. The diode was made by Professor R. J. Mattauch at the University of Virginia.

Manuscript received February 18, 1977; revised May 12, 1977.

D. N. Held was with the Department of Electrical Engineering, Columbia University, New York, NY 10027. He is now with the Jet Propulsion Laboratory, California Institute of Technology, Pasadena, CA 91103.

A. R. Kerr is with the NASA Institute for Space Studies, Goddard Space Flight Center, New York, NY 10025.

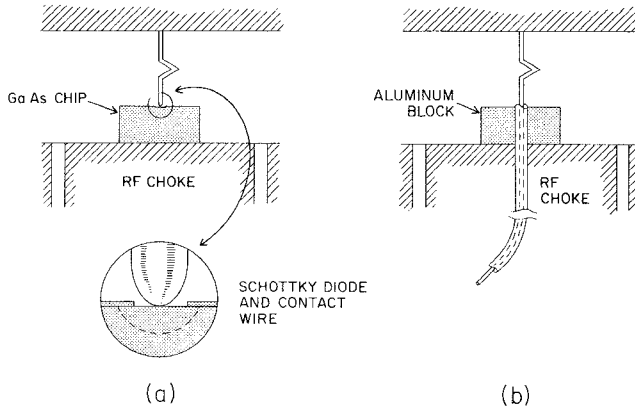


Fig. 2. Technique for measuring the embedding impedance seen by the diode. The diode in the real mixer (a) is replaced in the scale model (b) by the end of a small coaxial cable through which the embedding impedance can be measured directly.

## II. THE DIODE EMBEDDING IMPEDANCE

Eisenhart and Kahn [4], [5] have described a technique whereby it is possible to measure the embedding impedance seen by a waveguide-mounted diode. The diode is removed from its mount and replaced by a small coaxial cable, so the impedance seen by the end of the cable is essentially equal to the embedding impedance normally seen by the diode. The other end of the cable is connected to a slotted line or network analyzer which measures this impedance. Except for some small corrections due to differences in geometry in the region immediately surrounding the diode, the technique directly provides the desired embedding impedance. In order to make this technique practical for millimeter-wave mixer mounts, it is necessary to perform the measurements on a large-scale model of the mixer.

For the 80–120-GHz mixer used as an example in this paper, a  $65 \times$  scale model was constructed, including the stepped waveguide transformer, diode mount, RF choke, and backshort, shown in Fig. 1. The input waveguide was terminated in a matched multimode waveguide load, and the GaAs diode chip was modeled by an aluminum block as shown in Fig. 2. Using a Hewlett-Packard 8410A network analyzer it was then possible to measure the embedding impedance up to the sixth harmonic of the local oscillator. Because of the geometrical differences between the diode and the coaxial measuring probe, the measured embedding impedance had to be corrected for fringing effects. Equivalent circuits for the region close to the diode in the actual mixer and in the diode-less model are derived in [6], where it is shown that the correction to the measured embedding impedance is equivalent to adding a 0.63 fF (0.00063 pF) capacitor in shunt with the measured impedance (cf. the zero-bias diode capacitance  $C_{j0} \approx 7.0$  fF).

Typical embedding impedances measured at the scale-model equivalent of 87 GHz are illustrated in Fig. 3. The experimental results illustrated in this figure are presented as a function of the mixer backshort position, since in subsequent sections of this paper mixer performance will be evaluated as a function of backshort position. It is clear from

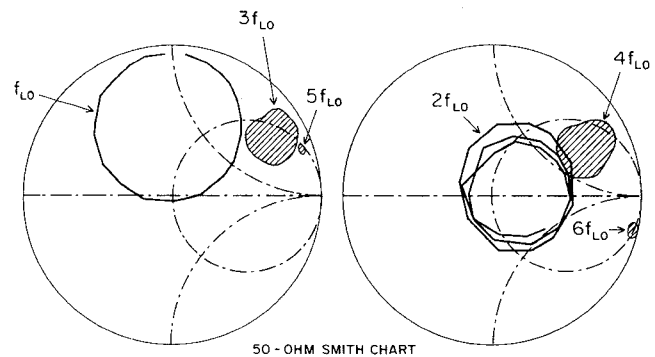


Fig. 3. The embedding impedance at harmonics of the LO frequency, for  $f_{LO} = 87$  GHz. The impedances are shown as functions of backshort position.

Fig. 3 that the embedding impedances at the harmonics of the local oscillator cannot be considered as open-circuits, short-circuits, or even simple reactive terminations, as has sometimes been assumed in the literature. In particular, the embedding impedance at the second harmonic has a substantial and widely varying real part.

## III. THE DIODE EQUIVALENT CIRCUIT

In Section V of Part 1 the characteristics of very small Schottky diodes were discussed. It was pointed out that the RF skin effect could contribute substantially to the series resistance, while nonuniform epilayer doping and fringing effects at the periphery of the depletion layer might cause the capacitance-law exponent  $\gamma$  to be voltage-dependent. It was further pointed out that scattering, observed in Schottky diodes at high-current levels, would effect mixer noise, and that thermal time constants must be taken into account when measuring the series resistance of a diode.

The equivalent circuit of a Schottky barrier diode, including noise sources, is shown in Fig. 4. In the following paragraphs procedures are described for determining the element values of this equivalent circuit, which are appropriate at millimeter wavelengths.

### A. Junction Capacitance

The capacitance of the junction as a function of voltage is given by [7]

$$C_j(v_j) = \frac{dQ}{dv_j} = C_{j0} \left(1 - \frac{v_j}{\phi}\right)^{-\gamma(v_j)} \quad (1)$$

where  $C_{j0}$  is the zero-voltage capacitance,  $\phi$  is the barrier potential, and  $\gamma(v_j)$  is related to the geometry of the junction and the semiconductor doping profile. If the junction can be considered planar, with negligible fringing effects, and if the epilayer doping is uniform, then  $\gamma = 0.5$ . However, when the diameter of the diode is not large compared with the thickness of the depletion layer, fringing effects at the edges of the diode may be significant, and will be most pronounced under reverse bias when the depletion layer is widest.

The junction capacitance can be measured at 1 MHz

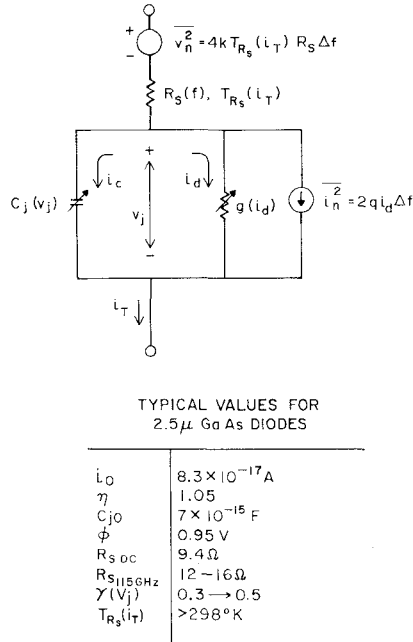


Fig. 4. The equivalent circuit of a Schottky diode, including frequency dependent series resistance and current dependent resistor noise temperature.

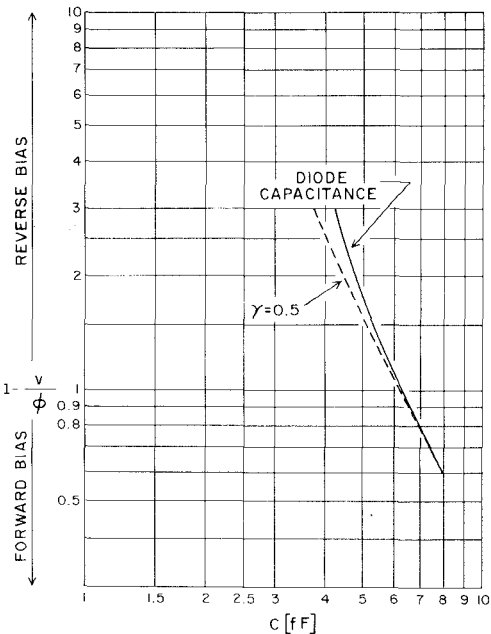


Fig. 5. Experimental  $C_j$  versus  $(1 - v_j/\phi)$  for a typical  $2.5\text{-}\mu\text{m}$  diode, illustrating the voltage dependence of  $\gamma$ .

using a capacitance bridge<sup>1</sup> [6], [8]. By plotting  $\log C_j$  versus  $\log (1 - v_j/\phi)$ , a line whose slope is equal to  $-\gamma$  is obtained. Experimental results indicate that the value of  $\gamma$  for some diodes exhibits a pronounced voltage dependence, a typical result being shown in Fig. 5.

The question arises as to whether the capacitance measured at 1 MHz is meaningful at 100 GHz and above. There is, however, no evidence to suggest any frequency

<sup>1</sup> A Boonton model 75D was used for this work.

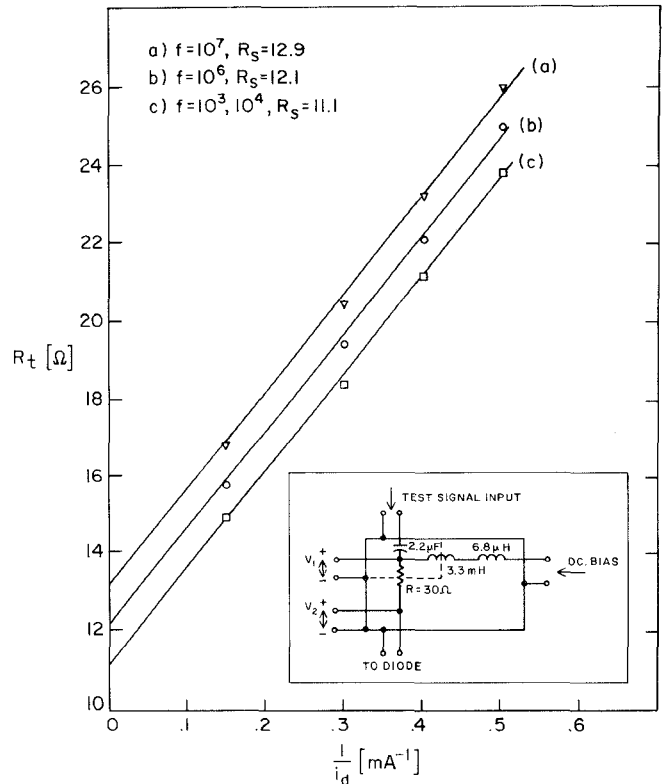


Fig. 6. Measured incremental resistance of a  $2.5\text{-}\mu\text{m}$  gallium arsenide diode as a function of reciprocal dc bias current, showing apparent frequency dependence of the series resistance (the y-axis intercept). This is due to heating effects. Inset: Circuit of device for measuring the incremental resistance  $R_t$  at frequencies up to 10 MHz.

dependence of the junction capacitance over this range of frequencies. There have been some papers [10]–[12] dealing with the effect of deep-level donors on frequency dependence of the transition capacitance of p-n junctions. However, the effect is only significant when the number of deep traps is comparable to the number of donors, which should not be the case for the heavily doped diodes under study. A second factor which can cause a frequency dependence of the junction capacitance is the scattering limited velocity of the electrons in the semiconductor. This limits the rate at which the depletion layer can be depleted or refilled, and is expected to have negligible effects below  $\sim 100$  GHz [13].

### B. The Barrier Resistance and the Series Resistance

It has been shown by Weinreb and Decker [14] that the conventional method of determining the series resistance  $R_s$  from the dc  $\log I-V$  curve contains an inherent error due to heating at the junction. To determine the true value of  $R_s$  measurements must be performed at frequencies greater than the reciprocal of the shortest thermal time constant of the diode and its mount. Measurements of these thermal time constants [14] indicate that errors should be negligible above  $\sim 20$  MHz.

A simple circuit, shown in Fig. 6, enables the incremental resistance  $R_t$  of a forward-biased diode to be measured in the frequency range 1 kHz–10 MHz. Measurements on a  $2.5\text{-}\mu\text{m}$  GaAs diode indicate that the resistance starts to increase above  $\sim 30$  kHz and levels off at  $\sim 10$  MHz. These

results are shown in Fig. 6 where  $R_s$  is plotted as a function of reciprocal bias current for several different frequencies; the value of  $R_s$  at each frequency is given by the y-axis intercept. It is seen that the resistance increases by  $\sim 2\text{--}3 \Omega$  between 10 kHz and 10 MHz. Further confirmation of these measurements comes from Weinreb and Decker [14] who measured the thermal time constants of the diode chip and mounting structure and found them to be approximately 1  $\mu\text{s}$  and 50 ms, respectively.

Another important phenomenon effecting the diode's series resistance is the RF skin effect. This effect occurs predominantly in the degenerately doped substrate of the diode chip and in the contacting whisker. The skin resistance has been calculated by several investigators [15], [16], [6] and for a 2.5- $\mu\text{m}$  diode is generally conceded to add about 2–3  $\Omega$  to the series resistance at 100 GHz. Direct measurement of the series resistance of a waveguide-mounted diode was performed using a new technique described in [6]. Values obtained for the series resistance at 115 GHz were typically 2  $\Omega$  larger than the low frequency values<sup>2</sup> as expected.

The results of these measurements of the series resistance are summarized in Table I. It is clear that the series resistance at millimeter wavelengths may be as much as twice the value obtained by the conventional dc method.

### C. Noise Temperature of the Series Resistance

It is well known that at electric field strengths in the vicinity of  $3 \times 10^3 \text{ V/cm}^3$ , bulk GaAs displays a nonlinear  $I$ - $V$  characteristic which is due primarily to central valley and intervalley phonon scattering.<sup>3</sup> It will be shown in Section IV that under normal mixer operating conditions the instantaneous value of the current through the series resistance of a diode can reach levels  $\sim 10 \text{ mA}$ . For the diodes used in this work it can be shown that the peak value of the electric field in the undepleted epitaxial material may then be as large as  $1.9 \times 10^3 \text{ V/cm}$ .<sup>4</sup> Although this value is comfortably below the critical field required for the onset of the Gunn effect at low frequencies, the field strength is sufficient to increase substantially the effective temperature of the electron gas in the GaAs and hence the noise temperature of the series resistance.

The noise temperature of the series resistance, measured at a frequency of 1.4 GHz on a dc biased diode, is shown in Fig. 7 as a function of the dc current. The noise temperature of the series resistance was derived by measuring the diode output temperature and correcting for the effect of the shot noise produced in the junction [6], [17]. Also shown in Fig. 7 are results reported by Baechtold [18] who measured the noise temperature of a bulk sample of GaAs. It is clear, then, that at high currents excess noise is generated in GaAs mixer

<sup>2</sup> Low-frequency values corrected for thermal time-constant effects.

<sup>3</sup> The critical field for highly doped GaAs is approximately  $5 \times 10^3 \text{ V/cm}$  [9], [18].

<sup>4</sup> This figure is based on the assumption of uniform current flow through a 2.5- $\mu\text{m}$  diameter diode, with a resistivity of 0.096  $\Omega\text{-cm}$  in the epilayer, corresponding to an impurity concentration of  $2.5 \times 10^{17}/\text{cm}^3$ .

TABLE I  
SERIES RESISTANCE VALUES

$R_s$ measured at DC (including thermal effects)	$6.8 \pm 0.1 \text{ ohm}$
$R_s$ measured at 10 MHz	$9.4 \pm 0.2 \text{ ohm}$
Thermal time-constant error	$-2.6 \pm 0.3 \text{ ohm}$

True low frequency $R_s$ (measured at 10 MHz)	$9.4 \pm 0.2 \text{ ohm}$
Calculated skin-effect at 115 GHz	$2.5 \pm 0.5 \text{ ohm}$
Predicted value of $R_s$ at 115 GHz	$11.9 \pm 0.7 \text{ ohm}$
Measured value of $R_s$ at 115 GHz	$11.2 \pm 2.0 \text{ ohm}$

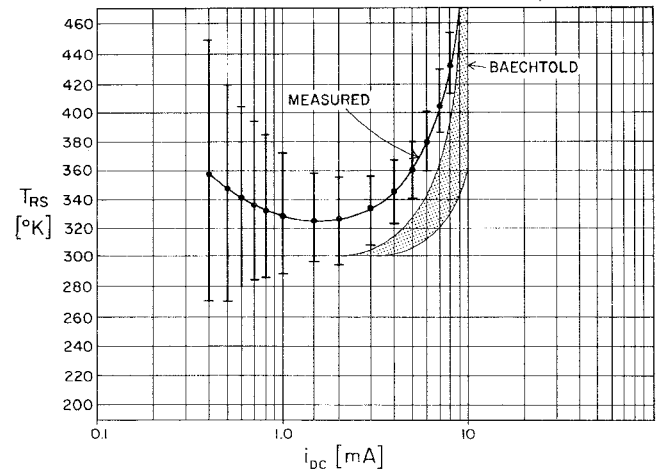


Fig. 7. Noise temperature of the series resistance at 1.4 GHz as a function of dc current. Also shown are Baechtold's results for an epilayer doping between 2 and  $3 \times 10^{17} \text{ cm}^{-3}$  (shaded region).

diodes due to scattering phenomena. Although the scattering noise has been measured at 1.4 GHz, the results should be valid in the millimeter-wave region since the effective intervalley scattering time constant in GaAs is on the order of  $2 \times 10^{-12} \text{ s}$  [19]–[21], and the central valley scattering time constant is assumed to be short compared with the dielectric relaxation time of the epitaxial layer which is  $\sim 10^{-14} \text{ s}$  [22], indicating a spectral density which is essentially uniform up to approximately 80 GHz, decreasing at higher frequencies.

When the diode is operating as a mixer the noise temperature of the series resistance will be a function of time, and the down-converted components of this noise will be partially correlated [1]. For a room-temperature mixer this correlation is expected to have a small effect, and it will be assumed here that scattering noise can be approximated by an increased average noise temperature of the series resistance,<sup>5</sup> an assumption supported by the good agreement obtained between theory and experiment in Section

<sup>5</sup> The average noise temperature is derived by integrating the measured noise temperature (Fig. 7) at the total diode current,  $i_T$  (Fig. 8), over the LO cycle. Typical average noise temperatures are approximately 60 K–100 K above ambient at room temperature.

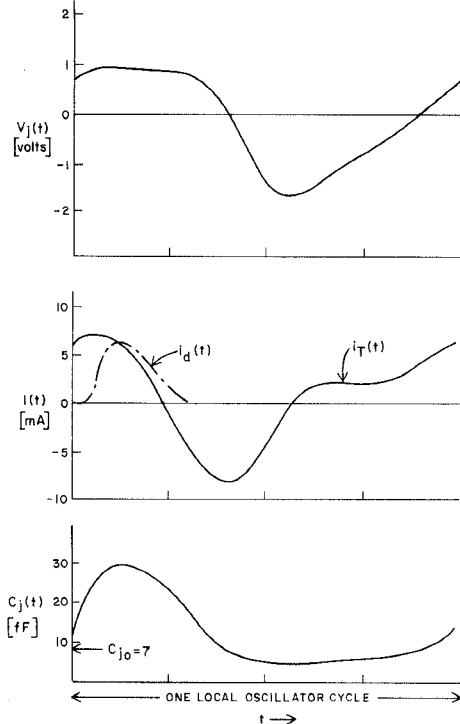


Fig. 8. Typical diode waveforms at 87 GHz. The junction voltage  $v_j(t)$ , total current in  $R_s$ ,  $i_T(t)$ , current in the diode conductance,  $i_d(t)$ , and junction capacitance  $C_j(t)$  are illustrated for a single local oscillator cycle. The dc bias conditions are:  $I_{dc} = 2.0$  mA,  $V_{dc} = 0.5$  V.

IV. In cryogenic mixers however, scattering noise and its partially correlated down-converted components are expected to be very significant and this simplifying assumption may be quite invalid.

#### IV. MIXER PERFORMANCE ANALYSIS

It was shown in Part 1 [1] that if the embedding impedance and the equivalent circuit of the diode are known, it is possible to solve the large-signal nonlinear problem to determine the LO waveforms at the diode, and then to determine the small-signal conversion loss and noise figure of the mixer. In this section the results of such an analysis are given for the 80–120 GHz mixer shown in Fig. 1 [3]. The embedding impedance was measured on a model, as described in Section II of the present paper, and the large-signal LO waveforms were computed as described in Section II of Part 1. Typical waveforms are shown in Fig. 8.

Knowing the LO waveforms, the conversion loss and noise temperature of the mixer can be determined as described in Sections II and III of Part 1. Since the mixer backshort setting has the strongest effect of all the external variables on mixer performance (other variables are dc bias and LO power), the measured and computed results given here are plotted as functions of backshort position. This serves not only to verify the accuracy of the computed solution for a wide variety of embedding impedances, but also provides useful insight into the behavior of the mixer. Typical sets of results are shown in Figs. 9 and 10 for 87 and 115 GHz. Computed results are shown for  $\gamma = 0.3\text{--}0.5$  and  $R_s(100 \text{ GHz}) = 12\text{--}16 \Omega$ ; these correspond to the likely

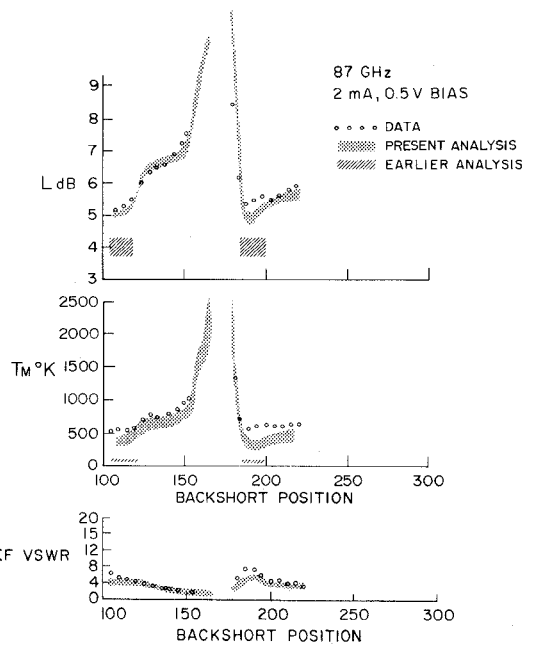


Fig. 9. Comparison of theoretical and experimental results at 87 GHz. The SSB conversion loss  $L$ , equivalent SSB input noise temperature  $T_M$  of the mixer (excluding IF amplifier noise), and IF VSWR with respect to  $50 \Omega$ , are shown as functions of backshort position. The theoretical results are computed for a broadband mixer (equal signal and image response) with the capacitance exponent  $\gamma = 0.3\text{--}0.5$  and the series resistance  $R_s(100 \text{ GHz}) = 12\text{--}16 \Omega$ . Also shown are the results of an earlier analysis [2], [3] which led to the observation of anomalous mixer noise.  $T_M$  is related to the noise temperature ratio  $t$  of a broad-band mixer by  $T_M = T_a(Lt - 2)$ , where  $T_a$  is the ambient temperature of the mixer and its input termination.

range of values of these quantities allowing for skin effect and fringing effects as discussed in Section III. It has been assumed in this work that  $\gamma(v_j)$  can be approximated by a voltage-independent mean value and that  $R_s$  exhibits the normal skin-effect type of frequency dependence. Also shown in Fig. 9 are the results of an earlier analysis [2], [3] which led to the observation of an anomalous component of mixer noise, thereby stimulating the present work.

The main sources of error in the computed results are expected to be due to high- $Q$  effects and to loss in the backshort. It was assumed for simplicity that the embedding impedance at a LO harmonic was equal to the impedance at the adjacent sideband frequencies, i.e.,  $Z_e(n\omega_p \pm \omega_{if}) = Z_e(n\omega_p)$ . Clearly this assumption will lead to errors if there are any sharp features on the loss or noise-temperature curves of Figs. 9 and 10. The conversion-loss minimum in Fig. 10 is an example of this and it can be seen that the measured and computed results differ most in this region. The backshort used in the experimental mixer was of the contacting spring-finger type, generally assumed to have low loss. Measurement of the loss of this particular backshort revealed a surprisingly large loss, equivalent to a resistance of  $\sim 8 \Omega$  at the plane of the short-circuit. At certain backshort positions this can contribute substantially to the measured conversion loss. Experimental repeatability was somewhat degraded by this backshort, presumably due to poor electrical contact with the waveguide. Experience during these measurements suggests experimental uncer-

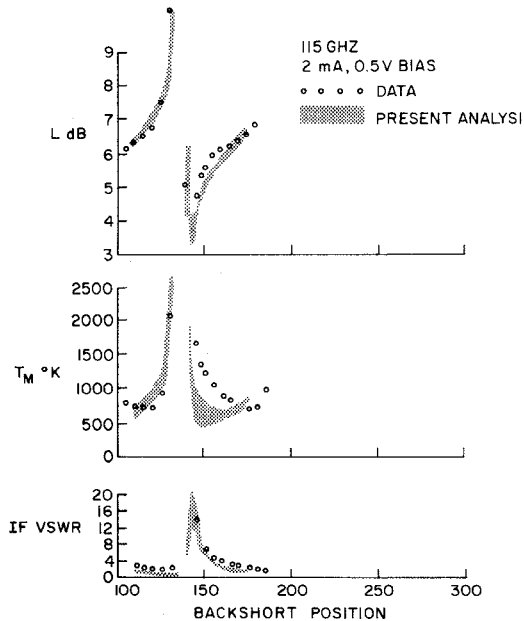


Fig. 10. Comparison of theoretical and experimental mixer performance at 115 GHz. See Fig. 9 caption for details.

tainties of  $\pm 0.3$  dB in  $L$  and  $\pm 130^\circ$  in  $T_M$  for most backshort settings, doubling in the vicinity of the sharp conversion-loss minimum. All measurements were performed using the 1.4-GHz IF radiometer/reflectometer apparatus described by Wienreb and Kerr [23].

## V. DISCUSSION

Having established that the performance of a mixer can be accurately predicted by the theory given in the companion paper [1], it is useful to evaluate the various contributions to the conversion loss and the mixer noise.

### A. Sources of Mixer Loss and Noise

In Fig. 11  $T_M$  and  $L$  are shown broken down into their constituent parts. The three major components of the conversion loss are 1) RF input mismatch loss, 2) dissipation in the series resistance at the signal and intermediate frequencies, and 3) loss in the junction, which includes power dissipated in the junction resistance at the signal and intermediate frequencies and also power lost by conversion to other frequencies. It should be noted that the mismatch loss can not necessarily be eliminated by RF tuning, since for broadband mixers the minimum overall conversion loss usually occurs for a mismatched input [24].

Noise in this room-temperature mixer is composed almost entirely of shot and thermal noise; the effect of the scattering mechanisms is fairly small. In the vicinity of the minimum of  $T_M$  the contributions from the shot and thermal sources are comparable.

### B. Power Flow in the Mixer

From the conversion loss analysis given in Part 1 it is possible to calculate the conversion loss between any two frequencies and to analyze the power flow in the mixer. A typical result is shown in Fig. 12 for two backshort positions at 115 GHz. It is interesting to observe from Fig. 12(a)

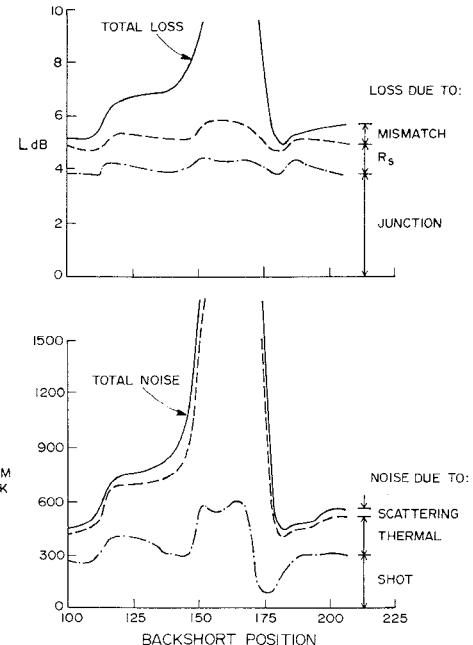


Fig. 11. Breakdown of mixer loss and noise at 87 GHz.

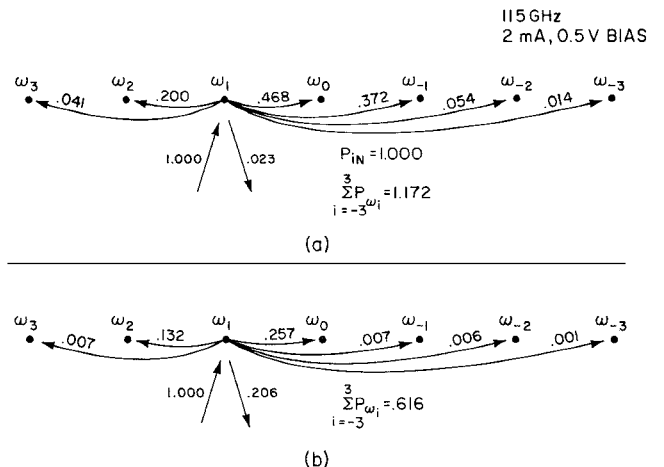


Fig. 12. Power flow at 115 GHz for two backshort positions. (a) Backshort position corresponding to minimum conversion loss. (b) Backshort position corresponding to minimum  $T_M$ .

that the mixer can behave as an active device, more small signal power being generated at the sideband frequencies than is incident at the signal frequency. This is a consequence of the time variation of the junction capacitance which produces "parametric" effects. It is also interesting to note that a substantial amount of power is dissipated at the sum frequency  $\omega_2 = 2\omega_p + \omega_0$ . Thus the embedding impedance at that frequency may be as important in mixer design as is the termination of the image frequency.

## VI. CONCLUSION AND SUMMARY

The theory given in Part 1 has been used to predict the conversion loss and noise of an 80–120-GHz mixer. Close agreement was obtained between measured and computed results for a variety of operating conditions. The analysis has demonstrated the following.

- 1) For a room temperature mixer the "anomalous" noise can be explained almost entirely by shot and thermal noise. The contribution due to scattering is typically only 10 percent.
- 2) The shot noise has components which, when down converted via the action of the mixer, are correlated.
- 3) The assumptions that the series resistance is time invariant and that scattering noise can be approximated by an increase in the noise temperature of the series resistance, are reasonable for this room-temperature mixer. This is not expected to be the case for cryogenic mixers, however, as scattering noise may be a substantial part of the overall noise.
- 4) The value of the series resistance in the vicinity of 100 GHz may be as much as twice its apparent dc value. This is due to the RF skin effect, and to an error, caused by thermal effects, inherent in the conventional method of determining the low-frequency series resistance from the dc log  $I-V$  characteristic of the diode. The difference between the apparent dc series resistance and the actual RF value accounts for approximately 1 dB of passive loss in the mixer used in this work.

#### ACKNOWLEDGMENT

The authors wish to thank the following for their substantial contributions to the work reported here: R. J. Mattauch and G. Green of the University of Virginia; S. Weinreb and D. R. Decker of the National Radio Astronomy Observatory; S. P. Schlessinger and E. Yang of Columbia University; and P. Thaddeus, J. Grange, I. Silverberg, and H. Miller of the Goddard Institute for Space Studies.

#### REFERENCES

- [1] D. N. Held and A. R. Kerr, "Conversion loss and noise of microwave and millimeter-wave mixers: Part 1—Theory," *IEEE Trans. Microwave Theory Tech.*, vol. MTT-26, Feb. 1978.
- [2] A. R. Kerr, "Anomalous noise in Schottky diode mixers at millimeter wavelengths," *IEEE MTT-S Int. Microwave Symp., Digest of Technical Papers*, 1975.
- [3] —, "Low-noise room-temperature and cryogenic mixers for 80–120 GHz," *IEEE Trans. Microwave Theory Tech.*, vol. MTT-23, pp. 781–787, 1975.
- [4] R. L. Eisenhart, "Impedance characterization of a waveguide microwave circuit," U.S. Army Electronics Command, Fort Monmouth, NJ, Technical Report 208, 1971.
- [5] R. L. Eisenhart and P. J. Kahn, "Theoretical and experimental analysis of a waveguide mounting structure," *IEEE Trans. Microwave Theory Tech.*, vol. MTT-19, pp. 706–719, 1971.
- [6] D. N. Held, "Analysis of room temperature millimeter-wave mixers using GaAs Schottky barrier diodes," Sc.D. dissertation, Columbia University, 1976.
- [7] S. M. Sze, *Physics of Semiconductor Devices*. New York: Wiley, 1969.
- [8] A. R. Kerr, R. J. Mattauch, and J. Grange, "A new mixer design for 140–220 GHz," *IEEE Trans. Microwave Theory Tech.*, vol. MTT-25, pp. 399–401, May 1977.
- [9] R. J. Mattauch, Private communication.
- [10] E. Schibli and A. G. Milnes, "Effects on deep impurities on n + p junction reverse-biased small-signal capacitance," *Solid State Electron.*, vol. 11, pp. 323–334, 1968.
- [11] W. Schultz, "A theoretical expression for the impedance of reverse-biased P-N junctions with deep traps," *Solid State Electron.*, vol. 14, pp. 227–231, 1971.
- [12] K. Hesse and H. Strack, "On the frequency dependence of GaAs Schottky barrier capacitances," *Solid State Electron.*, vol. 15, pp. 767–774, 1972.
- [13] J. C. Irvin, T. P. Lee, and D. R. Decker, "Varactor diodes," ch. in *Microwave Semiconductor Devices and their Circuit Application*, H. A. Watson, ed. New York: McGraw-Hill, 1969.
- [14] S. Weinreb and D. R. Decker, Private communication.
- [15] J. A. Calviello, J. L. Wallace, and P. R. Bie, "High performance GaAs quasi-planar varactors for millimeter waves," *IEEE Trans. Electron Devices*, vol. ED-21, pp. 624–630, Oct. 1974.
- [16] M. Schneider, Private communication.
- [17] R. J. Mattauch and T. J. Viola, "High frequency noise in Schottky barrier diodes," *Research Laboratories for the Engineering Sciences*, Univ. of Virginia, Report No. EE-4734-101-73U, 1973.
- [18] W. Baechtold, "Noise behavior of GaAs field-effect transistors with short gates," *IEEE Trans. Electron Devices*, vol. ED-19, pp. 674–680, 1972.
- [19] B. Culshaw and P. A. Blakey, "Intervalley scattering in gallium arsenide avalanche diodes," *Proc. IEEE (Lett.)*, vol. 64, pp. 569–571, 1976.
- [20] T. Ohmi, "A limitation on the frequency of Gunn effect due to the intervalley scattering time," *Proc. IEEE (Lett.)*, vol. 55, pp. 1739–1740, 1967.
- [21] V. Szekely and K. Tarnay, "Intervalley scattering model of the Gunn domain," *Electronics Letters*, vol. 4, pp. 592–594, 1968.
- [22] D. E. McCumber and A. G. Chynoweth, "Theory of negative conductance amplification and of Gunn instabilities in 'two-valley' semiconductors," *IEEE Trans. Electron Devices*, vol. ED-13, pp. 4–21, 1966.
- [23] S. Weinreb and A. R. Kerr, "Cryogenic cooling of mixers for millimeter and centimeter wavelengths," *IEEE Journal Solid State Circuits*, vol. SC-8, pp. 58–63, 1973.
- [24] A. A. M. Saleh, *Theory of Resistive Mixers*. Res. Monograph 64. Cambridge, MA: MIT Press, 1971.

# An Integrated-Circuit Balanced Mixer, Image and Sum Enhanced

LAWRENCE E. DICKENS, SENIOR MEMBER, IEEE, AND DOUGLAS W. MAKI, MEMBER, IEEE

**Abstract**—GaAs Schottky-barrier diodes with a zero-bias cutoff frequency of 800 GHz have been used in an integrated-circuit balanced diode mixer operating with a signal frequency centered at 9.3 GHz and a local-oscillator (LO) frequency at 7.8 GHz. For an instantaneous bandwidth of 1.0 GHz, the conversion loss (including all circuits and connector losses) was under 3.15 dB. Over the center 0.5 GHz of the band, the conversion loss was less than or equal to 2.8 dB. The conversion loss at the image-band edges was greater than 25 dB; the loss at the center of the image band was greater than 35 dB.

## I. INTRODUCTION

THIS PAPER reports generally on a microwave mixer for operation at *X* band, and more specifically on an integrated mixer circuit having very low conversion loss. Microwave diode mixers have been used for many years to obtain conversion of a signal at microwave frequencies to one at a much lower frequency. Such mixers have been the subject of much study and development. However, there is a continuing need for improvements which can result in better electrical performance, higher reliability, improved reproducibility, and lower production costs.

Well known [1]–[4] are the techniques for the enhancement of mixer operation by the proper control of the impedances at each of the mixer terminals and at each of the frequencies of importance. The frequencies of importance are the modulation products which exist according to the heterodyne principle by which the mixer operates. The received signal (RF), together with a higher level signal from a local oscillator (LO), are applied to a nonlinear element. The signal is mixed with the LO producing the sum frequency LO + RF, the difference (or intermediate) frequency (IF), LO – RF, and the image frequency 2LO – RF.

It has been known for some time that this loss in converting an RF signal to an IF signal can be minimized by properly terminating the sum and image frequencies. However, the realization of the proper termination can represent a severe problem. Prior integrated-circuit forms [3], [5] of image-enhanced mixers have generally been single-ended (unbalanced) mixers as opposed to balanced mixers, and have suffered the limitation of narrow-band

operation imposed by the use of a narrow-band filter for image termination control.

Image-enhanced mixers can yield substantial improvement in performance only if high-performance diodes are available. The measure of potential performance is indicated by the frequency cutoff of the diode. Very high frequency cutoff ( $f_{co}$ ) is required for low conversion loss. Until the advent of the Schottky-barrier diode, and in particular, the GaAs Schottky barrier, sufficiently high  $f_{co}$  diodes were not available and image-enhanced mixers were only an academic curiosity. Now such Schottky barriers are readily available and low-conversion-loss mixers are a reality.

## II. SCHOTTKY-BARRIER JUNCTION PROPERTIES

The Schottky barrier used for mixers primarily requires the variable resistance property of a junction, thus it is commonly called a varistor. The variation of resistance of a varistor as a function of applied voltage is dramatic. The reverse-bias resistance is on the order of many megohms. The resistance decreases rapidly with increasing forward bias until the forward-bias series resistance  $R_s$  dominates over the effect of the junction resistance.

The junction resistance is in parallel with a junction capacitance  $C_j$  which is also a voltage variable component. The varistor must be designed such that the junction capacitance is minimized for a given series-limiting resistance. To compare varistors of differing  $R_s$  and  $C_j$  values, it is useful to define a cutoff frequency,  $f_{co} = (2\pi C_j R_s)^{-1}$ . For this comparison the zero-bias value for  $f_{co}$  is useful. It has been found that this value correlates well with measured results.

Figs. 1 and 2 show the  $f_{co}$  as computed for silicon and GaAs Schottky barriers. The value for  $R_s$  is made up of two parts. The first is the resistance of the epitaxial region  $X_e$ , and the second is the parasitic resistance due to the spreading of the current from the epitaxial layer into a substrate of finite conductivity  $\rho_s$ . Two values of junction diameter  $D_j$  were assumed. Three values of  $X_e$  were assumed. The first curve shows the limiting value of  $f_{co}$  due to the junction alone (no substrate resistance), and the epi-layer thickness is taken to be  $X_e = W_B$ . The remaining curves assumed a substrate spreading resistance. The second curve was calculated assuming the epitaxial-layer thickness  $X_e$  to be just enough to accommodate the space charge region at breakdown  $W_B$ . The third and

Manuscript received April 22, 1974; revised September 27, 1974. This work was supported in part by the United States Army Electronics Command, Fort Monmouth, N. J., under Contract DAAB07-72-C-0221.

The authors are with the Systems Development Division, Westinghouse DESC, Baltimore, Md. 21203.

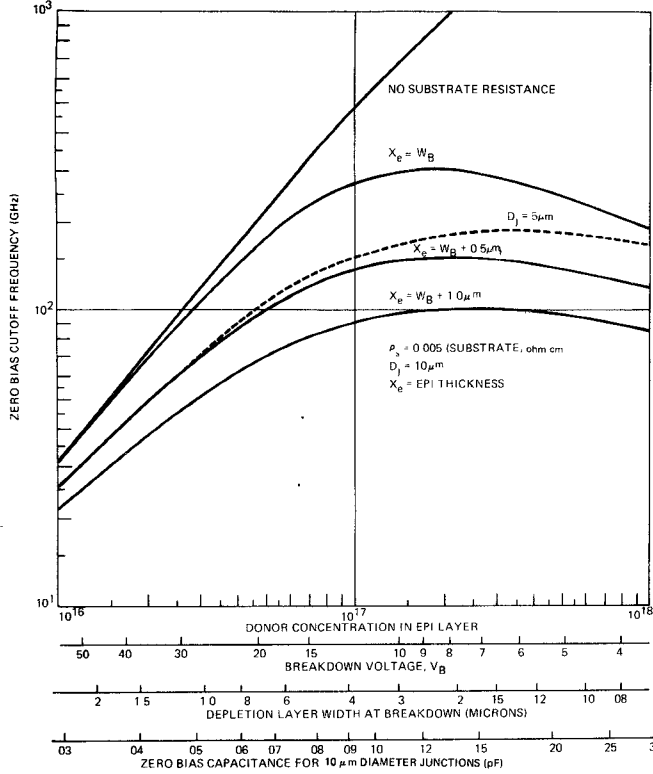


Fig. 1. Theoretical parameters of epitaxial silicon Schottky barriers.

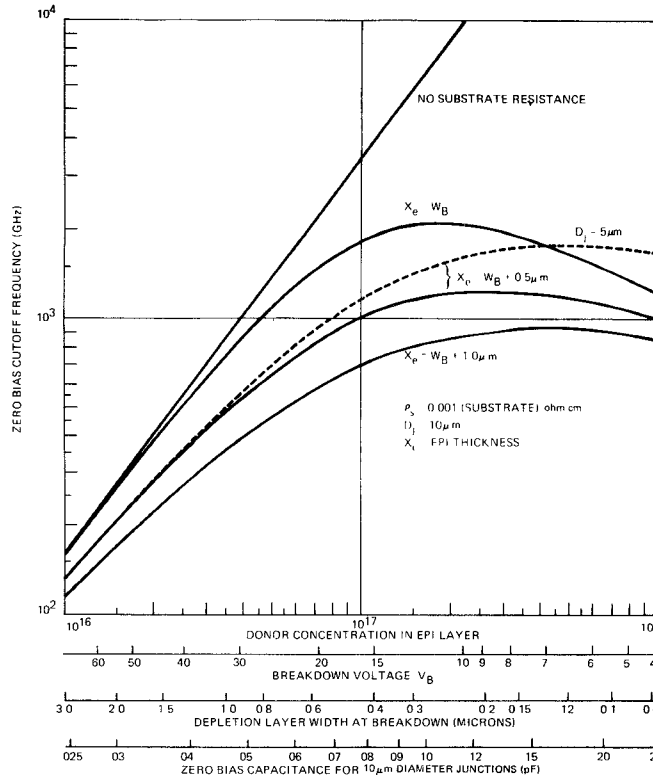


Fig. 2. Theoretical parameters of epitaxial GaAs Schottky barriers.

fourth curves make an allowance in the epi-layer thickness of 0.5 and 1.0  $\mu\text{m}$ , respectively.

The effect of the parasitic substrate resistance is clearly apparent in the figures, both in the drastically reduced

$f_{eo}$  and in the occurrence of a maximum in the curves [3]. The breakdown-voltage-impurity-density relationship of Sze and Gibbons [6] for an abrupt junction has been plotted also in the figures. These breakdown voltages represent bulk breakdown characteristics. Note that the  $f_{eo}$  calculation has been made assuming at least an epi-thickness sufficient to be fully depleted at breakdown. This allows maximum breakdown voltage for a given doping level. If a much reduced epi-thickness is used, then an improvement in  $f_{eo}$  can be obtained. Assume a GaAs epi-layer doping of  $10^{16}$  and a thickness of 0.5  $\mu\text{m}$ . Then one can calculate an  $f_{eo}$  (for the 10- $\mu\text{m}$ -diam junction on GaAs) of 2283 GHz, a breakdown voltage of 22 V, and a punch-through voltage of 2.0 V. The zero-bias capacitance is 0.024 pF. Now suppose that an excess of 0.5  $\mu\text{m}$  were left on this epi-layer (due to processing variables). Now the value for  $f_{eo}$  drops to 604 GHz, a drastic change in the value for  $R_s$ . Thus the epi-layer thickness for this diode becomes an extremely critical control parameter. However, such a thin-layer diode is attractive, especially for high-burnout diodes, because, for a given application, a junction diameter of 20  $\mu\text{m}$  on a 0.5- $\mu\text{m}$  epi-layer of  $10^{16}$  will give about the same impedance level and  $f_{eo}$  as a junction diameter of 10  $\mu\text{m}$  on a 0.5- $\mu\text{m}$  epi-layer of  $2 \times 10^{17}$ . Such a diode would have a two-to-one thermal impedance improvement over the smaller diode. The case for which the barrier depletion layer at zero bias extends through, or nearly through, the entire lightly doped epi-layer represents a special form of metal-semiconductor barrier known as a Mott barrier [3].

Note in Figs. 1 and 2 that there is an order of magnitude difference in the  $f_{eo}$  scales between Si and GaAs. Realistic substrate resistances have been assumed. It can be seen that if one assumes a nominal 0.5- $\mu\text{m}$  excess of epi-layer material for both Si and GaAs, that for 10- $\mu\text{m}$  junctions the Si devices will yield an  $f_{eo}$  of no more than 150 GHz; the GaAs devices can be expected with  $f_{eo}$  on the order of 1000 GHz. These numbers are realistic and have been readily approximated in practice. Thus GaAs is the natural choice for very low-conversion-loss mixers.

### III. DESIGN CONSIDERATIONS

Barber [4] has presented an analysis of microwave mixers and has shown that the pulse-duty ratio of the Schottky-diode current waveform is the most fundamental parameter for defining mixer operation because the diode current pulse retains its typical (switched) shape even when the voltage waveform becomes highly nonsinusoidal.

It can be shown that most microwave mixer diodes (adjusted for lowest conversion loss) behave as though the barrier itself were switched on and off at the LO rate, and that the resistance in the ON state is just that of the limiting series resistance ( $R_s$ ), and the impedance in the OFF state is just that expected of the series resistance  $R_s$  in series with the barrier capacitance  $C_j$ . Of course the barrier capacitance is a function of voltage and time, but good correlation with measured results are obtained if the

zero-bias capacitance value is used. Thus the frequency cutoff is  $f_{co} = (2\pi R_s C_s)^{-1}$ .

Using these considerations, an extension of Barber's analysis [7] has allowed the calculation of the conversion loss as a function of the pulse-duty ratio and as limited by the operating frequency to cutoff-frequency ratio ( $f/f_{co}$ ). Fig. 3 shows the expected mixer conversion loss that would be obtained for the broad-band case (wherein the image termination equals the signal termination). Fig. 4 shows the computed mixer conversion loss for the case wherein the image is short circuited.

Figs. 5, 6, and 7 show the computed values of mixer terminal impedances plotted as functions of the pulse-duty ratio ( $t$ ). In each case the RF-signal impedance  $R_{RF}$  has been chosen to minimize the mixer noise figure.

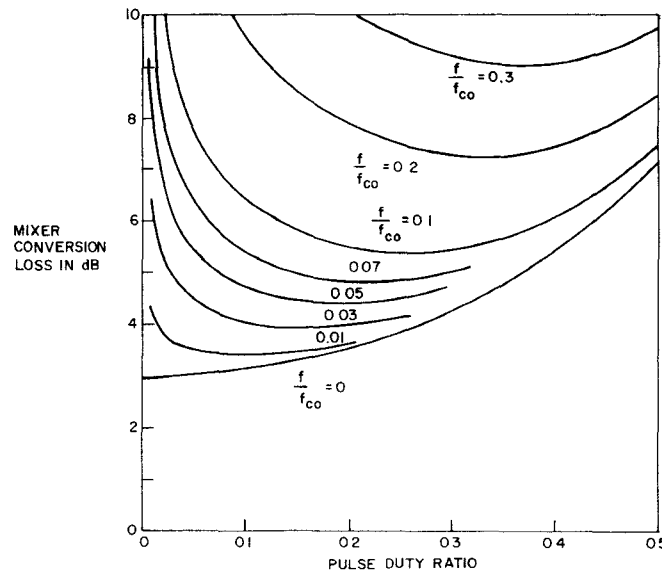


Fig. 3. Computed mixer conversion loss for the broad-band case.  
(Image termination equals signal termination.)

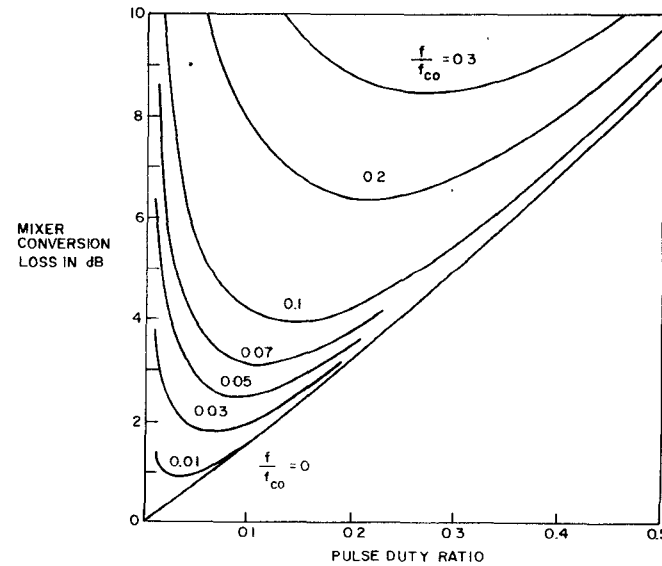


Fig. 4. Computed mixer conversion loss for the short-circuited image case.

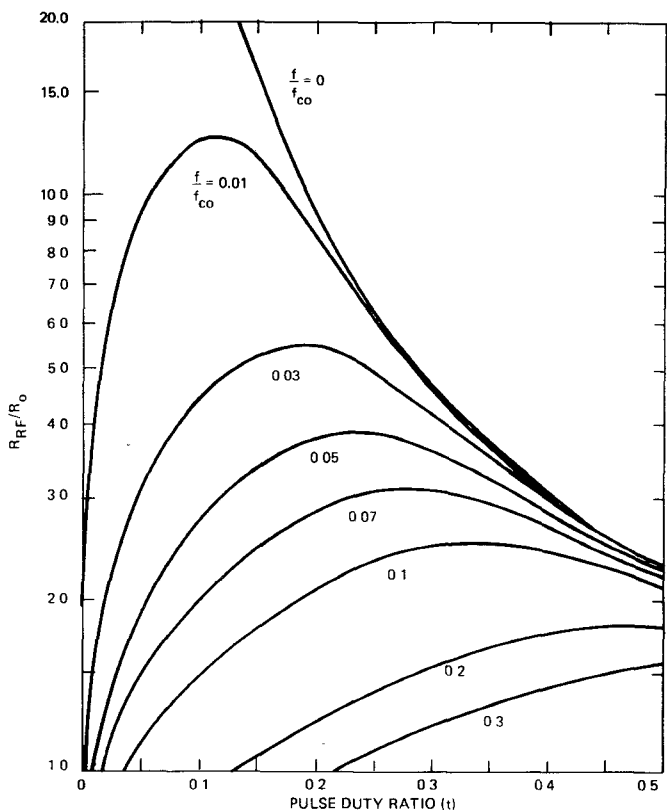


Fig. 5. Computed RF impedance for the broad-band case.

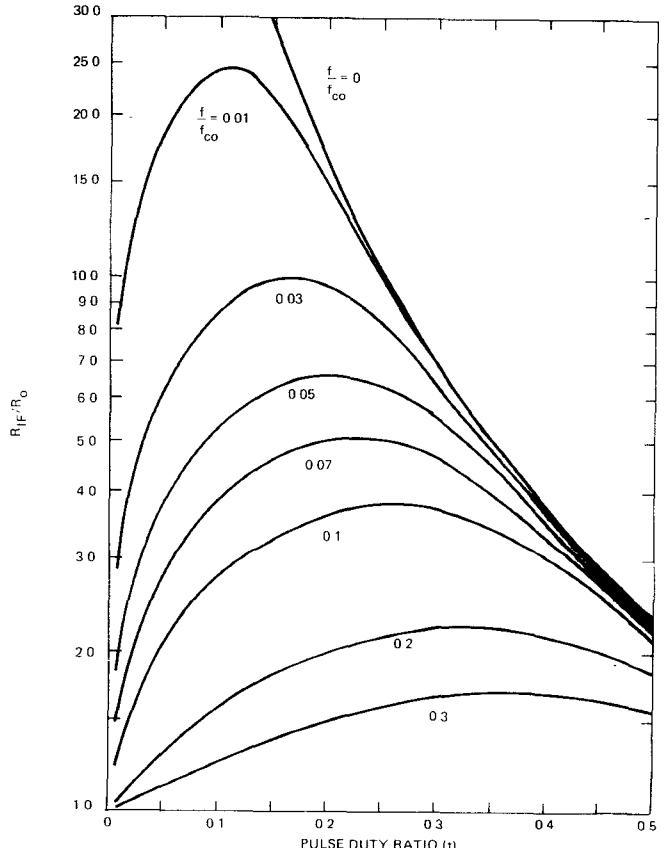


Fig. 6. Computed IF impedance for the broad-band case.

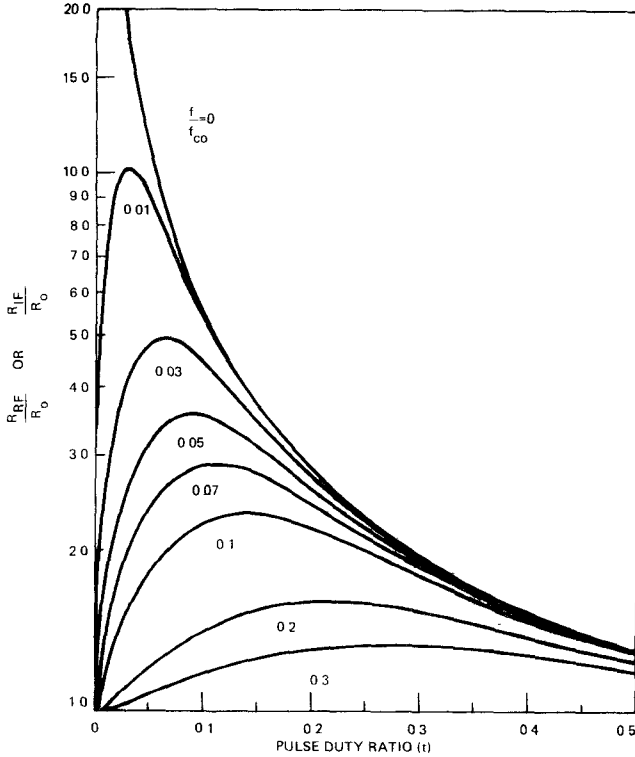


Fig. 7. Computed terminal impedance for the short-circuited image case.

This condition also results in an input impedance match. The RF and IF impedances have been computed as quantities normalized to  $R_0$ .  $R_0$  is the average diode impedance and is well approximated by the simple expression

$$R_0 = R_s/t. \quad (1)$$

This is the time-averaged diode impedance and thus is the impedance presented to the LO.

The rectified dc current is a useful quantity for checking mixer operation and can be calculated by using (2).

$$I_{dc} \cong \left( \frac{Pt}{R_s} \right)^{1/2} \left[ \frac{0.9 \sin(\pi t) - \sqrt{2}t \cos(\pi t)}{1+t} \right] \quad (2)$$

where  $P$  is the LO power,  $t$  is the pulse-duty ratio, and  $R_s$  is the diode-limiting resistance.

The LO power can be estimated by (3).

$$P = \frac{t(V_0 - V_b)^2}{R_s[1 + \cos(2\pi t)]} \quad (3)$$

where  $V_0$  is the forward potential drop of the Schottky barrier and  $V_b$  is the bias voltage. Typical values for  $V_0$  are 0.75 V (GaAs), 0.5 V (Si-Schottky barrier), and 0.15 V (Si-point contact).

#### IV. RESULTS

Fig. 8 shows the implemented design which allows complete realization of the desired image-enhanced balanced mixer using GaAs Schottky-barrier diodes. This is a plan view of the microwave-integrated-circuit (MIC) mixer as viewed from the ground-plane side of the alumina substrate. The RF signal of frequency 9.3 GHz enters the substrate on the right edge via the microstrip (signal-input) port. The RF is coupled to the diodes via a broadband microstrip-to-slot-line transition and through a bandpass image-reject impedance-matching filter consisting of microstrip lines coupled to the slot line. The pair of mixer diodes terminate this filter.

The LO at a frequency of 7.8 GHz is injected via the LO-input microstrip terminal. The LO power then passes through the directional filter and to the mixer diodes by way of a microstrip-to-coplanar-line transition (pin through the substrate). Slot-line stubs at the end of the

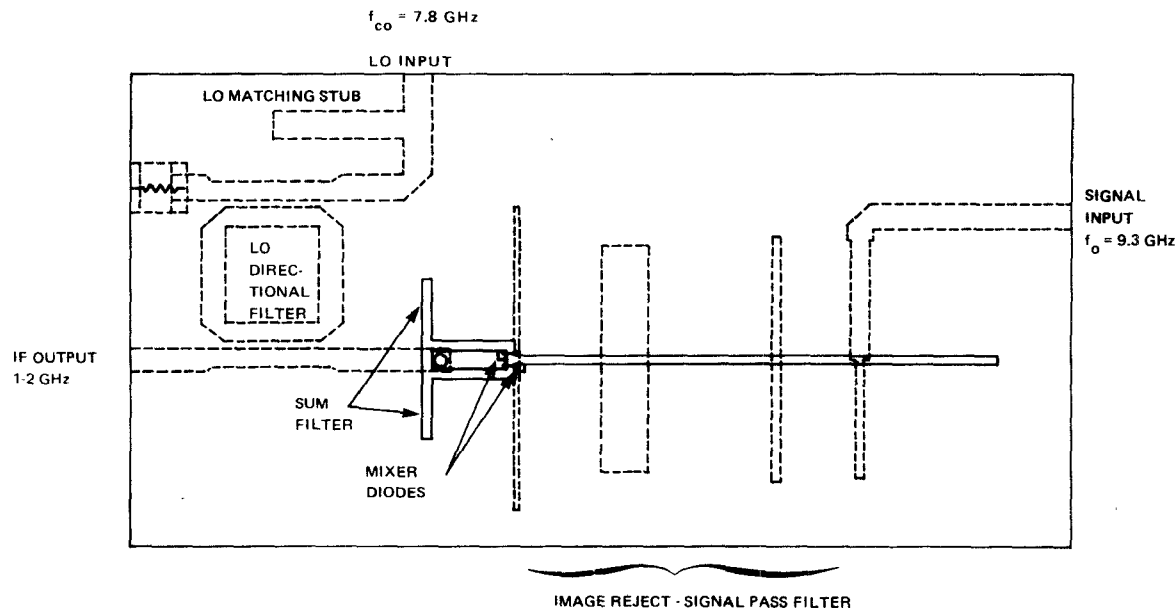


Fig. 8. X-band image-enhanced balanced mixer.

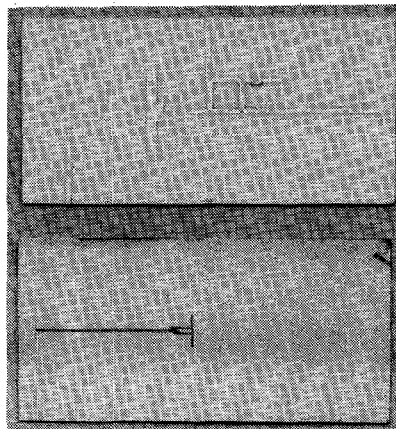


Fig. 9. Photograph of the X-band balanced mixer.

coplanar-line section present a short circuit to the mixer diodes at the sum frequency. The diodes are arranged such that the IF-output line is common with the LO input. The wide frequency separation of the IF and LO, and the directional- and frequency-selective properties of the directional filter allow very simple diplexing of the two signals with essentially zero bandwidth limiting of the IF port.

The two diodes are in parallel to the IF and LO ports, but in series to the signal port. As the conventional IF amplifier input impedance is nominally  $50 \Omega$ , the microstrip-to-coplanar-line characteristic impedance is set to  $50 \Omega$ . In a short-circuited image mixer the signal impedance is equal to the IF impedance. Thus the diode impedance must be  $100 \Omega$ , the two in parallel then matching the  $50\Omega$  line. But the two in series will present  $200 \Omega$  to the signal slot line. The slot line can readily be made with a characteristic impedance of nominally  $100 \Omega$ . The  $50\Omega$  microstrip to  $100\Omega$  slot-line transition has well in excess of 10-percent bandwidth. The signal filter then is designed to supply the impedance transformation required to match the  $200\Omega$  diode impedance to the  $100\Omega$  slot-line impedance.

Reference to Fig. 4 will show that a conversion loss of under  $2.0 \text{ dB}$  can be achieved with diodes of  $f_{co} \cong 800 \text{ GHz}$  and with PDR  $\cong 0.10$ . The signal-load impedance  $R_{RF}$  can be obtained from Fig. 7, and is found to be  $R_{RF} = 5.5 R_0$ . The impedance to the LO port is given by (1), so that if  $R_L = 100 \Omega$  and  $t = 0.10$ , then  $R_{LO} = 18.0 \Omega$ . The LO line will then have a VSWR  $\cong 5.5:1$ . As the directional filter is narrow-band and transparent to the LO power, the LO matching stub can be placed as shown in Fig. 8 without loss of performance.

Using (1), and the fact that  $R_L = 100 \Omega$ , one finds  $R_s = 1.8 \Omega$  for  $t = 0.10$ . Assuming a diode frequency cutoff of  $800 \text{ GHz}$ , the junction capacitance is found to be  $C_j = 0.11 \text{ pF}$ . A junction diameter of about  $10 \mu\text{m}$  will yield this value of  $C_j$  with an attendant  $f_{co} = 800 \text{ GHz}$ .

A computer program has been written which allows the analysis and optimization of microwave circuits with embedded mixer diodes. The diode model used was that which assumes that the Schottky diode can be represented

as a junction switched at the LO rate. In the ON condition the resistance is that of the limiting series resistance; and in the OFF state it is the series resistance in series with the barrier capacitance. The zero-bias capacitance was used for the analysis and appears to give good correlation with measured results. In this computer routine a three-frequency analysis is used. That is, the diodes are represented by black boxes with terminals at the RF, IF, and image frequencies with couplings set by the  $3 \times 3$  conductance matrix. All other frequencies generated are assumed to be short circuited. A nodal analysis routine is used to model the external circuitry at the three frequencies of interest and the diodes are added in parallel. An optimization program is then used to vary circuit values until the desired results are obtained. The computer results tracked the measured values within  $0.4 \text{ dB}$  over the band.

The signal filter loss was estimated to be  $\approx 0.85 \text{ dB}$ . The conversion loss was  $L_c \cong 1.6 \text{ dB}$ . The microstrip-to-slot-line transition is no more than  $0.05 \text{ dB}$  so that an overall conversion loss for the complete mixer should be about  $2.5 \text{ dB}$ . An additional loss of about  $0.2 \text{ dB}$  must be added for the 3-mm coaxial connectors used to bring in the RF-input signal and to remove the IF in the test fixture. Thus the total expected conversion loss (band center) is expected to be  $2.7 \text{ dB}$ .

An estimate for the LO power is obtained from (3). It is obvious by inspection of Fig. 8 that the diodes are dc short circuited and thus  $V_b = 0$ . For the GaAs devices being used,  $V_0 \cong 0.75 \text{ V}$ . Thus for the diode with  $R_s = 1.8 \Omega$ , an LO power of about  $17 \text{ mW}$  is required to attain the PDR = 0.1. As two diodes are being used, an available LO power of  $\approx 35 \text{ mW}$  is required for full modulation and attainment of reasonable impedance levels.

A mixer embodying the previously described design has been built. A photograph of the substrate with diodes mounted (top and bottom views of the substrate) is shown in Fig. 9. The following characteristics indicate the advancement of the state-of-the-art performance obtained. The measured curve of conversion loss versus frequency is shown in Fig. 10. These data (Table I) represent all circuit losses including connector losses.

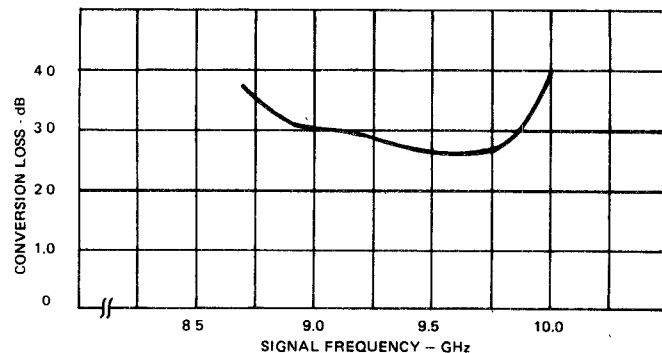


Fig. 10. Curve of conversion loss versus frequency.

TABLE I  
BALANCED MIXER PERFORMANCE

Signal frequency (center)	9.4 GHz
LO frequency	7.8 GHz
Signal bandwidth	1.0 GHz
Conversion loss (1.0-GHz band)	$\leq 3.15$ dB
Conversion loss (0.5-GHz band)	$\leq 2.8$ dB
Conversion loss (best point)	2.6 dB
LO power	$\approx 40$ mW
Dynamic range (input signal for 1.0-dB compression)	+ 13 dBm
Image band isolation	> 25 dB
VSWR (across signal band)	< 1.4:1

## REFERENCES

- [1] E. W. Herold *et al.*, "Conversion loss of diode mixers having image frequency impedance," *Proc. IRE*, vol. 33, pp. 603-609, Sept. 1945.
- [2] H. C. Torrey and C. A. Whitmer, *Crystal Rectifiers* (M.I.T. Radiation Lab. Series), vol. 15. New York: McGraw-Hill, 1948.
- [3] H. A. Watson, *Microwave Semiconductor Devices and Their Circuit Applications*. New York: McGraw-Hill, 1969.
- [4] M. R. Barber, "Noise figure and conversion loss of the Schottky barrier mixer diode," *IEEE Trans. Microwave Theory Tech.*, vol. MTT-15, pp. 629-635, Nov. 1967.
- [5] J. B. Cahalan *et al.*, "An integrated, X-band, image and sum frequency enhanced mixer with 1 GHz IF," in *1971 G-MTT Symp. Digest*, pp. 16-17, May 1971.
- [6] S. M. Sze and G. Gibbons, "Avalanche breakdown voltages of abrupt and linearly graded p-n junctions in Ge, Si, GaAs, and GaP," *Appl. Phys. Lett.*, vol. 8, pp. 111-113, Mar. 1966.
- [7] L. E. Dickens, "Low conversion loss millimeter wave mixers," in *1973 G-MTT Symp. Digest*, pp. 66-68, June 1973.

**APPENDIX VII-3**

**TRANSISTOR MIXERS**

## MESFET DRAIN MIXERS: ANALYSIS AND DESIGN

M. João Rosário, Pedro R. B. Vitor, J. Costa Freire

Centro de Electrónica Aplicada da UTL - INIC e Departamento de Engenharia  
Electrotécnica e Computadores - IST  
1096 Lisboa Portugal

### SUMMARY

A general and efficient nonlinear/linear analysis technique of MESFET drain mixers is presented. The study of conversion gain and matching impedances of the mixer is based on the Z-parameter conversion matrix. Using this approach, all the nonlinearities in the FET large signal equivalent circuit can be included and any number of local oscillator (LO) harmonics and mixing products can be considered. LO level and dc bias conditions for maximum gain are predicted.

### 1- INTRODUCTION

Theoretical analysis of mixer performance has been an important problem for more than thirty years. Since the early work of Torrey and Whitmar [1], a good deal of work [2] - [6] has been carried out in order to clarify the functioning of different mixer configurations.

Recently, the successful manufacturing of low-noise Ga As FETs for microwave applications, has created the possibility of developing mixers with performances that challenge those based on Schottky diodes.

The most common topologies are based on the IG(VGS) or ID(VDS) nonlinear characteristics. In the first case, the gate mixer, the local oscillator is connected between gate and source, while in the second case, the drain mixer, the local oscillator is applied between drain and source.

For the analysis of these two topologies, Maas [7] has presented a generalized theory based on the conversion matrices of each nonlinear element of the FET model. However, he has applied this theory only to gate mixers. A previous work by Begemann and Jacob [8] has presented the study of drain mixers considering only the transconductance and output resistance non linearities, but no experimental results were presented.

In this paper, a complete analysis of drain mixers is presented. A set of programs running on PCs was developed. This set, MIXAN (MIXer ANalysis), is based on the output results of SPICE transient analysis. It will give, for different values of DC operating points and different levels of local oscillator power  $P_{LO}$ , the conversion gain, the small signal input (RF) and output (IF) impedances. Thus, the dc bias and local oscillator level for maximum conversion gain can be determined. As a result of this analysis, the possibility of improving the conversion gain of drain mixers, by an appropriate choice of the IF and image` gate termination will be theoretically demonstrated. This approach is an

extension of the design technique previously proposed by the authors for diode mixers [9].

In order to ascertain the validity of the drain mixers analysis, a 11GHz-1GHz converter was designed and implemented in microstrip technology with soft substrate. The comparison between measured and theoretical results shows a good agreement what proves the usefulness of the proposed method as a design aid.

### 2. MESFET MODEL AND NONLINEAR ANALYSIS

The quasi-static nonlinear model used to simulate the behaviour of the MESFET under large-signal conditions is shown in Fig. 1. This model includes the nonlinearities which are essential to operation in drain mixers, namely the transconductance  $g_m$ , the drain resistance  $R_{ds}$  and the gate-drain capacitance  $C_{gd}$ . Are assumed to be linear all the other elements in the equivalent network, i.e. the parasitic resistances and inductances  $R_g$ ,  $R_s$ ,  $R_d$ ,  $L_g$ ,  $L_s$  and  $L_d$ , the gate resistance  $R_i$  and the gate-source capacitance  $C_{gs}$ , although slightly voltage dependent, due to the specificities of this topology.

Applying a large oscillator signal (LO) of frequency  $\omega_0$  between the drain and source terminals, the transconductance  $g_m$ , the drain resistance  $R_{ds}$  and the gate-drain capacitance  $C_{gd}$  become time varying functions of the same frequency. The voltage amplification factor  $\mu = g_m R_{ds}$  also becomes a time varying function that can be described by its Fourier series. Thus, we can write for each nonlinear element model

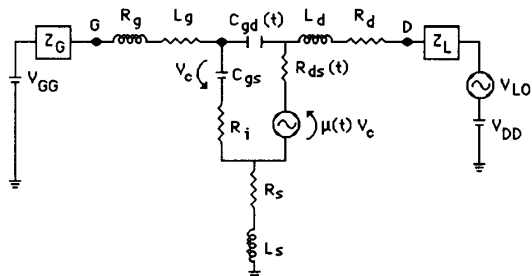


Fig 1 - MESFET nonlinear model

$$x(t) = \sum_{n=-\infty}^{\infty} X_n \exp(jnw_0 t) \quad (1)$$

where

$$X_n = 1/2\pi \int_{-\infty}^{+\infty} X(t) \exp(-jnw_0 t) dw_0 \quad (2)$$

### 3. LINEAR ANALYSIS

Under RF small-signal conditions, the frequencies present in the mixer are given by

$$f_n, m = f_0 + m f_s \quad (3)$$

where  $-\infty \leq n \leq \infty$ ,  $m=0, \pm 1$ , and  $f_0$  and  $f_s$  are the LO and RF frequencies, respectively.

According to this, all the magnitudes of currents and voltages in the circuit are of the form

$$\begin{aligned} x(t) &= \sum_{n=-\infty}^{\infty} \sum_{m=0}^{\infty} X_{n,m} \exp[j(nw_0 + mw_s)t] \quad (4) \\ &= x_{LO}(t) + x_{MX}(t) \end{aligned}$$

where  $x_{LO}(t)$  is the local oscillator component of  $x(t)$ ,

$$x_{LO}(t) = \sum_{n=-\infty}^{\infty} X_{n,0} \exp(jnw_0 t) \quad (5)$$

and  $x_{MX}(t)$  denotes the small-signal mixing products

$$x_{MX}(t) = \sum_{n=-\infty}^{\infty} \sum_{m=0}^{\infty} X_{n,m} \exp[j(nw_0 + mw_s)t]. \quad (6)$$

Since all the magnitudes involved in the above expressions are real,

$$X_{n,m} = (X_{-n,-m})^* \quad (7)$$

and it is only necessary to calculate one of these two complex coefficients.

Among the set of mixing products are the intermediate frequency (IF) and the image frequency (IM). Only these frequencies, together with RF, are considered in the complete mixer equivalent network of Fig. 2, in which the mixer is considered as a multiport with each port tuned to a single frequency. All the other mixing products are assumed to be suppressed by the filters  $F_k$ ,  $k=1 \dots 6$ , where the index  $k$  holds for the RF ( $k=1, k=4$ ), IF ( $k=2, k=5$ ) and IM ( $k=3, k=6$ ). The FET is loaded with complex impedances  $Z_k$ , with  $k$  denoted as above (the second subscript has been omitted for the sake of simplicity).

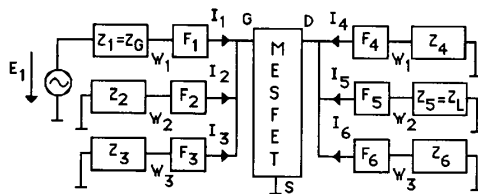


Fig 2 - Mixer configuration as a multiport

Conversion matrices relate the flowing current and applied voltage components, at different mixing frequencies in a harmonically time-varying element. For a time-varying resistance, the V-I relation is as follows [10]

$$V_K = [R] I_K. \quad (8)$$

Similarly, for a capacitor we have

$$I_K = j[\Omega][C]V_K \quad (9)$$

where  $I_K$  and  $V_K$  are the current and voltage for the mixing product frequency  $\omega_K$ . The elements of the conversion matrix  $[C]$  are the Fourier components of the time-varying element and  $[\Omega]$  is a diagonal matrix whose elements are the radian frequencies of the mixing products.

Since Kirchoff's laws hold for the frequency vectors in (8) and (9), we can write loop or node equations for the circuit of Fig. 2. In a way which is similar to that used for constant coefficient circuits we can write the Z matrix description of the multiport behaviour of the mixer as follows:

$$\begin{bmatrix} E_1 \\ 0 \\ 0 \\ 0 \\ 0 \\ 0 \end{bmatrix} = \begin{bmatrix} Z_T \\ \vdots \end{bmatrix} \cdot \begin{bmatrix} I_1 \\ I_2 \\ I_3^* \\ I_4 \\ I_5 \\ I_6^* \end{bmatrix} \quad (10)$$

where the conversion matrix  $Z_T$  can be partitioned as:

$$\begin{bmatrix} Z_T \\ \vdots \end{bmatrix} = \begin{bmatrix} Z_{11} & Z_{12} \\ Z_{21} & Z_{22} \end{bmatrix} \quad (10a)$$

The four sub-matrices in this partition are functions of the element conversion matrices of the model :

$$\begin{aligned} [Z_{11}] &= [Z_1] - [R][Z_3]^{-1}[Z_4] \\ [Z_{12}] &= [Z_2] + [R][Z_3]^{-1}[Rds] \\ [Z_{21}] &= [Z_3] + [Z_7][Z_3]^{-1}[Z_4] \\ [Z_{22}] &= [Z_5] - [Z_7][Z_3]^{-1}[Rds] \end{aligned} \quad (10b)$$

where

$$\begin{aligned} [R] &= R_i[I] + [Cgs]^{-1} \\ [Z_1] &= [Zni] + j[\Omega](Lg + Ls) + (Rg + Rs + R_i)[I] + [Cgs]^{-1} \\ [Z_2] &= Rs[I] + j[\Omega]Ls \\ [Z_3] &= [Rds] + R_i[I] + [Cgd]^{-1}([I] + [\mu]) [Cgs]^{-1} \\ [Z_4] &= R_i[I] + ([I] + [\mu]) [Cgs]^{-1} \\ [Z_5] &= [Zno] + j[\Omega](Ld + Ls) + [Rds] + (Rd + Rs)[I] \\ [Z_6] &= Rs[I] + j[\Omega]Ls - [\mu] [Cgs]^{-1} \\ [Z_7] &= [Rds] + [\mu] [Cgs]^{-1} \end{aligned} \quad (10c)$$

In the above expressions, we have made use of the following definitions:

$$\begin{aligned} [Zni] &= \text{diag}[Z_g(\omega_K)] \\ [Zno] &= \text{diag}[Z_L(\omega_K)] \\ [Cgs] &= j[\Omega]Cgs \end{aligned} \quad (10d)$$

$[Rds]$ ,  $[\mu]$  and  $[Cgd]$  are the matrix conversion for  $Rds(t)$ ,  $\mu(t)$  and  $Cgd(t)$ .  $[I]$  is the identity matrix.

From expressions (10) the conversion gain, the input impedance (RF) and the output impedance (IF) are

$$G_t = 4 |y_{51}|^2 \operatorname{Re}\{Z_G\} \operatorname{Re}\{Z_L\} \quad (11)$$

$$Z_{in} = 1/y_{11} - Z_G \quad (12)$$

$$Z_{out} = 1/y_{55} - Z_L \quad (13)$$

where the  $y_{yy'}$  are elements of the admittance matrix

$$[Y_T] = [Z_T]^{-1} \quad (14)$$

#### 4. CONVERSION GAIN AND MATCHING CONDITIONS IN A X-BAND MESFET DRAIN MIXER

In this section, the analysis technique previously presented is applied to the study of the conversion gain and matching conditions of a X-band MESFET drain mixer. The LO, RF and IF frequencies chosen are 10.0, 11.0, and 1.0GHz, respectively.

To optimum conversion gain, the input network must provide conjugate matching at the RF frequency and a short circuit at the IF and image frequencies, whilst the output network must conjugate match the device at IF and LO frequencies, while providing the filtering and LO-IF isolation.

In Figs. 3 and 4 the simulated values of the conversion gain, for several values of  $V_{GS}$ ,  $V_{DS}$  and  $P_{LO}$ , are sown. It can be noticed that for maximum conversion gain the device must be biased with  $V_{GS} = -0.3V$ ,  $V_{DS} = 0.7V$  and the local oscillator power should be 10.5dBm. For these values the RF input impedance is  $Z_{in}=6+j10\Omega$  and the output impedance is  $Z_{out}=78\Omega$  (IF frequency). From these values, the passive networks can be synthesized in order to achieve all optimal the conditions mentioned above.

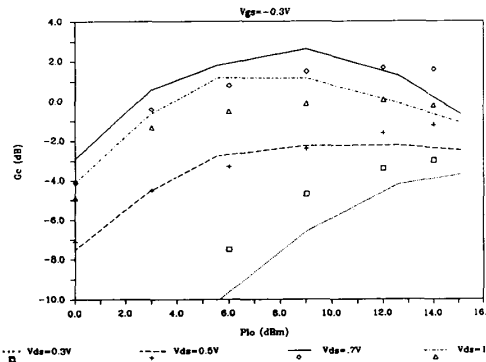


Fig 3 - Measured (symbols) and simulated (lines) conversion gain versus  $P_{LO}$  for several values of  $V_{DS}$

The circuit was implemented on a plastic substract using microstrip technology. Frequency dispersion and discontinuities were taken into consideration [11]. A schematic diagram of the mixer is shown in Fig.5.

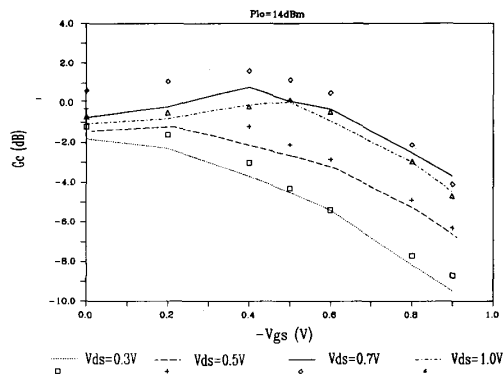


Fig 4 - Measured (symbols) and simulated (lines) conversion gain versus  $V_{GS}$  for maximum  $P_{LO}$

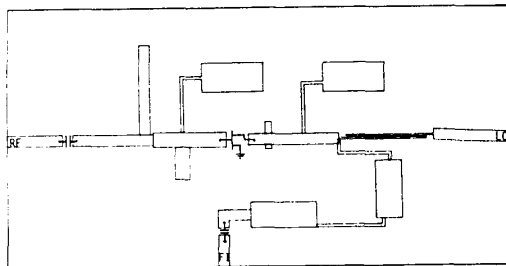


Fig 5 - Schematic diagram of the implemented mixer

The IF short circuit at the input is achieved by using, as gate biasing circuit, a high impedance short circuit stub that is one quarter-wavelength at the RF frequency. The rejection of the image frequency is achieved by means of an open stub with a quarter-wavelength at this frequency. The simulation of this network is presented in Fig. 6 and compared with the measured input reflection coefficient of the mixer.

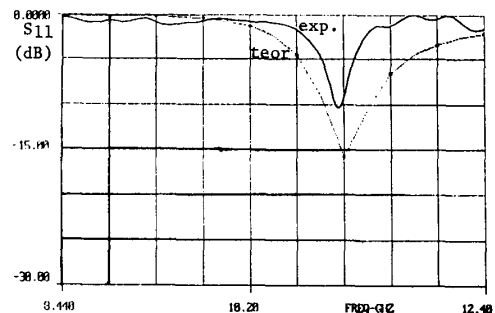


Fig 6 - Measured and simulated RF input reflection coefficient

The LO signal is injected through parallel coupled lines in order to decouple the drain bias and provide the LO-IF isolation. The output filter is based on a fourth order Tchebychev LC ladder filter. The asymmetry of this type of filter permits to match the mixer output impedance ( $78\Omega$ ) to the  $50\Omega$  IF termination. The design of the filter was optimized in order to assure short circuit at all the LO harmonics and higher order mixing frequencies. Fig. 7 shows the comparison between simulated input reflection coefficient of this network and measured reflection coefficient at the LO port.

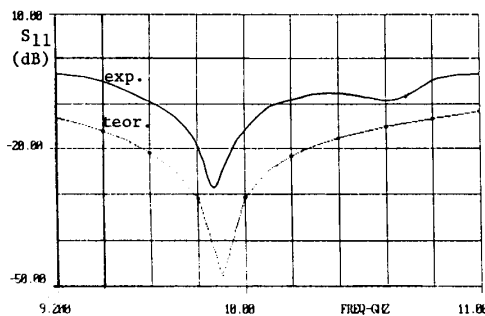


Fig 7 - Measured and simulated LO input reflection coefficient

The measured reflection at the IF port (-7dB) is higher than the predicted, (-12dB). This is due to the difficulty of obtaining experimentally the dependence of  $R_{ds}$  with  $V_{DS}$ .

In Figs. 3 and 4 was superposed to the above mentioned simulated curves of the conversion gain, the experimental. Absolute maximum conversion gain is achieved for the predicted dc bias point but for a LO level 3.5dB higher. In this condition, in Fig. 8, is presented the conversion gain v.s. frequency, to confirm  $F_{IM}$  and to measure mixer bandwidth.

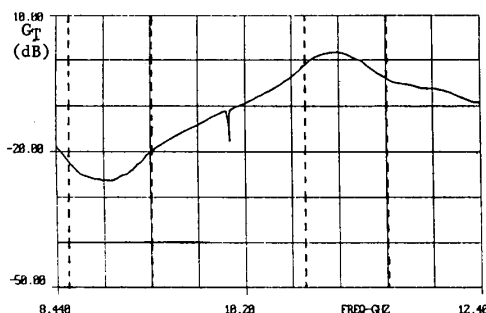


Fig 8 -Measured conversion gain versus frequency for optimal conditions

### 5 - CONCLUSIONS

A technique for drain mixers analysis was presented. This procedure determines the mixer conversion gain and the matching conditions as functions of the device bias and local oscillator level, from the results of a SPICE transient analysis.

This tool was used on the design and optimization of a X-band drain mixers. An example was presented for which the experimental and simulated results are in close agreement. The discrepancies noticed on LO level for maximum gain condition, can be associated with inaccuracies in the MESFET model parameters extraction. A 10% change in the values of  $R_{ds}$  and  $C_{gd}$  is sufficient to justify the differences between the experimental and theoretical values obtained for  $G_t$ ,  $Z_{in}$  and  $Z_{out}$ .

The MIXAN program was initially developed for the analysis of diode mixers. The extension of the MIXAN package to other classes of mixers is being developed at present by the authors.

### ACKNOWLEDGMENTS

The authors wish to thank the support of the Junta Nacional de Investigação Científica e Tecnológica (J. N. I. C. T. contract nº 219.85.62).

### REFERENCES

- [1] H. C. Torrey and C. A. Whitmer, "Crystal Rectifiers", (M.I.T.) Radiation Lab. Series, vol. 15, New York, McGraw Hill, 1948.
- [2] A. A. Saleh, "Theory of Resistive Mixers", Cambridge M. A.: M. I. T. Press, 1971.
- [3] M. R. Barber, "Noise Figure and Conversion Losses of the Schottky Barrier Mixer Diode" IEEE Trans. Microwave Theory and Tech., vol. MTT-22, May 1974.
- [4] R. A. Pucel, D. Masse and R. Bera, "Performance of Ga As MESFET Mixers at X-band", IEEE Trans. Microwave Theory and Tech., vol. MTT-24, June 1974.
- [5] O. Kurita and K. Morita, "Microwave MESFET Mixer", IEEE Trans. Microwave Theory and Tech., vol. MTT-24, June 1974.
- [6] P. Harrop and T. A. C. M. Claasen, "Modelling of an FET Mixer", Electron. Lett., Vol.14, nº12, 1978.
- [7] S. A. Maas, "Theory and Analysis of Ga As MESFET Mixers", IEEE Trans. Microwave Theory and Tech., vol. MTT-32, October 1984.
- [8] G. Begemann and A. Jacob, "Conversion Gain of MESFET Drain Mixers", Electron. Lett., vol. 15, nº18, 1979.
- [9] M. João Rosário and J. Costa Freire, "Microwave Mixers Analysis Based on Spice2", MELECON'87, Rome 1987.
- [10] S. Egami, "Nonlinear, Linear Analysis and Computer-aided Design of Resistive Mixers", IEEE Trans. Microwave Theory and Tech., vol. MTT-22, March 1974.
- [11] K. C. Gupta, R. Garg and R. Chadha, "Computer-Aided Design of Microwave Circuits", Artech House, 1981.

# Design Technique for MESFET Mixers for Maximum Conversion Gain

M. JOÃO ROSÁRIO, STUDENT MEMBER, IEEE, AND J. COSTA FREIRE, SENIOR MEMBER, IEEE

**Abstract**—A design technique for MESFET mixers is described. This technique is based on a mixer analysis program (MIXAN) designed to obtain the value of conversion gain and evaluate the influence of the embedding impedances for any local oscillator power and dc bias, in order to optimize the mixer performance. The MIXAN program, which uses SPICE as a “subroutine” to determine large-signal current and voltage waveforms, is able to obtain the operating conditions for maximum conversion gain. The good agreement between experimental and simulation results for  $X$ -band drain and gate mixers proves the validity of the design technique.

## I. INTRODUCTION

THE DESIGN procedure for MESFET mixers presented in this paper is based on a nonlinear/linear analysis technique (conversion matrices concept) [1]. It follows an approach which is similar to the design technique previously proposed by the authors for diode mixers [2], which led to the implementation of a first version of the MIXAN program (MIXers ANalysis). More elaborate auxiliary routines had to be developed and added to the initial MIXAN program in order to accommodate the two-port configuration of MESFET's.

In order to increase the accuracy of the method, a nonlinear MESFET model with a new parameter extraction technique was implemented. This technique is particularly appropriate for circuit designers since it is based only on dc and small-signal measurements (no physical parameters are required) and can be implemented through a linear analysis program incorporating an optimization routine such as TOUCHSTONE [3].

The time-domain analysis of the circuit is performed initially to obtain the control voltage waveforms of the model nonlinear elements when the MESFET is pumped by the local oscillator (LO). The widely used nonlinear CAD program SPICE is used for this purpose (PSPICE version 3.08 [4]).

After calculating the model time-varying parameters and their Fourier coefficients, the global mixer characteristics, such as conversion gain ( $G_c$ ), input impedance ( $Z_{in}$ ) at radio frequency (RF), and output impedance ( $Z_{out}$ ) at

intermediate frequency (IF), are calculated by the program MIXAN.

Based on the results produced by the program, an iterative design technique was set up for the two most common MESFET mixer topologies: **gate-mixer** (local oscillator connected between gate and source) based on the  $i_D(v_{GS})$  nonlinear characteristic in the saturation region ( $v_{DS} > v_{DSS}$ ); and **drain-mixer** (local oscillator connected between drain and source) based on the  $i_D(v_{DS})$  nonlinear characteristic at the triode region, in the neighborhood of the knee (low  $v_{DS}$ ).

Under large-signal operation, the nonlinear device behavior is strongly dependent on the embedding networks, due to their frequency selectivity. In order to optimize the mixer performance, a preliminary study of the embedding impedances, and of their influence on the conversion gain, is performed [5].

In order to ascertain the validity of the proposed methodology, 11 GHz to 1 GHz converters were designed and implemented in microstrip technology with soft substrate. Comparisons between measured and simulation results of the two prototypes, one for each MESFET mixer topology, are presented. The good agreement between theory and experiment proves the usefulness of the proposed method as a design aid.

## II. MESFET MODEL

The Curtice quasi-static large-signal model (Fig. 1) of the intrinsic MESFET [6] is used in the nonlinear analysis. This model exhibits a  $\pi$  topology with terminals  $G'D'S'$  and is resident in several versions of SPICE running on PC's, such as PSPICE version 3.08 [4], the program called from inside MIXAN.

The dc diode parameters are almost irrelevant for the present study, since the model is to be used with the gate–source and gate–drain junctions reverse biased. For this reason, default values are assigned to these parameters. The capacitances,  $C_{gd}$  and  $C_{gs}$ , are modeled through the classical relation [6]:

$$C = \frac{C_0}{\left(1 + \frac{v}{V_{bi}}\right)^M} \quad (1)$$

Manuscript received March 27, 1990; revised August 7, 1990.

The authors are with the Centro de Electrónica Aplicada de UTL-INIC and with the Department of Electrical and Computer Engineering, Instituto Superior Técnico, Av. Rovisco Pais, 1096 Lisboa, Portugal.

IEEE Log Number 9039247.

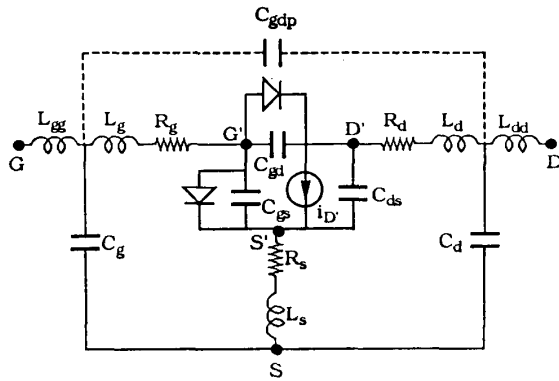


Fig. 1. MESFET nonlinear model.

where  $C = C_{gd}$ ,  $C_{gs}$ ;  $C_0 = C_{GD0}$ ,  $C_{GS0}$ ; and  $v = v_{G'D'}$ ,  $v_{G'S'}$ .

The other important nonlinear element (Fig. 1) is the  $i_{D'}$  current source, which, according to Curtice [6], can be expressed by the following relation (saturation region):

$$i_{D'} = \beta(1 + \lambda v_{D'S'}) \tanh(\alpha v_{D'S'})(v_{G'S'} - V_T)^2. \quad (2a)$$

The small-signal equivalent circuit of  $i_{D'}$  is formed by the parallel arrangement of a voltage-controlled current source of transconductance  $g_m$  and a conductance  $g_{d's'}$ :

$$g_m = \left[ \frac{\partial i_{D'}}{\partial v_{G'S'}} \right]_{V_{DS}} \quad (2b)$$

$$g_{d's'} = \left[ \frac{\partial i_{D'}}{\partial v_{D'S'}} \right]_{V_{GS}}. \quad (2c)$$

The other intrinsic capacitance,  $C_{ds}$ , the parasitics of the semiconductor access regions,  $R_g$ ,  $R_d$ , and  $R_s$ , and the mounting base parasitics,  $L_g$ ,  $L_d$ ,  $L_s$ ,  $L_{gg}$ ,  $L_{dd}$ ,  $C_g$ , and  $C_d$ , are regarded as constants.

The model parameter extraction procedure presented in this paper is based only on dc and small-signal measurements [7]. All parameters are obtained by fitting data to the model equations under different device operation conditions.

The drain-current-controlled source parameters,  $V_{T0}$ ,  $\beta$ ,  $\alpha$ , and  $\lambda$ , are obtained from the measured dc characteristics,  $I_D(V_{GS})$  for  $V_{GS} > V_{DSS}$  (saturation region) and  $I_D(V_{DS})$  for  $V_{GS} \approx V_{GS\max}/2$ . For this purpose, (2a) is fitted to data in different conditions, assuming that the drain current is low enough in order to neglect the parasitic resistances  $R_d$  and  $R_s$ : (i) Equation (2) predicts, for  $V_{DS}$  constant, a linear dependence of  $I_D^{1/2}$  on  $V_{GS}$ ; from this condition, the threshold voltage  $V_{T0}$  is obtained. (ii) For low  $V_{DS} (\lambda V_{DS} \ll 1)$ , the product  $\alpha\beta$  is obtained from the  $I_D(V_{DS})$  slope for constant  $V_{GS}$ . (iii) For high values of  $V_{DS}$  (saturation region),  $\tanh(\alpha V_{DS}) \approx 1$ , and  $\lambda$  and  $\beta$  can be obtained from the  $I_D(V_{DS})$  slope and  $I_D(0)$ , respectively. (iv) Finally, from (ii) and (iii),  $\alpha$  is calculated.

From the drain current equation, the small-signal parameters  $g_m$  and  $g_{d's'}$  are obtained for several dc bias conditions, appropriate to the model application (eqs.

TABLE I  
CFY18-23 MODEL PARAMETERS

STATIC PARAMETERS				DYNAMIC PARAMETERS				
$V_{TO}(V)$	$\beta(mAV^{-2})$	$\lambda(V^{-1})$	$\alpha(V^{-1})$	$C_{GS0}(pF)$	$C_{GD0}(pF)$	$V_{bi}(V)$	$M$	$t(pps)$
-1.959	9.22	0.253	4.55	0.945	0.029	0.125	0.5	3.203
PARASITIC					$C_{gd}(pF)$	$C_g(pF)$	$L_{gd}(nH)$	$L_{gg}(nH)$
$R_d(\Omega)$	$R_g(\Omega)$	$R_s(\Omega)$	$L_d(nH)$	$L_g(nH)$	0.084	0.153	0.180	0.312
1.14	2.24	0.252	0.350	0.357				0.132

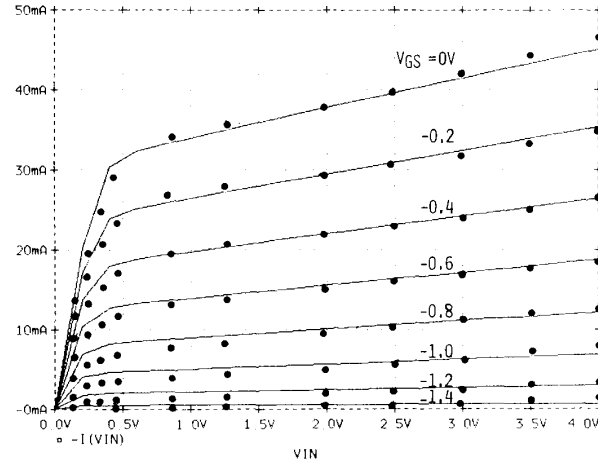


Fig. 2. MESFET dc output characteristics: model (lines) and experiments (symbols).

(2b) and (2c)). For these bias conditions, the remaining parameters of the small-signal model are obtained by fitting the  $S$  parameters to their measured values for the useful frequency range. This step of the extraction is performed with the help of a commercially available linear analysis CAD program that also performs parameter tuning [3].

We assume all model parameters to be constant except for the nonlinear input and feedback capacitances,  $C_{gs}$  and  $C_{gd}$ , and the already known  $g_m$  and  $g_{d's'}$ . At a first stage, all constant parameters are obtained by fitting for a typical dc bias condition. Using these values, new sets of values for  $C_{gs}$  and  $C_{gd}$  are obtained for other bias conditions. The pairs of values for these nonlinear capacitances are then used to obtain the parameters in expression (1) ( $C_{GS0}$ ,  $C_{GD0}$ ,  $M$ ,  $V_{bi}$ ) by a new fitting process.

Using this technique, a large-signal model for the commercially available CFY18-23 MESFET was obtained (Table I). A frequency range from 2 to 15 GHz was used to perform the parameter tuning. Only three quiescent points were considered for determining the parameters in the  $C_{gs}$  and  $C_{gd}$  equations.

Figs. 2 and 3 show a comparison between simulated characteristics and measurements. It can be seen that good agreement is obtained, in spite of the reduced number of bias conditions that were considered.

A better matching in the  $s_{12}$  phase can be obtained by introducing a parasitic capacitance  $C_{gd_p}$  (dashed line in Fig. 1). However, this element increases the complexity of

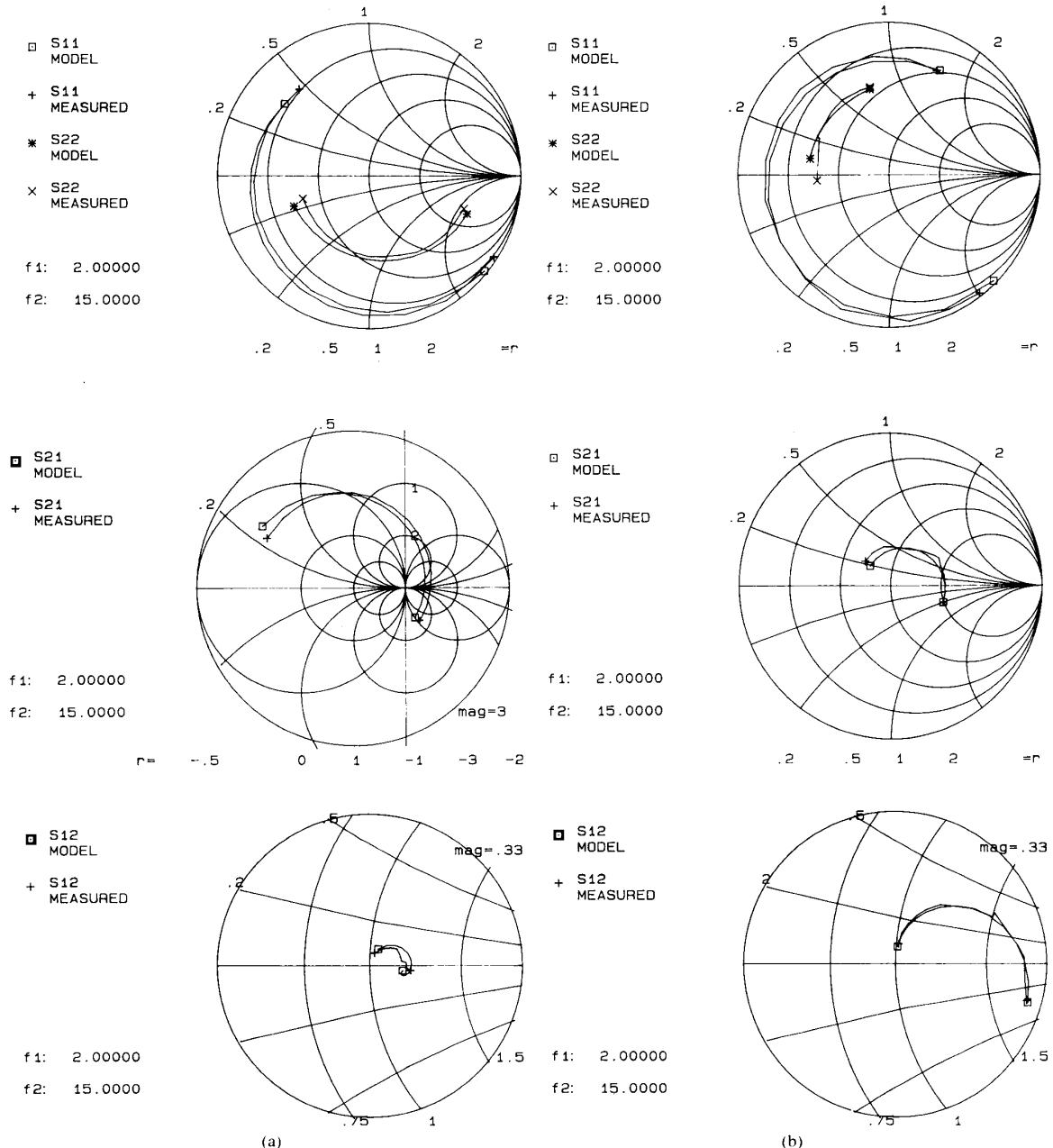


Fig. 3. MESFET  $S$  parameters: comparison between simulation and measurement for (a)  $V_{DS} = 0.2$  V and  $I_D = 10$  mA and (b)  $V_{DS} = 3$  V and  $I_D = 10$  mA.

the nonlinear/linear mixer analysis, without a significant change in accuracy.

### III. NONLINEAR ANALYSIS

In order to save computation time and avoid convergence problems, we have reduced, within the required accuracy, the number of nonlinear elements in the model. For drain mixers, only the feedback capacitance  $C_{gd}$  and

the voltage-dependent current source  $i_D(v_{GS}, v_{DS})$  were regarded as nonlinear. The input capacitance  $C_{gs}$  and the voltage-dependent current source  $i_D(v_{GS}, v_{DS})$  were assumed as the only nonlinear elements for the gate mixer.

In the nonlinear/linear analysis method followed in this paper, only the LO excitation needs to be considered to obtain the waveforms of the control variables  $v_{GS}$ ,  $v_{DS}$  of the intrinsic model. Under RF small-signal excitation,

the current source  $i_{D'}$  is modeled by a voltage-dependent current source  $g_m v_{g's'}$  and a conductance  $g_{d's'}$ . Since  $i_D(v_{G'S'}, v_{D'S'})$  is a nonlinear element, both  $g_m$  and  $g_{d's'}$  are time dependent.

From the waveforms of the control variables, we can write, for each nonlinear element ( $C_{gd}$ ,  $C_{gs}$ ,  $g_m$  and  $g_{d's'}$ ), a time-varying function which can be described by its Fourier series:

$$x(t) = \sum_{n=-\infty}^{\infty} X_n \exp(jn\omega_o t) \quad (3)$$

where

$$X_n = \frac{1}{2\pi} \int_0^{2\pi} x(t) \exp(-jn\omega_o t) d\omega_o t. \quad (4)$$

We assume that the frequencies present in the mixer are

$$f_{n,m} = nf_o + mf_s \quad (5)$$

where  $-\infty < n < \infty$ ,  $m = 0, \pm 1$ , and  $f_o$  and  $f_s$  are the LO and RF frequencies, respectively. According to this, the magnitudes of currents and voltages in the circuit are all of the form

$$\begin{aligned} x(t) &= \sum_{n=-\infty}^{+\infty} \sum_{m=-1}^{+1} X_{n,m} \exp[j(n\omega_o + m\omega_s)t] \\ &= x_{LO}(t) + x_{MX}(t) \end{aligned} \quad (6)$$

where  $x_{LO}(t)$  is the local oscillator component of  $x(t)$ :

$$x_{LO}(t) = \sum_{n=-\infty}^{+\infty} X_{n,0} \exp[jn\omega_o t] \quad (7)$$

and  $x_{MX}(t)$  denotes the small-signal mixing products:

$$x_{MX}(t) = \sum_{n=-\infty}^{+\infty} \sum_{m=-1}^{+1} X_{n,m} \exp[j(n\omega_o + m\omega_s)t] \quad (m \neq 0). \quad (8)$$

Since all the variables  $x(t)$  involved in the above expressions are real,

$$X_{n,m} = (X_{-n,-m})^* \quad (9)$$

only one of the two complex coefficients needs to be calculated.

The SPICE transient analysis gives, for fixed LO level, dc bias, and load conditions, the waveforms of  $v_{G'S'}(t)$ ,  $v_{D'S'}(t)$ , and  $v_{G'D'}(t)$ . From these waveforms and from (1), (2b), and (2c), we obtain the Fourier series coefficients (3) for  $C_{gd}(t)$ ,  $C_{gs}(t)$ ,  $g_m(t)$ , and  $g_{d's'}(t)$  by means of a FFT routine included in the MIXAN program.

#### IV. LINEAR ANALYSIS

Among the set of mixing products are the intermediate frequency (IF) and the image frequency (IM). Only these frequencies, together with RF, are considered in this study. However, the MIXAN program can support a higher number of mixing products at the cost of extra computer time. Therefore, the complete mixer equivalent network has the configuration shown in Fig. 4. In this configuration, the mixer is regarded as a linear multiport with each port tuned to a single frequency. All the other

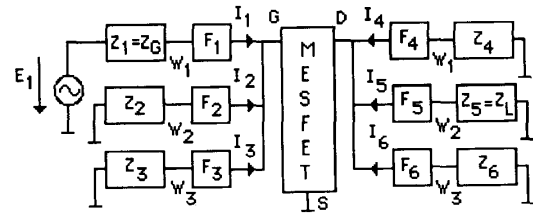


Fig. 4. Mixer configuration as a linear multiport.

mixing products are assumed to be suppressed by the filters  $F_k$ ,  $k = 1, \dots, 6$ , where the index  $k$  holds for RF ( $k = 1, k = 4$ ), IF ( $k = 2, k = 5$ ), and IM ( $k = 3, k = 6$ ). The FET is loaded with complex impedances  $Z_k$ .

At this point, we define conversion matrices which relate the current and voltage harmonics for each time-varying circuit element. The matrix elements are the Fourier coefficients obtained in the nonlinear analysis according to (1) and (2). For a time-varying resistance,  $R(t)$ , the  $V-I$  relationship is [8], [9]

$$[V_K] = [R][I_K] \quad (10)$$

where the vectors  $I_K$  and  $V_K$  are the current and voltage components for the mixing products of frequency  $\omega_K$ , and  $R$  is the conversion matrix, whose elements are the Fourier coefficients of  $R(t)$ . Similarly, for a capacitor we have

$$[I_K] = j[\Omega][C][V_K]. \quad (11)$$

The elements of the conversion matrix  $C$  are the Fourier components of the time-varying capacitance, and  $\Omega$  is a diagonal matrix whose elements are the radian frequencies of the mixing products.

Since Kirchhoff's laws hold for the current and voltage vectors in (10) and (11), we can write loop or node equations for the circuit of Fig. 4. In a way which is similar to that used for time-constant coefficient circuits, we can write the  $Z$  matrix description of the multiport behavior of the mixer as follows:

$$\begin{bmatrix} E_1 \\ 0 \\ 0 \\ 0 \\ 0 \\ 0 \end{bmatrix} = [Z_T] \cdot \begin{bmatrix} I_1 \\ I_2 \\ I_3^* \\ I_4 \\ I_5 \\ I_6^* \end{bmatrix} \quad (12a)$$

where the conversion matrix  $Z_T$  can be partitioned as

$$[Z_T] = \begin{bmatrix} [Z_{11}] & [Z_{12}] \\ [Z_{21}] & [Z_{22}] \end{bmatrix}. \quad (12b)$$

In this partition, the four submatrices are functions of the conversion matrices of each model element:

$$\begin{aligned} [Z_{11}] &= [Z_1] - [Z_{gs}][Z_3]^{-1}[Z_4] \\ [Z_{12}] &= [Z_2] + [Z_{gs}][Z_3]^{-1}[R_{ds}] \\ [Z_{21}] &= [Z_6] + [Z_7][Z_3]^{-1}[Z_4] \\ [Z_{22}] &= [Z_5] - [Z_7][Z_3]^{-1}[R_{ds}] \end{aligned} \quad (12c)$$

where

$$\begin{aligned}
 [Y_{gs}] &= j[\Omega][C_{gs}] \\
 [Y_{gd}] &= j[\Omega][C_{gd}] \\
 [Z_{gs}] &= [Y_{gs}]^{-1} \\
 [Z_1] &= [Z_{ni}] + [Y_{gs}]^{-1} \\
 [Z_2] &= R_s[I] + j[\Omega]L_s \\
 [Z_3] &= [R_{ds}] + [Y_{gd}]^{-1} + ([I] + [g_m][R_{ds}])[Y_{gs}]^{-1} \\
 [Z_4] &= ([I] + [g_m][R_{ds}])[Y_{gs}]^{-1} \\
 [Z_5] &= [Z_{no}] + [R_{ds}] + (R_s)[I] \\
 [Z_6] &= R_s[I] + j[\Omega]L_s - [g_m][R_{ds}][Y_{gs}]^{-1} \\
 [Z_7] &= [R_{ds}]( [I] + [g_m][Y_{gs}]^{-1} ). \quad (12d)
 \end{aligned}$$

In the above expressions, we have used the following definitions:

$$\begin{aligned}
 [Z_{ni}] &= \text{diag}[Z_G(\omega_k) + Z_{PI}(\omega_k)] \\
 [Z_{no}] &= \text{diag}[Z_L(\omega_k) + Z_{PO}(\omega_k)] \quad (12e)
 \end{aligned}$$

and  $[R_{ds}]$ ,  $[g_m]$ ,  $[C_{gd}]$ , and  $[C_{gs}]$  represent the conversion matrices for  $R_{ds}(t)$ ,  $g_m(t)$ ,  $C_{gd}(t)$ , and  $C_{gs}(t)$ .  $[I]$  is the identity matrix, and  $Z_{PI}(\omega_k)$  and  $Z_{PO}(\omega_k)$  are the impedances of the input and output parasitic elements, respectively.

From expressions (12), the conversion gain  $G_c$ , the input impedance  $Z_{in}$  (RF), and the output impedance  $Z_{out}$  (IF) are given by

$$G_c = 4|y_{S1}|^2 \cdot \text{Re}\{Z_G\} \cdot \text{Re}\{Z_L\} \quad (13)$$

$$Z_{in} = \frac{1}{y_{11}} - Z_G \quad (14)$$

$$Z_{out} = \frac{1}{y_{55}} - Z_L \quad (15)$$

where  $y_{ij}$  designates the generic element of the admittance matrix

$$[Y_T] = [Z_T]^{-1}. \quad (16)$$

## V. MIXAN PROGRAM

According to the nonlinear/linear analysis technique presented above, an auxiliary CAD program (MIXAN) was developed that calculates the input and output impedances and the conversion gain of MESFET mixers. The MIXAN program flowchart is represented in Fig. 5. In a first stage, it calls for SPICE transient analysis to determine the control voltages of the MESFET model elements when it is pumped by the local oscillator.

## VI. DESIGN TECHNIQUE

Under large-signal operation, the nonlinear device behavior is strongly dependent on the embedding networks, due to their frequency selectivity. However, in order to optimize the mixer performance, these networks must be designed with the device external characteristics taken into account. Accordingly, an iterative method for the design is required.

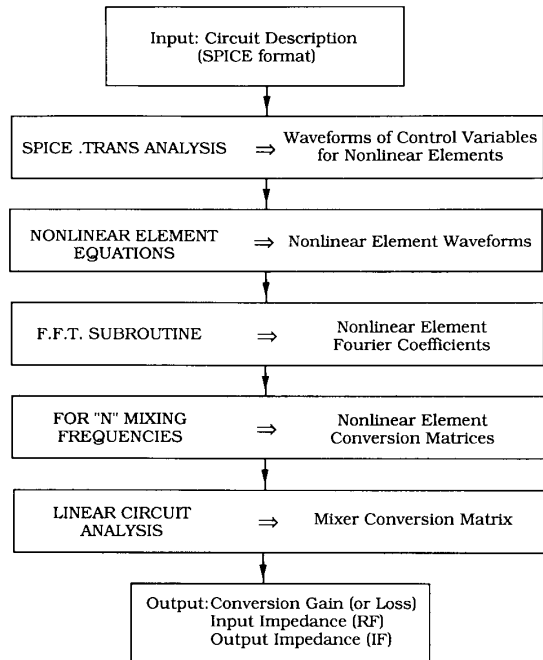


Fig. 5. MIXAN program flowchart.

The MESFET mixer's design procedure can be summarized as follows.

- 1) Measure the MESFET dc characteristics and small-signal  $S$  parameters.
- 2) Fit the large-signal model parameters to the experimental data obtained in step 1.
- 3) Design the MESFET selective loads. In order to increase power efficiency, only reactive impedances are considered, with the obvious exception of the RF impedance at input and the IF impedance at output. For this purpose, we design tuned networks at the three frequencies considered in the linear analysis and at  $f_o$  (LO) and  $2f_o$ , which are formed by a  $\lambda/4$  stub and a sliding transmission line that modifies the phase of the reflection coefficient.
- 4) Study the influence of the embedding impedances on conversion gain and stability. With the MESFET model obtained in step 2 and the networks designed in step 3, the three mixer parameters,  $Z_{in1}$ ,  $Z_{out1}$ , and  $G_{c1}$ , are obtained with the MIXAN program.
- 5) For the optimal load conditions (those leading to the highest gain within the stability region and technologically "acceptable" values for  $Z_{in}$  and  $Z_{out}$ ), design the input coupling network in order to obtain impedance matching at RF ( $50 \Omega \leftrightarrow Z_{in1}$ ) and design the output coupling network in order to match the impedance at IF ( $Z_{out} \leftrightarrow 50 \Omega$ ).
- 6) For the networks designed in step 5, new values for the three parameters,  $Z_{in2}$ ,  $Z_{out2}$ , and  $G_{c2}$ , are obtained.

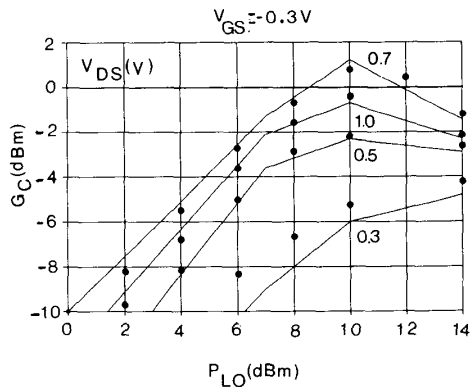


Fig. 6. Drain mixer: measured (symbols) and simulated (lines) conversion gains versus  $P_{LO}$  for different values of  $V_{DS}$ .

- 7) Design a new set of input and output coupling networks if  $Z_{in2} \neq Z_{in1}$  or  $Z_{out2} \neq Z_{out1}$ .
- 8) For the new set of input and output coupling networks, obtain the three mixer parameters with the MIXAN program:  $Z_{in3}$ ,  $Z_{out3}$ , and  $G_{c3}$ .
- 9) Repeat steps 7 and 8 until  $Z_{inj+1} \approx Z_{inj}$  and  $Z_{outj+1} \approx Z_{outj}$ . From our experience, we have noticed that two iterations for the input network and three iterations for the output network are usually sufficient.

Following this procedure for different LO power levels ( $P_{LO}$ ) and MESFET bias conditions, the conversion gain can be optimized.

## VII. EXPERIMENTAL RESULTS

The analysis technique presented above was applied to the study of the conversion gain and matching conditions of  $X$ -band MESFET mixers. Two prototypes, one for each MESFET mixer topology, were designed, mounted, and measured. The LO, RF, and IF frequencies chosen for this test were 10.0, 11.0, and 1.0 GHz, respectively. Both circuits were implemented on a plastic substrate using microstrip technology. Frequency dispersion and discontinuities were taken into consideration [10].

### A. Drain Mixer

To obtain optimum conversion gain, according to step 4 of the design technique, the input network must provide conjugate matching at RF and a short circuit at IF, while the output network must conjugate match the device at IF and provide a short circuit at LO frequencies ( $f_o, 2f_o$ ) while providing filtering and LO-IF isolation. The influence on conversion gain of the network impedance at image frequency has been proved negligible and, in accordance, a short circuit was assumed.

In Figs. 6 and 7, the values of the conversion gain obtained by simulation are shown for several values of  $V_{GS}$ ,  $V_{DS}$  and  $P_{LO}$ . It can be seen that for maximum conversion gain, the device should be biased with  $V_{GS} = -0.3$  V and  $V_{DS} = 0.7$  V and the local oscillator power should be 10.5 dBm. For these values, the RF input

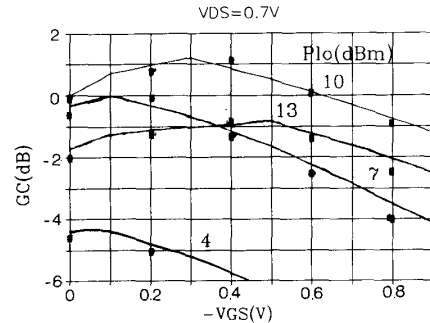


Fig. 7. Drain mixer: measured (symbols) and simulated (lines) conversion gains versus  $V_{GS}$  for different values of  $P_{LO}$ .

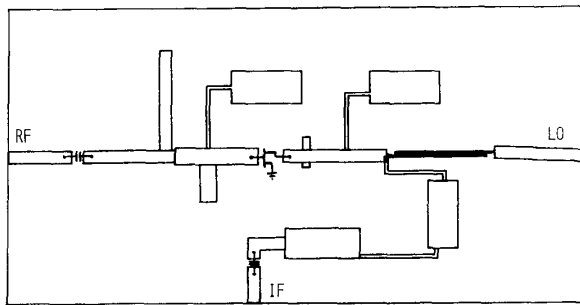


Fig. 8. Drain mixer: microstrip prototype.

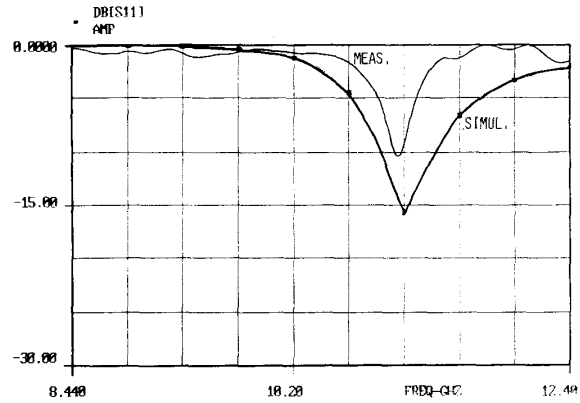


Fig. 9. Drain mixer: measured and simulated RF input reflection coefficients versus frequency.

impedance is  $Z_{in} = 6 + j10 \Omega$ , and the IF output impedance is  $Z_{out} = 78 \Omega$ . Based on these values, the passive networks can be synthesized in order to achieve all the conditions mentioned above (Fig. 8).

The IF short circuit at the input is implemented by using, as gate biasing circuit, a quarter-wavelength stub at RF frequency. The image frequency rejection is achieved by means of an open stub with a quarter wavelength at this frequency. The simulation of this network, assuming  $Z_{in}$  to be constant, is presented in Fig. 9 and compared with the measured input reflection coefficient of the mixer.

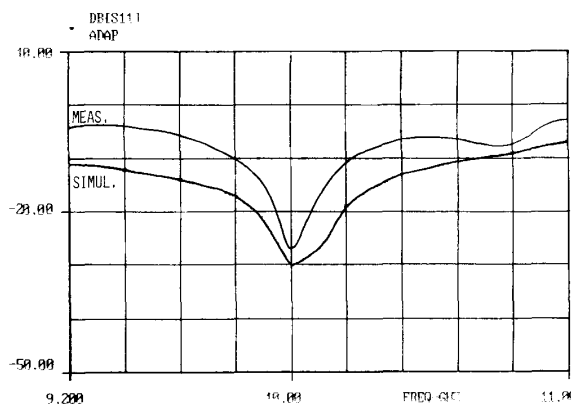


Fig. 10. Drain mixer: measured and simulated LO input reflection coefficients versus frequency.

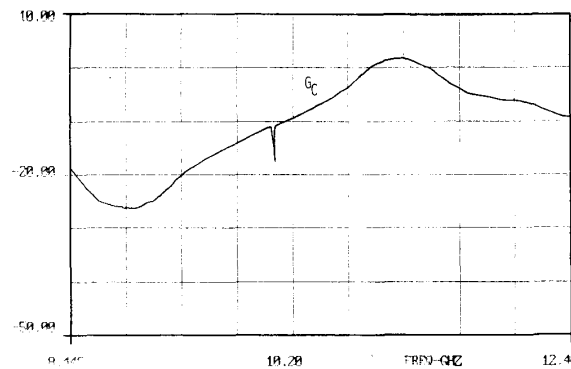


Fig. 11. Drain mixer: measured conversion gain versus frequency for optimal conditions.

The LO signal is injected through parallel coupled lines in order to decouple the drain bias and provide the LO-IF isolation. The output filter is based on a fourth-order Chebyshev *LC* ladder filter. The asymmetry of this type of filter makes it possible to match the mixer output impedance ( $78 \Omega$ ) to the  $50 \Omega$  IF termination. The design of the filter was optimized in order to ensure a short circuit at all LO harmonics and higher order mixing frequencies. Fig. 10 shows a comparison between the simulated input reflection coefficient of this network and the measured reflection coefficient at the LO port.

In Figs. 6 and 7, the experimental results were superimposed on the above-mentioned simulated curves of the conversion gain. Absolute maximum conversion gain is achieved for the predicted dc bias point but for a LO level 1.5 dB higher than the predicted one. The conversion gain versus frequency is presented for these conditions (Fig. 11) in order to confirm  $f_{IM}$  rejection and to determine mixer bandwidth.

#### B. Gate Mixer

Following the procedure described above, the optimal load conditions for a gate mixer were found to be IF short-circuited at the input with LO and harmonics

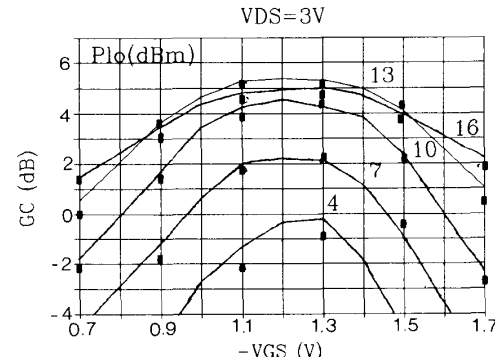


Fig. 12. Gate mixer: measured (symbols) and simulated (lines) conversion gains versus  $V_{GS}$  for different values of  $P_{LO}$ .

short-circuited at the output. The influence of the image frequency termination on the conversion gain was negligible. These results confirm the conclusions obtained by other authors [11], [12].

Maximum conversion gain is obtained with a drain load at RF that leads to unstable operation of the MESFET ( $\text{Re}\{Z_{in}\} < 0$  or  $\text{Re}\{Z_{out}\} < 0$ ). The introduction of a short circuit eliminates this undesirable situation at the cost of a lower  $G_c$ . To increase the gain, another alternative is an appropriate choice of gate load reflection at  $2f_o$ . With the CFY18 MESFET, this leads to an 1.8 dB increase in  $G_c$  without instability [5].

In Fig. 12, the simulated values of the conversion gain are depicted for several values of  $V_{GS}$  and  $P_{LO}$ . It can be seen that for maximum conversion gain, the device should be biased near pinch-off ( $V_{GS} = -1.3$  V,  $V_{DS} = 3$  V) and the local oscillator power should be 13 dBm. For these values, the RF input impedance is  $Z_{in} = 7 + j15 \Omega$  and the output impedance is  $Z_{out} = 387 + j129 \Omega$ .

The most critical point of the design of a gate mixer is the difficulty of synthesizing the output network, owing to the high output impedance of the MESFET. A network with a high-impedance microstrip transmission line and a short-circuit stub was used for this purpose. The LO and RF signals were applied through a directional filter that provides LO-IF isolation. Networks which are similar to those used in the drain mixer were chosen for the other load conditions (Fig. 13).

In Fig. 14, the conversion gain and the input reflection versus frequency are presented for maximum conversion gain conditions. The mixer presents a bandwidth of 300 MHz (at  $-3$  dB) with an input reflection better than  $-10$  dB.

#### VIII. CONCLUSIONS

A design technique for MESFET mixers has been presented. The technique is implemented by means of a program, MIXAN, that uses the nonlinear/linear analysis and the conversion matrix theory. The SPICE program is called for the nonlinear time-domain analysis.

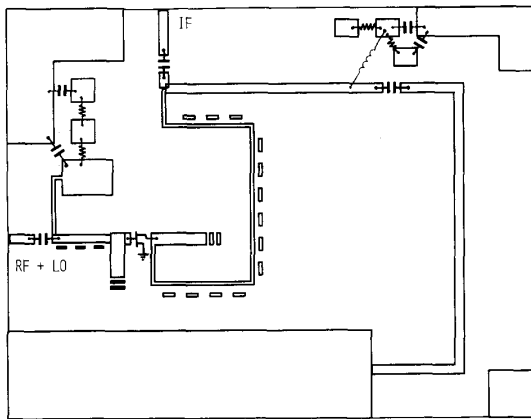


Fig. 13. Gate mixer: microstrip prototype.

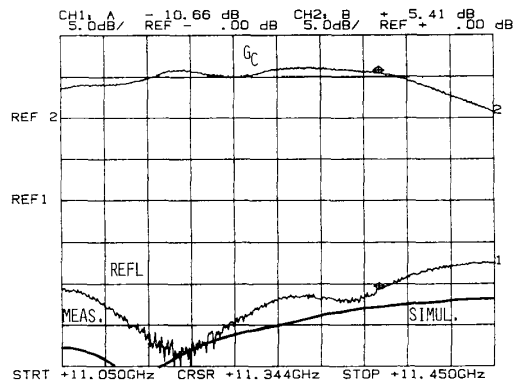


Fig. 14. Gate mixer: conversion gain and input reflection coefficient versus frequency for maximum conversion gain conditions.

The design technique starts with parameter extraction for a large-signal MESFET model (based only on dc and small-signal measurements) and with the evaluation of the influence of the embedding impedances on conversion gain and stability. This approach was then used to design X-band drain and gate mixers. Prototypes implemented in microstrip with soft substrates were mounted and measured. Predicted and experimental values, namely conversion gain, input and output reflection coefficients, and their dependence on bias conditions and LO level, were in close agreement. Although only MESFET drain gate mixers have been studied, the method can also be extended to the analysis of dual-gate and distributed MESFET mixers.

#### ACKNOWLEDGMENT

The authors are grateful to Prof. F. Pérez of E.T.S.I. Telecommunicacion of the Universidad Politecnica of Madrid for his helpful suggestions on the design of test loads and coupling networks.

#### REFERENCES

- [1] O. N. Held and A. R. Kerr, "Conversion loss and noise of microwave and millimeter-wave mixers," *IEEE Trans. Microwave Theory Tech.*, vol. MTT-26, pp. 49-55, Feb. 1978.
- [2] M. João Rosário and J. Costa Freire, "Microwave mixers analysis based on SPICE2," in *Proc. IEEE Mediterranean Electrotech. Conf.*, (Rome), 1987, pp. 337-340.
- [3] *Touchstone 1.5 User Guide*, EESof, Inc., Mar. 1987.
- [4] *PSPICE User's Guide*, MicroSim Corp., Oct. 1986.
- [5] M. João Rosário, P. Vitor, and J. Costa Freire, "Optimal CAD for microwave mixers," presented at 3rd Asia-Pacific Microwave Conf., Tokyo, Sept. 1990.
- [6] W. R. Curtice "A MESFET model for use in the design of GaAs integrated circuits," *IEEE Trans. Microwave Theory Tech.*, vol. MTT-28, pp. 448-456, May 1980.
- [7] M. João Rosário and J. Costa Freire, "Experimental characterization of MESFETs for nonlinear applications," in *Proc. Microwave and Opttronics Conf.*, (Stuttgart), April 1990, pp. 263-268.
- [8] S. A. Maas, "Theory and analysis of GaAs MESFET mixers," *IEEE Trans. Microwave Theory Tech.*, vol. MTT-32, pp. 1402-1406, Oct. 1984.
- [9] S. Egami, "Non-linear, linear analysis and computer-aided design of resistive mixers," *IEEE Trans. Microwave Theory Tech.*, vol. MTT-22, pp. 270-275, Mar. 1974.
- [10] K. C. Gupta, R. Garg, and R. Chadha, *Computer-Aided Design of Microwave Circuits*, Norwood, MA: Artech House, 1981.
- [11] P. Harrop and T. A. C. M. Clasen, "Modelling of an F.E.T. mixer," *Electron. Lett.*, vol. 14, no. 12, pp. 369-370, 1978.
- [12] C. Camacho-Péñalosa and C. S. Aitchison, "Analysis and design of MESFET gate mixers," *IEEE Trans. Microwave Theory Tech.*, vol. MTT-35, pp. 643-652, July 1987.

†

**M. João Rosário** (S'90) was born in Olhão, Portugal. She graduated from the Instituto Superior Técnico (Technical University of Lisbon) in 1978 and received the M.Sc. degree in electrical engineering there in 1986.



From 1979 to 1985 she was a Research Assistant at the Engineering Institute of Lisbon, and since October 1985 she has been a member of the teaching staff at the Electrical and Computer Engineering Department of the Instituto Superior Técnico. Since 1984 she has been engaged in research on microwave circuits at the Centro de Electrónica Aplicada of the Technical University of Lisbon, where she is currently working toward the Ph.D. degree in electrical and computer engineering. Her research interests are in the area of field-effect transistor modeling and the design of microwave mixers and filters.

‡

**J. Costa Freire** (S'81-M'84-SM'89) was born in Lisbon, Portugal. He graduated in electrical engineering in 1975 and received the Ph.D. degree in applied electronics from the Instituto Superior Técnico (Technical University of Lisbon) in 1984.



Since 1975, he has been a member of the teaching and research staff at the Electrical and Computer Engineering Department of the Instituto Superior Técnico (Research Assistant from 1975 to 1984, Assistant Professor from 1984 to 1989). Presently, he is an Associate Professor. Since 1984 he has led a research group on microwave electronics at the Centro de Electrónica Aplicada of the Technical University of Lisbon (CEAUTL). His main interests are in the areas of semiconductor device modeling and the design of nonlinear high-frequency and microwave circuits. He is currently head of CEAUTL.

Dr. Costa Freire has been an IEEE officer since 1985 at the section level, and since 1988 he has been an appointed representative to the Region 8 Committee.

# Nonlinear Models for the Intermodulation Analysis of FET Mixers

Solti Peng, *Student Member, IEEE*, Patrick J. McCleer, *Member, IEEE*, and George I. Haddad, *Fellow, IEEE*

**Abstract**—An accurate, detailed analysis program has been developed for intermodulation distortion (IMD) simulation of FET mixers. This program is very efficient at calculating the IMD from multiple RF inputs. We have proposed a simplified nonlinear model for IMD analysis of FET gate mixers. The accuracy of the simplified model has been verified experimentally using two different MESFET mixers and one HEMT mixer at *X* band. All the tests show good agreement between measured results and the calculated results for second- and third-order IMD. The simplified model is based on modeling the derivative of the device transconductance by a sum of a Gaussian function and a linear function of the gate voltage. Drain bias dependence is ignored. The advantage of this model is that it can be used for both MESFET and HEMT mixers, and its fitting parameters can be easily determined from a nonlinear characterization of the devices at low frequencies.

## I. INTRODUCTION

THE demand for a wide dynamic range in today's microwave and millimeter-wave receivers results in strict IMD performance requirements for the front-end mixers. MESFET mixers, due to their low intermodulation products and low noise, as well as the potential for conversion gain, are gaining favor over their counterparts, diode mixers, because they can be easily realized in MMIC's. In order to effectively describe the IMD performance of the FET mixers, an efficient and accurate analysis tool is required. In recent years, the harmonic balance technique [1]–[4] and Volterra series [5], [6] expansion have been widely used in the microwave nonlinear circuit simulations. Also, the general-purpose harmonic balance technique has been broadly implemented in commercial microwave nonlinear circuit simulators. Nonetheless, the IMD of FET mixers is still rarely included in the circuit simulation during the mixer design. The reasons are, since there are one large LO signal and two RF small signals occurring in the IMD analysis in mixers, the efficiency of the harmonic balance technique dramatically drops with the number of input signals, and the IMD from small signals under the presence of a large signal will be smeared out due to the numerical accuracy of computers. The Volterra series is very efficient at analyzing multiple inputs, but it is limited to moderate power inputs and not suitable for

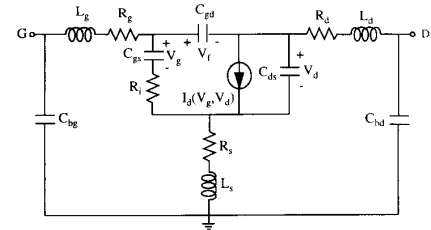


Fig. 1. FET large-signal equivalent circuit. Bonding parasitics are included.

the large signal input encountered in the mixer IMD analysis. The only way to avoid these problems is to analyze the large signal and small signals separately, using the harmonic balance technique for large-signal analysis and Volterra series for small-signal analysis. We have applied this technique to FET mixers. Our work is based on the pioneering work of Maas [7] who used this technique to calculate the two-tone IMD in diode mixers.

An accurate device circuit model is required for IMD analysis. This model must both include the nonlinear elements and account for the derivatives of functional dependence of these nonlinear elements at least up to third order [8], [9]. Most of the existing nonlinear models for FET's, however, are not in this category [10]–[13]. Two models [8], [14] consider the derivative terms, but do not include a good description of the third-order derivative. Also, the fitting of the derivatives of their models to the measured data is not intuitive. Therefore, a simple FET nonlinear model suitable for mixer IM analysis is sought.

A brief description of the analysis program is given in the next section. We apply this analysis program to study the nonlinear drain current source contribution to the overall IMD performance of MESFET mixers at *X* band. Then, we propose a nonlinear model which simplifies the derivatives fitting process, and also gives good agreement between the measured and fitted nonlinear element value and its derivatives. We then present experimental and calculated results of the IMD performance in two MESFET mixers and one HEMT mixer at *X* band.

## II. THE ANALYSIS PROGRAM

An efficient and accurate analysis program has been developed for IMD simulation of FET mixers. The technique used in this program is based on the *large-signal-small-signal*

Manuscript received April 5, 1994; revised July 18, 1994. This work was supported by the U.S. Army Research Office under the URI Program Grant DAAL03-92-G-0109.

The authors are with the Center for High Frequency Microelectronics, Solid State Electronics Laboratory, Department of Electrical Engineering and Computer Science, University of Michigan, Ann Arbor, MI 48109 USA.  
IEEE Log Number 9410324.

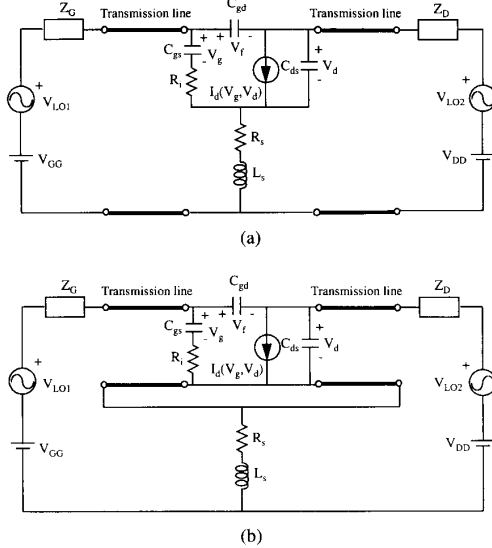


Fig. 2. (a) An intuitive FET circuit layout and (b) a modified FET circuit layout for large-signal harmonic balance analysis using the reflection algorithm.

analysis [15]. The equivalent circuit of the device used in the large signal analysis is shown in Fig. 1. The reflection algorithm [16], [17] is used for the large-signal harmonic-balance analysis to obtain the LO pumping waveforms for the voltages across the internal capacitors. This algorithm is constructed by using two ideal imaginary transmission lines, with their electrical lengths at the LO frequency equal to many half wavelengths to isolate the nonlinear device from the linear input and output circuits. The steady-state solution of the device is solved in the time domain. The voltage and current waveforms at the other end of the imaginary transmission lines are expanded into Fourier series at the LO harmonic components. In order to pursue the match of the impedance of the Fourier components to the impedance of the linear circuit at the LO harmonic frequencies, iterations are carried out by summing up the reflected waves due to the impedance mismatch until they are matched. An intuitive circuit topology [18] of this case is shown in Fig. 2(a). A drawback of this intuitive case is that the time-domain equation of the device is rather complicated. Theoretically, the imaginary transmission lines can be placed at any position in the circuit without altering the steady-state solution of the circuit. Therefore, we should keep the part of the time-domain equations as simple as possible. The best choice is to include only nonlinear elements and to move all linear elements to the other side of the imaginary transmission lines. The advantages are: saving computer running time, avoiding the possible numerical convergence problem, and the ease with which to include possible linear reactive elements without modifying the part of the time-domain equations. The new circuit topology for the large-signal analysis is shown in Fig. 2(b) which excludes the source impedance (series source resistance and source bonding inductance) from

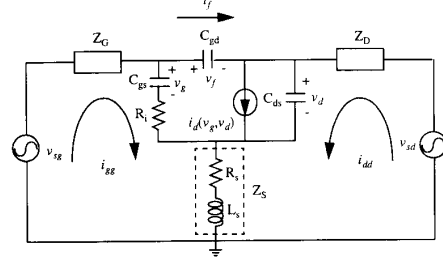


Fig. 3. The equivalent circuit for small-signal analysis.

the nonlinear part of the circuit. The capacitors \$C\_{gd}\$ and \$C\_{ds}\$, which can be treated as linear elements in the FET gate mixers, are still included in the nonlinear part of the circuit in order to increase the flexibility of the program, i.e., to include their nonlinearities, if needed. The internal voltage waveforms of \$V\_g\$, \$V\_f\$, and \$V\_d\$ are obtained by the reflection algorithm according to the new circuit topology.

The FET small-signal equivalent circuit is shown in Fig. 3. The small-signal incremental current loop equations can be written in the following matrix form:

$$\mathbf{ZI} = \mathbf{V} \quad (1)$$

where

$$\mathbf{Z} = \begin{pmatrix} Z_G + R_i + Z_S & Z_G & Z_S \\ Z_G & Z_G + Z_D & -Z_D \\ Z_S & -Z_D & Z_D + Z_S \end{pmatrix} \quad (2)$$

$$\mathbf{I} = \begin{pmatrix} i_{gg}(t) \\ i_f(t) \\ i_{dd}(t) \end{pmatrix} \quad (3)$$

$$\mathbf{V} = \begin{pmatrix} v_{sg}(t) - v_g(t) \\ v_{sg}(t) - v_{sd}(t) - v_f(t) \\ v_{sd}(t) - v_d(t) \end{pmatrix} \quad (4)$$

where \$i\_{gg}\$, \$i\_f\$, \$i\_{dd}\$ are small-signal incremental currents, \$v\_g\$, \$v\_f\$, \$v\_d\$ are small-signal incremental voltages, and \$v\_{sg}\$, \$v\_{sd}\$ are small-signal voltage sources at gate and drain, respectively.

Since the most significant nonlinear element in a MESFET gate mixer is the drain current, the nonlinear effects from the capacitors are ignored in our work. Thus, the small-signal incremental currents are

$$i_{gg} = \frac{d}{dt}(C_{gs}v_g(t)) \quad (5)$$

$$i_f = \frac{d}{dt}(C_{gd}v_f(t)) \quad (6)$$

$$i_{dd} = i_d(v_g, v_d) + \frac{d}{dt}(C_{ds}v_d(t)). \quad (7)$$

The small-signal drain current  $i_d(v_g, v_d)$ , expanded in Taylor's series up to third order, is as follows:

$$\begin{aligned} i_d(v_g, v_d) &= \frac{\partial I_d}{\partial V_g} v_g + \frac{\partial I_d}{\partial V_d} v_d + \frac{1}{2} \frac{\partial^2 I_d}{\partial V_g^2} v_g^2 \\ &\quad + \frac{\partial^2 I_d}{\partial V_g \partial V_d} v_g v_d + \frac{1}{2} \frac{\partial^2 I_d}{\partial V_d^2} v_d^2 \\ &\quad + \frac{1}{6} \frac{\partial^3 I_d}{\partial V_g^3} v_g^3 + \frac{1}{2} \frac{\partial^3 I_d}{\partial V_g^2 \partial V_d} v_g^2 v_d \\ &\quad + \frac{1}{2} \frac{\partial^3 I_d}{\partial V_g \partial V_d^2} v_g v_d^2 + \frac{1}{6} \frac{\partial^3 I_d}{\partial V_d^3} v_d^3 \\ &\equiv G_m v_g \\ &\quad + G_{ds} v_d + G_{m2} v_g^2 \\ &\quad + G_{m1d1} v_g v_d + G_{d2} v_d^2 \\ &\quad + G_{m3} v_g^3 + G_{m2d1} v_g^2 v_d + G_{m1d2} v_g v_d^2 + G_{d3} v_d^3. \end{aligned} \quad (8)$$

The time variable dependence has been dropped to shorten the notation. This small-signal drain current includes both the output conductance derivative terms ( $G_{d2}$  and  $G_{d3}$ ) and the cross-derivative terms ( $G_{m1d1}$ ,  $G_{m2d1}$ , and  $G_{m1d2}$ ) which have been ignored in most of the nonlinear analyses. We have implemented this complete model in our analysis program. A study has been carried out to theoretically examine the importance of this complete model compared with the conventional model (only  $G_m$ ,  $G_{m2}$ , and  $G_{m3}$  included) to the overall IMD performance of FET mixers. This is presented in the next section.

Due to the pump of the LO signal, all the coefficients in the Taylor's expansion are also time-varying functions. We expand the small-signal incremental voltages and limit consideration up to third order

$$v_p(t) = v_{p1}(t) + v_{p2}(t) + v_{p3}(t) \quad (9)$$

and

$$v_p^2(t) = v_{p1}^2(t) + 2v_{p1}(t)v_{p2}(t) \quad (10)$$

$$v_p^3(t) = v_{p1}^3(t) \quad (11)$$

where  $v_p$  represents  $v_g$ ,  $v_f$ , and  $v_d$ .

In order to analyze the circuit in the frequency domain, the time-varying functions due to the LO pump have to be Fourier expanded into the harmonic components of the LO frequency  $\omega_p$ . They have the form

$$G_x(t) = \sum_{h=-K}^K G_{x,h} e^{jh\omega_p t}. \quad (12)$$

In FET gate mixers, the RF signal is from the gate side, so  $v_{sd} = 0$ . The subscript  $g$  in the small-signal voltage source representing the source at the gate will be dropped. The small-signal voltage with  $Q$  input signals is

$$v_s(t) = \sum_{q=1}^Q 2V_{s,q} \cos(\omega_q t) = \sum_{\substack{q=-Q \\ q \neq 0}}^Q V_{s,q} e^{j\omega_q t} \quad (13)$$

where  $2V_{s,q}$  is the voltage peak value of the  $q$ th input signal with frequency  $\omega_q$ . Note that  $\omega_{-q}$  is equal to  $-\omega_q$ .

The Taylor's expansion of the small-signal drain current is substituted in (1), and all the time-varying functions are expanded in frequency domain. The circuit equations can then be separated into subcircuits for different orders. They have the form

$$[\mathbf{ZY} - \mathbf{1}] \mathbf{Vn} = \mathbf{Vs} \mathbf{n} \quad (14)$$

where

$$\mathbf{Y} = \begin{pmatrix} j\Omega C_{gs} & 0 & 0 \\ 0 & 0 & j\Omega C_{gd} \\ \mathbf{G}_m & 0 & \mathbf{G}_{ds} + j\Omega C_{ds} \end{pmatrix}. \quad (15)$$

$\mathbf{G}_m$  and  $\mathbf{G}_{ds}$  have the form of the conversion matrix in the conventional small-signal analysis of mixers. Note that the frequency matrix  $\Omega$  has to reflect the frequencies of different orders. The impedances in impedance matrix  $\mathbf{Z}$  also have to be evaluated at the corresponding frequencies of different orders. A short description of the subcircuits for different orders follows.

*First order* ( $n = 1$ ):

$$\mathbf{V}_1 = \begin{pmatrix} v_{g1} \\ v_{f1} \\ v_{d1} \end{pmatrix} \quad (16)$$

$$\mathbf{V}_{s1} = \begin{pmatrix} v_s \\ v_s \\ 0 \end{pmatrix}. \quad (17)$$

The first-order voltages in the frequency domain have the form

$$v_{p1}(t) = \sum_{m=-K}^K \sum_{\substack{q=-Q \\ q \neq 0}}^Q V_{p1,m,q} e^{j(m\omega_p + \omega_q)t} \quad (18)$$

which can be solved from the first-order circuit equations. The equivalent circuit for the first-order equations is shown in Fig. 4(a). After the first-order voltages are determined, the conversion gain/loss can be calculated between any two frequencies.

*Second order* ( $n = 2$ ):

$$\mathbf{V}_2 = \begin{pmatrix} v_{g2} \\ v_{f2} \\ v_{d2} \end{pmatrix} \quad (19)$$

$$\mathbf{V}_{s2} = -\mathbf{ZI}_{s2} \quad (20)$$

where

$$\mathbf{I}_{s2} = \begin{pmatrix} 0 \\ 0 \\ G_{m2} v_{g1}^2 + G_{d2} v_{d1}^2 + G_{m1d1} v_{g1} v_{d1} \end{pmatrix}. \quad (21)$$

Note that each element in matrices is a function of time. Since the first-order voltages have been solved, the second-order

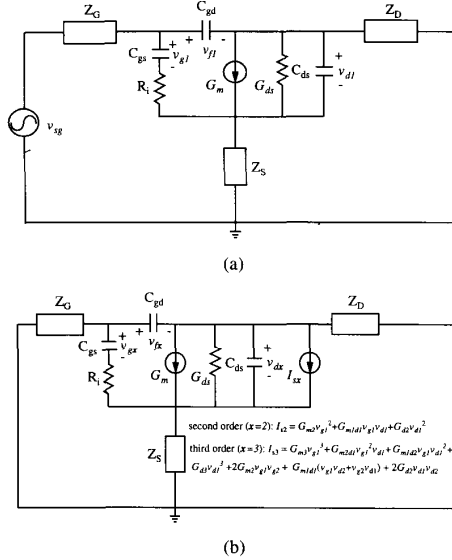


Fig. 4. (a) First-order small-signal equivalent circuit. (b) Second-order ( $x = 2$ ) and third-order ( $x = 3$ ) small-signal equivalent circuit.

nonlinear current source  $I_{s2}$  can be determined, where

$$G_{m2}(t)v_{g1}^2(t) = \sum_{h=-K}^K \sum_{m=-K}^K \sum_{n=-K}^K \sum_{\substack{q1=-Q \\ q1 \neq 0}}^Q \sum_{\substack{q2=-Q \\ q2 \neq 0}}^Q \cdot G_{m2,h} V_{g1,m,q1} V_{g1,n,q2} \cdot \exp(j[(h+m+n)\omega_p + \omega_{q1} + \omega_{q2}]t). \quad (22)$$

$G_{d2}v_{d1}^2$  and  $G_{m1d1}v_{g1}v_{d1}$  have similar forms. The second-order voltages can be written as

$$v_{p2}(t) = \sum_{m=-K}^K \sum_{\substack{q1=-Q \\ q1 \neq 0}}^Q \sum_{\substack{q2=-Q \\ q2 \neq 0}}^Q V_{p2,m,q1,q2} \cdot \exp(j(m\omega_p + \omega_{q1} + \omega_{q2})t) \quad (23)$$

which can be solved from the second-order circuit equations. The equivalent circuit for the second-order equation is shown in Fig. 4(b) (with  $x = 2$ ). Once the second-order voltages are known, the output power for any second-order distortion can be determined.

Third order ( $n = 3$ ):

$$\mathbf{V}_3 = \begin{pmatrix} v_{g3} \\ v_{f3} \\ v_{d3} \end{pmatrix} \quad (24)$$

$$\mathbf{V}_{s3} = -Z\mathbf{I}_{s3} \quad (25)$$

where

$$\mathbf{I}_{s3} = \begin{pmatrix} 0 \\ 0 \\ a+b \end{pmatrix} \quad (26)$$

with

$$a = 2G_{m2}v_{g1}v_{g2} + G_{m3}v_{g1}^3 + 2G_{d2}v_{d1}v_{d2} + G_{d3}v_{d1}^3 \quad (27)$$

$$b = G_{m1d1}(v_{g1}v_{d2} + v_{g2}v_{d1}) + G_{m2d1}v_{g1}^2v_{d1} + G_{m1d2}v_{g1}v_{d1}^2 \quad (28)$$

in which

$$\begin{aligned} & G_{m3}(t)v_{g1}^3(t) \\ &= \sum_{h=-K}^K \sum_{m=-K}^K \sum_{n=-K}^K \sum_{l=-K}^K \cdot \sum_{\substack{q1=-Q \\ q1 \neq 0}}^Q \sum_{\substack{q2=-Q \\ q2 \neq 0}}^Q \sum_{\substack{q3=-Q \\ q3 \neq 0}}^Q G_{m3,h} V_{g1,m,q1} \\ & \cdot V_{g1,n,q2} V_{g1,l,q3} \exp(j[(h+m+n+l)\omega_p \\ & + \omega_{q1} + \omega_{q2} + \omega_{q3}]t) \end{aligned} \quad (29)$$

$$\begin{aligned} & G_{m2}(t)v_{g1}(t)v_{g2}(t) \\ &= \sum_{h=-K}^K \sum_{m=-K}^K \sum_{n=-K}^K \sum_{\substack{q1=-Q \\ q1 \neq 0}}^Q \sum_{\substack{q2=-Q \\ q2 \neq 0}}^Q \sum_{\substack{q3=-Q \\ q3 \neq 0}}^Q G_{m2,h} \\ & \cdot V_{g1,m,q1} V_{g2,n,q2} V_{g2,l,q3} \exp(j[(h+m+n)\omega_p \\ & + \omega_{q1} + \omega_{q2} + \omega_{q3}]t) \end{aligned} \quad (30)$$

and the other elements can be expanded into the frequency domain accordingly. The equivalent circuit for the third-order equations is shown in Fig. 4(b) (with  $x = 3$ ).

The output power for any third-order IMD of interest can be determined from the third-order circuit equations. For instance, the frequency of the third-order IMD with two RF tones is either  $|2f_{IF2} - f_{IF1} - f_p|$  ( $q_1 = 2$ ,  $q_2 = 2$ , and  $q_3 = -1$ ) or  $|2f_{IF1} - f_{IF2} - f_p|$  ( $q_1 = 1$ ,  $q_2 = 1$ , and  $q_3 = -2$ ).

### III. NONLINEAR SOURCES IN MESFET GATE MIXERS

The most significant nonlinear element in a MESFET gate mixer is the drain current, which formally is a function of both gate ( $V_g$ ) and drain voltage ( $V_d$ ). The small-signal drain current expanded in Taylor's series up to third order has been given in (8).

Usually, the nonlinear transconductance ( $G_m$ ,  $G_{m2}$ , and  $G_{m3}$ ) is the only part of the nonlinear drain current which has been considered in the FET nonlinear applications. The influence from other terms in (8) on the overall nonlinear performance has been ignored. Recently, the authors of [8] proposed a technique to determine the values of  $G_m$ ,  $G_{m2}$ , and  $G_{m3}$  from the measurement data at low frequency (50 MHz). The authors of [19] and [20] then extended the measurement technique, and proposed a new measurement setup which is able to extract the values of all the coefficients in (8). They included all of these coefficients in their load pull IM distortion simulation. They also demonstrated that the influence from

terms other than  $G_m$ ,  $G_{m2}$ , and  $G_{m3}$  on the overall IM distortion of their load pull simulation is significant.

In order to determine the influence of all the terms in (8) on the overall IM distortion of FET gate mixers, we have carried out a simulation study using our analysis program. We have followed exactly the nonlinear characterization procedure at low frequency proposed in [19] and [20] to obtain all the coefficients in (8) for the device in our study. The sources we used for the low-frequency characterization were at 95 and 105 MHz. The device we used in this study is a MESFET fabricated in the Solid State Electronics Laboratory at the University of Michigan (the device will be denoted as SSEL in the rest of the text). This device has a gate geometry of  $0.25 \times 90 \mu\text{m}$ , a doping concentration of  $5 \times 10^{17} \text{ cm}^3$ , a 600-Å-thick channel, and a pinch-off voltage of  $-2.0 \text{ V}$ . We characterized this device at various gate and drain voltages. The gate voltage was varied from  $-3.0$  to  $0 \text{ V}$  by steps of  $0.1 \text{ V}$ . The drain voltage was varied from  $1.5$  to  $3.3 \text{ V}$  by steps of  $0.2 \text{ V}$ . The values of all the coefficients extracted from this low-frequency characterization were then numerically implemented in the analysis program discussed in Section II. Linear interpolation was used to determine the values between the measured data points. Single-tone IM of an  $X$ -band mixer with LO at  $10.8 \text{ GHz}$  and RF at  $11.1 \text{ GHz}$  was simulated for two different cases: one using all the coefficients, and the other only using the nonlinearity of the transconductance and its derivatives ( $G_m$ ,  $G_{m2}$ , and  $G_{m3}$ ). Simple  $50\Omega$  source and  $50\Omega$  load impedances were used in this study. A dc drain voltage of  $2.5 \text{ V}$  was chosen as a bias point to compare the theoretical results of this two cases. The signals at two times and three times the frequency of the IF signal, i.e.,  $600$  and  $900 \text{ MHz}$ , were the single-tone IM products at the output. In Fig. 5, we show the simulation results of these two cases for a  $4.63 \text{ dBm}$  LO power. The results show no significant difference between these two cases, which means the contributions from terms other than  $G_m$ ,  $G_{m2}$ , and  $G_{m3}$  to the overall IMD of the FET gate mixers are much smaller than those of the dominant terms,  $G_m$ ,  $G_{m2}$ , and  $G_{m3}$ . They, in effect, can be ignored.

#### IV. THE PROPOSED NONLINEAR MODEL

The essential issue of modeling the nonlinear drain current centers on how accurately the coefficients  $G_m$ ,  $G_{m2}$ , and  $G_{m3}$  can be described. A common approach is to model the drain current function itself [8], [10]–[14]. The drawback of this approach is that any error occurring in the drain current function will propagate down to all its derivatives. Most of the existing drain current models [10]–[13] did not take derivatives into consideration when they originally were proposed. Consequently, these models have an inadequate description of  $G_{m2}$  and  $G_{m3}$ , the second and third derivatives of the drain current function with respect to the gate voltage. Therefore, these models basically are not suitable for IM analysis. In order to avoid this shortcoming, we propose a direct model of the second derivative of the drain current with respect to gate voltage ( $G_{m2}$ ) instead of the drain current function, which greatly simplifies the fitting process of the

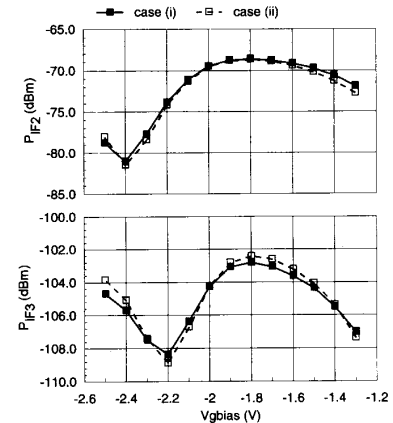


Fig. 5. Comparison of single-tone IM simulation of the SSEL MESFET gate mixer between two cases: case (i) with the full nonlinear drain current model in (8) and case (ii) with only  $G_m$ ,  $G_{m2}$ , and  $G_{m3}$  included. The mixer has a simple  $50\Omega$  source and a  $50\Omega$  load impedance.  $2.5 \text{ V}$  of the drain voltage is chosen.  $f_{LO} = 10.8 \text{ GHz}$ ,  $f_{RF} = 11.1 \text{ GHz}$ ,  $f_{IF2} = 600 \text{ MHz}$ , and  $f_{IF3} = 900 \text{ MHz}$ .  $P_{LO} = 4.63 \text{ dBm}$ , and  $P_{RF} = -20.66 \text{ dBm}$ .

model. The proposed functional dependence of the second derivative is a Gaussian function plus a linear modification term. The functions for  $G_m$  and  $G_{m3}$  are easily derived from  $G_{m2}$  by simple integration and differentiation with respect to the gate voltage. The proposed functions for  $G_m$ ,  $G_{m2}$ , and  $G_{m3}$  are as follows:

$$G_m = G'_{mx} v_{g\sigma} \sqrt{\pi} \left( 1 + \operatorname{erf} \left( \frac{v_g - v_{gp}}{v_{g\sigma}} \right) \right) + G''_{m0} (v_g - v_{g\gamma})^2 \quad (31)$$

$$G_{m2} = G'_{mx} e^{-((v_g - v_{gp})/v_{g\sigma})^2} + G''_{m0} (v_g - v_{g\gamma}) \quad (32)$$

$$G_{m3} = -\frac{2}{3} \frac{G'_{mx}}{v_{g\sigma}^2} (v_g - v_{gp}) e^{-((v_g - v_{gp})/v_{g\sigma})^2} + \frac{1}{3} G''_{m0}. \quad (33)$$

$G'_{mx}$ ,  $G''_{m0}$ ,  $v_{gp}$ ,  $v_{g\sigma}$ , and  $v_{g\gamma}$  are the fitting parameters.  $G'_{mx}$ ,  $v_{gp}$ , and  $v_{g\sigma}$ , which are the peak value, the location of the peak value, and the half-width of the Gaussian function, respectively, can be approximately determined just from the plot of data for  $G_{m2}$ . This simplifies the fitting between the model and the measurement data. All the parameters can be easily determined from a simple least-square fit to data determined from low-frequency measurements. The fitting results of  $G_m$ ,  $G_{m2}$ , and  $G_{m3}$  for the SSEL MESFET at  $V_D = 2.5 \text{ V}$  are shown in Fig. 6. The agreement between the model and the measurement data is considered excellent.

All of these fitting parameters are, strictly speaking, functions of drain voltage, but since, in the case of the gate mixer, the device is biased in the saturation region, the variation due to the drain voltage can be ignored.

Although this simplified model was originally constructed for the MESFET mixers, it can be used for HEMT mixers as well. Even though HEMT's have quite different characteristics of transconductance versus gate voltage compared to MESFET's this model also can fit  $G_m$ ,  $G_{m2}$ , and  $G_{m3}$  very well due to the extra linear function of gate voltage used in  $G_{m2}$ . The same low-frequency nonlinear characterization

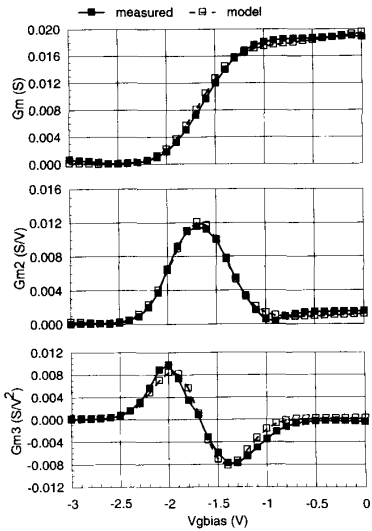


Fig. 6. Comparison of  $G_m$ ,  $G_{m2}$ , and  $G_{m3}$  between the measurement and the proposed model for the SSEL MESFET at  $V_D = 2.5$  V. The fitting parameters are:  $G'_{mx} = 0.01174$ ,  $G''_{m0} = 4.9 \times 10^4$ ,  $v_{gp} = -1.68$ ,  $v_{g\sigma} = 0.40$ , and  $v_{g\gamma} = -2.45$ .

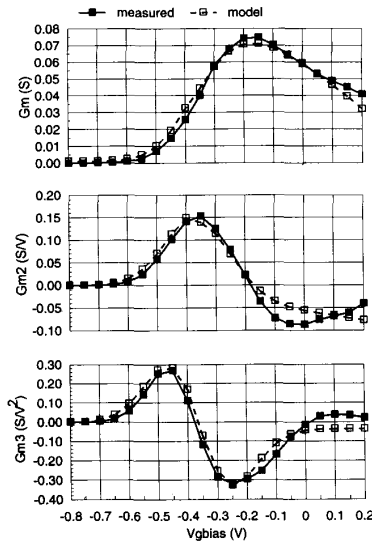


Fig. 7. Comparison of  $G_m$ ,  $G_{m2}$ , and  $G_{m3}$  between the measurement and the proposed model for the NE324 HEMT at  $V_D = 2.0$  V. The fitting parameters are:  $G'_{mx} = 0.160$ ,  $G''_{m0} = -0.105$ ,  $v_{gp} = -1.358$ ,  $v_{g\sigma} = 0.157$ , and  $v_{g\gamma} = -0.530$ .

procedure for MESFET was also applied to HEMT in order to obtain the values of  $G_m$ ,  $G_{m2}$ , and  $G_{m3}$  experimentally. The HEMT device used in this study is a commercial product from NEC, model NE324. In Fig. 7, the fitting result of the model is compared with the measurement data at  $V_D = 2.0$  V for  $G_m$ ,  $G_{m2}$ , and  $G_{m3}$ . In order to achieve better fit, the linear term in  $G_{m2}$  is only included for the gate voltage greater than  $v_{gp}$ . Good agreement between measurement and the proposed model is observed, which shows the ability of this model to fit the nonlinear transconductance of HEMT's.

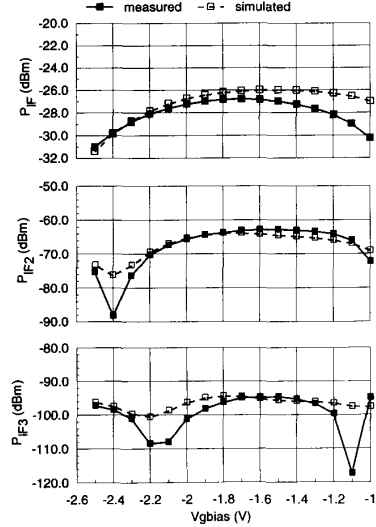


Fig. 8. Measured and calculated single-tone IM results of the SSEL MESFET gate mixer for  $V_D = 2.5$  V with a simple  $50\text{-}\Omega$  source and a  $50\text{-}\Omega$  load impedance.  $f_{LO} = 10.8$  GHz,  $f_{RF} = 11.1$  GHz,  $f_{IF1} = 300$  MHz,  $f_{IF2} = 600$  MHz, and  $f_{IF3} = 900$  MHz.  $P_{LO} = 4.63$  dBm and  $P_{RF} = -20.66$  dBm.

## V. X-BAND MIXER RESULTS

To verify the adequacy of the model for the IMD analysis of MESFET mixers, we made single-tone IM measurements on two different MESFET mixers, one using the SSEL MESFET, and the other a commercial MESFET (model NE71000 from NEC). The devices were bonded on chip carriers and measured in an  $X$ -band test fixture. The sole purpose of this measurement was to verify the validity of the proposed model. So, no matching was attempted for either input or output circuits. Both mixer circuits had a simple  $50\text{-}\Omega$  source and a  $50\text{-}\Omega$  load impedance. The LO and RF at 10.8 and 11.1 GHz, respectively, were applied to the gate and IF output at 300, 600, and 900 MHz were measured at the drain. The measured and calculated results for the SSEL MESFET mixer and the NE71000 MESFET mixer are shown in Figs. 8 and 9, respectively. In Fig. 10, we show the measured and calculated second-order and third-order output power versus RF input power for the SSEL MESFET mixer under the same bias and LO power condition as in Fig. 8. The calculated second-order and third-order intercept points ( $IP_2$  and  $IP_3$ , respectively) are also marked in the figure. All of the simulation results are obtained from the analysis program discussed in Section II. 12 harmonics of the LO frequency were chosen for all the simulations. Even though 12 harmonics were used, the simulation program required only about 1 min. of computation time for each point on a Sun/SPARC 10 workstation. Good agreement between the measured and calculated results was obtained for both mixers.

We then applied our simplified model to a two-tone IMD simulation. The two-tone IM measurement was performed on the NE71000 MESFET mixer. An additional RF source at 11.2 GHz was added to the gate of the previous setup, and the third-order IM product,  $2f_{IF2} - f_{IF1} - f_p$ , at 500 MHz was measured at the output. The results of this measurement along with the

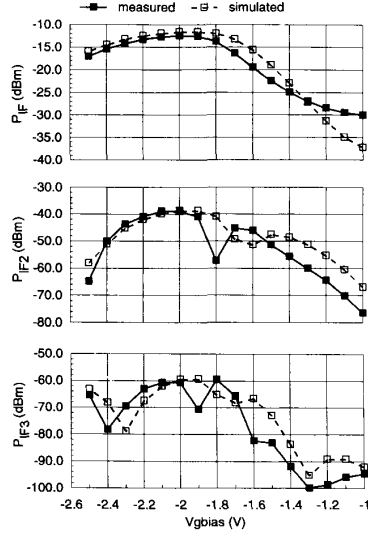


Fig. 9. Measured and calculated single-tone IM results of the NE71000 MESFET gate mixer for  $V_D = 2.7$  V with a simple  $50\Omega$  source and a  $50\Omega$  load impedance.  $f_{LO} = 10.8$  GHz,  $f_{RF1} = 11.1$  GHz,  $f_{IF} = 300$  MHz,  $f_{IF2} = 600$  MHz, and  $f_{IF3} = 900$  MHz.  $P_{LO} = 3.0$  dBm and  $P_{RF} = -10.22$  dBm.

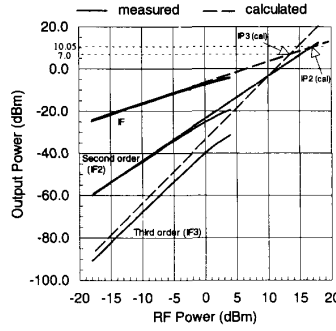


Fig. 10. Calculated single-tone  $IP_2$  and  $IP_3$  of the SSEL MESFET along with the measured data. Gate bias of  $-1.8$  V is chosen. Check Fig. 8 for the values of drain bias, LO power, and signal frequencies.

calculated results from the analysis program are shown in Fig. 11. The good agreement shown again supports the validity of the simplified model for the IM analysis of MESFET gate mixers and the accuracy of the analysis program for multitone IMD simulation.

We also made single-tone and two-tone IM measurements of a HEMT mixer at  $X$  band. The device used in the mixer measurement is the same device mentioned in Section IV. The device was bonded on the same type of chip carrier used for the MESFET's. The same measurement setup was also used.

The comparison of the calculated IF power, second- and third-order IM products for the single-tone case with the measurement results is shown in Fig. 12. The comparison for the third-order IM product for the two-tone case is shown in Fig. 13. The good agreement conforms the validity of the proposed simplified model applied to HEMT mixers.

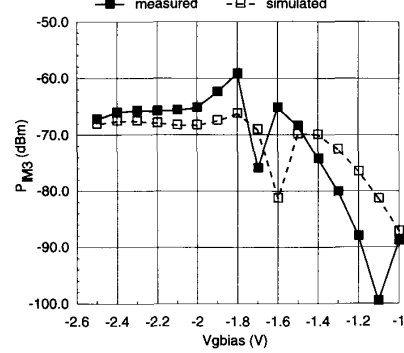


Fig. 11. Measured and calculated two-tone IM results of the NE71000 MESFET gate mixer for  $V_D = 2.7$  V with a simple  $50\Omega$  source and a  $50\Omega$  load impedance.  $f_{LO} = 10.8$  GHz,  $f_{RF1} = 11.1$  GHz,  $f_{RF2} = 11.2$  GHz, and  $f_{IM3} = 500$  MHz.  $P_{LO} = 3.0$  dBm,  $P_{RF1} = -17.0$  dBm, and  $P_{RF2} = -11.0$  dBm.

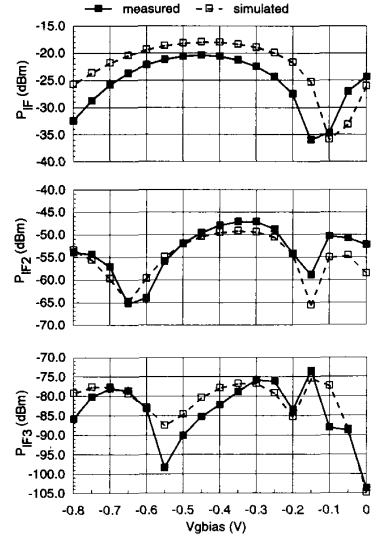


Fig. 12. Measured and calculated single-tone IM results of the NE324 HEMT gate mixer for  $V_D = 2.0$  V with a simple  $50\Omega$  source and a  $50\Omega$  load impedance.  $f_{LO} = 10.8$  GHz,  $f_{RF} = 11.1$  GHz,  $f_{IF} = 300$  MHz,  $f_{IF2} = 600$  MHz, and  $f_{IF3} = 900$  MHz.  $P_{LO} = -2.0$  dBm and  $P_{RF} = -21.67$  dBm.

## VI. CONCLUSION

An efficient and accurate analysis program has been developed for the IM simulation of FET mixers. The technique used in this program is based on the *large-signal-small-signal analysis*. This program can avoid the common problem encountered in the commercial microwave circuit simulators (e.g., LIBRA) for the IM analysis of mixers. Since these simulators use the general-purpose harmonic balance technique to analyze the LO and RF signals simultaneously, the third-order IM distortion from the much smaller RF signals, compared to the LO signal, will be smeared out by the large LO signal through the discrete Fourier transform due to the roundoff error of the computer. Even though multitone excitations are available in these simulators, the computer running time will

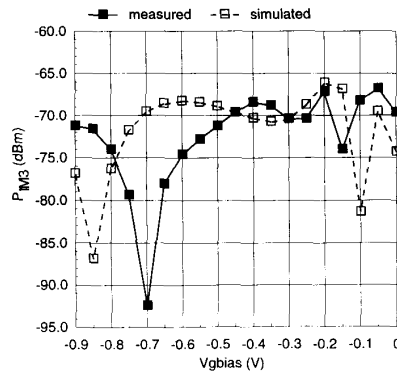


Fig. 13. Measured and calculated two-tone IM results for the NE324 HEMT gate mixer for  $V_D = 2.0$  V with a simple  $50\Omega$  source and a  $50\Omega$  load impedance.  $f_{LO} = 10.8$  GHz,  $f_{RF1} = 11.1$  GHz,  $f_{RF2} = 11.2$  GHz, and  $f_{IM3} = 500$  MHz.  $P_{LO} = -2.0$  dBm,  $P_{RF1} = -21.67$  dBm, and  $P_{RF2} = -22.70$  dBm.

be dramatically increased with the number of excitations. This makes the IM analysis of mixers almost impractical using these simulators.

A detailed study was carried out to examine the influence on the IM distortion of the MESFET gate mixers from the nonlinear factors in the drain current other than the nonlinearity of the transconductance with respect to gate voltage. The study shows that the influence is small, and the nonlinear transconductance alone is adequate to describe the IM distortion in the FET gate mixers. Then, a simplified nonlinear model for the transconductance was proposed. This model uses the sum of a Gaussian function and a linear function of gate voltage for the derivative of the transconductance ( $G_{m2}$ ). The fitting parameters of the model can be easily determined by an intuitive examination from the low-frequency characterization of the transconductance nonlinearity and a simple least square fit. The calculated results from this model are in good agreement with experimental data. The accuracy of the model for the IM analysis of FET mixers has been verified experimentally by two different MESFET mixers and one HEMT mixer at X band. The good agreement between the measurement and simulation shows the validity of the model for both MESFET and HEMT mixers.

#### ACKNOWLEDGMENT

The authors thank K. Moore for fabricating the SSEL MESFET's and C.-Y. Chi for device bonding.

#### REFERENCES

- [1] A. Ushida and L. Chua, "Frequency-domain analysis of nonlinear circuits driven by multitone signals," *IEEE Trans. Circuits Syst.*, vol. CAS-31, pp. 766-778, Sept. 1984.
- [2] R. Gilmore, "Nonlinear circuit design using the modified harmonic balance algorithm," *IEEE Trans. Microwave Theory Tech.*, vol. MTT-34, pp. 1294-1307, Dec. 1986.
- [3] W. R. Curtice, "Nonlinear analysis of GaAs MESFET amplifiers, mixers, and distributed amplifiers using the harmonic balance technique," *IEEE Trans. Microwave Theory Tech.*, vol. MTT-35, pp. 441-447, May 1987.
- [4] C. C. Pénalosa and C. S. Aitchison, "Analysis and design of MESFET gate mixers," *IEEE Trans. Microwave Theory Tech.*, vol. MTT-35, pp. 643-652, July 1987.
- [5] J. J. Bussgang, L. Ehrman, and J. W. Graham, "Analysis of nonlinear systems with multiple inputs," *Proc. IEEE*, vol. 62, pp. 1088-1119, Aug. 1974.
- [6] R. A. Minasian, "Volterra series analysis of MESFET mixers," *Int. J. Electron.*, vol. 50, no. 3, pp. 215-219, 1981.
- [7] S. A. Maas, "Two-tone intermodulation in diode mixers," *IEEE Trans. Microwave Theory Tech.*, vol. MTT-35, pp. 307-314, Mar. 1987.
- [8] S. A. Maas and D. Neilson, "Modeling MESFET's for intermodulation analysis of mixers and amplifiers," *IEEE Trans. Microwave Theory Tech.*, vol. 38, pp. 1964-1971, Dec. 1990.
- [9] S. A. Maas, "How to model intermodulation distortion," in *IEEE MTT Symp. Dig.*, 1991, pp. 149-151.
- [10] W. R. Curtice, "A MESFET model for use in the design of GaAs integrated circuits," *IEEE Trans. Microwave Theory Tech.*, vol. MTT-28, pp. 448-456, May 1980.
- [11] W. R. Curtice and M. Ettenberg, "A nonlinear GaAs FET model for use in the design of output circuits for power amplifiers," *IEEE Trans. Microwave Theory Tech.*, vol. MTT-33, pp. 1383-1394, Dec. 1985.
- [12] A. Materka and T. Kacprzak, "Computer calculation of large-signal GaAs FET amplifier characteristics," *IEEE Trans. Microwave Theory Tech.*, vol. MTT-33, pp. 129-135, Feb. 1985.
- [13] H. Statz, P. Newman, I. Smith, R. Pucel, and H. Haus, "GaAs FET device and circuit simulation in SPICE," *IEEE Trans. Electron Dev.*, vol. ED-34, pp. 160-169, Feb. 1987.
- [14] I. Angelov, H. Zirath, and N. Rorsman, "A new empirical nonlinear model for HEMT and MESFET devices," *IEEE Trans. Microwave Theory Tech.*, vol. 40, pp. 2258-2266, Dec. 1992.
- [15] S. A. Maas, *Nonlinear Microwave Circuits*. Norwood, MA: Artech House, 1988.
- [16] A. R. Kerr, "A technique for determining the local oscillator waveforms in a microwave mixer," *IEEE Trans. Microwave Theory Tech.*, vol. MTT-23, pp. 828-831, Oct. 1975.
- [17] P. H. Siegel and A. R. Kerr, "A user oriented computer program for the analysis of microwave mixers, and a study of the effects of the series inductance and diode capacitance on the performance on the performance of some simple mixers," NASA Tech. Memo. 80324, NASA Goddard Space Flight Center, Greenbelt, MD, July 1979.
- [18] S. A. Maas, *Microwave Mixers*, 1st ed. Norwood, MA: Artech House, 1985.
- [19] J. C. Pedro and J. Perez, "An improved MESFET model for prediction of intermodulation load-pull characterization," in *IEEE MTT-S Dig.*, 1992, pp. 825-828.
- [20] ———, "Accurate simulation of GaAs MESFET's intermodulation distortion using a new drain-source current model," *IEEE Trans. Microwave Theory Tech.*, vol. 42, pp. 25-33, Jan. 1994.



**Solti Peng** (S'90) was born in Kaohsung, Taiwan, on February 3, 1964. He received the B.S. degree in physics from the National Cheng-Kung University, Taiwan, in 1984, and the M.S. degree in electrical engineering from the University of Michigan, Ann Arbor, in 1990.

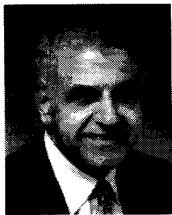
Since then, he has been working toward the Ph.D. degree in the Department of Electrical Engineering at the University of Michigan.



**Patrick J. McCleer** (S'67-M'69-S'71-M'71-S'75-S'78-M'78) received the B.S. degree from the University of Michigan, Ann Arbor, in 1969, the M.S. degree from M.I.T., Cambridge, in 1972, and the Ph.D. degree, also from the University of Michigan, in 1978, all in electrical engineering.

He is President of McCleer Power, Inc., a small firm in Jackson, MI, which specializes in research and development, and prototype fabrication of power electronic system and electrical machines. He is also a part time associate research scientist in the Department of Electrical Engineering, University of Michigan.

Dr. McCleer is a Registered Professional Engineer in the State of Michigan.



**George I. Haddad** (S'57-M'61-SM'66-F'72) received the B.S.E., M.S.E., and Ph.D. degrees in electrical engineering from the University of Michigan, Ann Arbor.

From 1957-1958 he was associated with the Engineering Research Institute of the University of Michigan, where he was engaged in research on electromagnetic accelerators. In 1958 he joined the Electron Physics Laboratory, where he was engaged in research on masers, parametric amplifiers, detectors, and electron-beam devices. From 1960-1969 he served successively as instructor, assistant professor, associate professor, and professor in the Electrical Engineering Department. He served as Director of the Electron Physics Laboratory from 1968-1975. From 1975-1987 he served as Chairman of the Department of Electrical Engineering and Computer Science. From 1987-1990 he was Director of both the Solid-State Electronics Laboratory and the Center for High-Frequency Microelectronics. He is currently the Robert J. Hiller Professor and Chairman of the Electrical Engineering and Computer Science Department and Director of the Center for High Frequency Microelectronics. His current research areas are microwave and millimeter-wave solid-state devices and monolithic integrated circuits, microwave-optical interactions, and optoelectronic devices and integrated circuits.

Dr. Haddad received the 1970 Curtis W. McGraw Research Award of the American Society for Engineering Education for outstanding achievements by an engineering teacher, the College of Engineering Excellence in Research Award (1985), the Distinguished Faculty Achievement Award (1986) of the University of Michigan, and the S. S. Attwood Award of the College of Engineering for Outstanding Contributions to Engineering Education, Research, and Administration. He is a member of Eta Kappa Nu, Sigma Xi, Phi Kappa Phi, Tau Beta Pi, and American Society for Engineering Education, and the American Physical Society. He is a member of the National Academy of Engineering.

# Resistive HEMT Mixers for 60-GHz Broad-Band Telecommunication

Mikko Varonen, Mikko Kärkkäinen, Jan Riska, Pekka Kangaslahti, *Member, IEEE*, and Kari A. I. Halonen, *Member, IEEE*

**Abstract**—We report two resistive mixers, i.e., a balanced and a balanced image-rejection (IR) mixer for the 60-GHz frequency range. A compact and wide-band method for the local-oscillator (LO) power division is presented. The 56-GHz LO signal, which propagates in a coplanar-waveguide mode, is divided in between the lines of two spiral baluns. Consequently, a smooth and compact transition from even-to-odd propagation mode and an in-phase power division for two singly balanced unit mixers is achieved. As a result, the developed IR mixer occupies only  $1.41\text{mm}^2$  of chip area. The balanced design achieved 11.5 dB of conversion loss from 57 to 67 GHz with a fixed IF of 5.3 GHz. The corresponding LO suppression was better than 34 dB with 8 dBm of LO power. The IR mixer achieved better than 19 dB of IR ratio and better than 36 dB of LO suppression for an RF frequency from 57 to 66 GHz. The corresponding conversion loss varies from 13 to 16 dB. The measured 1-dB compression point of the IR mixer was at a  $-13\text{dBm}$  output power level and the third-order intercept point was at a  $4\text{dBm}$  level.

**Index Terms**—Baluns, MIMICs, resistive mixers.

## I. INTRODUCTION

THE possibilities open to the 60-GHz frequency band are interesting because of the wide bandwidth that has been allocated globally for wireless networks; 5 GHz of spectral space has been assigned for multimedia services around 60 GHz with a global overlap of 3 GHz starting from 59 GHz and extending up to 62 GHz [1], [2].

For millimeter-wave communication systems, low-cost, reliable, and high-performance circuits are required. The mixer is one of the key components in a millimeter-wave transceiver. In a receiver or transmitter, the problem with the image frequency that comes up in the mixing process must be solved. If there is no image rejection (IR) present in the receiver, noise, and possible interference from the image band will degrade the overall performance of the receiver. In the case of the transmitter, the image frequency or, alternatively, the mirror frequency, may double the

power at the input of the power amplifier if it is not sufficiently suppressed. If a single-chip transmitter or receiver is to be developed, the filter has to be integrated on-chip. A compact sub-harmonic mixer integrated with an IR filter has been reported in [3]. However, it has a relative narrow passband at 60 GHz. Generally, the filter response determines the available local oscillator (LO) tuning range and prevents the overlapping of the desired RF and image bands. In addition, if the IF is low, the image band is close to the RF band, which makes the filter design more problematic. Therefore, the IR mixer configuration seems to be an appealing topology. Furthermore, by using a balanced design, we can suppress the LO leakage and spurious signals as well as reduce AM LO noise.

The field-effect transistor (FET) resistive mixer was first described in [4] and a balanced version was reported in [5]. Recently, a number of resistive mixers have been reported at V-band [6]–[10]. The advantages of the resistive FET mixer are very low distortion, low  $1/f$  noise, stability, no shot noise, and, in practice, no dc power consumption. Additionally, the resistive mixer can operate with relatively low LO power levels [11].

The aim of this paper is to present broad-band monolithic-microwave integrated-circuit (MMIC) mixers that operate without filters. This enables a wide-band LO tuning range. The prototype balanced mixer was reported in [12]; here, we present the design in detail and new broad-band measurement results. The excellent results of the prototype mixer encouraged us to develop a small-size high-performance mixer that provides both high IR and LO suppression without filters. We also demonstrate how to employ spiral transmission-line baluns at V-band. We present a wide-band and compact method for the transition from even to odd mode and in-phase LO power division for the mixer. This resulted in a small chip area of  $1.41\text{ mm}^2$  for the balanced IR mixer. The mixers were fabricated using a commercial pseudomorphic high electron-mobility transistor (pHEMT) technology from OMMIC, France.

Some of the essential design issues concerning resistive mixers are discussed in the beginning of Section II following the detailed design of the balanced prototype and IR mixers. The measurement setup for up-conversion measurements and the measurement results are presented in Section III. Finally, we present conclusions in Section IV.

## II. MIXER DESIGN

In a resistive FET mixer, the transistor is operated in its linear ohmic region, where the LO of the mixer is applied to the gate. The IF (or RF) is applied to the drain and, consequently, the

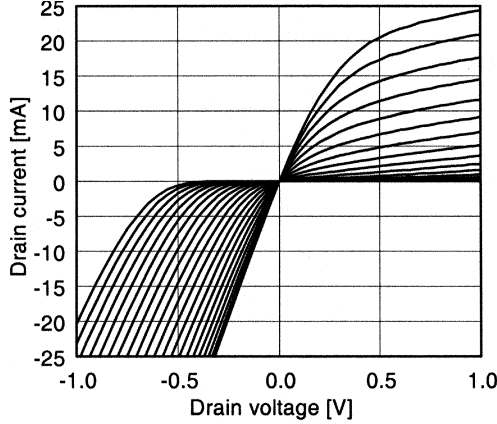
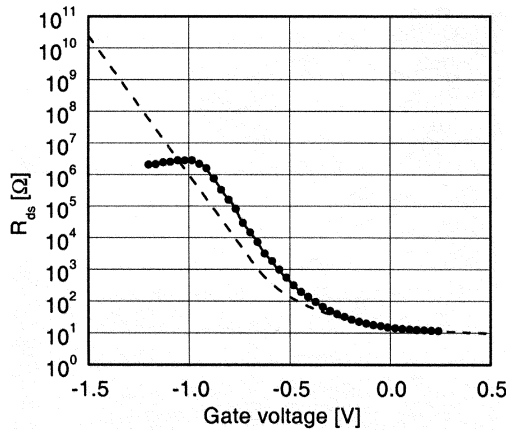
Manuscript received June 7, 2004; revised September 1, 2004. This work was supported by the Academy of Finland under the Millimono Project, by the Finnish Technology Development Centre, by Nokia Networks, by the Nokia Research Center, and by Ylinen Electronics.

M. Varonen, M. Kärkkäinen, and K. A. I. Halonen are with the Electronic Circuit Design Laboratory, Helsinki University of Technology, FI-02150 Espoo, Finland (e-mail: mva@ecdl.hut.fi).

J. Riska was with the Electronic Circuit Design Laboratory, Helsinki University of Technology, FI-02150 Espoo, Finland. He is now with Freescale Semiconductor, FI-02150 Espoo, Finland.

P. Kangaslahti was with the Electronic Circuit Design Laboratory, Helsinki University of Technology, FI-02150 Espoo, Finland. He is now with the Microwave Systems Section, Observational Systems Division, Jet Propulsion Laboratory, Pasadena, CA 91109 USA.

Digital Object Identifier 10.1109/TMTT.2005.845764

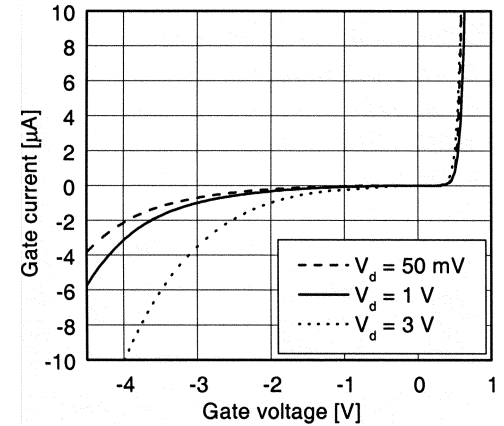
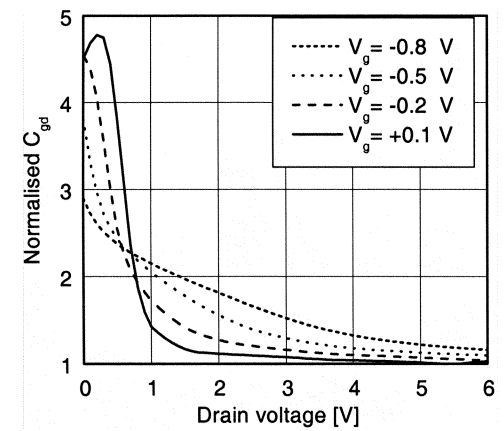
Fig. 1. Measured *IV* curves of a  $2 \times 50 \mu\text{m}$  HEMT.Fig. 2. Measured and simulated (dashed line) drain-to-source resistance of a  $2 \times 50 \mu\text{m}$  HEMT as a function of gate-to-source voltage ( $V_d = 50 \text{ mV}$ ).

RF (or IF) is filtered from the drain. No drain dc-bias voltage is applied to the transistor. The LO of the mixer is used to modulate the channel resistance of an HEMT. The measured *IV* curves of a  $2 \times 50 \mu\text{m}$  high electron-mobility transistor (HEMT) are shown in Fig. 1. The gate voltage  $V_g$  is swept from  $-1.0$  to  $0 \text{ V}$  in  $0.05\text{-V}$  steps. The channel resistance  $R_{\text{ch}}$  can be found from

$$R_{\text{ch}} = \frac{\partial V_d}{\partial I_d} \quad (1)$$

where  $V_d$  and  $I_d$  are the drain voltage and current, respectively. The measured and simulated drain-to-source resistance  $R_{\text{ds}}$  of a  $2 \times 50 \mu\text{m}$  HEMT is shown in Fig. 2. The measured gate current as a function of gate voltage is presented in Fig. 3. The minimum channel resistance is around  $1 \Omega \cdot \text{mm}$ . The measured  $R_{\text{ds}}$  saturates when the control voltage is set below  $-1 \text{ V}$ . This is due to gate-leakage effects. The required drive level can be reduced if the gate is biased toward pinchoff. It can be seen that the appropriate gate bias of the device is around  $-0.5 \text{ V}$ .

Since the drain of the transistor is unbiased, the gate-to-drain capacitance  $C_{\text{gd}}$  is greater than it would be if the drain were biased to the saturation region. This is shown in Fig. 4, where simulated normalized gate-to-drain capacitance as a function of the drain voltage for different gate bias voltages is shown. To prevent the LO from pumping the drain conductance, the RF- and IF-matching circuits have to be designed to short circuit the

Fig. 3. Measured gate current of a  $2 \times 50 \mu\text{m}$  HEMT as a function of gate voltage for different drain voltages.Fig. 4. Normalized gate-to-drain capacitance  $C_{\text{gd}}$  as a function of drain voltage for different gate bias voltages. The  $C_{\text{gd}}$  is normalized to open channel capacitance.

drain at LO frequency. A wide-band LO short can be realized by using a balanced design. Just as the LO couples through the gate-to-drain capacitance to the drain, so can the RF signal leak to the gate through this capacitance. However, it has been shown that the RF leakage is not a critical design factor [11].

#### A. Singly Balanced Resistive Mixer

The simplified circuit of the singly balanced resistive mixer is shown in Fig. 5. The LO is applied to a balun to generate the required  $180^\circ$  phase shift at the transistor gates. The drains are connected together through small valued metal-insulator-metal (MIM) capacitors. The connection point of the two drains is a virtual ground for the LO. In order to obtain the desired balanced mixing operation, the IF currents in the drains are out-of-phase and, thus, an external (off-chip) output balun or a hybrid must be used to combine them.

The circuit was designed using a  $0.25\text{-}\mu\text{m}$  pHEMT process and coplanar waveguides (CPWs). In this design, the CPW technology was chosen because the grounding of the transistor sources is easy while the drains are kept close together. By employing this method, we can obtain a good virtual ground for the LO at the output.

The gatewidth of the pHEMTs was chosen to be  $2 \times 35 \mu\text{m}$  in order to achieve good impedance matching at the RF port.

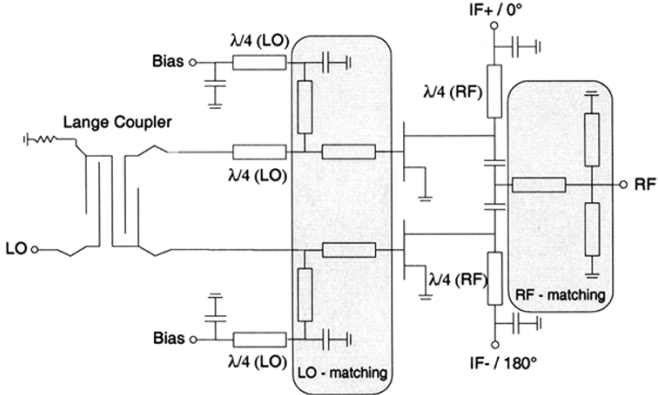


Fig. 5. Simplified schematic of the singly balanced resistive mixer. The IF+ and IF- ports are connected to an off-chip IF hybrid. The capacitors are short circuits at RF frequency and open circuits at IF frequency. A Lange coupler together with a  $\lambda/4$  transmission line is used to generate the out-of-phase LO signal at the gate of the transistors.

The RF port is matched with a symmetrical short-circuited shunt stub. Due to the symmetry and the  $180^\circ$  phase shift between the IF lines, any low-frequency disturbance coupled from the RF line will cancel out when they are combined in the off-chip balun.

The transistor gates are matched with short-circuited shunt stubs to  $50\ \Omega$ . A Lange coupler with 3-dB coupling in a microstrip configuration together with a  $\lambda/4$ -length CPW line were designed to realize the  $180^\circ$  phase shift of the LO signals at the transistor gates. In order to make the Lange coupler operate in microstrip mode, a gap of  $75\ \mu\text{m}$  to the ground-plane metallization was used.

A photograph of the fabricated singly balanced resistive mixer is shown in Fig. 6. The unwanted slotline mode is suppressed by placing air bridges around discontinuities [13]. Due to the relatively thin substrate and limited ground-plane width, the parasitic microstrip mode can be present. Vias are used for connecting the surface ground planes to zero potential to further reduce the possibility of propagating unwanted modes [14].

### B. Balanced Resistive IR Mixer

The design principle of the developed balanced resistive IR mixer is presented in Fig. 7. An off-chip differential  $90^\circ$  divider is used for the IF signal. The unit mixers are fed with in-phased LO signals, whereas the IF signal is applied  $90^\circ$  out-of-phase. The desired upper sideband (USB) RF signals from the unit mixers are combined in-phase by the Lange coupler. The undesired lower sideband (LSB) signals are combined out-of-phase and cancelled out. The nominal LO and IF frequencies are 56.0 and 5.3 GHz, respectively. The desired RF frequency (USB) is 61.3 GHz.

The simplified schematic of the unit mixer is shown in Fig. 8. The singly balanced resistive unit mixer consists of two  $2 \times 50\ \mu\text{m}$  pHEMTs. The LO is applied from the CPW to a spiral transmission-line balun to generate the required  $180^\circ$  phase shift at the transistor gates. The drains are connected together through small MIM capacitors. The connection point is a virtual ground for the LO and an open circuit for the IF. In order to obtain the desired balanced mixing operation, the IF

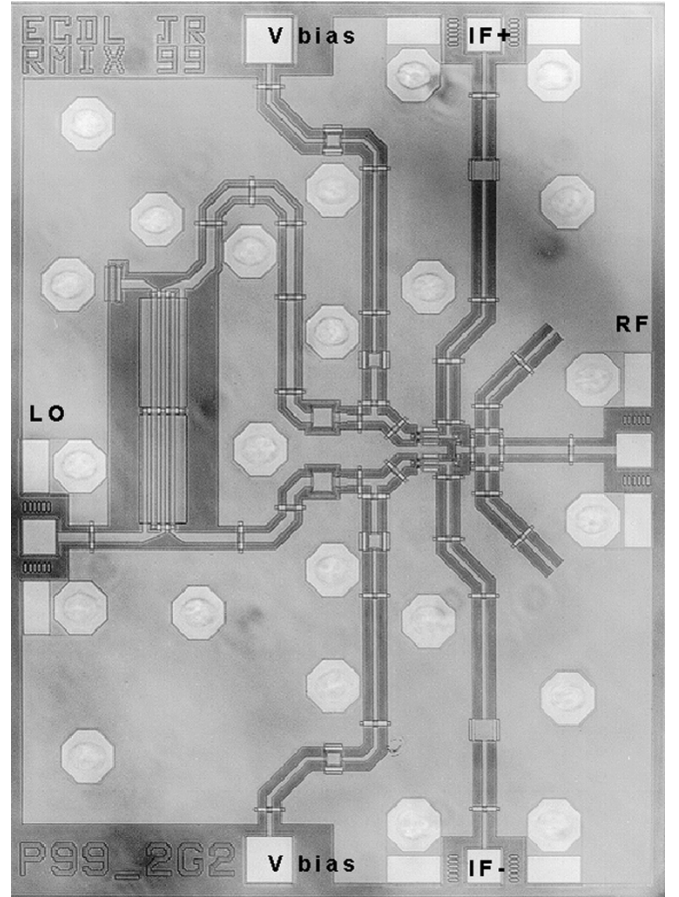


Fig. 6. Fabricated balanced resistive mixer (chip size:  $1.5\ \text{mm} \times 2.0\ \text{mm}$ ) from [12].

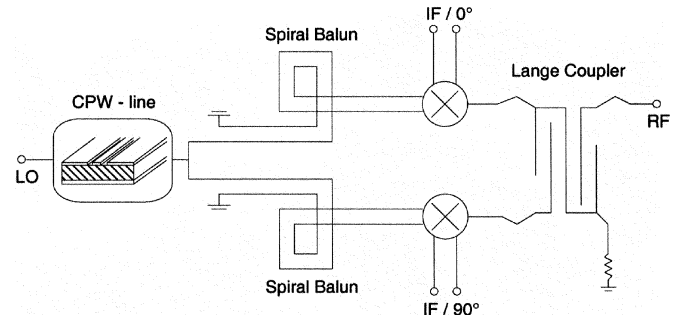


Fig. 7. Configuration of the balanced IR mixer.

signals are applied  $180^\circ$  out-of-phase to the drains. An off-chip hybrid is used for combining them. At RF frequency, the IF line is a quarter-wavelength short-circuited stub, which isolates the IF circuitry from the RF output. The RF short circuit is formed with a ground via-hole and a small valued capacitor.

The spiral transmission-line transformer is a compact and wide-bandwidth balun. The use of the spiral transmission-line transformers have been shown to be a successful solution in microwave mixer circuits [15]. We have demonstrated millimeter-wave frequency-doubler circuits using compact-size spiral baluns [16] and now apply these baluns in a V-band mixer.

The power division and the required  $180^\circ$  phase shift at the gates of the mixing devices are obtained by using two transmis-

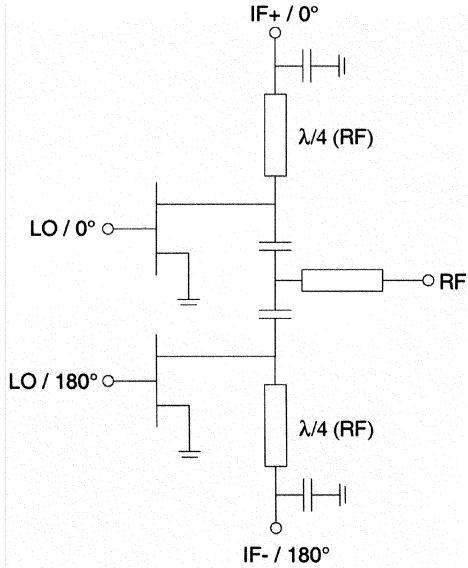


Fig. 8. Realization of the singly balanced unit mixer. The IF+ and IF- ports are connected to an off-chip IF hybrid. The capacitors are short circuits at RF frequency and open circuits at IF frequency.

sion-line baluns connected to CPW LO input. The LO signal propagates on-chip between the CPW slots. The propagating LO is smoothly divided in between the two lines of the spirals. For the signal to propagate in the odd mode, the balun has to rectify the even-mode propagation, which means that the even-mode impedance has to be several times higher than the odd-mode impedance. The even-mode impedance can be increased by wrapping the transmission-line balun in a spiral, as discussed in [15]. The spiral has a minimal effect on the odd-mode impedance. The number of turns of the spiral is limited by the parasitic capacitance, which may result in undesired resonances. This has to be taken into account, particularly at millimeter-wave frequencies. Therefore, we designed the spiral transformers to have one compact turn in order to minimize the parasitic capacitance.

The differential mode propagates in between the two lines of the spiral, thus, the characteristic impedance for these coupled lines should match the input impedance  $Z_0$  of the circuit to the resistive impedances  $Z_{in}$  of the matched HEMTs. The circuit is properly matched provided that the electrical length of the coupled lines in the odd mode is  $\lambda/4$  at the design frequency and the odd-mode impedance of the quarter-wave transformer  $Z_{odd}$  is

$$Z_{odd} = \sqrt{2Z_{in}Z_0}. \quad (2)$$

Since the exact values of even-mode and odd-mode impedances are not extremely critical, the analysis can be divided into two parts, as shown in Fig. 9. The even-mode impedance was calculated from the equivalent circuit of a characterized spiral inductor in which the lines of the balun are joined, and the odd-mode impedance and effective permittivity were calculated using finite-difference electromagnetic (EM) software for the coupled balun.

The connection of the CPW LO input and spiral baluns can be seen in Fig. 10, where a photograph of the test structure on

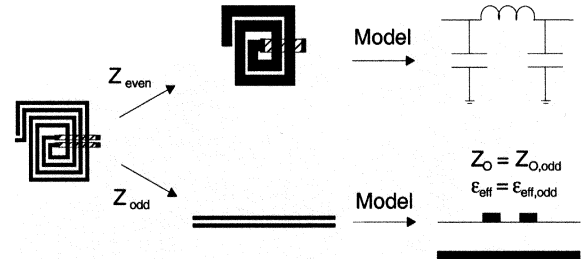


Fig. 9. Simulation of the spiral balun is divided to the characterization of the even-mode impedance  $Z_{even}$  with a spiral inductor and the EM analysis of the odd-mode impedance  $Z_{odd}$  by calculating the odd-mode properties of a straight section of coupled lines.

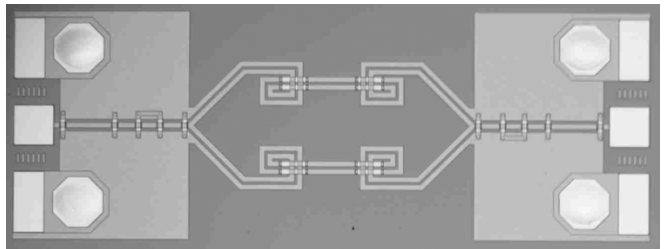


Fig. 10. Test structure on a microchip for the balun and power division of the balanced IR mixer.

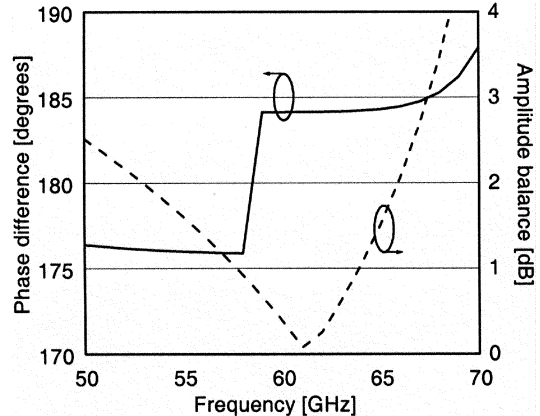


Fig. 11. Simulated phase difference and amplitude balance of the LO balun. The phase difference is  $180^\circ \pm 4^\circ$  from 50 to 65 GHz. The amplitude balance is 1.4 dB at 56 GHz.

a microchip is presented. The test structure includes the implementation of the in-phase power division and the transition from even to odd mode for the balanced IR mixer design. In the structure, the divided signal is converted back to CPW mode to easily measure the performance of the even- to odd-mode transition and the power division with coplanar RF probes. The width of the transmission lines of the balun are  $10 \mu\text{m}$  and the lines are separated by a  $5-\mu\text{m}$  gap.

The phase and amplitude balances of the LO power division circuit were simulated using finite-difference EM software; the results are shown in Fig. 11.

The measured and simulated scattering parameters of the test structure at V-band are shown in Fig. 12. The measurement indicates that the power division and the balun are realized successfully and there are no undesired resonances within the LO-frequency range.

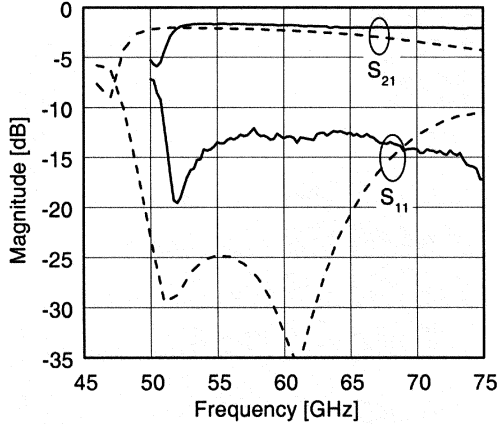


Fig. 12. Measured and simulated back-to-back response of the balun test structure. The dashed lines represent simulated values. The measured insertion loss of the test structure is 2 dB from 52 to 75 GHz.

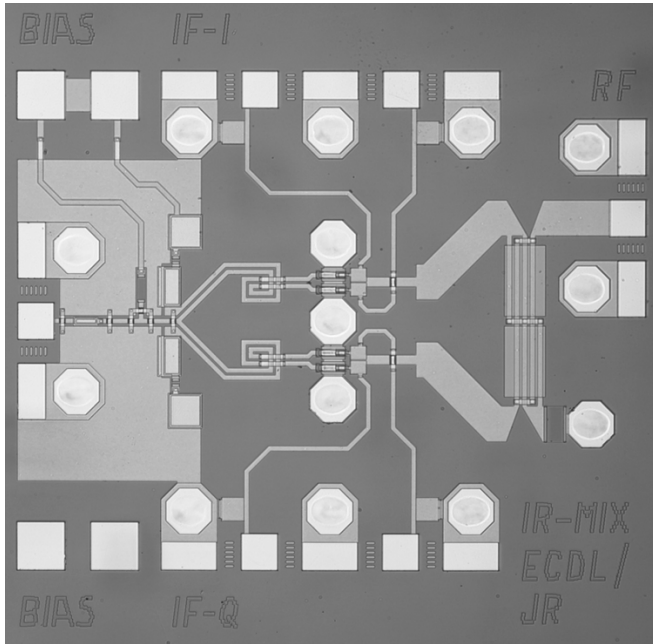


Fig. 13. Manufactured balanced IR mixer. The chip size is 1.5 mm  $\times$  1.5 mm. The mixer circuit fits within a 1.41-mm<sup>2</sup> area on chip.

A photograph of the balanced resistive IR mixer is presented in Fig. 13. The microchip was fabricated using a commercially available 0.15- $\mu$ m GaAs pHEMT process. The chip size is 1.5 mm  $\times$  1.5 mm, but the occupied chip area is only 1.41 mm<sup>2</sup> on a standard chip in multiuser processing.

### III. MEASURED MIXER PERFORMANCE

The measurement setup for the on-wafer measurements of the balanced resistive IR mixer is shown in Fig. 14. The same setup was used when the singly balanced mixer was measured. A 180° IF hybrid was used instead of differential 90° divider in the singly balanced mixer measurement setup. Since only one millimeter-wave frequency source was available for making the measurements, the mixer was measured in the up-conversion configuration. The required LO power was generated by multiplying the signal generator signal using a V-band quadrupler.

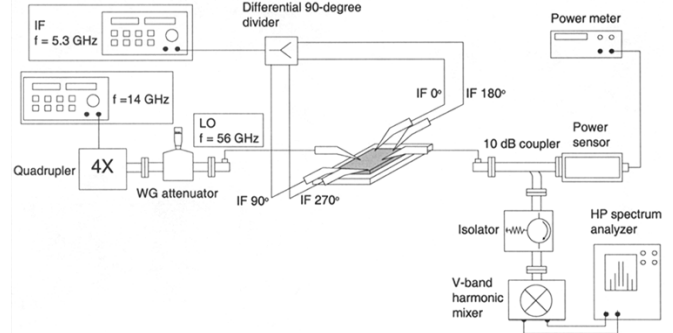


Fig. 14. Measurement setup for the balanced resistive IR mixer. The LO power was generated by multiplying the signal from the generator using a V-band quadrupler. An off-chip differential 90° divider was used for the IF signal. The RF spectrum is measured at the output with a spectrum analyzer. The bias (not shown) is brought to the chip with a dc probe.

The waveguide attenuator is used for power adjustment. The LO power was delivered to the chip using coplanar RF probes. The maximum output power of the quadrupler was approximately 10 dBm and the maximum LO power delivered to the chip was around 8 dBm.

An off-chip differential 90° divider was used for the IF signal. For test purposes, an external IF divider was fabricated on an FR4 substrate. The phase splitter consists of two 90° branch-line couplers and a 180° microstrip rat-race hybrid. The measured back-to-back attenuation of the hybrid was around 11 dB. The amplitude and phase imbalances of the splitter were 0.2 dB and 3.7° at 5.3 GHz, respectively. The loss of the external IF hybrid was subtracted from the measurement results. The output signal of the mixer was down-converted using an external V-band harmonic mixer and the RF spectrum was measured with a spectrum analyzer.

#### A. Measurement Results of the Singly Balanced Resistive Mixer

The mixer was measured as an up-converter having nominal 5.3-GHz IF frequency and 56-GHz LO frequency. Thus, the desired USB signal is at 61.3 GHz. The conversion loss was measured as a function of the applied gate bias and LO power in order to find the best up-conversion performance of the mixer. The measured and simulated results are presented in Figs. 15 and 16. The optimum conversion loss is achieved when the transistor is biased near the threshold voltage. When this happens, the LO pumps the channel resistance from its high value to its low value. The results show that the optimum gate voltage is around  $-0.55$  V. The highest RF output power is achieved with 8 dBm of LO power, although the mixer seems to be capable of delivering even more RF power with higher LO power levels.

The measured conversion loss and LO-to-RF isolation as a function of RF frequency is presented in Fig. 17. The IF is fixed at 5.3-GHz frequency and the LO power delivered on-chip is around 8 dBm. The measured conversion loss is 11.5 dB with a flatness of 1.4 dB.

The LO-to-RF isolation is better than 34 dB, which suggests that the generated 180° LO signal phase shift and the LO virtual ground on the drain side were realized successfully. In Fig. 18, the measured conversion loss is presented when the LO is fixed.

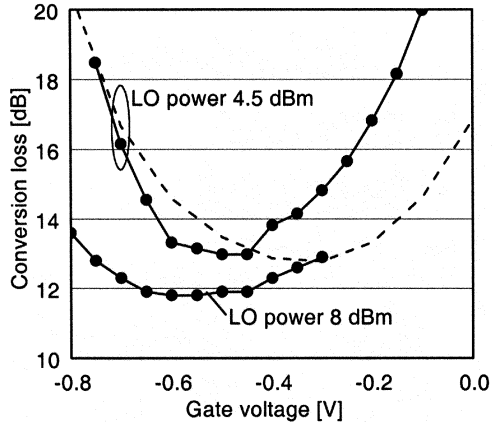


Fig. 15. Measured and simulated conversion loss of the singly balanced mixer as a function of applied gate bias. The dashed line represents the simulated value for LO power of 4.5 dBm.

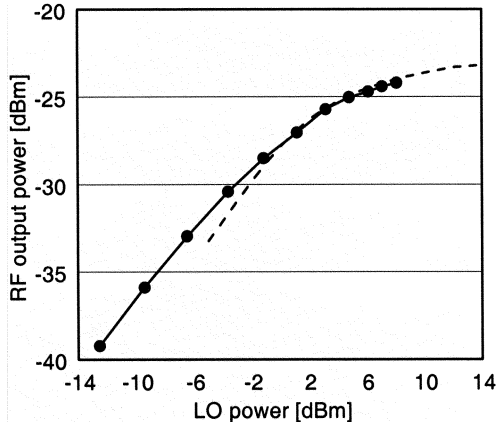


Fig. 16. Measured and simulated (dashed line) RF (61.3 GHz) output power of the singly balanced mixer as a function of applied LO power. The gate voltage is set to  $-0.55$  V.

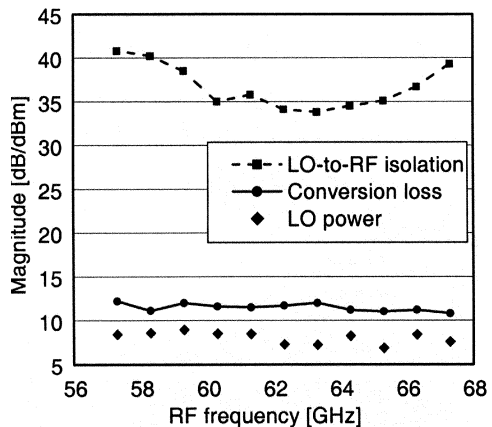


Fig. 17. Measured conversion loss and corresponding LO-to-RF isolation as a function of the RF frequency of the singly balanced mixer. The IF frequency is fixed at 5.3 GHz. The corresponding LO power delivered to the chip is also shown.

### B. Measured Results of the Balanced IR Mixer

To find the optimum up-conversion performance of the balanced resistive IR mixer, the conversion loss, LO-to-RF port isolation, and IR were measured as a function of the applied gate

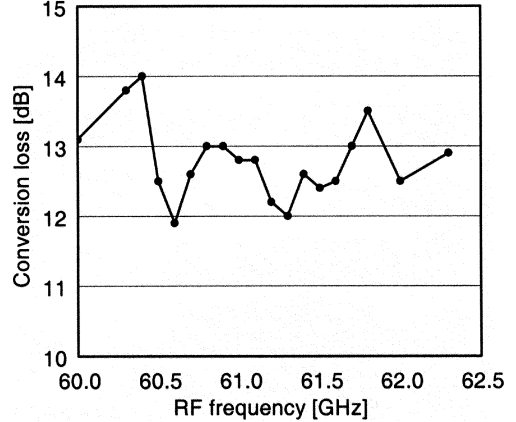


Fig. 18. Measured conversion loss at fixed LO frequency (56 GHz) of the singly balanced resistive mixer. The IF is swept from 4.0 to 6.3 GHz.

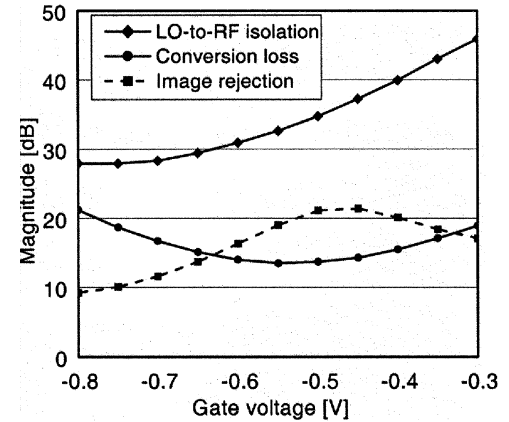


Fig. 19. Measured conversion loss, LO-to-RF isolation, and IR ratio of the balanced resistive IR mixer as a function of applied gate bias.

bias and LO power. The measured results are shown in Figs. 19 and 20, respectively. As with the singly balanced mixer, the lowest conversion loss is achieved at a gate voltage of  $-0.55$  V. On the other hand, the highest IR is achieved at a gate voltage of  $-0.45$  V. In addition, the LO-to-RF isolation increases when the transistor gate is biased further above threshold voltage. Therefore, the gate bias of the mixer was set to  $-0.45$  V for optimum mixer performance. The highest RF output power is achieved with LO power of 8 dBm, as shown in Fig. 20. The IR ratio improves at higher LO power levels. The return losses of the LO and RF ports were measured at V-band and the measurement results are shown in Fig. 21.

The measured conversion loss and IR ratio at a fixed IF frequency of 5.3 GHz are shown in Fig. 22 where the LO power delivered to the chip is also shown. The attenuation of the external IF splitter is not included in the measurement results. The conversion loss degrades as the LO power decreases and vice versa. With higher LO power levels, lower conversion loss and a flatter response are to be expected. The measured LO-to-RF isolation is presented in Fig. 23 and the measured conversion loss and IR ratio with fixed LO frequency (56 GHz) is shown in Fig. 24. Good LO suppression indicates that the power division and matching of the transistor gates using spiral transmission-line transformers and CPW input were realized successfully.

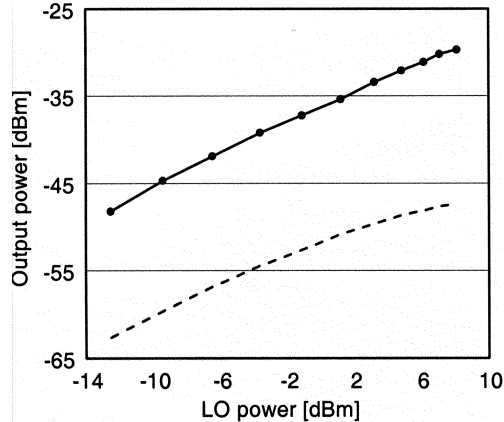


Fig. 20. Measured RF output power and image power (dashed line) of the balanced resistive IR mixer as a function of applied LO power. The gate voltage is set to  $-0.45$  V.

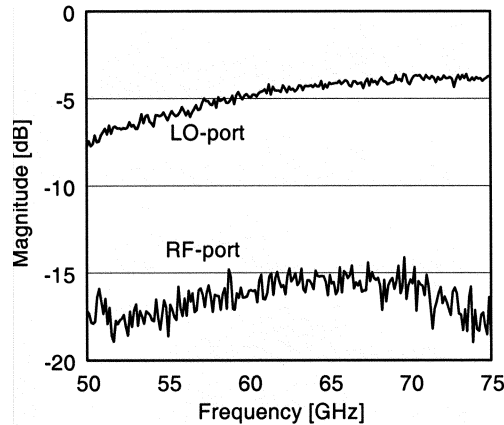


Fig. 21. Measured return losses of LO and RF ports of the balanced resistive IR mixer.

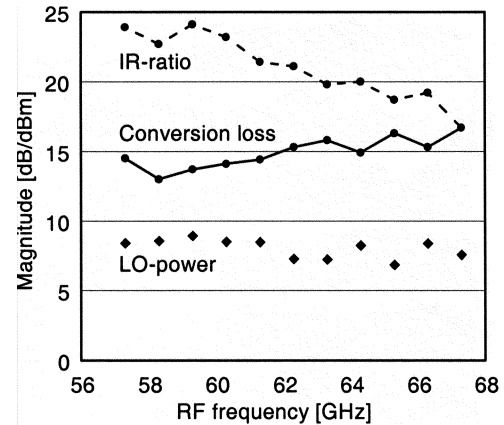


Fig. 22. Measured conversion loss and IR ratio at fixed IF frequency (5.3 GHz) of the balanced resistive IR mixer. The LO is swept from 52 to 62 GHz.

The measured amplitude and phase errors of the external FR4 test phase splitter are shown in Fig. 25, which are determined for the IF-input lines of the two unit mixer pairs. These results are used in the calculation of the IR ratio in Fig. 24; as expected, the IR is mostly determined by the external IF splitter.

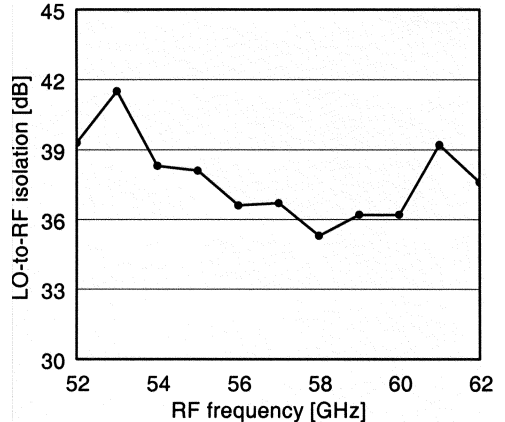


Fig. 23. Measured LO-to-RF isolation of the balanced IR mixer.

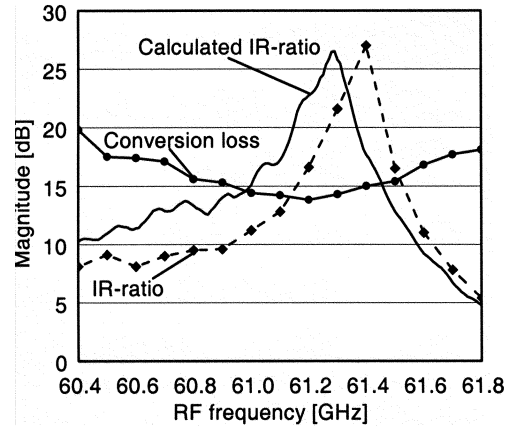


Fig. 24. Measured conversion loss and IR ratio at fixed LO frequency (56 GHz) of the balanced resistive IR mixer. The solid line represents the calculated IR ratio using the measured amplitude and phase errors of the IF test phase splitter. The IF is swept from 4.4 to 5.8 GHz.

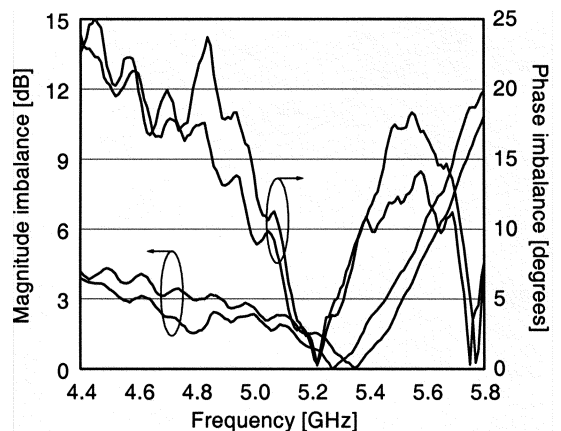


Fig. 25. Measured amplitude and phase error of the IF test phase splitter.

The linearity of the balanced IR mixer was defined by measuring the output compression point and the output third order intercept point (OIP3) of the mixer. In Fig. 26, the output third-order intermodulation product at 61.27 GHz and the fundamental signal at 61.29 GHz as a function of applied input

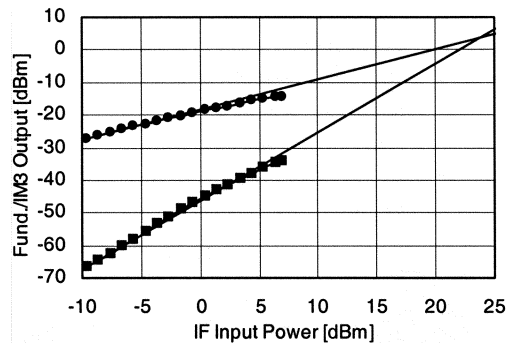


Fig. 26. Measured two-tone test result of the balanced resistive IR mixer. Two IF signals at 5.29 and 5.31 GHz were applied to the mixer. The LO frequency was set to its nominal value of 56 GHz. The OIP3 is at a 4-dBm power level. The measured 1-dB output compression point is at a -13-dBm power level.

TABLE I  
SUMMARY OF MEASURED RESULTS OF  
THE BALANCED IR MIXER

RF frequency	57...66 GHz
Conversion loss	13...16 dB
IR-ratio	> 19 dB
LO suppression	> 35 dB
OIP3	+ 4 dBm
1 dB output compression point	- 13 dBm

power are shown. The measured results of the balanced IR mixer are gathered in Table I.

#### IV. CONCLUSIONS

In this paper, we have presented the design of broad-band MMIC resistive pHEMT mixers. Based on the successful design of the prototype mixer, we have designed a resistive IR mixer with balanced unit mixers. In this design, we have presented a compact circuit for LO power division and transition from even to odd mode for the pHEMTs in the unit mixers. This resulted in a small chip area of 1.41 mm<sup>2</sup>.

The designed balanced IR mixer can significantly improve the performance and reduce the chip area of a 60-GHz telecommunication system. The high IR and LO suppression of the developed mixer enables the integration of the power amplifier and mixer on a single chip without a filter.

#### ACKNOWLEDGMENT

The authors are grateful to the MilliLab, European Space Agency External Laboratory, Espoo, Finland, for providing measurement equipment.

#### REFERENCES

- [1] P. Smulders, "Exploiting the 60 GHz band for local wireless multimedia access: Prospects and future directions," *IEEE Commun. Mag.*, vol. 40, pp. 140–147, Jan. 2002.
- [2] J. Mikkonen, "Emerging wireless broadband networks," *IEEE Commun. Mag.*, vol. 36, pp. 112–117, Feb. 1998.
- [3] A. Yamada, Y. Amano, Y. Motouchi, N. Takahashi, E. Suematsu, and H. Sato, "A compact 60 GHz sub-harmonically pumped mixer MMIC integrated with an image rejection filter," in *IEEE MTT-S Int. Microwave Symp. Dig.*, Seattle, WA, Jun. 2002, pp. 1733–1736.
- [4] S. A. Maas, "A GaAs MESFET mixer with very low intermodulation," *IEEE Trans. Microw. Theory Tech.*, vol. MTT-35, no. 4, pp. 425–429, Apr. 1987.

- [5] S. Maas, "A GaAs MESFET balanced mixer with very low intermodulation," in *IEEE MTT-S Int. Microwave Symp. Dig.*, Las Vegas, NV, Jun. 1987, pp. 895–898.
- [6] H. Zirath, "Development of 60 GHz front end circuits for high data rate communication systems in Sweden and Europe," in *IEEE Gallium Arsenide Integrated Circuit Symp. Dig.*, San Diego, CA, Nov. 2003, pp. 93–96.
- [7] M. Kimishima, T. Ataka, and H. Okabe, "A family of Q, V, and W-band monolithic resistive mixers," in *IEEE MTT-S Int. Microwave Symp. Dig.*, Phoenix, AZ, May 2001, pp. 115–118.
- [8] K. S. Ang, M. Chongcheawchanan, and I. D. Robertson, "Monolithic resistive mixers for 60 GHz direct conversion receivers," in *IEEE Radio Frequency Integrated Circuits Symp. Dig.*, Boston, MA, Jun. 2000, pp. 35–38.
- [9] T. Kashiwa, T. Katoh, T. Ishida, T. Ishikawa, and Y. Nakayama, "A V-band drain injected/resistive dual-mode monolithic mixer," in *IEEE Gallium Arsenide Integrated Circuit Symp. Dig.*, Monterey, CA, Oct. 1999, pp. 117–120.
- [10] M. Schefer, U. Lott, W. Patrick, H. Meier, and W. Bachtold, "Passive, coplanar V-band HEMT mixer," in *IEEE Int. Indium Phosphide and Related Materials Conf. Dig.*, Cape Cod, MA, May 1997, pp. 177–180.
- [11] S. Maas, *Nonlinear Microwave and RF Circuits*, 2nd ed. Norwood, MA: Artech House, 2003.
- [12] J. Riska, P. Kangaslahti, M. Kärkkäinen, and V. Porra, "Amplifiers and signal generation circuits for 60 GHz wireless broadband systems," presented at the Eur. Microwave Conf., Paris, France, Oct. 2000, Paper EuMc\_P3.
- [13] Y. Baeyens, L. Verweyen, W. Haydl, W. Marsetz, and M. Schlechtweg, "Design of compact millimeter-wave MMICs using CPW," in *IEE Design of RFICs and MMICs Tutorial Coll.*, 1987, Ref. 1997/391, pp. 3/1–3/6.
- [14] O. Salmela, "Wideband, single-mode coplanar waveguide operation," in *Proc. Asia-Pacific Microwave Conf.*, Yokohama, Japan, Dec. 1998, pp. 827–829.
- [15] S. Maas, F. Kintis, F. Fong, and M. Tan, "A broadband planar monolithic ring mixer," in *IEEE Microwave Millimeter-Wave Monolithic Circuits Symp. Dig.*, San Francisco, CA, Jun. 1996, pp. 51–54.
- [16] P. Kangaslahti, J. Riska, M. Kärkkäinen, P. Alinikula, and V. Porra, "Low phase noise signal generation circuits for 60 GHz wireless broadband system," in *IEEE MTT-S Int. Microwave Symp. Dig.*, Boston, MA, Jun. 2000, pp. 43–46.



**Mikko Varonen** received the M.Sc. degree in electrical engineering from the Helsinki University of Technology, Espoo, Finland, in 2002, and is currently working toward the Ph.D. degree in electrical engineering at the Helsinki University of Technology.

He is currently with the Electronic Circuit Design Laboratory, Helsinki University of Technology. His research interests involve millimeter-wave integrated circuits.



**Mikko Kärkkäinen** received the M.Sc. degree in electrical engineering from the Helsinki University of Technology, Espoo, Finland, in 2000, and is currently working toward the Ph.D. degree at the Helsinki University of Technology.

He is currently with the Electronic Circuit Design Laboratory, Helsinki University of Technology. His research interest is millimeter-wave circuit design.

**Jan Riska** was born in Porvoo, Finland, in 1973. He received the M.Sc. degree in electrical engineering and Licentiate's degree from the Helsinki University of Technology (HUT), Espoo, Finland, in 1998 and 2000, respectively.

He is currently with Freescale Semiconductor, Espoo, Finland.



**Pekka Kangaslahti** (S'94–M'98) received the M.Sc and Ph.D. degrees from the Helsinki University of Technology, Espoo, Finland, in 1992 and 1999, respectively.

He is currently a Senior Engineer with the Microwave Systems Section, Observational Systems Division, Jet Propulsion Laboratory, Pasadena, CA. He possesses over ten years of experience in MMIC design and measurement techniques. His current interest is in the development MMICs and millimeter-wave modules for large arrays.



**Kari A. I. Halonen** (M'02) was born in Helsinki, Finland, on May 23, 1958. He received the M.Sc. degree in electrical engineering from the Helsinki University of Technology (HUT), Espoo, Finland, in 1982, and the Ph.D. degree in electrical engineering from the Katholieke Universiteit Leuven, Heverlee, Belgium, in 1987.

From 1982 to 1984, he was an Assistant with HUT and a Research Assistant with the Technical Research Center of Finland. From 1984 to 1987, he was a Research Assistant with the Electronics, Systems, Automation, and Technology (ESAT) Laboratory, Katholieke Universiteit Leuven, under a temporary grant from the Academy of Finland. Since 1988, he has been with the Electronic Circuit Design Laboratory, HUT, as a Senior Assistant (1988–1990) and as the Director of the Integrated Circuit Design Unit of the Microelectronics Center (1990–1993). During the 1992–1993 academic year, he was on a leave of absence, acting as a Research and Development Manager with Fincitec Inc., Kemi, Finland. From 1993 to 1996, he was an Associate Professor and, since 1997, he has been a Full Professor with the Faculty of Electrical Engineering and Telecommunications, HUT. In 1998, he became the Head of the Electronic Circuit Design Laboratory. He has authored or coauthored over 150 international and national conference and journal publications on analog integrated circuits. He holds several patents on analog integrated circuits. His research interests are CMOS and BiCMOS analog integrated circuits, particularly for telecommunication applications.

Dr. Halonen was an associate editor for the IEEE TRANSACTIONS ON CIRCUITS AND SYSTEMS—PART I: FUNDAMENTAL THEORY AND APPLICATIONS (1997–1999). He has been a guest editor for the IEEE JOURNAL OF SOLID-STATE CIRCUITS. He was the Technical Program Committee Chairman for the European Solid-State Circuits Conference in 2000. He was the recipient of the Beatrice Winner Award presented at the 2002 IEEE International Solid-State Circuits Conference.



## Design Seminar



Agilent EEsof  
Customer Education  
and Applications

### RFIC MOS Gilbert Cell Mixer Design



**Agilent Technologies**  
Innovating the HP Way

#### Abstract

The Gilbert double-balanced mixer configuration is widely used in RFIC applications because of its compact layout and moderately high performance. This seminar will walk through the design of a CMOS Gilbert mixer focusing on the parameters that influence the linearity of the signal path, the noise, and therefore the spurious-free dynamic range of the mixer. We will explore design tradeoffs that include biasing and device sizing, LO power, conversion gain, gain compression, intermodulation distortion, and noise.



## About the Author



**Steve Long**

- University of California, Santa Barbara
- Professor, Electrical and Computer Engineering
- Consultant to Industry



Page 2

### BIOGRAPHICAL SKETCH

Stephen Long received his BS degree in Engineering Physics from UC Berkeley and MS and PhD in Electrical Engineering from Cornell University. He has been a professor of electrical and computer engineering at UC Santa Barbara since 1981. The central theme of his current research projects is rather practical: use unconventional digital and analog circuits, high performance devices and fabrication technologies to address significant problems in high speed electronics such as low power IC interconnections, very high speed digital ICs, and microwave analog integrated circuits for RF communications. He teaches classes on communication electronics and high speed digital IC design.

Prior to joining UCSB, from 1974 to 1977 he was a Senior Engineer at Varian Associates, Palo Alto, CA. From 1978 to 1981 he was employed by Rockwell International Science Center, Thousand Oaks, CA as a member of the technical staff.

Dr. Long received the IEEE Microwave Applications Award in 1978 for development of InP millimeter wave devices. In 1988 he was a research visitor at GEC Hirst Research Centre, U.K. In 1994 he was a Fulbright research visitor at the Signal Processing Laboratory, Tampere University of Technology, Finland and a visiting professor at the Electromagnetics Institute, Technical University of Denmark. He is a senior member of the IEEE and a member of the American Scientific Affiliation.



**Basic engineering problem:**

*Design of MOS RFIC mixers for large dynamic range...*

**Learning Objectives:**

- Understand operation of MOSFET Gilbert mixer
- Biasing considerations
- Design for stability, linearity and noise
- Specify performance: NF, P<sub>1dB</sub>, TOI, SFDR

[Always see the NOTES pages for Exercises throughout...](#)



There are many different mixer circuit topologies and implementations that are suitable for use in receiver and transmitter systems. We will select one of the widely used double-balanced mixer topologies as our example. The design process presented here will have more general applicability to other circuit approaches, both for mixers and amplifiers, in receiver applications.



## Design specifications



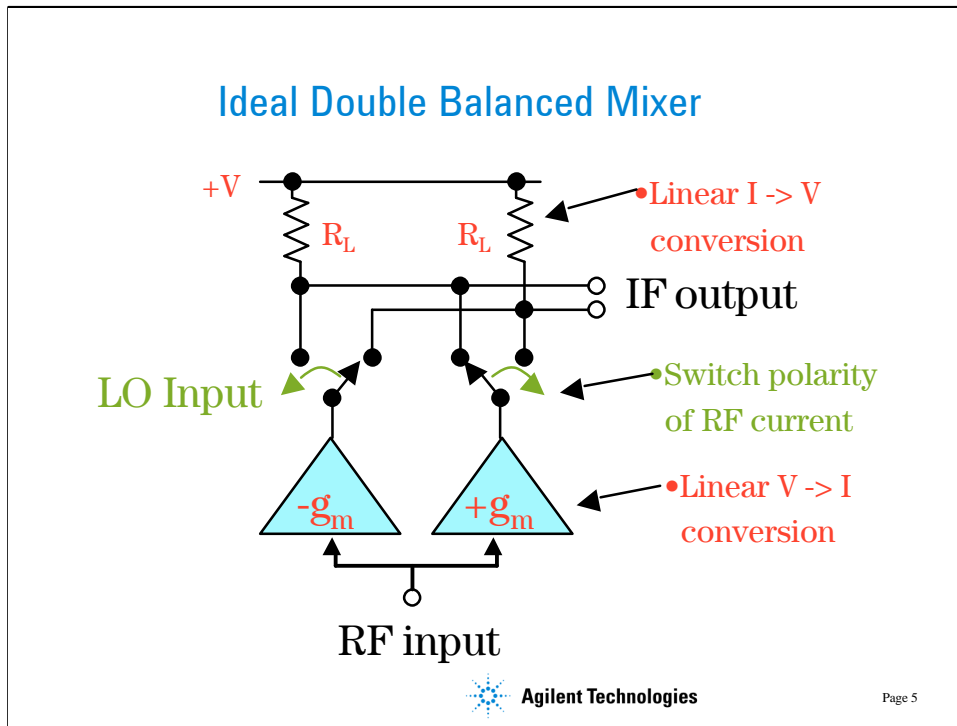
- Frequencies:
  - LO = 855 MHz
  - RF = 900 MHz
  - IF = 45 MHz
- Technology: 0.35 mm CMOS
- Supply voltage: 3.3V
- Input IP3 > - 6 dBm
- RF Input: matching off chip on PCB; single-ended
- LO Input: single-ended; on-chip LO buffer



Page 4

Here we have some representative, but somewhat arbitrary specifications for the mixer.

A BSIM 3.3 model was used for the 0.35  $\mu$ m CMOS process. Parameters for the model were obtained from a digital CMOS process, so absolute accuracy for more analog applications involving distortion and noise is not to be assumed. But, relative accuracy is sufficient for exploring many of the design details and revealing general trends.



An ideal double balanced mixer simply consists of a switch driven by the local oscillator that reverses the polarity of the RF input at the LO frequency[1]. To get the highest performance from the mixer we must make the RF to IF path as linear as possible and minimize the switching time of the LO switch. The ideal mixer above would not be troubled by noise (at the low end of the dynamic range) or intermodulation distortion (IMD) at the high end since the transconductors and resistors are linear and the switches are ideal.

The ideal balanced structure above cancels any output at the RF input frequency since it will average to zero. It also cancels out any LO frequency component since we are taking the IF output as a differential signal and the LO shows up as common mode. Therefore, to take full advantage of this design, an IF balun, either active (a differential amplifier) or passive (a transformer or hybrid), is required.



## How does it convert frequency?

- Let  $V_{RF}(t) = V_R \cos(w_{RF}t)$
- The circuit converts this into a current:  
$$I = g_m V_{RF}(t)$$
- Then, it multiplies I by the LO switching function  $T(t)$  defined in the next slide.
- $V_{IF}(t) = 2 g_m R_L T(t) V_{RF}(t) = A T(t) V_{RF}(t)$



Page 6

Mixers perform frequency translations (conversion) by multiplication of an RF input signal with an LO signal. The trig relationship

$$\cos x \sin y = (1/2) [\sin(x + y) - \sin(x - y)]$$

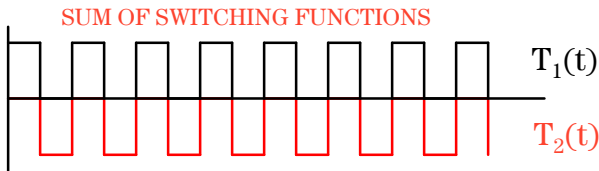
provides the desired up and down translations.



## LO Switching Function T(t)

$$T_1(t) = \frac{1}{2} + \frac{2}{p} \left[ \sin(\omega_{LO}t) + \frac{1}{3} \sin(3\omega_{LO}t) + \dots \right]$$

$$T_2(t) = -\frac{1}{2} + \frac{2}{p} \left[ \sin(\omega_{LO}t) + \frac{1}{3} \sin(3\omega_{LO}t) + \dots \right]$$

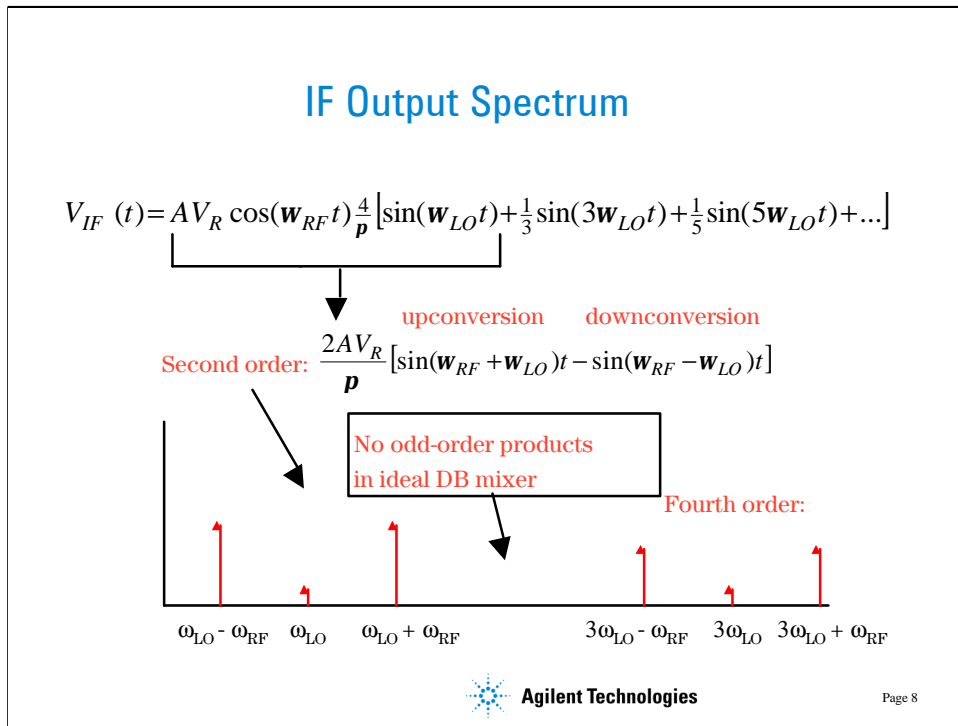


Agilent Technologies

Page 7

If the LO is a square wave with 50% duty cycle, it is easily represented by its Fourier Series. The symmetry causes the even-order harmonics to drop out of the LO spectrum. When multiplied by a single frequency cosine at  $\omega_{RF}$  the desired sum and difference outputs will be obtained as shown in the next slide.

There will be harmonics of the LO present at  $3\omega_{LO}$ ,  $5\omega_{LO}$ , etc. that will also mix to produce outputs called “spurs” (an abbreviation for spurious signals).



The second-order output spectral lines at  $\omega_{LO} \pm \omega_{RF}$  are the desired upconversion and downconversion products from the mixer. Typically, one of these outputs will be removed by IF filtering. Note that ideally there will not be any third-order or higher odd-order products in the mixer output since only odd LO harmonics are generated in a perfectly symmetric switching DB mixer. The DC component should also cancel. This reduces the number of spurious outputs when compared with other nonlinear or unbalanced mixer approaches making the selection of the LO and IF frequencies less restrictive.

Here we see that the ideal conversion gain  $(V_{IF}/V_R)^2 = A^2 (2/\pi)^2 = -4 \text{ dB}$  (if  $A=1$ ).

In real mixers, there is always some imbalance. This will produce some LO to IF or RF to IF feedthrough (thus, isolation is not perfect). Secondly, the RF to IF path is not perfectly linear. This will lead to intermodulation distortion. Odd-order distortion (typically third and fifth order are most significant) will cause spurs within the IF bandwidth or cross-modulation when strong signals are present. Also, the LO switches are not perfectly linear, especially while in the transition region. This can add more distortion to the IF output and will increase loss due to the resistance of the switches.



## Intermodulation distortion

- IMD consists of the higher order signal products that are generated when two RF signals are present at the mixer input. The IMD will be down and up converted by the LO as will the desired RF signal.
- IMD generation is a good indicator of large signal performance of a mixer.
- Absolute accuracy is highly dependent on the accuracy of the device model, but the relative accuracy is valuable for optimizing the circuit parameters for best IMD performance.



Page 9

Next we would like to evaluate how the distortion generated by the mixer signal path is affected by the choice of various design parameters.



## Design of MOS DB mixer

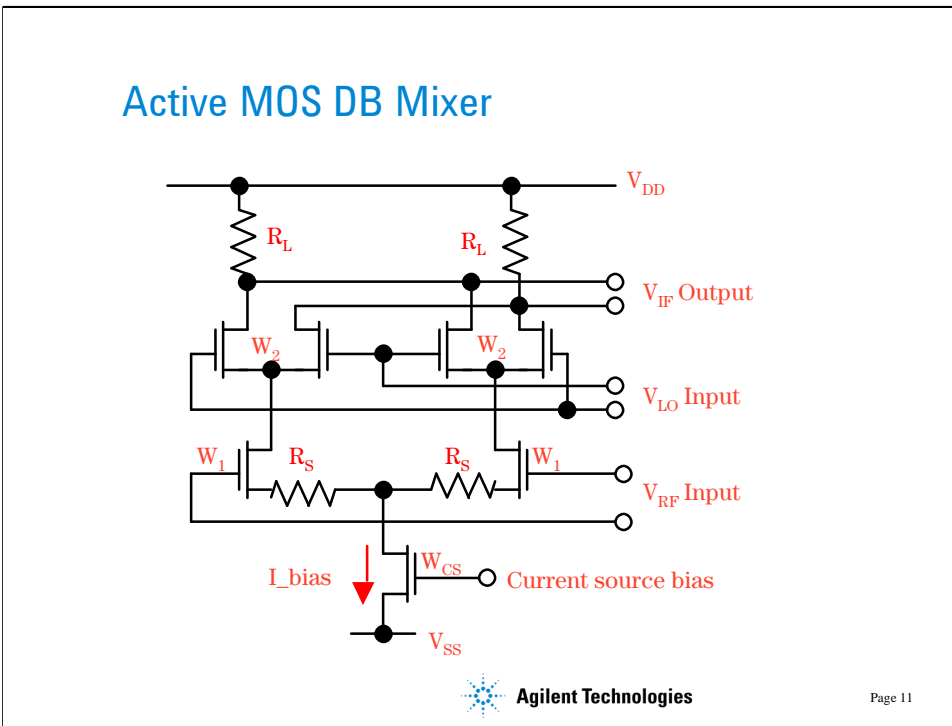


- Device width
- Biasing
- Linearity of transconductance amplifier
- Stability and input matching network
- Gain compression and IMD
- Noise figure
- Spurious Free Dynamic Range



Page 10

Our approach will emphasize the distortion-limited (large-signal) performance over noise-limited (small-signal) performance.



This is a schematic of a MOSFET version of the Gilbert active DB mixer (Gilbert claims that it was really first invented by H. E. Jones as a demodulator).[2] The upper FETs provide a fully balanced, phase-reversing current switch function. The lower FETs are the transconductance amplifier.

Many design decisions are possible.

**I bias and device widths  $W_1$  and  $W_2$ :** We need to choose a  $W_1$  that will provide high  $g_m$ , saturation at low  $V_{DS}$  (for low power supply operation), and low noise. Large widths are preferred for noise, and the optimum width for noise with power constraints can be estimated from the MOS device parameters [3]. Large widths also require large bias currents to obtain high  $g_m$ . Choosing  $W_1 = W_2$  is typically best. So, next we must investigate the minimum current required to keep all devices in saturation.

**Linearity of signal path:** Once the bias is determined, we will investigate linearization of the transconductance amplifier through source resistance and inductance. Resistance will increase the input voltage range where nearly linear gain can be obtained, but will reduce conversion gain to some degree. Source inductance will be used mainly to guarantee stability by forcing a positive real component into the input impedance. This also helps to make the input impedance easier to match.

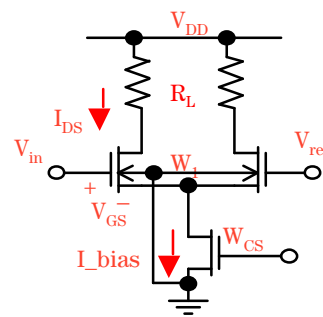


## Device width and bias current

- Width is estimated for noise[3]:  $W_{opt} \approx \frac{1}{3wLC_{ox}R_{gen}}$
- for CMOS with  $L = 0.35$  mm

and  $R_{gen} = 50\text{W}$ :  $W_{opt} = 800$  mm

- Determine suitable bias current
  - require:  $V_{DS} > V_{D_{sat}}$
  - caution:  $V_{SB}$  varies with current
  - use differential amp to evaluate device I-V &  $g_m$ . Use  $I_{bias}$  as the independent variable.



 Agilent Technologies

Page 12

The device width of 800  $\mu\text{m}$  is estimated from a MOSFET noise model[3]. For this width, you must make sure that  $I_{DS}$  is large enough to saturate the MOSFET ( $V_{DS} > V_{D_{sat}}$ ). At the same time, you want to design for low  $V_{DD}$  operation, so large  $V_{DS}$  is also undesirable. Finally, large  $V_{DS}$  will increase hot electron effects at the drain thereby increasing noise.

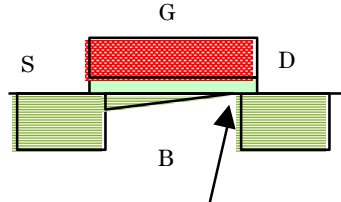
**Exercise:** set up a DC simulation of a MOSFET with width of 800  $\mu\text{m}$  and gate length of 0.35 $\mu\text{m}$  using the ADS design file **MOS\_curve\_tracer.dsn**. Note the size of  $V_{D_{sat}}$  for various gate voltages. Apply a positive source-to-substrate (bulk) potential and see how the device current varies with  $V_{SB}$ . This body effect will increase the threshold voltage  $V_T$  and reduce current for a given  $V_{GS}$ .

When  $I_{bias}$  is swept on the diff amp above, the source-to-bulk voltage changes. This changes the device I-V, so it's more efficient to evaluate the device I-V characteristics when configured as a diff amp. Now, the source is allowed to float to whatever bias is needed to support the current.

[see ADS design: diffpair\_dc1]

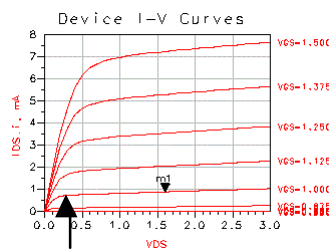


## MOSFET DC Characteristics



- Saturation occurs when channel pinches off at drain

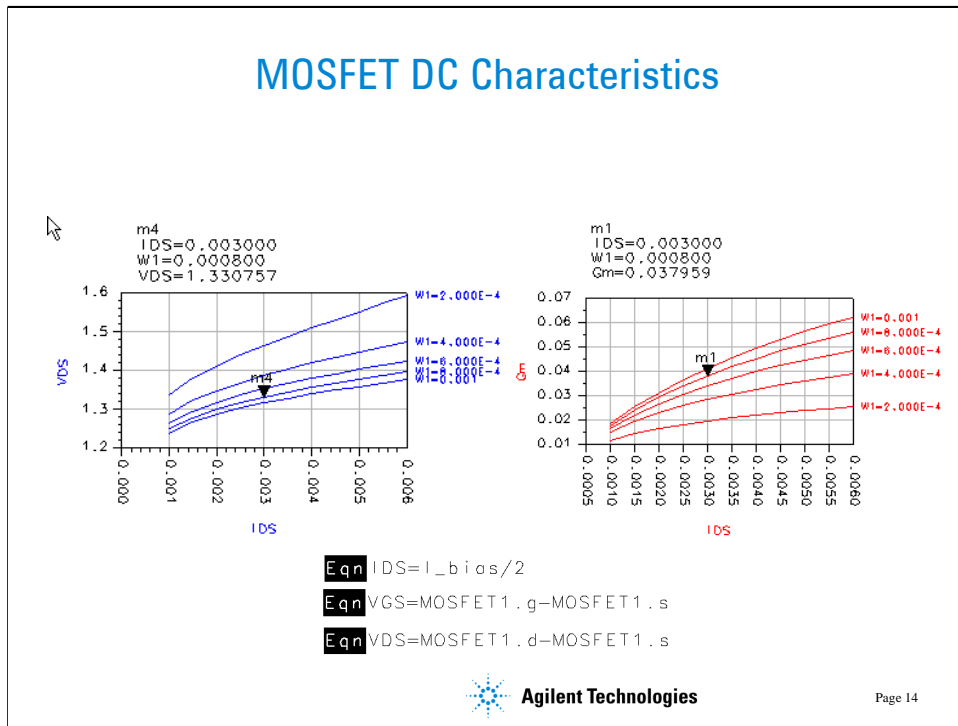
$$V_{DSat} = V_{GS} - V_T$$



Agilent Technologies

Page 13

$V_{DSat}$  is the drain voltage at which the channel first reaches saturation. At saturation, the drain current no longer increases rapidly with further increase in  $V_{DS}$  because the drain end of the channel has pinched off. It is necessary to insure that the device is in saturation in order to obtain high  $gm$  and low  $C_{gd}$ , beneficial for most active circuit implementations.



The plots above show  $V_{DS}$  and  $g_m$  as a function of  $I_{DS}$ .  $V_{DD} = 3.3V$  in this case, and the  $R_D$  value was varied with  $I_{DS}$  to maintain a constant drain voltage of 2.4V.

Since both inputs of the diff pair are at the same voltage (2V in this example) we define

$$I_{DS} = I_{bias}/2$$

as an *Eqn* in the display panel.  $I_{bias}$  is swept by controlling the current into a current mirror (not shown on previous slide) with an independent DC current source. The *PARAMETER SWEEP* controller can be used to vary  $W_1$ .

Also, we can include voltages at all device nodes in the data file by using the *OPTIONS* controller and setting *OutputInternalNodes=yes*.  $V_{DS}$  is defined by another *Eqn* as

$$V_{DS} = \text{MOSFET1.d} - \text{MOSFET1.s}$$

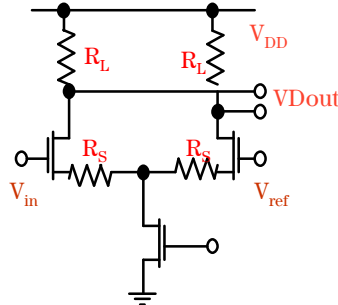
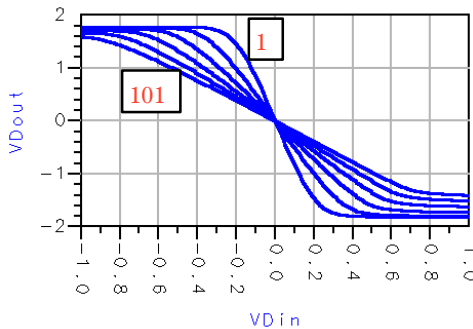
From the  $g_m$  plot, we can see that  $g_m$  increases directly with  $I_{DS}$  and with  $W_1$ . Also,  $V_{DS}$  is well above the saturation knee (roughly 0.5V) for all currents and widths. At currents below about 3 mA, there is little benefit to increasing  $W_1$  beyond 600  $\mu\text{m}$ , so we will choose this as our minimum bias current. We might expect to see conversion gain increase with higher drain currents at the cost of higher power dissipation.

[see ADS design files: diffpair\_dc1.dsn and MOS\_curve\_tracer.dsn]



## Linearity of signal path

- $R_s$  is varied from 1 to 101 ohms



NOTE:  $V_{Din} = V_{in} - V_{ref}$



Page 15

Now we will focus on the linearity of the signal path (RF to IF). A transfer characteristic is simulated by sweeping the DC input voltage

$$V_{Din} = V_{in} - V_{ref}$$

$V_{ref} = 2.0V$ . We would expect that by increasing the resistance  $R_s$ , adding negative feedback, we would linearize the transfer characteristic by exchanging gain for linearity. In the simulation shown,  $R_s$  values are stepped using a *PARAMETER SWEEP* controller from 1 to 101 ohms. We see that the gain (slope) becomes more linear over a wider input voltage range with increasing  $R_s$ .

**Exercise.** Evaluate how the choice of  $V_{ref}$  affects the transfer characteristic.

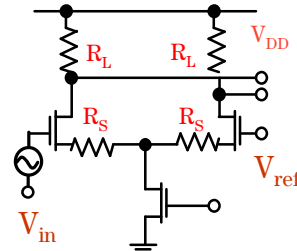
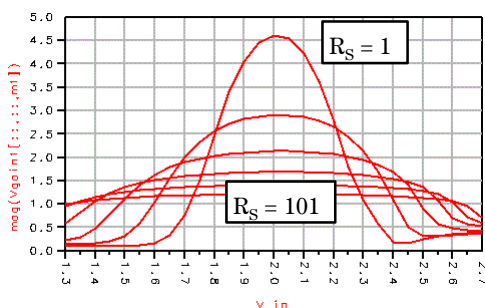
[See ADS design file: diffpair\_tc.dsn]



## Linearity of signal path

Incremental gain vs. input offset voltage:

AC simulation: sweep  $V_{in}$  and  $R_s$



NOTE:  $V_{ref} = 2$  volts



Agilent Technologies

Page 16

Another way of viewing the linearity of the amplifier is by doing an AC analysis of incremental voltage gain as a function of frequency with  $R_s$  as a parameter. The plot above illustrates that increasing  $R_s$  decreases gain but also reduces the relative gain variation with input offset voltage,  $V_{in}$ . In fact, this is the conventional first order treatment for improving linearity of a differential stage, albeit at the expense of gain and noise. But, because the mixer distortion will increase as the large signal input voltage increases, this simple technique is valuable. But, we can never get perfectly flat gain with this simple approach.

[Refer to ADS design files: diffpair\_tc.dsn and diffpair\_tcgain2.dsn]

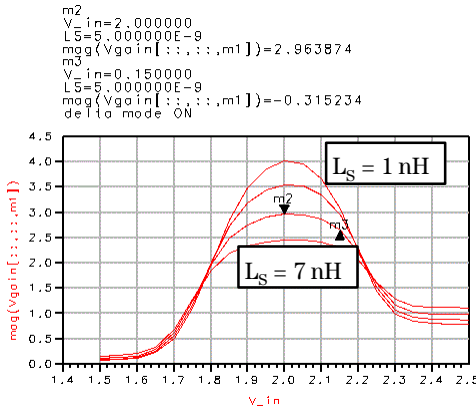
The asymmetry seen on the high input voltage side is due to the input MOSFET dropping out of saturation.

From this analysis, and if conversion gain and noise are not very important for your application, you would think that larger  $R_s$  would be better: more effective in reducing distortion. It turns out that this design has some peculiar properties in this regard, so watch for this later.

**Exercise:** 1. Evaluate how the small-signal gain vs.  $V_{in}$  varies with  $I_{bias}$  as a parameter. Compare your result with diffpair\_tcgain4.dsn.



## Linearization through $L_S$ ?



$$f = 900 \text{ MHz}$$

- Doesn't add noise
- Less voltage drop
- But, not as good for linearity
- Also, inductors on Si have low Q, so would have both  $R_S$  and  $L_S$ .



Agilent Technologies

Page 17

A popular technique in low voltage RFIC design is to substitute inductors for resistors. This has the advantages that the ideal inductor will not add noise to the circuit, and it reduces the supply voltage requirement for the circuit. The effectiveness of this approach is somewhat frequency dependent. At 900 MHz, the gain degeneration and linearity improvement for reasonable sized inductors is limited. It becomes more effective at higher frequencies.

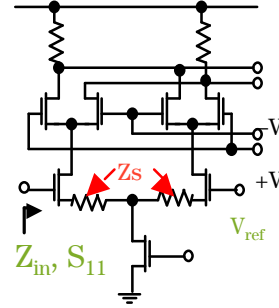
[See ADS design: diffpair\_tcgain5.dds. Try changing the frequency on the display screen and observe how the inductive degeneration varies.]

Also, inductors on Si substrates have low Q, on the order of 2 to 3. For a Q of 2.5, for example, a 5 nH inductor at 900 MHz would have a series resistance of about 10 ohms. Thus, we really are including both resistance and inductance. We will see that this is a good combination for modifying the input match.



## Stability of mixer input port

- dB  $|S_{11}| > 0$ : unstable. Why?



 Agilent Technologies

Page 18

We will do an S-parameter simulation of the Gilbert DB mixer to determine the input impedance as a function of  $R_S$ . The LO switch is biased on, thus the circuit resembles a cascode.

We see that as  $R_S$  is increased, the magnitude of  $S_{11}$  becomes greater than 1 ( $>0$ dB). This means that the real part of the input resistance is negative, a condition desirable for oscillators, not mixers. We also note that this condition gets worse at higher frequencies. Thus, we need to look more closely to find out why this is happening and find a way to guarantee stability.

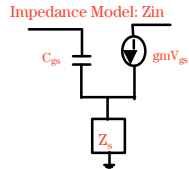
[Refer to ADS example files: gilmix\_sp.dsn and .dds]



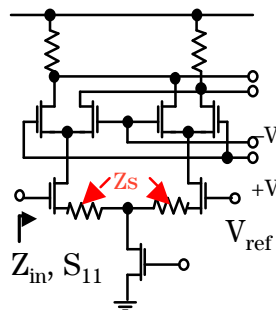
## Input impedance of mixer

$$Z_{in}(j\omega) = \frac{1}{j\omega C_{gs}} + Z_s + \frac{w_T}{j\omega} Z_s$$

NOTE:  $\omega_T$  is the unity current gain frequency =  $gm/C_{gs}$ .



Zs	Re{Zin} + Im{Zin}
R	$R + \left( \frac{w_T R}{j\omega} + \frac{1}{j\omega C_{gs}} \right)$
L	$w_T L + \left( \frac{1}{j\omega C_{gs}} + j\omega L \right)$
C	$-\frac{w_T}{\omega^2 C} + \left( \frac{1}{j\omega C_{gs}} + \frac{1}{j\omega C} \right)$



Agilent Technologies

Page 19

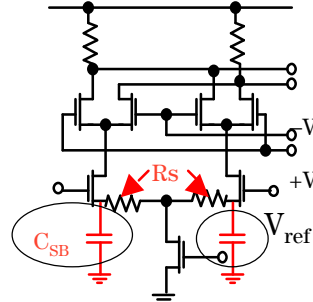
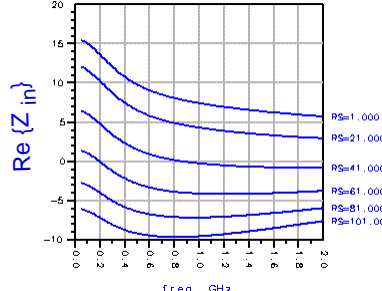
The equation above for input impedance was derived from a simple small-signal analysis neglecting  $C_{gd}$  and assuming that the node between the source resistors is at virtual ground. If the source node impedance  $Z_s$  was purely resistive, we should have a series equivalent input circuit that consists of R and two series capacitors. If R is large, the equivalent input series capacitive reactance is large and has a large effect on  $Z_{in}$ . The real part is clearly positive.

Similarly, we find that a series inductance L produces a non-frequency dependent positive real part and a series LC resonant network. Only the capacitor produces a negative resistance, and with an unusual frequency dependence.



## Input impedance of mixer

$$\text{Re}\{Z_{in}\} = \frac{R_S(1 - w_T R_S C_{SB})}{1 - w^2 R_S^2 C_{SB}^2}$$



Agilent Technologies

Page 20

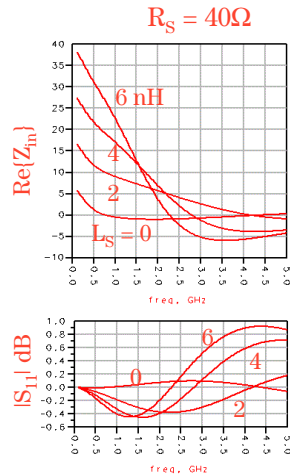
Since we are seeing  $|S_{11}| > 1$ , we must have a negative resistance in the input. Why? This is due to the parasitic source to bulk capacitance of the MOSFET. As  $R_S$  increases, the shunt  $C_{SB}$  has greater effect on the source impedance and therefore drives the input impedance negative. If  $\omega_T R_S C_{SB} > 1$ , we will have a negative real  $Z_{in}$ .

**Exercise:** Try adding extra shunt capacitance to the source nodes in the schematic gilmix\_sp and see how  $S_{11}$  and  $Z_{in}$  is affected.

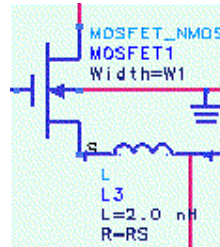
To compensate for the negative resistance, let's add some series inductance.



## Source inductance added



- Small  $L_S$  can improve input match at design frequency of 900 MHz
- It will also help with stability



 Agilent Technologies

Page 21

The addition of small amounts of source inductance in series with  $R_S$  (40 ohms in this example) helps improve the input match at the design frequency of 900 MHz. The 40 ohms was chosen as the largest series R that did not produce large negative resistances at the input.

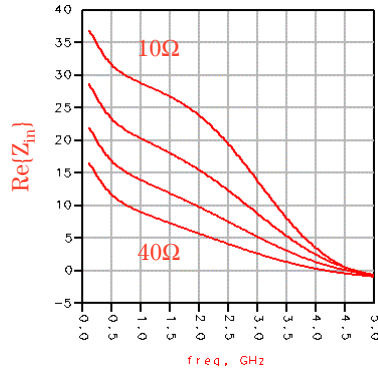
An  $L_S = 2$  nH raises  $\text{Re}\{Z_{in}\}$  without producing instability. We can see that above 4 GHz, a very small amount of series resistance on the input will yield unconditional stability. This would come from losses in the matching network. The larger  $\text{Re}\{Z_{in}\}$  will make the input matching network less sensitive to element values.

[ Refer to ADS example files: gilmix\_sp2]



## $Z_{in}$ with added source inductance

$$L_S = 2 \text{ nH}$$



- Input impedance varies with  $R_s$ .
- Since we will evaluate the effect of  $R_s$  on distortion, we must design a matching network for each  $R_s$  value selected.

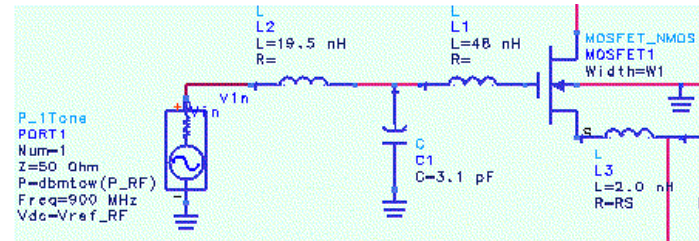


We now see that the additional inductance has eliminated the negative real part to the input impedance for  $R_s \leq 40\Omega$ .

But,  $R_s$  has a major effect on  $Z_{in}$ . Since we saw earlier that  $R_s$  may influence the linearity of the diff pair, we will want to investigate the dependence of distortion on  $R_s$ . Thus, we will need to design a matching network for each  $R_s$  value.



## Add input matching network



- Off chip - inductances are too large for on-chip fabrication
- Calculate components for each  $R_S$  value to be evaluated
- Add single frequency generator for harmonic balance simulation

NOTE: Other side is terminated with Vref\_RF.

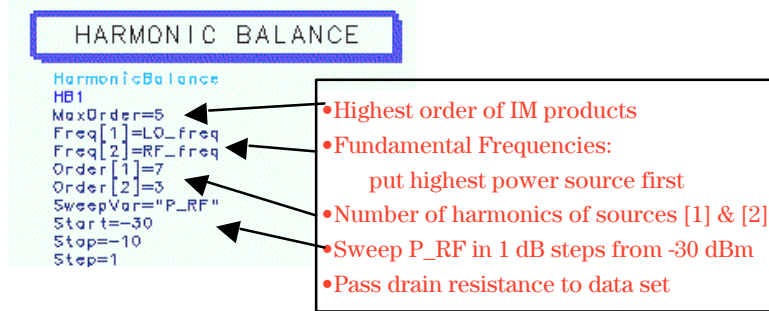


We have seen that  $Z_{in}$  will vary with  $R_S$  and  $L_S$ . For  $L_S = 2 \text{ nH}$ , we will design a T-network to match the 50 ohm off-chip generator to the mixer input for 3 values of  $R_S$ . (We will want to investigate the dependence of intermodulation on  $R_S$  in a later slide.)

$R_S (\Omega)$	$Z_{in} (\Omega)$	$L1$	$C1$	$L2$
10	$29.4-j183$	48nH	3.1pF	19.5nH
20	$20.8-j200$	46.4	4.1	15.7
40	$9.4-j221$	44.1	7.4	8.3



## Use Harmonic Balance simulation



Agilent Technologies

Page 24

Adding the input matching network shown on the previous slide for  $R_S = 10\Omega$  and  $L_S = 2 \text{ nH}$ , we can now calculate the conversion gain as a function of whatever parameters we wish to vary. In this example, the RF input power,  $P_{RF}$ , will be swept.

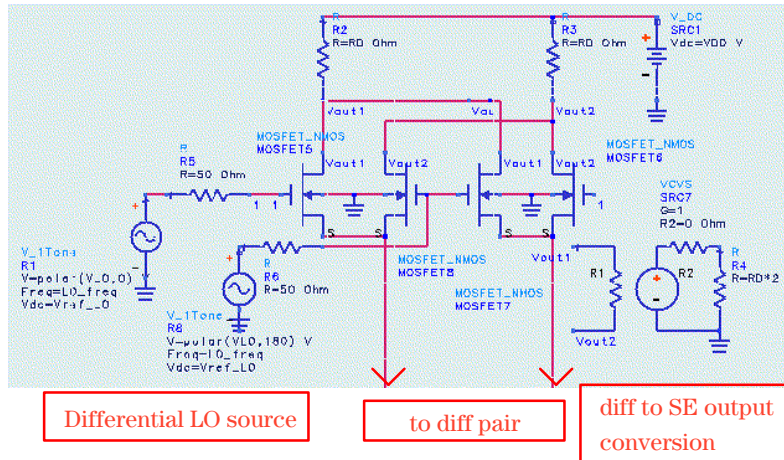
Harmonic balance is the method of choice for simulation of mixers. By specifying the number of harmonics to be considered for the LO and RF input frequencies and the maximum order (highest order of sums and differences) to be retained, you get the frequency domain result of the mixer at all relevant frequencies. To get this information using SPICE or other time domain simulators would require a very long simulation time since at least two complete periods of the lowest frequency component must be generated in order to get accurate FFT results. In addition, the time step must be compatible with the highest frequency component to be considered.

Maximum order corresponds to the highest order IM product ( $n + m$ ) to be considered ( $nf[1] \pm mf[2]$ ). The simulation will run faster with lower order and fewer harmonics of the sources, but may be less accurate. You should test this by checking if the result changes significantly as you increase order or harmonics.

The frequency with the highest power level (the LO) is always the first frequency to be designated in the harmonic balance controller. Other inputs follow sequencing from highest to lowest power.



## L0 switch



 Agilent Technologies

Page 25

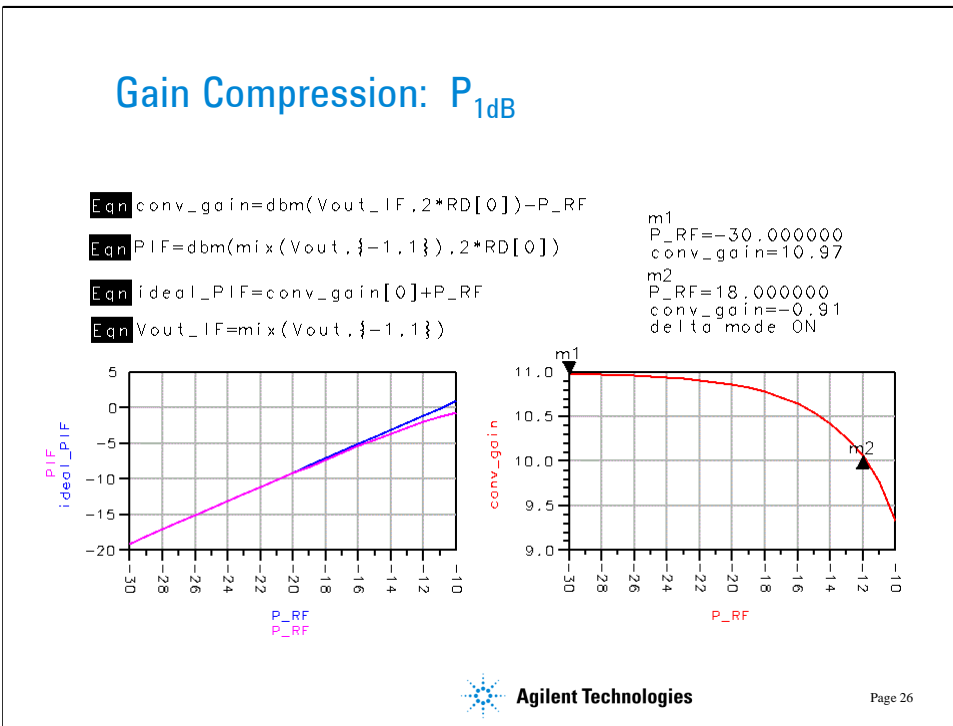
Differential LO drive is required if you need good LO to IF and LO to RF isolation. This is probably the case, otherwise you could get by with a simpler single-balanced design. Since the LO and RF frequencies are rather close together (in this example), you can't depend on the input matching network to attenuate the LO signal very much. The LO driver might typically be located on-chip as another diff amp, but to simplify the simulation, it is represented here as two voltage sources at 0 and 180 degrees phase with amplitude VLO. A DC offset of Vref\_LO is also needed to correctly bias the LO inputs. We will sweep VLO later to determine the LO amplitude for best IMD performance.

A differential output is also required in order to obtain the double-balanced properties. Your LO signal, which is common-mode for differential and thus cancels, will show up at full amplitude in the output if single-ended. For the simulation, we can use an ideal voltage-controlled-voltage-source to provide this conversion:

$$V_{out} = V_{out1} - V_{out2}$$

On-chip, we would use another diff amp for this purpose or off-chip, a transformer or balun.

[Refer to gilmix\_GC3 for this example]



Equations are added to the display panel which select the IF frequency, calculate the differential IF output power, convert it to dBm, then subtract the RF input power, also in dBm.

$$\text{conv\_gain} = \text{dBm}(V_{\text{IFout}}^2/(2*RD)) - P_{\text{RF}}$$

$V_{\text{IFout}}$  is the differential output voltage at the IF output frequency. This frequency is selected from the data set using the *mix* function. The downconverted IF at 45 MHz is selected with:

$$V_{\text{IFout}} = \text{mix}(V_{\text{out}}, \{-1,1\}).$$

The indices in the curly brackets are ordered according to fundamental frequencies. Thus,  $\{-1,1\}$  selects RF\_freq – LO\_freq.

Here we can identify the 1 dB gain compression power to be about  $-12$  dBm.

[Refer to ADS example gilmix\_GC3]



## Exercise...



- OK, now its your turn to run a simulation. Modify the schematic file gilmix\_hbGC3 to simulate how  $P_{1dB}$  varies as a function of LO voltage.
- To do this, add a PARAMETER SWEEP controller
- The LO voltage range from 0.05 to 0.25V amplitude will be of interest.

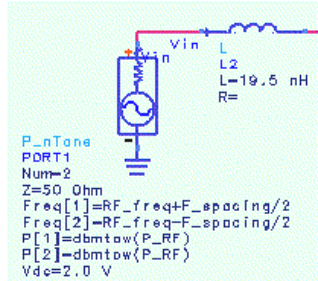


Agilent Technologies

Page 27



## IMD simulation



- Use a two-tone generator at the mixer input.
- The two input frequencies are separated by  $F_{spacing}$  and each have an input power of  $P_{RF}$  dBm.
- A DC offset  $V_{dc}$  is needed to properly bias the RF input.



Page 28

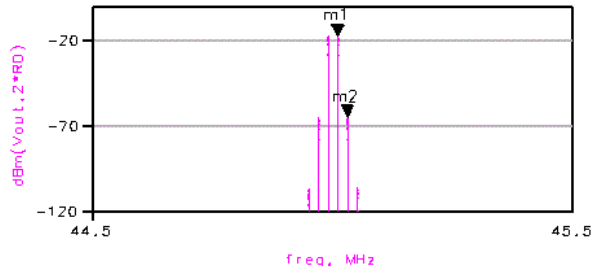
We will be mainly concerned with the third-order IMD. This is especially troublesome since it can occur at frequencies within the IF bandwidth. For example, suppose we have 2 input frequencies at 899.990 and 900.010 MHz. Third order products at  $2f_1 - f_2$  and  $2f_2 - f_1$  will be generated at 899.980 and 900.020 MHz. These may fall within the filter bandwidth of the IF filter and thus cause interference to a desired signal.

Other odd-order products will also be of interest, but may be less reliably predicted unless the device model is precise enough to give accurate nonlinearity in the transfer characteristics up to the  $2n-1^{\text{th}}$  order.

[Refer to ADS file gilmix\_hbTOI3]



## IF output spectrum



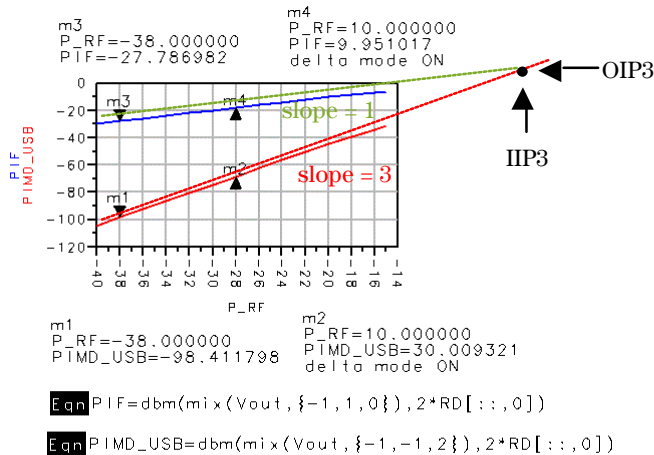
Third-order intermodulation products at  $2f_1 - f_2 - f_{\text{LO}}$  and  $2f_2 - f_1 - f_{\text{LO}}$  will be present in the IF output.



Note that the third-order ( $m_2$ ) and fifth-order products are quite close in frequency to the desired signal ( $m_1$ ). This means that they are often impossible to remove by filtering.



## Third-order intercept definition



Agilent Technologies

Page 30

A widely-used figure of merit for IMD is the third-order intercept (TOI) point. This is a fictitious signal level at which the fundamental and third-order product terms would intersect. In reality, the intercept power is 10 to 15 dBm higher than the  $P_{1dB}$  gain compression power, so the circuit does not amplify or operate correctly at the IIP3 input level. The higher the TOI, the better the large signal capability of the mixer.

It is common practice to extrapolate or calculate the intercept point from data taken at least 10 dBm below  $P_{1dB}$ . One should check the slopes to verify that the data obeys the expected slope = 1 or slope = 3 behavior. When this is true,

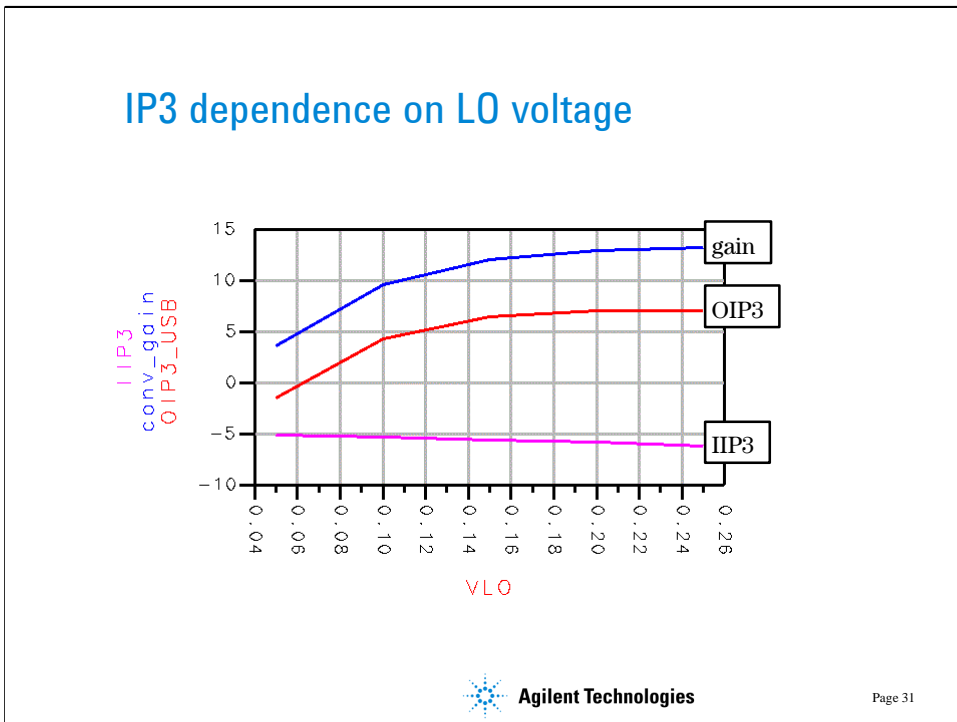
$$\text{OIP3} = (\text{PIF} - \text{PIMD})/2 + \text{PIF}.$$

Also, the input and output intercepts are simply related by the gain:

$$\text{OIP3} = \text{IIP3} + \text{conversion gain}.$$

In the data display above, equations are used to select out the IF fundamental tone and the IMD tone, in this case, the upper sideband. The mix function now has 3 indices since there are 3 frequencies present: LO, RF1 and RF2. The dBm conversion again takes into account the actual differential output load resistance.

The two IMD sidebands should be approximately of equal power if the simulation is correct. If not, increase the order of the LO in the HB controller and see if this makes the sidebands more symmetric.



Agilent Technologies

Page 31

Now we can begin to investigate the third-order intercept (TOI) sensitivity to various design parameters. The LO voltage (amplitude) dependence is shown above. Clearly, it is beneficial to provide sufficient LO voltage to fully switch the upper transistors. The larger voltage decreases the distortion by increasing the slew rate at the switch input. The switch thus spends less time in a nonlinear intermediate state. We reach a point of diminishing returns somewhere around 0.15 to 0.20 V in this case. IIP3 is actually declining because the conversion gain is increasing with VLO. It takes less input power to obtain the output intercept power when gain is higher.

[Refer to ADS file gilmix\_hbTOI3]



## TOI dependence on $R_S$

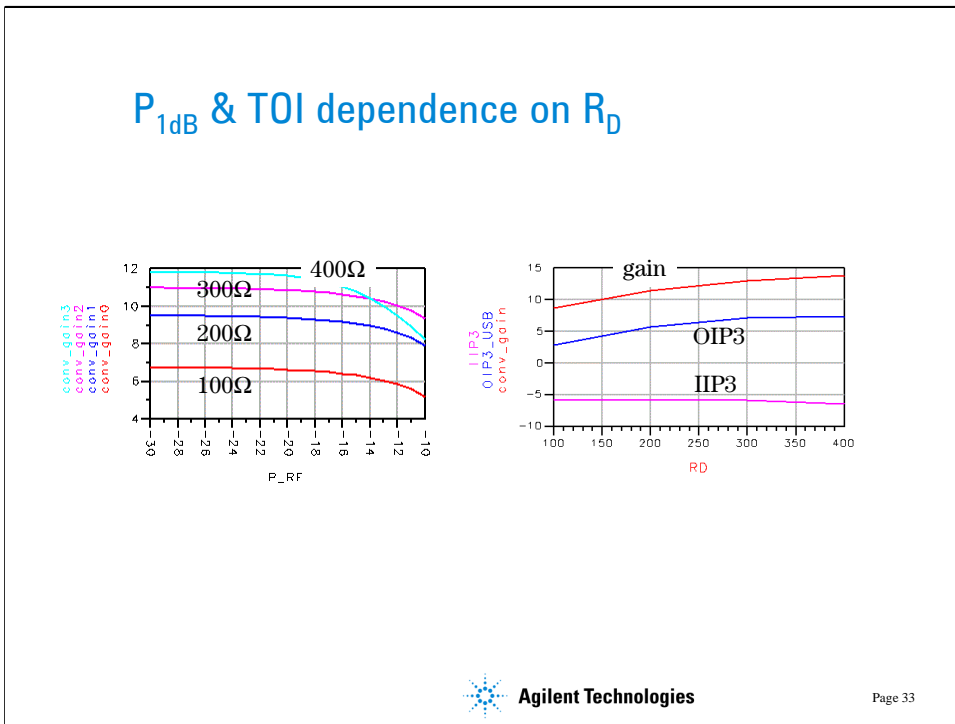
OIP gets worse with  $R_S$

$R_S$	Gain	OIP3	IIP3	Vgate
10 ohms	12.9 dB	7.1 dBm	-5.8 dBm	0.048V
20	13.1	6.0	-7.1	0.061
40	14.3	3.1	-11.2	0.098



Remember our earlier simulations of diffamp gain and linearity vs.  $R_S$ ? We found improvement in the linearity and reduced gain as the source resistance was increased. In fact, this is a standard method for linearizing diffamps! Why isn't it working here? We see quite the opposite trend.

When the input impedance was simulated, we found rapid variation with  $R_S$ . A different input matching network is needed for each  $R_S$  value to provide a conjugate match and maximum transducer gain. As  $R_S$  increases,  $\text{Re}\{Z_{in}\}$  gets smaller, and the voltage on the gate for a given input power increases. We also find the conversion gain increasing. It is this passive gain in the input matching network that is degrading the TOI properties of the mixer. The RF voltage increases more rapidly with  $R_S$  than the inherent gain of the amplifier itself decreases due to feedback.



Another design parameter of interest is the drain resistance,  $R_D$ . Clearly, it will have a big effect on the conversion gain as confirmed above. But, what about TOI? We find that the OIP3 and IIP3 simulation shows steadily increasing intercept power with increased  $R_D$ . Does this make sense? We might expect the higher open-loop gain with large  $R_D$  to suppress distortion, but we would also expect it to degrade the ultimate large signal capability of the mixer as reflected in  $P_{1dB}$ . Indeed, when  $P_{1dB}$  is simulated, we find that the highest  $R_D$  value severely cramps the large signal capability. The upper FETs are running out of headroom at large signal levels. The TOI simulation didn't predict this because it was extrapolating the intercept from low RF input power levels. It never took into account the nonideality that could occur if the biasing of the FETs was not maintained. Thus, to get the complete picture, both simulations are important.

[Refer to ADS files: gilmix\_GC4 and gilmix\_hbTOI4]



## Exercise



- Using the ADS files as templates, simulate the TOI and gain compression of the mixer while varying:
  - $V_{DD}$
  - $I_{bias}$
- Note: when you vary  $I_{bias}$ , you should keep the drain voltage constant by varying the  $R_D$  value. This can be done by defining  $R_D(I_{bias})$  with VarEqn statement in the schematic window. See how much you can improve TOI with larger bias current.



Agilent Technologies

Page 34

You can check your answers with files gilmix\_hbTOI5 and gilmix\_hbTOI7



## Isolation between ports

- The mixer is not perfectly unilateral -  
leakage between:
  - LO to IF
  - LO to RF
  - RF to IF
- Determine the magnitude of these leakage components at the IF and RF ports using the mix function to select frequencies.



Page 35

Isolation can be quite important for certain mixer applications. For example, LO to RF leakage can be quite serious in direct conversion receiver architectures because it will remix with the RF and produce a DC offset. Large LO to IF leakage can degrade the performance of a mixer postamp.



## Isolation between ports

```

Eqn LO2IF=dbm(mix({vout,{1,0,0}},2*RD[0,0])-PLO
Eqn LO2RF=dbm(mix({vin,{1,0,0}}))-PLO
Eqn RF2IF=dbm(mix({vout,{0,1,0}},2*RD[0,0])-dbm(mix({vin,{0,1,0}})))

```

VLO	LO2IF	LO2RF	RF2IF
0.050	-46.010	-174.276	-145.932
0.100	-36.222	-180.604	-138.323
0.150	-31.264	-170.031	-135.508
0.200	-29.297	-145.849	-106.122
0.250	-28.788	-143.350	-99.695

UNREALISTIC !



Agilent Technologies

Page 36

The excellent isolation between ports on double balanced mixers depends on precise balance. The simulation is using ideal components that are perfectly matched and gives grossly optimistic estimates of LO2RF and RF2IF isolation. In real implementations, the MOSFETs and resistors may have slight variations in their parameters that could unbalance the mixer enough to degrade performance.



## Isolation with imbalance

- Imbalance in  $R_D$  is added:  $R_D \pm \Delta R_D$
- $V_{LO} = 0.20V$

DRD	LO2IF	LO2RF	RF2IF	percent
5.000	-29.298	-75.699	-59.372	1.667
10.000	-29.301	-69.678	-53.340	3.333
15.000	-29.304	-66.154	-49.807	5.000
20.000	-29.309	-63.654	-47.296	6.667
25.000	-29.316	-61.713	-45.342	8.333



Page 37

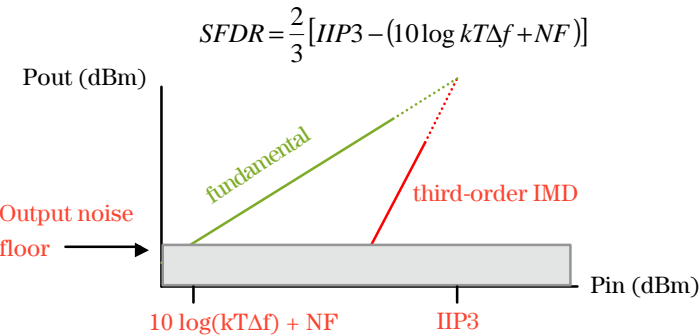
The drain resistors are intentionally skewed by an offset resistance  $\Delta RD$  to illustrate the sensitivity of LO2RF and RF2IF isolation to imbalance. The predictions become more realistic.

[See ADS file gilmix\_iso]



## Noise figure & SFDR

- We have been concentrating on the large signal limitations of the mixer. Noise determines the other end of the mixer dynamic range.
- Spurious-free dynamic range:



 Agilent Technologies

Page 38

Noise figure is defined as the ratio between the input and output S/N ratio.

$$NF (\text{dB}) = 10 \log[(S/N)_{in}] / [(S/N)_{out}]$$

Any real mixer or amplifier will degrade S/N because noise is added to the signal. The minimum input signal power is determined by noise. The noise is represented by a NF.

The maximum signal power is limited by distortion, which we describe by IIP3. The SFDR is a commonly used figure of merit to describe the dynamic range of an RF system. If the signal power is increased beyond the point where the IMD rises above the noise floor, then the signal-to-distortion ratio dominates and degrades by 3 dB for every 1 dB increase in signal power. If we are concerned with the third-order distortion, the SFDR is calculated from the geometric 2/3 relationship between the input intercept and the IMD.

It is important to note that the SFDR depends directly on the bandwidth  $\Delta f$ . It has no meaning without specifying bandwidth.



## Determining Noise Figure

- Use harmonic balance simulator for mixer NF.
  - takes into account any nonlinearities and harmonics that could mix noise down into the IF band.
  - If  $P_{RF} \ll P_{LO}$ , either a 1-tone generator or a passive termination can be used at the input with equal accuracy.
  - Noise Figure is calculated.
    - Ideal filter (centered on RF) is added in simulation.
    - Noise contributions within mixer added.
    - $NF = 5.7 \text{ dB}$ .
    - $SFDR = 112 \text{ dB}$  (with 100 kHz BW).



The harmonic balance simulator will take into account wideband noise that is generated in the mixer. Some of this noise gets mixed down to the IF frequency from the harmonics of the LO. If the RF signal is of small amplitude, the harmonics that it might generate can be neglected, and either a 1-tone generator or a passive termination can be used. The predictions will be the same.



## Final mixer specs



- IIP3 = - 6 dBm
- P<sub>1dB</sub> = - 12 dBm
- Conversion gain = 13 dB
- NF = 5.7 dB
- SFDR = 112 dB (100 kHz BW)
- Power dissipation = 20 mW



Agilent Technologies

Page 40

Here are the final mixer performance specifications that have resulted from this example. We have clearly not exhausted the design space, and there are many other factors that could be considered that might have further influence on the results.

In the next slide, there is a list of other circuits that we should also include if time permitted.



## What's next?



- We would also need to design:
  - LO buffer for single-ended to differential
  - IF buffer for differential to single-ended
  - biasing for the RF and LO inputs



Agilent Technologies

Page 41



## Conclusion



### Learning objectives:

- Understand operation of MOSFET Gilbert mixer
- Biasing considerations
- Design for stability, linearity and noise
- Specify performance: NF,  $P_{1\text{dB}}$ , TOI, SFDR

### Further resources:

- Now, go through the ADS example files, modify them for your application. Use them as templates for your own design work.



Agilent Technologies

Page 42



## References



- [1] Gray, P. R. and Meyer, R. G., *Design of Analog Integrated Circuits*, 3rd Ed., Chap. 10, Wiley, 1993.
- [2] Gilbert, B., "Design Considerations for BJT Active Mixers", *Analog Devices*, 1995.
- [3] Lee, T. H., *The Design of CMOS Radio-Frequency Integrated Circuits*, Chap. 11, Cambridge U. Press, 1998.



Page 43

## References

- [1] Gray, P. R. and Meyer, R. G., *Design of Analog Integrated Circuits*, 3rd Ed., Chap. 10, Wiley, 1993.
- [2] Gilbert, B., "Design Considerations for BJT Active Mixers", *Analog Devices*, 1995.
- [3] Lee, T. H., *The Design of CMOS Radio-Frequency Integrated Circuits*, Chap. 11, Cambridge U. Press, 1998.



End of Design Seminar...



Agilent Technologies

Page 44

**Stephen Long**  
Professor, Electrical and Computer Engineering,  
University of California, Santa Barbara

## RFIC Mixer Design with ADS



## About the Author



**Steve Long**

- University of California, Santa Barbara
- Professor, Electrical and Computer Engineering

### BIOGRAPHICAL SKETCH

Stephen Long received his BS degree in Engineering Physics from UC Berkeley and MS and PhD in Electrical Engineering from Cornell University. He has been a professor of electrical and computer engineering at UC Santa Barbara since 1981. The central theme of his current research projects is rather practical: use unconventional digital and analog circuits, high performance devices and fabrication technologies to address significant problems in high speed electronics such as low power IC interconnections, very high speed digital ICs, and microwave analog integrated circuits for RF communications. He teaches classes on communication electronics and high speed digital IC design.

Prior to joining UCSB, from 1974 to 1977 he was a Senior Engineer at Varian Associates, Palo Alto, CA. From 1978 to 1981 he was employed by Rockwell International Science Center, Thousand Oaks, CA as a member of the technical staff.

Dr. Long received the IEEE Microwave Applications Award in 1978 for development of InP millimeter wave devices. In 1988 he was a research visitor at GEC Hirst Research Centre, U.K. In 1994 he was a Fulbright research visitor at the Signal Processing Laboratory, Tampere University of Technology, Finland and a visiting professor at the Electromagnetics Institute, Technical University of Denmark. He is a senior member of the IEEE and a member of the American Scientific Affiliation.

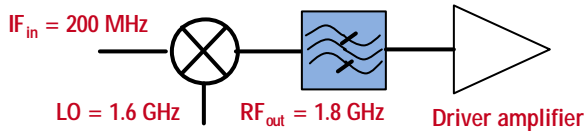
## Motivation – Why ADS for RFIC mixer design?

- Mixer DesignGuide provides analysis tools for:
  - DC, RF spectrum, impedance matching, gain, gain compression, N\_db compression, IMD and TOI, noise figure, dynamic range, ACPR
  - Parameter, frequency, RF and LO power sweeps
  - Library of mixer examples
- Speeds up learning curve for ADS –
  - Become effective more quickly
  - Set up complicated simulations that would take days to prepare in a few minutes

The mixer DesignGuide is intended to enhance productivity of RF designers by providing an extensive collection of analysis tools that can be easily loaded into your project from a pulldown menu. Each pair of these analysis network and displays, which could take days to set up and verify, can be easily adapted for your mixer circuit simulation requirements.

## Introduction

- Design sequence very dependent on application
  - Upconversion application selected as example: base station
  - Gilbert cell MOSFET double-balanced differential mixer



- 0.35 mm CMOS process; 3.3 volt supply
- Design for largest dynamic range
- Convert to single-ended output

RFIC Mixer Design with ADS  
19 April, 2001



Page 4

A transmit mixer application is selected to illustrate a design procedure that is enabled by the Mixer DesignGuide. The input baseband or IF signal is centered at 200 MHz. The output is at 1.8 GHz. We will assume that the mixer is intended for a base station power amplifier application.

The mixer will use 0.35  $\mu$ m MOSFETs with a default device model parameter set. Of course, you will need to substitute your own verified MOSFET model parameters for the default set. Otherwise, there would be no hope of any correspondence between simulation and measurement for the mixer characteristics that are more sensitive to model nonlinearities. This would especially be true for intermodulation simulations and noise.

## Learning Objectives:



*Design a high dynamic range mixer for transmit applications*

- Learn how to make use of the Agilent ADS Mixer DesignGuide
- Understand the important design and analysis tools for this application
- Specify performance: Gain, NF, P<sub>1dB</sub>, TOI, Dynamic Range
- Improve the design: add resonator and convert to single-ended output

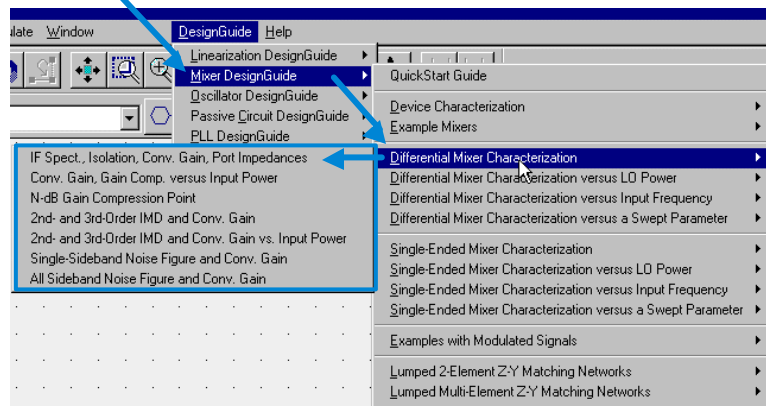
[Always see the NOTES pages for additional information throughout...](#)

There are many different performance specifications for mixers. Some are of interest for receive applications where the input signal level is not under the control of the designer. In this case, the maximum linearity under large signal drive conditions is often very critical. Noise figure may be of secondary concern.

For the transmit application used here as an illustration, the designer has control of the signal level. Then, the design strategy shifts to trading off noise and IMD behavior in order to achieve the largest useable dynamic range.

As an extra illustration, after the intrinsic mixer performance is evaluated, the design will be modified to improve conversion gain and image rejection by tuning the mixer output. Secondly, a differential-to-single ended converter will be added to interface to an off-chip bandpass filter.

## Using the ADS Mixer DesignGuide: First, select the analysis type...



RFIC Mixer Design with ADS  
19 April, 2001

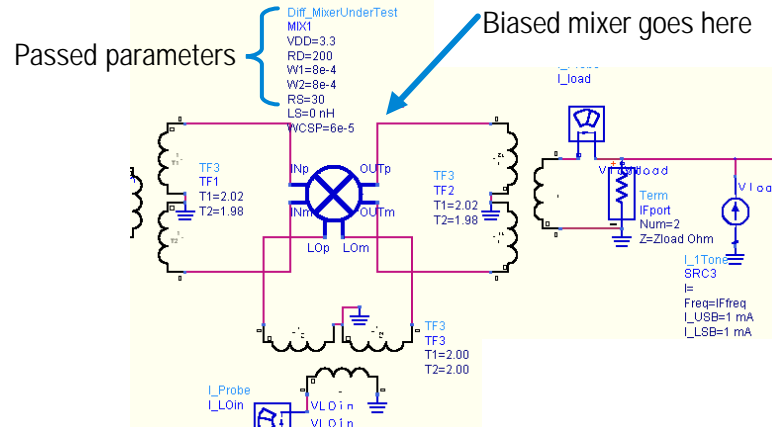
 Agilent Technologies

Page 6

The analysis tools are accessible by the DesignGuide pulldown menu. Select Mixer DesignGuide, then scroll through the list to find the relevant analysis. Then, the schematic and display panels will be loaded into your project.

## Differential Mixer Test Bench Example

Proceed by replacing the default mixer circuit with your mixer  
Set parameters and select the analysis schematic template  
from the DesignGuide pulldown menu.



RFIC Mixer Design with ADS  
19 April, 2001



Page 7

The mixer under test is constructed as an ADS subnetwork. The mixer itself can be replaced with or modified to become your own design. Select the mixer, push down into the subnetwork, and replace the circuit with your own design. If you use the Diff\_MixerUnderTest as your subnetwork, and insert your design, the design is automatically inserted into all of the analysis circuit templates. Or, you can save your design under a different name, select it using the component library icon on the toolbar, and replace the default mixer with your own.

You can declare any of the circuit parameters to be accessible outside of the subnetwork by using the File > Design Parameters panel. In this example, VDD, RD (drain resistance), WCSP (current source control width), W1 and W2 (transconductance and switch MOSFET widths), and source degeneration resistance (RS) and inductance (LS) are all available for a parameter sweep.

## Set up the simulation conditions

- Set variables and simulation controller sweep range

```
VAR
R2
LOfreq=1600 MHz
RFfreq=200 MHz
P_RF=-30
Zload=400+j*0
Set the following parameters:
1) LO frequency, LOfreq
2) Input frequency, RFfreq
3) Input power, P_RF
4) Load impedance, Zload

HB1
MaxOrder=14
Freq[1]=LOfreq
Freq[2]=RFfreq
Order[1]=11
Order[2]=3
SS_MixerMode=yes
SS_Freq=1.0 kHz
UseKrylov=yes
}
} Set Order for the LO and RF inputs

SweepVar="P_LO"
Start=0
Stop=6
Step=1
Set the range of values
for the LO power sweep
Mix_Diff(CG)_LoSwp
```

RFIC Mixer Design with ADS  
19 April, 2001



Page 8

You then will configure the simulation controller, HB in this example, with the appropriate parameters.

Order[1] number of LO harmonics - should be large for switching mixers

Order[2] number of harmonics at the mixer signal input - small if input amplitude is small; larger if you are simulating the mixer near the 1 dB compression point

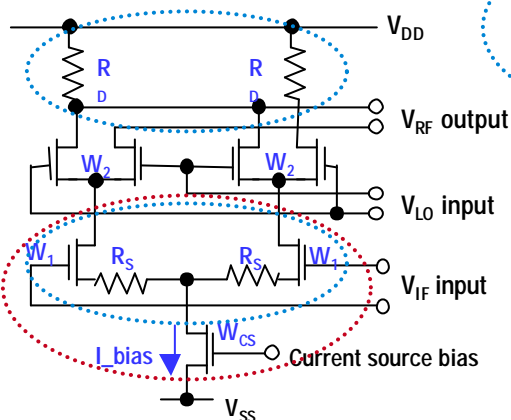
MaxOrder maximum sum of the LO and Input harmonics considered in the solution. Generally, you would use the sum: Order[1]+Order[2]

SweepVar: This is the swept parameter, in this example the LO power. Set the range and step size used for the simulation.

Note that the data file size will increase with the order and with the number of sweep steps.

## Gilbert cell double-balanced mixer

### Up conversion application example



### Trade-offs:

Conversion gain,  
Gain compression,  
Bandwidth

Noise figure

RFIC Mixer Design with ADS  
19 April, 2001

Agilent Technologies

Page 9

We will utilize the DesignGuide mixer library as a starting point for the design exercise. This is a schematic of a MOSFET version of the Gilbert active double-balanced mixer. The lower FET diff pair serves as a transconductance amplifier. The upper FETs provide a fully balanced, phase-reversing current switch. A DC bias generator is included (not shown) which will keep the MOSFETs in their active region.

The large signal handling capability of the mixer will depend mainly upon the linearity of the transconductance amplifier, and is measured by determining the maximum input voltage (or power in some cases) that causes a 1 dB compression in the conversion gain. The maximum linear input voltage range can be increased by increasing the source degeneration resistors,  $R_S$ . While source inductance can also provide beneficial degeneration, in this case, we have a very low input IF frequency, 200 MHz. The inductance values required would be too large for RFIC implementation, thus we are stuck with the resistors (they will add noise). The load resistors could also cause gain compression if the voltage swing at the drains is large enough to cause the output to clip under large signal drive conditions.

The double-balanced design rejects IF and LO feedthrough to the output if the output is taken differentially. This is because the LO component in the output is a common mode signal while the RF output is differential.

For a more complete explanation of how the Gilbert cell mixer operates, refer to the reference list at the end of this presentation.

## Design procedure

The example design sequence is suited for an upconversion mixer. Our goal is to increase dynamic range. Conversion gain and matching are not as critical.

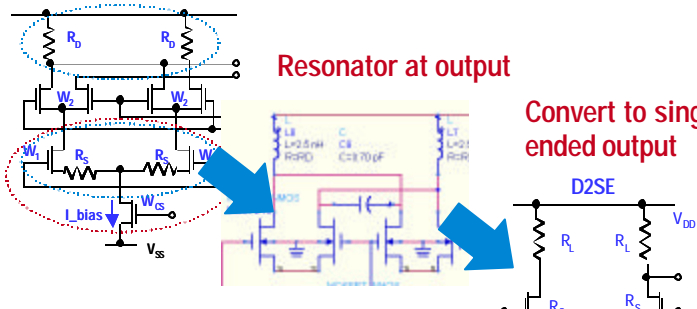
1. LO amplitude: Conversion gain,  $V_{in}$  at 1 dB gain compression
2. Gain Compression: source resistance  $R_s$ , drain resistance,  $R_d$
3. Noise figure:  $R_s$ ,  $I_{bias}$
4. Dynamic Range vs. Input Voltage
5. Spectral spreading and ACPR with digital modulation

A mixer that is to be used for base station transmit applications requires high linearity and low noise so that the least amount of spurious power is spread into the adjacent channel. We will optimize our mixer in the following sequence:

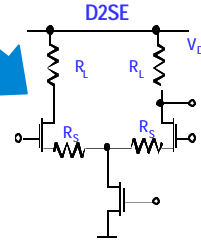
1. LO amplitude. You want to make sure the mixer commutating switch is fully activated. Excess distortion can be produced with a weakly conducting or slowly activated switch. Use the conversion transducer gain and 1 dB gain compression input level to determine when the LO voltage is sufficient.
2. Evaluate the influence of source and drain resistance on the 1 dB compression level. This will give insight into the principal mechanisms that limit linearity.
3. The added noise of the mixer will affect the minimum signal level and thus limit dynamic range. There will be a tradeoff between noise, gain, and gain compression.
4. The two-tone 3rd order intermodulation distortion power and the noise figure determine the mixer dynamic range vs. input voltage. Since for transmit applications you have complete control over your input voltage, find the optimum dynamic range - the mixer's "sweet spot" for best performance. Or, alternatively, if you have a fixed signal level, design the mixer to provide the best dynamic range at that signal level.
5. Finally, test the mixer under more realistic signal excitation - using a CDMA source, for example, to emulate a multicarrier environment. This is a more severe test than the two-tone IMD one, and is much more time consuming to simulate since a large number of symbols must be used for accurate results.

## Design sequence

### Gilbert cell - resistively loaded



Convert to single-ended output



*Let's get started!*

RFIC Mixer Design with ADS  
19 April, 2001

Agilent Technologies

Page 11

Once the basic resistively loaded Gilbert cell mixer is characterized, two modifications will be employed to improve performance. First, the mixer drain nodes will be tuned with inductors and a capacitor for resonance at the output frequency. This improves conversion gain if inductors with reasonable Qu can be fabricated. It also decreases the amplitude of the undesired output image because of its bandpass transfer function. The image must be removed anyway, and its presence can only degrade the distortion of the output stage by increasing the peak voltage present at its input.

The output of the mixer will need to be filtered off-chip with a SAW filter before further amplification, so a single ended output is more efficient. The last stage is added to perform a differential to single ended conversion. It must have good common mode rejection to suppress LO feedthrough and good linearity so that it doesn't degrade dynamic range.

## 1. Determine LO voltage: Conversion gain & gain compression

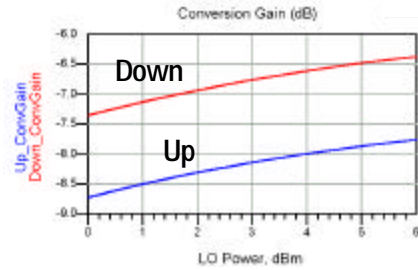
- Sweep LO power

Sweep parameters  
Sweep plan "P\_LO"  
Start=0  
Stop=6  
Step=1  
Set the range of values  
for the LO power sweep  
Mix\_DIFF\_CG\_LOwp

Differential Mixer Characterization versus LO Power

Isolation, Conv. Gain, Port Impedances

N-dB Gain Compression Point



LO Power dBm	LO voltage @ LOfreq	1.0 dB gain compression input power level (dBm)	Conversion gain
0.000	0.589 / -22.529	-6.825	-9.721
2.000	0.743 / -21.791	-6.891	-9.306
4.000	0.938 / -21.168	-6.924	-8.993
6.000	1.182 / -20.857	-6.957	-8.753

RFIC Mixer Design with ADS  
19 April, 2001



Page 12

The first step is to determine a suitable LO voltage that provides a reasonable compromise between conversion gain and LO power and at the same time does not limit the 1 dB gain compression input voltage. The MOSFETs forming the commutating switch (upper level) must be driven hard enough to present a low series resistance to the load. Most of the mixer analysis schematic and display templates available in the DesignGuide library include an LO power sweep capability. Use the menu as shown to select a conversion gain simulation as a function of LO power. Also, a NdB Gain Compression analysis can be used to evaluate the dependence of gain compression on LO drive.

From these simulations, we see that the input power at which gain compresses by 1 dB (P1dB) is not a strong function of LO voltage, but conversion gain is somewhat dependent. The more gate voltage applied to the upper tier of MOSFETs, the lower their series resistance relative to the drain resistance and thus the higher the conversion gain. We also can see that there is a conversion loss which gets worse at the higher output RF frequency of 1.8 GHz, but we can improve on this later by tuning the RF output of the mixer.

## 2. $V_{1dB}$ dependence on $R_S$ , $R_D$

Differential Mixer Characterization versus a Swept Parameter

N-dB Gain Compression Point

- We can see a strong dependence of gain compression on  $R_S$
- $R_D$  has little effect on compression, so limiting is occurring at the input

Swept Parameter	1.0 dB gain compression input (dBm)	input (Volts)	Conversion gain	Nearly constant output (Volts)
$R_S$	10.000	-11.118	0.172 / -2.405	-4.969
	20.000	-8.738	0.227 / -2.116	-6.935
	30.000	-7.007	0.277 / -1.928	-8.500
	40.000	-5.386	0.334 / -1.780	-9.879
Swept Parameter	1.0 dB gain compression input (dBm)	input (Volts)	Conversion gain	output (Volts)
$R_D$	100.000	-7.007	0.277 / -1.928	-8.500
	200.000	-7.007	0.277 / -1.928	-9.110
	300.000	-7.007	0.277 / -1.928	-10.313

RFIC Mixer Design with ADS  
19 April, 2001

Agilent Technologies

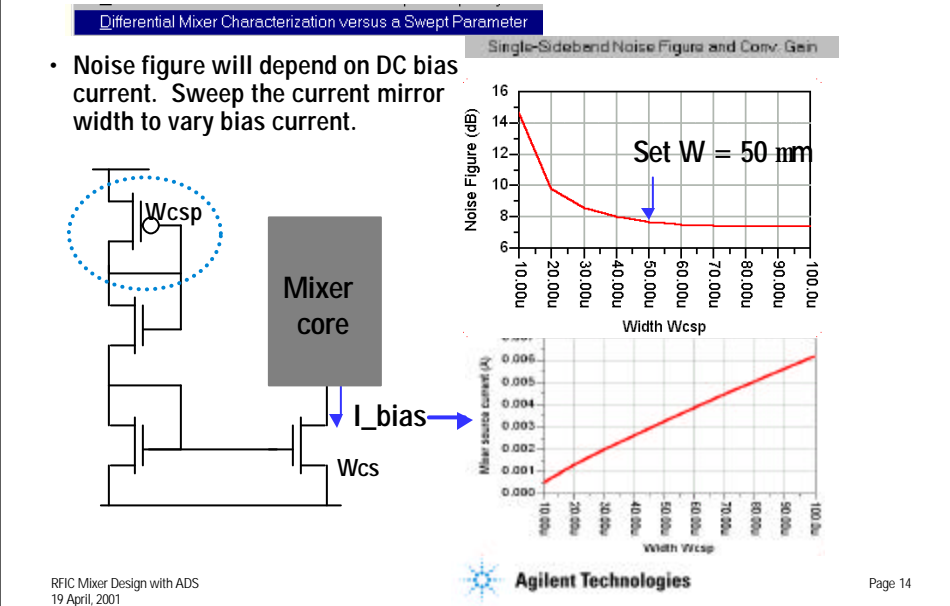
Page 13

Gain compression is evaluated using the N-dB Gain Compression Point analysis schematic. The 1dB gain compression input power and input voltage are found for swept parameters. In this case, the influence of  $R_S$  and  $R_D$  on  $V_{1dB}$  was determined. The  $R_S$  sweep used  $R_D = 100\Omega$ . The  $R_D$  sweep set  $R_S = 30\Omega$ . Conversion gain is measured at the 1 dB compressed level. Alternatively, a two-dimensional sweep could also be set up using an extra Parameter Sweep controller.

In an RFIC mixer where the input might not be matched to a source impedance, the input voltage is a more important metric of gain compression than the input available power ( $P_{1dB}$ ) since available power assumes a conjugately matched source and load. Also, in a multi-signal environment, the peak input voltage can be quite large at the instant in time when all signals add in phase. It is this peak voltage that determines the distortion limits of the mixer. For example, the two-tone IMD simulations will predict a 1 dB compression power 6 dB lower than single tone simulations because the peak voltage will be twice as high for the same power per tone.

It is also interesting to note that the conversion power gain depends inversely on  $R_D$ . In the simulation, the external load resistance was set to  $2 R_D$  so that the output power (power absorbed in the load) is also the available output power,  $P_{out} = V_{out}^2 / 4R_D$ . The voltage gain would be expected to follow  $R_D/R_S$  but increases less rapidly than anticipated, probably due to the output RC time constant bandwidth limitations.

### 3a. Noise Figure dependence on I\_bias



We can simulate the mixer single-sideband noise figure as a function of DC bias current through the Gilbert cell (mixer core). The DC current is varied by sweeping the width of the PMOS current source  $W_{csp}$  and the mixer current mirror width  $W_{cs}$  using a parameter sweep.

SSB noise figure is appropriate because only one input frequency is applied to the mixer, but wideband noise at the image frequency and from LO harmonics is included in the signal to noise calculation. We find that the NF is reduced with increasing  $I_{bias}$ , but reaches a point of diminishing returns. Thus, a width of 50  $\mu\text{m}$  was selected as a compromise between power and noise.

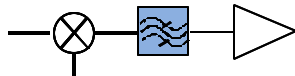
The device widths in this mixer have been selected to minimize noise [3].

### 3b. Noise Figure dependence on $R_s$

- The noise figure will also be strongly affected by  $R_s$ .

Swept Parameter Value	Noise Figure, dB	Down Conversion Gain, dB	Up Conversion Gain, dB
10.00	6.48	-2.55	-3.18
20.00	7.97	-4.71	-5.35
30.00	8.22	-8.43	-7.07
40.00	10.80	-7.88	-8.60

- We find that we must trade off NF and V1dB. This will influence dynamic range



- Noise floor = MDS =  $-174 \text{ dBm/Hz} + 10 \log \text{BW} + \text{NF}$
- Conversion gain is also varied, and may affect input referred noise

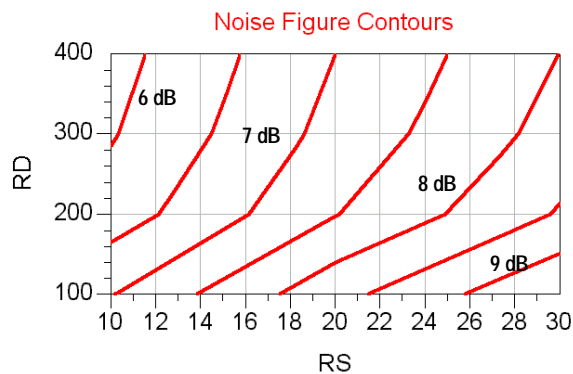
We also find a strong dependence of SSB NF on the source resistance. This is expected because the thermal noise contributed by the resistor is directly in the input voltage loop of the differential pair. Thus, we will need to trade off V1dB and noise figure to obtain the largest dynamic range of the mixer.

The dynamic range at low input signal power levels will be limited by the carrier to noise ratio. The noise power for a minimum detectable signal ( $S/N = 1$ ) depends on both NF and the noise bandwidth. This bandwidth will normally be set by an external SAW filter between the mixer and the driver amplifier. The filter is also required to reject the output difference ( $F_{LO} - F_{IN}$ ) image frequency at 1.4 GHz.

The conversion gain (a loss in this case) may also increase the noise figure because the drain resistor thermal noise is input referred through the gain. Thus, we will also want to investigate a tuned output to eliminate some of this noise.

### 3c. Noise Figure dependence on $R_S$ , $R_D$

- You can perform a two parameter sweep and plot contours of noise figure.



RFIC Mixer Design with ADS  
19 April, 2001

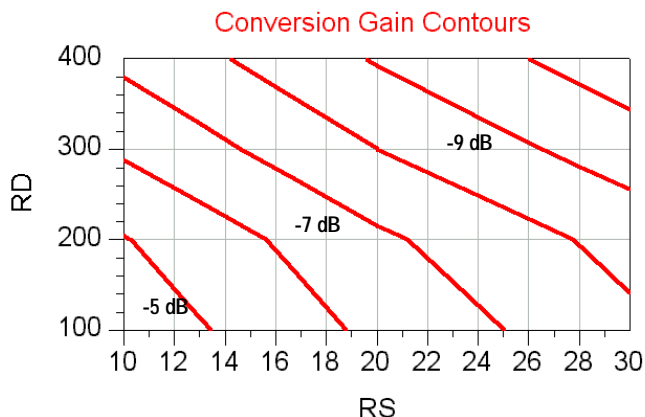


Page 16

You can also perform a two parameter sweep by selecting a second Parameter Sweep controller. In this example, the variation in noise figure with RS and RD that was displayed in tables on the previous slide can now be plotted as constant NF contours using the contour function in the function library.

### 3d. Up Conversion Gain dependence on $R_S$ , $R_D$

- And also a contour plot for conversion gain:



RFIC Mixer Design with ADS  
19 April, 2001

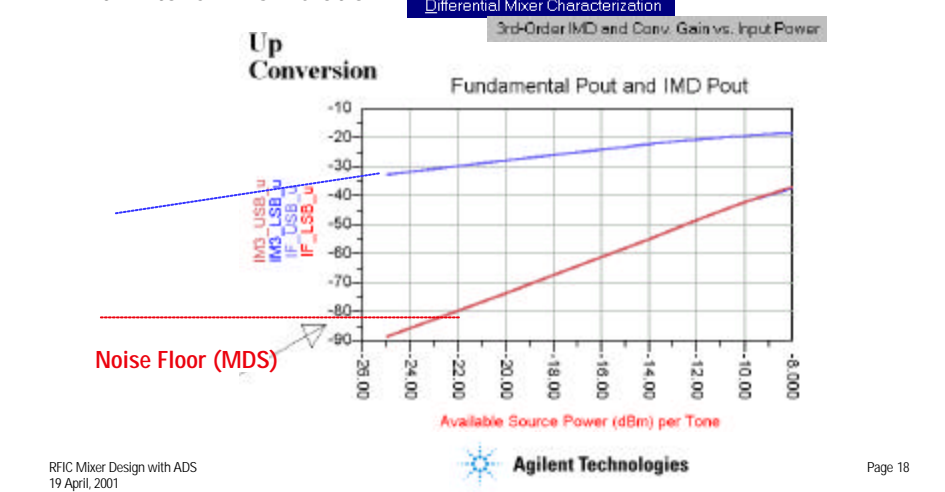


Page 17

You can do the same thing with the conversion gain data.

#### 4a. Carrier to IMD ratio

- Both carrier/noise and carrier/IMD can limit dynamic range
- Determine the 3<sup>rd</sup> order IMD power vs. input voltage or power with 2-tone HB simulation.



At higher input signal levels, the dynamic range of the mixer is limited by the distortion. The third-order intermodulation distortion products are the most damaging because they show up in-band and cannot be rejected by the filter.

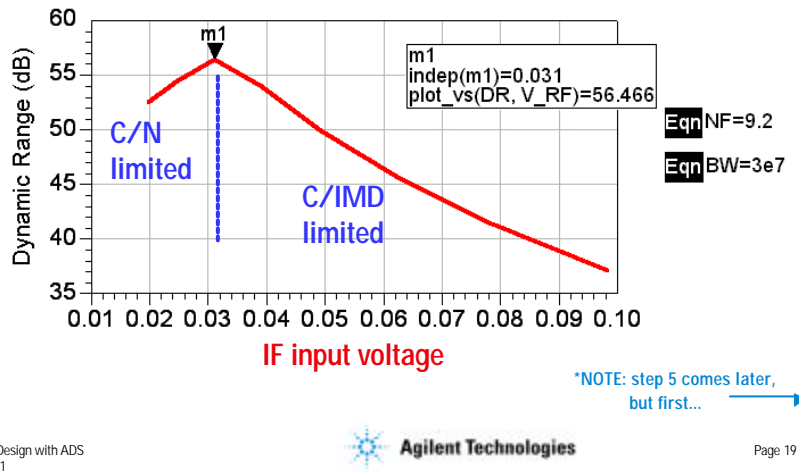
A two-tone third-order IMD simulation with an RF power sweep can be used to display the carrier-to-IMD power ratio. The IMD power present in the output will increase at 3 times the rate of increase of input power. Thus, the difference between output power and IMD power shrinks with increasing input.

At low input signal levels, the noise floor, set by the mixer noise figure and the noise bandwidth of the mixer-bandpass filter-amplifier cascade, will set a lower limit to the output power from the mixer. The dotted lines above show this noise floor in red. The blue dotted line represents the mixer output power vs. RF input power at this lower input regime. It has a slope of 1. You can see that the difference between output power and noise floor shrinks as the power decreases.

The maximum dynamic range is found at the inflection point.

## 4b. Calculate dynamic range vs input voltage

- Combine data from IMD RF power sweep and SSB NF simulations
- Plot dynamic range for  $R_S = 30W$



RFIC Mixer Design with ADS  
19 April, 2001

Agilent Technologies

Page 19

Here, we have taken outputs from two simulations: IMD RF power sweep and the SSB NF. The dynamic range is controlled by the least of these two conditions:

$$DR = P_{out} (\text{dBm}) - MDS (\text{dBm}) \quad \text{for low input levels} \\ (\text{noise limited})$$

$$DR = P_{out} (\text{dBm}) - PIMD (\text{dBm}) \quad \text{for higher input levels} \\ (\text{distortion limited})$$

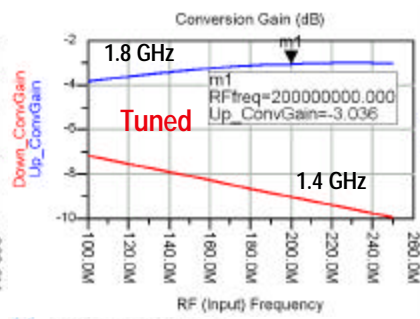
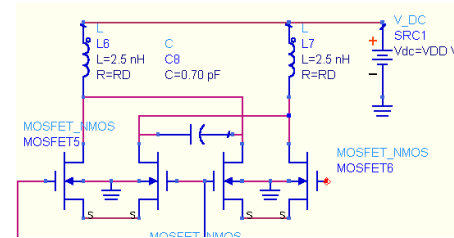
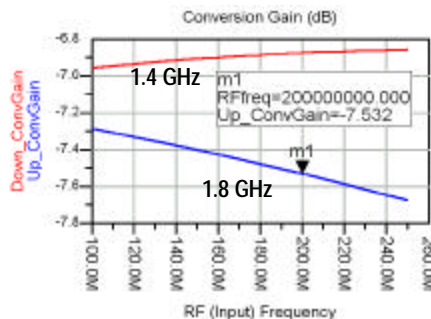
$R_S$	DR (dB)	$V_{in}$ (V)	NF (dB)
(differential)			
10	57.7	0.017	6.5
20	57.3	0.025	8
30	56.4	0.031	9.2
40	56.0	0.039	10.3

The dynamic range peak will depend on the noise bandwidth. For narrower bandwidths, the noise floor will drop and the peak DR will increase but shift to lower differential input voltage. The 30 MHz noise bandwidth was chosen because of the base station application. The transmitter should be capable of covering an entire frequency band.

## Improve mixer conversion gain and noise figure

- Tune the output of the mixer
  - Absorb capacitance
- Frequency sweep

### Resistive load



RFIC Mixer Design with ADS  
19 April, 2001

Agilent Technologies

Page 20

The low conversion gain of the resistively loaded mixer will cause higher noise due to the drain resistors. By resonating the output at 1.8 GHz, the conversion gain is increased and the gain at the image (1.4 GHz) is reduced. The comparison between the resistive loaded case and the tuned case shows an increase in conversion gain by about 3.5 dB.

You can perform an RF frequency sweep to find the resonant frequency. From that, you can calculate how much capacitance is contributed by the drain-to-substrate junction and absorb it into the resonator.

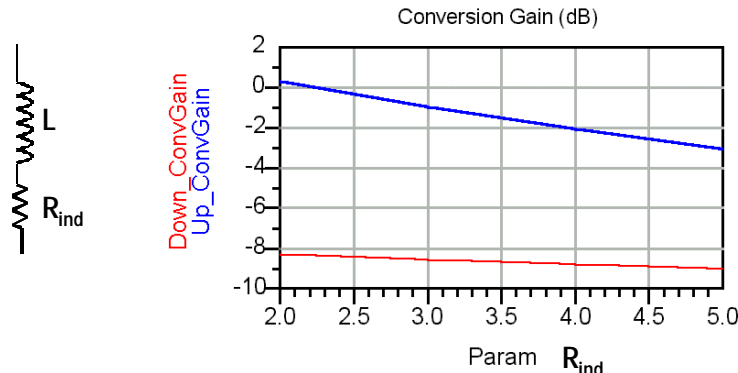
An unloaded Q = 5 is assumed for the inductor.

## Gain reduction due to inductor Q

Differential Mixer Characterization versus a Swept Parameter

Isolation, Conv. Gain, PortImpedances

- We do find, however, that the gain is sensitive to the unloaded Q of the inductor.  $R_{ind}$  represents the series resistance of the inductor.
- Q unloaded is varied from 12 down to 5.



RFIC Mixer Design with ADS  
19 April, 2001

Agilent Technologies

Page 21

On chip inductor Q is limited by metal losses and substrate conduction in bulk silicon processes. An ordinary digital IC process will produce low Qu in spiral inductors. CMOS or BiCMOS RFIC processes can achieve higher Q inductors by using thicker dielectrics and thicker metal. Q values in the range of 5 to 15 are typical.

The low conversion gain is also due in both cases to an unmatched input. We will consider this later.

## Tuned output - noise figure

Differential Mixer Characterization versus a Swept Parameter

Single-Sideband Noise Figure and Conv. Gain

- The noise figure is reduced by about 0.5 to 1 dB when the output of the mixer is tuned. Again, this depends on the inductor Q.

Swept Parameter Value	Noise Figure, dB	Down Conversion Gain, dB	Up Conversion Gain, dB
20.00	7.00	-6.74	1.42
30.00	8.08	-8.38	-0.22
40.00	9.01	-9.75	-1.59

RFIC Mixer Design with ADS  
19 April, 2001



Page 22

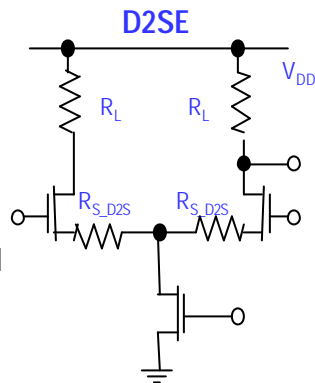
RD = 2.5 RL = 400

Unfortunately, for realistic unloaded inductor Q values (on bulk Silicon) of the order of 5, the benefits of tuned output are diminished. The conversion gain is improved by about 4 dB and the noise figure by only 0.5 dB. There would be much more benefit on a CMOS RF Analog, SOI or GaAs processes where higher Q values can be obtained.

Having said that, we will continue to evaluate the tuned solution.

## Active Balun: differential to single-ended RF out

- Connect differential amplifier stage to output of tuned mixer.
- Choose either direct output as shown (with off-chip load resistor) or use a source follower.
- Size the MOSFETs according to the output current and voltage required. Their input capacitance can be absorbed in the mixer tank circuit.
- Determine  $R_{S\_D2S}$  so that the D2SE block does not degrade the dynamic range.



RFIC Mixer Design with ADS  
19 April, 2001

 Agilent Technologies

Page 23

The next step will be to convert the RF output from a differential signal to single-ended with an active balun. You must perform this conversion rather than just taking one output from the mixer because the mixer differential output is necessary for rejection of LO feedthrough. Since we need a SAW filter between the mixer output and the driver stage, a single-ended output is sufficient. While passive baluns can be made for 1.8 GHz, we will benefit in cost and size by placing an active balun on-chip. This differential amplifier stage is used to convert the differential output of the tuned mixer to a single output. The gate capacitances of the D2SE stage can be absorbed into the resonator at the mixer drain nodes. The D2SE stage must also be designed so that it does not dominate the IMD generation of the mixer.  $R_{S\_D2SE}$  can be adjusted to set the  $V_{1dB}$  level.

The output driver could use an off-chip load resistor with open drain output connection as suggested by the circuit simulated here. The load resistance will probably be determined either by the filter impedance or by transmission line impedance. The bias current for the D2SE converter stage will be dictated by this impedance level. The device widths must also be chosen so that they can handle the necessary drain current and provide adequate voltage gain. The addition of a source follower to the output is another option.

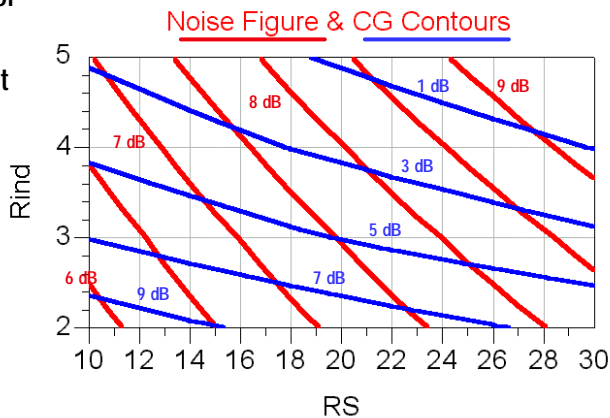
## Evaluate mixer with D2SE stage

- First simulate with differential mixer analysis tools to compare with resistively loaded and tuned mixer performance
  - Noise figure and conversion gain
  - IMD and dynamic range
- Then, adapt single-ended (SE) mixer analysis tools from the DesignGuide to evaluate with SE input and output

For the initial design evaluation, we will continue to measure the differential output so that comparisons can be made between the differential tuned mixer and the mixer with output buffer. Then, the mixer will be evaluated in a single-ended configuration.

## Noise Figure and Conversion Gain Contours

- Large dependence of gain and NF on RS
- Gain very dependent on Rind



RFIC Mixer Design with ADS  
19 April, 2001

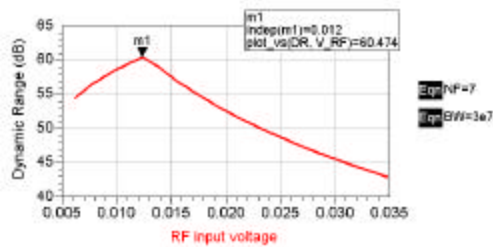
 Agilent Technologies

Page 25

The SSB noise figure simulation is performed again with parameter sweeps for RS and Rind. We can see that there is little noise sensitivity to Rind, however, it strongly affects the conversion gain. RS affects both NF and conversion gain and it also will also affect the carrier-to-IMD ratio vs. IF input voltage.

## Dynamic range simulations

- Dynamic range vs. RS of mixer.  $R_{ind} = 5 \text{ W}$
- Noise figure dominates over the IMD behavior at this bandwidth since DR improves with smaller RS
- Dynamic range also improves with reduction in  $R_{ind}$ .



RS	NF (dB)	DR (dB)	Vin (mV)
10	7	60.5	12
20	8.5	59.8	17
30	9.7	59.2	22

RFIC Mixer Design with ADS  
19 April, 2001

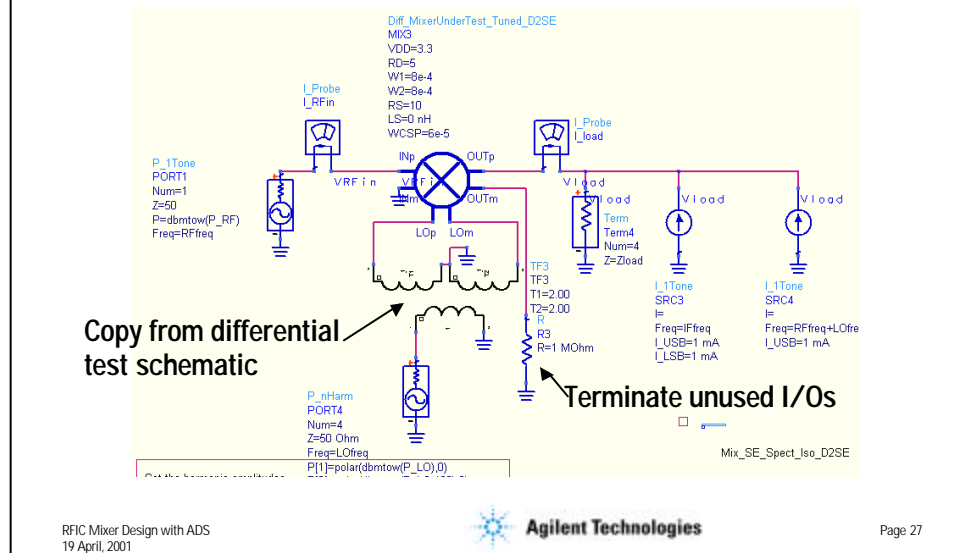
 Agilent Technologies

Page 26

The Mixer TOI/IMD simulation is performed again for RS of 10, 20, and 30 ohms. We can see that the dynamic range slowly improves for smaller RS. This will be very dependent on the noise bandwidth, however. For our simulations, a 30 MHz bandwidth was assumed.

## Test as single ended mixer

Modify SE schematic to evaluate our mixer



A DesignGuide schematic intended for evaluation of single-ended mixers was copied from the menu and modified. Our tuned mixer with the D2SE output stage was inserted from the component library. Unused inputs were terminated: the input was grounded and the output terminated in a large resistance.

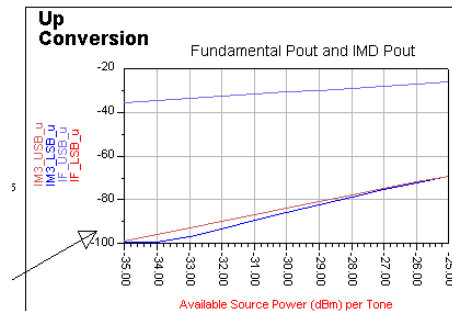
The LO is differential. A transformer and source was copied from a differential test schematic and pasted into this schematic. An active LO SE to differential stage could also be designed and added to the mixer if desired.

## Single-ended NF and IMD performance

Single-Ended Mixer Characterization versus a Swept Parameter

- NF higher; CG lower than differential mixer
- Use NF and IMD vs RF power to calculate dynamic range for the single-ended mixer connection

Swept Parameter Value	Noise Figure, dB	Down Conversion Gain, dB	Up Conversion Gain, dB
10.00	7.89	-9.48	-0.36
20.00	9.46	-11.49	-2.37
30.00	10.78	-13.11	-4.00



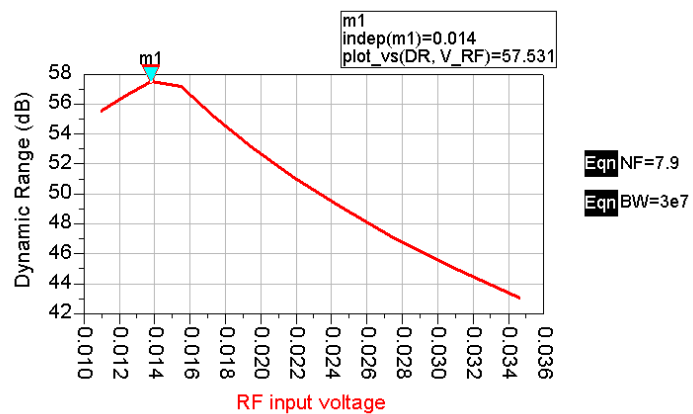
RFIC Mixer Design with ADS  
19 April, 2001

 Agilent Technologies

Page 28

Again, noise figure and IMD vs RF power sweeps were performed for a range of RS values from 10 to 30 ohms. This is combined to determine dynamic range on the next slide.

## Single-ended mixer: dynamic range



RFIC Mixer Design with ADS  
19 April, 2001



Page 29

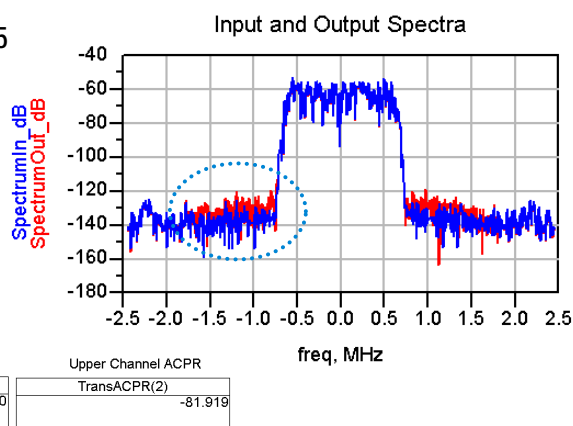
The best result was for the RS = 10 ohm case. We see a peak dynamic range of 57.5 dB at an input voltage of 14 mV.

## 5. Simulate mixer with CDMA input

Examples with Modulated Signals

Simulation with CDMA Source

- Circuit envelope simulation with IS-95 CDMA modulation
- 128 symbols
- ACPR increased
- $V_{in} = 12 \text{ mV } (-33 \text{ dBm})$



Lower Channel ACPR		Upper Channel ACPR	
TransACPR(1)	-82.470	TransACPR(2)	-81.919

RFIC Mixer Design with ADS  
19 April, 2001

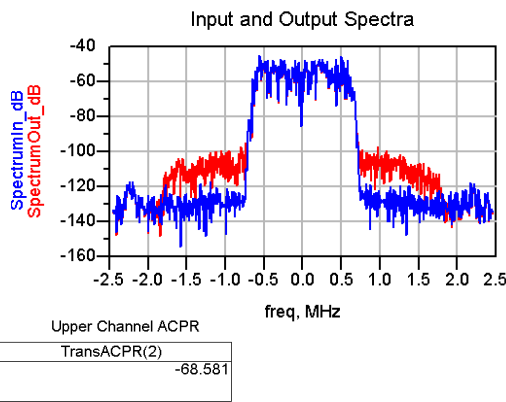
 Agilent Technologies

Page 30

A more severe test of linearity requires simulation with a digital signal source such as this CDMA example. An IS-95 CDMA source with very good ACPR was used to drive the mixer input. When the input RF signal level was set to the optimum value for mixer dynamic range, relatively little spectral regrowth is observed. To save time, only 128 symbols were used in the circuit envelope simulation. A more accurate simulation might require in excess of 1000 symbols.

## Evaluate at higher drive level

- Input available power increased to -25 dBm
- Effects of IMD generation and gain compression effects are evident with wideband source – ACPR is much higher



RFIC Mixer Design with ADS  
19 April, 2001



Page 31

When the signal level is increased, there is much more distortion evident. The input level in this simulation corresponds to about 30 mV of drive voltage.

## IF input impedance

Single-Ended Mixer Characterization

IF Spect., Isolation, Conv. Gain, Port Impedances

- The RF input port impedance can be matched if baseband/IF generation is from off-chip.
- We can see at 200 MHz, the input impedance is dominated by capacitive reactance.

Reference Impedance for Rho  
(rereflection coefficient) and  
VSWR calculations.  $\text{Eqn } Z_0=50$

Looking into the RF (Input) Port:

Frequency	Impedance	Reflection Coefficient	VSWR
200.MHz	8.47 - j1.40E2	0.96 / -39.20	52.28

RFIC Mixer Design with ADS  
19 April, 2001



Page 32

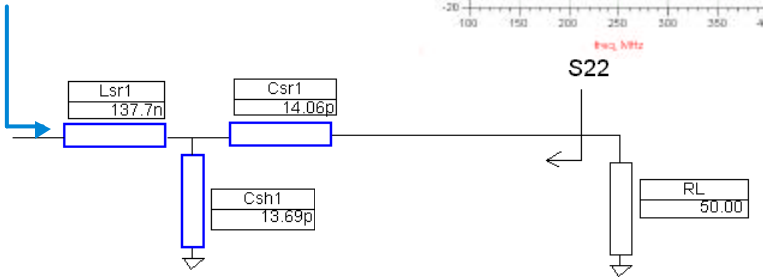
We noted earlier that the input of the mixer is badly mismatched. This may not be of much concern if the baseband and IF driver circuits are on the same chip with the upconversion mixer. In that case, the voltage levels are more of interest.

If you are interested in driving from off chip, we can see above that the input impedance is dominated by capacitive reactance. A matching network could increase the conversion gain significantly if this were of interest.

## Impedance matching utility

Lumped Multi-Element Z-Y Matching Networks

- Specify  $Z_{desired} = Z_{in^*}$



RFIC Mixer Design with ADS  
19 April, 2001

 Agilent Technologies

Page 33

The Mixer DesignGuide contains several impedance matching utilities that could be used to design and evaluate matching networks.

## Conclusion

### Learning objectives met:

- Learn how to make use of the Agilent ADS Mixer DesignGuide
- Understand the important design and analysis tools for this application
- Specify performance: Gain, NF,  $P_{1\text{dB}}$ , TOI, Dynamic Range
- Improve the design: add resonator and convert to single-ended output

We have now completed a design study of an upconversion transmit mixer. The procedure illustrated here is by no means unique, and you may find ways of getting the same information by other sequences of steps.

Also, the DesignGuide analysis schematics can be further modified to include nested sweeps. These can provide a two-dimensional perspective on the design space to gain further insight (in exchange for increased simulation time and data file size).

You can also make use of the ADS optimizer to automatically achieve the design goals. This could require combining the simulations on more than one analysis schematic onto a single multi-level schematic, or possibly creating a look-up table and interpolation function for one of the critical performance parameters to speed up the optimization process.

## References



- Gray, P. R. and Meyer, R. G., *Design of Analog Integrated Circuits*, 4th Ed., Chap. 10, Wiley, 2001.
- Gilbert, B., "Design Considerations for BJT Active Mixers", Analog Devices, 1995.
- Lee, T. H., *The Design of CMOS Radio-Frequency Integrated Circuits*, Chap. 11, Cambridge U. Press, 1998.
- Agilent EESof Design Seminar, "Fundamentals of Mixer Design," 1999.
- Agilent EESof Design Seminar, "RFIC Mixer Design", 1999.